MYCOBACTERIA-HOST INTERACTIONS: GENETICS, IMMUNITY, PATHOLOGY

EDITED BY: Alexander S. Apt, Igor Kramnik and David Neil McMurray
PUBLISHED IN: Frontiers in Cellular and Infection Microbiology and Frontiers in Immunology

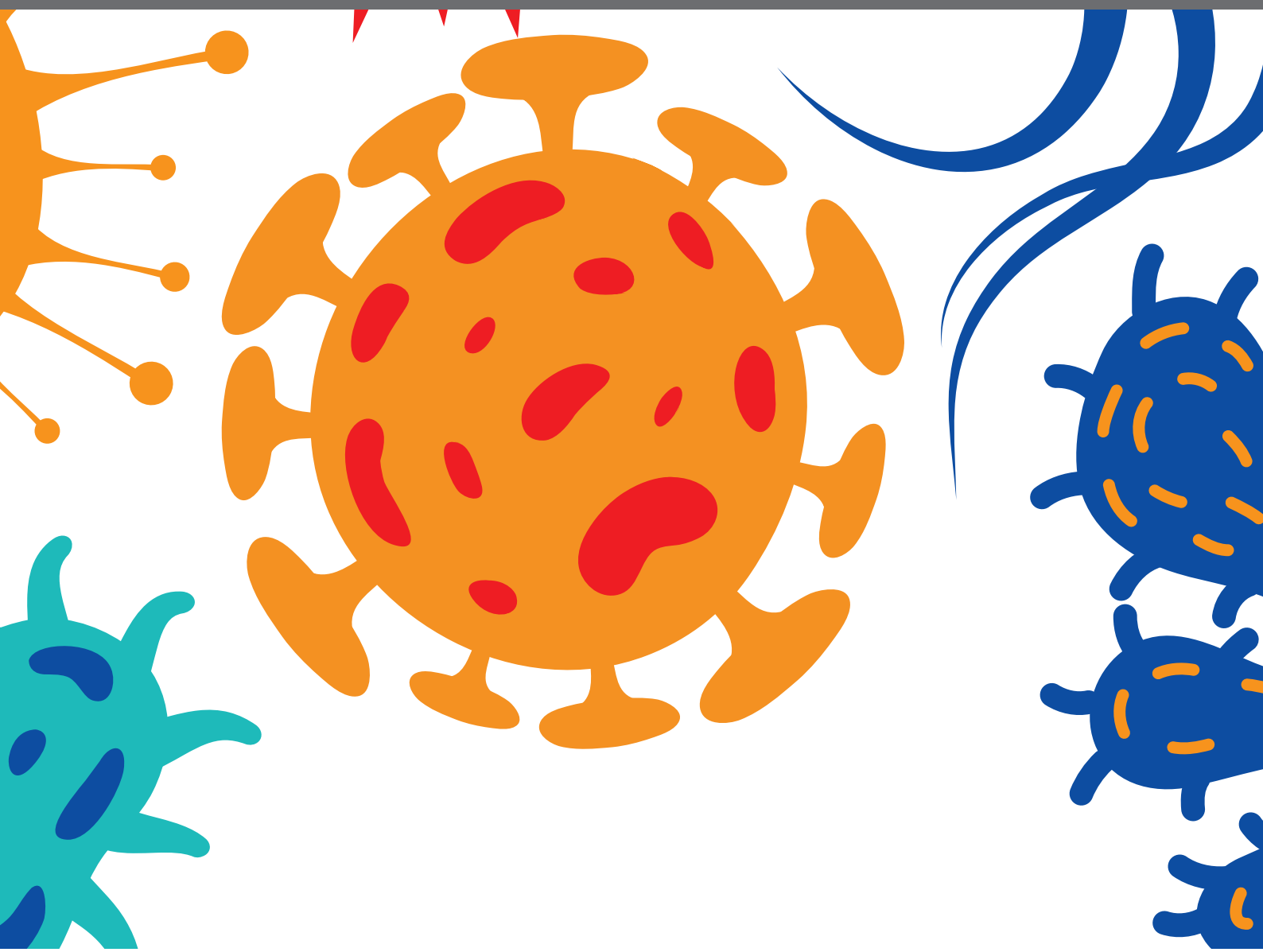

frontiers Research Topics

frontiers

ISSN 1664-8714
ISBN 978-2-88966-298-2
DOI 10.3389/978-2-88966-298-2

About Frontiers

Frontiers is more than just an open-access publisher of scholarly articles: it is a pioneering approach to the world of academia, radically improving the way scholarly research is managed. The grand vision of Frontiers is a world where all people have an equal opportunity to seek, share and generate knowledge. Frontiers provides immediate and permanent online open access to all its publications, but this alone is not enough to realize our grand goals.

Frontiers Journal Series

The Frontiers Journal Series is a multi-tier and interdisciplinary set of open-access, online journals, promising a paradigm shift from the current review, selection and dissemination processes in academic publishing. All Frontiers journals are driven by researchers for researchers; therefore, they constitute a service to the scholarly community. At the same time, the Frontiers Journal Series operates on a revolutionary invention, the tiered publishing system, initially addressing specific communities of scholars, and gradually climbing up to broader public understanding, thus serving the interests of the lay society, too.

Dedication to Quality

Each Frontiers article is a landmark of the highest quality, thanks to genuinely collaborative interactions between authors and review editors, who include some of the world's best academicians. Research must be certified by peers before entering a stream of knowledge that may eventually reach the public - and shape society; therefore, Frontiers only applies the most rigorous and unbiased reviews.
Frontiers revolutionizes research publishing by freely delivering the most outstanding research, evaluated with no bias from both the academic and social point of view. By applying the most advanced information technologies, Frontiers is catapulting scholarly publishing into a new generation.

What are Frontiers Research Topics?

Frontiers Research Topics are very popular trademarks of the Frontiers Journals Series: they are collections of at least ten articles, all centered on a particular subject. With their unique mix of varied contributions from Original Research to Review Articles, Frontiers Research Topics unify the most influential researchers, the latest key findings and historical advances in a hot research area! Find out more on how to host your own Frontiers Research Topic or contribute to one as an author by contacting the Frontiers Editorial Office: researchtopics@frontiersin.org

MYCOBACTERIA-HOST INTERACTIONS: GENETICS, IMMUNITY, PATHOLOGY

Topic Editors:
Alexander S. Apt, Central Tuberculosis Research Institute (RAMS), Russia
Igor Kramnik, Boston University, United States
David Neil McMurray, Texas A&M Health Science Center, United States

Citation: Apt, A. S., Kramnik, I., McMurray, D. N., eds. (2020). Mycobacteria-Host Interactions: Genetics, Immunity, Pathology. Lausanne: Frontiers Media SA.
doi: 10.3389/978-2-88966-298-2

Table of Contents

frontiers in Cellular and Infection Microbiology

EDITORIAL
published: 30 October 2020
doi: 10.3389/fcimb.2020.611216

Editorial: Mycobacteria-Host Interactions: Genetics, Immunity, Pathology

Alexander S. Apt[1], *Igor Kramnik*[2] *and David Neil McMurray*[3]*

[1] Central Tuberculosis Research Institute, Moscow, Russia, [2] Boston University, Boston, MA, United States, [3] Texas A & M Health Science Center, Bryan, TX, United States

Keywords: mycobacteria, pathogenesis, immunity, genetic, vaccine

Editorial on the Research Topic

Mycobacteria-Host Interactions: Genetics, Immunity, Pathology

This research topic consists of 13 manuscripts that focus on some aspect of the interaction between mycobacteria and their hosts. Many report novel experimental data, while others are minireviews of the pertinent literature. A few of the manuscripts reflect the unique perspectives of the authors on issues in tuberculosis (TB) of some controversy.

For purposes of this editorial, we have organized the manuscripts into discrete sub-topics with the indicated number of papers in each: TB-comorbidities [diabetes (2); TB and HIV (2)]; aspects of TB pathogenesis [dormancy (2) and dissemination (2)]; innate (2) and adaptive (2) immunity; and a provocative paper on the application of personalized or precision medicine in TB (1).

Segura-Cerda et al. have reviewed the literature that establishes Type 2 diabetes (T2D) as an important co-morbidity that increases the risk 2–4 fold for the development of pulmonary TB. In this manuscript, the authors focus on the putative mechanisms that might explain this synergistic relationship. They highlight dyslipidemia and hyperglycemia as two of the conditions associated with T2D that exacerbate TB. Several hormonal changes (e.g., decreases in leptin, ghrelin, and reactive oxygen species) and vitamin D deficiency are also discussed as they relate to increased susceptibility to TB. A related paper (Kumar et al.) reports the significant associations that they observed between plasma eicosanoid levels, lung pathology and bacterial burden in human patients with TB–T2D co-morbidity and speculate about potential mechanisms.

HIV infection is a risk factor for relapse following failed chemotherapy in treated TB patients, but the mechanisms involved are not understood. Huante et al. have adapted a humanized mouse model of TB–HIV co-infection to study the effect of HIV on relapse in mice with post-chemotherapy pauci-bacillary infection. The authors used the so-called "Cornell" approach to drive infection levels down with rifampin and isoniazid, and then infected the mice with HIV. Relapsing co-infected mice exhibited increase bacterial and viral burdens in the lungs. This novel model has great potential to elucidate the synergistic effects of these two pathogens on the host. In a second paper related to TB–HIV co-infection, Naqvi and Endsley review the roles of C-type lectin receptor (CLR) recognition. CLRs such as the mannose receptor, Mincle, Dectin 1 & 2, DC-SIGN, and others may play important roles in protective immunity and immune evasion in TB/HIV and their genetic polymorphisms in populations may influence disease susceptibility in co-infected individuals.

OPEN ACCESS

Edited and reviewed by:
Nahed Ismail,
University of Illinois at Chicago, United States

***Correspondence:**
David Neil McMurray
mcmurray@medicine.tamhsc.edu

Specialty section:
This article was submitted to Clinical Microbiology, a section of the journal Frontiers in Cellular and Infection Microbiology

Received: *28 September 2020*
Accepted: *13 October 2020*
Published: *30 October 2020*

Citation:
Apt AS, Kramnik I and McMurray DN (2020) Editorial: Mycobacteria-Host Interactions: Genetics, Immunity, Pathology. Front. Cell. Infect. Microbiol. 10:611216. doi: 10.3389/fcimb.2020.611216

There is perhaps no aspect of TB pathogenesis more intriguing or controversial than latency or dormancy. Two papers in this Research Topic address that issue. Trutneva et al. created dormant *Mycobacterium tuberculosis* H37Rv using established culture procedures and studied the protein profiles of the non-replicating bacilli over a 13-month period. The proteome of the dormant bacilli differed markedly from that of metabolically active cells but, despite the substantially diminished size of the dormant cells, they contained numerous intact proteins. The authors speculate that the presence of chaperones, DNA-stabilizing proteins, and enzymes involved in protection from oxidative stress were responsible for the preservation of many proteins in dormant *M. tuberculosis*. In the second paper, Salina et al. identified an NO-inducible small mycobacterial RNA (MTS1338) that apparently regulates a shift in the transcriptome profile consistent with adaptation to the environment within the macrophage. The authors speculate that MTS1338 may be involved in the transition to the non-replicating, dormant state within host cells.

Although pulmonary disease is the most common clinical presentation of TB, there are several extra-pulmonary manifestations that present both diagnostic and therapeutic challenges. Moule and Cirillo have reviewed the literature on disseminated TB [e.g., lymphadenitis, spinal infection (Pott's Disease), pleurisy, and central nervous system (CNS) disease] and have focused on the mechanisms by which mycobacteria may escape from the lung. They examine the potential roles of lung epithelial cells, dendritic cells, alveolar and infiltrating macrophages in the escape of bacilli from the lung and suggest that extra-pulmonary spread may be a common consequence of all TB lung infections. A second paper (Kumar et al.) focuses on CNS TB using a well-established rabbit model of meningitis in which different strains of *M. tuberculosis* were injected intra-cisternally. The authors report that blocking pro-inflammatory cytokines (e.g., TNFα, IL-6, IL-1β) improves the clinical outcome and suggest that phosphodiesterase-4 inhibitors may have therapeutic potential for treatment of humans with TB meningitis.

Four of the manuscripts in this Research Topic discuss the mechanisms by which innate host responses and adaptive immunity contribute to a successful host response to mycobacterial infection. Two of the papers have examined the role of Th-17 cells that produce IL-17A, a cytokine which plays a protective role early in infection but drives tissue destruction later in the course of disease when it becomes unregulated. Leisching reviews the importance of PI3-Kinase pathways in driving a Th-17 response and that the p110δ and p110γ isoforms have opposite effects on Th-17 cell populations. The author speculates that inhalable PI3-Kinase inhibitors might have therapeutic benefit in TB by dampening the unregulated IL-17A response. Huang et al. report that Interleukin-2-inducible T-cell kinase (ITK) is involved in early protection against pulmonary TB in mice. ITK-deficient mice developed increased bacterial burdens and pathology in the lungs accompanied by a defect in the development of IL-17A-producing γδT cells. They also demonstrated that pulmonary granulomas from active TB patients contained increased levels of ITK mRNA compared to normal lung tissue using laser capture microdissection. The authors suggest that enhancing ITK activity may be a viable host-directed therapeutic approach.

Kang et al. utilized a novel ethyl cinnamate method for clarifying mouse lung tissues to examine the localization of different types of innate immune cells (e.g., neutrophils, alveolar and infiltrating macrophages, etc.) within pulmonary granulomas. The mice were infected with *M. tuberculosis* by the aerosol route and the lungs were removed after 4 weeks. The clarified tissues were imaged using light sheet fluorescence microscopy and 3D images of the infected lungs were created.

Le Moigne et al. used both *in vitro* and *in vivo* approaches to examine the involvement of a TLR-2 activating factor in the pathogenesis of *Mycobacterium abscessus*, an important pulmonary pathogen in cystic fibrosis (CF) patients. Antibodies against the factor were found in the sera of CF patients. However, vaccination with the TLR-2 activating factor (a mixture of several lipoproteins) exhibited no protection against aerosol infection of mice with *M. abscessus*, but provided modest protection when mice were challenged intravenously.

The final paper in this Research Topic is a thought-provoking minireview/perspective written by Azad et al. The authors have reviewed the genetic basis for considerable human-to-human variation in cellular, inflammatory and immune responses to TB. They advocate for a "personalized" or "precision" medicine approach to compensate for those differences but admit that this approach is fraught with challenges. These include the lack of sufficient genetic data in many ethnic groups and the difficulty in delivering individualized therapies in high-burden, low-resource settings.

We believe that the manuscripts in this Research Topic reflect novel approaches to filling some of the most vexing gaps in our understanding of the interactions between mycobacteria and their hosts. Several of the papers have clear translational significance which bodes well for the application of this knowledge to improved TB prevention and control going forward.

AUTHOR CONTRIBUTIONS

All three authors contributed equally to this editorial. All authors contributed to the article and approved the submitted version.

Conflict of Interest: The authors declare that the research was conducted in the absence of any commercial or financial relationships that could be construed as a potential conflict of interest.

frontiers in Cellular and Infection Microbiology

ORIGINAL RESEARCH
published: 01 October 2019
doi: 10.3389/fcimb.2019.00335

Plasma Eicosanoid Levels in Tuberculosis and Tuberculosis-Diabetes Co-morbidity Are Associated With Lung Pathology and Bacterial Burden

Nathella Pavan Kumar[1]*, *Kadar Moideen*[1], *Arul Nancy*[1,2], *Vijay Viswanathan*[2], *Basavaradhya S. Shruthi*[2], *Sivakumar Shanmugam*[3], *Syed Hissar*[4], *Hardy Kornfeld*[5] and *Subash Babu*[1,6]

[1] National Institutes of Health—NIRT—International Center for Excellence in Research, Chennai, India, [2] Prof. M. Viswanathan Diabetes Research Center, Chennai, India, [3] Department of Bacteriology, National Institute for Research in Tuberculosis, Chennai, India, [4] Department of Clinical Research, National Institute for Research in Tuberculosis, Chennai, India, [5] University of Massachusetts Medical School, Worcester, MA, United States, [6] Laboratory of Parasitic Diseases, National Institutes of Allergy and Infectious Diseases, National Institutes of Health, Bethesda, MD, United States

OPEN ACCESS

Edited by:
Alexander S. Apt,
Central Tuberculosis Research Institute (RAMS), Russia

Reviewed by:
Anna Upton,
TB Alliance, United States
Mohtashem Samsam,
University of Central Florida College of Medicine, United States

***Correspondence:**
Nathella Pavan Kumar
pavankumarn@nirt.res.in

Specialty section:
This article was submitted to Clinical Microbiology, a section of the journal Frontiers in Cellular and Infection Microbiology

Received: 24 July 2019
Accepted: 18 September 2019
Published: 01 October 2019

Citation:
Pavan Kumar N, Moideen K, Nancy A, Viswanathan V, Shruthi BS, Shanmugam S, Hissar S, Kornfeld H and Babu S (2019) Plasma Eicosanoid Levels in Tuberculosis and Tuberculosis-Diabetes Co-morbidity Are Associated With Lung Pathology and Bacterial Burden. Front. Cell. Infect. Microbiol. 9:335. doi: 10.3389/fcimb.2019.00335

Host eicosanoids are lipid mediators of inflammation that are commonly accepted as important modulators of the host immune response in *Mycobacterium tuberculosis* infection. During active tuberculosis (TB), eicosanoids may play an important role in the regulation of inflammatory responses. However, a detailed investigation of the relationship of eicosanoids in TB and TB-diabetes comorbidity (TB-DM) and association to disease pathology or bacterial burdens has not been studied. To study this, we examined the plasma levels of Lipoxin A4 (LXA4), 15-epi-LXA4, Leukotriene B4 (LTB4), and Prostaglandin E2 (PGE2) in individuals with either TB-DM, TB, diabetes mellitus (DM) or healthy controls (HC). Plasma levels of LXA4, 15-epi-LXA4, and PGE2 were significantly increased while the levels of LTB4 were significantly decreased in TB-DM and TB group compared to DM and HC. The ratio of LXA4 to LTB4 and 15-epiLXA4 to LTB4 was significantly enhanced in TB-DM compared to TB. Moreover, the levels of LXA4, 15-epi-LXA4 and the ratios of LXA4 to LTB4 and 15-epiLX4 to LTB4 were significantly increased in TB individuals with bilateral or cavitary disease and these markers also revealed a significant positive relationship with bacterial burden. At the completion of anti-tuberculosis therapy (ATT), levels of LXA4, 15-epi-LXA4, and PGE2 in TB-DM and TB groups were diminished and levels of LTB4 were enhanced in the TB group compared to pre-treatment. Our data imply that alteration and upregulation of eicosanoids are standard characteristics of TB-DM co-morbidity. Our data also demonstrate that modulation in the eicosanoid levels reflect disease severity and extent in TB and TB-DM and are modulated by ATT.

Keywords: ***Mycobacterium tuberculosis*, diabetes mellitus, eicosanoids, anti-TB treatment, cytokines**

INTRODUCTION

Tuberculosis (TB) and diabetes mellitus (DM) are two of the most common diseases worldwide and often occur in the same geographical regions (Dooley and Chaisson, 2009). The occurrence of this co-morbidity poses a major threat to the global program for elimination of tuberculosis (Lonnroth et al., 2015). While a variety of clinical and epidemiological studies have been performed in this dual disease process, very few immunological or translational insights are available. The presence of a hyper-inflammatory milieu is highly characteristic of TB-DM co-morbidity and provides an opportunity for host-directed therapies to function as an adjunct measure to control this threat (Prada-Medina et al., 2017).

Eicosanoids are arachidonic acid derived lipid mediators that elicit a panel of pro- and anti-inflammatory responses and include prostaglandins, lipoxins, leukotrienes, and resolvins (Tobin et al., 2013). The enzyme 5-lipoxygenase is essential for the generation of lipoxin and leukotriene mediators from arachidonic acid, while the enzymes cyclooxygenase−1 and 2 are required for the generation of prostaglandins (Das, 2017). These lipid mediators have been shown to exert major influence on the outcomes of experimental *M. tuberculosis* (*M. tb)* infection (Mayer-Barber and Sher, 2015). Published studies have reported that leukotriene B4 (LTB4) and prostaglandin E2 (PGE2) play a host protective role by mediating bacterial clearance, while lipoxin A4 (LXA4) and 15-epi-lipoxin A4 (15-epi-LXA4) play a pathogenic role by hampering the host inflammatory response in TB (Mayer-Barber et al., 2014). Moreover, pro- and anti-inflammatory eicosanoid ratios are associated with the modulation of the host response to *M. tb* infection (Bafica et al., 2005; Tobin et al., 2012). Published studies have also reported that eicosanoid ratios in plasma were significantly increased in active TB patients compared to latent TB or healthy controls (Mayer-Barber et al., 2014). However, the role in eicosanoids in human TB and more specifically TB-DM co-morbidity has been poorly explored.

In this study, we elucidated the systemic levels of eicosanoids at baseline and at the end of anti-tuberculosis treatment (ATT). Our data reveal that DM differentially modulates the eicosanoid levels in individuals with TB before and after completion of treatment. Our data also show that certain eicosanoid levels reflect baseline disease severity and extent in TB and TB-DM and are modulated by ATT.

MATERIALS AND METHODS

Ethics Statement

The Ethics Committees of the Prof. M. Viswanathan Diabetes Research Center and National Institute for Research in Tuberculosis provided approval for this study. Informed written consent was obtained from all individuals recruited for the study.

Study Population

Plasma samples were collected from 44 participants with active pulmonary TB with diabetes mellitus (TB-DM) and 44 participants with active pulmonary TB (TB), 44 participants with diabetes mellitus (DM), 30 healthy control participants with no TB or diabetes (HC) recruited in Chennai, India. Pulmonary TB was diagnosed based on smear and culture positivity for *M. tb*. Chest X-rays were used to define cavitary disease (n = 23) and non-cavitary disease (n = 65) as well as unilateral (n = 49) vs. bilateral (n = 39) lung involvement. Smear grades were used to estimate bacterial burdens and classified as 1+ (n = 33), 2+ (n = 33) and 3+ (n = 22). All participants with active TB had no record of prior TB disease or ATT at the time of enrolment. Oral glucose tolerance test and/or glycated hemoglobin (HbA1c) levels (for known diabetics) was used to diagnose glycemic status (DM or normoglycemia), according to the WHO criteria. All the enrolled DM and HC participants were Quantiferon TB gold assay negative, asymptomatic and with normal chest X-rays. Standard ATT was administered to TB-DM and TB participants using the directly observed treatment, short course (DOTS) strategy. Fresh plasma samples were obtained again from TB-DM and TB participants at the end of ATT (6 months). All TB-DM and TB participants were culture negative for *M. tb* at this time point.

ELISA

Plasma levels of LXA4, 15-epi-LXA4, PGE2, and LTB4 were measured using the MyBioSource.com quantitative measurement kit and plasma levels of IL-1α, IL-1β, IFNγ, and TNFα were measured using Bio-Plex multiplex cytokine assay system (Bio-Rad, Hercules, CA). The lowest detection limits were as follows LXA4, 0.156 ng/mL; 15-epi-LXA4, 0.312 ng/mL; PGE2, 7.8 pg/mL; LTB4, 15.6 pg/mL; IL-1α, 5.23 pg/mL; IL-1β, 3.96 pg/mL; IFNγ, 4.39 pg/mL, and TNFα, 3.24 pg/mL.

Statistical Analysis

Geometric means (GM) were used for measurements of central tendency. Statistically significant differences between the four groups were analyzed using the Kruskal-Wallis test with Dunn's correction for multiple comparisons. The Mann-Whitney test was used to compare eicosanoid concentrations in TB individuals with unilateral or bilateral lung lesions and cavitary or non-cavitary disease. Linear trend post-test was used to compare eicosanoid concentrations with smear grades (reflecting bacterial burdens) and Spearman rank correlation was used to compare eicosanoid concentrations with HbA1c levels. Analyses were performed using GraphPad PRISM Version 8.

RESULTS

Study Population Characteristics

Table 1 depicts the demographic and biochemical features of the study population. As shown, the TB-DM and TB groups did not differ significantly in age, sex, smear, or culture grades at baseline (**Table 1**).

Plasma Levels of Eicosanoids and Ratios in TB and TB-DM

To determine the impact of TB and DM on eicosanoid expression, we measured the plasma levels of LXA4, 15-epiLXA4, PGE2, and LTB4 in TB-DM, TB, DM, and HC participants

TABLE 1 | Demographic and clinical variables of the study groups and biochemical parameters in TB-DM, TB, DM, and HC.

Study demographics	TB-DM	TB	DM	HC
No. of subjects recruited	44	44	44	30
Gender (male/female)	34/10	27/17	30/14	15/15
Median age (range)	47 (25–70)	39 (24–67)	44 (33–68)	34 (23–55)
Smear grade: 0/1+/2+/3+	0/14/19/11	0/19/18/7	NA	NA
Cavitary disease (Y/N)	13/31	10/34	NA	NA
Lung lesions (unilateral/bilateral)	24/20	25/19	NA	NA
Fasting blood glucose, mg/dL	154 (111–417)	93 (73–103)	140 (95–311)	75 (70–109)
Glycated hemoglobin level, %	10.3 (7.3–15.6)	5.6 (5.0–5.8)	10 (6.9–12.5)	5.5 (5.0–5.9)

The values represent the geometric mean (and the 95% confidence intervals) except for age where the median (and the range) are depicted.

(**Figure 1A**). The levels of LXA4 (Geometric Mean (GM) 11.3 ng/ml in TB-DM vs. 6.6 ng/ml in TB, 1.3 pg/ml in DM and 2.04 pg/ml in HC), 15-epiLXA4 (GM 6.8 ng/ml in TB-DM vs. 3.9 ng/ml in TB, 1.4 ng/ml in DM and 1.7 ng/ml in HC), and PGE2 (GM 10 pg/ml in TB-DM vs. 5.9 pg/ml in TB, 2.5 pg/ml in DM and 2.4 pg/ml in HC) were significantly elevated in TB-DM and DM group in comparison with TB and HC group. In contrast, the levels of LTB4 (GM 170.3 pg/ml in TB-DM vs. 220.3 pg/ml in TB, 357.8 pg/ml in DM and 329.8 pg/ml in HC) was significantly decreased in TB-DM and DM group in comparison with TB and HC individuals. Thus, TB-DM and TB were associated with significantly altered plasma levels of eicosanoids. Next, to examine the association of eicosanoid ratios with TB-DM and TB, we measured the ratios of LXA4:LTB4, 15-epi-LXA4:LTB4, LXA4:PGE2, 15-epi-LXA4:PGE2, and PGE2:LTB4 in TB-DM and TB individuals (**Figure 1B**). The ratios of LXA4:LTB4 (GM 0.06643 in TB-DM vs. 0.02994 in TB), 15-epi-LXA4:LTB4 (GM 0.03992 in TB-DM vs. 0.01744 in TB), and PGE2:LTB4 (GM 0.05873 in TB-DM vs. 0.02691 in TB) were significantly increased in TB-DM compared to TB. Thus, balance between lipid mediators is associated with differences in TB and TB-DM.

LXA4 and 15-epiLXA4 Are Markers of Disease Severity in TB and TB-DM

To determine the relationship among the plasma levels of eicosanoids and disease severity in TB and TB-DM, we compared plasma levels of LXA4, 15-epiLXA4, PGE2, and LTB4 in all TB study participants with unilateral vs. bilateral disease and cavitary vs. non-cavitary disease based on chest X-ray. As shown in **Figure 2A**, the plasma levels of LXA4 (GM 14 ng/ml in cavitary vs. 9 ng/ml in non-cavitary disease) and 15-epiLXA4 (GM 8.2 ng/ml in cavitary vs. 4.4 ng/ml in non-cavitary) were significantly elevated in TB-DM and TB participants with cavitary disease compared to those without. Similarly, as shown in **Figure 2B**, the plasma levels of LXA4 (GM 12 ng/ml in bilateral vs. 9 ng/ml in unilateral disease) were significantly elevated in TB-DM participants with bilateral disease compared to those with unilateral disease. To elucidate the relationship between the ratios of eicosanoids and disease severity in TB and TB-DM, we compared ratios of LXA4:LTB4, 15-epi-LXA4:LTB4, LXA4:PGE2, 15-epi-LXA4:PGE2, and PGE2:LTB4 in all TB study participants with unilateral vs. bilateral disease and cavitary vs. non-cavitary disease based on chest X-ray. As shown in **Figure 2C**, the ratios of LXA4:LTB4 (GM 0.06902 in cavitary vs. 0.0303550 in non-cavitary disease) and 15-epi-LXA4:LTB4 (GM 0.04095 in cavitary vs. 0.02299 in non-cavitary) were significantly elevated in TB-DM and TB participants with cavitary disease compared to those without. Similarly, as shown in **Figure 2D**, the ratios of LXA4:LTB4 (GM 0.05959 in bilateral vs. 0.03628 in unilateral disease) and 15-epi-LXA4:LTB4 (GM 0.03531 in bilateral vs. 0.02140 in unilateral disease) were significantly elevated in TB-DM and TB participants with bilateral disease compared to those with unilateral disease. Thus, disease severity assessed radiographically in TB-DM and TB was associated with elevated plasma levels of certain eicosanoids, most notably LXA4 and altered ratios of LXA4 or epi-LXA4 to LTB4.

LXA4 and 15-epiLXA4 Are Markers of Bacterial Burden in TB and TB-DM

To determine the association of the plasma levels of eicosanoids and bacterial burdens, we studied a correlation of the plasma levels of LXA4, 15-epiLXA4, PGE2, and LTB4 in TB-DM and TB study participants with smear grades from 1+ to 3+. As shown in **Figure 3A**, LXA4 and 15-epiLXA4 showed a significant positive correlation with smear grades in TB-DM and TB participants, indicating a positive relationship of these factors with bacterial burdens. To elucidate the relationship of the ratios of eicosanoids and bacterial burdens, we studied the correlation of the ratios of LXA4:LTB4, 15-epi-LXA4:LTB4, LXA4:PGE2, 15-epi-LXA4:PGE2, and PGE2:LTB4 in TB-DM and TB participants with smear grades. As shown in **Figure 3B**, LXA4:LTB4 and 15-epi-LXA4:LTB4 showed a significant positive relationship with smear grades in TB-DM and TB participants, demonstrating a positive association of these factors with bacterial burdens. Thus, disease severity by estimated bacterial burden in TB-DM and TB was associated with increased systemic levels of certain eicosanoids, most notably LXA4 and altered ratios of LXA4 or epi-LXA4 to LTB4.

Decreased Plasma Levels of Eicosanoids in TB-DM Following ATT

To determine whether the eicosanoid levels were altered by ATT, we examined the plasma levels of eicosanoids in TB-DM

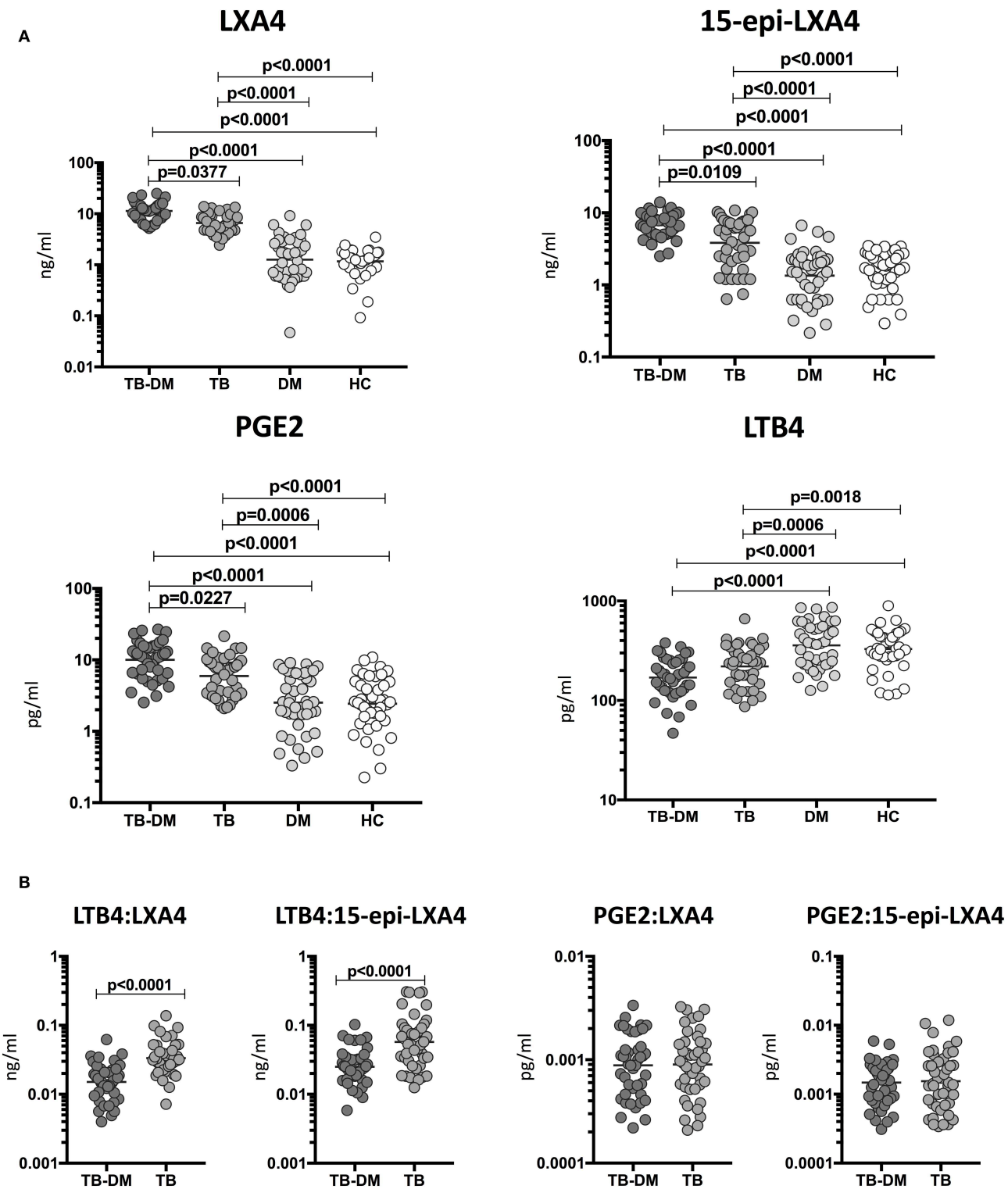

FIGURE 1 | Altered plasma levels of eicosanoids in TB-DM and TB individuals. **(A)** The plasma levels of LXA4, 15-epi-LXA4, PGE2, and LTB4 were measured in TB-DM ($n = 44$), TB ($n = 44$), DM ($n = 44$), and HC ($n = 44$) individuals at baseline. **(B)** Ratios of LXA4:LTB4, 15-epi-LXA4:LTB4, LXA4:PGE2, 15-epi-LXA4:PGE2, and PGE2:LTB4 in TB-DM and TB individuals at baseline. The data are represented as scatter plots with each circle representing a single individual. **(A)** *P*-values were calculated using the Kruskal-Wallis test with Dunn's *post-hoc* for multiple comparisons. **(B)** *P*-values were calculated using Mann-Whitney test.

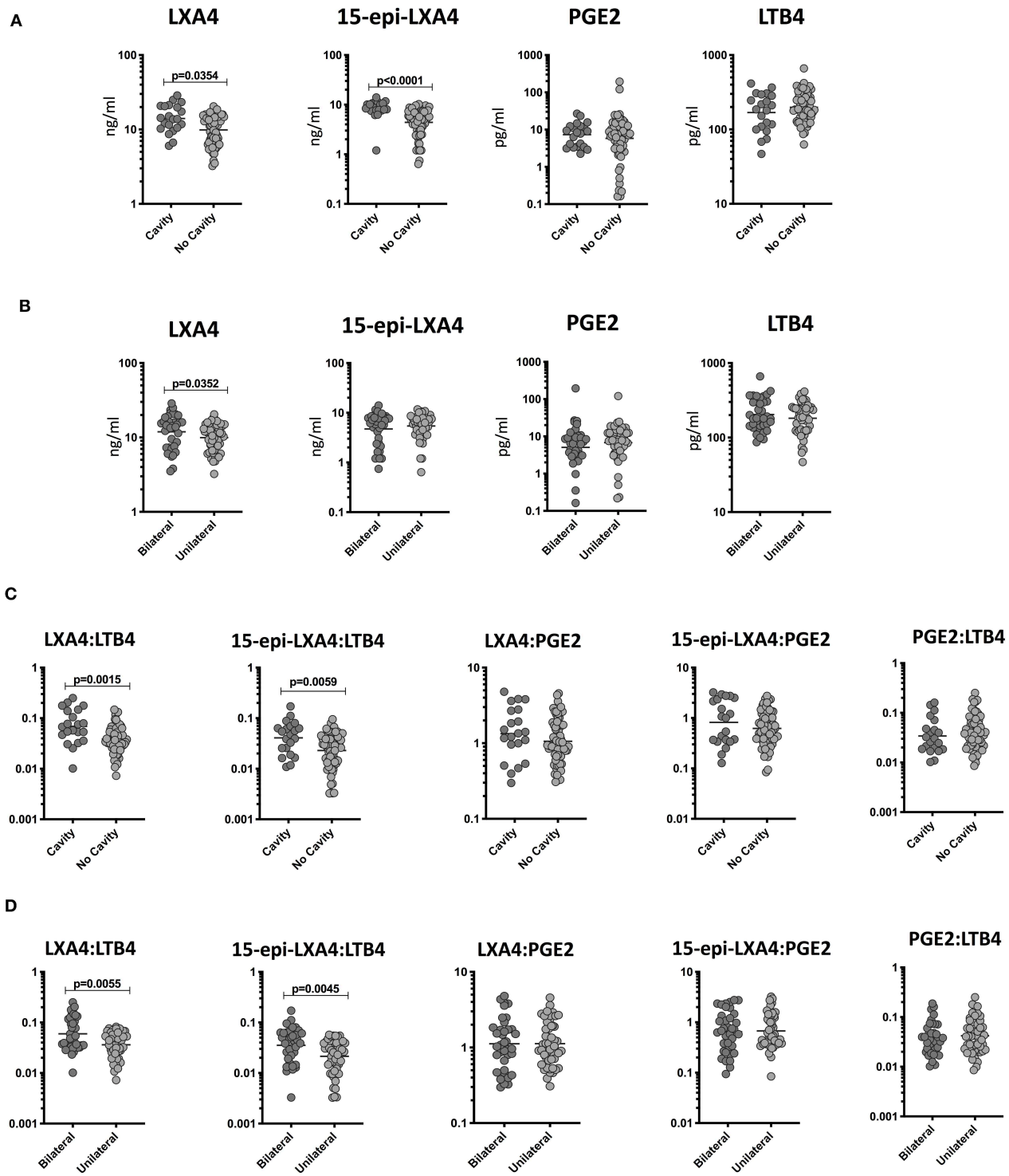

FIGURE 2 | Elevated plasma levels of eicosanoids in cavitary and bilateral disease and relationship to bacterial burden in TB-DM and TB individuals. **(A)** The plasma levels of LXA4, 15-epi-LXA4, PGE2, and LTB4 were measured in TB-DM and TB individuals with cavitary vs. non-cavitary disease. **(B)** The plasma levels of LXA4, 15-epi-LXA4, PGE2, and LTB4 were measured in TB-DM and TB individuals with bilateral vs. unilateral disease. **(C)** The ratios of LXA4:LTB4, 15-epi-LXA4:LTB4, LXA4:PGE2, 15-epi-LXA4:PGE2, and PGE2:LTB4 were measured in TB-DM and TB individuals with cavitary vs. non-cavitary disease **(D)** The ratios of LXA4:LTB4, 15-epi-LXA4:LTB4, LXA4:PGE2, 15-epi-LXA4:PGE2, and PGE2:LTB4 were measured in TB-DM and TB individuals with bilateral vs. unilateral disease. The data are represented as scatter plots with each circle representing a single individual. *P*-values were calculated using the Mann-Whitney test with Holm's correction for multiple comparisons.

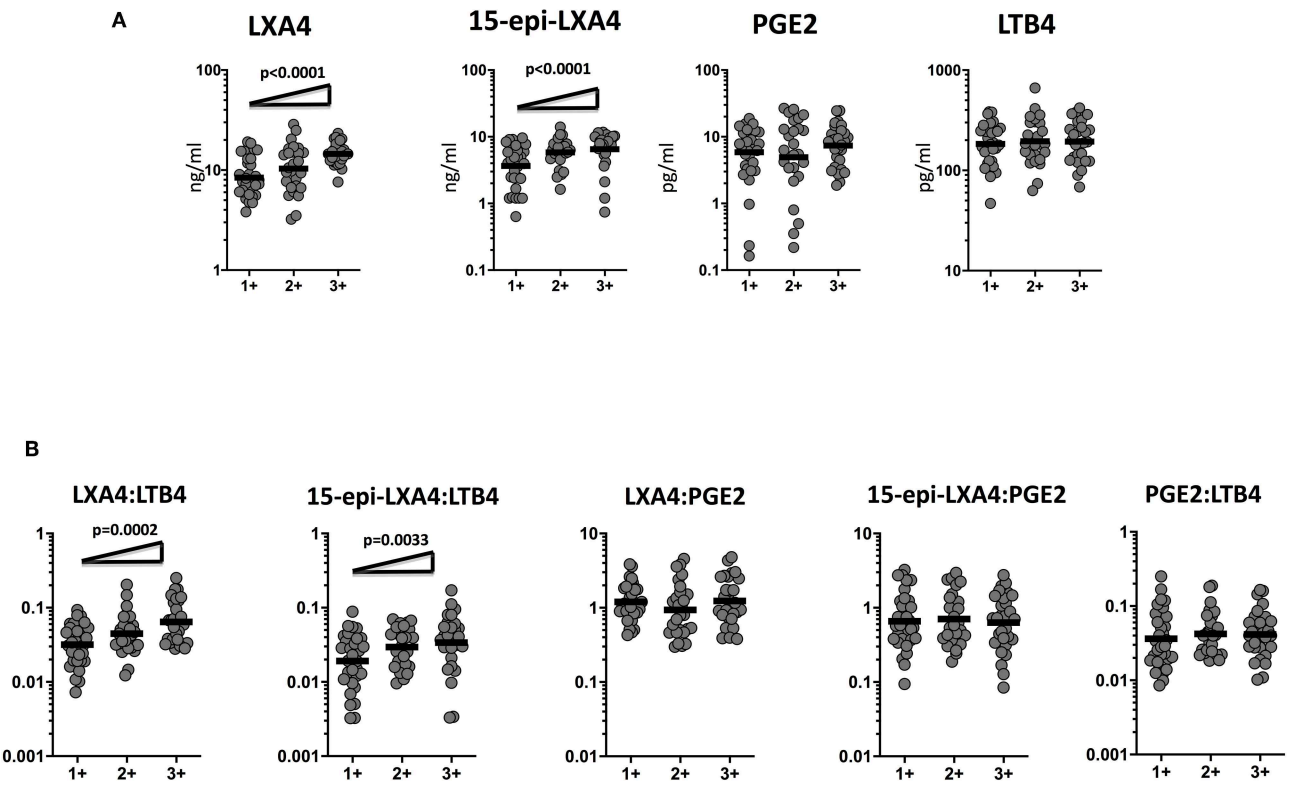

FIGURE 3 | Eicosanoid are markers of bacterial burden in TB and TB-DM. **(A)** The relationship between the plasma levels of LXA4, 15-epi-LXA4, PGE2, and LTB4 and smear grades as estimated by sputum smears was examined in TB-DM and TB individuals. **(B)** The relationship between the ratios of LXA4:LTB4, 15-epi-LXA4:LTB4, LXA4:PGE2, 15-epi-LXA4:PGE2, and PGE2:LTB4 and smear grades as estimated by sputum smears was examined in TB-DM and TB individuals. The data are represented as scatter plots with each circle representing a single individual. For bacterial burden correlation *P*-values were calculated using the Linear trend post-test.

at baseline (pre-T) and at the completion of ATT (post-T). As shown in **Figure 4A**, ATT resulted in significantly decreased levels of LXA4 (GM of 11.31 ng/ml at pre-T vs. 6.1 ng/ml at post-T), 15-epiLXA4 (GM of 6.7 ng/ml at pre-T vs. 1.2 ng/ml at post-T) and PGE2 (GM of 10 pg/ml at pre-T vs. 6.3 pg/ml at post-T) in TB-DM individuals. To elucidate whether the eicosanoid ratios were also modulated by ATT, we examined the eicosanoid ratios in TB-DM and TB at baseline (pre-T) and at the completion of ATT (post-T). As shown in **Figure 4B**, ATT resulted in significantly decreased ratios of LXA4:LTB4 (GM of 0.06643 at pre-T vs. 0.03306 at post-T), 15-epi-LXA4:LTB4 (GM of 0.03992 at pre-T vs. 0.004554 at post-T), 15-epi-LXA4:PGE2 (GM of 0.6798 at pre-T vs. 0.1326 at post-T), and PGE2:LTB4 (GM of 0.05873 at pre-T vs. 0.03434 at post-T) in TB-DM individuals. Thus, eicosanoid levels and eicosanoid ratios are significantly altered in TB-DM by ATT.

Decreased Plasma Levels of Eicosanoids in TB Following ATT

To examine whether the eicosanoid levels were modulated by ATT, we studied the eicosanoid ratios in TB at baseline (pre-T) and at the completion of ATT (post-T). As shown in **Figure 5A**, ATT resulted in significantly decreased levels of LXA4 (GM of 6.5 ng/ml at pre-T vs. 3.1 ng/ml at post-T), 15-epiLXA4 (GM of 3.8 ng/ml at pre-T vs. 0.77 ng/ml at post-T), and PGE2 (GM of 5.9 pg/ml at pre-T vs. 3.5 pg/ml at post-T) and significantly increased levels of LTB4 (GM of 220.3 pg/ml at pre-T vs. 283.8 pg/ml at post-T) in TB individuals. Similarly, as shown in **Figure 5B**, ATT resulted in significantly decreased levels of LXA4:LTB4 (GM of 0.02994 at pre-T vs. 0.01124 at post-T), 15-epi-LXA4:LTB4 (GM of 0.01744 at pre-T vs. 0.002713 at post-T), 15-epi-LXA4:PGE2 (GM of 0.6479 at pre-T vs. 0.1883 at post-T), and PGE2:LTB4 (GM of 0.02691 at pre-T vs. 0.01441 at post-T) in TB individuals. Thus, eicosanoid levels and eicosanoid ratios are significantly altered in TB by ATT.

Circulating Eicosanoids Exhibit Relationship With Pro-Inflammatory Cytokines

We have previously measured the circulating levels of pro-inflammatory cytokines (IL-1α, IL-1β, IFNγ, and TNFα) in these individuals and shown that IL-1β, IFNγ, and TNFα were significantly increased in TB patients with DM compared to TB individuals (Kumar et al., 2013; Prada-Medina et al., 2017). Since, LXA4, LTB4, and PGE2 have been described to be associated with pro-inflammatory cytokine modulation in

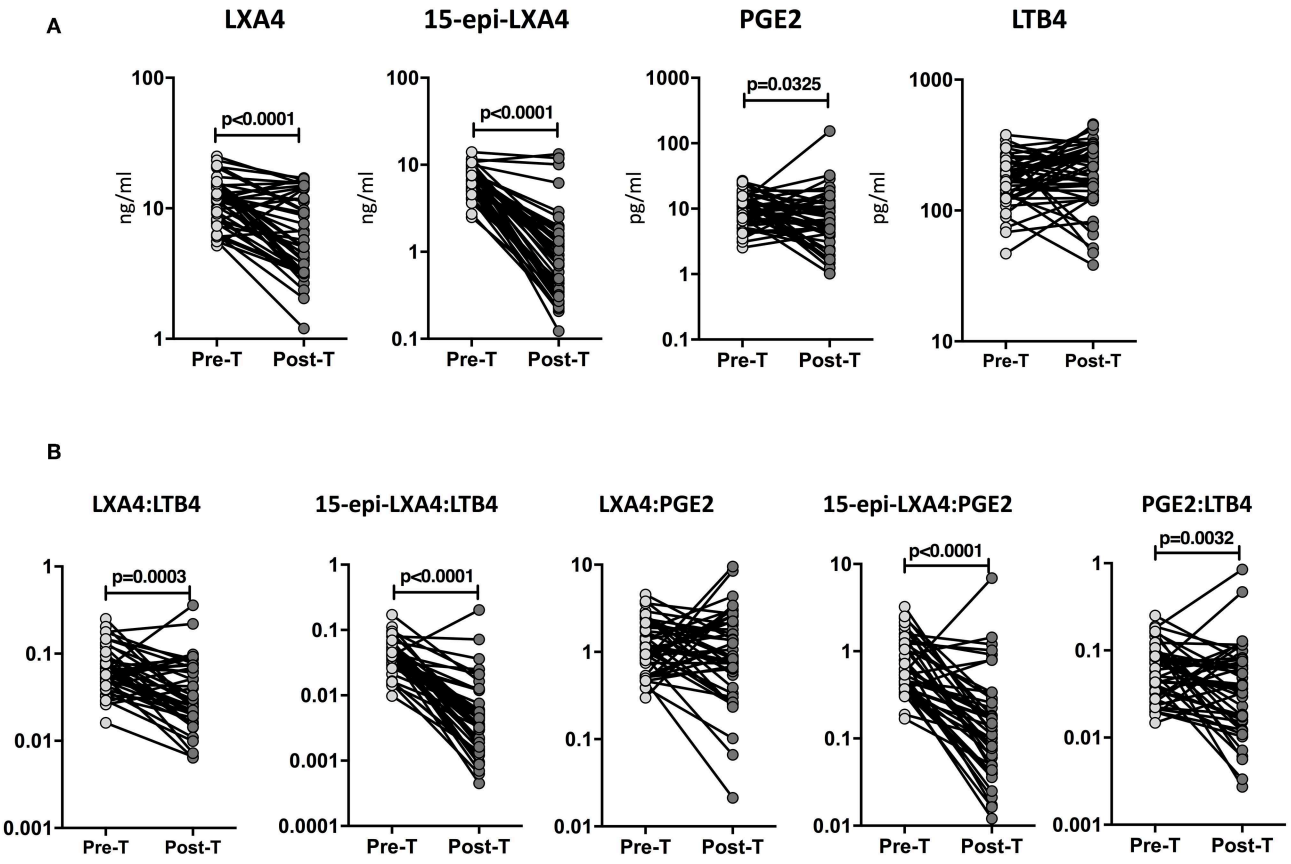

FIGURE 4 | Altered plasma levels of eicosanoids at the end of standard anti-tuberculosis therapy in TB-DM individuals. **(A)** The plasma levels of LXA4, 15-epi-LXA4, PGE2, and LTB4 were measured in TB-DM individuals at baseline (pre-T) and at 6 months of ATT (post-T). **(B)** The ratios of LXA4:LTB4, 15-epi-LXA4:LTB4, LXA4:PGE2, 15-epi-LXA4:PGE2, and PGE2:LTB4 were measured in TB-DM individuals at baseline (pre-T) and at 6 months of ATT (post-T). The data are presented as line graphs with each line representing a single individual. *P*-values were calculated using the Wilcoxon signed rank test.

TB, we examined the association between the plasma levels of eicosanoids in all TB individuals with pro-inflammatory cytokines (**Figure 6**). As shown, the circulating levels of LXA4 showed a significant positive correlation, with IFNγ, TNFα IL-1β and negative correlation with IL-1α levels. In addition, LTB4 exhibited a significant negative relationship with IFNγ and IL-1β in all TB participants with and without DM at baseline, indicating a significant involvement of these factors with cytokines.

DISCUSSION

Eicosanoids and prostaglandins are major lipid moieties of considerable interest in metabolic biology. However, it is being gradually accepted that these lipid molecules have the capability to shape the immune response to infectious pathogens. Lipid mediators of the eicosanoid family have been proven to have influence on the outcome of the *M. tb* infection (Mayer-Barber and Sher, 2015). Previously published studies have also reveal that *M. tb* can also alter the host eicosanoid metabolism as a survival strategy (Divangahi et al., 2010). The interplay among the eicosanoids, PGE2 and LXA4 is known to affect the type of cell death in infected macrophages. LXA4 enhances macrophage necrosis, resulting in cell death and escape of *M. tb* to the extracellular milieu. PGE2 stimulates macrophage apoptosis, resulting in membrane integrity, bacillary containment and heightened immunity (Chen et al., 2008). LTB4, via the regulation of TNFα production (Tobin et al., 2012), can enhance attraction of neutrophils (Lammermann et al., 2013) and lead to macrophage necrosis (Tobin et al., 2012). Our findings clearly demonstrate the presence of elevated levels of LXA4, 15-epiLXA4, and PGE2 in TB-DM and TB at baseline, with only LTB4 being present at lower levels compared to controls. Our data also demonstrate a positive relationship between LXA4 and pro-inflammatory cytokines and a negative relationship between LTB4 and pro-inflammatory cytokines, suggesting a cross-regulation of eicosanoids with cytokine levels in TB.

Published findings report that high LXA4 favors the mycobacterial infection (Amaral et al., 2013). Specifically, LXA4 can induce necrotic cell death of the infected macrophages (Bafica et al., 2005). We have previously reported that LXA4 and 15-epi-LXA4 are significantly increased in the active TB group compered to latent and healthy controls (Mayer-Barber et al., 2014). In agreement with this report, our present finding also confirms the presence of elevated levels of LXA4 and

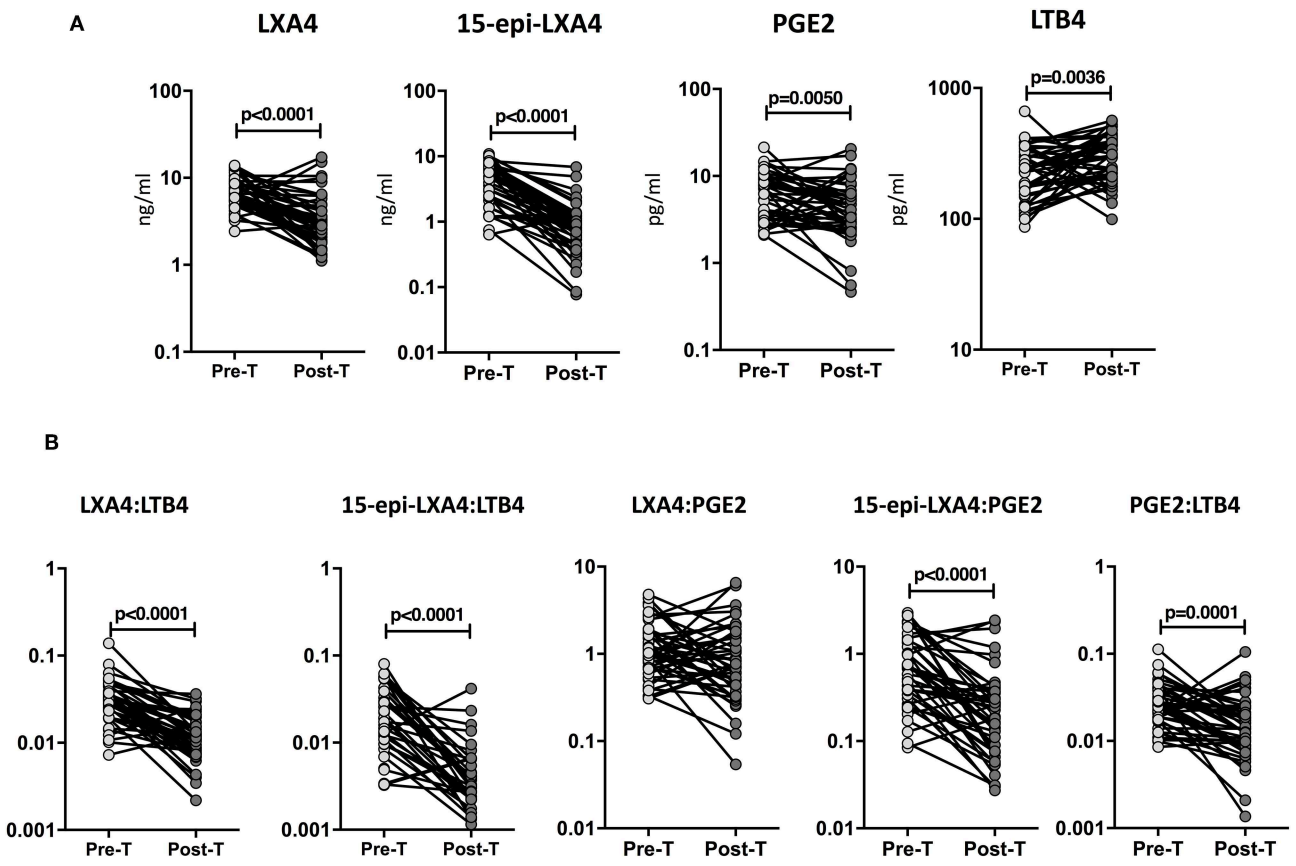

FIGURE 5 | Increased eicosanoids ratios at the end of standard anti-tuberculosis therapy in TB-DM and TB individuals. **(A)** The plasma levels of LXA4, 15-epi-LXA4, PGE2, and LTB4 were measured in TB individuals at baseline (pre-T) and at 6 months of ATT (post-T). **(B)** The ratios of LXA4:LTB4, 15-epi-LXA4:LTB4, LXA4:PGE2, 15-epi-LXA4:PGE2, and PGE2:LTB4 were measured in TB individuals at baseline (pre-T) and at 6 months of ATT (post-T). The data are presented as line graphs with each line representing a single individual. *P*-values were calculated using the Wilcoxon signed rank test.

15-epi-LXA4 in TB individuals who are with and without diabetes compared to DM and HC. More interestingly, our data also highlight an important involvement of LXA4 and 15-epi-LXA4 with both the amount of pathology in TB as well as the degree of disease. Finally, our data disclose a direct correlation of LXA4 and 15-epi-LXA4 levels with bacterial burdens, perhaps suggesting that high LXA4 and 15-epi-LXA4 reflect an inflammatory environment favorable for *M. tb* replication. This is further corroborated by the fact that LXA4 and 15-epi-LXA4 levels are significantly reduced following successful chemotherapy. Interestingly, our data also reveal that only LXA4 and not 15-epiLXA exhibits a significant positive relationship with pro-inflammatory cytokines—IL-1β, IFNγ, and TNFα. Thus, LXA4 in TB-DM and TB is a major biomarker of disease severity and bacterial burden.

Earlier studies have reported that excess LTB4 production leads to increased TNF dependent macrophage cell death, while diminished levels LTB4 leads to a relative increase in LXA4, which in turn results in cell death due to loss of bacterial control (Tobin et al., 2012). Our current finding also reveals the presence of diminished levels of LTB4 in TB individuals who are with and without diabetes compared to DM and HC. Moreover, our findings reveal certain important features of eicosanoid imbalance and its association with TB-DM and DM. Thus, the ratios of LXA4: LTB4 and 15epiLXA4: LTB4 are significantly increased in TB-DM compared to TB alone. Our data also reveal that the ratio of LXA4 to LTB4 levels and of 15-epiLXA4 to LTB4 levels appear to be associated with both disease severity/extent as well as bacterial burdens in TB-DM and TB. Hence, eicosanoid balance between the lipoxins and LTB4 seems to be associative factors with lung pathology and bacterial burden in TB-DM and TB. This is further corroborated by the decrease in the ratios following ATT in both TB-DM and TB. Finally, LTB4 levels in TB-DM and TB individuals is negatively associated with the levels of the pro-inflammatory cytokines—IL-1α and IL-1β.

Animal model studies have reported PGE2 confers resistance against *M. tb* infection, while LXA4 promotes bacterial growth (Bafica et al., 2005; Chen et al., 2008; Divangahi et al., 2009). Thus, during *M. tb* infection, the balance of PGE2 and LXA4 is important in regulating the relative amounts of apoptosis and necrosis, which is an important feature in the control of intracellular infection. Moreover, studies using the genetic analysis of the susceptibility of zebrafish to *M. marinum* have validated the important role of these host lipid pathways in

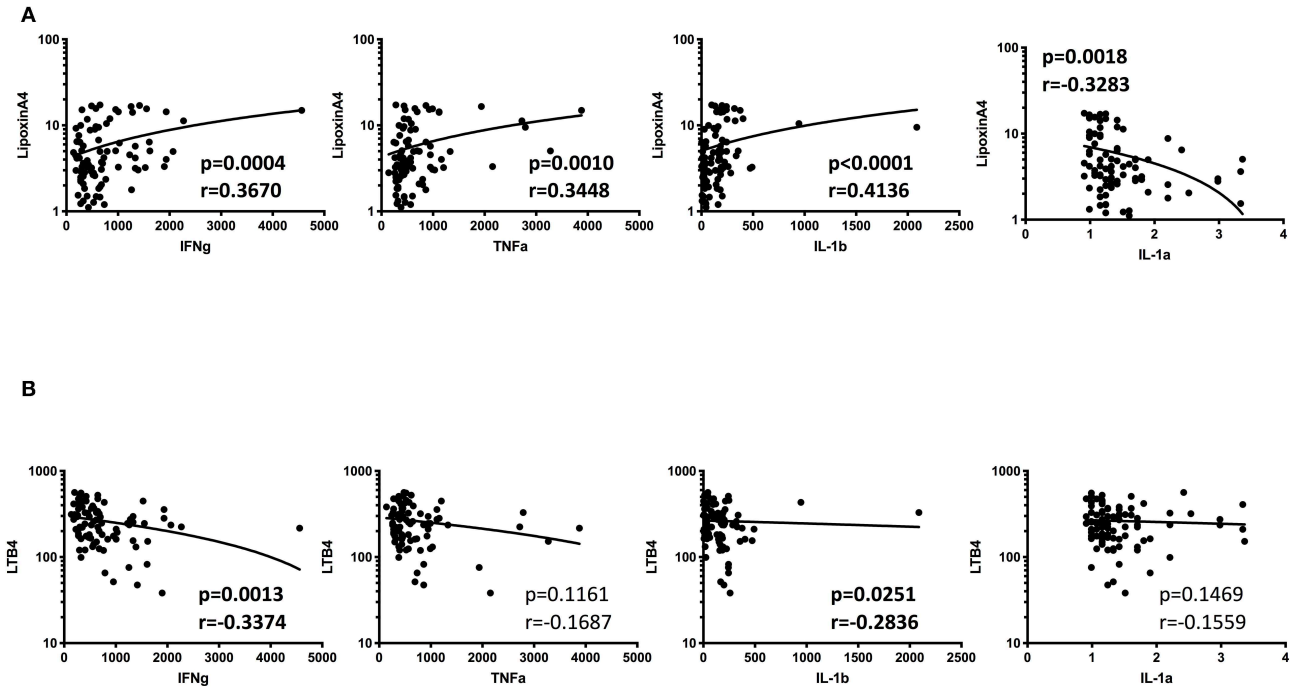

FIGURE 6 | Significant correlation between plasma levels of eicosanoids and pro-inflammatory cytokines in all TB individuals. **(A)** The relationship between the plasma levels of lipoxin A4 and cytokines was examined in all TB individuals with and without DM at baseline. **(B)** The relationship between the plasma levels of LTB4 and cytokines was examined in all TB individuals with and without DM at baseline The data are represented as scatter plots with each circle representing a single individual. *P*-values were calculated using the Spearman Rank Correlation.

innate immunity (Tobin et al., 2010). Our data clearly shows that the presence of elevated levels of PGE2 are observed in TB individuals who are with and without diabetes compared to DM and HC, but our data do not reveal a direct correlation of PGE2 with lung pathology or bacterial burdens. However, we do observe significantly decrease levels of PGE2 following ATT in both TB-DM and TB individuals, suggesting that PGE2 is an important factor in TB disease. Our data also reveal no association of lipoxin to PGE2 or PGE2 to LTB4 ratios in the pathology of TB-DM and TB. Thus, PGE2 appears to play a less important associative role with disease pathology or bacterial burden in TB-DM and TB. Moreover, our data did not reveal any significant association between PGE2 levels and pro-inflammatory cytokines in TB or TB-DM.

There is an increasing appreciation of the distinct roles that lipid mediators play in regulating inflammatory responses during *M. tb* infection (Tobin and Ramakrishnan, 2013). To define the outcome and severity of mycobacterial infection, the balance between the lipid mediators are important (Pedruzzi et al., 2016). In this study, we report that ratios of LXA4:LTB4, 15-epi-LXA4:LTB4, and PGE2:LTB4 were significantly enhanced in TB-DM and correlated with disease severity and in-turn diminished following ATT. The limitations of our study are the limited sample size, the estimation of eicosanoid levels only in the plasma and the absence of mechanistic insights. Despite this, our study contributes to the growing body of literature on the regulation of innate immune responses in TB-DM co-morbidity. To our knowledge, no studies have reported correlation of LXA4:LTB4 and 15-epi-LXA4:LTB4 with disease severity in TB-DM comorbidity. Our data clearly reveals that changes in eicosanoids might reflect a perfectly balanced host response needed to control imbalance in TB diabetes comorbidity linked with outcome of *M. tb* infection. Finally, our data also complements the growing understanding of pathophysiology in TB diabetes comorbidity.

DATA AVAILABILITY STATEMENT

The datasets analyzed in this manuscript are not publicly available. Requests to access the datasets should be directed to pavankumarn@nirt.res.in.

ETHICS STATEMENT

The studies involving human participants were reviewed and approved by Ethics Committees of the Prof. M. Viswanathan Diabetes Research Center and National Institute for Research in Tuberculosis. The patients/participants provided their written informed consent to participate in this study.

AUTHOR CONTRIBUTIONS

SB and NP designed the study. NP, KM, and AN conducted experiments. NP and KM acquired data. NP, KM, and SS analyzed

data. VV, HK, and SB funding acquisition. BS and SH project administration. NP and SB wrote the manuscript.

FUNDING

This project has been funded in whole or in part with Federal funds from the Government of India's (GOI) Department of Biotechnology (DBT), the Indian Council of Medical Research (ICMR), the United States National Institutes of Health (NIH), National Institute of Allergy and Infectious Diseases (NIAID), Office of AIDS Research (OAR), and distributed in part by CRDF Global [grant USB1-31149-XX-13]. This work was also funded by CRDF Global RePORT India Consortium Supplemental Funding [grant OISE-17-62911-1]. The contents of this publication are solely the responsibility of the authors and do not represent the official views of the DBT, the ICMR, the NIH, or CRDF Global. This work was also funded in part by the Division of Intramural Research, NIAID, NIH.

ACKNOWLEDGMENTS

We thank the staff of Department of Clinical Research and the Department of Bacteriology, NIRT for valuable assistance in bacterial cultures and radiology and the staff of MVDRC, RNTCP and Chennai corporation for valuable assistance in recruiting the patients for this study. Data in this manuscript were collected as part of the Regional Prospective Observational Research for Tuberculosis (RePORT) India Consortium.

REFERENCES

Amaral, J. J., Antunes, L. C., de Macedo, C. S., Mattos, K. A., Han, J., Pan, J., et al. (2013). Metabonomics reveals drastic changes in anti-inflammatory/pro-resolving polyunsaturated fatty acids-derived lipid mediators in leprosy disease. *PLoS Negl. Trop. Dis.*7:e2381. doi: 10.1371/journal.pntd.0002381

Bafica, A., Scanga, C. A., Serhan, C., Machado, F., White, S., Sher, A., et al. (2005). Host control of *Mycobacterium tuberculosis* is regulated by 5-lipoxygenase-dependent lipoxin production. *J. Clin. Invest.* 115, 1601–1606. doi: 10.1172/JCI23949

Chen, M., Divangahi, M., Gan, H., Shin, D. S., Hong, S., Lee, D. M., et al. (2008). Lipid mediators in innate immunity against tuberculosis: opposing roles of PGE2 and LXA4 in the induction of macrophage death. *J. Exp. Med.* 205, 2791–2801. doi: 10.1084/jem.20080767

Das, U. N. (2017). Lipoxin A4 as a possible mediator of the beneficial actions of phosphodiesterase-5 enzyme inhibitors. *Arch. Med. Sci.* 13, 263–266. doi: 10.5114/aoms.2017.64723

Divangahi, M., Chen, M., Gan, H., Desjardins, D., Hickman, T. T., Lee, D. M., et al. (2009). *Mycobacterium tuberculosis* evades macrophage defenses by inhibiting plasma membrane repair. *Nat. Immunol.* 10, 899–906. doi: 10.1038/ni.1758

Divangahi, M., Desjardins, D., Nunes-Alves, C., Remold, H. G., and Behar, S. M. (2010). Eicosanoid pathways regulate adaptive immunity to *Mycobacterium tuberculosis*. *Nat. Immunol.* 11, 751–758. doi: 10.1038/ni.1904

Dooley, K. E., and Chaisson, R. E. (2009). Tuberculosis and diabetes mellitus: convergence of two epidemics. *Lancet Infect. Dis.* 9, 737–746. doi: 10.1016/S1473-3099(09)70282-8

Kumar, N. P., Sridhar, R., Banurekha, V. V., Jawahar, M. S., Fay, M. P., Nutman, T. B., et al. (2013). Type 2 diabetes mellitus coincident with pulmonary tuberculosis is associated with heightened systemic type 1, type 17, and other proinflammatory cytokines. *Ann. Am. Thorac. Soc.* 10, 441–449. doi: 10.1513/AnnalsATS.201305-112OC

Lammermann, T., Afonso, P. V., Angermann, B. R., Wang, J. M., Kastenmuller, W., Parent, C. A., et al. (2013). Neutrophil swarms require LTB4 and integrins at sites of cell death *in vivo*. *Nature* 498, 371–375. doi: 10.1038/nature12175

Lonnroth, K., Migliori, G. B., Abubakar, I., D'Ambrosio, L., de Vries, G., Diel, R., et al. (2015). Towards tuberculosis elimination: an action framework for low-incidence countries. *Eur. Respir. J.* 45, 928–952. doi: 10.1183/09031936.00214014

Mayer-Barber, K. D., Andrade, B. B., Oland, S. D., Amaral, E. P., Barber, D. L., Gonzales, J., et al. (2014). Host-directed therapy of tuberculosis based on interleukin-1 and type I interferon crosstalk. *Nature* 511, 99–103. doi: 10.1038/nature13489

Mayer-Barber, K. D., and Sher, A. (2015). Cytokine and lipid mediator networks in tuberculosis. *Immunol. Rev.* 264, 264–275. doi: 10.1111/imr.12249

Pedruzzi, G., Das, P. N., Rao, K. V., and Chatterjee, S. (2016). Understanding PGE2, LXA4 and LTB4 balance during *Mycobacterium tuberculosis* infection through mathematical model. *J. Theor. Biol.* 389, 159–170. doi: 10.1016/j.jtbi.2015.10.025

Prada-Medina, C. A., Fukutani, K. F., Pavan Kumar, N., Gil-Santana, L., Babu, S., Lichtenstein, F., et al. (2017). Systems immunology of diabetes-tuberculosis comorbidity reveals signatures of disease complications. *Sci. Rep.* 7:1999. doi: 10.1038/s41598-017-01767-4

Tobin, D. M., and Ramakrishnan, L. (2013). TB: the Yin and Yang of lipid mediators. *Curr. Opin. Pharmacol.* 13, 641–645. doi: 10.1016/j.coph.2013.06.007

Tobin, D. M., Roca, F. J., Oh, S. F., McFarland, R., Vickery, T. W., Ray, J. P., et al. (2012). Host genotype-specific therapies can optimize the inflammatory response to mycobacterial infections. *Cell* 148, 434–446. doi: 10.1016/j.cell.2011.12.023

Tobin, D. M., Roca, F. J., Ray, J. P., Ko, D. C., and Ramakrishnan, L. (2013). An enzyme that inactivates the inflammatory mediator leukotriene b4 restricts mycobacterial infection. *PLoS ONE* 8:e67828. doi: 10.1371/journal.pone.0067828

Tobin, D. M., Vary, J. C. Jr., Ray, J. P., Walsh, G. S., Dunstan, S. J., Bang, N. D., et al. (2010). The lta4h locus modulates susceptibility to mycobacterial infection in zebrafish and humans. *Cell* 140, 717–730. doi: 10.1016/j.cell.2010.02.013

Conflict of Interest: The authors declare that the research was conducted in the absence of any commercial or financial relationships that could be construed as a potential conflict of interest.

frontiers in Cellular and Infection Microbiology

REVIEW
published: 04 October 2019
doi: 10.3389/fcimb.2019.00342

Changes in Host Response to *Mycobacterium tuberculosis* Infection Associated With Type 2 Diabetes: Beyond Hyperglycemia

Cristian Alfredo Segura-Cerda[1,2], *Wendy López-Romero*[2] and *Mario Alberto Flores-Valdez*[2*]

[1] Doctorado en Farmacología, Universidad de Guadalajara, Guadalajara, Mexico, [2] Biotecnología Médica y Farmacéutica, Centro de Investigación y Asistencia en Tecnología y Diseño del Estado de Jalisco, Guadalajara, Mexico

Tuberculosis (TB) remains as the first cause of death among infectious diseases worldwide. Global incidence of tuberculosis is in part coincident with incidence of type 2 diabetes (T2D). Incidence of T2D is recognized as a high-risk factor that may contribute to tuberculosis dissemination. However, mechanisms which favor infection under T2D are just starting to emerge. Here, we first discuss the evidences that are available to support a metabolic connection between TB and T2D. Then, we analyze the evidences of metabolic changes which occur during T2D gathered thus far for its influence on susceptibility to *M. tuberculosis* infection and TB progression, such as hyperglycemia, increase of 1AC levels, increase of triglycerides levels, reduction of HDL-cholesterol levels, increased concentration of lipoproteins, and modification of the activity of some hormones related to the control of metabolic homeostasis. Finally, we recognize possible advantages of metabolic management of immunity to develop new strategies for treatment, diagnosis, and prevention of tuberculosis.

Keywords: ***Mycobacterium tuberculosis*** **infection, type 2 diabetes, hyperglycemia, diabetic dyslipidemia, hormones**

OPEN ACCESS

Edited by:
Igor Kramnik,
Boston University, United States

Reviewed by:
Kai Huang,
University of Texas Medical Branch at Galveston, United States
Robert Cody Sharp,
University of Florida Health, United States

***Correspondence:**
Mario Alberto Flores-Valdez
floresv@ciatej.mx;
floresvz91@gmail.com

Specialty section:
This article was submitted to Clinical Microbiology, a section of the journal Frontiers in Cellular and Infection Microbiology

Received: *03 July 2019*
Accepted: *23 September 2019*
Published: *04 October 2019*

Citation:
Segura-Cerda CA, López-Romero W and Flores-Valdez MA (2019) Changes in Host Response to Mycobacterium tuberculosis Infection Associated With Type 2 Diabetes: Beyond Hyperglycemia. Front. Cell. Infect. Microbiol. 9:342. doi: 10.3389/fcimb.2019.00342

INTRODUCTION

Infection with *Mycobacterium tuberculosis*, which in susceptible people leads to either active or latent tuberculosis (TB), remains as a high-burden health problem globally. It is calculated that in 2017, TB caused 1.3 millions deaths, and 10.0 million new cases were reported (WHO, 2018). Some disorders have been recognized as risk factors to develop pulmonary TB, such as HIV coinfection, malnutrition, tobacco smoking, and type 2 diabetes (T2D) (WHO, 2018).

T2D is a chronic metabolic disorder that essentially affect the function of pancreatic β-cells, resulting in progressive development of insuline resistance and chronic inflammation (Defronzo et al., 2015). Several meta-analysis show that T2D is associated with a two- to four-fold increased risk of active TB, even multidrug-resistant TB (Amare et al., 2013; Al-Rifai et al., 2017; Liu et al., 2017; Hayashi and Chandramohan, 2018). As a risk factor for developing TB, T2D has attracted attention by its projected increase and its prevalente worldwide. In 2018, it was estimated that T2D affected one of each 10 individuals globally (425 million people around the world) and it is projected that the number of cases of T2D may increase by 40% in 2045 (IDF, 2017). Hence, an increase in the global burden of T2D poses a higher risk of TB spread worldwide in the upcoming years.

Epidemiological data about comorbidity between TB and T2D show that there is a close relationship between both diseases. A recent meta-analysis showed that 16% of newly-diagnosed TB patients have T2D and up to 4.1% of T2D patients develop TB (Wilkinson et al., 2017). In 2017, close to 800,000 newly-diagnosed TB cases were attributed to T2D, and T2D was the risk factor that contributed to most TB cases in countries like China and India, even above HIV infection (WHO, 2018). However, the incidence of TB-T2D can be higher than reported, because the American Association of Diabetes (ADA) estimates that around 50% of T2D patients remain undiagnosed and the WHO has found higher rates of undiagnosed TB mainly in low-income countries (American Diabetes Association, 2018a; WHO, 2018). Both WHO and the International Union against Tuberculosis and Lung Disease recommend to diagnose T2D in newly-diagnosed TB patients, with the aim of generating pharmacological strategies that effectively contribute to the clinical management of T2D and TB (Liu et al., 2019).

In addition to its importance on TB prevalence, patients with T2D have more severe manifestations of TB than non-T2D ones (Carreira et al., 2012; **Figure 1A**) and have a lower response to anti-TB treatment (OR 2.93) (Viswanathan and Gawde, 2014) compared to patients without T2D. Moreover, the recurrence and reactivation of LTBI, which potentially contributes to TB dissemination, is higher in T2D patients than in non-T2D ones (OR = 1.83) (Jimenez-Corona et al., 2013).

Some relevant innate and adaptive immunity mechanisms that are necessaries for *M. tuberculosis* clearance have been shown to be compromised in patients with TD2M, as recently reviewed (Restrepo, 2016; Kumar Nathella and Babu, 2017; Rao et al., 2019). However, a causal relationship between T2D and TB has not been completely addressed. Even though the role of hyperglycemia on the immunity against *M. tuberculosis* has been widely described (Magee et al., 2018), new evidences about other metabolic changes that occur during T2D progression are emerging, such as the effects of dyslipidemia, vitamin deficiency, and changes in hormonal activity, which will be discussed in specific sections below. Here, we discuss diverse findings ranging from *in vitro* studies to clinical research, which support the connection between T2D progression and TB susceptibility in a metabolic-dependent way and present a global connection of feasible events that may occur during this comorbidity, which might create an appropriate environment to *M. tuberculosis* infection, and we also present evidences of the role of the treatment of T2D on this response.

PREDIABETES AND PROGRESSION TO TB

Prediabetes is defined as a stage where glucose levels do not meet with the criteria for T2D but are too high to be considered as normal. Prediabetes is diagnosed by a fasting blood glucose (FBG) values between 100 and 125 mg/dL or 2 h oral glucose tolerance test (OGTT) between 140 and 199 mg/dL or Hemoglobin 1AC between 5.7 and 6.4% (American Diabetes Association, 2019a). Even though a time-regulated interaction between T2D and TB remains unresolved, some evidences suggest that progression from prediabetes to T2D may influence the susceptibility to *M. tuberculosis* infection (**Figure 1B**). An study of household contacts of active TB patients (who had a higher risk to develop TB) showed that prediabetes is present in at least 27% of them (Shivakumar et al., 2018), while another study in western India that included 1,073 participants, revealed that more than one-half of newly diagnosed TB patients had T2D or pre-T2D (Mave et al., 2017).

Prediabetes induces changes in cytokines production that are related to control of *M. tuberculosis* infection. A study in prediabetic-TB patients showed that they had higher circulating concentrations of IFN-γ, TNF-α, IL-12, IL-17, IL-1β, GM-CSF (cytokines that favors Th1 response) and also had higher concentrations of IL-5, IL-10, and TGF-β (cytokines related to regulation of cytokine response) than TB patients without prediabetes (Kumar et al., 2014). This dysregulation of cytokines levels found in plasma may compromise the immune response against *M. tuberculosis*, and suggest that progressive changes in immune response related to T2D progression may influence the susceptibility to TB.

Progression of T2D in obese patients produces changes that can be related to an increased TB susceptibility through modulation of adypocytokines such as the C1q tumor necrosis factor related protein-3 (C1qTNF3 or CTRP-3). C1qTNF3 is a cytokine produced by macrophages and adipocytes that reduces inflammation generated by adipocytes (Kopp et al., 2010; Schmid et al., 2014). A study in obese patients showed that T2D induces a reduction in the plasmatic concentrations of this cytokine as compared with non-T2D patients (Elsaid et al., 2019). A study conducted in South Africa and Gambia, showed that patients who progress from a Latent TB Infection (LTBI) to active TB (LTBI defined as TST+, Quantiferon TB assay+) have lower concentrations of C1qTNF3 in plasma than LTBI patients who did not progress to TB during a more than 1 year follow-up (Penn-Nicholson et al., 2019). These findings suggest that the reduction in C1qTNF3 might be a potential contributor to the increased risk for TB in people with T2D, and might be a factor worth evaluating in the clinic.

In formally established T2D (as opposed to pre-T2D), some additional disorders in metabolism may occur, such as hyperglycemia, dyslipidemia, changes in lipoprotein concentrations, and changes in hormonal profiles (Olokoba et al., 2012; Carrera Boada and Martinez-Moreno, 2013). These alterations seem to be an adequate environment for *M. tuberculosis* infection to thrive in T2D subjects, likely improving persistence of mycobacteria and allowing them to consolidate the pulmonar infection and its effects (**Figure 1C**).

CLINICAL FEATURES OF T2D AND THEIR EFFECTS ON RESPONSE TO *M. tuberculosis* INFECTION

Effect of Hyperglycemia on Susceptibility to *M. tuberculosis* During T2D

T2D is characterized by an increase in blood concentration of glucose (measured as FBG >126 mg/dL or measured as 2 h

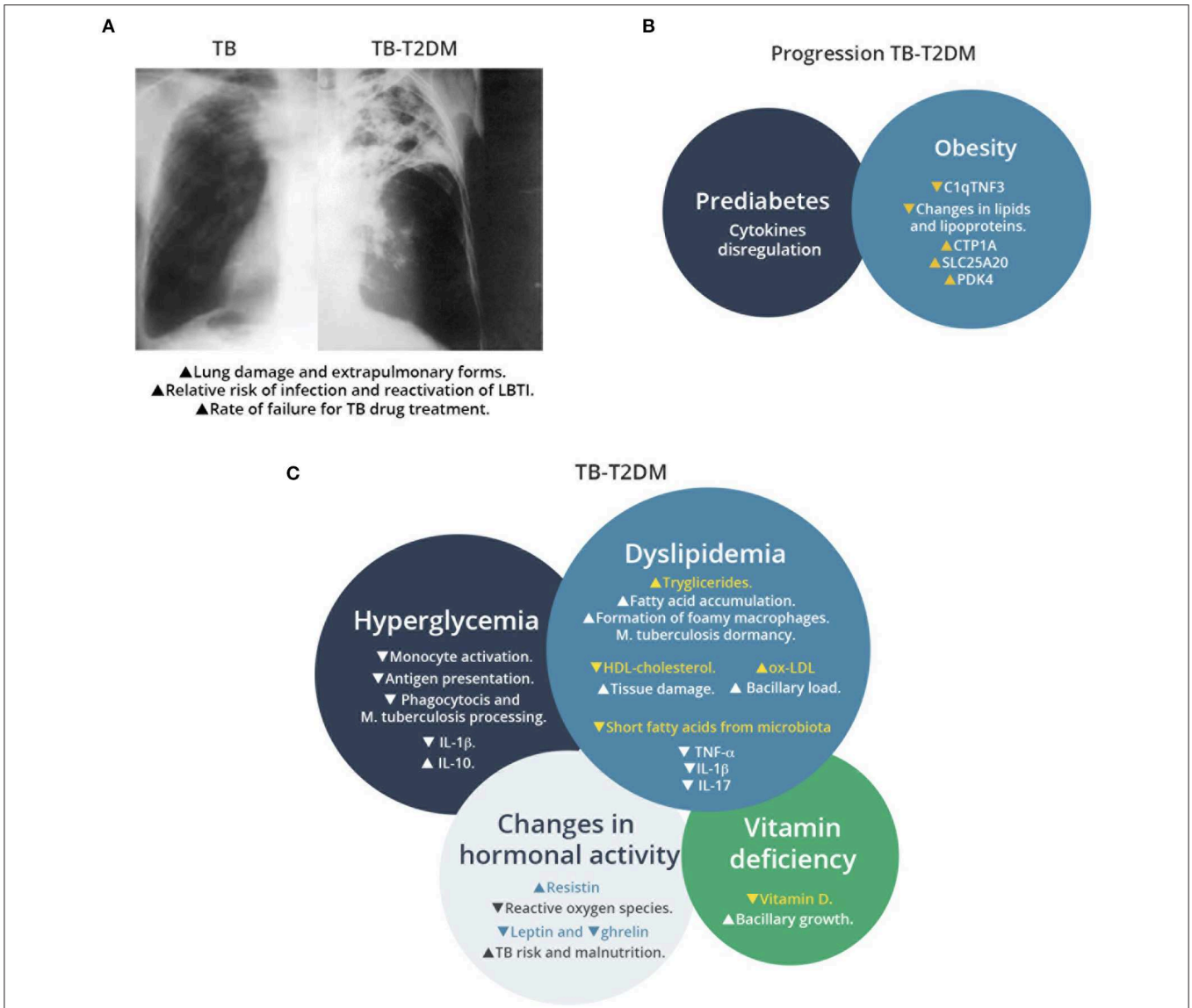

FIGURE 1 | Overview of TB-T2D comorbidity, factors associated to T2D that increase susceptibility to *M. tuberculosis* infection, and metabolic changes that affect the host immune response. **(A)** Schematic representation of chest radiography of *M. tuberculosis* infected lung in patients with or without T2D. Comorbidity increases the lung damage associated to *M. tuberculosis* infection. **(B)** Factors associated to progression of TB in T2D patients. Prediabetes and obesity contribute to TB susceptibility with progressive changes in T2D patients, as recent signatures for TB progression have revealed recently. **(C)** Effects of metabolic changes in TB-T2D on the host response *to M. tuberculosis* infection. TB-T2D patients suffer hyperglycemia, dyslipidemia, changes in hormonal activity and vitamin deficiency. These conditions result in higher manifestations of *M. tuberculosis* infection.

postprandial glucose >200 mg/dL), known as hyperglycemia, and higher proportions of 1AC in blood (>6.5%) (American Diabetes Association, 2018a).

High glucose concentration in blood has been related to defects in host response against *M. tuberculosis* infection. An study in Japan, where FBG levels in 522 TB-confirmed patients were tested, showed a positive association (+1.31) between glucose intolerance and the development of TB (OR 3.15, C.I. 1.12–8.88; Hayashi et al., 2014). This positive association was also found in an a cross-sectional study in African individuals, where subjects with random blood glucose (RBG) concentration ≥11.1 mmol/L had 2.15 times the odds of prevalent TB than individuals with a RBG concentration <11.1 mmol/L (Bailey et al., 2016).

Rationale dissection of the effect of hyperglycemia indicates that it can affect the activity of macrophages. Macrophages are one of the first cells to encounter mycobacteria and are the main cells where mycobacteria resides during infection (Srivastava et al., 2014).

Montoya-Rosales and collaborators (Montoya-Rosales et al., 2016) cultured monocyte-derived macrophages from human U-937 cell line in the presence of different concentrations of glucose in the medium, and observed a negative correlation between

glucose concentration and phagocytosis of *M. tuberculosis*. In the same system, the authors described a positive correlation between glucose concentration and induction of LL-37 antimicrobial peptide, and with the induction of anti-inflammatory cytokines such as TGF-β and IL-10 (Montoya-Rosales et al., 2016).

Another defect in macrophage function caused by hyperglycemia is the expression of receptors related to antigen presentation and related to T cell activation. A study where alveolar macrophages from T2D patients were infected with *M. tuberculosis* H37Rv, reported reduced levels of expression of CD86, CD80, and HLA-DR, molecules that participate in antigen presentation and Th response; and also a reduced induction of IL-6, IL-1β, IL-10, and IL-12 before and after the infection (Lopez-Lopez et al., 2018). Taken together, the works by Montoya-Rosales et al. (2016) and Lopez-Lopez et al. (2018) suggest a potential mechanistic explanation that contribute to partially explain the influence of hyperglycemia on the susceptibility to M. tuberculosis infection in T2D patients, but studies *in vivo* are needed to clearly establish the role of hyperglycemia on TB during TB-T2D comorbidity.

Glycemic control is commonly measured by hemoglobin 1AC because it represents the concentration of glucose found in blood 2 or 3 months before the actual measurement has been done (American Diabetes Association, 2018a). A glycemic level over the recommended by ADA (1AC <7%, preprandial capillary glucose between 83 and 130 mg/dL and peak postprandial capillary plasma glucose <180 mg/dL; American Diabetes Association, 2019b) has been correlated with higher prevalence of TB among T2D patients (Almeida-Junior et al., 2016) and with extended lung damage caused by TB, detected by computed tomography (Xia et al., 2018), or by radiological examinations (Huang et al., 2017) in patients with TB-T2D. However, a mechanistic explanation about the role of 1AC in promoting lung pathology in TB-T2D remains undescribed.

Regarding the role of an increase in 1AC levels and its effects on innate immune response, a study in India determined the levels of monocyte activator markers (CD164, sCD163, and CRP) in plasma of TB, T2D, T2D, and healthy controls (Kumar et al., 2019). In this study, 1AC of either TB or TB-T2D patients was positively correlated with levels of these markers. In addition, authors demonstrated that in patients who were diabetic before developing TB, the levels of these markers were increased compared with those of healthy controls, suggesting that changes in monocyte activation marker profiles coincident with changes in 1AC may be progressive. In another study conducted in Indonesia, cytokines in blood were determined in two defined groups of patients depending on their 1AC levels (<7 and >7%). Patients with 1AC >7% had the same levels of IFN-γ and IL-12 than the patients with 1AC <7%, but had lower levels of vitamin A (Ginandjar et al., 2016). Deficiency in vitamin A levels has been recently associated to a higher risk of TB in Moroccan patients (Qrafli et al., 2017), and this vitamin was found in lower levels in TB patients than in healthy controls (Oh et al., 2017). Whether or not there is a correlation between low 1AC levels and decreased vitamin A (or vice versa) remains to be determined.

Even though 1AC levels have not been found to be related to anti-TB treatment success in both T2D and non-T2D patients (Tabarsi et al., 2014), recent evidence suggest that higher levels of 1AC in TB patients may produce a delayed time to sputum conversion in TB patients receiving anti-TB treatment (Nurwidya et al., 2018). More efforts are needed to better understand the relationship between 1AC and the susceptibility to *M. tuberculosis* infection.

Effect of Diabetic Dyslipidemia on Susceptibility to *M. tuberculosis* During T2D

T2D is associated with some alterations in lipid of lipids and lipoproteins, a condition described as diabetic dyslipidemia (Carmena, 2008). This disorder comprises high levels of triglycerides, reduction of high-density lipoprotein (HDL) cholesterol concentrations and high levels of low-density lipoproteins (LDL) in blood (Wu and Parhofer, 2014; Cuevas et al., 2016).

A recent analysis by ^{1}H-Nuclear Magnetic Resonance of lipid metabolic markers (lipoproteins, fatty acids, glycerides, amino acids, and glycolytic molecules) in plasma samples from TB, T2D, and TB-T2D patients showed that TB-T2D comorbidity displays characteristics of both diseases, such as reduced concentration of amino acids (indicator of waste) and lower dyslipidemia than expected only in T2D (Vrieling et al., 2018). In the same study, authors recognized that there were differences in the profiles among individuals, perhaps attributable to the chronicity of T2D and the time lapse of comorbidity TB-T2D. This suggested that there is a dynamism between both diseases that generates differences in lipid environments, which, in turn, could lead to different responses against infection.

As for the effects of triglycerides on TB, an *in vitro* study using PBMC-derived macrophages and THP-1 derived macrophages, showed that *M. tuberculosis* incorporates triglycerides from the host to infection sites in conditions of hypoxia (Daniel et al., 2011; Guerrini et al., 2018). This condition creates a fatty acid-rich environment for *M. tuberculosis* that favor the use of lipids as the major source of energy during *M. tuberculosis* infection, as documented in granulomas in rabbits, marmosets, and humans (Guerrini et al., 2018). A recent systematic review and meta-analysis has reinforced this concept by finding a positive correlation between latent infection by *M. tuberculosis* (defined as TST+ or IGRA+) with T2D, OR = 1.18 (1.06–1.30; Lee et al., 2017).

Accumulation of lipids in macrophages leads to formation of cytokine secreting foam cells in T2D patients. A study where J774 murine macrophages were exposed to serum of T2D patients, showed that serum triglycerides levels correlated with induction of lipid accumulation in these cells and consequently, in the formation of foamy macrophages (Cui et al., 2010). It is known that formation of foamy macrophages contributes to persistence of bacteria and to the tissue pathology during TB (Russell et al., 2009). Nevertheless, the direct effect of high levels of triglycerides in T2D patients on the formation of foamy macrophages during TB infection has not been addressed in clinical studies.

The observed reduction in HDL-cholesterol in T2D patients, has also been observed in patients with pulmonary tuberculosis (Deniz et al., 2007; Rao, 2009). This reduction in HDL-cholesterol was recently identified as a risk factor for severe lung lesions in patients with TB-T2D (Dong et al., 2018). However, the role of the reduction in HDL-cholesterol on the host response against *M. tuberculosis* is still unaddressed, and need to be explored in future studies.

Further to the above mentioned increase in concentration of triglycerides in T2D patients, they had higher concentrations of oxidized-LDL (Ox-LDL) in serum than healthy controls (Vrieling et al., 2019). In guinea pigs, it has been demonstrated that ox-LDL accumulates in lungs during active infection by *M. tuberculosis* (Parish et al., 2012), which is in line with findings *in vitro* that indicates that ox-LDL is taken up by macrophages in environments rich in glucose (Hayek et al., 2005). The effect of ox-LDL on bacilli activity was addressed by Parish and collaborators, who performed a study using alveolar macrophages obtained from guinea pigs loaded with Ox-LDL and then infected with *M. tuberculosis H37Rv*. They observed that Ox-LDL-treated macrophages had higher bacillary loads than untreated macrophages after 3 days of culture (Parish et al., 2012). Coincidentally, this effect has also been observed in primary human macrophages exposed to Ox-LDL before infection with *M. tuberculosis* H37Rv, where there was an increase of the bacterial burden in a dose-dependent manner within macrophages *in vitro* (Vrieling et al., 2019). These evidences reinforce the fact that the higher concentrations of Ox-LDL found in T2D patients may contribute to a higher susceptibility to TB progression and suggest that diabetic dyslipidemia is closely related to TB susceptibility.

PHYSIOPATHOLOGICAL MECHANISMS ALTERED IN T2D AND THEIR RELATIONSHIP WITH TB SUSCEPTIBILITY

Hormones Related to Blood Glucose Control and Their Possible Roles During TB-T2D

Leptin and ghrelin are two hormones related to control of blood glucose concentration that are related to malnutrition during TB (Chang et al., 2013; Mexitalia et al., 2017). In a study where the concentration of leptin and ghrelin in blood was measured in TB, TB-T2D, and healthy Chinese people, there were found lower levels of leptin in TB-T2D patients as compared with TB patients, and higher levels of ghrelin were observed in TB-T2D patients than in TB patients (Zheng et al., 2013). These data suggest that T2D may increase susceptibility to TB through affecting appetite through these changes in ghrelin and leptin, which are related to a higher susceptibility to *M. tuberculosis* infection (Buyukoglan et al., 2007).

Resistin is a protein suggested to be part of the development of insulin resistance in humans and mice (Benomar et al., 2013), and it has been recognized as a key molecule that links obesity and T2D (Steppan et al., 2001). Resistin participates in increasing expression of proinflammatory cytokines such as TNF-α, IL-6, IL-12, and monocyte chemoattractant protein (MCP)-1 in PBMCs, macrophages, and hepatic stellate cells via the nuclear factor-κB (NF-κB) pathway (Bokarewa et al., 2005). It was shown that patients with T2D had higher levels of resistin in serum and this increase correlated with a diminished capability of THP-1 human macrophages to induce the production of reactive species of oxygen (ROS) *in vitro* against a challenge with *M. tuberculosis* (Chao et al., 2015). Another study in patients without T2D, found higher concentrations of serum resistin in TB patients than in healthy controls, and this concentration diminishes during 6 months of treatment with a standard anti-tuberculosis treatment (Ehtesham et al., 2011). These evidences suggest TB induces a metabolic change in the production of resistin, which has effects in both metabolic and immunologic response and derives in macrophage defective functions.

Production of intestinal incretins, proteins released after food intake and which stimulate insulin secretion (Nauck and Meier, 2018), such as GLP (glucagon-like peptide) is reduced in patients with T2D (Mannucci et al., 2000). GLP is degraded by the enzyme dipeptidyl peptidase IV (DPP-4) and as a part of the antidiabetic treatment, blockers of DPP4 are commonly used for glucose control (Deacon, 2019). A recent study found a negative correlation in blood levels of DPP4 and the chemoattraction of cells to lung in TB infected humans (Blauenfeldt et al., 2018). According to this study, TB patients had a lower amount of DPP4 than healthy controls and this was correlated with TB pathology through the recruitment of Th1 T cells to the site of infection. Even though the effect on blood glucose levels through the use of DPP4 blockers during TB-T2D on the host response to *M. tuberculosis* infection has not been addressed, the hormonal control of appetite and blood glucose may cause modulation of the of immune response.

Modifications in Microbiota in T2D Patients and Its Role on Immunity Against Mycobacteria

Patients with T2D have modifications in the composition of their intestinal microbiota that may lead to tuberculosis susceptibility (Zhang et al., 2013). In T2D patients, there is a significant reduction in the numbers of bacteria that produces short-chain fatty acids (SCFA) (Larsen et al., 2010; Morrison and Preston, 2016). The role of SCFA in response to *M. tuberculosis* was explored *in vitro* by Lachmandas and collaborators by exposing isolated Peripheral Blood Mononuclear Cells (PBMCs) to SCFA (acetate, propionate or butyrate) and measuring cytokines that participate in the proinflammatory and anti-inflammatory response against a stimulus with *M. tuberculosis* H37Rv lysates *in vitro*. Treatment with SCFA decreased induction of TNF-α, IL-1β, and IL-17, while it did not modify the induction of IL-6, IFN-γ, or IL-22 (Lachmandas et al., 2016). A reduced production of TNF-α or IL-1β is related with higher bacillary burden, while a reduced production in IL-17 has been related to lower migration of T cells to the site of infection, conducting to severe scenarios of infection (Domingo-Gonzalez et al., 2016). Even though Lachmandas and collaborators did not demonstrate that SCFA

concentrations affected bacillary load in this *in vitro* model, it was clear that they affected host response against *M. tuberculosis* infection and left open the opportunity to experimentally address their influence *in vivo* using suitable models.

Vitamin D Deficiency in T2D and Its Effect on Immune Response Against Mycobacteria

Vitamin D is known to play a role in the control of TB infection (Kearns and Tangpricha, 2014). In addition, vitamin D is related with the control of blood glucose in T2D though modulation of insulin resistance and insulin secretion (Norman et al., 1980). Vitamin D deficiency is common in T2D patients, and some studies have related this deficiency with an increased risk of TB. A recent study has correlated the presence of pre-T2D and T2D with lower levels of vitamin D in TB patients in China (Zhao et al., 2017). Another study in recently diagnosed TB patients in China, either with TB or TB-T2D, revealed that there is an association between diminished vitamin D levels in serum and TB (OR = 3.26, C.I. 1.56–6.82) or TB-T2D (OR = 2.27, C.I. 1.05–4.92) (Wang et al., 2017).

Regarding the evidences linking vitamin D deficiency to a higher risk of TB, an study in Tanzania, revealed that vitamin D deficiency is related to an increased risk of TB only in patients with persistent hyperglycemia (OR = 4.0, C.I. 0.86–18.54) (Boillat-Blanco et al., 2016), and another study in China showed that patients with more than 10 years of T2D diagnosis have lower levels of vitamin D (Zhao et al., 2018). In addition to these data, an study in Chinese patients showed that both T2D and pre-T2D people have lower levels of vitamin D in serum (Zhao et al., 2017). These results suggest that there is a time-dependent relationship between vitamin D, hyperglycemia and TB risk.

A study in Mexico, where monocytes obtained from T2D patients (with confirmed vitamin D deficiency) were infected with *M. tuberculosis* H37Ra, showed that bacterial replication was higher in monocytes from T2D patients than in monocytes from healthy controls (Herrera et al., 2017), suggesting that vitamin D (among other possible defects as already described above) contribute to reduced control of *M. tuberculosis* in cells derived from T2D patients.

TREATMENT OF T2D AND ITS IMPACT ON TB SUSCEPTIBILITY

Effect of Anti-hyperglycemic Drugs on the Host Response to *M. tuberculosis* Infection

According to ADA, metformin is the preferred initial treatment for hyperglycemia in T2D patients (American Diabetes Association, 2018b) and, even though a recent systematic review found evidence that suggest the glycemic control may have a favorable effect on anti-TB treatments outcomes (Shewade et al., 2017), its influence on the host response against *M. tuberculosis* is controversial.

Two recent retrospective studies in Taiwan showed that the treatment of hyperglycemia with metformin is a factor that prevents TB in T2D patients [HR 0.552, 95% C.I. 0.493–0.617 (Tseng, 2018) and HR 0.84, 95% C.I. 0.74–0.96 (Lee M. C. et al., 2018)]. In spite of its protective role, there is no conclusive information about the effectiveness of adjunctive therapy with metformin and anti-TB treatment. A recent report suggest that metformin acts by reducing concentration of circulating metalloproteinases (MPP-1, -2, and -8), and it is correlated with reduced bacterial burden in TB-T2D patients treated with metformin and antibiotics (Kumar et al., 2018). However, a study conducted in Seoul showed that treatment of TB-T2D patients with metformin plus the anti-TB treatment, did not have an effect on the sputum culture conversion nor TB recurrence within 1 year after treatment completion (Lee Y. J. et al., 2018), which is in line of findings of not increased efficacy of TB treatment by administration of metformin in mice (Dutta et al., 2017). These evidences suggest that control of hyperglycemia may contribute to the maintenance of a metabolic environment that may be able to reduce the susceptibility to TB throughout mechanisms that act independently of antibiotic activity.

A study where PBMCs from healthy controls were cultured with glibenclamide, a sulphonylurea also used to reduce hyperglycemia, produced a reduction in M1 markers (CD14+ CD16–), and increased M2 markers (CD14+ CD16+) in these cells independently of infection with BCG. Moreover, when PBMC obtained from subjects who were treated with oral glibenclamide were infected with *M. tuberculosis*, they exhibited an impaired capability to kill bacilli (Kewcharoenwong et al., 2018). While to date, there are no studies reported that correlate the use of glibenclamide with TB susceptibility or anti-TB treatment efficacy, some studies in healthy subjects have demonstrated that there are pharmacological interactions between glibenclamide and glimepiride (another sulphonylurea used to control of hyperglycemia) (Surekha et al., 1997; Niemi et al., 2000). Future studies in this regard are needed to clarify the role of glibenclamide on TB treatment efficacy.

Effect of Pharmacological Treatment of, or Vaccination With BCG, on Diabetic Dyslipidemia and Host Response to *M. tuberculosis* Infection

As we described above, some metabolic changes associated with diabetic dyslipidemia can be actively implicated in the susceptibility of the host to *M. tuberculosis* infection. Treatment of dyslipidemia has been shown to influence the capability to respond to *M. tuberculosis* infection. Lee and collaborators identified in a retrospective study that Taiwanese individuals with T2D and treated with statins had a lower risk of developing active TB (RR 0.76, 95% C.I. 0.60–0.97), than individuals with T2D and no treatment with statins (Lee et al., 2015). However, treatment of dyslipidemia had no influence on the efficacy of a combined therapy formed by antibiotic-treatment and statins or fibrates against TB, as a cohort study showed recently (Chen et al., 2019). These evidences suggest that control of diabetic dyslipidemia should have different effects on the host response to *M. tuberculosis* depending on the stage of TB, before activation of infection, or when infection is established.

Vaccination with BCG produces changes on parameters related to diabetic dyslipidemia. An study where guinea pigs were vaccinated or not with BCG, showed that vaccination produces a lower accumulation of Ox-LDL at the site of infection after challenge with *M. tuberculosis* H37Rv than accumulation observed in unvaccinated guinea pigs (Parish et al., 2012). This effect regarding the accumulation of ox-LDL is in agreement with results obtained with peritoneal macrophages isolated from hyperlipidemic APOE*Leiden. CETP mice vaccinated with BCG, which after vaccination, had lower concentrations of non-HDL cholesterol than unvaccinated mice, and this event correlated with lower formation of foamy cells (Van Dam et al., 2016). These data suggest that immunization with BCG has also an effect on lipid metabolism and may contribute to the protection afforded against TB by pathways other than those directly involved in immune responses.

CONCLUDING REMARKS

Recently, a systematic review showed that more than 70% of new drug efficacy trials have not considered the T2D population in their protocols (Lutfiana et al., 2019). We strongly believe research in TB should encompass efforts to understand how the presence of risk factors like T2D may compromise the efficacy and/or immunogenicity of vaccines, or affect the sensibility of diagnostic methods, or even the therapeutic effect of new drugs.

As a mathematical modeling of TB-T2D shows, control of T2D may lead to a significant reduction in TB incidence, and the uncontrolled raise of T2D should have the opposite effect (Pan et al., 2015). We think that a better understanding of the mechanisms that couple metabolic changes with TB susceptibility will lead to the design of better therapies, which would focus on the management of the TB-T2D comorbidity. We do not rule out the use of drugs that are traditionally used in the T2D treatment as a host-directed therapy against TB, as metformin and statins, even though further studies are needed to fully ascertain their efficacy as a complement for the treatment of TB. Furthermore, we suggest that the design and evaluation of current and future vaccine candidates against TB, or diagnostic methods that aim to early diagnose TB before the onset of overt disease in T2D patients, should consider including their evaluation in T2D preclinical models, as well as in human volunteers whenever a clinical trial is designed and performed.

T2D patients undergo some metabolic modifications that may facilitate the establishment, maintenance, and progression of *M. tuberculosis* infection. Since the onset of a prediabetic stage, the metabolic environment compromises the host response and produces changes that allows infection and favors disease progression and its worsening. In this sense, identification of biomarkers of progression to TB in prediabetic patients is needed to better understand the transition point between progression or not to TB. Recent efforts to elucidate a metabolic signature of progression to TB revealed that some metabolic networks may be related to progression to TB (Duffy et al., 2019). In particular, genes that encode for molecules that participate in fatty-acid metabolism and protein catabolism resulted as significantly associated to TB progression: *CTP1A*, which codes for carnitine palmitoyltransferase 1A was downregulated in obesity (Orellana-Gavalda et al., 2011); *SLC25A20*, which codes for carnitine acyl-carnitine translocase and has been observed to contribute to insulin secretion in mouse models of obesity (Soni et al., 2014); and *PDK4*, which codes for pyruvate dehydrogenase kinase, a key enzyme that participates in control of blood glucose in an insuline-dependent manner (Lee, 2014), and is increased in diabetic rats (Wu et al., 1998).

During T2D and TB comorbidity, the basal levels of glucose, 1AC, triglycerides, HDL-cholesterol, lipoproteins, and hormones related to the control of metabolic parameters creates an environment that supports bacterial survival and their spread (**Figure 1**). Finally, we contend that a better understanding of how immunity is modulated by metabolic signatures, will allow us to identify targets for treatment of TB-T2D patients, which lead to an improved control of T2D and resolution of TB disease by an enhanced clearance of *M. tuberculosis* from infected cells.

AUTHOR CONTRIBUTIONS

CS-C and MF-V extensively discussed the manuscript. All authors wrote the manuscript, reviewed drafts, and approved submission of this work.

FUNDING

CS-C and WL-R received financial support from CONACYT, Ph.D. fellowship 432019 and 337689, respectively.

ACKNOWLEDGMENTS

The effect of T2D on humoral response to TB is being evaluated thanks to project FONCICYT-GACD265796 (MF-V).

REFERENCES

Almeida-Junior, J. L., Gil-Santana, L., Oliveira, C. A., Castro, S., Cafezeiro, A. S., Daltro, C., et al. (2016). Glucose metabolism disorder is associated with pulmonary tuberculosis in individuals with respiratory symptoms from Brazil. *PLoS ONE* 11:e0153590. doi: 10.1371/journal.pone.0153590

Al-Rifai, R. H., Pearson, F., Critchley, J. A., and Abu-Raddad, L. J. (2017). Association between diabetes mellitus and active tuberculosis: a systematic review and meta-analysis. *PLoS ONE* 12:e0187967. doi: 10.1371/journal.pone.0187967

Amare, H., Gelaw, A., Anagaw, B., and Gelaw, B. (2013). Smear positive pulmonary tuberculosis among diabetic patients at the Dessie referral hospital, Northeast Ethiopia. *Infect. Dis. Poverty* 2:6. doi: 10.1186/2049-9957-2-6

American Diabetes Association (2018a). 2. Classification and diagnosis of diabetes: standards of medical care in diabetes-2018. *Diabetes Care* 41, S13–S27. doi: 10.2337/dc18-S002

American Diabetes Association (2018b). 8. Pharmacologic approaches to glycemic treatment: standards of medical care in diabetes-2018. *Diabetes Care* 41, S73–S85. doi: 10.2337/dc18-S008

American Diabetes Association (2019a). 2. Classification and diagnosis of diabetes: standards of medical care in diabetes-2019. *Diabetes Care* 42, S13–S28. doi: 10.2337/dc19-S002

American Diabetes Association (2019b). 6. Glycemic targets: standards of medical care in diabetes-2019. *Diabetes Care* 42, S61–S70. doi: 10.2337/dc19-S006

Bailey, S. L., Ayles, H., Beyers, N., Godfrey-Faussett, P., Muyoyeta, M., Du Toit, E., et al. (2016). The association of hyperglycaemia with prevalent tuberculosis: a population-based cross-sectional study. *BMC Infect. Dis.* 16:733. doi: 10.1186/s12879-016-2066-1

Benomar, Y., Gertler, A., De Lacy, P., Crepin, D., Ould Hamouda, H., Riffault, L., et al. (2013). Central resistin overexposure induces insulin resistance through Toll-like receptor 4. *Diabetes* 62, 102–114. doi: 10.2337/db12-0237

Blauenfeldt, T., Petrone, L., Del Nonno, F., Baiocchini, A., Falasca, L., Chiacchio, T., et al. (2018). Interplay of DDP4 and IP-10 as a potential mechanism for cell recruitment to tuberculosis lesions. *Front. Immunol.* 9:1456. doi: 10.3389/fimmu.2018.01456

Boillat-Blanco, N., Bovet, P., Ramaiya, K. L., Mganga, M., Minja, L. T., Saleh, L., et al. (2016). Association between tuberculosis, diabetes and 25 hydroxyvitamin D in Tanzania: a longitudinal case control study. *BMC Infect. Dis.* 16:626. doi: 10.1186/s12879-016-1960-x

Bokarewa, M., Nagaev, I., Dahlberg, L., Smith, U., and Tarkowski, A. (2005). Resistin, an adipokine with potent proinflammatory properties. *J. Immunol.* 174, 5789–5795. doi: 10.4049/jimmunol.174.9.5789

Buyukoglan, H., Gulmez, I., Kelestimur, F., Kart, L., Oymak, F. S., Demir, R., et al. (2007). Leptin levels in various manifestations of pulmonary tuberculosis. *Mediators Inflamm.* 2007:64859. doi: 10.1155/2007/64859

Carmena, R. (2008). Riesgo elevado de disfunción lipoproteica en la diabetes mellitus tipo 2. *Rev Esp Cardiol Supl.* 8, 19C—26C. doi: 10.1016/S1131-3587(08)73551-9

Carreira, S., Costeira, J., Gomes, C., Andre, J. M., and Diogo, N. (2012). Impact of diabetes on the presenting features of tuberculosis in hospitalized patients. *Rev. Port. Pneumol.* 18, 239–243. doi: 10.1016/j.rppneu.2012.04.001

Carrera Boada, C. A., and Martinez-Moreno, J. M. (2013). Pathophysiology of diabetes mellitus type 2: beyond the duo "insulin resistance-secretion deficit". *Nutr. Hosp.* 28(Suppl. 2), 78–87. doi: 10.3305/nh.2013.28.sup2.6717

Chang, S. W., Pan, W. S., Lozano Beltran, D., Oleyda Baldelomar, L., Solano, M. A., Tuero, I., et al. (2013). Gut hormones, appetite suppression and cachexia in patients with pulmonary TB. *PLoS ONE* 8:e54564. doi: 10.1371/journal.pone.0054564

Chao, W. C., Yen, C. L., Wu, Y. H., Chen, S. Y., Hsieh, C. Y., Chang, T. C., et al. (2015). Increased resistin may suppress reactive oxygen species production and inflammasome activation in type 2 diabetic patients with pulmonary tuberculosis infection. *Microbes Infect.* 17, 195–204. doi: 10.1016/j.micinf.2014.11.009

Chen, Y. T., Kuo, S. C., Chao, P. W., and Chang, Y. Y. (2019). Use of lipid-lowering agents is not associated with improved outcomes for tuberculosis patients on standard-course therapy: a population-based cohort study. *PLoS ONE* 14:e0210479. doi: 10.1371/journal.pone.0210479

Cuevas, M., A., and Alonso, K. R. (2016). Dislipidemia diabética. *Rev. Méd. Clín. Las Condes* 27, 152–159. doi: 10.1016/j.rmclc.2016.04.004

Cui, X., Kushiyama, A., Yoneda, M., Nakatsu, Y., Guo, Y., Zhang, J., et al. (2010). Macrophage foam cell formation is augmented in serum from patients with diabetic angiopathy. *Diabetes Res. Clin. Pract.* 87, 57–63. doi: 10.1016/j.diabres.2009.10.011

Daniel, J., Maamar, H., Deb, C., Sirakova, T. D., and Kolattukudy, P. E. (2011). *Mycobacterium tuberculosis* uses host triacylglycerol to accumulate lipid droplets and acquires a dormancy-like phenotype in lipid-loaded macrophages. *PLoS Pathog.* 7:e1002093. doi: 10.1371/journal.ppat.1002093

Deacon, C. F. (2019). Physiology and pharmacology of DPP-4 in glucose homeostasis and the treatment of type 2 diabetes. *Front. Endocrinol.* 10:80. doi: 10.3389/fendo.2019.00080

Defronzo, R. A., Ferrannini, E., Groop, L., Henry, R. R., Herman, W. H., Holst, J. J., et al. (2015). Type 2 diabetes mellitus. *Nat. Rev. Dis. Primers* 1:15019. doi: 10.1038/nrdp.2015.19

Deniz, O., Gumus, S., Yaman, H., Ciftci, F., Ors, F., Cakir, E., et al. (2007). Serum total cholesterol, HDL-C and LDL-C concentrations significantly correlate with the radiological extent of disease and the degree of smear positivity in patients with pulmonary tuberculosis. *Clin. Biochem.* 40, 162–166. doi: 10.1016/j.clinbiochem.2006.10.015

Domingo-Gonzalez, R., Prince, O., Cooper, A., and Khader, S. A. (2016). Cytokines and chemokines in *Mycobacterium tuberculosis* infection. *Microbiol. Spectr.* 4:TBTB2-0018-2016. doi: 10.1128/microbiolspec.TBTB2-0018-2016

Dong, Z., Shi, J., Dorhoi, A., Zhang, J., Soodeen-Lalloo, A. K., Tan, W., et al. (2018). Hemostasis and lipoprotein indices signify exacerbated lung injury in TB with diabetes comorbidity. *Chest* 153, 1187–1200. doi: 10.1016/j.chest.2017.11.029

Duffy, F. J., Weiner, J. III, Hansen, S., Tabb, D. L., Suliman, S., Thompson, E., Maertzdorf, J., et al. (2019). Immunometabolic signatures predict risk of progression to active tuberculosis and disease outcome. *Front. Immunol.* 10:527. doi: 10.3389/fimmu.2019.00527

Dutta, N. K., Pinn, M. L., and Karakousis, P. C. (2017). Metformin adjunctive therapy does not improve the sterilizing activity of the first-line antitubercular regimen in mice. *Antimicrob. Agents Chemother.* 61:e00652-17. doi: 10.1128/AAC.00652-17

Ehtesham, N. Z., Nasiruddin, M., Alvi, A., Kumar, B. K., Ahmed, N., Peri, S., et al. (2011). Treatment end point determinants for pulmonary tuberculosis: human resistin as a surrogate biomarker. *Tuberculosis* 91, 293–299. doi: 10.1016/j.tube.2011.04.007

Elsaid, H. H., Elgohary, M. N., and Elshabrawy, A. M. (2019). Complement c1q tumor necrosis factor-related protein 3 a novel adipokine, protect against diabetes mellitus in young adult Egyptians. *Diabetes Metab. Syndr.* 13, 434–438. doi: 10.1016/j.dsx.2018.10.004

Ginandjar, P., Saraswati, L. D., and Widjanarko, B. (2016). Profile of glycated-hemoglobin, antioxidant vitamin and cytokine levels in pulmonary tuberculosis patients: a cross sectional study at Pulmonary Diseases Center Semarang City, Indonesia. *Biomed. J.* 39, 354–360. doi: 10.1016/j.bj.2016.01.011

Guerrini, V., Prideaux, B., Blanc, L., Bruiners, N., Arrigucci, R., Singh, S., et al. (2018). Storage lipid studies in tuberculosis reveal that foam cell biogenesis is disease-specific. *PLoS Pathog.* 14:e1007223. doi: 10.1371/journal.ppat.1007223

Hayashi, S., and Chandramohan, D. (2018). Risk of active tuberculosis among people with diabetes mellitus: systematic review and meta-analysis. *Trop. Med. Int. Health* 23, 1058–1070. doi: 10.1111/tmi.13133

Hayashi, S., Takeuchi, M., Hatsuda, K., Ogata, K., Kurata, M., Nakayama, T., et al. (2014). The impact of nutrition and glucose intolerance on the development of tuberculosis in Japan. *Int. J. Tuberc. Lung Dis.* 18, 84–88. doi: 10.5588/ijtld.13.0495

Hayek, T., Hussein, K., Aviram, M., Coleman, R., Keidar, S., Pavoltzky, E., et al. (2005). Macrophage foam-cell formation in streptozotocin-induced diabetic mice: stimulatory effect of glucose. *Atherosclerosis* 183, 25–33. doi: 10.1016/j.atherosclerosis.2005.02.018

Herrera, M. T., Gonzalez, Y., Hernandez-Sanchez, F., Fabian-San Miguel, G., and Torres, M. (2017). Low serum vitamin D levels in type 2 diabetes patients are associated with decreased mycobacterial activity. *BMC Infect. Dis.* 17:610. doi: 10.1186/s12879-017-2705-1

Huang, L. K., Wang, H. H., Lai, Y. C., and Chang, S. C. (2017). The impact of glycemic status on radiological manifestations of pulmonary tuberculosis in diabetic patients. *PLoS ONE* 12:e0179750. doi: 10.1371/journal.pone.0179750

IDF (2017). *IDF Diabetes Atlas.* Available online at: https://www.diabetesatlas.org

Jimenez-Corona, M. E., Cruz-Hervert, L. P., Garcia-Garcia, L., Ferreyra-Reyes, L., Delgado-Sanchez, G., Bobadilla-Del-Valle, M., et al. (2013). Association of diabetes and tuberculosis: impact on treatment and post-treatment outcomes. *Thorax* 68, 214–220. doi: 10.1136/thoraxjnl-2012-201756

Kearns, M. D., and Tangpricha, V. (2014). The role of vitamin D in tuberculosis. *J. Clin. Transl. Endocrinol.* 1, 167–169. doi: 10.1016/j.jcte.2014.08.002

Kewcharoenwong, C., Prabowo, S. A., Bancroft, G. J., Fletcher, H. A., and Lertmemongkolchai, G. (2018). Glibenclamide reduces primary human monocyte functions against tuberculosis infection by enhancing M2 polarization. *Front. Immunol.* 9:2109. doi: 10.3389/fimmu.2018.02109

Kopp, A., Bala, M., Buechler, C., Falk, W., Gross, P., Neumeier, M., et al. (2010). C1q/TNF-related protein-3 represents a novel and endogenous lipopolysaccharide antagonist of the adipose tissue. *Endocrinology* 151, 5267–5278. doi: 10.1210/en.2010-0571

Kumar Nathella, P., and Babu, S. (2017). Influence of diabetes mellitus on immunity to human tuberculosis. *Immunology* 152, 13–24. doi: 10.1111/imm.12762

Kumar, N. P., Banurekha, V. V., Nair, D., Sridhar, R., Kornfeld, H., Nutman, T. B., et al. (2014). Coincident pre-diabetes is associated with dysregulated cytokine responses in pulmonary tuberculosis. *PLoS ONE* 9:e112108. doi: 10.1371/journal.pone.0112108

Kumar, N. P., Moideen, K., Bhootra, Y., Nancy, A., Viswanathan, V., Shruthi, B. S., et al. (2019). Elevated circulating levels of monocyte activation markers among tuberculosis patients with diabetes co-morbidity. *Immunology* 156, 249–258. doi: 10.1111/imm.13023

Kumar, N. P., Moideen, K., Viswanathan, V., Shruthi, B. S., Sivakumar, S., Menon, P. A., et al. (2018). Elevated levels of matrix metalloproteinases reflect severity and extent of disease in tuberculosis-diabetes co-morbidity and are predominantly reversed following standard anti-tuberculosis or metformin treatment. *BMC Infect. Dis.* 18:345. doi: 10.1186/s12879-018-3246-y

Lachmandas, E., Van Den Heuvel, C. N., Damen, M. S., Cleophas, M. C., Netea, M. G., and Van Crevel, R. (2016). Diabetes mellitus and increased tuberculosis susceptibility: the role of short-chain fatty acids. *J. Diabetes Res.* 2016:6014631. doi: 10.1155/2016/6014631

Larsen, N., Vogensen, F. K., Van Den Berg, F. W., Nielsen, D. S., Andreasen, A. S., Pedersen, B. K., et al. (2010). Gut microbiota in human adults with type 2 diabetes differs from non-diabetic adults. *PLoS ONE* 5:e9085. doi: 10.1371/journal.pone.0009085

Lee, I. K. (2014). The role of pyruvate dehydrogenase kinase in diabetes and obesity. *Diabetes Metab. J.* 38, 181–186. doi: 10.4093/dmj.2014.38.3.181

Lee, M. C., Chiang, C. Y., Lee, C. H., Ho, C. M., Chang, C. H., Wang, J. Y., et al. (2018). Metformin use is associated with a low risk of tuberculosis among newly diagnosed diabetes mellitus patients with normal renal function: a nationwide cohort study with validated diagnostic criteria. *PLoS ONE* 13:e0205807. doi: 10.1371/journal.pone.0205807

Lee, M. R., Huang, Y. P., Kuo, Y. T., Luo, C. H., Shih, Y. J., Shu, C. C., et al. (2017). Diabetes mellitus and latent tuberculosis infection: a systematic review and metaanalysis. *Clin. Infect. Dis.* 64, 719–727. doi: 10.1093/cid/ciw836

Lee, M. Y., Lin, K. D., Hsu, W. H., Chang, H. L., Yang, Y. H., Hsiao, P. J., et al. (2015). Statin, calcium channel blocker and Beta blocker therapy may decrease the incidence of tuberculosis infection in elderly Taiwanese patients with type 2 diabetes. *Int. J. Mol. Sci.* 16, 11369–11384. doi: 10.3390/ijms160511369

Lee, Y. J., Han, S. K., Park, J. H., Lee, J. K., Kim, D. K., Chung, H. S., et al. (2018). The effect of metformin on culture conversion in tuberculosis patients with diabetes mellitus. *Korean J. Intern. Med.* 33, 933–940. doi: 10.3904/kjim.2017.249

Liu, M., Liu, S. W., Wang, L. J., Bai, Y. M., Zeng, X. Y., Guo, H. B., et al. (2019). Burden of diabetes, hyperglycaemia in China from to 2016: findings from the 1990 to 2016, global burden of disease study. *Diabetes Metab.* 45, 286–293. doi: 10.1016/j.diabet.2018.08.008

Liu, Q., Li, W., Xue, M., Chen, Y., Du, X., Wang, C., et al. (2017). Diabetes mellitus and the risk of multidrug resistant tuberculosis: a meta-analysis. *Sci. Rep.* 7:1090. doi: 10.1038/s41598-017-01213-5

Lopez-Lopez, N., Martinez, A. G. R., Garcia-Hernandez, M. H., Hernandez-Pando, R., Castaneda-Delgado, J. E., Lugo-Villarino, G., et al. (2018). Type-2 diabetes alters the basal phenotype of human macrophages and diminishes their capacity to respond, internalise, and control *Mycobacterium tuberculosis*. *Mem. Inst. Oswaldo Cruz* 113:e170326. doi: 10.1590/0074-02760170326

Lutfiana, N. C., Van Boven, J. F. M., Masoom Zubair, M. A., Pena, M. J., and Alffenaar, J. C. (2019). Diabetes mellitus comorbidity in patients enrolled in tuberculosis drug efficacy trials around the world: a systematic review. *Br. J. Clin. Pharmacol.* 85, 1407–1417. doi: 10.1111/bcp.13935

Magee, M. J., Salindri, A. D., Kyaw, N. T. T., Auld, S. C., Haw, J. S., and Umpierrez, G. E. (2018). Stress hyperglycemia in patients with tuberculosis disease: epidemiology and clinical implications. *Curr. Diab. Rep.* 18:71. doi: 10.1007/s11892-018-1036-y

Mannucci, E., Ognibene, A., Cremasco, F., Bardini, G., Mencucci, A., Pierazzuoli, E., et al. (2000). Glucagon-like peptide (GLP)-1 and leptin concentrations in obese patients with Type 2 diabetes mellitus. *Diabetic Med.* 17, 713–719. doi: 10.1046/j.1464-5491.2000.00367.x

Mave, V., Meshram, S., Lokhande, R., Kadam, D., Dharmshale, S., Bharadwaj, R., et al. (2017). Prevalence of dysglycemia and clinical presentation of pulmonary tuberculosis in Western India. *Int. J. Tuberc. Lung Dis.* 21, 1280–1287. doi: 10.5588/ijtld.17.0474

Mexitalia, M., Dewi, Y. O., Pramono, A., and Anam, M. S. (2017). Effect of tuberculosis treatment on leptin levels, weight gain, and percentage body fat in Indonesian children. *Korean J. Pediatr.* 60, 118–123. doi: 10.3345/kjp.2017.60.4.118

Montoya-Rosales, A., Castro-Garcia, P., Torres-Juarez, F., Enciso-Moreno, J. A., and Rivas-Santiago, B. (2016). Glucose levels affect LL-37 expression in monocyte-derived macrophages altering the *Mycobacterium tuberculosis* intracellular growth control. *Microb. Pathog.* 97, 148–153. doi: 10.1016/j.micpath.2016.06.002

Morrison, D. J., and Preston, T. (2016). Formation of short chain fatty acids by the gut microbiota and their impact on human metabolism. *Gut Microbes* 7, 189–200. doi: 10.1080/19490976.2015.1134082

Nauck, M. A., and Meier, J. J. (2018). Incretin hormones: their role in health and disease. *Diabetes Obes. Metab.* 20(Suppl. 1), 5–21. doi: 10.1111/dom.13129

Niemi, M., Kivisto, K. T., Backman, J. T., and Neuvonen, P. J. (2000). Effect of rifampicin on the pharmacokinetics and pharmacodynamics of glimepiride. *Br. J. Clin. Pharmacol.* 50, 591–595. doi: 10.1046/j.1365-2125.2000.00295.x

Norman, A. W., Frankel, J. B., Heldt, A. M., and Grodsky, G. M. (1980). Vitamin D deficiency inhibits pancreatic secretion of insulin. *Science* 209, 823–825. doi: 10.1126/science.6250216

Nurwidya, F., Ratnawati, Wijaya, D., Nazaruddin, A., and Burhan, E. (2018). The relationship between hemoglobin A1C levels and sputum conversion time in indonesian patients with new cases of pulmonary tuberculosis. *J. Nat. Sci. Biol. Med.* 9, 217–221. doi: 10.4103/jnsbm.JNSBM_24_18

Oh, J., Choi, R., Park, H. D., Lee, H., Jeong, B. H., Park, H. Y., et al. (2017). Evaluation of vitamin status in patients with pulmonary tuberculosis. *J. Infect.* 74, 272–280. doi: 10.1016/j.jinf.2016.10.009

Olokoba, A. B., Obateru, O. A., and Olokoba, L. B. (2012). Type 2 diabetes mellitus: a review of current trends. *Oman Med. J.* 27, 269–273. doi: 10.5001/omj.2012.68

Orellana-Gavalda, J. M., Herrero, L., Malandrino, M. I., Paneda, A., Sol Rodriguez-Pena, M., Petry, H., et al. (2011). Molecular therapy for obesity and diabetes based on a long-term increase in hepatic fatty-acid oxidation. *Hepatology* 53, 821–832. doi: 10.1002/hep.24140

Pan, S.-C., Ku, C.-C., Kao, D., Ezzati, M., Fang, C.-T., and Lin, H.-H. (2015). Effect of diabetes on tuberculosis control in 13 countries with high tuberculosis: a modelling study. *Lancet Diabetes Endocrinol.* 3, 323–330. doi: 10.1016/S2213-8587(15)00042-X

Parish, T., Palanisamy, G. S., Kirk, N. M., Ackart, D. F., Obregón-Henao, A., Shanley, C. A., et al. (2012). Uptake and accumulation of oxidized low-density lipoprotein during *Mycobacterium tuberculosis* infection in guinea pigs. *PLoS ONE* 7:34148. doi: 10.1371/journal.pone.0034148

Penn-Nicholson, A., Hraha, T., Thompson, E. G., Sterling, D., Mbandi, S. K., Wall, K. M., et al. (2019). Discovery and validation of a prognostic proteomic signature for tuberculosis progression: a prospective cohort study. *PLoS Med.* 16:e1002781. doi: 10.1371/journal.pmed.1002781

Qrafli, M., El Kari, K., Aguenaou, H., Bourkadi, J. E., Sadki, K., and El Mzibri, M. (2017). Low plasma vitamin A concentration is associated with tuberculosis in Moroccan population: a preliminary case control study. *BMC Res. Notes* 10:421. doi: 10.1186/s13104-017-2737-z

Rao, S. (2009). Serum cholesterol, HDL, LDL levels in pulmonary tuberculosis. *Infect. Dis. Clin. Pract.* 17, 99–101. doi: 10.1097/IPC.0b013e3181934367

Rao, S., R. M., Iqbal, K., Haroon, F., and Hasan, Z. (2019). Impact of diabetes on mechanisms of immunity against *Mycobacterium tuberculosis*. *J Pak Med Assoc.* 69, 94–98. Available online at: https://jpma.org.pk/article-details/9007?article_id=9007

Restrepo, B. I. (2016). Diabetes and tuberculosis. *Microbiol. Spectr.* 4, 595–606. doi: 10.1128/microbiolspec.TNMI7-0023-2016

Russell, D. G., Cardona, P. J., Kim, M. J., Allain, S., and Altare, F. (2009). Foamy macrophages and the progression of the human tuberculosis granuloma. *Nat. Immunol.* 10, 943–948. doi: 10.1038/ni.1781

Schmid, A., Kopp, A., Hanses, F., Karrasch, T., and Schaffler, A. (2014). C1q/TNF-related protein-3 (CTRP-3) attenuates lipopolysaccharide (LPS)-induced systemic inflammation and adipose tissue Erk-1/-2 phosphorylation in mice *in vivo*. *Biochem. Biophys. Res. Commun.* 452, 8–13. doi: 10.1016/j.bbrc.2014.06.054

Shewade, H. D., Jeyashree, K., Mahajan, P., Shah, A. N., Kirubakaran, R., Rao, R., et al. (2017). Effect of glycemic control and type of diabetes treatment

on unsuccessful TB treatment outcomes among people with TB-Diabetes: a systematic review. *PLoS ONE* 12:e0186697. doi: 10.1371/journal.pone.0186697

Shivakumar, S., Chandrasekaran, P., Kumar, A. M. V., Paradkar, M., Dhanasekaran, K., Suryavarshini, N., et al. (2018). Diabetes and pre-diabetes among household contacts of tuberculosis patients in India: is it time to screen them all? *Int. J. Tuberc. Lung Dis.* 22, 686–694. doi: 10.5588/ijtld.17.0598

Soni, M. S., Rabaglia, M. E., Bhatnagar, S., Shang, J., Ilkayeva, O., Mynatt, R., et al. (2014). Downregulation of carnitine acyl-carnitine translocase by miRNAs 132 and 212 amplifies glucose-stimulated insulin secretion. *Diabetes* 63, 3805–3814. doi: 10.2337/db13-1677

Srivastava, S., Ernst, J. D., and Desvignes, L. (2014). Beyond macrophages: the diversity of mononuclear cells in tuberculosis. *Immunol. Rev.* 262, 179–192. doi: 10.1111/imr.12217

Steppan, C. M., Bailey, S. T., Bhat, S., Brown, E. J., Banerjee, R. R., Wright, C. M., et al. (2001). The hormone resistin links obesity to diabetes. *Nature* 409, 307–312. doi: 10.1038/35053000

Surekha, V., Peter, J. V., Jeyaseelan, L., and Cherian, A. M. (1997). Drug interaction: rifampicin and glibenclamide. *Natl. Med. J. India* 10, 2.

Tabarsi, P., Baghaei, P., Marjani, M., Vollmer, W. M., Masjedi, M. R., and Harries, A. D. (2014). Changes in glycosylated haemoglobin and treatment outcomes in patients with tuberculosis in Iran: a cohort study. *J. Diabetes Metab. Disord.* 13:123. doi: 10.1186/s40200-014-0123-0

Tseng, C. H. (2018). Metformin decreases risk of tuberculosis infection in type 2 diabetes patients. *J. Clin. Med.* 7:264. doi: 10.3390/jcm7090264

Van Dam, A. D., Bekkering, S., Crasborn, M., Van Beek, L., Van Den Berg, S. M., Vrieling, F., et al. (2016). BCG lowers plasma cholesterol levels and delays atherosclerotic lesion progression in mice. *Atherosclerosis* 251, 6–14. doi: 10.1016/j.atherosclerosis.2016.05.031

Viswanathan, A. A., and Gawde, N. C. (2014). Effect of type II diabetes mellitus on treatment outcomes of tuberculosis. *Lung India* 31, 244–248. doi: 10.4103/0970-2113.135764

Vrieling, F., Ronacher, K., Kleynhans, L., Van Den Akker, E., Walzl, G., Ottenhoff, T. H. M., et al. (2018). Patients with concurrent tuberculosis and diabetes have a pro-atherogenic plasma lipid profile. *EBioMedicine* 32, 192–200. doi: 10.1016/j.ebiom.2018.05.011

Vrieling, F., Wilson, L., Rensen, P. C. N., Walzl, G., Ottenhoff, T. H. M., and Joosten, S. A. (2019). Oxidized low-density lipoprotein (oxLDL) supports *Mycobacterium tuberculosis* survival in macrophages by inducing lysosomal dysfunction. *PLoS Pathog.* 15:e1007724. doi: 10.1371/journal.ppat.1007724

Wang, Q., Ma, A., Han, X., Zhang, H., Zhao, S., Liang, H., et al. (2017). Is low serum 25-hydroxyvitamin D a possible link between pulmonary tuberculosis and type 2 diabetes? *Asia Pac. J. Clin. Nutr.* 26, 241–246. doi: 10.6133/apjcn.032016.02

WHO (2018). *Global Tuberculosis Report*.

Wilkinson, K. A., Workneh, M. H., Bjune, G. A., and Yimer, S. A. (2017). Prevalence and associated factors of tuberculosis and diabetes mellitus comorbidity: a systematic review. *PLoS ONE* 12:e0175925. doi: 10.1371/journal.pone.0175925

Wu, L., and Parhofer, K. G. (2014). Diabetic dyslipidemia. *Metab. Clin. Exp.* 63, 1469–1479. doi: 10.1016/j.metabol.2014.08.010

Wu, P., Sato, J., Zhao, Y., Jaskiewicz, J., Popov, K. M., and Harris, R. A. (1998). Starvation and diabetes increase the amount of pyruvate dehydrogenase kinase isoenzyme 4 in rat heart. *Biochem. J.* 329, 197–201. doi: 10.1042/bj3290197

Xia, L. L., Li, S. F., Shao, K., Zhang, X., and Huang, S. (2018). The correlation between CT features and glycosylated hemoglobin level in patients with T2DM complicated with primary pulmonary tuberculosis. *Infect. Drug Resist.* 11, 187–193. doi: 10.2147/IDR.S146741

Zhang, X., Shen, D., Fang, Z., Jie, Z., Qiu, X., Zhang, C., et al. (2013). Human gut microbiota changes reveal the progression of glucose intolerance. *PLoS ONE* 8:e71108. doi: 10.1371/journal.pone.0071108

Zhao, X., Yuan, Y., Lin, Y., Zhang, T., Bai, Y., Kang, D., et al. (2018). Vitamin D status of tuberculosis patients with diabetes mellitus in different economic areas and associated factors in China. *PLoS ONE* 13:e0206372. doi: 10.1371/journal.pone.0206372

Zhao, X., Yuan, Y., Lin, Y., Zhang, T., Ma, J., Kang, W., et al. (2017). Vitamin D status in tuberculosis patients with diabetes, prediabetes and normal blood glucose in China: a cross-sectional study. *BMJ Open* 7:e017557. doi: 10.1136/bmjopen-2017-017557

Zheng, Y., Ma, A., Wang, Q., Han, X., Cai, J., Schouten, E. G., et al. (2013). Relation of leptin, ghrelin and inflammatory cytokines with body mass index in pulmonary tuberculosis patients with and without type 2 diabetes mellitus. *PLoS ONE* 8:e80122. doi: 10.1371/journal.pone.0080122

Conflict of Interest: The authors declare that the research was conducted in the absence of any commercial or financial relationships that could be construed as a potential conflict of interest.

frontiers in Immunology

MINI REVIEW
published: 01 November 2019
doi: 10.3389/fimmu.2019.02583

PI3-Kinase δγ Catalytic Isoforms Regulate the Th-17 Response in Tuberculosis

*Gina R. Leisching**

SA MRC Centre for TB Research, DST-NRF Centre of Excellence for Biomedical Tuberculosis Research, Division of Molecular Biology and Human Genetics, Faculty of Medicine and Health Sciences, Stellenbosch University, Cape Town, South Africa

Although IL17A plays a protective role at the mucosal surface, when IL17A signaling becomes dysregulated, a pathological response is locally induced. At the early stages of *Mycobacterium tuberculosis* (*M.tb*) infection, IL17A contributes to granuloma formation and pathogen containment. In contrast, during disease progression, a dysregulated IL17A hyperinflammatory response drives tissue destruction through enhanced neutrophil recruitment. Cumulative research has implicated the PI3-Kinase pathways as one of the most relevant in the pathophysiology of inflammation. Evidence shows that IL-17A secretion and the expansion of the Th17 population is dependant in PI3-Kinase signaling, with the p110δ and p110γ isoforms playing a prominent role. The p110γ isoform promotes disease progression through dampening of the Th17 response, preventing pathogen clearance and containment. The p110γ gene, *PIK3CG* is downregulated in TB patients during late-stage disease when compared to healthy controls, demonstrating an important modulatory role for this isoform during TB. Conversely, the p110δ isoform induces IL-17A release from pulmonary γδ T-cells, committed Th17 cells and promotes neutrophil recruitment to the lung. Inhibiting this isoform not only suppresses IL-17A secretion from Th17 cells, but it also inhibits cytokine production from multiple T-helper cell types. Since increased IL-17A levels are observed to be localized in the lung compartments (BAL and lymphocytes) in comparison to circulating levels, an inhalable PI3Kδ inhibitor, which is currently utilized for inflammatory airway diseases characterized by IL-17A over-secretion, may be a therapeutic option for active TB disease.

Keywords: tuberculosis, IL-17A, PI3-Kinase, Th17, neutrophils, airway inflammation

OPEN ACCESS

Edited by:
Alexander S. Apt, Central Tuberculosis Research Institute (RAMS), Russia

Reviewed by:
Christoph Hölscher, Research Center Borstel (LG), Germany
Javier Rangel-Moreno, University of Rochester, United States

***Correspondence:**
Gina R. Leisching
gina.leisching@gmail.com

Specialty section:
This article was submitted to T Cell Biology, a section of the journal Frontiers in Immunology

Received: *19 June 2019*
Accepted: *18 October 2019*
Published: *01 November 2019*

Citation:
Leisching GR (2019) PI3-Kinase δγ Catalytic Isoforms Regulate the Th-17 Response in Tuberculosis. Front. Immunol. 10:2583. doi: 10.3389/fimmu.2019.02583

INTRODUCTION

IL-17A is mostly active at mucosal sites and plays a primarily protective role at the lung surface through bridging the gap between the innate and adaptive immune responses (1, 2). Dysregulated signaling upstream or downstream may therefore greatly affect feedback loops during an inflammatory or infectious episode. Its potential of IL-17A to mediate a pathological immune response is especially observed at the intestinal, skin, and lung mucosa. Diseases such as colitis, inflammatory bowel disease (IBD), dermatitis, psoriasis, asthma, and chronic obstructive

pulmonary disease (COPD) caused by chronic inflammation are rooted by dysregulated IL-17A signaling (3–7). Its role in potentiating chronic inflammatory diseases is so significant, that targeting of the IL-17A pathway is a major focus of anti-inflammatory drug development (8).

The immunopathological potential of IL-17A during autoimmune and infectious episodes suggests that IL-17A may have a detrimental effect in chronic bacterial infections such as tuberculosis (TB), particularly during late stages of disease (9). In resistant hosts, IL-17A contributes to the formation of a mature granuloma (10, 11) which constrains the multiplication of *Mycobacterium tuberculosis* (*M.tb*) clinical isolates and plays a protective role (12).This is particularly observed during infection with hypervirulent *M.tb* strains. A recent paper by Erdmann and colleagues describes the ability of IL-17A to contribute to the expansion of IFN-γ-, IL-2- and TNF-secreting multifunctional T cells in IL-27Rα$^{-/-}$ mice, and that the level of IL-17A induction is essential for the accumulation of these cells during infection (13, 14). It was also observed that IL-17A, but not IFN-γ, is critical for mucosal vaccine–induced immunity against *M.tb* (14). On the other hand, Th17 cells have been implicated in the pathology of TB through inducing exacerbated neutrophil recruitment which enhances inflammation and pleural tissue damage in during disease (3). Even though IL-17 production may be required for early granuloma formation, it's chronic or exacerbated secretion may also be detrimental as it promotes neutrophil accumulation which compromises the generation of a stable mononuclear granuloma. Granuloma turnover then becomes dysregulated which leads to liquefactive necrosis and pathological scarring (15–17). Cumulative evidence suggests that IL-17A-induced pathology is significant during late-stage disease rather than during early infection (3, 18, 19), however delineating IL-17A signaling during both stages could promote the development of specific immunotherapeutic interventions that target key molecules within this pathway, and in doing so, improve current treatment regimes.

It has been observed that in patients with active TB, not only do they have a lower proportion of circulating Th17 cells (20), but plasma levels of IL-17A are also lower when compared to healthy individuals or those with latent TB infection (LTBI) (21). IL-17A is found to be increased in bronchoalveolar lavage (BAL) fluid of TB patients (17) and in lymphocytes surrounding pulmonary granulomas (17). In mice studies, it was observed that IL-17RA (IL-17A receptor) is expressed in non-hematopoietic cells (endothelial and epithelial cells, as well as fibroblasts) in the lungs of *M.tb* infected mice (18, 22). Thus, during late-stage disease, IL-17A appears to play a predominant role within the lung microenvironment and through complex signaling cascades, not only promotes neutrophil influx into the pleural space, thereby promoting the damaging hyperinflammatory environment, but simultaneously drives tissue destruction through upregulating matrix metalloproteases (MMPs) (17).

The literature indicates that various PI3-K isoforms play a significant role in shaping the Th17 response, however signaling through the various isoforms is still unclear, as well as the role they play in IL-17A secretion in TB (4, 23, 24). It is established that IL-17A secretion and the expansion of the Th17 population is dependent on IL-23 (16), however downstream signaling is mediated by members of the PI3-Kinase family. Studies have shown that the PI3-Kinase pathway activates and is activated by IL-17A during a number of inflammatory diseases (25, 26), including TB (17, 27). It is noteworthy that transcriptomic studies have revealed that various members of the PI3-kinase family, such as *PIK3CD*, *PIK3IP1*, *PIK3C2B* are aberrantly expressed in patients with active TB compared to uninfected controls (28, 29). This review aims to clarify PI3-Kinase-mediated IL-17A signaling in the context of TB disease in various cell types and indicate how it mediates the Th17 response. In addition, the possibility of utilizing PI3K-isoform specific drugs which could hinder Th17 differentiation, and therefore IL-17A secretion during late-stage TB disease as a possible therapeutic option is explored.

PI3-KINASES REGULATE IL-17 SECRETION AND T-CELL EXPANSION

PI3-Kinases are fundamental intermediaries in immune cell signaling networks. They generate a phosphatidylinositol (3,4,5)-trisphosphate second messenger molecule which recruits protein kinases and other proteins to the plasma membrane, where they activate other downstream mediators that are important in cell differentiation, proliferation, migration, and survival. The class IA PI3Ks, namely PI3Kα, PI3Kβ, and PI3Kδ bind tyrosines phosphorylated by receptor-associated kinases, whereas PI3Kγ, the only class IB PI3K, is activated by G protein-coupled receptors (30). PI3Kδ and PI3Kγ are expressed predominantly in leukocytes and have been studied intensively in the context of immune-mediated diseases. Further, both isoforms are required in some cellular responses such as the generation of ROS by neutrophils and the degranulation of mast cells, which suggests that the contribution of each isoform is coordinated at different stages (31–33).

The role of these isoforms in the context of the Th17 response in TB has been better defined in the last few years where the immunomodulatory role early on in infection is observed. Briefly, the presence of inhaled mycobacteria in the lung activates local bronchial epithelial cells (34) and phagocytosis by alveolar macrophages mediated by various receptors marks the commencement of the innate immune response during the early stages of infection (35). Fine orchestration of the release of chemokines and cytokines from these cells quickly recruits circulating immune cells such as neutrophils and lung γδ T-cells to the site of infection which is then followed by effector T-cell populations (**Figure 1A**). Naïve CD4^{+} T-cells differentiate into Th17 cells after exposure to IL-1β and IL-23 (36), which in turn stimulate the secretion of IL-17A. TB-reactive T-cells residing in the lungs before *M.tb* exposure and those located systemically are recruited to the site of infection shortly after pulmonary *M.tb* exposure, which is where the control of the initial infection begins (37). Activation of PI3-kinase signaling is initiated downstream of the T-cell receptor after its engagement with an antigen. The increment in T-cell populations and the related cytokines is a hallmark of the majority of immunological diseases, including TB. The significance of PI3-kinases in regulating the

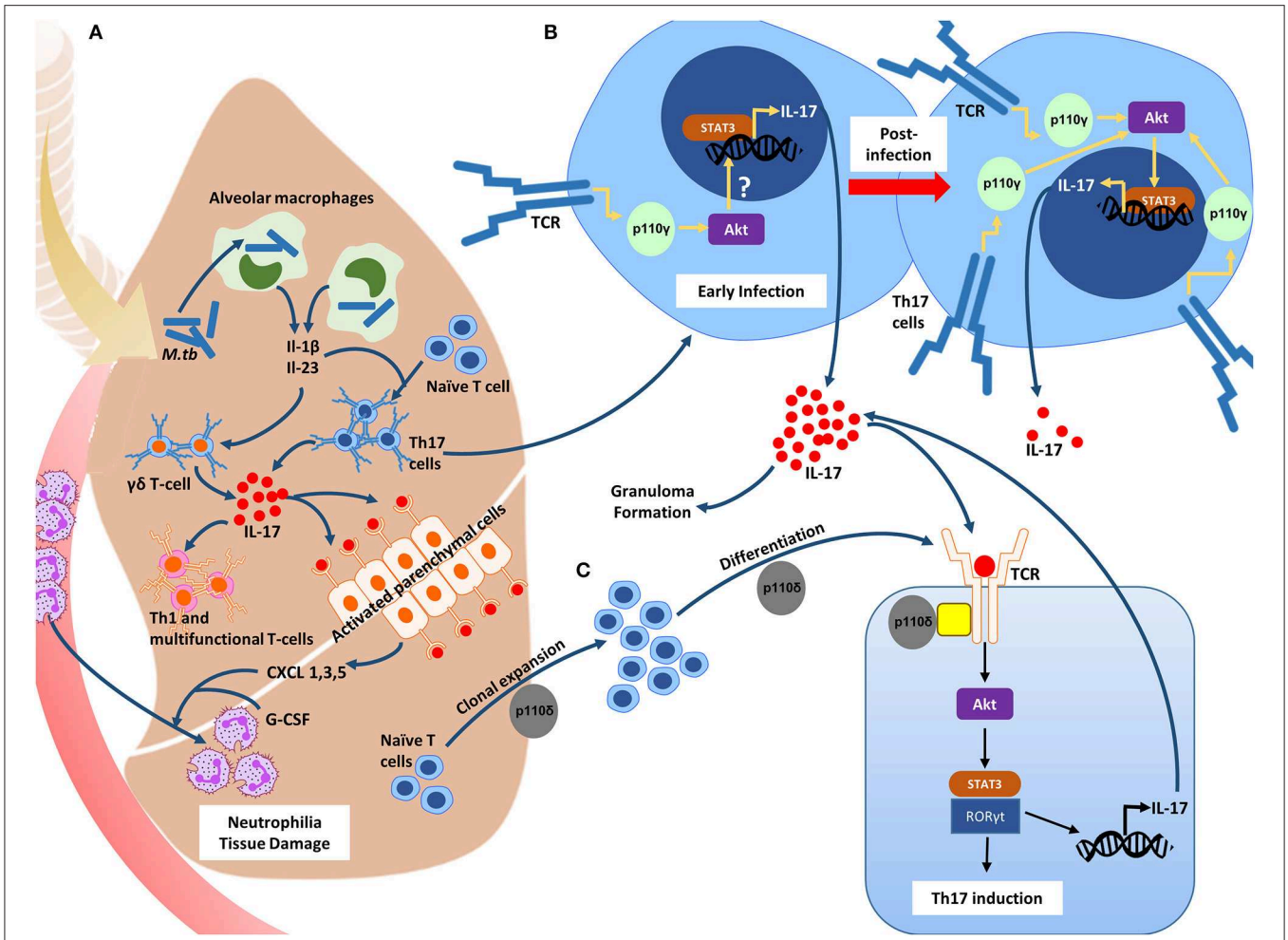

FIGURE 1 | The role of the PI3-K δγ catalytic isoforms in inducing the Th17 phenotype during *M.tb* infection. **(A)** Inhaled mycobacteria in the lung is phagocytosed by resident alveolar macrophages, inducing the release of IL-1β and Il-23. These cytokines, as well as others cause the recruitment of circulating immune cells such as neutrophils and lung γδ T-cells. IL-17A is then released from the γδ T-cells causing the activation of the parenchymal cells which through the release of both CXCL1, 3, and 5, and G-CSF, promote an influx of neutrophils. IL-17A levels are essential for the recruitment of Th1 and multifunctional T-cells. **(B)** The PI3-K p110γ isoform is downregulated in activated Th17 cells during the initial stages of infection, and through an unknown downstream mechanism, results in enhanced *IL17A* transcription, and subsequent IL-17A release. In resistant hosts, this results in granuloma formation and effective containment of the bacilli. PI3-K p110γ expression returns to homeostatic levels, leading to the suppression of *IL17A* transcription. In susceptible hosts, PI3-K p110γ expression remains downregulated, resulting in increased IL-17A secretion and pathology. **(C)** The PI3-K p110δ isoform is required for the clonal expansion and differentiation of Th17 cells +.

development, survival and differentiation of Th1, Th2, and Th17 cell subsets has been demonstrated.

PI3-K p110γ Inhibits IL-17A Secretion During TB

PI3Kγ, a class IB isoform belonging to the PI3-Kinase family plays a prominent role in shaping the Th17 response during early infection with *M.tb* (**Figure 1B**). Studies in gene-deficient mice suggest that the presence of the p110γ isoform may promote susceptibility to infection and subsequent development of TB disease through dampening of the Th17 response (38–40). It was observed that PI3Kγ$^{-/-}$ mice challenged intranasally with LPS had increased concentrations of IL-17A in their bronchoalveolar lavage fluid (39). Another group showed that spleen cell cultures stimulated with LPS revealed increased production of IL-17A by PI3Kγ- deficient T-cells (40). More recently, Cavalcanti-Neto et al. observed that mice deficient in this enzyme were resistant to *M.tb* infection and exhibited a robust Th17 response to which they attributed the improved resistance (38). In line with this, transcriptomics reveal that in patients with active TB, *PIK3CG* is downregulated compared to healthy controls (41), and those with latent TB (42) indicating a modulatory role for this isoform even during late stage disease. This data suggests that in resistant hosts, PI3Kγ may be downregulated initially in order to facilitate granuloma formation and resolution of the infection through IL-17A upregulation, and then regain homeostatic levels of expression after the resolution of the infection. In hosts which are susceptible to progress toward active disease, PI3Kγ may be downregulated from the initial point of infection throughout the progression and establishment of disease resulting in the over

secretion and therefore pathological potential of IL-17A. This dysregulated expression may be as a result of inherited genetic alterations in *PIK3CG* and/or dysregulation in the upstream or downstream signaling components which govern PI3Kγ activation. This requires further investigation. Nevertheless, lower levels of the p110γ isoform likely contributes to the over-secretion and therefore the immunopathology of the IL-17A response during TB, and raises the question of whether PI3Kγ classifies as a negative regulator of IL-17A during natural protective immunity toward *M.tb* infection.

PI3-K p110δ Is a Target of *M.tb* and Shapes the Th17 Response During TB

Pharmacological studies together with genetic evidence have implicated dysfunctional PI3K signaling in airway inflammation, and studies exploring the potential therapeutic benefit of PI3Kδ (class IA isoform) have yielded encouraging results (43). PI3Kδ is an isoform of PI3Kγ and lies downstream of tyrosine kinase-associated receptors, T cell receptors (TCR), co-stimulatory, and cytokine receptors, depending on the cell type. The role of PI3Kδ in macrophages and T-cells during *M.tb* infection is discussed below.

Recent work has found that during macrophage infection, *M.tb* upregulates miRNAs that target mRNAs encoding PI3Kδ, mTORC-1, and MNK-1 (44). By disrupting the genes encoding PI3-K δ/AKT/mTORC1 and MNK regulatory pathways, matrix metalloproteinase (MMP) expression, specifically MMP-1, is upregulated. In doing so, *M.tb* alters the normal protective response of the macrophage toward a tissue destructive phenotype through MMP expression. In the same study the authors observed that the expression of PI3Kδ is globally absent throughout TB granulomas, but present in normal lung tissue from healthy individuals (44). Knock-out studies found that p110γ/$\delta^{-/-}$ mice had increased IL-17A serum concentrations and frequencies of IL-17A+ splenic T-cells and that a deficiency in either the γ or δ isoform disrupts the IL-17A/G-CSF axis which results in neutrophilia (27). Evidence suggests that this decrease or loss in function of PI3Kδ enhances IL-17A and IL-17A-producing T-cells. In contrast, inhibition of PI3Kδ suppresses IL-17A expression through the regulation of NF-kB activity in a murine model of asthma (45) and in imiquimod-induced psoriasis-like dermatitis (6). Recently, a disease related to a gain of function mutation in PI3Kδ was described (46). In activated PI3Kδ syndrome (APDS), over expression of PI3Kδ in these individuals predisposes them to respiratory infections and airway damage. Thus, both a gain or loss in function of PI3Kδ significantly affects the Th17 response during an infectious or inflammatory episode and plays an important role in immunopathology of various disease states.

The signaling pathways responsible for T-cell differentiation are numerous, however the importance of the PI3-Kinase pathway in orchestrating differentiation of these cells has been noted previously (25, 26, 47–50). PI3Kδ specifically is of interest since its preferentially expressed in leukocytes and is essential for $CD4^+$ T-cell clonal expansion and differentiation (51). Naïve cells differentiate into Th17 cells following stimulation of their T-cell receptor (TCR) by antigen exposure or to IL-1β and IL-23 stimulation (36). Upon stimulation, the TCR causes PI3-K δ activation through TCR costimulatory and adaptor proteins (51, 52) which then generates phosphatidylinositol-3,4,5-trisphosphate (PIP3) by phosphorylating phosphatidylinositol-4,5-bisphosphate at the plasma membrane. PIP3 then recruits AKT to the plasma membrane inducing its phosphorylation where it initiates various cellular functions. Recently it was observed that PI3Kδ induces IL-17A secretion from committed Th17 cells (**Figure 1C**), and that inhibiting this isoform not only suppresses IL-17A secretion from Th17 cells, but also inhibits cytokine production from multiple T-helper cell types (48). The same study confirmed that PI3Kδ mediated IL-17A release from pulmonary γδ T-cells, and thus appears to be a key molecule in the IL-17A signaling cascade. Inhibition of PI3-K δ *in vivo* also resulted in a decrease in neutrophil recruitment to the lung and therefore in the BAL fluid of mice. No effect was observed in macrophages and other cells which demonstrates the link between PI3Kδ, IL-17A, and neutrophil trafficking (48).

As a consequence of dysregulated IL-17A signaling resulting from changes in the expression of PI3Kδ or PI3Kγ, exacerbated neutrophil influx into the pleural space is commonly observed during late stage TB (53). Further, aberrant expression of these genes and other PI3-K family members cause disruptions in neutrophil trafficking that lead to neutrophil hyperreactivity through directly compromising their migratory accuracy. This results in prolonged tissue transit time which leads to bystander tissue injury mediated by surface-associated neutrophil proteases and further secretion of IL-17A (54). Targeting of the p110δ isoform that control neutrophil influx and IL-17A may be a therapeutic option for patients with TB.

IS THE INHIBITION OF P110δ ISOFORM AN OPTION FOR THE TREATMENT OF TB?

The benefit of targeting PI3K isoforms has received considerable attention and is being viewed as a viable therapeutic option in inflammatory and infectious lung disorders. The comprehensive role of PI3Kδ and PI3Kγ in the ordinance of immunological mechanisms has presented them as potential targets for the treatment of immunological diseases such as autoimmune and allergic diseases (55, 56). Examples of this include PI3Kδ inhibitors to suppress the progression of inflammation and reduce the severity of rheumatoid arthritis and systemic lupus erythematosus in murine models (57). The selective PI3Kγ inhibitor AS605240 was shown *in vitro* and *in vivo* to reverse autoimmune diabetes in non-obese diabetic mice and inhibit T-cell cytokine release (58). In the context of TB, Th1 along with Th17 are the main effector populations which mediate both protection and pathology during the early and late stages of disease progression (9, 59). Thorough investigation of the functions of PI3Kδ and PI3Kγ in tuberculosis and other disease models, as well as in patient tissues, will be crucial to validate them as targets for the treatment of a range of inflammatory diseases. As mentioned previously, dysregulated IL-17A secretion

is also observed to be increased in the airways of COPD patients and severe asthmatics which coordinate neutrophilic inflammation in these diseases. Although neutrophilia is an overwhelming feature of these diseases, targeting of these cells may not be effective. It was observed that therapies directed at neutrophil-derived products have limited efficacy and are only effective exceptional circumstances (60, 61). The p110δ isoform has been implicated in airway inflammation, with selective targeting of this isoform yielding promising results in COPD and asthma by broadly reducing lymphocyte-derived cytokines such as IL-17A, and suppressing ROS release from neutrophils (43, 62, 63). Specifically, p110δ inhibition demonstrates that T lymphocyte-derived cytokine generation can be suppressed with multiple T-cell lineages targeted (48), as well as Th17 differentiation (48). Recently, a clinical study on APDS patients was conducted using the oral PI3Kδ selective inhibitor Leniolisib which aimed to "normalize" the augmented PI3Kδ activity rather than to completely inhibit it. This resulted in some clinical benefit in a short-term study, without significant toxicity to the patient (64).

In TB patients it is imperative that IL-17A secretion is not completely abolished as this cytokine is required for a certain level of *M.tb* control and granuloma turn over. Further, an inhalable form of this inhibitor, for use in asthma patients may be a viable option. The above evidence suggests that targeting of this isoform may yield positive results. It is more likely that by dampening the Th17 response, which includes neutrophil influx, tissue damage will be reduced. In this way, long-term pulmonary damage from fibrotic scar tissue development may be subverted, however the resulting effect on *M.tb* survival is unclear and requires further investigation. Although IL-17A does exhibit protective effects, particularly against hypervirulent *M.tb* strains, the option of enhancing IL-17, particularly during late-stage TB disease may potentiate and exacerbate auto-immune responses and chronic inflammation. Further investigation into the Th17 response during late-stage TB is required to increase our understanding on the dynamic changes in IL17 signaling during this complex disease.

OUTSTANDING QUESTIONS AND CHALLENGES

An important step would begin with investigations in the lung and pulmonary compartment of TB patients as this will reveal unique characteristics of this niche which are distinct from what is observed in the blood. For example there is evidence supporting the fact that Th17-like cells and Th17- related cytokines are remarkably different from those observed from the blood in TB patients (64). Thus, better characterization of the Th17 cellular response in TB pulmonary compartments is needed. Since Th17 cells and their related cytokines are increased in pulmonary tissue and BAL during late-stage disease (17), an inhalable p110δ isoform inhibitor is a therapeutic treatment option as an adjunct to standard antibiotics. To date, the use of p110δ isoform inhibitors as an adjunct to standard therapy have not been proposed for the treatment of TB, thus many unanswered questions remain as to whether this is a viable option. Inflammatory airway diseases with an inflammatory cytokine profile similar to that of TB, which is driven specifically by IL-17A oversecretion, appear to be resolved with the use of a p110δ inhibitor such as Leniolisib. Extended studies are required to evaluate outcomes such as respiratory infection and inflammation, and to establish the safety of long-term treatment of the drug. Evidence suggests that PI3Kδ and PI3Kγ synchronize in distinct, yet interdependent signaling pathways in many immune cells. Their fine-tuned integration gives rise to pro-inflammatory events in the multistep pathogenic process of inflammation. To date, it is unknown how the expression of these isoforms are regulated in response to one another, as well as other isoforms, particularly during TB. A key question that remains is whether both PI3Kδ and PI3Kγ are valid targets for the treatment of chronic inflammatory diseases such as tuberculosis or whether one would be more suitable than the other. Further, the presence of *M.tb* in the lungs of TB patients receiving the proposed treatment raises further questions: (1) will a reduction in IL-17A levels provide a niche more suitable for *M.tb* replication, or (2) will it reduce neutrophil recruitment to the lung compartment, thereby promoting the generation of a stable mononuclear granuloma?

AUTHOR CONTRIBUTIONS

The author confirms being the sole contributor of this work and has approved it for publication.

FUNDING

This work was funded by the South African Medical Research Council and the National Research Foundation of South Africa.

REFERENCES

1. Happel KI, Dubin PJ, Zheng M, Ghilardi N, Lockhart C, Quinton LJ, et al. Divergent roles of IL-23 and IL-12 in host defense against Klebsiella pneumoniae. *J Exp Med*. (2005) 202:761–9. doi: 10.1084/jem.20050193
2. Ye P, Garvey PB, Zhang P, Nelson S, Bagby G, Summer WR, et al. Interleukin-17 and lung host defense against Klebsiella pneumoniae infection. *Am J Respir Cell Mol Biol*. (2001) 25:335–40. doi: 10.1165/ajrcmb.25.3.4424
3. Fogli LK, Sundrud MS, Goel S, Bajwa S, Jensen K, Derudder E, et al. T cell–derived IL-17 mediates epithelial changes in the airway and drives pulmonary neutrophilia. *J Immunol*. (2013) 2013:1301360. doi: 10.4049/jimmunol.1390058
4. Song X, Qian Y. IL-17 family cytokines mediated signaling in the pathogenesis of inflammatory diseases. *Cell Signal*. (2013) 25:2335–47. doi: 10.1016/j.cellsig.2013.07.021
5. Chen F, Cao A, Yao S, Evans-Marin HL, Liu H, Wu W, et al. mTOR mediates IL-23 induction of neutrophil IL-17 and IL-22 production. *J Immunol*. (2016) 196:4390–9. doi: 10.4049/jimmunol.1501541
6. Roller A, Perino A, Dapavo P, Soro E, Okkenhaug K, Hirsch E, et al. Blockade of phosphatidylinositol 3-kinase (PI3K) δ or PI3Kγ reduces IL-17

and ameliorates imiquimod-induced psoriasis-like dermatitis. *J Immunol*. (2012) 189:4612–20. doi: 10.4049/jimmunol.1103173
7. McGeachy MJ, Cua DJ, Gaffen SL. The IL-17 family of cytokines in health and disease. *Immunity*. (2019) 50:892–906. doi: 10.1016/j.immuni.2019.03.021
8. Jones SA, Sutton CE, Cua D, Mills KH. Therapeutic potential of targeting IL-17. *Nat Immunol*. (2012) 13:1022–5. doi: 10.1038/ni.2450
9. Torrado E, Cooper AM. IL-17 and Th17 cells in tuberculosis. *Cytokine Growth Factor Rev*. (2010) 21:455–62. doi: 10.1016/j.cytogfr.2010.10.004
10. Yoshida YO, Umemura M, Yahagi A, O'Brien RL, Ikuta K, Kishihara K, et al. Essential role of IL-17A in the formation of a mycobacterial infection-induced granuloma in the lung. *J Immunol*. (2010) 184:4414–22. doi: 10.4049/jimmunol.0903332
11. Umemura M, Yahagi A, Hamada S, Begum MD, Watanabe H, Kawakami K, et al. IL-17-mediated regulation of innate and acquired immune response against pulmonary *Mycobacterium bovis* bacille Calmette-Guerin infection. *J Immunol*. (2007) 178:3786–96. doi: 10.4049/jimmunol.178.6.3786
12. Gopal R, Monin L, Slight S, Uche U, Blanchard E, Junecko BAF, et al. Unexpected role for IL-17 in protective immunity against hypervirulent *Mycobacterium tuberculosis* HN878 infection. *PLoS Pathog*. (2014) 10:e1004099. doi: 10.1371/journal.ppat.1004099
13. Erdmann H, Behrends J, Ritter K, Hölscher A, Volz J, Rosenkrands I, et al. The increased protection and pathology in *Mycobacterium tuberculosis*-infected IL-27R-alpha-deficient mice is supported by IL-17A and is associated with the IL-17A-induced expansion of multifunctional T cells. *Mucosal Immunol*. (2018) 11:1168–80. doi: 10.1038/s41385-018-0026-3
14. Gopal R, Rangel-Moreno J, Slight S, Lin Y, Nawar HF, Junecko BF, et al. Interleukin-17-dependent CXCL13 mediates mucosal vaccine–induced immunity against tuberculosis. *Mucosal Immunol*. (2013) 6:972. doi: 10.1038/mi.2012.135
15. Cruz A, Fraga AG, Fountain JJ, Rangel-Moreno J, Torrado E, Saraiva M, et al. Pathological role of interleukin 17 in mice subjected to repeated BCG vaccination after infection with *Mycobacterium tuberculosis*. *J Exp Med*. (2010) 207:1609–16. doi: 10.1084/jem.20100265
16. Khader SA, Cooper AM. IL-23 and IL-17 in tuberculosis. *Cytokine*. (2008) 41:79–83. doi: 10.1016/j.cyto.2007.11.022
17. Singh S, Maniakis-Grivas G, Singh UK, Asher RM, Mauri F, Elkington PT, et al. Interleukin-17 regulates matrix metalloproteinase activity in human pulmonary tuberculosis. *J Pathol*. (2018) 244:311–22. doi: 10.1002/path.5013
18. Lombard R, Doz E, Carreras F, Epardaud M, Le Vern Y, Buzoni-Gatel D, et al. IL-17RA in non-hematopoietic cells controls CXCL-1 and 5 critical to recruit neutrophils to the lung of mycobacteria-infected mice during the adaptive immune response. *PLoS ONE*. (2016) 11:e0149455. doi: 10.1371/journal.pone.0149455
19. Xu L, Cui G, Jia H, Zhu Y, Ding Y, Chen J, et al. Decreased IL-17 during treatment of sputum smear-positive pulmonary tuberculosis due to increased regulatory T cells and IL-10. *J Transl Med*. (2016) 14:179. doi: 10.1186/s12967-016-0909-6
20. Coulter F, Parrish A, Manning D, Kampmann B, Mendy J, Garand M, et al. IL-17 production from T helper 17, mucosal-associated invariant T, and γδ cells in tuberculosis infection and disease. *Front Immunol*. (2017) 8:1252. doi: 10.3389/fimmu.2017.01252
21. Li Q, Li J, Tian J, Zhu B, Zhang Y, Yang K, et al. IL-17 and IFN-γ production in peripheral blood following BCG vaccination and *Mycobacterium tuberculosis* infection in human. *Eur Rev Med Pharmacol Sci*. (2012) 16:2029–36.
22. Keller C, Hoffmann R, Lang R, Brandau S, Hermann C, Ehlers S. Genetically determined susceptibility to tuberculosis in mice causally involves accelerated and enhanced recruitment of granulocytes. *Infect Immun*. (2006) 74:4295–309. doi: 10.1128/IAI.00057-06
23. Song C, Hsu K, Yamen E, Yan W, Fock J, Witting PK, et al. Serum amyloid A induction of cytokines in monocytes/macrophages and lymphocytes. *Atherosclerosis*. (2009) 207:374–83. doi: 10.1016/j.atherosclerosis.2009.05.007
24. Huang F, Kao C-Y, Wachi S, Thai P, Ryu J, Wu R. Requirement for both JAK-mediated PI3K signaling and ACT1/TRAF6/TAK1-dependent NF-κB activation by IL-17A in enhancing cytokine expression in human airway epithelial cells. *J Immunol*. (2007) 179:6504–13. doi: 10.4049/jimmunol.179.10.6504
25. Handi J, Patterson SJ, Levings M. The role of the PI3K signaling pathway in CD4+ T cell differentiation and function. *Front Immunol*. (2012) 3:245. doi: 10.3389/fimmu.2012.00245
26. Kurebayashi Y, Nagai S, Ikejiri A, Ohtani M, Ichiyama K, Baba Y, et al. PI3K-Akt-mTORC1-S6K1/2 axis controls Th17 differentiation by regulating Gfi1 expression and nuclear translocation of RORγ. *Cell Rep*. (2012) 1:360–73. doi: 10.1016/j.celrep.2012.02.007
27. Bucher K, Schmitt F, Mothes B, Blumendeller C, Schäll D, Piekorz R, et al. Deficiency of PI3-Kinase catalytic isoforms p110γ and p110δ in mice enhances the IL-17/G-CSF axis and induces neutrophilia. *Cell Commun Signal*. (2017) 15:28. doi: 10.1186/s12964-017-0185-y
28. Leisching GR. Susceptibility to tuberculosis is associated with PI3K-dependent increased mobilization of neutrophils. *Front Immunol*. (2018) 9:1669. doi: 10.3389/fimmu.2018.01669
29. Maertzdorf J, Repsilber D, Parida SK, Stanley K, Roberts T, Black G, et al. Human gene expression profiles of susceptibility and resistance in tuberculosis. *Genes Immun*. (2011) 12:15. doi: 10.1038/gene.2010.51
30. Rommel C, Camps M, Ji H. PI3Kδ and PI3Kγ: partners in crime in inflammation in rheumatoid arthritis and beyond? *Nat Rev Immunol*. (2007) 7:191–201. doi: 10.1038/nri2036
31. Sasaki T, Irie-Sasaki J, Jones RG, Oliveira-dos-Santos AJ, Stanford WL, Bolon B, et al. Function of PI3Kγ in thymocyte development, T cell activation, and neutrophil migration. *Science*. (2000) 287:1040–6. doi: 10.1126/science.287.5455.1040
32. Ali K, Bilancio A, Thomas M, Pearce W, Gilfillan AM, Tkaczyk C, et al. Essential role for the p110δ phosphoinositide 3-kinase in the allergic response. *Nature*. (2004) 431:1007. doi: 10.1038/nature02991
33. Laffargue M, Calvez R, Finan P, Trifilieff A, Barbier M, Altruda F, et al. Phosphoinositide 3-kinase γ is an essential amplifier of mast cell function. *Immunity*. (2002) 16:441–51. doi: 10.1016/S1074-7613(02)00282-0
34. Sauty A, Dziejman M, Taha RA, Iarossi AS, Neote K, Garcia-Zepeda EA, et al. The T cell-specific CXC chemokines IP-10, Mig, and I-TAC are expressed by activated human bronchial epithelial cells. *J Immunol*. (1999) 162:3549–58.
35. Ernst JD. Macrophage receptors for *Mycobacterium tuberculosis*. *Infect Immun*. (1998) 66:1277–81.
36. McGeachy MJ, Cua DJ. Th17 cell differentiation: the long and winding road. *Immunity*. (2008) 28:445–53. doi: 10.1016/j.immuni.2008.03.001
37. Cooper AM. T cells in mycobacterial infection and disease. *Curr Opin Immunol*. (2009) 21:378–84. doi: 10.1016/j.coi.2009.06.004
38. Cavalcanti-Neto M, Prado R, Piñeros A, Sérgio C, Bertolini T, Gembre A, et al. Improvement of the resistance against early *Mycobacterium tuberculosis*-infection in the absence of PI3Kγ enzyme is associated with increase of CD4+ IL-17+ cells and neutrophils. *Tuberculosis*. (2018) 113:1–9. doi: 10.1016/j.tube.2018.08.009
39. Xu Y, Loison F, Luo HR. Neutrophil spontaneous death is mediated by down-regulation of autocrine signaling through GPCR, PI3Kγ, ROS, and actin. *Proc Natl Acad Sci USA*. (2010) 107:2950–5. doi: 10.1073/pnas.0912717107
40. Harris SJ, Ciuclan L, Finan PM, Wymann MP, Walker C, Westwick J, et al. Genetic ablation of PI3Kγ results in defective IL-17RA signaling in T lymphocytes and increased IL-17 levels. *Eur J Immunol*. (2012) 42:3394–404. doi: 10.1002/eji.201242463
41. Lesho E, Forestiero FJ, Hirata MH, Hirata RD, Cecon L, Melo FF, et al. Transcriptional responses of host peripheral blood cells to tuberculosis infection. *Tuberculosis*. (2011) 91:390–9. doi: 10.1016/j.tube.2011.07.002
42. Lee S-W, Wu LS-H, Huang G-M, Huang K-Y, Lee T-Y, Weng JT-Y. Gene expression profiling identifies candidate biomarkers for active and latent tuberculosis. *BMC Bioinformatics*. (2016) 17:S3. doi: 10.1186/s12859-015-0848-x
43. Stokes CA, Condliffe AM. Phosphoinositide 3-kinase δ (PI3Kδ) in respiratory disease. *Biochem Soc Transl*. (2018) 46:361–9. doi: 10.1042/BST20170467
44. Brace PT, Tezera LB, Bielecka MK, Mellows T, Garay D, Tian S, et al. Mycobacterium tuberculosis subverts negative regulatory pathways in human macrophages to drive immunopathology. *PLoS Pathog*. (2017) 13:e1006367. doi: 10.1371/journal.ppat.1006367
45. Park S-J, Lee KS, Kim SR, Min KH, Moon H, Lee MH, et al. Phosphoinositide 3-kinase δ inhibitor suppresses interleukin-17 expression in a murine asthma model. *Eur Respir J*. (2010) 36:1448–59. doi: 10.1183/09031936.00106609

46. Angulo I, Vadas O, Garçon F, Banham-Hall E, Plagnol V, Leahy TR, et al. Phosphoinositide 3-kinase δ gene mutation predisposes to respiratory infection and airway damage. *Science*. (2013) 342:866–71. doi: 10.1126/science.1243292
47. Nagai S, Kurebayashi Y, Koyasu S. Role of PI3K/Akt and mTOR complexes in Th17 cell differentiation. *Ann N Y Acad Sci*. (2013) 1280:30–4. doi: 10.1111/nyas.12059
48. Way EE, Trevejo-Nunez G, Kane LP, Steiner BH, Puri KD, Kolls JK, et al. Dose-dependent suppression of cytokine production from T cells by a novel phosphoinositide 3-kinase delta inhibitor. *Sci Rep*. (2016) 6:30384. doi: 10.1038/srep30384
49. Chen X, Guo Y, Han R, Liu H, Ding Y, Shi Y, et al. Class I PI3K inhibitor ZSTK474 attenuates experimental autoimmune neuritis by decreasing the frequency of Th1/Th17 cells and reducing the production of proinflammatory cytokines. *Cell Immunol*. (2018) 329:41–9. doi: 10.1016/j.cellimm.2018.04.011
50. Yin N, Wang Y, Lu X, Liu R, Zhang L, Zhao W, et al. hPMSC transplantation restoring ovarian function in premature ovarian failure mice is associated with change of Th17/Tc17 and Th17/Treg cell ratios through the PI3K/Akt signal pathway. *Stem Cell Res Ther*. (2018) 9:37. doi: 10.1186/s13287-018-0772-x
51. Okkenhaug K, Vanhaesebroeck B. PI3K in lymphocyte development, differentiation and activation. *Nat Rev Immunol*. (2003) 3:317. doi: 10.1038/nri1056
52. Okkenhaug K, Patton DT, Bilancio A, Garçon F, Rowan WC, Vanhaesebroeck B. The p110δ isoform of phosphoinositide 3-kinase controls clonal expansion and differentiation of Th cells. *J Immunol*. (2006) 177:5122–8. doi: 10.4049/jimmunol.177.8.5122
53. Philips JA. Neutrophils: double agents for TB. *Sci Transl Med*. (2017) 9:eaan6195. doi: 10.1126/scitranslmed.aan6195
54. Sapey E, Greenwood H, Walton G, Mann E, Love A, Aaronson N, et al. Phosphoinositide 3-kinase inhibition restores neutrophil accuracy in the elderly: toward targeted treatments for immunosenescence. *Blood*. (2014) 123:239–48. doi: 10.1182/blood-2013-08-519520
55. Randis TM, Puri KD, Zhou H, Diacovo TG. Role of PI3Kδ and PI3Kγ in inflammatory arthritis and tissue localization of neutrophils. *Eur J Immunol*. (2008) 38:1215–24. doi: 10.1002/eji.200838266
56. Maxwell MJ, Tsantikos E, Kong AM, Vanhaesebroeck B, Tarlinton DM, Hibbs ML. Attenuation of phosphoinositide 3-kinase δ signaling restrains autoimmune disease. *J Autoimmun*. (2012) 38:381–91. doi: 10.1016/j.jaut.2012.04.001
57. Haselmayer P, Camps M, Muzerelle M, El Bawab S, Waltzinger C, Bruns L, et al. Characterization of novel PI3Kδ inhibitors as potential therapeutics for SLE and lupus nephritis in pre-clinical studies. *Front Immunol*. (2014) 5:233. doi: 10.3389/fimmu.2014.00233
58. Azzi J, Moore RF, Elyaman W, Mounayar M, El Haddad N, Yang S, et al. The novel therapeutic effect of phosphoinositide 3-kinase-γ inhibitor AS605240 in autoimmune diabetes. *Diabetes*. (2012) 61:1509–18. doi: 10.2337/db11-0134
59. Freches D, Korf H, Denis O, Havaux X, Huygen K, Romano M. Mice genetically inactivated in interleukin-17 A receptor are defective in long-term control of *Mycobacterium tuberculosis* infection. *Immunology*. (2013) 140:220–31. doi: 10.1111/imm.12130
60. Nordenmark LH, Taylor R, Jorup C. Feasibility of computed tomography in a multicenter COPD trial: a study of the effect of AZD9668 on structural airway changes. *Adv Ther*. (2015) 32:548–66. doi: 10.1007/s12325-015-0215-3
61. Stockley R, De Soyza A, Gunawardena K, Perrett J, Forsman-Semb K, Entwistle N, et al. Phase II study of a neutrophil elastase inhibitor (AZD9668) in patients with bronchiectasis. *Respir Med*. (2013) 107:524–33. doi: 10.1016/j.rmed.2012.12.009
62. Southworth T, Plumb J, Gupta V, Pearson J, Ramis I, Lehner MD, et al. Anti-inflammatory potential of PI3Kδ and JAK inhibitors in asthma patients. *Respir Res*. (2016) 17:124. doi: 10.1186/s12931-016-0436-2
63. Khan A, Southworth T, Worsley S, Sriskantharajah S, Amour A, Hessel EM, et al. An investigation of the anti-inflammatory effects and a potential biomarker of PI3Kδ inhibition in COPD T cells. *Clin Exp Pharmacol Physiol*. (2017) 44:932–40. doi: 10.1111/1440-1681.12784
64. Rao VK, Webster S, Dalm VA, Šedivá A, van Hagen PM, Holland S, et al. Effective "activated PI3Kδ syndrome"–targeted therapy with the PI3Kδ inhibitor leniolisib. *Blood*. (2017) 130:2307–16. doi: 10.1182/blood-2017-08-801191

Conflict of Interest: The author declares that the research was conducted in the absence of any commercial or financial relationships that could be construed as a potential conflict of interest.

frontiers in Cellular and Infection Microbiology

ORIGINAL RESEARCH
published: 26 November 2019
doi: 10.3389/fcimb.2019.00405

MTS1338, A Small *Mycobacterium tuberculosis* RNA, Regulates Transcriptional Shifts Consistent With Bacterial Adaptation for Entering Into Dormancy and Survival Within Host Macrophages

Elena G. Salina[1†], Artem Grigorov[2†], Yulia Skvortsova[2], Konstantin Majorov[3], Oksana Bychenko[2], Albina Ostrik[1], Nadezhda Logunova[3], Dmitriy Ignatov[2‡], Arseny Kaprelyants[1], Alexander Apt[3] and Tatyana Azhikina[2]*

[1] Laboratory of Biochemistry of Stresses in Microorganisms, Bach Institute of Biochemistry, Research Center of Biotechnology, Moscow, Russia, [2] Laboratory of Regulatory Transcriptomics, Department of Genomics and Postgenomic Technologies, Shemyakin and Ovchinnikov Institute of Bioorganic Chemistry, Moscow, Russia, [3] Laboratory for Immunogenetics, Department of Immunology, Central Institute for Tuberculosis, Moscow, Russia

Small non-coding RNAs play a significant role in bacterial adaptation to changing environmental conditions. We investigated the dynamics of expression of MTS1338, a small non-coding RNA of *Mycobacterium tuberculosis*, in the mouse model *in vivo*, regulation of its expression in the infected macrophages, and the consequences of its overexpression in bacterial cultures. Here we demonstrate that MTS1338 significantly contributes to host-pathogen interactions. Activation of the host immune system triggered NO-inducible up-regulation of MTS1338 in macrophage-engulfed mycobacteria. Constitutive overexpression of MTS1338 in cultured mycobacteria improved their survival *in vitro* under low pH conditions. MTS1338 up-regulation launched a spectrum of shifts in the transcriptome profile similar to those reported for *M. tuberculosis* adaptation to hostile intra-macrophage environment. Using the RNA-seq approach, we demonstrate that gene expression changes accompanying MTS1338 overexpression indicate reduction in translational activity and bacterial growth. These changes indicate mycobacteria entering the dormant state. Taken together, our results suggest a direct involvement of this sRNA in the interplay between mycobacteria and the host immune system during infectious process.

Keywords: ***Mycobacterium tuberculosis*, tuberculosis, small RNA MTS1338, RNA-seq, infection**

OPEN ACCESS

Edited by:
Anthony Baughn, University of Minnesota Twin Cities, United States

Reviewed by:
Subramanian Dhandayuthapani, Texas Tech University Health Sciences Center, United States
Evgeniya V. Nazarova, Genentech, United States

***Correspondence:**
Tatyana Azhikina
tatazhik@ibch.ru

[†] These authors have contributed equally to this work

[‡] Present address:
Dmitriy Ignatov, Max Planck Unit for the Science of Pathogens, Berlin, Germany

Specialty section:
This article was submitted to Molecular Bacterial Pathogenesis, a section of the journal Frontiers in Cellular and Infection Microbiology

Received: *03 October 2019*
Accepted: *12 November 2019*
Published: *26 November 2019*

Citation:
Salina EG, Grigorov A, Skvortsova Y, Majorov K, Bychenko O, Ostrik A, Logunova N, Ignatov D, Kaprelyants A, Apt A and Azhikina T (2019) MTS1338, A Small Mycobacterium tuberculosis RNA, Regulates Transcriptional Shifts Consistent With Bacterial Adaptation for Entering Into Dormancy and Survival Within Host Macrophages. Front. Cell. Infect. Microbiol. 9:405. doi: 10.3389/fcimb.2019.00405

INTRODUCTION

M. tuberculosis persistence in the infected host involves several stages and may have different manifestations: initial infection followed by semi-acute or chronic diseases; latent infection characterized by the presence of viable bacteria with slow-to-no level of replication and the lack of clinical manifestations; and transition from the latent state to reactivation processes

(Stewart et al., 2003; Russell, 2007). The spectrum of the disease manifestations depends upon a dynamic balance between protective host responses and defensive strategies of *M. tuberculosis*. Identification of molecular mechanisms of *M. tuberculosis* adaptation to the host immune defense during its persistence within macrophages is an important scientific and medical problem.

Long co-evolution of *M. tuberculosis* and its human host allowed the pathogen to develop strategies that can effectively combat host defense systems. Regulatory proteins, non-coding RNAs and their targets constitute complex adaptive metabolic networks that allow the pathogen to resist host response at different stages of infection. Bacterial sRNAs participate in regulation of transcription and translation by affecting the level of gene expression and mRNA stability. Mostly, sRNAs are expressed in response to the external factors, helping bacteria to adaptively react to the changing environmental conditions and regulate the key stages of pathogenesis (Holmqvist and Wagner, 2017; Dutta and Srivastava, 2018; Hör et al., 2018).

Application of the high throughput sequencing and computer algorithm approaches allowed identification of dozens of sRNAs in mycobacterial species (Haning et al., 2014; Schwenk and Arnvig, 2018; Taneja and Dutta, 2019). Several *in vitro* studies have elucidated the functioning of sRNAs in *M. tuberculosis* (Arnvig et al., 2011; Solans et al., 2014; Moores et al., 2017; Gerrick et al., 2018; Mai et al., 2019). However, dissecting the role of a particular sRNA in mycobacterial physiology appeared to be difficult, especially in *in vivo* settings.

One of such RNAs, MTS1338 (DosR-associated sRNA, ncRv11733), is highly expressed during the stationary phase of growth (Arnvig and Young, 2012), and the dormancy state (Ignatov et al., 2015). This sRNA is present only in genomes of highly pathogenic mycobacteria and is very conservative. *In vitro* experiments demonstrated that its transcription is controlled by the transcriptional regulator DosR and is activated under hypoxic and NO-induced stresses (Moores et al., 2017), suggesting that MTS1338 may play a role during the stable phase of infection, when host responses confront mycobacterial multiplication more or less successfully. Indeed, we and others demonstrated a striking increase in the MTS1338 transcription in animal models of chronic infection (Arnvig and Young, 2012; Ignatov et al., 2014). Thus, it seems likely that MTS1338 triggers adaptive biochemical cascades for intracellular persistence.

Here, we characterize the dynamic changes in the MTS1338 expression in mycobacteria obtained from the lungs of genetically susceptible and resistant TB-infected mice, and provide a direct evidence that the level of expression is regulated by the IFN-γ-dependent NO production. Using high-throughput technologies, we describe changes in the genome transcription profile that accompany an increased MTS1338 transcription. Overexpression of MTS1338 leads to transcriptional shifts consistent with decreased bacterial metabolism, cell division and adaptation to host immune responses experienced by mycobacteria residing within host macrophages. Taken together, our results demonstrate that the small non-coding MTS1338 RNA regulates molecular mechanisms providing *M. tuberculosis* inter-macrophage survival.

MATERIALS AND METHODS

Bacterial Strains, Media, and Growth Conditions

For *in vitro* experiments, *M. tuberculosis* H37Rv (WT), pMV (empty plasmid control) and OVER (MTS1338 overexpressing) *M. tuberculosis* strains were initially grown from frozen stocks for 10 days in Sauton medium. Medium content (per liter): 0.5 g KH_2PO_4, 1.4 g $MgSO_4 \times 7H_2O$, 4 g L-asparagine, 60 ml glycerol, 0.05 g ferric ammonium citrate, 2 g sodium citrate, 0.1 ml 1% $ZnSO_4$, pH 7.0 (adjusted with 1M NaOH). Supplements: ADC growth supplement (Connell, 1994), 0.05% Tween 80 and 50 μg/ml kanamycin (Sigma-Aldrich, USA). Growth conditions: 37°C with agitation (200 rpm). The starter cultures were inoculated into fresh medium (the same composition) and grown up to stationary phase for RNA-seq experiments and stress survival experiments.

For cloning procedures, *Escherichia coli* DH5α was grown in Luria Bertani (LB) broth and LB-agar. When required, antibiotics were added at the following concentrations: kanamycin (Sigma-Aldrich), 50 μg/ml (*M. tuberculosis*); ampicillin (Invitrogen, USA), 100 μg/ml (*E. coli*).

M. tuberculosis Over and pMV (Control) Strains Establishment

The MTS1338 gene-containing vector was constructed on the basis of the pMV261 (Stover et al., 1991) as described by Ignatov et al. (2015). The plasmid was transferred into mycobacteria by electroporation. MTS1338 overexpression was confirmed by quantitative PCR. The control strain was produced using an empty pMV261 vector.

Growth Inhibition *in vitro* by NO, H_2O_2, and Low pH

Bacterial cultures were grown up to the stationary phase, washed up with PBS and diluted to $OD_{600} = 0.2$ (10^7 CFU/ml) by (i) Sauton medium (pH 5.5) with ADC growth supplement and 0.05% Tween for low pH stress; (ii) by the culture supernatant to study inhibitory effects of NO (provided by the DETA/NO donor, 0.5 mM) and H_2O_2 (10 mM). Cell viability after 24 h and 48 h of stresses exposure were measured by incorporation of [^{3}H]-uracil label. Two microliters of 5,6,-[^{3}H]-uracil (2 μCi) were added to 1-ml culture samples and incubated at 37°C with agitation for 20 h. Two hundred microliters of culture were put in 3 ml 7% ice-cold CCl_3COOH, incubated at 0° C for 15 min and filtered through glass microfiber filters (Whatman, USA). Precipitated cells were washed with 3 ml 7% CCl_3COOH and 3 ml 96% ethanol. Filters were put in 10 ml of scintillation mixture; CPM were determined by LS analyser (Beckman Instruments Inc., USA).

RNA Extraction From Cultured Mycobacteria

Bacterial cultures were grown up to the stationary phase, rapidly cooled on ice, centrifuged, and total RNA was isolated by phenol-chloroform extraction after cell disruption by Bead Beater with 0.1 mm zirconia beads (BioSpec Products, USA) as previously described (Rustad et al., 2009). After isolation, RNA was treated

with Turbo DNase (Life Technologies, USA) to remove traces of genomic DNA, and purified with the RNeasy mini kit (Qiagen, Netherlands). Amounts and purity of RNA were determined spectrophotometrically; integrity of RNA was assessed in 1% agarose gel.

Libraries for RNA-Seq and RNA-Seq Data Analyses

RNA samples were depleted of 16S and 23S rRNA using RiboMinus™ Transcriptome Isolation Kit, bacteria (Invitrogen, USA). Sequencing libraries were generated using the resulting ribosomal transcript-depleted RNA and NEBNext Ultra II Directional RNA Library Prep Kit (NEB, USA) according to the manufacturers' protocol. Sequencing was performed using the Illumina NovaSeq as the single-ended 100 nt-long reads. Experiments were performed in triplicates.

After quality control evaluation and trimming of bad qualitative reads the reads were mapped on the reference *M. tuberculosis* genome (AL123456.3, http://www.ncbi.nlm.nih.gov/) by Bowtie2 (Langmead and Salzberg, 2012). The alignment was performed with the "-local" option, which allows leaving 5′ and 3′ ends uncharted. Calculation of the mapped reads for all genes was performed using functions of the featureCounts package (Liao et al., 2014) built into the author's script. Resulting statistics were visualized as transcription profiles using the Artemis genome browser (Carver et al., 2012).

Differentially expressed genes were identified by the software package DESeq2 (Love et al., 2014). The genes were considered to be differentially expressed, if the *p*-value was less than 0.05, the expected measure of false deviations (FDR) was not higher than 0.1, and the expression change module (FC, Fold change) was not less than 3. Further distribution of genes according functional categories was performed using the Mycobrowser database (https://mycobrowser.epfl.ch/).

Quantitative Reverse Transcription-PCR (qRT-PCR)

One microgram of total RNA was used for cDNA synthesis with random hexanucleotides and SuperScript III reverse transcriptase (Life Technologies, USA). Quantitative PCR was performed using qPCRmix-HS SYBR (Evrogen, Russia) and the Light Cycler 480 real-time PCR system (Roche, Switzerland); cycling conditions were as follows: 95°C for 20 s, 61°C for 20 s, 72°C for 30 s, repeat 40 times; primers are listed in **Supplementary Table 1**. In the end of amplification, a dissociation curve was plotted to confirm specificity of the product. All real-time experiments were repeated in triplicate. The results were normalized against the 16S rRNA gene. Calculations were performed according to (Ganger et al., 2017) for the relative expression ratio.

Infections of Peritoneal Macrophages and *in vivo*

Mycobacteria

For infection of mice and macrophage cultures, *M. tuberculosis* H37Rv (substrain Pasteur) from the collection of CIT were used. Mycobacteria were prepared to infect mice and macrophages as described previously (Lyadova et al., 2000). Briefly, to obtain log-phase bacteria for challenge, 50 μl from a thawed aliquot was added to 30 ml of Dubos broth (BD Bioscience, USA) supplemented with 0.5% Fatty Acid-Poor BSA (Calbiochem-Behring Corp., USA) and incubated for 2 weeks at 37°C. The resulting suspension was washed two times at 3,000 g, 20 min, 4°C with Ca^{2+}- and Mg^{2+}-free PBS containing 0,2 mM EDTA and 0,025% Tween 80. Cultures were filtered through a 5 μm-pore-size filter (Millipore, USA) to remove clumps. To estimate the CFU content in the filtrate, 20 μl from each 5-fold serial dilution was plated onto Dubos agar (BD), and the total number of micro-colonies in the spot was calculated under an inverted microscope (200^x magnification) after being cultured for 3 days at 37°C. The bulk of the filtered culture was stored at 4°C, and it was found that no change in the CFU content occurred during this storage period.

Mice

C57BL/6Ycit (B6) and I/StSnEgYCit strain (I/St) mice were kept under conventional, non-SPF conditions in the Animal Facilities of the Central Research Institute of Tuberculosis (CIT, Moscow, Russia) in accordance with the guidelines from the Russian Ministry of Health # 755, and under the NIH Office of Laboratory Animal Welfare (OLAW) Assurance #A5502-11. Female mice aged 2.5–3.0 months were used. All experimental procedures were approved by the Bioethics Committee of the Central Research Institute of Tuberculosis (IACUC), protocols # 2, 3, 7, 8, 11 approved on March 6, 2016.

Infection of Mice, RNA Extraction

To infect mice, mycobacteria were re-suspended in supplemented PBS. Mice were infected via respiratory tract with ∼100 viable CFU/mouse using an Inhalation Exposure System (Glas-Col, USA), as described in Radaeva et al. (2005, 2008). The size of challenging dose was confirmed in preliminary experiments by plating serial 2-fold dilutions of 2-ml homogenates of the whole lungs obtained from B6 and I/St females at 2 h post-exposure onto Dubos agar and counting colonies after 3-wk incubation at 37°C. To assess CFU counts, lungs from individual mice were homogenized in 2.0 ml of sterile saline, and 10-fold serial dilutions were plated on Dubos agar and incubated at 37°C for 20–22 days.

To extract total RNA, lungs of infected mice were homogenized in Trizol reagent (Life Technologies, USA), and RNA was isolated according to a standard protocol using BeadBeater with 0.1 mm zirconia beads (BioSpec Products, USA) (Rustad et al., 2009).

Infection of Peritoneal Macrophages, iNOS Activation, RNA Extraction

To obtain peritoneal macrophages, B6 mice were injected intraperitoneally with 3% peptone (Sigma-Aldrich) in saline. Five days later, peritoneal exudate cells (PEC) were eluted from the peritoneal cavities with Ca^{2+}- and Mg^{2+}-free PBS supplemented with 2% FCS and 10 U/ml heparin, washed twice with PBS, and resuspended in RPMI 1640 containing 5% FCS, 10 mM HEPES

and 2 mM L-glutamine. The content of nonspecific esterase-positive cells in PEC exceeded 85%. PEC were plated onto 90 mm Petri dishes (Costar, Corning Inc., USA) at 10×10^6 cells/dish in 10 ml of RPMI-1640 containing 5% FCS, 10 mM HEPES and 2 mM L-glutamine to obtain macrophage monolayers. The cells were allowed to adhere for 2 h at 37°C, 5% CO_2 before mycobacteria were added in 10 ml of supplemented RPMI-1640 at MOI = 20, 15, and 5 for 2-, 4- and 24-h incubation, respectively. Macrophage-free mycobacterial cultures served as controls.

To activate macrophages, monolayers were treated with murine rIFN-γ (100 U/ml, Sigma) for 14 h before adding mycobacteria. To block iNOS, 100 μM L-NIL (Sigma) was added 1 h before rIFN-γ administration.

To extract RNA, dishes with cell monolayers were gently shaken, culture medium was completely aspirated and macrophages were lysed with 5 ml/dish of Trizol (Invitrogen) as recommended by the manufacturer. Mycobacteria alone in control cultures were suspended by pipetting and centrifuged at 3,000 g, 20 min, 4°C. Pellets were suspended in 1 ml of Trizol. RNA was isolated by bacterial cell disruption and phenol-chloroform extraction as described in Rustad et al. (2009).

Statistics

Statistical analysis was performed using ANOVA test and *t*-test by GraphPad Prism6.0 software (GraphPad Software, San Diego, CA, USA). $P < 0.05$ was considered statistically significant.

RESULTS

MTS1338 Expression in TB-Infected Mice

Earlier it was demonstrated that several *M. tuberculosis* non-coding RNAs, including MTS1338, are highly transcribed *in vivo* (Arnvig et al., 2011; Ignatov et al., 2014). Here, we investigated the dynamical transcription profile of MTS1338 in mycobacteria persisting in the mouse lungs from initial to terminal phases of infection. Aerosol infection with low doses of WT strain leads to a chronic and temporary effectively controlled infection in genetically resistant B6 mice, whilst in susceptible I/St mice fatal pulmonary pathology develops relatively rapidly (Kondratieva et al., 2010). Differences in mycobacterial lung CFU counts between I/St and B6 mice reached about 1.2 logs during the first 2 months post challenge and remained stable until I/St mice succumbed to infection (**Figure 1A**). We isolated total RNA from the mouse lungs, and profiled the MTS1338 expression in the lung mycobacterial population by quantitative real-time PCR (**Figure 1B**). The highest level of expression was observed at week 10 post-challenge. In B6 mice, it remained high throughout the experiment, although slowly decreased at the very late phase of infection. At week 10 of infection, when I/St mice start to lose control of the disease progression, the level of MTS1338 expression in their lung mycobacterial population was significantly higher ($P < 0.01$) than that in more resistant B6 mice (**Figure 1B**). Overall, at the stage of flourishing infection, the MTS1338 expression level in the lung-residing bacteria was more

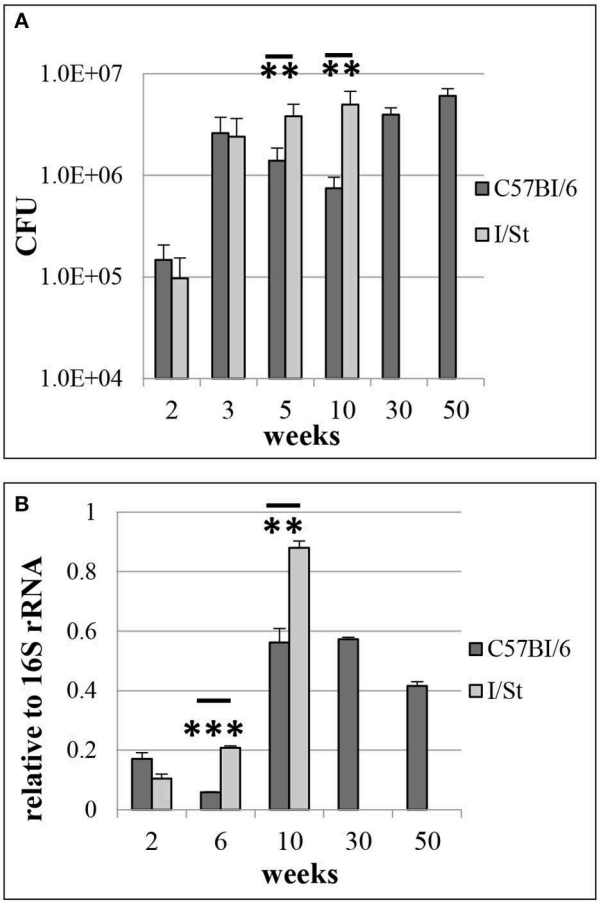

FIGURE 1 | *M. tuberculosis* WT infection in resistant B6 and susceptible I/St mice. **(A)** Lung CFU counts along the disease progression (**$P < 0.01$ at 5- and 10-weeks post challenge, ANOVA). **(B)** MTS1338 expression levels of at different time points (**$P < 0.01$ and ***$P < 0.001$, unpaired *t*-test). At indicated time points, samples of total RNA were analyzed by quantitative real-time PCR, and the MTS1338 expression levels were normalized to those of 16S rRNA (ΔCt data). The data are presented as the mean ± SD of three independent experiments.

then 1,000-fold higher compared to its expression level during stationary phase of growth *in vitro* (Ignatov et al., 2014).

The Expression of MTS1338 Is Regulated by iNOS

Our *in vivo* experiments demonstrated that the level of MTS1338 expression peaks at the stage of fully developed adaptive immune response against mycobacteria. At this stage, B6 mice display significantly higher levels of IFN-γ production compare to their I/St counterparts (Eruslanov et al., 2004; Radaeva et al., 2005; Logunova et al., 2015). Since IFN-γ is the key cytokine activating macrophages for intracellular mycobacterial killing (Cooper, 2009), we compared MTS1338 expression levels in peritoneal B6 macrophages, infected WT, either activated by the external IFN-γ, or not. The level of MTS1338 expression was assessed in dynamics at 2, 4, and 24

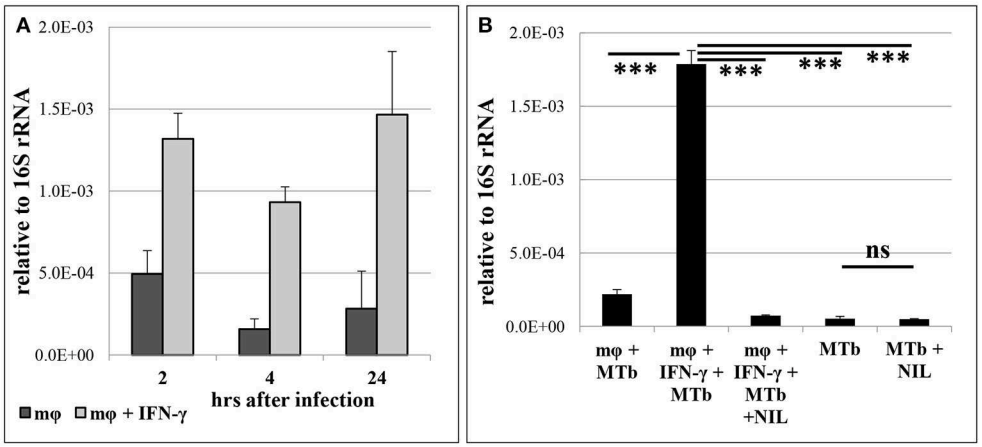

FIGURE 2 | MTS1338 transcription is NO-dependent and correlates with activation of infected macrophages. **(A)** The MTS1338 transcription dynamics in peritoneal macrophages of B6 mice infected by WT strain. **(B)** The level of MTS1338 transcription at 24 h post infection: control (mφ +MTb), IFN-γ-activated (mφ +MTb + INF-γ), IFN-γ-activated and L-NIL treated (mφ +MTb + INF-γ + NIL). The levels of MTS1338 transcription in pure WT cultures (MTb) and L-NIL-treated cultures (MTb + NIL) serve as controls for the assessment of possible L-NIL influence onto cultured mycobacteria. The data calculated as ΔCt are presented as the mean ± SD of three independent experiments; ***P <0.005, ns – not significant, unpaired t-test).

hours of macrophage infection (**Figure 2A**). In IFN-γ-activated macrophages, MTS1338 expression was significantly ($P < 0.001$, unpaired t-test) higher than in control macrophages at every time point, and the difference reached more than 10-fold at 24 hours post infection. Thus, pre-activation of macrophages with IFN-γ induced up-regulation of the MTS1338 expression in engulfed mycobacteria. Given that the efficacy of mycobacterial killing by peritoneal macrophages significantly increases in the presence of IFN-γ (Majorov et al., 2003), this result suggests that the level of MTS1338 expression correlates with the level of pressure emanating from macrophage antibacterial systems.

Since the active nitrogen oxidative derivatives serve as the major trigger of MTS1338 transcription activation *in vitro* (Moores et al., 2017), we decided to test whether this is true for the infected macrophage system. Nitrogen oxidative derivatives production in macrophages depends upon inducible NO-synthase (iNOS2), thus we compared mycobacteria-infected IFN-γ-activated and control macrophages cultured for 24 hours in the presence or absence of L-NIL [N6-(1-iminoethyl)-L-lysine hydrochloride]—a selective inhibitor of iNOS2. Inhibition of NO production in IFN-γ-activated macrophages completely abrogated elevation in the MTS1338 expression. L-NIL itself did not affect MTS1338 expression in pure WT cultures (**Figure 2B**). Thus, in macrophages, nitrogen oxidative derivatives are an important trigger of MTS1338 expression.

Survival Under *in vitro* Stresses

To check whether elevated transcription of MTS1338 protects *M. tuberculosis* against hostile stressful environment, we compared survival of the OVER and pMV strains in cultures subjected to different type of stresses: low pH or elevated levels of NO and H_2O_2. Inhibitory effects of external NO, H_2O_2 and pH = 5.5 on mycobacteria were estimated by the level of incorporation of [^{3}H]-uracil after 24 and 48 h of stress exposure (**Figure 3**). Uracil incorporation directly and strongly ($\rho > 99$) correlates with CFU counts in mycobacterial cultures (Hu et al., 2000; Majorov et al., 2003). In the absence of stress, the OVER strain grew slightly slower than the pMV one ($P < 0.01$ at the 48-h time point), which is consistent with earlier observations (Arnvig et al., 2011; Ignatov et al., 2015). Treatment of cultures with external NO or H_2O_2 had marginal to no effect on mycobacterial growth. However, overexpression of MTS1338 provided significant level of protection against acidic conditions: at pH = 5.5, uracil incorporation by the OVER strain was significantly higher both at 24 h ($P < 0.05$), and 48 h ($P < 0.01$) of culturing.

Transcriptome Changes Induced by the MTS1338 Overexpression Are Consistent With Mycobacterial Adaptation to Persistence

To assess how overexpression of MTS1338 influences mycobacterial adaptation, we compared transcriptomes of the OVER and pMV strains at the phase of stationary growth in liquid culture using RNA-seq approaches. The MTS1338 expression level in the OVER strain in these experiments was more than 10-fold higher compared to the pMV strain as confirmed by qRT-PCR (**Supplementary Figure 1A**).

Mapping the processed reads against the reference *M. tuberculosis* H37Rv genome (AL123456.3, http://www.ncbi.nlm.nih.gov/), provided the following numbers of mapped reads: 18940746 (96.91%), 19931958 (97.27%) and 20528207 (97.68%) for the OVER strains and 18671706 (97.04%), 16003598 (96.36%) and 15540058 (96.85%) for the pMV strain. The percentage of the protein-encoding part of the genome deduced from all mapped reads comprised 13.97% (2609191), 20.04% (3207752) and 15.52% (2411509) for pMV, and 10.9% (2065273), 15.39% (3067710), and 20.11% (4127293) for OVER (12.8×10^6 reads).

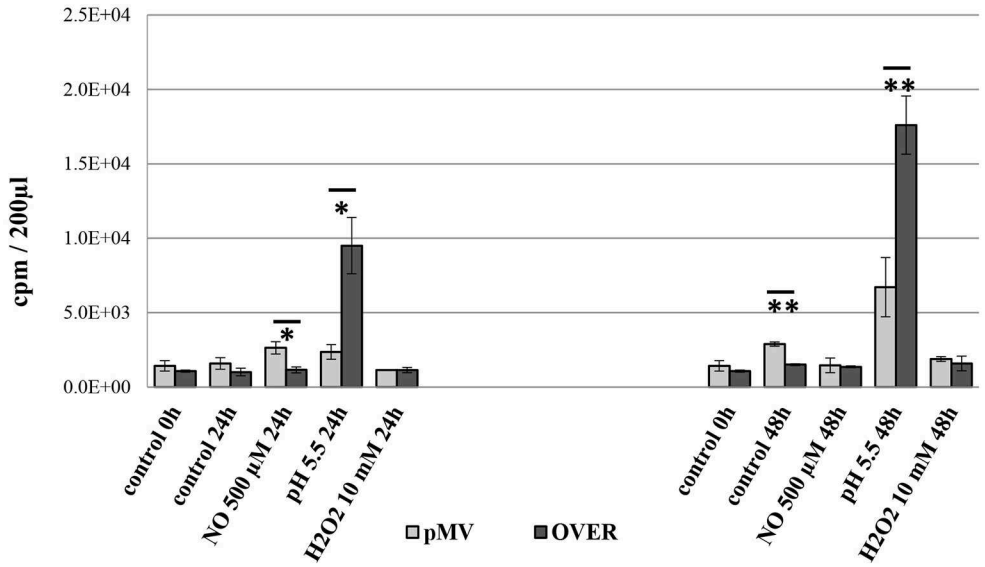

FIGURE 3 | Viability of the OVER and pMV *M. tuberculosis* strains under stressful conditions *in vitro*. Stationary phase mycobacteria were subjected to pH = 5.5 or elevated levels of NO and H_2O_2 in 24- and 48-h cultures. The effect of stresses was measured by [^{3}H]-uracil incorporation in three independent experiments and expresses as mean CPM ± SD. *$P < 0.05$, **$P < 0.01$, unpaired *t*-test). The data are presented as the mean ± SD of three independent experiments.

Using the software package DESeq2 (Love et al., 2014), we identified genes the expression of which differed between the two strains. Unexpectedly, only 28 genes were found to change their expression more then 1.5-fold under the MTS1338 overexpression conditions, with 15 genes demonstrating a decreased and 13 genes an increased expression. Further ascribing of genes to functional categories was performed using the Mycobrowser database. The list of differentially expressed genes (DEGs) is displayed in **Table 1**. Complete data on RNA-seq are displayed in **Supplementary Table 2**. Possible functional consequences of particular shifts in gene expression profiles are provided in the Discussion section. Differential expression of six randomly chosen genes was confirmed by the quantitative RT-PCR (**Supplementary Figure 1B**).

DISCUSSION

In mycobacteria, sRNAs have been discovered much later then in many other bacterial species (Haning et al., 2014), and their functions mostly remain unknown. However, recent high-throughput transcriptional profiling of cultured *M. tuberculosis* exposed to relevant stresses identified a pool of both known and novel mycobacterial sRNAs involved in response to stress conditions *in vitro* (Gerrick et al., 2018).

Here, we present functional characteristics of the sRNA MTS1338, one of highly expressed in *M. tuberculosis* during the stationary growth phase (Arnvig et al., 2011) and at dormancy (Ignatov et al., 2015), suggesting its role in the maintenance of *M. tuberculosis* survival under unfavorable conditions. Since these observations suggest that high levels of MTS1338 expression are required for its functional activity, we constructed the *M. tuberculosis* strain overexpressing MTS1338 for identification of its *in vitro* phenotype, as well as transcriptional changes triggered by this small RNA. Earlier it was demonstrated that MTS1338 expression is NO-inducible and is activated by transcriptional regulator DosR under hypoxic cultural conditions (Moores et al., 2017), as well as under starvation, oxidative and low pH stresses (Gerrick et al., 2018). Our experiments demonstrate that the strain constitutively overexpressing MTS1338 is more resistant to low pH than the control (pMV) strain (**Figure 3**).

Overexpression of MTS1338 dramatically changes the bacterial growth rate (Arnvig et al., 2011; Ignatov et al., 2015). Our experiments with *M. tuberculosis* dormancy and resuscitation *in vitro* demonstrated that MTS1338 participates in entering dormancy (Ignatov et al., 2015), but is not involved in the resuscitation process (Salina et al., 2019). *In vivo*, high levels of MTS1338 transcription were reported for *M. tuberculosis* residing in chronically infected mouse lungs (Arnvig et al., 2011; Ignatov et al., 2014). In the present work, using a mouse model of infection, we demonstrate that MTS1338 up-regulation strictly follows activation of iNOS in macrophages. Importantly, at the stage of advanced infection the level of expression was significantly higher in genetically TB-susceptible I/St mice compared to more resistant B6 animals. This may reflect an attempt of mycobacteria residing in the I/St lungs to rapidly turn down metabolism, facing severe functional failure in the surrounding tissue, providing aggressive, highly hypoxic and necrotic conditions to a large proportion of mycobacterial population (Kondratieva et al., 2010). We anticipated that an abundant expression of MTS1338 leads to shifts of the whole genome transcriptional profile toward preparation of mycobacteria to stress-induced metabolic slowdown, thereby helping survival in hostile intra-macrophage surrounding.

TABLE 1 | List of genes, differentially expressed in OVER strain vs. pMV strain.

Gene		Function (according to Mycobrowser)	Functional category	Essentiality *in vitro* (Sassetti et al., 2003; Griffin et al., 2011)	Fold Change
rv0079			Conserved hypotheticals		8.2
rv0080			Conserved hypotheticals		10
rv0081			Regulatory proteins		4.9
rv0082		Probable oxidoreductase	Intermediary metabolism and respiration		6.1
rv0083		Probable oxidoreductase	Intermediary metabolism and respiration		5.7
rv0084	*hycD*	Possible formate hydrogenlyase HycD	Intermediary metabolism and respiration		4
rv0085	*hycP*	Possible hydrogenase HycP	Intermediary metabolism and respiration	ES	6.2
rv0086	*hycQ*	Possible hydrogenase HycQ	Intermediary metabolism and respiration	ES	5.2
rv0087	*hycE*	Possible formate hydrogenase HycE	Intermediary metabolism and respiration		4.2
rv0440	*groEL2*	60 kDa chaperonin 2 GroEL2 (protein CPN60-2) (GroEL protein 2) (65 kDa antigen) (heat shock protein 65) (cell wall protein A) (antigen A)	Virulence, detoxification, adaptation	ES	0.2
rv0516c		Possible anti-anti-sigma factor	Information pathways		2.9
rv1158c		Conserved hypothetical ala-, pro-rich protein	Conserved hypotheticals		0.05
rv1469	*ctpD*	Probable cation transporter P-type ATPase D CtpD	Cell wall and cell processes		0.4
rv1620c	*cydC*	Probable component linked with the assembly of cytochrome transport transmembrane ATP-binding protein ABC transporter CydC	Intermediary metabolism and respiration	ES	7.4
rv1621c	*cydD*	Probable component linked with the assembly of cytochrome transport transmembrane ATP-binding protein ABC transporter CydD	Intermediary metabolism and respiration		5.7
rv1622c	*cydB*	Probable integral membrane cytochrome D ubiquinol oxidase (subunit II) CydB (cytochrome BD-I oxidase subunit II)	Intermediary metabolism and respiration	ES	5.7
rv1690	*lprJ*	Probable lipoprotein LprJ	Cell wall and cell processes		0.3
rv1772			Conserved hypotheticals		0.3
rv2033c			Conserved hypotheticals		0.2
rv2812		Probable transposase	Insertion seqs and phages		0,1
rv2947c	*pks15*	Probable polyketide synthase Pks15	Lipid metabolism		0.2
rv2986c	*hupB*	DNA-binding protein HU homolog HupB (histone-like protein) (HLP) (21-kDa laminin-2-binding protein)	Information pathways	ES	0.2
rv2987c	*leuD*	Probable 3-isopropylmalate dehydratase (small subunit) LeuD (isopropylmalate isomerase) (alpha-IPM isomerase) (IPMI)	Intermediary metabolism and respiration	ES	0.2
rv2988c	*leuC*	Probable 3-isopropylmalate dehydratase (large subunit) LeuC (isopropylmalate isomerase) (alpha-IPM isomerase) (IPMI)	Intermediary metabolism and respiration		0.3
rv3019c	*esxR*	Secreted ESAT-6 like protein EsxR (TB10.3) (ESAT-6 like protein 9)	Cell wall and cell processes		0.3
rv3136	*PPE51*	PPE family protein PPE51	Pe/ppe		0.1
rv3260c	*whiB2*	Probable transcriptional regulatory protein WhiB-like WhiB2	Regulatory proteins	ES	0.2
rv3767c		Possible S-adenosylmethionine-dependent methyltransferase	Lipid metabolism		0.3

Orange boxes stand for up-regulated DEGs; green, down-regulated DEGs.

However, RNA-seq transcriptome evaluation demonstrated that the number of DEGs in MTS1338-overexpressing and pMV strains is relatively small. MTS1338 overexpression resulted in elevated expression of three operons—*rv0079-rv0081*, *rv0082-rv0087,* and *rv1620c-rv1622c*. *rv0079-0081* genes belong to the DosR regulon which activates under hypoxic conditions (Voskuil et al., 2003). *rv0079* expression was shown to be regulated by *rv0081* (Chauhan et al., 2011). In *E. coli* and *M. bovis*, homologous protein significantly inhibits cell growth, apparently interacting with the 30S ribosome subunit and inhibiting translation—the phenotype typical for transition to dormancy (Kumar et al., 2012). *rv0080* encodes a conservative hypothetical protein with unknown functions. It contains a domain of pyridoxine 5′-phosphate (PNP) oxidase-like (PNPOx-like)

superfamily, which catalyze flavin mononucleotide-mediated redox reactions. *rv0081* is one of two key transcriptional factors mediating early response to hypoxia (Galagan et al., 2013). As an important "metabolic hub" working in concert with other transcription regulators, *rv0081* is associated with the processes of lipid metabolism, protein degradation, and cholesterol biosynthesis (Rodriguez et al., 2014; Aguilar-Ayala et al., 2017).

The genes of other two operons encode proteins of the functional category "Intermediary metabolism and respiration." *rv0082-rv0087* genes are also regulated by *rv0081* (He et al., 2011), but not included in the DosR regulon. The *rv0082–rv0087* locus in *M. tuberculosis* encodes a putative [NiFe]-hydrogenase complex (Berney et al., 2014). In *E. coli*, homologous proteins are involved in the conversion of formate to CO_2 and H_2 under conditions of anaerobic respiration in the absence of an external terminal electron acceptor (Leonhartsberger et al., 2002). Facultative H_2 metabolism is central for mycobacterial persistence. Mycobacteria enhance long-term survival by up-regulating hydrogenases during energy and oxygen limitations (Greening and Cook, 2014).

rv1620c-rv1622c (*cydC, D, B* respectively) encode proteins, which are involved in the cytochrome biogenesis and active transport across the membrane of components involved in the assembly of cytochrome. The expression of *CydDC* is linked to the incorporation of heme cofactors into a variety of periplasmic cytochromes, as well as the bd-type respiratory oxidases. CydB is the component of the aerobic respiratory chain that is supposedly predominant when cells are grown at low aeration, and is up-regulated under low pH (Baker et al., 2014). It has been reported that the presence of bd-type oxidases is correlated with bacterial virulence. For example, growth of mycobacteria at low oxygen tensions enhances both the expression of a bd-type oxidase and cell invasion (Bermudez et al., 1997).

Down-regulated genes belong to different functional categories. Among them, three genes with chaperone functions attract special attention. All these genes are essential for *M. tuberculosis* growth *in vitro* (Sassetti et al., 2003; Griffin et al., 2011). *rv0440* encodes GroEL2, the chaperone belonging to the HSP60 family. Its chaperone-like functions provide resistance to stress (Qamra et al., 2004) and modulate host immune responses (Lewthwaite et al., 2007; Naffin-Olivos et al., 2014). GroEL2 is highly induced in response to environmental cues during infection like heat shock, oxidative stress, growth in macrophages, and hypoxia (Qamra et al., 2005). The HupB protein encoded by *rv2986c* belongs to the histone-like family of prokaryotic DNA-binding proteins capable of wrapping DNA to stabilize it, and prevent DNA denaturation under extreme environmental conditions (Kumar et al., 2010). It is involved in controlling the transfer of mycolic acids to sugars by the Ag85 complex (Katsube et al., 2007), as well as siderophore biosynthesis, and is essential for mycobacteria growth in macrophages (Pandey et al., 2014).

WhiB2 encoded by *rv3260c* belongs to the WhiB family of transcriptional regulators. Its apo-form displays a chaperone activity, preventing aggregation and providing correct refolding of proteins; this activity does not require ATP and is independent of its own oxidized or reduced status and co-chaperones (Konar et al., 2012). The homolog of whiB2 in *M. smegmatis*, WhmD, participates in septa formation during cell division. WhmD overexpression decreases the linear size of *M. smegmatis* cells (Raghunand and Bishai, 2006). In addition, the newly formed cell walls are more susceptible to lysis (Gomez and Bishai, 2000). It was suggested that WhiB2 is involved in the assembly and

TABLE 2 | DEGs, and their correlation with expression of different functional categories (according to COG).

Gene		Product	Genes with correlated expression, categories enriched	
			Positive correlation	Negative correlation
rv0079			T	
rv0080			T	C, J
rv0087	*hycE*	Possible formate hydrogenase HycE		J
rv0440	*groEL2*	60 kDa chaperonin 2 GroEL2	J	
rv1158c		Conserved hypothetical ala-, pro-rich protein	C, M	
rv1620c	*cydC*	Probable "component linked with the assembly of cytochrome" transport transmembrane ATP-binding protein ABC transporter CydC		J
rv1621c	*cydD*	Probable "component linked with the assembly of cytochrome" transport transmembrane ATP-binding protein ABC transporter CydD		J
rv1622c	*cydB*	Probable integral membrane cytochrome D ubiquinol oxidase (subunit II) CydB (cytochrome BD-I oxidase subunit II)		J
rv2947c	*pks15*	Probable polyketide synthase Pks15	J	K
rv2986c	*hupB*	DNA-binding protein HU homolog HupB (histone-like protein)	J	
rv2988c	*leuC*	Probable 3-isopropylmalate dehydratase (large subunit) LeuC (isopropylmalate isomerase) (alpha-IPM isomerase) (IPMI)	K	
rv3019c	*esxR*	Secreted ESAT-6 like protein EsxR (TB10.3) (ESAT-6 like protein 9)	C, O	
rv3136	*PPE51*	PPE family protein PPE51	J	

C, energy production and conversion; J, Translation, ribosomal structure and biogenesis; K, transcription; M, cell envelope biogenesis, outer membrane; O, posttranslational modifications, protein turnover, chaperones; T, signal transduction mechanisms. Orange boxes stand for up-regulated DEGs; green, down-regulated DEGs.

stabilization of the FtsZ ring around the cell septum during division (Huang et al., 2013).

Two other down-regulated genes, *rv2987c* and *rv2988c*, encode subunits of putative 3-isopropylmalate dehydratase and are involved in leucine biosynthesis. *In vivo* and *in vitro* studies demonstrate that leucine-auxotrophic *M. tuberculosis* strains do not replicate inside host cells (Hondalus et al., 2000).

Overall, up-regulated genes fall into "intermediate metabolism and respiration" functional category, and either belong to the DosR regulon directly (*rv0079-rv0081*), or are connected through DosR-regulated transcriptional factor *rv0081* (*rv0082-rv0087*). All up-regulated genes are thought to be involved into mycobacterial survival inside macrophages.

The list of down-regulated genes is functionally more diverse. Of interest is a decreased of genes encoding chaperone proteins, such as GroEL2, HupB, WhiB2. Theoretically, their expression should be rather increased under unfavorable conditions. To find an explanation of this paradox, we studied TB databases (http://genome.tbdb.org), concentrating on groups of genes co-expressed with these chaperones genes. It appeared that the majority of DEGs, including *groEL2, hupB,* and *whiB2*, are co-expressed with genes of the functional category J: Translation, ribosomal structure and biogenesis (Clusters of Orthologous Groups, COG, Tatusov et al., 2000). In all cases, irrespective to up- or down-regulation of DEGs, there was reversed correlation with genes of the J category (**Table 2**). These data suggest that the MTS1338 overexpression leads to transcriptional changes that correlate with a translation slowdown.

Summarizing, our results suggest an important potential role of MTS1338 in pathogenesis of mycobacteria-triggered diseases. An increase in MTS1338 production during infection *in vivo* and in activated macrophages, changes in the expression of genes important for mycobacterial metabolism and a better survival under low pH accompanying MTS1338 overexpression—all suggest that this sRNA may well contribute to successful persistence of *M. tuberculosis* within host cells.

DATA AVAILABILITY STATEMENT

The data sets supporting the results of this article are available in the GEO data repository under the accession number GSE137857.

ETHICS STATEMENT

The animal study was reviewed and approved by Bioethics Committee of the Central Research Institute of Tuberculosis (IACUC).

AUTHOR CONTRIBUTIONS

ES, DI, AK, AA, and TA conceived the idea and designed the experiments. ES, AG, YS, KM, OB, AO, and NL performed the experiments. ES, AK, AA, and TA analyzed the data and wrote the paper.

FUNDING

This work was supported by the Russian Science Foundation grant no. 18-15-00332 to TA (new *M. tuberculosis* strains, RNA-seq experiments and analyses, stresses *in vitro*, infection analyses); grant no. 18-45-04015 to AA (*in vivo* and macrophages infection experiments).

SUPPLEMENTARY MATERIAL

The Supplementary Material for this article can be found online at: https://www.frontiersin.org/articles/10.3389/fcimb.2019.00405/full#supplementary-material

Supplementary Table 1 | Oligonucleotides used in the study.

Supplementary Table 2 | RNA-seq data.

Supplementary Figure 1 | (A) MTS1338 transcription level in samples used for RNA-seq. pMV stands for control *M. tuberculosis* strains. Cl2, cl8, cl4—OVER strains, independent clones. **(B)** Validation of RNA-seq data by qRT-PCR.

REFERENCES

Aguilar-Ayala, D. A., Palomino, J. C., Vandamme, P., Martin, A., and Gonzalez-Y-Merchand, Y. A. (2017). Genetic regulation of *Mycobacterium tuberculosis* in a lipid-rich environment. *Infect. Genet. Evol.* 55, 392–402. doi: 10.1016/j.meegid.2016.10.015

Arnvig, K., and Young, D. (2012). Non-coding RNA and its potential role in *Mycobacterium tuberculosis* pathogenesis. *RNA Biol.* 9, 427–436. doi: 10.4161/rna.20105

Arnvig, K. B., Comas, I., Thomson, N. R., Houghton, J., Boshoff, H. I., Croucher, N. J., et al. (2011). Sequence-based analysis uncovers an abundance of non-coding RNA in the total transcriptome of *Mycobacterium tuberculosis*. *PLoS Pathog.* 7:e1002342. doi: 10.1371/journal.ppat.1002342

Baker, J. J., Johnson, B. K., and Abramovitch, R. B. (2014). Slow growth of *Mycobacterium tuberculosis* at acidic pH is regulated by phoPR and host-associated carbon sources. *Mol. Microbiol.* 94, 56–69. doi: 10.1111/mmi.12688

Bermudez, L. E., Petrofsky, M., and Goodman, J. (1997). Exposure to low oxygen tension and increased osmolarity enhance the ability of *Mycobacterium avium* to enter intestinal epithelial (HT-29) cells. *Infect. Immun.* 65, 3768–3773.

Berney, M., Greening, C., Hards, K., Collins, D., and Cook, G. M. (2014). Three different [NiFe] hydrogenases confer metabolic flexibility in the obligate aerobe *Mycobacterium smegmatis*. *Environ. Microbiol.* 16, 318–330. doi: 10.1111/1462-2920.12320

Carver, T., Harris, S. R., Berriman, M., Parkhill, J., and McQuillan, J. A. (2012). Artemis: an integrated platform for visualization and analysis of high-throughput sequence-based experimental data. *Bioinformatics* 28, 464–469. doi: 10.1093/bioinformatics/btr703

Chauhan, S., Sharma, D., Singh, A., Surolia, A., and Tyagi, J. S. (2011). Comprehensive insights into *Mycobacterium tuberculosis* DevR (DosR) regulon activation switch. *Nucleic Acids Res.* 39, 7400–7414. doi: 10.1093/nar/gkr375

Connell, N. D. (1994). Mycobacterium: isolation, maintenance, transformation, and mutant selection. *Methods Cell Biol.* 45, 107–125. doi: 10.1016/S0091-679X(08)61848-8

Cooper, A. M. (2009). Cell-mediated immune responses in tuberculosis. *Annu. Rev. Immunol.* 27, 393–422. doi: 10.1146/annurev.immunol.021908.132703

Dutta, T., and Srivastava, S. (2018). Small RNA-mediated regulation in bacteria: a growing palette of diverse mechanisms. *Gene* 656, 60–72. doi: 10.1016/j.gene.2018.02.068

Eruslanov, E. B., Majorov, K. B., Orlova, M. O., Mischenko, V. V., Kondratieva, T. K., Apt, A. S., et al. (2004). Lung cell responses to *M. tuberculosis* in genetically susceptible and resistant mice following intratracheal challenge. *Clin. Exp. Immunol.* 135, 19–28. doi: 10.1111/j.1365-2249.2004.02328.x

Galagan, J. E., Minch, K., Peterson, M., Lyubetskaya, A., Azizi, E., Sweet, L., et al. (2013). The *Mycobacterium tuberculosis* regulatory network and hypoxia. *Nature* 499, 178–183. doi: 10.1038/nature12337

Ganger, M. T., Dietz, G. D., and Ewing, S. J. (2017). A common base method for analysis of qPCR data and the application of simple blocking in qPCR experiments. *BMC Bioinformatics* 18:534. doi: 10.1186/s12859-017-1949-5

Gerrick, E. R., Barbier, T., Chase, M. R., Xu, R., François, J., Lin, V. H., et al. (2018). Small RNA profiling in *Mycobacterium tuberculosis* identifies MrsI as necessary for an anticipatory iron sparing response. *Proc. Natl. Acad. Sci. U.S.A.* 115, 6464–6469. doi: 10.1073/pnas.1718003115

Gomez, J. E., and Bishai, W. R. (2000). whmD is an essential mycobacterial gene required for proper septation and cell division. *Proc. Natl. Acad. Sci. U.S.A.* 97, 8554–8559. doi: 10.1073/pnas.140225297

Greening, C., and Cook, G. M. (2014). Integration of hydrogenase expression and hydrogen sensing in bacterial cell physiology. *Curr. Opin. Microbiol.* 18, 30–38. doi: 10.1016/j.mib.2014.02.001

Griffin, J. E., Gawronski, J. D., DeJesus, M. A., Ioerger, T. R., Akerley, B. J., and Sassetti, C. M. (2011). High-resolution phenotypic profiling defines genes essential for mycobacterial growth and cholesterol catabolism. *PLoS Pathog.* 7:e1002251. doi: 10.1371/journal.ppat.1002251

Haning, K., Cho, S. H., and Contreras, L. M. (2014). Small RNAs in mycobacteria: an unfolding story. *Front. Cell Infect. Microbiol.* 4:96. doi: 10.3389/fcimb.2014.00096

He, H., Bretl, D. J., Penoske, R. M., Anderson, D. M., and Zahrt, T. C. (2011). Components of the Rv0081-Rv0088 locus, which encodes a predicted formate hydrogenlyase complex, are coregulated by Rv0081, MprA, and DosR in *Mycobacterium tuberculosis*. *J. Bacteriol.* 193, 5105–5118. doi: 10.1128/JB.05562-11

Holmqvist, E., and Wagner, E. G. H. (2017). Impact of bacterial sRNAs in stress responses. *Biochem. Soc. Trans.* 45, 1203–1212. doi: 10.1042/BST20160363

Hondalus, M. K., Bardarov, S., Russell, R., Chan, J., Jacobs, W. R., and Bloom, B. R. (2000). Attenuation of and protection induced by a leucine auxotroph of *Mycobacterium tuberculosis*. *Infect. Immun.* 68, 2888–2898. doi: 10.1128/IAI.68.5.2888-2898.2000

Hör, J., Gorski, S. A., and Vogel, J. (2018). Bacterial RNA biology on a genome scale. *Mol. Cell* 70, 785–799. doi: 10.1016/j.molcel.2017.12.023

Hu, Y., Mangan, J. A., Dhillon, J., Sole, K. M., Mitchison, D. A., Butcher, P. D., et al. (2000). Detection of mRNA transcripts and active transcription in persistent *Mycobacterium tuberculosis* induced by exposure to rifampin or pyrazinamide. *J. Bacteriol.* 182, 6358–6365. doi: 10.1128/JB.182.22.6358-6365.2000

Huang, K. H., Durand-Heredia, J., and Janakiraman, A. (2013). FtsZ ring stability: of bundles, tubules, crosslinks, and curves. *J. Bacteriol.* 195, 1859–1868. doi: 10.1128/JB.02157-12

Ignatov, D. V., Salina, E. G., Fursov, M. V., Skvortsov, T. A., Azhikina, T. L., and Kaprelyants, A. S. (2015). Dormant non-culturable *Mycobacterium tuberculosis* retains stable low-abundant mRNA. *BMC Genomics* 16:954. doi: 10.1186/s12864-015-2197-6

Ignatov, D. V., Timoshina, O. Y., Logunova, N. N., Skvortsov, T. A., and Azhikina, T. L. (2014). Expression of small RNAs of *Mycobacterium tuberculosis* in murine models of Tuberculosis infection. *Russ. J. Bioorg. Chem.* 40, 233–235. doi: 10.1134/S1068162014020058

Katsube, T., Matsumoto, S., Takatsuka, M., Okuyama, M., Ozeki, Y., Naito, M., et al. (2007). Control of cell wall assembly by a histone-like protein in Mycobacteria. *J. Bacteriol.* 189, 8241–8249. doi: 10.1128/JB.00550-07

Konar, M., Alam, M. S., Arora, C., and Agrawal, P. (2012). WhiB2/Rv3260c, a cell division-associated protein of Mycobacterium tuberculosis H37Rv, has properties of a chaperone. *FEBS J.* 279, 2781–2792. doi: 10.1111/j.1742-4658.2012.08662.x

Kondratieva, E., Logunova, N., Majorov, K., Averbakh, M., and Apt, A. (2010). Host genetics in granuloma formation: human-like lung pathology in mice with reciprocal genetic susceptibility to *M. tuberculosis and M. avium*. *PLoS ONE* 5:e10515. doi: 10.1371/journal.pone.0010515

Kumar, A., Majid, M., Kunisch, R., Rani, P. S., Qureshi, I. A., Lewin, A., et al. (2012). *Mycobacterium tuberculosis* DosR regulon gene Rv0079 encodes a putative, 'dormancy associated translation inhibitor (DATIN)'. *PLoS ONE* 7:e38709. doi: 10.1371/journal.pone.0038709

Kumar, S., Sardesai, A. A., Basu, D., Muniyappa, K., and Hasnain, S. E. (2010). DNA clasping by mycobacterial HU: the C-terminal region of HupB mediates increased specificity of DNA binding. *PLoS One* 5:e12551. doi: 10.1371/journal.pone.0012551

Langmead, B., and Salzberg, S. L. (2012). Fast gapped-read alignment with bowtie 2. *Nat. Methods* 9, 357–359. doi: 10.1038/nmeth.1923

Leonhartsberger, S., Korsa, I., and Böck, A. (2002). The molecular biology of formate metabolism in enterobacteria. *J. Mol. Microbiol. Biotechnol.* 4, 269–276.

Lewthwaite, J. C., Clarkin, C. E., Coates, A. R., Poole, S., Lawrence, R. A., Wheeler-Jones, C. P., et al. (2007). Highly homologous *Mycobacterium tuberculosis* chaperonin 60 proteins with differential CD14 dependencies stimulate cytokine production by human monocytes through cooperative activation of p38 and ERK1/2 mitogen-activated protein kinases. *Int. Immunopharmacol.* 7, 230–240. doi: 10.1016/j.intimp.2006.10.005

Liao, Y., Smyth, G. K., and Shi, W. (2014). Featurecounts: an efficient general purpose program for assigning sequence reads to genomic features. *Bioinformatics* 30, 923–930. doi: 10.1093/bioinformatics/btt656

Logunova, N., Korotetskaya, M., Polshakov, V., and Apt, A. (2015). The QTL within the H2 complex involved in the control of Tuberculosis infection in mice is the classical class II H2-Ab1 Gene. *PLoS Genet.* 11:e1005672. doi: 10.1371/journal.pgen.1005672

Love, M. I., Huber, W., and Anders, S. (2014). Moderated estimation of fold change and dispersion for RNA-seq data with DESeq2. *Genome Biol.* 15:550. doi: 10.1186/s13059-014-0550-8

Lyadova, I. V., Eruslanov, E. B., Khaidukov, S. V., Yeremeev, V. V., Majorov, K. B., Pichugin, A. V., et al. (2000). Comparative analysis of T lymphocytes recovered from the lungs of mice genetically susceptible, resistant, and hyperresistant to *Mycobacterium tuberculosis*-triggered disease. *J. Immunol.* 165, 5921–5931. doi: 10.4049/jimmunol.165.10.5921

Mai, J., Rao, C., Watt, J., Sun, X., Lin, C., Zhang, L., et al. (2019). *Mycobacterium tuberculosis* 6C sRNA binds multiple mRNA targets via C-rich loops independent of RNA chaperones. *Nucleic Acids Res.* 47, 4292–4307. doi: 10.1093/nar/gkz149

Majorov, K. B., Lyadova, I. V., Kondratieva, T. K., Eruslanov, E. B., Rubakova, E. I., Orlova, M. O., et al. (2003). Different innate ability of I/St and A/Sn mice to combat virulent *Mycobacterium tuberculosis*: phenotypes expressed in lung and extrapulmonary macrophages. *Infect. Immun.* 71, 697–707. doi: 10.1128/IAI.71.2.697-707.2003

Moores, A., Riesco, A. B., Schwenk, S., and Arnvig, K. B. (2017). Expression, maturation and turnover of DrrS, an unusually stable, DosR regulated small RNA in *Mycobacterium tuberculosis*. *PLoS ONE* 12:e0174079. doi: 10.1371/journal.pone.0174079

Naffin-Olivos, J. L., Georgieva, M., Goldfarb, N., Madan-Lala, R., Dong, L., Bizzell, E., et al. (2014). Mycobacterium tuberculosis Hip1 modulates macrophage responses through proteolysis of GroEL2. *PLoS Pathog.* 10:e1004132. doi: 10.1371/journal.ppat.1004132

Pandey, S. D., Choudhury, M., Yousuf, S., Wheeler, P. R., Gordon, S. V., Ranjan, A., et al. (2014). Iron-regulated protein HupB of Mycobacterium tuberculosis positively regulates siderophore biosynthesis and is essential for growth in macrophages. *J. Bacteriol.* 196, 1853–1865. doi: 10.1128/JB.01483-13

Qamra, R., Mande, S. C., Coates, A. R., and Henderson, B. (2005). The unusual chaperonins of *Mycobacterium tuberculosis*. *Tuberculosis* 85, 385–394. doi: 10.1016/j.tube.2005.08.014

Qamra, R., Srinivas, V., and Mande, S. C. (2004). *Mycobacterium tuberculosis* GroEL homologues unusually exist as lower oligomers and retain the ability to suppress aggregation of substrate proteins. *J. Mol. Biol.* 342, 605–617. doi: 10.1016/j.jmb.2004.07.066

Radaeva, T. V., Kondratieva, E. V., Sosunov, V. V., Majorov, K. B., and Apt, A. (2008). A human-like TB in genetically susceptible mice followed by the true dormancy in a Cornell-like model. *Tuberculosis* 88, 576–585. doi: 10.1016/j.tube.2008.05.003

Radaeva, T. V., Nikonenko, B. V., Mischenko, V. V., Averbakh, M. M. Jr., and Apt, A. S. (2005). Direct comparison of low-dose and Cornell-like models of chronic

and reactivation tuberculosis in genetically susceptible I/St and resistant B6 mice. *Tuberculosis* 85, 65–72. doi: 10.1016/j.tube.2004.09.014

Raghunand, T. R., and Bishai, W. R. (2006). Mycobacterium smegmatis whmD and its homologue Mycobacterium tuberculosis whiB2 are functionally equivalent. *Microbiol.* 152, 2735–2747. doi: 10.1099/mic.0.28911-0

Rodriguez, J. G., Hernández, A. C., Helguera-Repetto, C., Aguilar Ayala, D., Guadarrama-Medina, R., Anzóla, J. M., et al. (2014). Global adaptation to a lipid environment triggers the dormancy-related phenotype of *Mycobacterium tuberculosis*. *MBio* 5:e01125-14. doi: 10.1128/mBio.01125-14

Russell, D. G. (2007). Who puts the tubercle in tuberculosis? *Nat. Rev. Microbiol.* 5, 39–47. doi: 10.1038/nrmicro1538

Rustad, T. R., Roberts, D. M., Liao, R. P., and Sherman, D. R. (2009). Isolation of mycobacterial RNA. *Methods Mol. Biol.* 465, 13–21. doi: 10.1007/978-1-59745-207-6_2

Salina, E. G., Grigorov, A., Bychenko, O., Skvortsova, Y., Mamedov, I., Azhikina, T., et al. (2019). Resuscitation of dormant "Non-culturable" mycobacterium tuberculosis is characterized by immediate transcriptional burst. *Front. Cell Infect. Microbiol.* 9:272. doi: 10.3389/fcimb.2019.00272

Sassetti, C. M., Boyd, D. H., and Rubin, E. J. (2003). Genes required for mycobacterial growth defined by high density mutagenesis. *Mol. Microbiol.* 48, 77–84. doi: 10.1046/j.1365-2958.2003.03425.x

Schwenk, S., and Arnvig, K. B. (2018). Regulatory RNA in *Mycobacterium tuberculosis*, back to basics. *Pathog. Dis.* 76:fty035. doi: 10.1093/femspd/fty035

Solans, L., Gonzalo-Asensio, J., Sala, C., Benjak, A., Uplekar, S., Rougemont, J., et al. (2014). The PhoP-dependent ncRNA Mcr7 modulates the TAT secretion system in *Mycobacterium tuberculosis*. *PLoS Pathog.* 10:e1004183. doi: 10.1371/journal.ppat.1004183

Stewart, G. R., Robertson, B. D., and Young, D. B. (2003). Tuberculosis: a problem with persistence. *Nat. Rev. Microbiol.* 1, 97–105. doi: 10.1038/nrmicro749

Stover, C. K., de la Cruz, V. F., Fuerst, T. R., Burlein, J. E., Benson, L. A., Bennett, L. T., et al. (1991). New use of BCG for recombinant vaccines. *Nature* 351, 456–60. doi: 10.1038/351456a0

Taneja, S., and Dutta, T. (2019). On a stake-out: Mycobacterial small RNA identification and regulation. *Non coding RNA Res.* 4, 86–95. doi: 10.1016/j.ncrna.2019.05.001

Tatusov, R. L., Galperin, M. Y., Natale, D. A., and Koonin, E. V. (2000). The COG database: a tool for genome-scale analysis of protein functions and evolution. *Nucleic Acids Res.* 28, 33–6. doi: 10.1093/nar/28.1.33

Voskuil, M. I., Schnappinger, D., Visconti, K. C., Harrell, M. I., Dolganov, G. M., Sherman, D. R., et al. (2003). Inhibition of respiration by nitric oxide induces a *Mycobacterium tuberculosis* dormancy program. *J. Exp. Med.* 198, 705–13. doi: 10.1084/jem.20030205

Conflict of Interest: The authors declare that the research was conducted in the absence of any commercial or financial relationships that could be construed as a potential conflict of interest.

frontiers in Cellular and Infection Microbiology

REVIEW
published: 14 January 2020
doi: 10.3389/fcimb.2019.00450

Thalidomide and Phosphodiesterase 4 Inhibitors as Host Directed Therapeutics for Tuberculous Meningitis: Insights From the Rabbit Model

Ranjeet Kumar[1], *Afsal Kolloli*[1†], *Pooja Singh*[1†], *Christopher Vinnard*[1], *Gilla Kaplan*[2] *and Selvakumar Subbian*[1*]

[1] New Jersey Medical School, Rutgers, Public Health Research Institute, The State University of New Jersey, Newark, NJ, United States, [2] University of Cape Town, Cape Town, South Africa

OPEN ACCESS

Edited by:
Igor Kramnik,
Boston University, United States

Reviewed by:
Brian Weinrick,
Trudeau Institute, United States
Randall Basaraba,
Colorado State University, United States
Gregory T. Robertson,
Colorado State University, United States

***Correspondence:**
Selvakumar Subbian
subbiase@njms.rutgers.edu

[†]These authors have contributed equally to this work

Specialty section:
This article was submitted to Clinical Microbiology, a section of the journal Frontiers in Cellular and Infection Microbiology

Received: 01 October 2019
Accepted: 12 December 2019
Published: 14 January 2020

Citation:
Kumar R, Kolloli A, Singh P, Vinnard C, Kaplan G and Subbian S (2020) Thalidomide and Phosphodiesterase 4 Inhibitors as Host Directed Therapeutics for Tuberculous Meningitis: Insights From the Rabbit Model. Front. Cell. Infect. Microbiol. 9:450. doi: 10.3389/fcimb.2019.00450

Tuberculous meningitis (TBM) is the most devastating form of extrapulmonary *Mycobacterium tuberculosis* infection in humans. Severe inflammation and extensive tissue damage drive the morbidity and mortality of this manifestation of tuberculosis (TB). Antibiotic treatment is ineffective at curing TBM due to variable and incomplete drug penetration across the blood-brain barrier (BBB) and blood-cerebrospinal fluid (CSF) barriers. Adjunctive corticosteroid therapy, used to dampen the inflammation, and the pathologic manifestation of TBM, improves overall survival but does not entirely prevent the morbidity of the disease and has significant toxicities, including immune-suppression. The rabbit has served as a fit for purpose experimental model of human TBM since the early 1900s due to the similarity in the developmental processes of the brain, including neuronal development, myelination, and microglial functions between humans and rabbits. Consistent with the observations made in humans, proinflammatory cytokines, including TNF-α, play a critical role in the pathogenesis of TBM in rabbits focusing the attention on the utility of TNF-α inhibitors in treating the disease. Thalidomide, an inhibitor of monocyte-derived TNF-α, was evaluated in the rabbit model of TBM and shown to improve survival and reduce inflammation of the brain and the meninges. Clinical studies in humans have also shown a beneficial response to thalidomide. However, the teratogenicity and T-cell activation function of the drug limit the use of thalidomide in the clinic. Thus, new drugs with more selective anti-inflammatory properties and a better safety profile are being developed. Some of these candidate drugs, such as phosphodiesterase-4 inhibitors, have been shown to reduce the morbidity and increase the survival of rabbits with TBM. Future studies are needed to assess the beneficial effects of these drugs for their potential to improve the current treatment strategy for TBM in humans.

Keywords: tuberculosis, mycobacterium, cerebrospinal fluid, phosphodiesterase-4 inhibitors, inflammation, corticosteroid, tumor necrosis factor-alpha

INTRODUCTION

Mycobacterium tuberculosis (Mtb), the causative agent of tuberculosis (TB), is transmitted via aerosols exhaled by patients with active disease and acquired by new contacts via inhalation of infectious droplets, resulting in the establishment of infection in the lungs. However, the bacteria can be transported by infected macrophages/dendritic cells from the lungs to other organs, such as lymph nodes, the spine, and the brain, resulting in disseminated extrapulmonary disease (Krishnan et al., 2010). Tuberculous meningitis (TBM), a common manifestation of Mtb-infection of the central nervous system (CNS), is associated with non-suppurative inflammation of the dura mater and meninges. TBM constitutes ∼5–10% of all extrapulmonary TB cases and thus represents less than 1% of all active TB cases. However, it is the deadliest form of TB with frequent mortality and severe morbidity (Farer et al., 1979; Torok, 2015). TBM is most commonly seen in children under the age of 4 years and older people. In addition, immune-suppression such as that seen in HIV-infection is associated with a significantly higher frequency of Mtb dissemination from the lungs to extrapulmonary sites, including the CNS (Dube et al., 1992; Thwaites et al., 2005; Marais et al., 2010; Ducomble et al., 2013; Heemskerk et al., 2016). A recent meta-analysis of the global TBM burden has reported about a 40% mortality rate within 6 months of TBM diagnosis with progressively deteriorating disease (van Laarhoven et al., 2019).

CLINICAL SYMPTOMS OF HUMAN TBM

Following Mtb dissemination and establishment of infection in the CNS, slow-progressive meningitis develops with symptoms such as headache, fever, vomiting, and neck stiffness, which are not easily distinguishable from other forms of meningitis (Wilkinson et al., 2017). If untreated, TBM progresses to more severe clinical symptoms such as unconsciousness, focal neurological deficits, seizures, raised intracranial pressure, hemiparesis, and cranial nerve palsies. Many of these symptoms are driven by the exacerbated inflammatory response to Mtb infection and mediated by the cytokines released into the CNS from infected immune cells, including TNF-α (Davis et al., 2019). In ∼50% of patients with advanced TBM, the fifth and third cranial nerves are affected, and about 10% of patients report limb weakness (either hemiplegia or paraplegia). At this stage, death is almost inevitable in the absence of any therapeutic interventions (Dastur et al., 1995; Thwaites et al., 2000). Key laboratory findings in the CSF of patients with TBM include pleocytosis with lymphocyte predominance (150–1,000 leukocytes/μl with a mixed population of neutrophils and lymphocytes), high protein content (0.8–2.0 g/dl) and low glucose levels (CSF: plasma glucose ratios of <0.5). TBM in patients with HIV co-infection is characterized by the absence of mononuclear leukocytes and/or the presence of a large number of neutrophils ($>1{,}000$ cells/μl), mimicking acute pyogenic bacterial meningitis (Torok, 2015). Elevated levels of inflammatory cytokines are commonly seen in the CSF and plasma of patients with TBM. Radiographic features in TBM patients include basal meningeal exudates, infarction, tuberculomas, and hydrocephalus.

THE CURRENT STRATEGY FOR TBM TREATMENT

The current TBM treatment strategy includes concurrent administration of standard anti-TB drugs and corticosteroid (Uhlin et al., 2012). Even though antibiotic therapy reduces mortality among TBM cases, the poor penetration of the drugs across the BBB and the associated exacerbation of the inflammatory response to the antibiotic-mediated killing of Mtb results in the inefficient cure of TBM. Since clinical manifestations of TBM are primarily driven by severe inflammation in the confined space of the cranium, anti-inflammatory drugs, such as corticosteroids, have been widely used as adjunctive therapy (Wasserman et al., 2019). Several studies, including a randomized-controlled clinical trial, have reported that treatment with corticosteroid helps to control exacerbated inflammation in TBM cases (Thwaites et al., 2004). The combination therapy of standard anti-TB drugs, along with dexamethasone, has been shown to prolong the survival and reduce mortality among HIV-negative TBM cases (Prasad et al., 2016). However, no significant difference was noted in severity of vasculitis among TBM cases treated with adjunctive corticosteroids compared to the placebo-treated cases (Schoeman et al., 1997). Moreover, adjunctive corticosteroid with antibiotic therapy did not affect the elevated levels of inflammatory cytokines such as TNF-α in the CSF of TBM patients (Donald et al., 1995).

Contradictory findings have been published on the utility of corticosteroids to reduce TBM-associated disability in patients (Nguyen et al., 2007). In some of these studies, a high dose of adjunctive corticosteroid administration controlled the inflammation and reduced other neurological complications associated with TBM in 50% of patients (Prasad et al., 2016). In other studies, adjunctive corticosteroid treatment did not alter or even worsened the clinical condition of the patients and failed to prevent neurological disability associated with TBM (Garg et al., 2014). These findings underlie the necessity of exploring additional adjunctive anti-inflammatory drugs, which can better dampen excessive inflammation caused by Mtb and provide beneficial effects when combined with antibiotics, as host-directed therapy for TBM.

ALTERNATIVE ANTI-INFLAMMATORY DRUGS FOR TBM TREATMENT

The limited efficacy of the standard use of corticosteroids as adjunctive therapy for TBM patients has led to attempts to identify alternative, improved host-directed therapeutic (HDT) treatment modalities for this disease. Thus, aspirin and thalidomide, both known to have anti-inflammatory properties, have been tested for their ability to control pathogen-mediated inflammation in TBM (Uhlin et al., 2012).

One of the clinical manifestations of TBM in children is the development of arterial stroke, which is associated with poor outcome of this disease (Schoeman et al., 2011). Aspirin, an anti-inflammatory, anti-thrombotic, and anti-ischemic drug, was evaluated for its potency in the treatment of arterial stroke associated with pediatric TBM. Data from a randomized, open-label clinical study conducted with 118 TBM patients in India show that adjunctive aspirin treatment (150 mg/day) significantly reduced the 3 month mortality rate (21.7%) and reduced the risk of stroke (19.1%), compared to the placebo-treated patients (Misra et al., 2010). However, no beneficial effect was found for aspirin treatment in another randomized clinical study conducted in South Africa with 146 pediatric TBM cases (Schoeman et al., 2011). In the South African study, the host-modulating functions of aspirin was dose-dependent, and all doses were well-tolerated. However, aspirin did not significantly reduce the morbidity of pediatric TBM patients (Schoeman et al., 2011). A meta-analysis that reviewed four randomized clinical studies totaling 546 TBM cases concluded that compared to the placebo-group, adjunctive aspirin treatment reduced the risk of new infarctions significantly, but not the mortality rate. The measurable adverse events were comparable between the placebo- and aspirin-treatment groups (Rizvi et al., 2019). However, the beneficial effect of adjunctive aspirin treatment in TBM cases with different levels of disease severity remains unclear.

Another anti-inflammatory drug that has been tested as an adjunctive to antibiotics for TBM treatment is thalidomide (α-N-[phthalimido] glutarimide). This non-barbiturate sedative, shown to be a potent antiemetic drug was widely prescribed for the treatment of morning sickness among pregnant women during the early 1960s. Although it became commonly used in Europe and Asia, the US Food and Drug Administration did not approve the sale of thalidomide in the US, due to concerns about the safety of the drug. This concern was later compounded by the finding that administration of thalidomide to pregnant women resulted in teratogenic effects, such as limb malformation in the newborns (Melchert and List, 2007). However, in the 90s, thalidomide treatment was shown to reduce TNF-α-associated inflammation significantly in patients with erythema nodosum leprosum (ENL) (Sampaio et al., 1991). Thereafter, a number of studies have confirmed these observations and demonstrated that ENL patients experience significantly improved clinical outcomes (Sampaio et al., 1993; Corral and Kaplan, 1999; Haslett et al., 2005; Millrine and Kishimoto, 2017).

The TNF-α inhibitory capacity of thalidomide prompted the evaluation of the drug's ability to control the inflammation in the CNS during TBM (Schoeman et al., 2000). In general, results from these studies suggest that thalidomide has a beneficial effect on TBM during antibiotic treatment in children and adults (Schoeman et al., 2000; Roberts et al., 2003). A dose-escalation study reported that administration of 6–24 mg/kg/day of thalidomide was well-tolerated among children suffering from stage-2 TBM (Schoeman et al., 2010). In contrast to treatment with anti-TB drugs with/without adjunctive corticosteroid treatment, pediatric TBM cases treated with adjunctive thalidomide showed significant improvement in disease manifestations; they did not develop new infarcts, as evidenced by CT scan analysis, and showed resolution of basal exudate. Moreover, thalidomide-treated TBM patients showed significantly reduced TNF-α levels in the CSF (Schoeman et al., 2010). Clinical case studies in pediatric meningitis have also demonstrated beneficial effects of thalidomide. A case-study of adjunctive thalidomide administration (4–5 mg/kg for 3–8 months) reported remarkable clinical recovery in four children suffering from TBM-related optochiasmatic arachnoiditis, which is a consequence of intracranial pressure and/or inflammation of the basal arachnoid (Schoeman et al., 2010). A double-blind, randomized clinical study of adjunctive high dose thalidomide treatment (24 mg/kg/day for 1 month) in stage-2 and -3 TBM cases did not significantly improve treatment efficacy, compared to the placebo group (Schoeman et al., 2004). However, in this study, the TBM cases in the adjunctive thalidomide treatment group had higher disease severity at baseline, compared to the placebo group (Schoeman et al., 2004). Recently, two clinical case studies revealed the beneficial role of thalidomide in controlling the neuroinflammation observed during CNS TB. Administration of thalidomide, in combination with anti-TB drugs and corticosteroids, was shown to improve the clinical outcome of patients with chronic TBM symptoms (Keddie et al., 2018). Another case study reported that adjunctive thalidomide (1.2 mg/kg/day) therapy with standard anti-TB drugs (HRZ) and low dose corticosteroid significantly improved the clinical status of the patient, after 5 months of treatment (Caraffa et al., 2018). These observations suggest that thalidomide might improve patient responses to antibiotic treatment, especially where traditional high dose corticosteroid therapy fails to control chronic inflammation and other neurological complications associated with TBM.

Although thalidomide is effective in reducing inflammation associated with infection in such conditions as ENL, the potential of this drug to activate T-cells may interfere with the anti-inflammatory property of the drug (Haslett et al., 1998, 1999). Studies conducted using animal models, and human peripheral blood samples show that thalidomide can function as a co-stimulatory signal to activate T cells. This increase in T cell proliferation is associated with elevated production of IL-2 and IFN-γ by these cells. Thus, thalidomide treatment can contribute to the development of immune reconstitution inflammatory syndrome (IRIS) in pulmonary TB patients with or without co-infection with HIV (Haslett et al., 1998, 1999; Corral and Kaplan, 1999). Consequently, there is a need to develop alternative compounds that are safe, retain the anti-TNF-α activity of the parent drug, but do not activate T-cell mediated immunity. Future studies are required to evaluate new derivatives of thalidomide for their potential to change and/or to improve the current treatment strategy for TBM.

THE RABBIT AS A PRECLINICAL MODEL TO ASSESS THE PATHOGENESIS AND NEW THERAPIES IN TBM

The rabbit, as an experimental TBM model of human disease, was established in 1923 (Kasahara, 1924). The first TBM rabbit model involved the atlanto-occipital inoculation of human

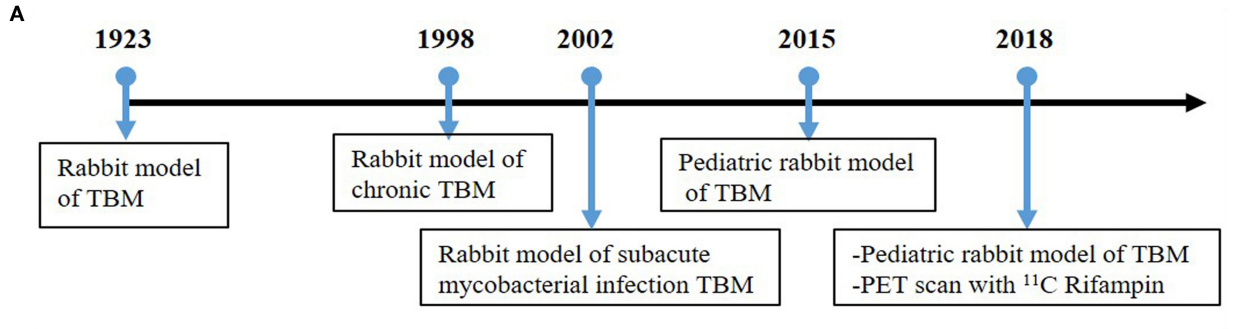

B

Disease presentation in rabbit model of TBM

Agent of infection	*Mtb HN878* ($5x10^5$ CFU)	*Mtb CDC1551* ($5x10^5$ CFU)	*Mtb H37Rv* (~$5x10^5$ CFU)	*M. bovis* Ravenal	
				2×10^7 CFU (*High dose*)	5×10^5 CFU (*Low dose*)
Disease manifestation					
Bacterial load	High	High	High	High	Low
Clinical symptoms / Disease pathology	Early; Acute	Delayed; Subacute	Early; Acute	Early; Acute	Delayed; Subacute
Dissemination of Mtb	Yes	No	Yes	Yes	No
Type of granuloma	Necrotizing	No necrosis	Necrotizing	Necrotizing	Non-necrotizing
Inflammation of meninges	High	Moderate	High	High	Low
Leukocytosis	High	Moderate	High	High	Low
Level of inflammatory cytokines (TNF-α, IL-1β)	High	Low	High	High	Low

FIGURE 1 | (A) Timeline of rabbit model TBM development. The first experimental model of rabbit TBM was established in 1923 using intra-cisternal inoculation of pathogenic mycobacteria. This model shows the presence of *Mycobacteria* in the meninges (Rich foci), disease progression with various infection/inoculum doses of different mycobacterial strains (chronic and subacute TBM) and the efficacy of anti-inflammatory drugs, such as thalidomide, on TBM. Since the TBM has a high mortality rate among children, a pediatric model of rabbit TBM was also developed and evaluated for disease progression in this population. Recent developments with the rabbit TBM model have introduced imaging techniques, such as PET scan (^{124}*I-DPA-713*), which is vital in understanding host-drug interactions during TBM treatment. **(B)** Disease presentation in rabbit model of TBM. The rabbit model of TBM have used different strains of pathogenic *Mycobacterium*, which demonstrated heterogeneity in the outcome of infection. High- and low-inoculum doses differ in their onset of disease symptoms and the rate of progression of infection. The laboratory Mtb strain H37Rv, clinical Mtb isolate HN878 and a high dose *M. bovis* Ravenal infection led to elevated cytokine response and severe inflammation of the meninges. These animals had early and robust disease pathology, accompanied by the presence of necrotizing granulomas and dissemination of Mtb to other organs of the body. In contrast, infection by Mtb CDC1551 and a low-dose *M. bovis* Ravenal, displayed a delayed and moderate-to-low inflammatory response without bacillary dissemination to other organs of the infected animals.

tubercle bacilli (presumably Mtb), avian tubercle bacilli, and bovine tubercle bacilli into the subarachnoid space (**Figure 1**). The inoculum, prepared in a saline solution, did not cause any initial visible reaction in the rabbits. However, at 6–15 days post-inoculation, tubercles had formed in the meninges, accompanied by signs of TBM, such as paralysis, followed by death. This early study demonstrated the resemblance of disease progression and immunopathology between human TBM and

TABLE 1 | Comparison of CSF characteristics between human and rabbit during normal and TBM conditions.

Species	Normal	TBM
Human	Clear and colorless	Opalescent, turbid and slightly yellow in color
	No Coagulation	Coagulation
	Total cell count: Adult- 0–5 cells/mm^3 Infants- 0–30 cells/mm^3	Total cell count: 10–1000 cells/mm^3 (Mainly monocytes, lymphocytes predominate and neutrophils present in the early stages)
	Glucose: 45–85 mg/dl	Glucose: <45 mg/dl
	Protein: 15–45 mg/dl	Protein: 100–500 mg/dl
	Specific gravity: 1.004–1.007	
Rabbit	Clear and colorless	Turbid, cloudy and off-white in color
	No Coagulation	Coagulation
	Total cell count: 0–10 cells/mm^3	Total cell count: 0–1500 cell/mm^3 PMN: 80–400/mm^3 Lymphocyte: 300–1200/mm^3
	Protein- albumin: 0.015–0.019% Globulin: Absent	Protein: 0.03–0.8%
	Glucose: 0.054%	Glucose: 0.042–0.01%
	Specific gravity: 1.005	

the rabbit model. The tubercles were mostly present at the base of the cerebrum and cerebellum, and less frequently on the spinal cord (Kasahara, 1924). This study also determined the chemical composition and physical appearance of CSF from rabbits with TBM and compared it to that of healthy animals (**Table 1**). Rabbits with TBM showed a decrease in CSF glucose content, an increase in protein levels and lymphocyte counts, and loss of anticoagulant properties. Clinical signs, such as loss of coordination, head tremor, rigidity of neck and back muscles, head retraction and ataxia, convulsions, and paralysis of the legs, marked the course of progressive disease pathology in rabbits with TBM (Kasahara, 1924). A classic study compared TBM disease pathology between children and the rabbit model, demonstrating that the presence of Mtb in the meningeal space directly leads to progressive TBM in both animals and humans (Rich and McCordock, 1933). Importantly, the clinical and CSF findings in the rabbit TBM model are very similar to human disease, with a predominance of lymphocytes, high protein levels, and viscous CSF consistency (**Table 1**). Moreover, basal meningeal enhancement and hydrocephalus are common abnormalities seen both in the rabbit model of TBM and in human TBM cases (Torok, 2015).

Another similarity between humans and the rabbit model of TBM is the cellular response underlying brain infection by Mtb. Microglial cells play an essential role in eliciting an immune response against Mtb in the case of TBM (Curto et al., 2004; Rock et al., 2008). Infected human microglial cells produce cytokines and chemokines *in vitro*, including TNF-α, IL-6, IL-1β, CCL2, CCL5, and CXCL10 (Rock et al., 2008). A recent study reported elevated production of inflammatory cytokines, including TNF-α and IFN-γ in whole blood from TBM patients upon *in vitro* stimulation with Mtb (van Laarhoven et al., 2019). Similar to the human conditions, mycobacterial invasion of microglia cells/macrophages leads to the release of pro-inflammatory cytokines in the rabbit model of TBM (Tsenova et al., 1998).

Although TNF-α has a protective role against Mtb infection, increased levels of this proinflammatory cytokine in TBM exacerbate inflammation that contributes to tissue destruction, increased protein, and decreased glucose levels (Tsenova et al., 1999). In the rabbit model of TBM, administration of a recombinant human TNF-α impaired the transportation of compounds/drugs across the BBB into the brain, and led to CSF leukocytosis, protein influx, and lactate accumulation.

The rabbit model of TBM also displays Mtb strain-specific immunopathology, which can contribute to our understanding of protective vs. permissive host responses to infection. For example, intra-cisternal infection of rabbits with the clinical Mtb isolates HN878 vs. CDC1551, produces significantly different disease outcome (Tsenova et al., 2005). Severe disease manifestations with higher bacterial loads in the CSF and brain were evident after 8 weeks of intra-cisternal inoculation with the clinical Mtb strain HN878. These animals also had necrotizing granulomatous meningitis, encephalitis, and vasculitis within the cortex of the brain. Progressive meningitis led to the loss of coordination and limb paralysis by 3 weeks post-infection (Tsenova et al., 2005). In contrast, the bacterial load in the CSF of rabbits infected with the clinical Mtb isolate CDC1551 was significantly lower, with no bacterial dissemination to other organs after 7 days of infection. These differences disappeared by the end of 4 weeks post-inoculation. Elevated proinflammatory cytokine levels and high protein levels, as well as leukocytosis, were observed in the CSF upon the establishment of infection with both Mtb isolates. However, at 6 weeks post-infection, rabbits infected with the clinical Mtb isolate CDC1551 had reduced TNF-α levels, concomitant with a reduced bacterial count, and no clinical signs of disease progression. Similarly, histologic examination of brain tissue from CDC1551 infected animals confirmed the moderate inflammation of the meninges, limited leukocytic infiltration and no necrosis (Tsenova et al., 2005).

In addition to the nature of the infecting Mtb strain, the inoculum dose of pathogenic mycobacteria used for infection can also affect the clinical outcome of TBM. Using this approach, a subacute model of mycobacterial CNS infection, with a delayed onset of disease, was established (Tsenova et al., 2002). In this model, intra-cisternal inoculation of rabbits with 5 x 10^4 CFU of *M. bovis* Ravenel induced progressive subacute meningitis characterized by high CSF leukocytosis, protein influx, and release of TNF-α, with substantial meningeal inflammation by 28 days post-infection. This rabbit model of subacute TBM was further refined by titrating different inoculum doses of Mtb and observing the temporal kinetics of bacterial growth and disease progression (Tsenova et al., 2002).

The developmental stages of the brain in children makes them highly vulnerable to TBM. To understand the pathogenesis of TB during early brain development, a pediatric rabbit model of TBM was created (Tucker et al., 2016). In this model, 4–8 day old NZW rabbits were inoculated with Mtb into the subarachnoid space, and the animals were monitored for 35 days post-infection.

In these animals, disease symptoms appeared by the 7th day post-infection, characterized by neurologic manifestations of TBM, including inability of the animals to move and balance their body parts and loss of head and body elevation. Further, disease scores from the neurobehavioral testing of these animals suggested a gradual loss of motor function and decreased maturity associated with progressive disease. Activation of microglia, the primary cells in brain that harbor Mtb during infection was tracked using a PET radiotracer for macrophage-associated inflammation (^{124}*I-DPA-713*) and confirmed with the presence of Iba-1, a marker of microglia. A PET-imaging study of pediatric rabbits with TBM revealed localization of the tracer around TB lesions in the brain and the site of injection at the 21st-day post-infection. In these animals, enlargement of the TB lesion was noted with time. The bacterial burden in brains, with superficial medial tuberculoma, increased until 14 days of infection after which it remained stable. Gradual dissemination of Mtb into the lungs was observed until 21 days that became stable with no significant increase until 35 days post-infection. At this time, microscopic examination revealed deep tuberculomas with increased Mtb CFU.

The penetration of antibiotics across the BBB during a multi-drug treatment regimen was evaluated in the pediatric rabbit TBM model (Tucker et al., 2018). In this study, 4–8 days postnatal rabbits infected in the subarachnoid space with Mtb H37Rv were treated after 21 days of infection with a combination of ^{11}C rifampin, isoniazid, and rifampicin for 6 weeks, followed by PET imaging. Results from this study revealed limited penetration of rifampin that diminished as early as 2 weeks post-treatment. PET scans also unveiled absence of antibiotics at the site of TB lesions (Tucker et al., 2018). Thus, a pediatric rabbit model of TBM infection provided a vital tool for our understanding of the effect of Mtb infection and disease progression on neuronal development, myelination, and microglia present in major white matter tracts, since these processes are very similar between rabbit and human brain development.

Taken together, the rabbit model of TBM recapitulates the pathologic manifestations seen in human disease. This model is useful to test therapeutic interventions after the development of clinical signs and to evaluate the effect of different regimens of anti-TB and immunomodulatory treatments on the course of the disease (Sampaio et al., 1991, 1993; Moreira et al., 1993; Tramontana et al., 1995; Tsenova et al., 2002).

Although the rabbit model recapitulates several clinical and pathologic manifestations of TBM in humans, it has some limitations. In the rabbit model, Mtb is inoculated directly into the intra-cisternal region. This may not reflect the natural dissemination that occur in patients with TBM. Similarly, disease manifestations of TBM in rabbits are associated with the nature of the mycobacterial strains and the infectious inoculum used. However such associations are not well-established in human patients. Therefore, future studies should fine-tune the rabbit and potentially other animal models of TBM, to mimic the natural route of Mtb transmission, without compromising the pathology of human disease. Nonetheless, experimental TBM in outbred rabbits displays the heterogeneity in host response, as seen in human patients (Tsenova et al., 2006).

DISCOVERY OF NEXT-GENERATION ANTI-INFLAMMATORY DRUGS AS HDT FOR TB

During the last decade, several structural analogs of thalidomide have been synthesized and evaluated for their potency as selective TNF-α inhibitors (Corral et al., 1996; Muller et al., 1996, 1999; Gordon and Goggin, 2003). Ultimately, two classes of novel compounds with TNF-α inhibitory activity were identified: Selective Cytokine Inhibitory Drugs (SelCIDs) and Immunomodulatory Drugs (IMiDs) (Corral and Kaplan, 1999; Marriott et al., 2001). The IMiDs were shown to be more potent inhibitors of TNF-α than the parent drug thalidomide. These IMiDs, such as Lenalidomide, CC5013 (Revlimid) and CC4047 (Actimid) (Celgene Corp.) decreased TNF-α expression by about 2,000 to 50,000-fold. The efficacy of these compounds has been evaluated in hematologic malignancies, including myelodysplastic syndrome (MDS) and multiple myeloma (MM) (Bartlett et al., 2004; Millrine and Kishimoto, 2017). In addition to TNF-α, IMiDs inhibit the expression of diverse pro-inflammatory cytokines, including IL-1β, IL-6, and IL-12. Similar to thalidomide, IMiDs stimulate differentiation and proliferation of T-cells; treatment of human PBMCs with IMiD CC-4047 upregulated the expression of CD40 ligands on T-cells, co-stimulated T-cell proliferation, and induced IFN-γ and IL-2 expression (Keifer et al., 2001). The IMiDs were also shown to be teratogenic.

A rabbit study of sub-acute CNS mycobacterial infection, established by intra-cisternal injection of low-dose pathogenic *M. bovis*, was shown to recapitulate the pathophysiology of human TBM (Tsenova et al., 2002). In these animals, treatment with anti-TB drugs did not improve the clinical deterioration; nearly 50% of animals showed signs of progressive neurologic disease and death, although the bacillary load was reduced in the brain and in the CSF. Disease manifestations were associated with elevated TNF-α levels in the CSF. In contrast, treatment of rabbits with TBM with antibiotics plus adjunctive IMiD3 CC-5013 (lenalidomide) improved the clinical outcome and reduced mortality. The beneficial effect of IMiD3 has been attributed to its ability to dampen TNF-α, IL-1β, IL-6, and other inflammatory cytokines. Additionally, IMiD3 has been shown to cross the BBB effectively and accumulates in CSF at sufficient concentrations without interfering with the penetration of anti-TB drugs into the CSF (Tsenova et al., 2002). Thus, IMiDs may be promising adjunctive drugs in treating TBM in humans. However, the IMiDs, similar to thalidomide, are teratogenic and, therefore, may not be the treatment of choice for an infectious disease such as TBM.

In contrast to IMiDs, SelCIDs selectively inhibit TNF-α production and do not stimulate lymphocyte proliferation; they have minimal effect on the production of other pro-inflammatory monocyte cytokines (Gordon and Goggin, 2003). The SelCIDs inhibit host phosphodiesterase-4 (PDE-4), an enzyme that hydrolyzes cyclic adenosine and guanosine monophosphates (cAMP and cGMP) to yield AMP and GMP, respectively (**Figure 2**). Both cAMP and cGMP transduce signals by interacting with protein kinase A (PKA) and PKG,

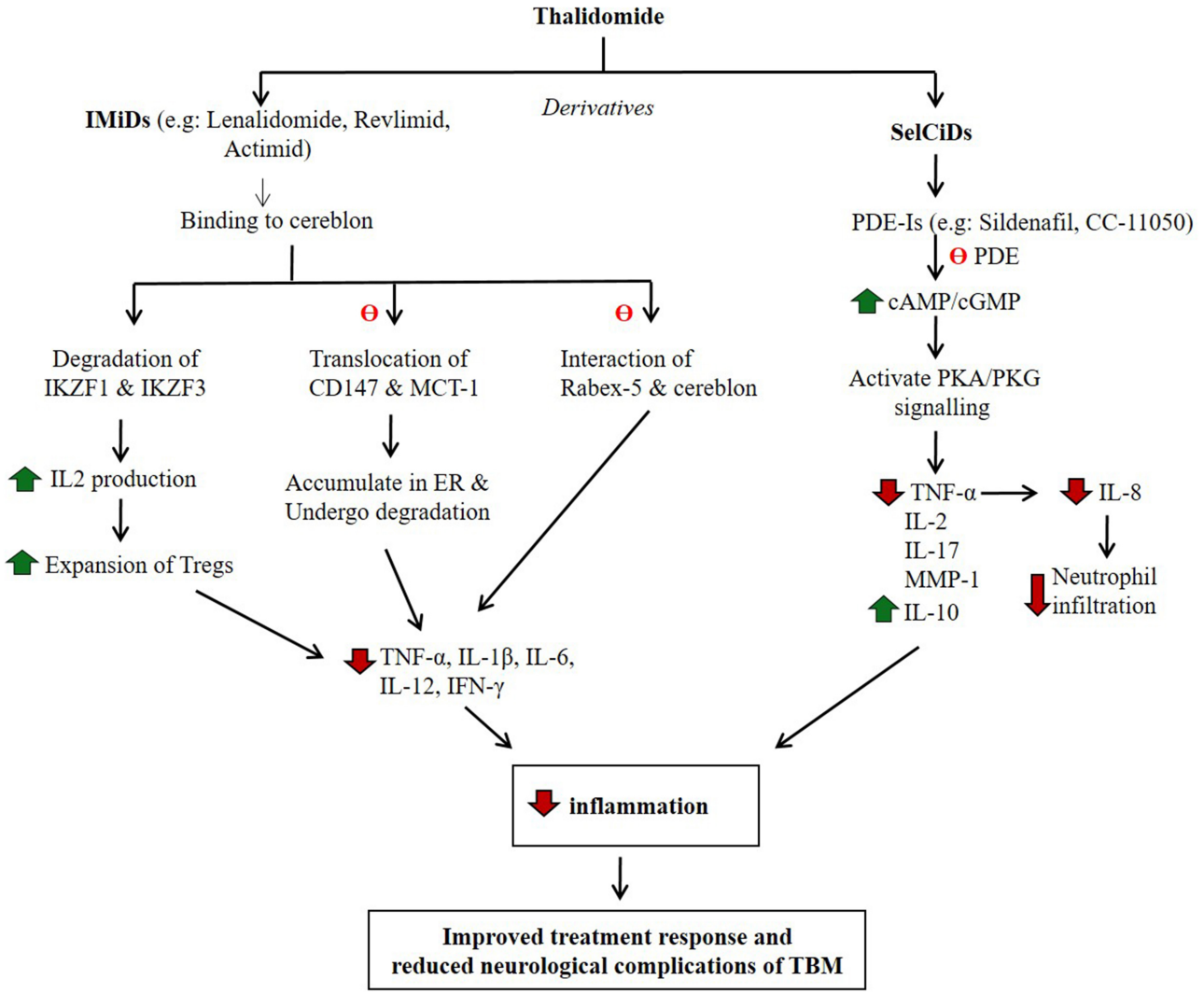

FIGURE 2 | Potential mode of action of thalidomide and its derivatives in regulating host inflammatory response. IMiDs and SelCiDs are derivatives of thalidomide with anti-inflammatory properties. However, compounds of these two classes of anti-inflammatory agents function differentially as shown. Red arrow indicates down-regulation and green arrow indicate up-regulation. θ indicates inhibition of the pathway.

respectively, and thereby modulate many physiological functions, including cell proliferation and differentiation, inflammation, and several metabolic pathways (Keravis and Lugnier, 2012). Inhibition of PDE4, the predominant PDE of monocytes and macrophages, results in dampening of the overly aggressive inflammatory responses in diverse diseases, including chronic obstructive pulmonary disease (COPD), asthma, pulmonary fibrosis, psoriatic arthritis, pulmonary TB, and others (Maurice et al., 2014). In both the mouse and rabbit models of pulmonary TB, administration of adjunctive PDE4 inhibitors (PDE4i), including CC-3052 and CC-11050, significantly reduced the bacillary load, macrophage activation, and the expression of pro-inflammatory molecules in the lungs (Koo et al., 2011; Subbian et al., 2011a,b, 2016a,b). Animals treated with PDE4i in combination with antibiotics showed accelerated clearance of Mtb infection, reduced fibrosis and reduction in lung granuloma size and numbers (Koo et al., 2011; Subbian et al., 2011a,b, 2016a,b). Similarly, another study reported that the PDE4i roflumilast and rolipram decreased the production of TNF-α, IL-6, CXCL1, and CXCL2/3, thus controlling neutrophil infiltration and subsequent lung inflammation in a rabbit model of pulmonary TB (Konrad et al., 2015). The efficacy of PDE4i, while evaluated extensively in preclinical models as well as in humans with newly diagnosed pulmonary TB and patients with ENL, has not been tested as adjunctive therapy for TBM.

CONCLUSION

Since TBM continues to have an unacceptably high morbidity and mortality rate, particularly in young children, there is an

urgent need for new, efficient adjunctive therapies for this devastating manifestation of TB. Results from the published literature suggest that the rabbit model of TBM can provide a useful tool for expanding our understanding of the pathologic process of CNS infection and disease. This preclinical model can facilitate the selection of optimal candidate adjunctive therapies to control the disease and improve the outcome of Mtb infection in the CNS of humans. The safety profile of PDE4i, described in this review, and their selective inhibition of monocyte-derived TNF-α, identify them as potantially efficacious adjunctive drugs to be used with antibiotics for the successful treatment of human TBM.

AUTHOR CONTRIBUTIONS

CV and SS conceived the concept. GK and SS designed the framework. RK, PS, AK, CV, GK, and SS wrote the manuscript. CV, GK, and SS edited the manuscript. All authors have read and agreed to publish the manuscript.

ACKNOWLEDGMENTS

The authors acknowledge the Celgene Global Health team and Dr. Vikram Khetani for their valuable discussions on thalidomide analogs.

REFERENCES

Bartlett, J. B., Dredge, K., and Dalgleish, A. G. (2004). The evolution of thalidomide and its IMiD derivatives as anticancer agents. *Nat. Rev. Cancer* 4, 314–322. doi: 10.1038/nrc1323

Caraffa, E., Russo, G., Vita, S., Lichtner, M., Massetti, A. P., Mastroianni, C. M., et al. (2018). Intracranial tuberculous mass lesions treated with thalidomide in an immunocompetent child from a low tuberculosis endemic country: a case report. *Medicine* 97:e11186. doi: 10.1097/MD.0000000000011186

Corral, L. G., and Kaplan, G. (1999). Immunomodulation by thalidomide and thalidomide analogues. *Ann. Rheum. Dis.* 58(Suppl. 1), I107–113. doi: 10.1136/ard.58.2008.i107

Corral, L. G., Muller, G. W., Moreira, A. L., Chen, Y., Wu, M., et al. (1996). Selection of novel analogues of thalidomide with enhanced TNF-α inhibitory activity. *Mol. Med.* 2, 506–515.

Curto, M., Reali, C., Palmieri, G., Scintu, F., Schivo, M. L., Sogos, V., et al. (2004). Inhibition of cytokines expression in human microglia infected by virulent and non-virulent mycobacteria. *Neurochem. Int.* 44, 381–392. doi: 10.1016/j.neuint.2003.08.012

Dastur, D. K., Manghani, D. K., and Udani, P. M. (1995). Pathology and pathogenetic mechanisms in neurotuberculosis. *Radiol. Clin. North Am.* 33, 733–752.

Davis, A. G., Rohlwink, U. K., Proust, A., Figaji, A. A., and Wilkinson, R. J. (2019). The pathogenesis of tuberculous meningitis. *J. Leukoc. Biol.* 105, 267–280. doi: 10.1002/JLB.MR0318-102R

Donald, P. R., Schoeman, J. F., Beyers, N., Nel, E. D., Carlini, S. M., Olsen, K. D., et al. (1995). Concentrations of interferon gamma, tumor necrosis factor alpha, and interleukin-1 beta in the cerebrospinal fluid of children treated for tuberculous meningitis. *Clin. Infect. Dis.* 21, 924–929. doi: 10.1093/clinids/21.4.924

Dube, M. P., Holtom, P. D., and Larsen, R. A. (1992). Tuberculous meningitis in patients with and without human immunodeficiency virus infection. *Am. J. Med.* 93, 520–524. doi: 10.1016/0002-9343(92)90579-Z

Ducomble, T., Tolksdorf, K., Karagiannis, I., Hauer, B., Brodhun, B., Haas, W., et al. (2013). The burden of extrapulmonary and meningitis tuberculosis: an investigation of national surveillance data, Germany, 2002 to 2009. *Euro Surveill.* 18:20436.

Farer, L. S., Lowell, A. M., and Meador, M. P. (1979). Extrapulmonary tuberculosis in the United States. *Am. J. Epidemiol.* 109, 205–217. doi: 10.1093/oxfordjournals.aje.a112675

Garg, R. K., Malhotra, H. S., and Kumar, N. (2014). Paradoxical reaction in HIV negative tuberculous meningitis. *J. Neurol. Sci.* 340, 26–36. doi: 10.1016/j.jns.2014.03.025

Gordon, J. N., and Goggin, P. M. (2003). Thalidomide and its derivatives: emerging from the wilderness. *Postgrad. Med. J.* 79, 127–132. doi: 10.1136/pmj.79.929.127

Haslett, P. A., Corral, L. G., Albert, M., and Kaplan, G. (1998). Thalidomide costimulates primary human T lymphocytes, preferentially inducing proliferation, cytokine production, and cytotoxic responses in the CD8+ subset. *J. Exp. Med.* 187, 1885–1892. doi: 10.1084/jem.187.11.1885

Haslett, P. A., Klausner, J. D., Makonkawkeyoon, S., Moreira, A., Metatratip, P., Boyle, B., et al. (1999). Thalidomide stimulates T cell responses and interleukin 12 production in HIV-infected patients. *AIDS Res. Hum. Retroviruses* 15, 1169–1179. doi: 10.1089/088922299310269

Haslett, P. A. J., Roche, P., Butlin, R., Macdonald, M., Shrestha, N., Manandhar, R., et al. (2005). Effective treatment of erythema nodosum leprosum with thalidomide is associated with immune stimulation. *J. Infect. Dis.* 192, 2045–2053. doi: 10.1086/498216

Heemskerk, A. D., Bang, N. D., Mai, N. T., Chau, T. T., Phu, N. H., Loc, P. P., et al. (2016). Intensified antituberculosis therapy in adults with tuberculous meningitis. *N. Engl. J. Med.* 374, 124–134. doi: 10.1056/NEJMoa1507062

Kasahara, M. (1924). The Production of tuberculous meningitis in the rabbit and the changes in its cerebrospinal fluid. *Am. J. Dis. Child.* 27, 428–432. doi: 10.1001/archpedi.1924.01920110009002

Keddie, S., Bharambe, V., Jayakumar, A., Shah, A., Sanchez, V., Adams, A., et al. (2018). Clinical perspectives into the use of thalidomide for central nervous system tuberculosis. *Eur. J. Neurol.* 25, 1345–1351. doi: 10.1111/ene.13732

Keifer, J. A., Guttridge, D. C., Ashburner, B. P., and Baldwin, A. S. Jr. (2001). Inhibition of NF-kappa B activity by thalidomide through suppression of IkappaB kinase activity. *J. Biol. Chem.* 276, 22382–22387. doi: 10.1074/jbc.M100938200

Keravis, T., and Lugnier, C. (2012). Cyclic nucleotide phosphodiesterase (PDE) isozymes as targets of the intracellular signalling network: benefits of PDE inhibitors in various diseases and perspectives for future therapeutic developments. *Br. J. Pharmacol.* 165, 1288–1305. doi: 10.1111/j.1476-5381.2011.01729.x

Konrad, F. M., Bury, A., Schick, M. A., Ngamsri, K. C., and Reutershan, J. (2015). The unrecognized effects of phosphodiesterase 4 on epithelial cells in pulmonary inflammation. *PLoS ONE* 10:e0121725. doi: 10.1371/journal.pone.0121725

Koo, M. S., Manca, C., Yang, G., O'Brien, P., Sung, N., Tsenova, L., et al. (2011). Phosphodiesterase 4 inhibition reduces innate immunity and improves isoniazid clearance of *Mycobacterium tuberculosis* in the lungs of infected mice. *PLoS ONE* 6:e17091. doi: 10.1371/journal.pone.0017091

Krishnan, N., Robertson, B. D., and Thwaites, G. (2010). The mechanisms and consequences of the extra-pulmonary dissemination of *Mycobacterium tuberculosis*. *Tuberculosis* 90, 361–366. doi: 10.1016/j.tube.2010.08.005

Marais, S., Thwaites, G., Schoeman, J. F., Torok, M. E., Misra, U. K., Prasad, K., et al. (2010). Tuberculous meningitis: a uniform case definition for use in clinical research. *Lancet Infect. Dis.* 10, 803–812. doi: 10.1016/S1473-3099(10)70138-9

Marriott, J. B., Muller, G., Stirling, D., and Dalgleish, A. G. (2001). Immunotherapeutic and antitumour potential of thalidomide analogues. *Expert Opin. Biol. Ther.* 1, 675–682. doi: 10.1517/14712598.1.4.675

Maurice, D. H., Ke, H., Ahmad, F., Wang, Y., Chung, J., and Manganiello, V. C. (2014). Advances in targeting cyclic nucleotide phosphodiesterases. *Nat. Rev. Drug Discov.* 13, 290–314. doi: 10.1038/nrd4228

Melchert, M., and List, A. (2007). The thalidomide saga. *Int. J. Biochem. Cell Biol.* 39, 1489–1499. doi: 10.1016/j.biocel.2007.01.022

Millrine, D., and Kishimoto, T. (2017). A brighter side to thalidomide: its potential use in immunological disorders. *Trends Mol. Med.* 23, 348–361. doi: 10.1016/j.molmed.2017.02.006

Misra, U. K., Kalita, J., and Nair, P. P. (2010). Role of aspirin in tuberculous meningitis: a randomized open label placebo controlled trial. *J. Neurol. Sci.* 293, 12–17. doi: 10.1016/j.jns.2010.03.025

Moreira, A. L., Sampaio, E. P., Zmuidzinas, A., Frindt, P., Smith, K. A., and Kaplan, G. (1993). Thalidomide exerts its inhibitory action on tumor necrosis

factor alpha by enhancing mRNA degradation. *J. Exp. Med.* 177, 1675–1680. doi: 10.1084/jem.177.6.1675

Muller, G. W., Chen, R., Huang, S.-Y., Corral, L. G., Wong, L. M., Patterson, R. T., et al. (1999). Amino-substituted thalidomide analogues: potent inhibitors of TNF-α production. *Bioorg. Med. Chem. Lett.* 9, 1625–1630. doi: 10.1016/s0960-894x(99)00250-4

Muller, G. W., Corral, L. G., Shire, M. G., Wang, H., Moreira, A., Kaplan, G., et al. (1996). Structural modifications of thalidomide produce analogs with enhanced TNF inhibitory activity. *J. Med. Chem.* 39, 3238–3240. doi: 10.1021/jm9603328

Nguyen, T. H., Tran, T. H., Thwaites, G., Ly, V. C., Dinh, X. S., Ho Dang, T. N., et al. (2007). Dexamethasone in Vietnamese adolescents and adults with bacterial meningitis. *N. Engl. J. Med.* 357, 2431–2440. doi: 10.1056/NEJMoa070852

Prasad, K., Singh, M. B., and Ryan, H. (2016). Corticosteroids for managing tuberculous meningitis. *Cochrane Database Syst. Rev.* 4:CD002244. doi: 10.1002/14651858.CD002244.pub4

Rich, A. R., and McCordock, H. A. (1933). The pathogenesis of tuberculous meningitis. *Bull. John Hopkins Hosp.* 52, 5–7.

Rizvi, I., Garg, R. K., Malhotra, H. S., Kumar, N., and Uniyal, R. (2019). Role of aspirin in tuberculous meningitis: a systematic review and meta-analysis. *Neurol. India* 67, 993–1002. doi: 10.4103/0028-3886.266232

Roberts, M. T., Mendelson, M., Meyer, P., Carmichael, A., and Lever, A. M. (2003). The use of thalidomide in the treatment of intracranial tuberculomas in adults: two case reports. *J. Infect.* 47, 251–255. doi: 10.1016/S0163-4453(03)00077-X

Rock, R. B., Olin, M., Baker, C. A., Molitor, T. W., and Peterson, P. K. (2008). Central nervous system tuberculosis: pathogenesis and clinical aspects. *Clin. Microbiol. Rev.* 21, 243–261. doi: 10.1128/CMR.00042-07

Sampaio, E. P., Kaplan, G., Miranda, A., Nery, J. A., Miguel, C. P., Viana, S. M., et al. (1993). The influence of thalidomide on the clinical and immunologic manifestation of erythema nodosum leprosum. *J. Infect. Dis.* 168, 408–414. doi: 10.1093/infdis/168.2.408

Sampaio, E. P., Sarno, E. N., Galilly, R., Cohn, Z. A., and Kaplan, G. (1991). Thalidomide selectively inhibits tumor necrosis factor alpha production by stimulated human monocytes. *J. Exp. Med.* 173, 699–703. doi: 10.1084/jem.173.3.699

Schoeman, J. F., Andronikou, S., Stefan, D. C., Freeman, N., and van Toorn, R. (2010). Tuberculous meningitis-related optic neuritis: recovery of vision with thalidomide in 4 consecutive cases. *J. Child Neurol.* 25, 822–828. doi: 10.1177/0883073809350507

Schoeman, J. F., Janse van Rensburg, A., Laubscher, J. A., and Springer, P. (2011). The role of aspirin in childhood tuberculous meningitis. *J. Child Neurol.* 26, 956–962. doi: 10.1177/0883073811398132

Schoeman, J. F., Springer, P., Ravenscroft, A., Donald, P. R., Bekker, L. G., van Rensburg, A. J., et al. (2000). Adjunctive thalidomide therapy of childhood tuberculous meningitis: possible anti-inflammatory role. *J. Child Neurol.* 15, 497–503. doi: 10.1177/088307380001500801

Schoeman, J. F., Springer, P., van Rensburg, A. J., Swanevelder, S., Hanekom, W. A., Haslett, P. A., et al. (2004). Adjunctive thalidomide therapy for childhood tuberculous meningitis: results of a randomized study. *J. Child Neurol.* 19, 250–257. doi: 10.1177/088307380401900402

Schoeman, J. F., Van Zyl, L. E., Laubscher, J. A., and Donald, P. R. (1997). Effect of corticosteroids on intracranial pressure, computed tomographic findings, and clinical outcome in young children with tuberculous meningitis. *Pediatrics* 99, 226–231. doi: 10.1542/peds.99.2.226

Subbian, S., Koo, M. S., Tsenova, L., Khetani, V., Zeldis, J. B., Fallows, D., et al. (2016a). Pharmacologic inhibition of host phosphodiesterase-4 improves isoniazid-mediated clearance of *Mycobacterium tuberculosis*. *Front. Immunol.* 7:238. doi: 10.3389/fimmu.2016.00238

Subbian, S., Tsenova, L., Holloway, J., Peixoto, B., O'Brien, P., Dartois, V., et al. (2016b). Adjunctive phosphodiesterase-4 inhibitor therapy improves antibiotic response to pulmonary tuberculosis in a rabbit model. *EBiomedicine* 4, 104–114. doi: 10.1016/j.ebiom.2016.01.015

Subbian, S., Tsenova, L., O'Brien, P., Yang, G., Koo, M. S., Peixoto, B., et al. (2011a). Phosphodiesterase-4 inhibition alters gene expression and improves isoniazid-mediated clearance of *Mycobacterium tuberculosis* in rabbit lungs. *PLoS Pathog.* 7:e1002262. doi: 10.1371/journal.ppat.1002262

Subbian, S., Tsenova, L., O'Brien, P., Yang, G., Koo, M. S., Peixoto, B., et al. (2011b). Phosphodiesterase-4 inhibition combined with isoniazid treatment of rabbits with pulmonary tuberculosis reduces macrophage activation and lung pathology. *Am. J. Pathol.* 179, 289–301. doi: 10.1016/j.ajpath.2011.03.039

Thwaites, G., Chau, T. T., Mai, N. T., Drobniewski, F., McAdam, K., and Farrar, J. (2000). Tuberculous meningitis. *J. Neurol. Neurosurg. Psychiatr.* 68, 289–299. doi: 10.1136/jnnp.68.3.289

Thwaites, G. E., Duc Bang, N., Huy Dung, N., Thi Quy, H., Thi Tuong Oanh, D., Thi Cam Thoa, N., et al. (2005). The influence of HIV infection on clinical presentation, response to treatment, and outcome in adults with Tuberculous meningitis. *J. Infect. Dis.* 192, 2134–2141. doi: 10.1086/498220

Thwaites, G. E., Nguyen, D. B., Nguyen, H. D., Hoang, T. Q., Do, T. T., Nguyen, T. C., et al. (2004). Dexamethasone for the treatment of tuberculous meningitis in adolescents and adults. *N. Engl. J. Med.* 351, 1741–1751. doi: 10.1056/NEJMoa040573

Torok, M. E. (2015). Tuberculous meningitis: advances in diagnosis and treatment. *Br. Med. Bull.* 113, 117–131. doi: 10.1093/bmb/ldv003

Tramontana, J. M., Utaipat, U., Molloy, A., Akarasewi, P., Burroughs, M., Makonkawkeyoon, S., et al. (1995). Thalidomide treatment reduces tumor necrosis factor alpha production and enhances weight gain in patients with pulmonary tuberculosis. *Mol. Med.* 1, 384–397. doi: 10.1007/BF03401576

Tsenova, L., Bergtold, A., Freedman, V. H., Young, R. A., and Kaplan, G. (1999). Tumor necrosis factor alpha is a determinant of pathogenesis and disease progression in mycobacterial infection in the central nervous system. *Proc. Natl. Acad. Sci. U.S.A.* 96, 5657–5662. doi: 10.1073/pnas.96.10.5657

Tsenova, L., Ellison, E., Harbacheuski, R., Moreira, A. L., Kurepina, N., Reed, M. B., et al. (2005). Virulence of selected *Mycobacterium tuberculosis* clinical isolates in the rabbit model of meningitis is dependent on phenolic glycolipid produced by the bacilli. *J. Infect. Dis.* 192, 98–106. doi: 10.1086/430614

Tsenova, L., Harbacheuski, R., Moreira, A. L., Ellison, E., Dalemans, W., Alderson, M. R., et al. (2006). Evaluation of the Mtb72F polyprotein vaccine in a rabbit model of tuberculous meningitis. *Infect Immun.* 74, 2392–401. doi: 10.1128/IAI.74.4.2392-2401.2006

Tsenova, L., Mangaliso, B., Muller, G., Chen, Y., Freedman, V. H., Stirling, D., et al. (2002). Use of IMiD3, a thalidomide analog, as an adjunct to therapy for experimental tuberculous meningitis. *Antimicrob. Agents Chemother.* 46, 1887–1895. doi: 10.1128/AAC.46.6.1887-1895.2002

Tsenova, L., Sokol, K., Freedman, V. H., and Kaplan, G. (1998). A combination of thalidomide plus antibiotics protects rabbits from mycobacterial meningitis-associated death. *J. Infect. Dis.* 177, 1563–1572. doi: 10.1086/515327

Tucker, E. W., Guglieri-Lopez, B., Ordonez, A. A., Ritchie, B., Klunk, M. H., Sharma, R., et al. (2018). Noninvasive (11)C-rifampin positron emission tomography reveals drug biodistribution in tuberculous meningitis. *Sci. Transl. Med.* 10:eaau0965. doi: 10.1126/scitranslmed.aau0965

Tucker, E. W., Pokkali, S., Zhang, Z., DeMarco, V. P., Klunk, M., Smith, E. S., et al. (2016). Microglia activation in a pediatric rabbit model of tuberculous meningitis. *Dis. Model. Mech.* 9, 1497–1506. doi: 10.1242/dmm.027326

Uhlin, M., Andersson, J., Zumla, A., and Maeurer, M. (2012). Adjunct immunotherapies for tuberculosis. *J. Infect. Dis.* 205(Suppl. 2), S325–S334. doi: 10.1093/infdis/jis197

van Laarhoven, A., Dian, S., van Dorp, S., Purnama, F., Koeken, V., Diandini, E., et al. (2019). Immune cell characteristics and cytokine responses in adult HIV-negative tuberculous meningitis: an observational cohort study. *Sci. Rep.* 9:884. doi: 10.1038/s41598-018-36696-3

Wasserman, S., Davis, A., Wilkinson, R. J., and Meintjes, G. (2019). Key considerations in the pharmacotherapy of tuberculous meningitis. *Expert Opin. Pharmacother.* 20, 1791–1795. doi: 10.1080/14656566.2019.1638912

Wilkinson, R. J., Rohlwink, U., Misra, U. K., van Crevel, R., Mai, N. T. H., Dooley, K. E., et al. (2017). Tuberculous meningitis. *Nat. Rev. Neurol.* 13, 581–598. doi: 10.1038/nrneurol.2017.120

Conflict of Interest: GK was a member of the board of directors of Celgene corporation from 1998-2018.

The remaining authors declare that the research was conducted in the absence of any commercial or financial relationships that could be construed as a potential conflict of interest.

frontiers in Immunology

ORIGINAL RESEARCH
published: 24 January 2020
doi: 10.3389/fimmu.2019.03103

Interleukin-2-Inducible T-Cell Kinase Deficiency Impairs Early Pulmonary Protection Against *Mycobacterium tuberculosis* Infection

Lu Huang[1], Kaixiong Ye[2,3], Michael C. McGee[4], Natalie F. Nidetz[4], Jessica P. Elmore[1], Candice B. Limper[1], Teresa L. Southard[5], David G. Russell[1], Avery August[1] and Weishan Huang[1,4]**

[1] Department of Microbiology and Immunology, College of Veterinary Medicine, Cornell University, Ithaca, NY, United States, [2] Department of Genetics, University of Georgia, Athens, GA, United States, [3] Institute of Bioinformatics, University of Georgia, Athens, GA, United States, [4] Department of Pathobiological Sciences, School of Veterinary Medicine, Louisiana State University, Baton Rouge, LA, United States, [5] Department of Biomedical Sciences, College of Veterinary Medicine, Cornell University, Ithaca, NY, United States

OPEN ACCESS

Edited by:
Igor Kramnik,
Boston University, United States

Reviewed by:
Chinnaswamy Jagannath,
University of Texas Health Science Center at Houston, United States
António Gil Castro,
University of Minho, Portugal

***Correspondence:**
Avery August
averyaugust@cornell.edu
Weishan Huang
huang1@lsu.edu

Specialty section:
This article was submitted to T Cell Biology, a section of the journal Frontiers in Immunology

Received: 30 October 2019
Accepted: 19 December 2019
Published: 24 January 2020

Citation:
Huang L, Ye K, McGee MC, Nidetz NF, Elmore JP, Limper CB, Southard TL, Russell DG, August A and Huang W (2020) Interleukin-2-Inducible T-Cell Kinase Deficiency Impairs Early Pulmonary Protection Against Mycobacterium tuberculosis Infection. Front. Immunol. 10:3103. doi: 10.3389/fimmu.2019.03103

Interleukin-2 (IL-2) inducible T-cell kinase (ITK) is a non-receptor tyrosine kinase highly expressed in T-cell lineages and regulates multiple aspects of T-cell development and function, mainly through its function downstream of the T-cell receptor. *Itk* deficiency can lead to CD4 lymphopenia and Epstein-Bar virus (EBV)-associated lymphoproliferation and recurrent pulmonary infections in humans. However, the role of the ITK signaling pathway in pulmonary responses in active tuberculosis due to *Mtb* infection is not known. We show here that human lungs with active tuberculosis exhibit altered T-cell receptor/ITK signaling and that *Itk* deficiency impaired early protection against *Mtb* in mice, accompanied by defective development of IL-17A-producing γδ T cells in the lungs. These findings have important implications of human genetics associated with susceptibility to *Mtb* due to altered immune responses and molecular signals modulating host immunity that controls *Mtb* activity. Enhancing ITK signaling pathways may be an alternative strategy to target *Mtb* infection, especially in cases with highly virulent strains in which IL-17A plays an essential protective role.

Keywords: active tuberculosis, transcriptomic analysis, non-receptor tyrosine kinase, IL-17A, IFN-γ, γδ T cells

INTRODUCTION

Mycobacterium tuberculosis (*Mtb*) is the causative agent of what remains one of the most insidious and invasive human infections, responsible for millions of cases of active lung diseases and deaths per year in the world [WHO Global Tuberculosis Report, (1) and O'Garra et al. (2)]. The immune responses by macrophages, neutrophils, and T-cell populations contribute to protective immunity controlling *Mtb* expansion in the host and transmission to others (2, 3). Genetic and environmental factors of the host associated with primary and acquired immunodeficiency can lead to an increased risk of developing active tuberculosis that presents severe pulmonary illness in the clinic (2, 4). Our knowledge of the molecular pathways of innate and adaptive immune effector functions remains incomplete, and a better understanding of potential host factors underlying the pulmonary complications could lead to the development of more innovative therapeutic strategies.

Interleukin-2 (IL-2)-inducible T-cell kinase (ITK) is a non-receptor tyrosine kinase highly expressed in T cells. ITK functions downstream of the T-cell receptor (TCR) and regulates multiple aspects of T-cell development and function (5). *ITK* deficiency in humans is associated with primary immunodeficiency, progressive natural killer T (NKT) and $CD4^+$ T-cell lymphopenia, elevated susceptibility to Epstein-Bar virus (EBV), and EBV-driven lymphoproliferative diseases, in which frequent pulmonary involvement has emerged as a clinical hallmark (6–13). Recurrent progressive pulmonary infection, airway obstruction, and respiratory failure in *ITK*-deficient patients pose significant threats that can eventually result in deaths of the patients at their early ages (12). Human T cells from patients with *ITK* deficiency exhibit impaired responses to TCR activation, with reduced generation of Th17 cells and production of the associated cytokines IL-17A, IL-22, and granulocyte-macrophage colony-stimulating factor (14). A murine model of *Itk* deficiency reveals a similar NKT and T-cell lymphopenia as observed in human patients with *ITK* deficiency. Mice lacking *Itk* have a marked reduction in NKT cells (15–18). Despite relatively normal number (trending the lower range) of $CD8^+$ αβ T cells, $Itk^{-/-}$ mice exhibited $CD4^+$ αβ T-cell lymphopenia, with reduced proportion of naive and increased memory αβ T cells (19–31). In the absence of *Itk*, mouse $CD4^+$ T cells are impaired in Th2 (producing IL-4/5/13) (32–38), Th9 (producing IL-9) (39), Th17 (producing IL-17) (35, 40–42), and Tr1 (producing IL-10) cell responses (43), while they are enhanced in Th1 (producing IFN-γ) cell response (32, 34, 38, 44, 45). Analysis of $Itk^{-/-}$ mice also reveals altered γδ T-cell development (46–49); however, the presence and function of γδ T cells has not been evaluated in *ITK*-deficient humans.

Epidemiological analysis of single-nucleotide polymorphism has also revealed a connection between greater *ITK* promoter activity and higher risk of asthmatic incidence in humans, which might be associated with the function of ITK in promoting T-cell activation (50). In murine models of allergic asthma, the expression of ITK is critical for the activation and development of Th2 and Th17 cells and the associated airway and tracheal inflammation (40, 51). Interestingly, a genome-wide association study of susceptibility to *Mycobacterium avium* subspecies *paratuberculosis* in Holstein cattle identified chromosomal regions that included the *ITK* gene (52). However, the role of ITK signaling pathway in pulmonary responses in active tuberculosis due to *Mtb* infection is unknown.

Here, we show that the TCR/ITK signaling pathway is enriched in human lungs with active tuberculosis and that *Itk* deficiency impaired early protection against *Mtb* in mice, accompanied by defective development of IL-17A-producing γδ T cells in the lungs. Furthermore, ITK appears to regulate the dynamics of lung myeloid cells, which may further contribute to immune control of *Mtb* at the early stage of infection.

Abbreviations: CFU, colony-forming unit; GSEA, gene set enrichment analysis; ITK, IL-2-inducible T-cell kinase; *Mtb*, *Mycobacterium tuberculosis*; NK, natural killer; TCR, T-cell receptor; Treg cells, Foxp3-expressing regulatory T cells.

MATERIALS AND METHODS

Mice

All mice were on the C57BL/6 background. Both female and male mice at the age of 6–12 weeks were used. All experiments were approved by the Office of Research Protections Institutional Animal Care and Use Committee at Cornell University.

Microarray and Data Analyses

Microarray data from lung normal tissue and caseous granulomas from active tuberculosis (TB) patient was generated as previously described (53, 54). Microarray data is available in the Gene Expression Omnibus under accession number GSE20050. In brief, tissues were fixed, and areas of interest were dissected using laser capture microdissection on the Leica AS LMD system (Leica, Buffalo Grove, IL). Total RNA was isolated and used on the GeneChip Human X3P Array (Affymetrix, Santa Clare, CA) following the manufacturer's instruction. Data analysis was performed in R (version 3.5.3) and Bioconductor (version 3.8). Probe intensities were $\log_2$ transformed and median centered. Differentially expressed genes were identified with limma (version 3.38.3) (55). In the case of multiple probes mapped to a gene, the probe with the maximum fold change was selected to represent the gene. Gene set enrichment analyses (GSEA) to determine over- and underrepresented gene sets were performed using the Kyoto Encyclopedia of Genes and Genomes pathway database as reference in gage (version 2.32.1) (56). All pathways that exhibited an up- or downregulated trend in caseum samples compared to normal tissues are summarized in the Supplementary Material (**Supplementary Table 1**). Enrichment score and core genes that drive the score are determined using the GSEA platform developed by the Broad Institute (57). Visualization of TCR signaling pathway with differential gene expression was performed in pathview (version 1.22.3) (**Supplementary Figure 1**) (58).

Mtb Infection and Colony-Forming Unit Counts

Mice were inoculated intranasally with ∼1,000 CFUs of Erdman *Mtb* constitutively expressing mCherry (mCherry-*Mtb*) (59) in 25 μl of phosphate-buffered saline (PBS) containing 0.05% Tween-80. Mice were euthanized after 2 and 4 weeks of infection. The left lung lobe and the accessory lobe of the right lung were removed and homogenized in PBS containing 0.05% Tween-80. Bacterial loads were determined by plating serial dilutions of the homogenates on 7H10 agar plates.

Histology and Pathogenic Scoring

Lung samples were fixed in 4% paraformaldehyde overnight, followed by hematoxylin and eosin (H&E) staining. Histological images were analyzed using DP2-BSW software (Olympus, Waltham, MA) to quantify the percentage of affected tissue area and score the severity of pathology (60).

Isolation of Lung Cells

Mice were euthanized at the indicated time points, and lungs were aseptically removed. To obtain a single-cell suspension, lungs were minced and digested in 5% fetal bovine serum/PBS solution containing 250 U/ml collagenase IV (Worthington, Lakewood, NJ) and 20 U/ml DNase (Roche, Indianapolis, IN) for 30 min at 37°C. Lung digestions were then passed through a 70-μm cell strainer, and red blood cells were lysed with ammonium-chloride-potassium buffer.

Fluorescent Mouse Antibodies

Fluorescent antibodies are listed in the format of "Fluorophore-target (clone)": eFluor 450-CD4 (GK1.5), Phycoerythrin (PE)-Foxp3 (FJK-16s), PE-eFluor 610-NK1.1 (PK136), allophycocyanin (APC)-IL-17A (eBio17B7), APC-CD11c (N418), PerCP-eFluor 710-CD49b (DX5), PE-Cy7-NK1.1 (PK136), PE-Cy7-IFN-γ (XMG1.2), and APC-eFluor 780-MHCII (M5/114.15.2) were from eBioscience (San Diego, CA). CD16/32 (93; i.e., Fc block), Brilliant Violet 421-CD64 (X54-5/7.1), Alexa Fluor 488-TCRγδ (GL3), and APC-Cy7-TCRβ (H57-597) were from BioLegend (San Diego, CA). FITC-Ly6G (1A8), PE-Siglec-F (E50-2440), PE-TNF-α (MP6-XT22), PE-CF594 CD8α (53-6.7), Alexa Fluor 700-Ki67 (B56), PerCP-Cy5.5-CD8α (53-6.7), and PerCP-Cy5.5-CD11b (M1/70) were from BD Biosciences (San Jose, CA).

T-Cell Stimulation

To activate bulk T cells, cells were stimulated with phorbol 12-myristate 13-acetate (PMA) (50 ng/ml, Sigma) and Ionomycin (0.5 μM, Sigma); to activate *Mtb*-specific $CD4^+$ T cells, cells were stimulated with ESAT-6_{4-17} peptide (MHCII-restricted presentation; synthesized by GenScript, purity > 95%; 5 μg/ml); to activate *Mtb*-specific $CD8^+$ T cells, cells were stimulated with TB10.4_{4-11} peptide (MHCI-restricted presentation; synthesized by GenScript, purity > 95%; 5 μg/ml). All stimulations were done in full RPMI-1640 media in the presence of Brefeldin A (5 μg/ml, Sigma) and Monensin (2 μM, Sigma), at 37°C for 5 h.

Flow Cytometry

Surface protein staining was done with antibodies for surface markers in PBS, in the presence of Fc Block (BioLegend) and fixable viability dye (Tonbo Biosciences). To determine cytokine production, cells were stimulated as indicated, followed by surface staining, then were fixed with 4% paraformaldehyde (Electron Microscopy Sciences, Hatfield, PA), and permeabilized and stained with antibodies in PBS containing 0.3% saponin

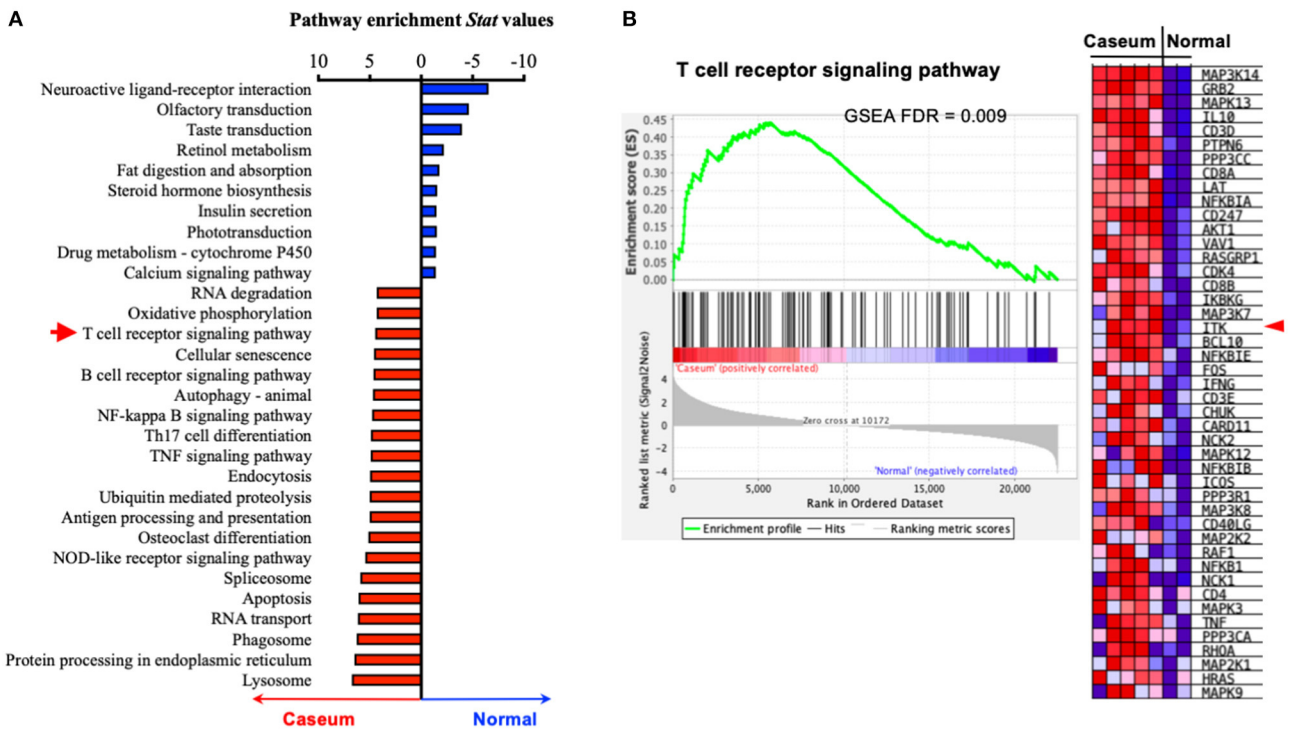

FIGURE 1 | ITK expression is altered in human lungs with active TB. **(A)** Pathway enrichment analyses of human lung tissues with active TB ("Caseum," $N = 5$), compared to normal lung tissues ("Normal," $N = 2$). Pathway enrichment statistical values were for pathways enriched in "Caseum" group were shown as positive values (upregulated in "Caseum" compared to "Normal"), while those enriched in normal lungs were shown as negative values (upregulated in "Normal" compared to "Caseum"). Twenty most enriched pathways in the "Caseum" group (out of 145 pathways with FDR < 0.05), and 10 most enriched pathways in "Normal" group (out of 11 pathways with FDR < 0.05) are shown. Red arrow indicates T-cell receptor signaling pathway. **(B)** Gene set enrichment score, profile of T-cell signaling receptor pathway and heatmap of the levels of expression of the score-driving genes in T-cell receptor signaling pathway. Red arrow indicates ITK. FDR, false discover rate.

(Sigma). To stain for nuclear transcription factors Foxp3 and Ki67, following surface staining, cells were fixed, permeabilized, and stained using Foxp3 staining buffer set (eBioscience). All flow cytometry data were acquired on LSRII (BD Biosciences) and analyzed in FlowJo (Tree Star, Ashland, OR).

Statistical Analysis

Two-tailed Student's *t*-test and two-way analysis of variance (ANOVA) between groups were performed using Prism (GraphPad, San Diego, CA), with $p < 0.05$ considered statistically significant. "NS" indicates differences that are not significant.

RESULTS

TCR/ITK Signaling Components Are Upregulated in Active Tuberculosis in Humans

The progression of human active TB disease and transmission involves the development of the caseous granuloma, in which both *Mtb* and the immune response are active (53). We have previously isolated human granulomata from patients with active TB (Caseum) and analyzed the transcriptomic profile in comparison to uninvolved lung tissue (normal) (53). Using pathway enrichment analyses, we found that genes of the TCR signaling were significantly enriched in the caseum tissue that was subjected to active TB, compared to uninvolved lung tissue (**Figure 1**). Among the enrichment score-driving critical genes of the TCR signaling, the levels of transcripts for ITK and its signaling components (5) such as LCK, GRB2, SLP76, NCK1, FYN, and PLCG are significantly upregulated in caseated granulomas compared to uninvolved lung tissue (**Figure 1B**). Among the genes that are significantly enriched in active TB, ITK locates in the hub of the TCR signaling pathway (**Supplementary Figure 1**). These data imply a role for ITK signaling in host immune activity during active TB.

Itk Deficiency Results in Impaired *Mtb* Clearance and Increased Lung Pathology

Given the observation that the TCR signaling pathway was upregulated in the face of active TB in human lungs and that ITK is a critical score-driving gene for the pathway enrichment (**Figure 1**), we sought to determine the role of ITK in host responses to *Mtb* infection. In murine models of *Itk* deficiency, despite no difference in animal mortality, we found that *Mtb* bacterial burden was significantly higher in the lungs in the absence of ITK 4 weeks post-*Mtb* infection (**Figure 2A**). Moreover, pulmonary pathology was elevated in the absence of ITK, with significantly larger areas in the airway affected at higher pathological scores (**Figure 2B**). Notably, compared to wild-type (WT) mice, the relative kinetics of bacterial growth in the lungs of $Itk^{-/-}$ and $Rag^{-/-}$ mice are similar (61, 62). These data suggest that the TCR/ITK signaling pathway regulates immune responses that contribute to limiting *Mtb* growth and controlling pulmonary inflammation 4 weeks postinfection.

Itk-Deficient Mice Exhibit Altered Early Immune Responses to *Mtb* Infection

The progression of human active TB disease and transmission involves the development of both innate and adaptive immunity. The relative abundance of lung phagocyte populations is extremely dynamic at the early stage of *Mtb* infection (63). Importantly, the various phagocytes in the lung provide different environments for *Mtb* and reveal distinct permissiveness for the growth of *Mtb* (64, 65). We thus analyzed populations of innate immune cells in both WT and *Itk*-deficient mice infected with *Mtb* that constitutively express fluorescent protein mCherry, which allows mapping of the cellular location of intracellular bacteria. During early-stage infection, we

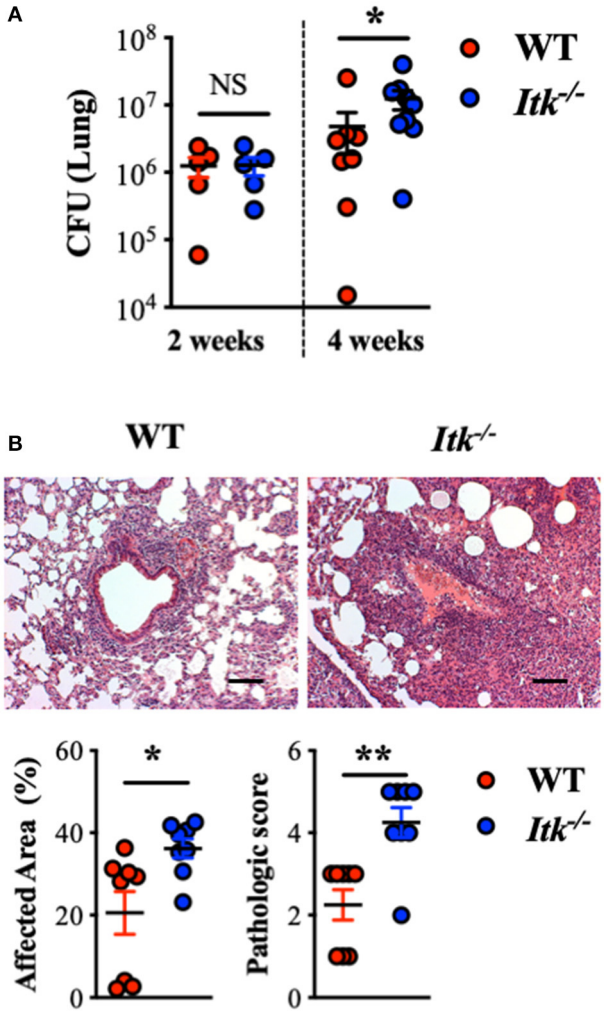

FIGURE 2 | *Itk* deficiency results in impaired bacterial clearance and increased pulmonary pathology post-*Mtb* infection in mice. WT and $Itk^{-/-}$ mice were infected with 10^3 CFU of *Mtb* (intranasal delivery) and analyzed 2 and 4 weeks postinfection. **(A)** CFU in WT and $Itk^{-/-}$ mice 2 and 4 weeks postinfection. **(B)** Representative histology, summary of affected area, and histological scoring of WT and $Itk^{-/-}$ lungs of mice 4 weeks post-*Mtb* infection. $^*p < 0.05$, $^{**}p < 0.01$ by Student's *t*-test. Scale bar = 100 μm. $N = 5$–10. Data were presented as mean ± SEM and represent results of three independent experiments.

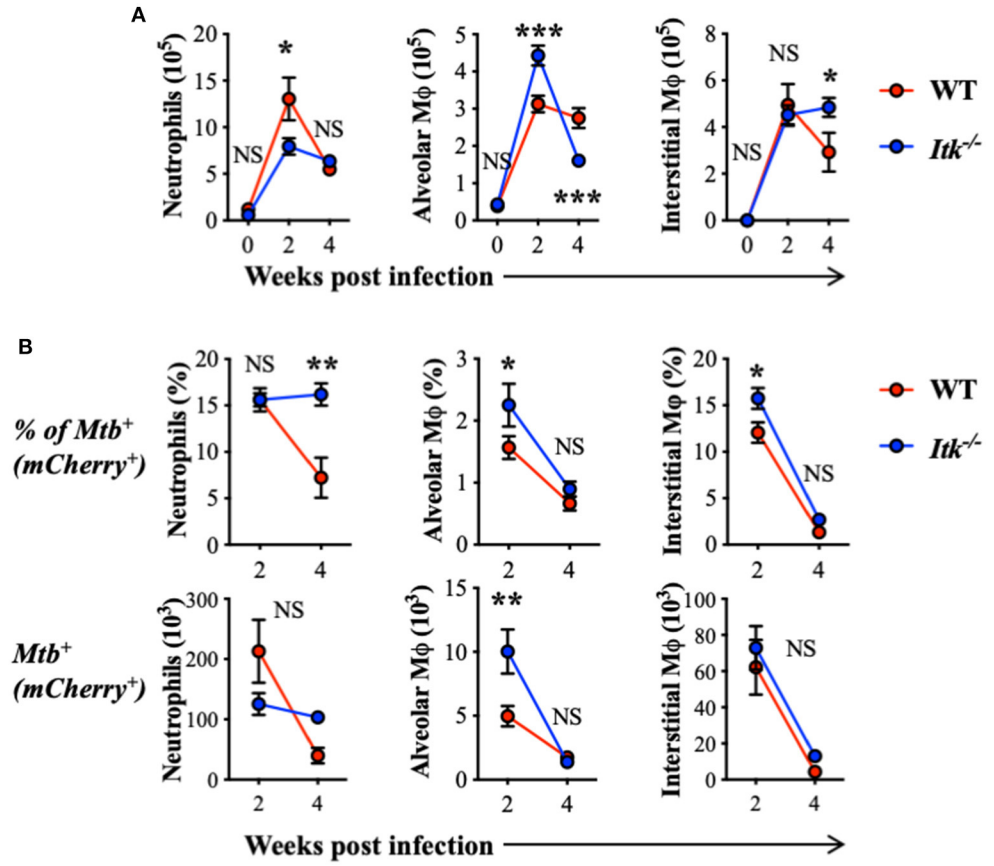

FIGURE 3 | ITK regulates innate myeloid immune response in mice during *Mtb* infection. WT and *Itk*$^{-/-}$ mice were infected with 10^3 CFU of mCherry-*Mtb*, and lungs were analyzed at the indicated time points. After gating on viable singlet cells, neutrophils (Ly6G$^+$CD11b$^+$), alveolar macrophages (Ly6G$^-$CD11c$^+$Siglec-F$^+$), and interstitial macrophages (Ly6G$^-$Siglec-F$^-$ CD11b$^+$MHCII$^+$CD64$^+$) were analyzed. **(A)** Number of total neutrophils, alveolar macrophages, and interstitial macrophages isolated from the lungs of infected mice. **(B)** Percentage and number of mCherry-*Mtb* positive neutrophils, alveolar macrophages, and interstitial macrophages in the lung of the infected mice. NS, not significant; *$p < 0.05$, **$p < 0.01$, ***$p < 0.001$ by two-way ANOVA with *post hoc* test. $N = 5$. Data were presented as mean ± SEM and represent results of three independent experiments.

observed increased total numbers of neutrophils and alveolar macrophages in the lung at 2 weeks postinfection in both WT and *Itk*$^{-/-}$ mice (**Figure 3A**). Further analysis of the pulmonary immune cell populations revealed that, in the absence of ITK, the proportion of *Mtb*-infected alveolar and interstitial macrophages was significantly higher early after infection (2 weeks); in addition, the proportion of *Mtb*-infected neutrophils was significantly higher 4 weeks after infection (**Figure 3**). Effective removal of *Mtb*-infected apoptotic neutrophils by macrophages, or efferocytosis, is considered beneficial for host defense (66). The failed clearance of infected neutrophils in *Itk*-deficient mice at 4 weeks suggests that Itk may be involved in regulating efferocytosis of lung macrophages. Both alveolar macrophages and neutrophils have been demonstrated as permissive cell types in *Mtb* infection by providing a hospitable environment for optimal bacterial growth (64, 65). The increased proportion of *Mtb*-infected neutrophils in the absence of ITK is associated with the increased bacterial burden at 4 weeks, suggesting that bacterial burden may be attributed to this difference. Therefore, these data suggest that ITK regulates the dynamic of lung phagocytes and contributes to host protection against *Mtb* infection.

ITK is highly expressed in T-cell lineages including γδ and αβ T cells. To further determine whether the absence of ITK affects T-cell and other related lymphocyte responses during *Mtb* infection, we also analyzed the abundance of γδ T cells, NK cells, NKT cells, and αβ T cells, including total αβ T cells, CD4$^+$ conventional αβ T cells, CD8$^+$ αβ T cells, and CD4$^+$ Foxp3$^+$ regulatory T (Treg) cells. Comparable numbers of γδ T cells, NKT cells, and CD8$^+$ αβ T cells were observed in WT and *Itk*-deficient mice infected with *Mtb*, while NK cells and CD4$^+$ αβ T cells were significantly increased, and Foxp3$^+$ Treg cells were significantly reduced in the absence of ITK (**Figure 4**). These results seemed surprising, as a reduced number of Treg cells accompanied by increased numbers of CD4$^+$ αβ T cells may suggest a more active immune response. The hosts' ability to limit bacterial growth and control pulmonary

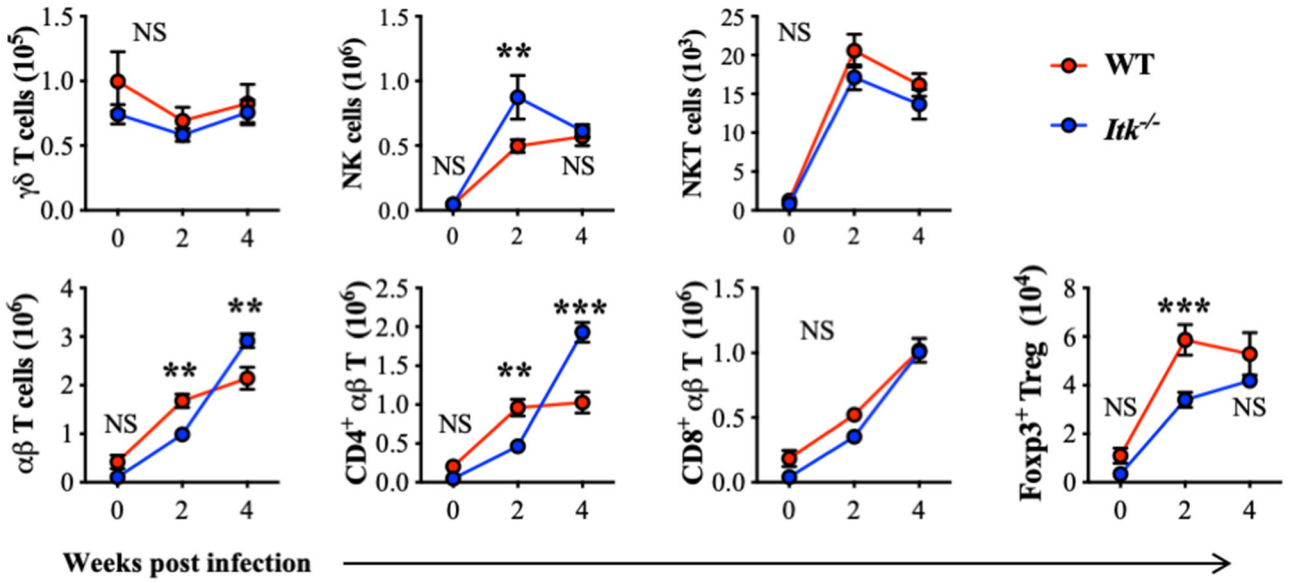

FIGURE 4 | *Itk* deficiency alters lymphocyte profile in the lung during *Mtb* infection. WT and *Itk*$^{-/-}$ mice were infected as in **Figure 3**, and lungs were analyzed at the indicated time points. After gating on viable singlet cells, lymphocytes including γδT cells (TCRγδ$^+$TCRβ$^-$), NK cells (TCRγδ$^-$TCRβ$^-$NK1.1$^+$), NKT cells (TCRγδ$^-$TCRβ$^+$NK1.1$^+$), and αβT cells (TCRγδ$^-$TCRβ$^+$), and among αβT cells, CD4$^+$ conventional T cells, CD8$^+$ cells, and CD4$^+$ Foxp3$^+$ Treg cells were analyzed. *N* = 5–9. Numbers of the indicated cell types were presented as mean ± SEM and represent results of three independent experiments. NS, not significant; $^{**}p < 0.01$, $^{***}p < 0.001$ by two-way ANOVA with *post hoc* test.

inflammation was, however, impaired in the absence of ITK. A possible explanation could be that the effector activity of the lymphocytes observed in the infected airway against *Mtb* may differ. These effector immune responses could involve innate lymphocyte activities, as well as *Mtb* antigen-specific adaptive lymphocyte functions.

ITK Is Critical for γδ T-Cell-Derived IL-17A Production During *Mtb* Infection

It has been reported that IL-17A is protective during primary infection of virulent *Mtb* (67), and IL-17A is predominantly produced by γδ T cells in the lungs early after *Mtb* infection (68). Indeed, while we detected significant IL-17A production by γδ T cells in the lungs of WT mice infected with *Mtb* (red foreground in **Figures 5A–C**), very limited IL-17A was produced by the conventional CD4$^+$ αβ Th17 cells (gray background in **Figure 5A**, as well as in **Figure 5D**). Interestingly, in the absence of ITK, there was a marked reduction in IL-17A-producing γδ T cells in the lung (**Figures 5A–C**). In contrast to the significant levels of IL-17A production in γδ T cells, IL-17A production by CD4$^+$ and CD8$^+$ αβ T cells during *Mtb* infection was minimal (**Figure 5B** vs. **Figure 5D**). Furthermore, in the absence of ITK, unlike γδ T-cell-derived IL-17A that was significantly impaired, IL-17A production by CD4$^+$ and CD8$^+$ αβ T cells did not exhibit overt differences, although the proportion of those cells making IL-17A was quite low (**Figure 5D**).

Itk Deficiency Has Minimal Impact on Antigen-Specific αβ T-Cell Responses During *Mtb* Infection

Our data above supports a strong role of ITK in promoting the IL-17A-producing effector γδ T cells during *Mtb* infection. It is possible that αβ T-cell effector functions were also altered in the absence of ITK and further contributed to the impaired bacterial clearance and enhanced lung pathology as observed in **Figure 2**. To determine whether ITK regulates αβ T-cell effector function, we stimulated cells isolated from the lungs of the infected mice 4 weeks postinfection. We found that bulk T-cell activation by PMA and ionomycin suggested that ITK is not required for CD4$^+$ and CD8$^+$ αβ T cells to produce effector cytokines tumor necrosis factor alpha (TNF-α) and interferon-gamma (IFN-γ) during *Mtb* infection (**Figure 6A**). Moreover, to our surprise, stimulation of *Mtb* antigen-specific CD4$^+$ αβ T cells with ESAT-6$_{4-17}$ (MHCII-restricted epitope), or CD8$^+$ αβ T cells with TB10.4$_{4-11}$ (MHCI-restricted epitope) revealed no difference in production of TNF-α and IFN-γ by these cells in the absence of ITK (**Figure 6B**). Along with the data above, our results suggest that the major protective role of ITK during *Mtb* infection might be executed through ITK-mediated IL-17A production by γδ T cells.

Itk Regulates γδ T Cell but Not αβ T-Cell Proliferation During *Mtb* Infection

Itk deficiency led to significantly impaired effector γδ T cells (**Figure 5**) but not αβ T cells (**Figure 6**). These might be

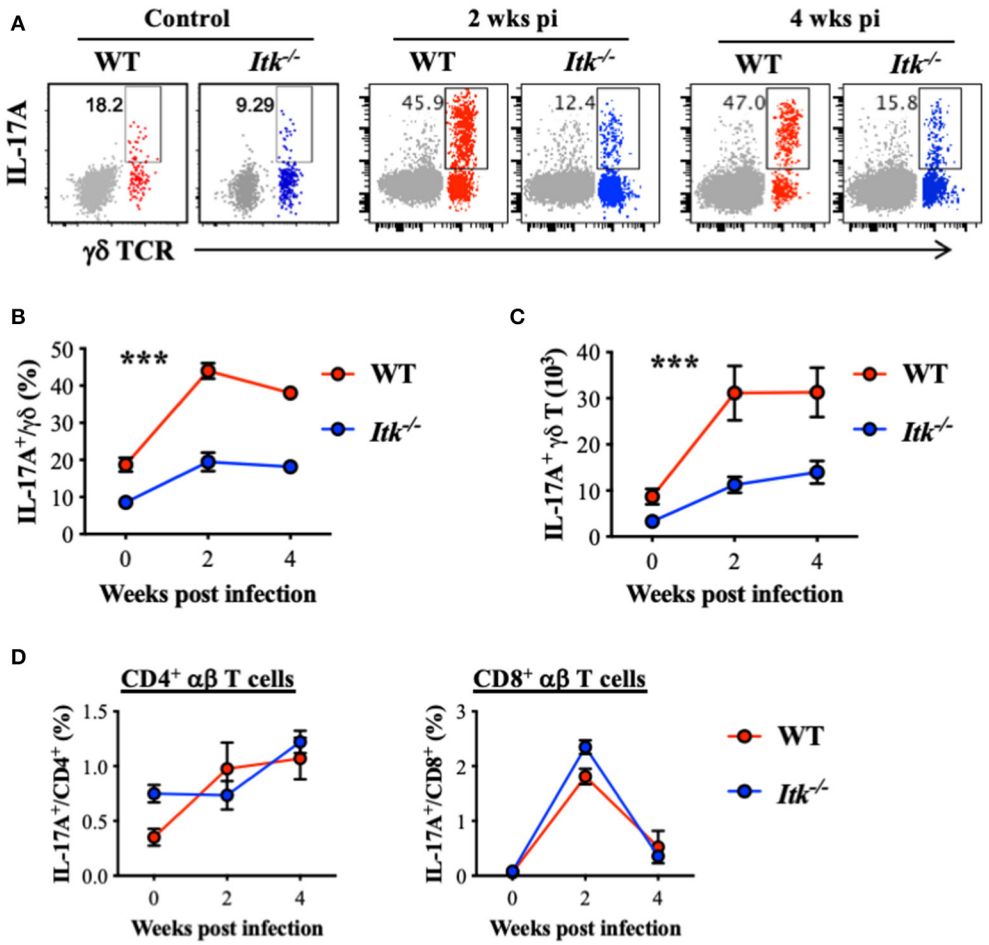

FIGURE 5 | *Itk* deficiency impairs lung γδ T-cell-derived IL-17A production during *Mtb* infection. WT and *Itk*$^{-/-}$ mice were infected as in **Figure 3**, and lungs were analyzed at the indicated time points. Cells isolated from the lungs were stimulated with PMA and ionomycin, in the presence of BFA and monensin, followed by intracellular cytokine staining. **(A)** Representative FACS plots for IL-17A production by γδ T cells. Production of CD4^{+} αβ T cells is shown as gray background. **(B)** Percentages and **(C)** number of IL-17A-producing γδ T cells. **(D)** Percentages of IL-17A-producing CD4^{+} and CD8^{+} αβ T cells. ***$p < 0.001$ by two-way ANOVA with *post hoc* test. $N = 5$–9. Numbers of the indicated cell types were presented as mean ± SEM and represent results of three independent experiments.

the results of differential requirement of ITK signaling in T-cell expansion. Using proliferative maker Ki67 to detect T-cell proliferation, we found that *Mtb*-driven early proliferation of γδ T cells was severely impaired in *ITK* deficiency (**Figure 7**, top panel), but not the CD4^{+} and CD8^{+} αβ T-cell subsets (**Figure 7**, middle and bottom panels). These data, in part, explain the selective defect of effector γδ T-cell development in *Itk*-deficient mice during *Mtb* infection.

DISCUSSION

The immune cells that control *Mtb* include macrophages, neutrophils, and T-cell populations (2, 3). The TCR pathway is elevated in active *Mtb* infection in human lung, and ITK is a major component of this pathway; however, its role in the T-cell response to *Mtb* is not known. Here, we demonstrate a protective role of ITK in *Mtb* infections in murine models, with a particular role in the ability of lung γδ T cells to produce IL-17A, which is associated with *Mtb* residence in lung neutrophils. These findings have important implications for understanding the T-cell immune response to *Mtb* and the role of ITK in this process.

In humans, *Mtb* infects *via* inhalation of a low dose of aerosolized bacteria; therefore, low-dose aerosol inoculation would better mimic the nature of *Mtb* infection in humans. However, in the absence of the ability to perform aerosolized infections, the standard experimental protocol of *Mtb* infection in mice is 1,000 CFU *via* intranasal inoculation (69–72). Monocytes play an essential role in initiating T-cell responses in the lung against *Mtb* infection (73), and using this standard protocol of *Mtb* infection in mice, we previously observed monocytosis (64), similar to what has been reported in other studies using aerosolized low-dose infection protocols (74, 75). Using intranasal inoculation with 1,000 CFU of *Mtb* in mice, we observed that the numbers of host myeloid cells infiltrating to the lung during *Mtb* infection are significantly altered in the absence of ITK. Alveolar macrophages are considered as the preferred replicating niche for *Mtb* and promote the early

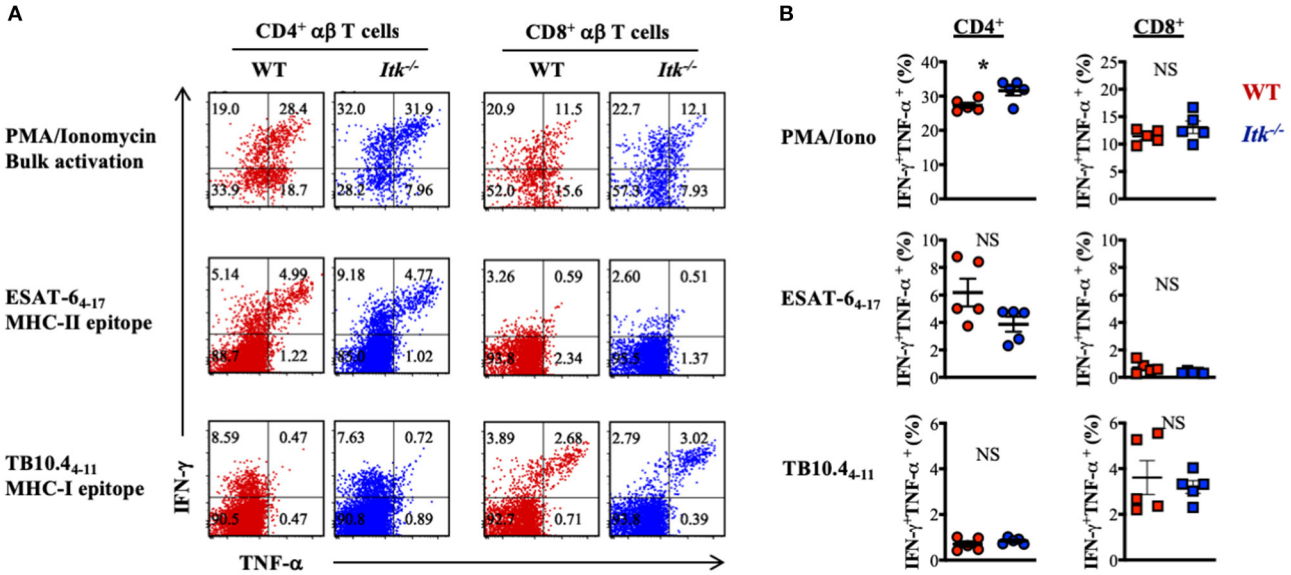

FIGURE 6 | *Itk* deficiency has minimal impact on lung antigen-specific αβ effector T cells during *Mtb* infection. WT and *Itk*$^{-/-}$ mice were infected as in **Figure 3** and analyzed 4 weeks postinfection. Cells isolated from the lungs were stimulated with PMA and ionomycin (for bulk T-cell activation), MHCII-restricted *Mtb* epitope ESAT-6_{4-17} (for antigen-specific CD4$^+$ T-cell activation), or MHCI- restricted *Mtb* epitope TB10.4_{4-11} (for antigen-specific CD8$^+$ T-cell activation), in the presence of BFA and monensin, followed by intracellular cytokine staining. **(A)** Representative FACS plots for IFN-γ and TNF-α production by CD4$^+$ and CD8$^+$ αβ T cells under the indicated stimulating conditions. **(B)** Summary of percentages of IFN-γ and TNF-α-producing CD4$^+$ and CD8$^+$ αβ T cells under the indicated stimulating conditions. $N = 5$. Data were presented as mean ± SEM and represent results of three independent experiments. NS, not significant; $^*p < 0.05$ by Student's *t*-test.

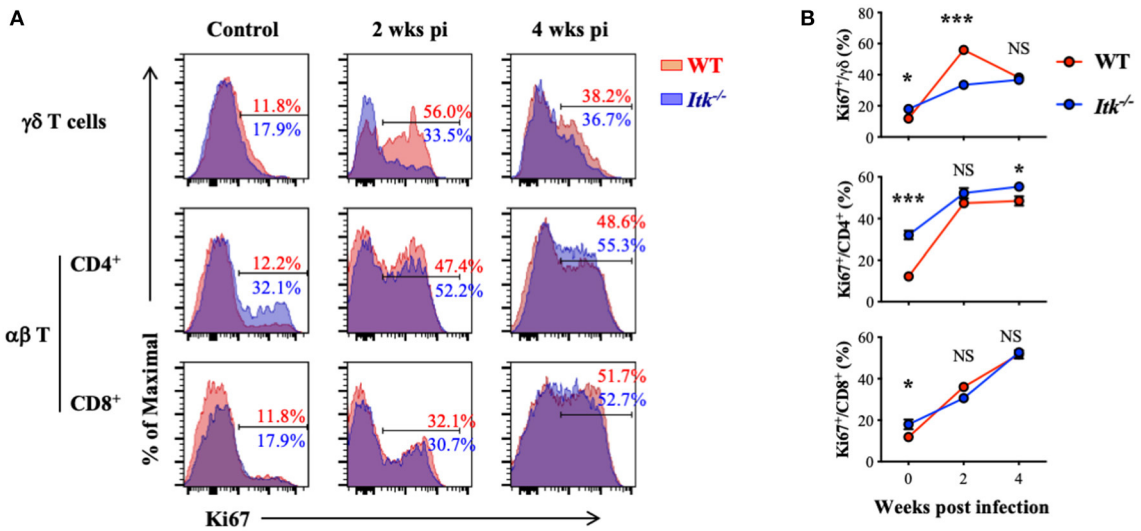

FIGURE 7 | *Itk* deficiency impairs lung γδ but not αβ T-cell proliferation during *Mtb* infection. WT and *Itk*$^{-/-}$ mice were infected as in **Figure 3** and analyzed at the indicated time points. Cells isolated from the lungs were analyzed via nuclear staining. **(A)** Representative FACS plots for Ki67 expression by γδ T cells and CD4$^+$ and CD8$^+$ αβ T cells at the indicated time points postinfection. **(B)** Summary of percentages of KI67$^+$ cells among γδ T cells and CD4$^+$ and CD8$^+$ αβ T cells. $N = 5$–9. Data were presented as mean ± SEM and represent results of three independent experiments. NS, not significant; $^*p < 0.05$, $^{***}p < 0.001$ by two-way ANOVA with *post hoc* test.

stage of infection (64, 76). In *Itk*-deficient mice, there are more alveolar macrophages harboring *Mtb*, suggesting a more permissive cellular environment in the lung. Moreover, although fewer neutrophils are present in the lung in the absence of ITK, there are more *Mtb* resident in neutrophils at 4 weeks postinfection. The redistribution of *Mtb* in different phagocytes in the absence of ITK appears to correlate with the increased bacterial burden in the lung 4 weeks postinfection. Other than

T cells, ITK has been indicated to regulate functions of innate immune cells such as mast cells (77, 78). However, potential intrinsic functions of ITK in lung macrophages and neutrophils during *Mtb* infection would merit further studies.

Activation of γδ T cells for IL-17A production is severely impaired in *Itk*-deficient mice and very likely responsible for the resultant neutrophil recruitment early after infection(s), as well as the increased neutrophil resident *Mtb* population later in infection. Indeed, we have shown that ITK can regulate γδ T cell development and function in mouse (48), and while there was no apparent difference in peripheral blood γδ T-cell numbers in humans carrying *ITK* mutations (12), the normal range for γδ T cells varies quite widely by anatomical location, as well as by geography and ethnicity (79). Despite relatively normal antigen-specific αβ T-cell responses, our results identify ITK signaling as an essential player for the IL-17A production by γδ T cells, the predominant source of IL-17A in *Mtb*-infected lungs (68). ITK exhibited a γδ T cell-specific function, as compared to αβ T cells, in driving T-cell proliferation during early immune responses to *Mtb* infections. Our work suggests that *ITK* deficiency in humans may lead to γδ T-cell deficiency in expansion and production of IL-17A, in the face of *Mtb* infection.

We and others have previously reported a role for ITK signaling in regulating $Foxp3^+$ regulatory T (Treg) cell development and function (41, 80). In the absence of ITK, the proportion of Treg cells among $CD4^+$ T cells in the lymphoid organs of naive mice is increased, and the differentiation of inducible Treg cells from $CD4^+$ naive T cells *in vitro* is also enhanced (41, 80). The role of ITK in Treg cell responses in the lung during *Mtb* infection was, however, unclear. In mouse model of *Mtb* infection, we observed higher *Mtb* burdens, higher lung pathological scores and reduced numbers of Treg cells found in the lungs in *Itk*-deficient mice, compared to those in the infected WT mice (**Figure 4**). Tissue damage may be explained by excessive growth of the pathogen and/or immunopathology. Indeed, we observed impaired γδ T cell expansion and γδ T cell-derived IL-17A production in *Mtb*-infected *Itk*-deficient mice but no overt differences in other immune effectors. The decrease in Treg numbers in the lung during *Mtb* infection in the absence of ITK may explain higher levels of immunopathology potentially due to impaired immunomodulatory function. Future research using murine models with conditional deletion of *Itk* specifically in $Foxp3^+$ Treg cells would allow more in-depth investigation of the role of ITK in Treg cells during *Mtb* infection.

Taken together, these findings suggest a potential role for ITK in active TB in humans, in addition to its known connection with primary immunodeficiency, susceptibility to EBV, lymphoproliferative diseases, and asthma (12, 50, 51). These findings also have important implications for human genetics associated with susceptibility to *Mtb* due to altered immune responses and molecular signals modulating host immunity that controls the progression of active tuberculosis.

Our findings support a role of ITK signaling in promoting protective immune responses against *Mtb*, in particular, γδ T cell expansion and production of IL-17A, which could contribute to the modulation of tuberculosis, especially in infections with highly virulent bacterial strains in which IL-17A has been shown to play an essential protective role (67). However, our work also sounds a note of caution for the potential use of compounds such as Ibrutinib that inhibit the related kinase BTK as well as ITK (81). Given the potential for inhibition of ITK, patients being treated with Ibrutinib may need to be monitored for infection or potential reactivation of latent *Mtb*.

DATA AVAILABILITY STATEMENT

The datasets generated for this study can be found in the Gene Expression Omnibus under accession number GSE20050.

ETHICS STATEMENT

The animal study was reviewed and approved by the Institutional Animal Care and Use Committees at Cornell University.

AUTHOR CONTRIBUTIONS

LH, MM, NN, JE, CL, and WH performed the experiments. LH, TS, AA, and WH analyzed and interpreted data. LH, AA, and WH wrote the manuscript. KY performed bioinformatic analyses. DR contributed reagents and intellectual input. AA and WH conceived research and designed experiments.

FUNDING

This work was supported in part by grants from the National Institutes of Health (AI120701 and AI138570 to AA, AI129422 to AA and WH, GM130555 Sub-6610 to WH, and AI134183 to DR), and a Pilot Grant (to WH) from LSU-Tulane COBRE Center for Experimental Infectious Disease Research (funded by NIH P30GM110760). JE was supported by a training program in Biomedical and Bioengineering at Cornell University (funded by NIH T32EB023860). MM is a recipient of the Pathobiological Sciences Graduate Program Fellowship in the School of Veterinary Medicine at the Louisiana State University.

ACKNOWLEDGMENTS

We thank Amie Redko for the animal care and Ling Zhang for the technical assistance.

SUPPLEMENTARY MATERIAL

The Supplementary Material for this article can be found online at: https://www.frontiersin.org/articles/10.3389/fimmu.2019.03103/full#supplementary-material

Supplementary Figure 1 | Gene enrichment profile of the TCR/ITK signaling in human lungs with active TB. Genes in the TCR signaling pathways were rendered with their positions and connections in the pathway, with colored codes indicating the log_2-fold change comparing levels of gene expression in caseous to those in normal tissues. Red indicates upregulation in caseous samples while blue indicates downregulation. Note that ITK is one of the central components of the TCR signaling pathway.

Supplementary Table 1 | Summary of pathways that exhibited an up- or down-regulated trend in caseum samples compared to normal tissues.

REFERENCES

1. *Global Tuberculosis Report 2019*. Geneva: World Health Organization (2019).
2. O'Garra A, Redford PS, McNab FW, Bloom CI, Wilkinson RJ, Berry MP. The immune response in tuberculosis. *Annu Rev Immunol.* (2013) 31:475–527. doi: 10.1146/annurev-immunol-032712-095939
3. de Martino M, Lodi L, Galli L, Chiappini E. Immune response to *Mycobacterium tuberculosis*: a narrative review. *Front Pediatr.* (2019) 7:350. doi: 10.3389/fped.2019.00350
4. Boisson-Dupuis S, Bustamante J, El-Baghdadi J, Camcioglu Y, Parvaneh N, El Azbaoui S, et al. Inherited and acquired immunodeficiencies underlying tuberculosis in childhood. *Immunol Rev.* (2015) 264:103–20. doi: 10.1111/imr.12272
5. Andreotti AH, Schwartzberg PL, Joseph RE, Berg LJ. T-cell signaling regulated by the Tec family kinase, Itk. *Cold Spring Harb Perspect Biol.* (2010) 2:a002287. doi: 10.1101/cshperspect.a002287
6. Tangye SG, Palendira U, Edwards ES. Human immunity against EBV-lessons from the clinic. *J Exp Med.* (2017) 214:269–83. doi: 10.1084/jem.20161846
7. Mansouri D, Mahdaviani SA, Khalilzadeh S, Mohajerani SA, Hasanzad M, Sadr S, et al. IL-2-inducible T-cell kinase deficiency with pulmonary manifestations due to disseminated Epstein-Barr virus infection. *Int Arch Allergy Immunol.* (2012) 158:418–22. doi: 10.1159/000333472
8. Linka RM, Risse SL, Bienemann K, Werner M, Linka Y, Krux F, et al. Loss-of-function mutations within the IL-2 inducible kinase ITK in patients with EBV-associated lymphoproliferative diseases. *Leukemia.* (2012) 26:963–71. doi: 10.1038/leu.2011.371
9. Huck K, Feyen O, Niehues T, Ruschendorf F, Hubner N, Laws HJ, et al. Girls homozygous for an IL-2-inducible T cell kinase mutation that leads to protein deficiency develop fatal EBV-associated lymphoproliferation. *J Clin Invest.* (2009) 119:1350–8. doi: 10.1172/JCI37901
10. Bienemann K, Borkhardt A, Klapper W, Oschlies I. High incidence of Epstein-Barr virus (EBV)-positive Hodgkin lymphoma and Hodgkin lymphoma-like B-cell lymphoproliferations with EBV latency profile 2 in children with interleukin-2-inducible T-cell kinase deficiency. *Histopathology.* (2015) 67:607–16. doi: 10.1111/his.12677
11. Veillette A, Perez-Quintero LA, Latour S. X-linked lymphoproliferative syndromes and related autosomal recessive disorders. *Curr Opin Allergy Clin Immunol.* (2013) 13:614–22. doi: 10.1097/ACI.0000000000000008
12. Ghosh S, Bienemann K, Boztug K, Borkhardt A. Interleukin-2-inducible T-cell kinase (ITK) deficiency - clinical and molecular aspects. *J Clin Immunol.* (2014) 34:892–9. doi: 10.1007/s10875-014-0110-8
13. Cohen JI. Primary immunodeficiencies associated with EBV disease. *Curr Top Microbiol Immunol.* (2015) 390:241–65. doi: 10.1007/978-3-319-22822-8_10
14. Eken A, Cansever M, Somekh I, Mizoguchi Y, Zietara N, Okus FZ, et al. Genetic deficiency and biochemical inhibition of ITK affect human Th17, Treg, and innate lymphoid cells. *J Clin Immunol.* (2019) 39:391–400. doi: 10.1007/s10875-019-00632-5
15. Qi Q, Huang W, Bai Y, Balmus G, Weiss RS, August A. A unique role for ITK in survival of invariant NKT cells associated with the p53-dependent pathway in mice. *J Immunol.* (2012) 188:3611–9. doi: 10.4049/jimmunol.1102475
16. Qi Q, Xia M, Bai Y, Yu S, Cantorna M, August A. Interleukin-2-inducible T cell kinase (Itk) network edge dependence for the maturation of iNKT cell. *J Biol Chem.* (2011) 286:138–46. doi: 10.1074/jbc.M110.148205
17. Felices M, Berg LJ. The Tec kinases Itk and Rlk regulate NKT cell maturation, cytokine production, and survival. *J Immunol.* (2008) 180:3007–18. doi: 10.4049/jimmunol.180.5.3007
18. Gadue P, Stein PL. NK T cell precursors exhibit differential cytokine regulation and require Itk for efficient maturation. *J Immunol.* (2002) 169:2397–406. doi: 10.4049/jimmunol.169.5.2397
19. Liao XC, Littman DR. Altered T cell receptor signaling and disrupted T cell development in mice lacking Itk. *Immunity.* (1995) 3:757–69. doi: 10.1016/1074-7613(95)90065-9
20. Bachmann MF, Littman DR, Liao XC. Antiviral immune responses in Itk-deficient mice. *J Virol.* (1997) 71:7253–7. doi: 10.1128/JVI.71.10.7253-7257.1997
21. Liao XC, Littman DR, Weiss A. Itk and Fyn make independent contributions to T cell activation. *J Exp Med.* (1997) 186:2069–73. doi: 10.1084/jem.186.12.2069
22. Schaeffer EM, Debnath J, Yap G, McVicar D, Liao XC, Littman DR, et al. Requirement for Tec kinases Rlk and Itk in T cell receptor signaling and immunity. *Science.* (1999) 284:638–41. doi: 10.1126/science.284.5414.638
23. Liu KQ, Bunnell SC, Gurniak CB, Berg LJ. T cell receptor-initiated calcium release is uncoupled from capacitative calcium entry in Itk-deficient T cells. *J Exp Med.* (1998) 187:1721–7. doi: 10.1084/jem.187.10.1721
24. Atherly LO, Lucas JA, Felices M, Yin CC, Reiner SL, Berg LJ. The Tec family tyrosine kinases Itk and Rlk regulate the development of conventional $CD8^+$ T cells. *Immunity.* (2006) 25:79–91. doi: 10.1016/j.immuni.2006.05.012
25. Broussard C, Fleischacker C, Horai R, Chetana M, Venegas AM, Sharp LL, et al. Altered development of $CD8^+$ T cell lineages in mice deficient for the Tec kinases Itk and Rlk. *Immunity.* (2006) 25:93–104. doi: 10.1016/j.immuni.2006.05.011
26. Prince AL, Yin CC, Enos ME, Felices M, Berg LJ. The Tec kinases Itk and Rlk regulate conventional versus innate T-cell development. *Immunol Rev.* (2009) 228:115–31. doi: 10.1111/j.1600-065X.2008.00746.x
27. Prince AL, Watkin LB, Yin CC, Selin LK, Kang J, Schwartzberg PL, et al. Innate $PLZF^+CD4^+$ alphabeta T cells develop and expand in the absence of Itk. *J Immunol.* (2014) 193:673–87. doi: 10.4049/jimmunol.1302058
28. Prince AL, Kraus Z, Carty SA, Ng C, Yin CC, Jordan MS, et al. Development of innate $CD4^+$ and $CD8^+$ T cells in Itk-deficient mice is regulated by distinct pathways. *J Immunol.* (2014) 193:688–99. doi: 10.4049/jimmunol.1302059
29. Hu J, Sahu N, Walsh E, August A. Memory phenotype $CD8^+$ T cells with innate function selectively develop in the absence of active Itk. *Eur J Immunol.* (2007) 37:2892–9. doi: 10.1002/eji.200737311
30. Hu J, August A. Naive and innate memory phenotype $CD4^+$ T cells have different requirements for active Itk for their development. *J Immunol.* (2008) 180:6544–52. doi: 10.4049/jimmunol.180.10.6544
31. Huang W, Huang F, Kannan AK, Hu J, August A. ITK tunes IL-4-induced development of innate memory $CD8^+$ T cells in a gammadelta T and invariant NKT cell-independent manner. *J Leukoc Biol.* (2014) 96:55–63. doi: 10.1189/jlb.1AB0913-484RR
32. Miller A, Wilcox H, Lai Z, Berg L. Signaling through Itk promotes T helper 2 differentiation via negative regulation of T-bet. *Immunity.* (2004) 21:67–80. doi: 10.1016/j.immuni.2004.06.009
33. Mueller C, August A. Attenuation of immunological symptoms of allergic asthma in mice lacking the tyrosine kinase ITK. *J Immunol.* (2003) 170:5056–63. doi: 10.4049/jimmunol.170.10.5056
34. Kannan A, Sahu N, Mohanan S, Mohinta S, August A. Itk modulates allergic airway inflammation by suppressing IFNγ in naïve $CD4^+$ T-cells. *J Allergy Clin Immunol.* (2013) 132:811–20.e1–5. doi: 10.1016/j.jaci.2013.04.033
35. Kannan A, Lee Y, Qi Q, Huang W, Jeong AR, Ohnigian S, et al. Allele-sensitive mutant, Itkas, reveals that Itk kinase activity is required for Th1, Th2, Th17, and iNKT-cell cytokine production. *Eur J Immunol.* (2015) 45:2276–85. doi: 10.1002/eji.201445087
36. Sahu N, Venegas AM, Jankovic D, Mitzner W, Gomez-Rodriguez J, Cannons JL, et al. Selective expression rather than specific function of Txk and Itk regulate Th1 and Th2 responses. *J Immunol.* (2008) 181:6125–31. doi: 10.4049/jimmunol.181.9.6125
37. Sahu N, Mueller C, Fischer A, August A. Differential sensitivity to Itk kinase signals for T helper 2 cytokine production and chemokine-mediated migration. *J Immunol.* (2008) 180:3833–8. doi: 10.4049/jimmunol.180.6.3833
38. Schaeffer EM, Yap GS, Lewis CM, Czar MJ, McVicar DW, Cheever AW, et al. Mutation of Tec family kinases alters T helper cell differentiation. *Nat Immunol.* (2001) 2:1183–8. doi: 10.1038/ni734
39. Gomez-Rodriguez J, Meylan F, Handon R, Hayes ET, Anderson SM, Kirby MR, et al. Itk is required for Th9 differentiation via TCR-mediated induction of IL-2 and IRF4. *Nat Commun.* (2016) 7:10857. doi: 10.1038/ncomms10857
40. Gomez-Rodriguez J, Sahu N, Handon R, Davidson TS, Anderson SM, Kirby MR, et al. Differential expression of interleukin-17A and−17F is coupled to T cell receptor signaling via inducible T cell kinase. *Immunity.* (2009) 31:587–97. doi: 10.1016/j.immuni.2009.07.009
41. Gomez-Rodriguez J, Wohlfert EA, Handon R, Meylan F, Wu JZ, Anderson SM, et al. Itk-mediated integration of T cell receptor and cytokine signaling regulates the balance between Th17 and regulatory T cells. *J Exp Med.* (2014) 211:529–43. doi: 10.1084/jem.20131459
42. Kannan AK, Kim DG, August A, Bynoe MS. Itk signals promote neuroinflammation by regulating $CD4^+$ T-cell activation and

trafficking. *J Neurosci.* (2015) 35:221–33. doi: 10.1523/JNEUROSCI.1957-14.2015
43. Huang W, Solouki S, Koylass N, Zheng SG, August A. ITK signalling via the Ras/IRF4 pathway regulates the development and function of Tr1 cells. *Nat Commun.* (2017) 8:15871. doi: 10.1038/ncomms15871
44. Kannan AK, Mohinta S, Huang W, Huang L, Koylass N, Appleton JA, et al. T-Bet independent development of IFNgamma secreting natural T helper 1 cell population in the absence of Itk. *Sci Rep.* (2017) 7:45935. doi: 10.1038/srep45935
45. Czar MJ, Debnath J, Schaeffer EM, Lewis CM, Schwartzberg PL. Biochemical and genetic analyses of the Tec kinases Itk and Rlk/Txk. *Biochem Soc Trans.* (2001) 29:863–7. doi: 10.1042/bst0290863
46. Yin CC, Cho OH, Sylvia KE, Narayan K, Prince AL, Evans JW, et al. The Tec kinase ITK regulates thymic expansion, emigration, and maturation of gammadelta NKT cells. *J Immunol.* (2013) 190:2659–69. doi: 10.4049/jimmunol.1202531
47. Felices M, Yin C, Kosaka Y, Kang J, Berg L. Tec kinase Itk in gammadelta T cells is pivotal for controlling IgE production *in vivo*. *Proc Natl Acad Sci USA.* (2009) 106:8308–13. doi: 10.1073/pnas.0808459106
48. Qi Q, Xia M, Hu J, Hicks E, Iyer A, Xiong N, et al. Enhanced development of $CD4^+$ gammadelta T cells in the absence of Itk results in elevated IgE production. *Blood*. (2009) 114:564–71. doi: 10.1182/blood-2008-12-196345
49. Xia M, Qi Q, Jin Y, Wiest DL, August A, Xiong N. Differential roles of IL-2-inducible T cell kinase-mediated TCR signals in tissue-specific localization and maintenance of skin intraepithelial T cells. *J Immunol.* (2010) 184:6807–14. doi: 10.4049/jimmunol.1000453
50. Lee SH, Chang HS, Jang AS, Park SW, Park JS, Uh ST, et al. The association of a single-nucleotide polymorphism of the IL-2 inducible T-cell Kinase gene with asthma. *Ann Hum Genet.* (2011) 75:359–69. doi: 10.1111/j.1469-1809.2010.00637.x
51. Ferrara TJ, Mueller C, Sahu N, Ben-Jebria A, August A. Reduced airway hyperresponsiveness and tracheal responses during allergic asthma in mice lacking tyrosine kinase inducible T-cell kinase. *J Allergy Clin Immunol.* (2006) 117:780–6. doi: 10.1016/j.jaci.2005.12.1330
52. Alpay F, Zare Y, Kamalludin MH, Huang X, Shi X, Shook GE, et al. Genome-wide association study of susceptibility to infection by *Mycobacterium avium* subspecies *paratuberculosis* in Holstein cattle. *PLoS ONE.* (2014) 9:e111704. doi: 10.1371/journal.pone.0111704
53. Kim MJ, Wainwright HC, Locketz M, Bekker LG, Walther GB, Dittrich C, et al. Caseation of human tuberculosis granulomas correlates with elevated host lipid metabolism. *EMBO Mol Med.* (2010) 2:258–74. doi: 10.1002/emmm.201000079
54. Seimon TA, Kim MJ, Blumenthal A, Koo J, Ehrt S, Wainwright H, et al. Induction of ER stress in macrophages of tuberculosis granulomas. *PLoS ONE.* (2010) 5:e12772. doi: 10.1371/journal.pone.0012772
55. Ritchie ME, Phipson B, Wu D, Hu Y, Law CW, Shi W, et al. limma powers differential expression analyses for RNA-sequencing and microarray studies. *Nucleic Acids Res.* (2015) 43:e47. doi: 10.1093/nar/gkv007
56. Luo W, Friedman MS, Shedden K, Hankenson KD, Woolf PJ. GAGE: generally applicable gene set enrichment for pathway analysis. *BMC Bioinformatics.* (2009) 10:161. doi: 10.1186/1471-2105-10-161
57. Subramanian A, Tamayo P, Mootha VK, Mukherjee S, Ebert BL, Gillette MA, et al. Gene set enrichment analysis: a knowledge-based approach for interpreting genome-wide expression profiles. *Proc Natl Acad Sci USA.* (2005) 102:15545–50. doi: 10.1073/pnas.0506580102
58. Luo W, Brouwer C. Pathview: an R/Bioconductor package for pathway-based data integration and visualization. *Bioinformatics.* (2013) 29:1830–1. doi: 10.1093/bioinformatics/btt285
59. Carroll P, Schreuder LJ, Muwanguzi-Karugaba J, Wiles S, Robertson BD, Ripoll J, et al. Sensitive detection of gene expression in mycobacteria under replicating and non-replicating conditions using optimized far-red reporters. *PLoS ONE.* (2010) 5:e9823. doi: 10.1371/journal.pone.0009823
60. Reece JJ, Siracusa MC, Southard TL, Brayton CF, Urban JF Jr, Scott AL. Hookworm-induced persistent changes to the immunological environment of the lung. *Infect Immun.* (2008) 76:3511–24. doi: 10.1128/IAI.00192-08
61. Chackerian AA, Alt JM, Perera TV, Dascher CC, Behar SM. Dissemination of *Mycobacterium tuberculosis* is influenced by host factors and precedes the initiation of T-cell immunity. *Infect Immun.* (2002) 70:4501–9. doi: 10.1128/IAI.70.8.4501-4509.2002
62. Feng CG, Kaviratne M, Rothfuchs AG, Cheever A, Hieny S, Young HA, et al. NK cell-derived IFN-gamma differentially regulates innate resistance and neutrophil response in T cell-deficient hosts infected with *Mycobacterium tuberculosis*. *J Immunol.* (2006) 177:7086–93. doi: 10.4049/jimmunol.177.10.7086
63. Srivastava S, Ernst JD, Desvignes L. Beyond macrophages: the diversity of mononuclear cells in tuberculosis. *Immunol Rev.* (2014) 262:179–92. doi: 10.1111/imr.12217
64. Huang L, Nazarova EV, Tan S, Liu Y, Russell DG. Growth of *Mycobacterium tuberculosis in vivo* segregates with host macrophage metabolism and ontogeny. *J Exp Med.* (2018) 215:1135–52. doi: 10.1084/jem.20172020
65. Mishra BB, Lovewell RR, Olive AJ, Zhang G, Wang W, Eugenin E, et al. Nitric oxide prevents a pathogen-permissive granulocytic inflammation during tuberculosis. *Nat Microbiol.* (2017) 2:17072. doi: 10.1038/nmicrobiol.2017.72
66. Dallenga T, Repnik U, Corleis B, Eich J, Reimer R, Griffiths GW, et al. *M. tuberculosis*-induced necrosis of infected neutrophils promotes bacterial growth following phagocytosis by macrophages. *Cell Host Microbe.* (2017) 22:519–30.e3. doi: 10.1016/j.chom.2017.09.003
67. Gopal R, Monin L, Slight S, Uche U, Blanchard E, Fallert Junecko BA, et al. Unexpected role for IL-17 in protective immunity against hypervirulent *Mycobacterium tuberculosis* HN878 infection. *PLoS Pathog.* (2014) 10:e1004099. doi: 10.1371/journal.ppat.1004099
68. Lockhart E, Green AM, Flynn JL. IL-17 production is dominated by gammadelta T cells rather than CD4 T cells during *Mycobacterium tuberculosis* infection. *J Immunol.* (2006) 177:4662–9. doi: 10.4049/jimmunol.177.7.4662
69. Horvath CN, Shaler CR, Jeyanathan M, Zganiacz A, Xing Z. Mechanisms of delayed anti-tuberculosis protection in the lung of parenteral BCG-vaccinated hosts: a critical role of airway luminal T cells. *Mucosal Immunol.* (2012) 5:420–31. doi: 10.1038/mi.2012.19
70. Segueni N, Tritto E, Bourigault ML, Rose S, Erard F, Le Bert M, et al. Controlled *Mycobacterium tuberculosis* infection in mice under treatment with anti-IL-17A or IL-17F antibodies, in contrast to TNFalpha neutralization. *Sci Rep.* (2016) 6:36923. doi: 10.1038/srep36923
71. Segueni N, Benmerzoug S, Rose S, Gauthier A, Bourigault ML, Reverchon F, et al. Innate myeloid cell TNFR1 mediates first line defence against primary *Mycobacterium tuberculosis* infection. *Sci Rep.* (2016) 6:22454. doi: 10.1038/srep22454
72. Benmerzoug S, Bounab B, Rose S, Gosset D, Biet F, Cochard T, et al. Sterile lung inflammation induced by silica exacerbates *Mycobacterium tuberculosis* infection via STING-dependent type 2 immunity. *Cell Rep.* (2019) 27:2649–64.e5. doi: 10.1016/j.celrep.2019.04.110
73. Samstein M, Schreiber HA, Leiner IM, Susac B, Glickman MS, Pamer EG. Essential yet limited role for CCR2(+) inflammatory monocytes during *Mycobacterium tuberculosis*-specific T cell priming. *Elife.* (2013) 2:e01086. doi: 10.7554/eLife.01086.013
74. Antonelli LR, Gigliotti Rothfuchs A, Goncalves R, Roffe E, Cheever AW, Bafica A, et al. Intranasal Poly-IC treatment exacerbates tuberculosis in mice through the pulmonary recruitment of a pathogen-permissive monocyte/macrophage population. *J Clin Invest.* (2010) 120:1674–82. doi: 10.1172/JCI40817
75. La Manna MP, Orlando V, Dieli F, Di Carlo P, Cascio A, Cuzzi G, et al. Quantitative and qualitative profiles of circulating monocytes may help identifying tuberculosis infection and disease stages. *PLoS ONE.* (2017) 12:e0171358. doi: 10.1371/journal.pone.0171358
76. Cohen SB, Gern BH, Delahaye JL, Adams KN, Plumlee CR, Winkler JK, et al. Alveolar macrophages provide an early *Mycobacterium tuberculosis* niche and initiate dissemination. *Cell Host Microbe.* (2018) 24:439–46.e4. doi: 10.1016/j.chom.2018.08.001
77. Huang W, Morales JL, Gazivoda VP, August A. Nonreceptor tyrosine kinases ITK and BTK negatively regulate mast cell proinflammatory responses to lipopolysaccharide. *J Allergy Clin Immunol.* (2016) 137:1197–205. doi: 10.1016/j.jaci.2015.08.056
78. Iyer AS, Morales JL, Huang W, Ojo F, Ning G, Wills E, et al. Absence of Tec family kinases interleukin-2 inducible T cell kinase (Itk) and Bruton's tyrosine

kinase (Btk) severely impairs Fc epsilonRI-dependent mast cell responses. *J Biol Chem.* (2011) 286:9503–13. doi: 10.1074/jbc.M110.165613
79. Esin S, Shigematsu M, Nagai S, Eklund A, Wigzell H, Grunewald J. Different percentages of peripheral blood gamma delta + T cells in healthy individuals from different areas of the world. *Scand J Immunol.* (1996) 43:593–6. doi: 10.1046/j.1365-3083.1996.d01-79.x
80. Huang W, Jeong AR, Kannan AK, Huang L, August A. IL-2-inducible T cell kinase tunes T regulatory cell development and is required for suppressive function. *J Immunol.* (2014) 193:2267–72. doi: 10.4049/jimmunol.1400968
81. Sagiv-Barfi I, Kohrt HE, Czerwinski DK, Ng PP, Chang BY, Levy R. Therapeutic antitumor immunity by checkpoint blockade is enhanced by ibrutinib, an inhibitor of both BTK and ITK. *Proc Natl Acad Sci USA.* (2015) 112:E966–72. doi: 10.1073/pnas.1500712112

Conflict of Interest: AA receives research support from 3M Corporation.

The remaining authors declare that the research was conducted in the absence of any commercial or financial relationships that could be construed as a potential conflict of interest.

frontiers in Cellular and Infection Microbiology

ORIGINAL RESEARCH
published: 31 January 2020
doi: 10.3389/fcimb.2020.00026

One-Year Old Dormant, "Non-culturable" *Mycobacterium tuberculosis* Preserves Significantly Diverse Protein Profile

Kseniya A. Trutneva*, Margarita O. Shleeva, Galina R. Demina, Galina N. Vostroknutova and Arseny S. Kaprelyans

Federal Research Centre "Fundamentals of Biotechnology" of the Russian Academy of Sciences, A.N. Bach Institute of Biochemistry, Moscow, Russia

OPEN ACCESS

Edited by:
David Neil McMurray, Texas A&M Health Science Center, United States

Reviewed by:
Pankaj Kumar, Jamia Hamdard University, India
Andrey Mulyukin, Winogradsky Institute of Microbiology (RAS), Russia
Martin I. Voskuil, University of Colorado Denver, United States

****Correspondence:***
Kseniya A. Trutneva
trutneva-k@mail.ru

Specialty section:
This article was submitted to Molecular Bacterial Pathogenesis, a section of the journal Frontiers in Cellular and Infection Microbiology

Received: *07 August 2019*
Accepted: *15 January 2020*
Published: *31 January 2020*

Citation:
Trutneva KA, Shleeva MO, Demina GR, Vostroknutova GN and Kaprelyans AS (2020) One-Year Old Dormant, "Non-culturable" Mycobacterium tuberculosis Preserves Significantly Diverse Protein Profile. Front. Cell. Infect. Microbiol. 10:26. doi: 10.3389/fcimb.2020.00026

For adaptation to stressful conditions, *Mycobacterium tuberculosis* (*Mtb*) is prone to transit to a dormant, non-replicative state, which is believed to be the basis of the latent form of tuberculosis infection. Dormant bacteria persist in the host for a long period without multiplication, cannot be detected from biological samples by microbiological methods, however, their "non-culturable" state is reversible. Mechanisms supporting very long capacity of mycobacteria for resuscitation and further multiplication after prolonged survival in a dormant phase remain unclear. Using methods of 2D electrophoresis and MALDI-TOF analysis, in this study we characterized changes in the proteomic profile of *Mtb* stored for more than a year as dormant, non-replicating cells with a negligible metabolic activity, full resistance to antibiotics, and altered morphology (ovoid forms). Despite some protein degradation, the proteome of 1-year-old dormant mycobacteria retained numerous intact proteins. Their protein profile differed profoundly from that of metabolically active cells, but was similar to the proteome of the 4-month-old dormant bacteria. Such protein stability is likely to be due to the presence of a significant number of enzymes involved in the protection from oxidative stress (katG/Rv1908, sodA/Rv3846, sodC/Rv0432, bpoC/Rv0554), as well as chaperones (dnaJ1/Rv0352, htpG/Rv2299, groEL2/Rv0440, dnaK/Rv0350, groES/Rv3418, groEL1/Rv3417, HtpG/Rv2299c, hspX/Rv2031), and DNA-stabilizing proteins. In addition, dormant cells proteome contains enzymes involved in specific metabolic pathways (glycolytic reactions, shortened TCA cycle, degradative processes) potentially providing a low-level metabolism, or these proteins could be "frozen" for usage in the reactivation process before biosynthetic processes start. The observed stability of proteins in a dormant state could be a basis for the long-term preservation of *Mtb* cell vitality and hence for latent tuberculosis.

Keywords: dormant cells, non-culturable cells, *Mycobacterium tuberculosis*, 2D electrophoresis, proteomic profile

INTRODUCTION

Mycobacterium tuberculosis (*Mtb*) is a most successful pathogen that may persist in a dormant state in a human body for decades and can reactivate to the active stage of disease after a long period of time (Flynn and Chan, 2001). Dormancy has been defined as a reversible state of low metabolic activity in which cells could survive for a long time without replication (Young et al., 2005). However, little is known about the biochemical processes which might occur in cells in the dormant state that provide long-lasting survival. Proteomic studies could potentially bring valuable information in this respect. Because only very little amounts of dormant *Mtb* cells can be recovered from the organs of infected individuals for such analysis, models which imitate the dormant state have been explored. Indeed, proteomic studies of dormancy models were performed using 2D electrophoresis (Florczyk et al., 2001; Betts et al., 2002; Rosenkrands et al., 2002; Starck et al., 2004; Devasundaram et al., 2016) and more advanced methods such us LC-MS/MS and SWATH (Albrethsen et al., 2013; Schubert et al., 2015). However, all known proteomic studies of dormant *Mtb* cells were performed on "short-term" models, such as the hypoxic Wayne model (formation of non-replicative form due to gradual depletion of oxygen in the growth medium) (Wayne, 1994) and the Loebel model based on starvation of cells in PBS buffer (Loebel et al., 1933), where the time of stress does not exceed 6 weeks. Moreover, the dormant cells obtained in these dormancy models don't mimic the true latent state *in vivo*, where cells are characterized by "non-culturability" (transient inability to grow on the non-selective solid media) and resistance to antibiotics (Khomenko and Golyshevskaya, 1984; Dhillon et al., 2004; Chao and Rubin, 2010). We have developed a model of the transition of *Mtb* cells into the dormant state based on the gradual acidification of the culture medium (Shleeva et al., 2011). The cells obtained in this model are characterized by a thickened cell wall, ovoid morphology, negligible metabolic activity, and resistance to antibiotics (Shleeva et al., 2011). In our study we explore proteomic profiling of *Mtb* dormant cells after 4 and 13 months of storage using 2D electrophoresis followed by MALDI-TOF analysis to characterize proteins (if any) of dormant cells that stored well after such a long period of time. The 2D electrophoresis method for proteome characterization was used in this study since this method allows the determining of intact proteins in the presence of the products of protein degradation which is highly possible after long storage.

MATERIALS AND METHODS

Bacterial Strains, Growth Media, and Culture Conditions

Inoculum was initially growth from frozen stock stored at −70°C in 40% glycerine. *Mtb* strain H37Rv was grown for 8 days (up to $OD_{600} = 2.0$) in Middlebrook 7H9 liquid medium (Himedia, India) supplemented with 0.05% Tween 80 and 10% growth supplement ADC (albumin, dextrose, catalase) (Himedia, India). One milliliter of the initial culture was added to 200 ml of modified Sauton medium contained (per liter): KH_2PO_4, 0.5 g; $MgSO_4.7H_2O$, 1.4 g; L-asparagine, 4 g; glycerol, 2 ml; ferric ammonium citrate, 0.05 g; citric acid, 2 g; 1% $ZnSO_4.7H_2O$, 0.1 ml; pH 6.0–6.2 (adjusted with 1 M NaOH) and supplemented with 0.5% BSA (Cohn Analog, Sigma), 0.025% tyloxapol and 5% glucose. Cultures were incubated in 500 ml flasks contained 200 ml modified Sauton medium at 37°C with shaking at 200 rpm (Innova, New Branswick) for 30–50 days, and pH values were periodically measured. In log phase pH of the culture reached 7.5–8 and then decrease in stationary phase. When the medium in post-stationary phase *Mtb* cultures reached pH 6.0–6.2 (after 30–45 d of incubation for different experiments), cultures (50 ml) were transferred to 50 ml plastic tightened capped tubes and kept under static conditions, without agitation, at room temperature for up to 13 months post inoculation. At the time of transfer 2-(N-morpholino) ethanesulfonic acid (MES) was added in a final concentration 100 mM to dormant cell cultures to prevent fast acidification of the spent medium during long-term storage.

Cyclic AMP Determination

Cell cultures at different stages of growth and storage were centrifuged at 13,000 g for 5 min. The cell pellets were treated with 1 ml 0.1 N HCl, heated at 95°C for 10 min and frozen immediately. The collected samples were disrupted by using a bead homogeniser FastPrep- 24, bacterial debris were removed by centrifugation, and aliquots of the supernatant were taken for the estimation of cAMP. To neutralize acidic sample Na_2CO_3 in concentration 2 M was used immediately before the samples were applied to the plates (Dass et al., 2008). cAMP levels were measured by ELISA using 96-well plates (96 Well ELISA Microplate, Greiner bio-one, Austria). Protein G (Imtek, Russia) (40 μg/ml) in PBS pH 7.4 was added to each well of 96-well plates and incubated for 2 h at the room temperature. Plates were washed using PBS containing 0.05% Triton X-100 (PBST). One hundred microliters of rabbit cAMP antibody (1:5,000) (GenScript, United States) and cAMP-HRP (1:20,000) (cAMP- peroxidase conjugate, GenScript, United States) was added to each well-followed by the addition of 50 μl of neutralized sample. After incubation for 2 h at room temperature microplates were washed with PBS. One hundred microliters of freshly prepared substrate contained 0.4 mM 3.3′,5.5′-tetramethylbenzidine (TMB, Sigma) in sodium citrate buffer (pH 4.0; 100 mM) with 3 mM H_2O_2 was added to each well and plates were incubated at room temperature for 30–40 min. The reaction was stopped by adding 100 μl 1M H_2SO_4. The results were registered at 450 nm with a Zenyth 3,100 microplate reader (Anthos Labtec Instruments, Austria). Three independent replicates were performed for each sample.

Respiration, DCPIP Reduction

Endogenous respiratory chain activity (complex I) was determined by reduction of DCPIP (2,6-dichlorophenolindophenol) in the presence of menadione monitored spectrophotometrically at 600 nm. The reaction mixture (4 ml) contained 0.2 μmol 2,6-DCPIP, 0.6 μmol menadione, and 400 μl of the cell suspension in Sauton medium (pH 7.4).

Microscopy

Phase–contrast epifluorescence microscopy was carried out on a Nikon eclipse Ni-U microscope, magnification 1,500×. Photos were taken using Nikon DS Qi2 camera (Japan).

Viability Evaluation by MPN

Most probable number (MPN) assays of *Mtb* were performed in 48-well plastic plates (Corning) containing 1 ml special media for the most effective reactivation of dormant *Mtb* cells. This media contains 3.25 g nutrient broth dissolved in 1 liter of mixture of Sauton medium (0.5 g KH_2PO_4; 1.4 g $MgSO_4.7H_2O$; 4 g L-asparagine; 0.05 g ferric ammonium citrate; 2 g sodium citrate; 0.01% (w/v) $ZnSO_4.7H_2O$ per liter pH 7.0), Middlebrook 7H9 liquid medium (Himedia, India) and RPMI (Thermo Fisher Scientific, USA) (1:1:1) supplemented with 0.5% v/v glycerol, 0.05% v/v Tween 80, 10% ADC (Himedia, India).

Mtb cells were serially 10-fold diluted in the reactivation medium. Appropriate five serial dilutions of *Mtb* cells (100 μl) were added to each well-contained the same medium in triplicate. Plates were incubated at 37°C with agitation at 130 rpm for 21 days. Wells with visible bacterial growth were counted as positive, and MPN values were calculated using standard statistical methods (de Man, 1974).

Viability Evaluation by CFU

Bacterial suspensions were serially diluted in fresh Sauton medium with 0.05%, and three replicates of 10 μl samples from each dilution were spotted on Middlebrook 7H9 liquid medium (Himedia, India) supplemented 1.5% (w/v) agar and 10% (v/v) ADC (Himedia, India). Plates were incubated at 37°C for 30 days, and CFUs were counted. The lower limit of detection was 10 CFU/ml.

Metabolic Activity Estimation

Cell metabolic activity was determined by incorporation of 1 μl of [5,6-^{3}H]-uracil (1 μCi, 0.02 μmol) as well as L-[U-^{14}C]-asparagine (4 MBq) into cells (1 ml). Cell suspension was incubated for 24 h at 37°C with agitation (for active cells) or at room temperature without agitation (for dormant cells). Cells (200 μl) were then harvested on glass microfiber GF/CTM filters (Whatman, UK) and washed with 3 ml 7% trichloroacetic acid followed by 3 ml absolute ethanol. Air-dried filters were placed in scintillation liquid (Ultima GoldTM, Perkin Elmer, USA), and the radioactivity incorporation was measured with a scintillation counter LS6500 (Beckman, USA).

Sample Preparation for 2D Electrophoresis

Active and dormant cells obtained in four biological replicates were pooled (total volume 200 ml for each replicate, cell amount was ca 3.5 g wet weight) for 2D electrophoretic analysis. It is known that pooling allows to obtain an average expression of a particular protein which matches the mean expression of that protein after averaging of several individual replicates (Diz et al., 2009). The pooling should reduce influence of the technical factors (especially during the destruction of dormant cells and extraction of proteins) on the result of 2D electrophoresis. This approach has been previously used in mycobacterial proteomic studies (Betts et al., 2002; Trutneva et al., 2018). Bacteria were harvested by centrifugation at 8,000 g for 15 min and washed 10 times with a buffer containing (per liter) 8 g NaCl, 0.2 g KCl, and 0.24 g Na_2HPO_4 (pH 7.4). The bacterial pellet was re-suspended in ice-cold 100 mM HEPES (4-(2-hydroxyethyl)-1-piperazineethanesulphonic acid) buffer (pH 8.0) containing complete protease inhibitor cocktail (Sigma, USA) and PMSF (Phenylmethanesulphonyl fluoride) then disrupted with zirconium beads on a bead beater homogeniser (MP Biomedicals FastPrep-24) for 1 min, 5 times for active cells and 10 times for dormant cells. The bacterial lysate was centrifuged at 25,000 g for 15 min at 4°C. The supernatant was separated into membrane and cytosolic fractions using ultracentrifugation at 100,000 g for 2 h (Parish and Roberts, 2015). The membrane fraction was washed with HEPES buffer three times using ultracentrifugation. To isolate the proteins from membrane fraction extraction was performed using the strong anionic detergent sodium dodecyl sulfate (SDS) (2% w/v). The cytosolic fraction and membrane extract were precipitated using the ReadyPrep 2-D cleanup kit (BioRad, USA) to remove ionic contaminants such as detergents, lipids, and phenolic compounds from protein samples. This kind of precipitation allows resuspension of the protein pellet in isoelectric focusing buffer contains 8 M urea, 2 M thiourea, 10 mM 1,4-dithiothreitol (DTT), 2 mM TCEP (Tris(2-carboxyethyl)-phosphine-hydrochloride), 1% (w/v) CHAPS, 1% (w/v) Triton X-100, 1% (w/v) amidosulphobetaine-14 (ASB), and 0.4% (v/v) ampholytes (pH 3–10).

Protein Amount Determination

Flores quantitative estimation of protein was used to check protein amount (Flores, 1978). Into 180 μl of the reaction mixture containing the bromophenol blue (0.0075%) dissolved in a solution of 15% ethanol and 2.5% glacial acetic acid was added 20 μl of sample in 100 mM Hepes (for cytosol) or in 100 mM Hepes in buffer (pH 8.0) contained 2% SDS dissolved (for membrane extracts). The absorbance at 610 nm was determined and adjusted to the calibration curve of the bovine serum albumin. Corresponding buffer was used for control.

Two-Dimensional Electrophoresis

Isoelectric focusing was performed in a 5% acrylamide gel (30% (w/v) acrylamide/bisacrylamide, 8 M urea, 2% (v/v) ampholyte pH 3–10 and 4–6 (1:4), 1% (w/v) CHAPS, 1% (w/v) Triton X-100, 0.4% (w/v) ASB) using 2.4 mm ID glass tubes in a Tube Cell (Model 175, BioRad, USA) until 3,700 Vhrs were attained. One hundred micrograms of total protein amount of each sample was used for analysis. After focusing, gels were extracted from the glass tubes and fixed in equilibration buffer 1 (0.375 M Tris-HCl, pH 6.8, 2 M urea, 20% (v/v) glycerol, 2% (w/v) SDS, 2% (w/v) DTT) and equilibration buffer 2 (0.375 M Tris-HCl, pH 6.8, 2 M urea, 20% (v/v) glycerol, 2% (w/v) SDS and 0.01% (w/v) bromophenol blue) for 15 min each. Second-dimension separation was performed as described by O'Farrell (O'Farrell, 1975) in large format (20 × 20 cm), 1.5 mm thick 12% SDS-PAGE gels in standard Tris-glycine buffer in a PROTEAN II xi cell for vertical electrophoresis (BioRad, USA). The gels were stained

by Coomassie CBBG-250 (Roti-Blue Carl Roth, Germany) followed by silver staining (https://www.alphalyse.com/wp-content/uploads/2015/09/Silver-staining-protocol.pdf).

The gels images were captured using Syngene G:BOX Gel & Blot Imaging Systems (Syngene, UK). Gel images stained by Coomassie were analyzed using TotalLab TL120 software to calculate spot density.

Each visible protein spot was excised manually from the gel and analyzed using MALDI-TOF. The MS/MS data obtained from MALDI-TOF were subjected to a Mascot Protein Database (MSDB) search to identify proteins. Proteins with coverage $< 10\%$ were not further considered. Protein functional roles for *Mtb* were obtained from the Mycobrowser database (https://mycobrowser.epfl.ch). Each sample for 2D analysis was performed in two technical replicates.

Protein Identification by MALDI-TOF

All fractions excised from 2D electrophoresis slab gels were hydrolyzed by trypsin digestion. The extracted tryptic peptides were analyzed by MALDI-TOF as described previously, with some modifications. A sample (0.5 μl) was mixed with the same volume of 20% (v/v) acetonitrile solution containing 0.1% (v/v) trifluoroacetic acid and 20 mg/ml 2,5-dihydroxybenzoic acid and then air-dried. Mass spectras were obtained on a Reflex III MALDI-TOF mass spectrometer with a UV laser (336 nm) in positive-ion mode in the range of 500–8,000 Da. Calibration was performed in accordance with the known peaks of trypsin autolysis.

For MS/MS analysis, the mass spectra of fragments were recorded with a Bruker Ultraflex MALDI-TOF mass spectrometer in tandem mode (TOF-TOF) with detection of positive ions. The proteins were identified using Mascot software in Peptide Fingerprint mode (Matrix Science, Boston, MA, USA). The accuracy of the mass measurement MH+ was 0.01% (with a possibility of modifying cysteine by acrylamide and methionine oxidation). Raw data and search results could be found on PeptideAtlas: http://www.peptideatlas.org/PASS/PASS01450.

RESULTS

Active cells for proteome analysis were obtained in the early stationary phase after 10 days of cell growth under agitation (culture "A") in standard Sauton medium (Connell, 1994). Dormant *Mtb* cells in the prolonged stationary phase were obtained by gradual acidification of the medium according to a published protocol (Shleeva et al., 2011) with some minor modifications (see M&M). Dormant cells were kept in plastic-capped tubes to avoid evaporation in the dark at room temperature for 4.5 months (culture "D1") and 13 months (culture "D2"). Under these conditions cells remain aerobic as the methylene blue did not decolorize and hence oxygen was not completely depleted (Shleeva et al., 2011). In addition, cytochrome composition of respiratory chain for culture D1 did not differ from active cells (Nikitushkin, personal communication) which indicates aerobic condition in contrast to Wayne cells where increased *bd* cytochrome oxidase as a terminal acceptor under oxygen depletion has been found (Kana et al., 2001; Shi et al., 2005). The estimated viability of stored dormant cells by CFU was about 10^4 cells/ml for D1 and zero for D2 mycobacteria (**Table 1**). The MPN (Most probable number) assay (estimation of viability in liquid medium) revealed a viable cell number higher than CFU, reflecting the reversible "non-culturablity" of these dormant cells on the solid media after this storage period (**Table 1**). According to the biochemical studies, dormant cells did not show transcriptional (by ^{3}H-uracil incorporation) and translational activity (by ^{14}C-asparigine incorporation), and they were characterized by a significant decrease in the activity of endogenous DCPIP (2,6-dichlorophenolindophenol) reduction reflecting respiratory activity (complex I) (**Table 1**).

We also checked the intracellular concentration of cAMP. Previously we found that the transition of *Mtb* to the dormant "non-culturable" state correlates with a decrease in the cAMP concentration (Shleeva et al., 2017a). Alternatively, cAMP concentration increases in *Msm* cells under resuscitation (Shleeva et al., 2013). Accordingly, we found a decrease in the cAMP concentration in *Mtb* cells after 4.5 months of storage which accompanied the significant developing of "non culturability" (**Table 1**).

Dormant cells were washed 10 times using PBS to remove dead cells. This approach results in ∼60% intact cells in the population according to PI (propidium iodide) staining (not shown). Such cells appeared small and ovoid in comparison to the rod-shaped cells typical of multiplying bacteria (**Figure 1**). These dormant cells contained less protein per mg wet cell weight in comparison to active cells. This was more evident for the membrane fraction than for the cytoplasm (**Table 1**). Obtained dormant cells were used for proteomic analysis. In each

TABLE 1 | Some properties of active and dormant *Mtb* cells.

Characteristic	Active cells	Dormant cells 4.5 months (D1)	Dormant cells 13 months (D2)
CFU, cells/ml	$(5 \pm 2) \times 10^7$	$(1 \pm 0.5) \times 10^4$	0
MPN, cells/ml	1.2×10^8-mean 3.7×10^7-low* 4.2×10^8-high*	9.3×10^7-mean 1.8×10^7-low* 4.2×10^8-high*	1.5×10^6-mean 4.5×10^5-low* 4.2×10^6-high*
H^3- Uracil inc. rate, CPM/mg wet cell weight	3,623 ± 52	0	0
cAMP, pmol/mg wet cell weight	124 ± 4	2 ± 1	0
^{14}C-asparigine inc. rate CPM/mg wet cell weight	340 ± 20	0	0
DCPIP reduction, nmol DCPIP min^{-1} mg^{-1} wet cell weight	0.11 ± 0.03	0.016 ± 0.003	0
Protein amounts in cytosol, mg/g wet cell weight	3.6 ± 0.2	2.13 ± 0.2**	2.55 ± 0.2**
Protein amounts in membrane fraction, μg/g wet cell weight	76.2 ± 5	39 ± 5**	20.7 ± 5**

95 percent confidence intervals.

***Dormant cells were 10 times washed before protein determination.*

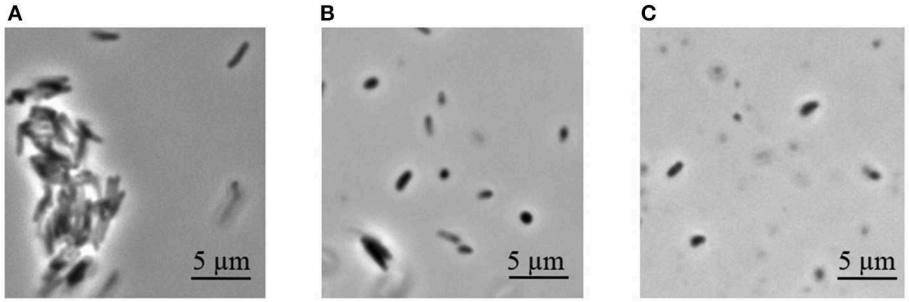

FIGURE 1 | Phase contrast microscopy of *M. tuberculosis* cells (magnification 1.500). **(A)** Active cells in early stationary phase. **(B)** Dormant cells after 4.5 months storage at room temperature. **(C)** Dormant cells after 13 months storage.

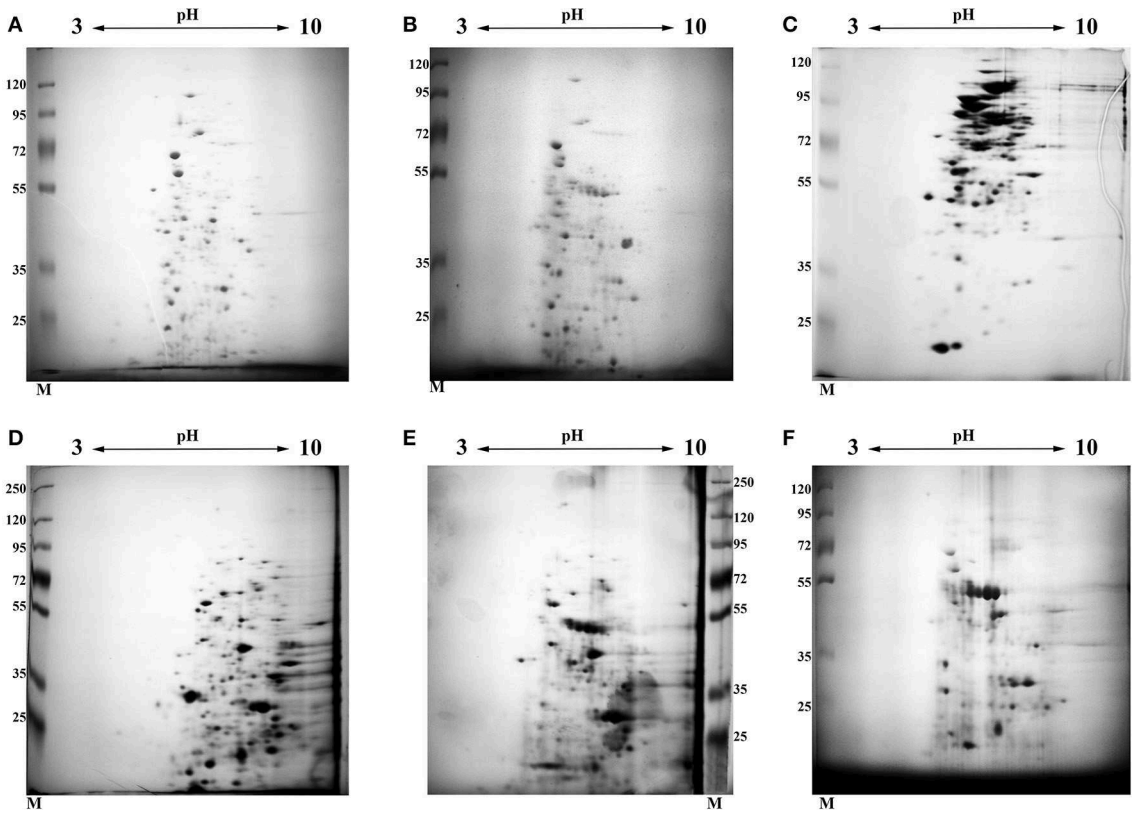

FIGURE 2 | 2D electrophoresis of different fractions obtained from active and dormant *M. tuberculosis* cells. Each gel was stained by Coomassie followed by silver staining. **(A)** Cytosol fraction of active, early stationary phase cells. **(B)** Cytosol fraction of dormant cells after 4.5 months storage at room temperature (D1). **(C)** Cytosol fraction of dormant cells after 13 months storage at room temperature (D2). **(D)** Membrane fraction extracted by SDS of active, early stationary phase cells. **(E)** Membrane fraction extracted by SDS of dormant cells after 4.5 months storage at room temperature (D1). **(F)** Membrane fraction extracted by SDS of dormant cells after 13 months storage at room temperature (D2). The gel photo represents one out of two identical technical replicates.

experiment the protein amount used for the first dimension was identical for both types of cells, although the total amount of protein isolated from active cells was different.

In order to elucidate and characterize the pool of proteins which are presented in "early" –(D1, 4.5 months of storage when significant decrease in metabolic activity judged by uracil incorporation was found) and "late" (13 month of storage D2) dormant cells, we analyzed the protein composition of different fractions (cytosol and membranes) by 2D electrophoresis. The results of these experiments are shown in **Figure 2** (2D photo). Manual excision of each spot from the gel followed by MALDI TOF allowed us to uncover a total of 21,703 peptides (12,318 cytosol + 9,385 membranes) in all 3 types of cells including protein repeats in the different spots. According to the Mascot

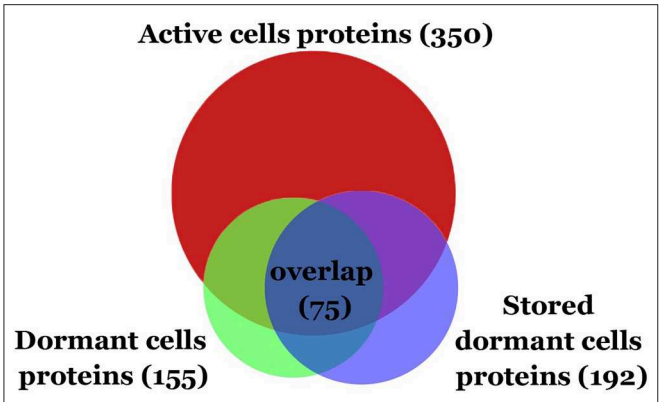

FIGURE 3 | Venn diagram showing the protein overlap between active, dormant (D1), and stored dormant cells (D2).

database those peptides belonged to 1,131 individual proteins (629 for cytosol and 502 for membranes) including repeating proteins in different types of cells (**Table S1**). Out of these, 446 could be linked to proteins with a different Rv (Uniprot) number (305 for cytosol and 243 for membranes). Each spot contained from 1–4 different proteins (on average 2.2 proteins for all types of cells) in one spot.

Comparative analysis revealed the reduction of protein diversity (350 proteins for active cells, 155 for D1 and 192 for D2 cells) (**Figure 3**), which could be apparently associated with protein degradation during cell transition to the dormant state followed by a long storage. Most significant degradation of proteins was found for cytosol fraction (243 proteins for active cells, 77 for D1 and 92 for D2 cells). In contrast, membrane proteins exhibited more stability (108 proteins for active cells, 79 for D1 and 102 for D2 cells). Protein degradation was visible in the increasing of a front line upon electrophoresis containing evidently degraded material (**Figure 2**). Most likely degradation of proteins into peptides that give a contribution to total protein measuring is responsible for the comparably small difference in protein amount per mg of cells vs. active cells found especially in the cytosolic fraction (**Table 1**).

Only small changes in proteins diversity could be found between early dormant cells and stored dormant cells and more than 50% of the protein is shared between two types of cells (**Figure 3**). This comparison reveals a pool of highly stable proteins in dormant state. At the same time, old dormant cells proteome (D2) contained proteins that are detected neither in the active nor in the early dormant proteome (**Table S2**). Apparently, these are stable proteins but in minor abundance in active cells. 53 proteins in D1, which are not presented in the dormant D2 proteome, were evidently degraded during the late phase of storage. From these, 43 proteins were found neither in active nor in stored dormant culture proteomes, probably reflecting their importance in the transition from multiplying to dormant state.

Identified proteins were ranked by their representation in the whole proteome, on the basis of the spot density (**Table S1**). This analysis allows comparing individual protein abundance in different cell types under conditions when total amount of protein per cell is not equal (**Table 1**).

A similar approach has been used previously for the comparative proteomic analysis of active and dormant *Msm* cells (Trutneva et al., 2018).

This analysis allows to find a cohort of proteins with substantially changed abundance in dormant vs. active cells [totally 139 increased proteins and 248 decreased proteins (**Table S3**)]. Remarkably, that majority of proteins found in 10 most abundant spots in D2 culture are more abundant or even ≪unique≫ in comparison with active culture (**Table 2**). We also analyzed the proteins with the aim of determining their stability after long storageand to elucidate metabolic pathways in which they could participate.

Such analysis of D2 proteins and their sorting according to their participation in particular metabolic reactions was represented in **Table S4**. Among them quite a few proteins were found to belong to the tricarboxylic acid (TCA) cycle (in contrast to the active cell proteome where all components were found). Namely, enzymes which facilitate the conversion of oxaloacetate to succinate via fumarate (mdh/Rv1240, fum/Rv1098, succinate dehydrogenase/Rv0247, Rv0248), compose the reductive branch of the TCA cycle which could potentially be used for the TCA cycle functioning in the opposite direction with formation of succinate as an end product (Zimmermann et al., 2015). The D2 proteome contains enzymes involved in the glycolytic pathway (glucose-6-phosphate isomerase/Rv0946, fructose-bisphosphate aldolase/Rv0363, phosphoglycerate kinase/Rv1437, enolase/Rv1023, pyruvate kinase/Rv1617), biosynthesis of fatty acids, cell wall and amino acid interconversion. A significant proportion (18 proteins) of the D2 proteome were found to participate in the hydrolysis of lipids, proteins and amino acids (**Table S4**).

Among the 192 proteins found in D2 cells a substantial number (19 proteins) belong to enzymes involved in defense mechanisms. Enzymes with catalase/peroxidase/superoxide dismutase activities (katG/Rv1908, sodA/Rv3846, sodC/Rv0432, bpoC/Rv0554) were presented in D2 cells. DNA binding histone-like protein (hupB/Rv2986) (**Table 2**) is capable of stabilizing DNA and prevents its denaturation under stress conditions (Enany et al., 2017). Previously it was found that HupB ortholog in *Msm* (Hlp) can provide compactization of the nucleoid during dormancy (Anuchin et al., 2010). It is interesting that a major protein found in the membrane fraction in D2 cells is Rv0341(iniB, **Table 2**) with unknown function that could also modify DNA topology due to its ability to interact with DNA (Shleeva et al., 2018) via a DNA-binding domain presented in the molecular structure according to Uniprot data base annotation.

The thioredoxin system of Rv3913/Rv3914, a well-known antioxidant defense system that participates in the virulence-determining mechanism in *Mtb* (Budde et al., 2004) was found "uniquely" in the proteome of dormant cells. In addition, the thioredoxin system and the protein with unknown function Rv2466c ("unique" for dormant cells as well) is controlled by SigH sigma factor, which is involved in the adaptation of *Mtb* to heat shock, oxidative and nitrosive stress (Raman et al., 2001). However, neither SigH nor other sigma factors

TABLE 2 | Proteins found in 10 most abundant spots in D2 proteome profile.

Fraction	Product	Gene	Place, active	Place, D2
Membrane	Probable iron-regulated elongation factor TU Tuf (EF-TU)	Rv0685	2	1
Cytosol	Probable 5-methyltetrahydropteroyltriglutamate–homocysteine methyltransferase MetE (methionine synthase, vitamin-B12 independent isozyme)	Rv1133c	85	1
Cytosol	Transketolase Tkt (TK)	Rv1449c	N/D	1
Cytosol	Malate synthase G GlcB	Rv1837c	134	1
Cytosol	Catalase-peroxidase-peroxynitritase T KatG	Rv1908c	85	1
Cytosol	Probable chaperone protein DnaK (heat shock protein 70) (heat shock 70 kDa protein) (HSP70)	Rv0350	5	2
Cytosol	60 kDa chaperonin 2 GroEL2 (protein CPN60-2) (GroEL protein 2) (65 kDa antigen) (heat shock protein 65) (cell wall protein A) (antigen A)	Rv0440	3	2
Membrane	Conserved 35 kDa alanine rich protein	Rv2744c	9	2
Cytosol	Maltokinase Mak	Rv0127	N/D	3
Membrane	Isoniazid inductible gene protein IniB	Rv0341	N/D	3
Membrane	Conserved protein	Rv1232c	41	3
Cytosol	Glutamine synthetase GlnA1 (glutamine synthase) (GS-I)	Rv2220	122	3
Cytosol	Probable adenosylhomocysteinase SahH (S-adenosyl-L-homocysteine hydrolase) (adohcyase)	Rv3248c	N/D	3
Cytosol	10 kDa chaperonin GroES (protein CPN10) (protein GroES) (BCG-a heat shock protein) (10 kDa antigen)	Rv3418c	N/D	4
Membrane	Probable bifunctional protein acetyl-/propionyl-coenzyme A carboxylase (alpha chain) AccA3: biotin carboxylase + biotin carboxyl carrier protein (BCCP)	Rv3285	83	5
Membrane	60 kDa chaperonin 1 GroEL1 (protein CPN60-1) (GroEL protein 1)	Rv3417c	48	6
Cytosol	Probable iron-regulated phosphoenolpyruvate carboxykinase [GTP] PckA (phosphoenolpyruvate carboxylase) (PEPCK)(pep carboxykinase)	Rv0211	130	7
Membrane	Probable short-chain type oxidoreductase	Rv0484c	N/D	7
Membrane	Possible ketoacyl reductase	Rv1544	N/D	7
Membrane	DNA-binding protein HU homolog HupB (histone-like protein) (HLP) (21-kDa laminin-2-binding protein)	Rv2986c	N/D	7
Cytosol	Probable acetohydroxyacid synthase IlvX (acetolactate synthase)	Rv3509c	83	8
Cytosol	Probable NAD(P) transhydrogenase (subunit alpha) PntAa [first part; catalytic part] (pyridine nucleotide transhydrogenase subunit alpha) (nicotinamide nucleotide transhydrogenase subunit alpha)	Rv0155	94	9
Membrane	Probable succinate dehydrogenase [iron-sulfur subunit] (succinic dehydrogenase)	Rv0247c	12	9
Cytosol	Probable succinyl-CoA synthetase (beta chain) SucC (SCS-beta)	Rv0951	119	9
Cytosol	Probable phosphoglycerate kinase Pgk	Rv1437	94	9
Membrane	Probable catechol-O-methyltransferase	Rv1703c	N/D	9
Membrane	Conserved protein	Rv3205c	N/D	9
Membrane	Probable O-antigen/lipopolysaccharide transport ATP-binding protein ABC transporter RfbE	Rv3781	N/D	9
Membrane	Probable short-chain type dehydrogenase/reductase	Rv0148	N/D	10
Membrane	Periplasmic superoxide dismutase [Cu-Zn] SodC	Rv0432	5	10
Cytosol	Probable citrate synthase I GltA2	Rv0896	N/D	10

In the columns marked as "place," proteins were arranged according to their spot density. See also M&M. Proteins with increased abundance in D2 cells vs. active cells (place for active cells proteome minus place for D2 > 10) are highlighted including proteins which were virtually absent in the active cells proteome (marked as "ND").

were found, possibly due to their low concentrations in the cell.

Several chaperone proteins were found to be highly presented in D2 (dnaJ1/Rv0352, htpG/Rv2299, groEL2/Rv0440, dnaK/Rv0350, groES/Rv3418, groEL1/Rv3417, HtpG/Rv2299c, hspX/Rv2031). It is not a surprise that Heat shock protein (HspX/Rv2031c), a member of the DosR regulon, was found to be increased in the dormant cells, since its significant accumulation was found in all other dormancy models (Florczyk et al., 2001; Betts et al., 2002; Rosenkrands et al., 2002; Starck et al., 2004; Mishra and Sarkar, 2015; Devasundaram et al., 2016). Apart from HspX, among 48 proteins belonging to the DosR regulon, several universal stress proteins (Rv2623, Rv1996, Rv2624) and several proteins with unknown functions (Rv2004, Rv2629) were only found.

Secreted antigen 85-B FbpB/Rv1886c that possesses mycolyltransferase activity required for the biogenesis of trehalose dimycolate (cord factor), a dominant structure necessary for maintaining cell wall integrity (Nguyen et al., 2005) was found in D2.

A number of proteins that participate in transcription and translation processes were represented in D1/D2 despite negligible activity of these processes under dormancy (**Table S1**). Other proteins involved in different metabolic reactions, transport activity and transcriptional regulation were shown in **Table S1**. It is interesting that despite the almost zero

level of respiratory chain activity [by DCPIP (**Table 1**) and by methylene blue (Shleeva et al., 2011) reduction] its components as well as H^+-ATPase (Rv1308, Rv1309, Rv1310) were found in dormant cells.

Among proteins with increased abundance in dormant cells (**Table S3**) mycobacterial persistence regulator MprA/Rv0981, the response regulator and part of two-component histidine-kinase system was found in D1. Under stress conditions, MprAB induces sigE transcription, which leads to an increase in the level of relA and, as a consequence, an increase in the level of (p)ppGpp eliciting the stringent response. Such a mechanism, in which the cascade of reactions begins with MprAB activation, is a specific pathway for mycobacteria (e.g., *M. smegmatis*; Sureka et al., 2008), since in other bacteria the first stage is strictly associated with the synthesis of relA (Magnusson et al., 2005). Expression of Rv0981 on the transcriptional level has been found in non-culturable deep dormant *Mtb* cells (Ignatov et al., 2015) whilst short-term dormant Wayn's cells did not show changes in the expression of this gene neither on transcriptional (Galagan et al., 2013) nor proteomic level (Schubert et al., 2015).

Another two-component PhoPR system regulates the *espA* gene cluster which is essential for virulence (Pang et al., 2013; Zhang et al., 2018). In our case, the level of phoP/Rv0757 increased in D1 and D2. It is known that this system is activated when cells enter a low pH environment resulting in the activation of a cluster of genes that help the cell to cope with oxidative stress (García et al., 2018). PhoPR has recently been shown to be a negative regulator of the DosRS (DevRS) system (Vashist et al., 2018). Perhaps that is a reason for the absence of the DevR regulator itself and other proteins belonging to DosR regulon in our model. This is in line with unchanged regulation of the expression of Rv0757 on both transcriptional (Galagan et al., 2013) and proteomic level (Schubert et al., 2015) in short-term Wayne dormancy. Whilst in more prolonged hypoxic conditions (enduring response) transcription of this gene was found to be up-regulated resulting in suppression of DosR regulon expression (Rustad et al., 2008).

A transcription regulator found upregulated in dormant cells is Diviva family protein Wag31 (Rv2145), which regulates cell shape and cell wall synthesis in *Mtb* through a molecular mechanism by which the activity of Wag31 can be modulated in response to environmental signals (Kang et al., 2008). In addition, Wag31 is one substrate of PknA and PknB kinases (Lee et al., 2014). Increased expression of Rv2145 was found on transcriptional level in non-culturable deep dormant *Mtb* cells (Ignatov et al., 2015) and in prolonged starvation model on proteomic level (Albrethsen et al., 2013). However it did not show expression changes in anaerobic cells (Rustad et al., 2008; Galagan et al., 2013; Schubert et al., 2015).

Elongation factor TU (Ef-Tu)/Rv0685, which is normally responsible for the selection and binding of the cognate aminoacyl-tRNA was found in large amounts in all types of cells. The activity of Ef-Tu is dependent on its interaction with GTP which, in turn, depends on Ef-Tu phosphorylation by protein kinases. Such phosphorylation results in a reduction in protein synthesis followed by a reduction of cell growth (Sajid et al., 2011). High amounts of Ef-Tu while phosphorylated could probably cause protein synthesis arrest during the dormant phase. Dephosphorylation of Ef-Tu under resuscitation of dormant *Mtb* cells would result in protein synthesis beginning.

Comparative proteomic analysis revealed that the diversity of active transporters dramatically decreased in dormant cells (**Table S3**). The proteomic profile of the late stage of dormancy (D2) contains only a few transporters comparative to active cells that contain protein, amino acids, oligopeptide, sugar and ion transporters. Similarly, the level of cAMP synthase (Rv1264) was found significantly decreased in D1 and D2 proteomes (**Table S3**). It was established that level of cAMP negatively correlates with storage time of dormant cells (**Table 1**).

The enzymes involved in biosynthesis of cell wall-found in dormant cells proteome were characterized by decreased abundance (**Table S3**).

DISCUSSION

Despite long-term storage the dormant *Mtb* cells' proteome remained enriched with a large diversity of proteins. This is the first investigation where the proteome of dormant *Mtb* cells stored for over a year was examined. Other dormant cells' proteome studies were carried out on cells after 20 days of hypoxic conditions (Schubert et al., 2015) or 6 weeks during starvation (Albrethsen et al., 2013). These short-term proteomic studies had a large overlap between active and dormant cell proteins. Thus, 69 and 66% of the first 200 most represented proteins were identical in those two models, respectively. However, in the present study we have a greater difference in the proteomes of active vs. dormant cells, and the overlap is only 47%. This discrepancy is evidently associated with a deeper dormancy state developed after more than 1 year of storage where cells, in contrast to "short" models, are characterized by "non-culturability" and negligible metabolic activity (**Table 1**). Presumably, long storage of cells results in the selection of the proteins which are most stable during the long period of dormancy and are not degraded within D2 cells and were thus available for analysis.

Comparative analysis of the 200 most abundant proteins in our dormancy model with proteins in Wayne (Schubert et al., 2015) and Loebel (Albrethsen et al., 2013) dormancy models reveals 58 "consensus" proteins (**Table 3**, **Table S5**). Eleven proteins from this list are involved in defense mechanisms and 14 proteins participate in central metabolic pathways (tricarboxylic acid cycle, glycolysis, respiratory chain, and ATPase). DNA-dependent RNA polymerase (alpha and beta chain) as well as elongation factors (Tu/Rv0685, Ts/Rv2889c) also presented in the 200 most abundant proteins shared between the three dormancy models. Obviously, these "consensus" proteins have unique stability in all dormant models despite different inducing factors and may play special roles in the maintaining of cell viability under stress conditions. It is interesting that proteins belonging to the DosR regulon were poorly represented both in D1 and D2, which highlights the difference between the Wayne anaerobic model and the model used in this study. This is also true for the Wayne vs. the Loebel model (Albrethsen et al., 2013). Evidently, due to the low metabolic activity of dormant

TABLE 3 | "Consensus" proteins shared between the 3 *Mtb* dormancy models found in the first 200 most abundant.

Gene number	Product
Rv1908c	Catalase-peroxidase-peroxynitritase T KatG
Rv1837c	Malate synthase G GlcB
Rv1133c	Probable 5-methyltetrahydropteroyltriglutamate–homocysteine methyltransferase MetE (methionine synthase, vitamin-B12 independent isozyme)
Rv0685	Probable iron-regulated elongation factor TU Tuf (EF-TU)
Rv1449c	Transketolase Tkt (TK)
Rv0440	60 kDa chaperonin 2 GroEL2
Rv2744c	Conserved 35 kDa alanine rich protein
Rv0350	Probable chaperone protein DnaK (heat shock protein 70) (heat shock 70 kDa protein) (HSP70)
Rv2220	Glutamine synthetase GlnA1 (glutamine synthase) (GS-I)
Rv3248c	Probable adenosylhomocysteinase SahH (S-adenosyl-L-homocysteine hydrolase) (adohcyase)
Rv3418c	10 kDa chaperonin GroES (protein CPN10) (protein GroES) (BCG-a heat shock protein) (10 kDa antigen)
Rv3285	Probable bifunctional protein acetyl-/propionyl-coenzyme A carboxylase (alpha chain) AccA3: biotin carboxylase + biotin carboxyl carrier protein (BCCP)
Rv3417c	60 kDa chaperonin 1 GroEL1 (protein CPN60-1) (GroEL protein 1)
Rv0211	Probable iron-regulated phosphoenolpyruvate carboxykinase [GTP] PckA
Rv0951	Probable succinyl-CoA synthetase (beta chain) SucC (SCS-beta)
Rv0896	Probable citrate synthase I GltA2
Rv1074c	Probable beta-ketoacyl CoA thiolase FadA3
Rv0363c	Probable fructose-bisphosphate aldolase Fba
Rv1617	Probable pyruvate kinase PykA
Rv1017c	Probable ribose-phosphate pyrophosphokinase PrsA (phosphoribosyl pyrophosphate synthetase)
Rv1310	Probable ATP synthase beta chain AtpD
Rv2280	Probable dehydrogenase
Rv2145c	Diviva family protein Wag31
Rv3028c	Probable electron transfer flavoprotein (alpha-subunit) FixB (alpha-ETF) (electron transfer flavoprotein large subunit) (ETFLS)
Rv1886c	Secreted antigen 85-B FbpB (85B) (antigen 85 complex B) (mycolyl transferase 85B) (fibronectin-binding protein B) (extracellular alpha-antigen)
Rv1094	Possible acyl-[acyl-carrier protein] desaturase DesA2 (acyl-[ACP] desaturase) (stearoyl-ACP desaturase)
Rv1023	Probable enolase Eno
Rv1475c	Probable iron-regulated aconitate hydratase Acn (citrate hydro-lyase) (aconitase)
Rv0815c	Probable thiosulfate sulfurtransferase CysA2
Rv3246c	Two component sensory transduction transcriptional regulatory protein MtrA
Rv1436	Probable glyceraldehyde 3-phosphate dehydrogenase Gap (GAPDH)
Rv3224	Possible iron-regulated short-chain dehydrogenase/reductase
Rv2996c	Probable D-3-phosphoglycerate dehydrogenase SerA1 (PGDH)
Rv0860	Probable fatty oxidation protein FadB
Rv3841	Bacterioferritin BfrB
Rv0831c	Conserved protein
Rv0242c	Probable 3-oxoacyl-[acyl-carrier protein] reductase FabG4
Rv2971	Probable oxidoreductase
Rv3280	Probable propionyl-CoA carboxylase beta chain 5 AccD5 (pccase) (propanoyl-CoA:carbon dioxide ligase)
Rv3457c	Probable DNA-directed RNA polymerase (alpha chain) RpoA
Rv1308	Probable ATP synthase alpha chain AtpA
Rv3846	Superoxide dismutase [FE] SodA
Rv3274c	Probable acyl-CoA dehydrogenase FadE25
Rv1630	30S ribosomal protein S1 RpsA
Rv2780	Secreted L-alanine dehydrogenase Ald (40 kDa antigen) (TB43)
Rv3914	Thioredoxin TrxC (TRX) (MPT46)
Rv0667	DNA-directed RNA polymerase (beta chain) RpoB (transcriptase beta chain)
Rv2140c	Conserved protein TB18.6
Rv0468	3-hydroxybutyryl-CoA dehydrogenase FadB2
Rv3596c	Probable ATP-dependent protease ATP-binding subunit ClpC1
Rv2334	Cysteine synthase a CysK1
Rv0462	Dihydrolipoamide dehydrogenase LpdC
Rv0684	Probable elongation factor G FusA1 (EF-G)
Rv0632c	Probable enoyl-CoA hydratase EchA3
Rv2031c	Heat shock protein HspX (alpha-crystallin homolog) (14 kDa antigen) (HSP16.3)
Rv2889c	Probable elongation factor Tsf (EF-ts)
Rv2215	DlaT, dihydrolipoamide acyltransferase, E2 component of pyruvate dehydrogenase
Rv2299c	Probable chaperone protein HtpG (heat shock protein)

cells, a large number of proteins (enzymes) found in the late phase of dormancy (D2) are not functionally active. For example, ATPase is unable to perform the synthesis of ATP because of the extremely low activity of the respiratory chain which results in low ATP level (Shleeva et al., 2011). The same is applicable for enzymes involved in transcription and translation. At the same time, such inactive D2 proteins can be considered as a reserve which can be used in the early stages of reactivation before transcription and protein synthesis *de novo*. Indeed, the beginning of the transcription takes place not at the first moment of reactivation of long-stored dormant cells, but much later, 4 days after reactivation (not shown). On the other hand, some D2 proteins could be functionally active, providing some level of metabolism maintenance. In addition, some degradative enzymes could be potentially active to provide metabolic substrates to maintain some level of metabolism and cell vitality ("catabolic survival"). For example, we found that in *Msm* dormant cells, trehalose could be used as a source of glucose assimilated in the glycolytic pathway (Shleeva et al., 2017b), the enzymes of which were found in D2 *Mtb* proteome. We cannot exclude that the reductive branch of the TCA cycle is functional in dormant *Mtb* resulting in extracellular accumulation of succinate that makes it possible to oxidize reductive equivalents formed in glycolysis (Zimmermann et al., 2015).

One of the most remarkable features of long-stored dormant cells is their enrichment by enzymes that protect cells

against oxidative stress (superoxide dismutases, catalases, and peroxidases) and prevent protein aggregation (chaperones). In addition, the found DNA binding proteins (hupB/Rv2986, iniB /Rv0341) could possibly provide stabilization of DNA therefore contributing to overall cell vitality and preventing its denaturation under stress conditions.

Previously, we performed similar experiments with dormant *Msm* cells obtained after gradual acidification of the media in a prolonged stationary phase (Trutneva et al., 2018).

Upon comparison of proteome profile of dormant Mtb and *Msm* cells, we may see both similarities and differences in protein composition. The most evident difference is significant reduction of total amount of proteins found in *Mtb* "dormant proteome" (44–55% from "active proteome") in comparison with dormant *Msm* (96% from active proteome).

Comparison of protein composition of dormant cells for two species reveal significant amount of enzymes in *Msm* participated in different metabolic pathways which normally belong to active metabolism (biosynthesis of aminoacids, purines, and pyrimidines, fatty acids, trehalose, porphyrines, cell wall, transport, and replication processes). It is highly unlikely that those enzymes and corresponding processes could take place under non-replicative state with low metabolic activity. We suggested that such proteins are comparatively stable during transition and storage and could be used under resuscitation, that makes dormant *Msm* easy to recover and therefore to be culturable (Trutneva et al., 2018) in contrast to *Mtb*.

Whilst there is a significant difference in protein diversity in two species in dormancy (dormant D2 *Mtb* proteome profile contains only 27% orthologs found in *Msm* proteome profile) we may find a cohort of functionally identical proteins in the two proteomes. Considering annotated protein orthologists in two species (280 dormant *Msm* and 192 in D2 *Mtb* culture), this cohort contains 78 proteins belonging to central metabolic pathways like glycolysis and the TCA cycle. The overlapped *Msm*/*Mtb* dormant proteome profile is similarly enriched with chaperones and proteins that provide degradative reaction and defense mechanisms against stresses (**Table S6**). Such cohort of functionally identical proteins could maintain "minimal metabolism" in dormant state providing cell survival and stress defense without multiplication.

Thus, the two studies reveal a partially similar response of *Mtb* and its non-pathogenic relative *Msm* to adaptation to dormancy at the proteome level making the found proteomic changes general for the dormant state in mycobacteria.

In summary, this study demonstrates that *Mtb* cells under long-term storage in a dormant, "non-culturable" state contain significant amounts of stable proteins with different functional activities. Despite the mechanisms of such unique stability in the absence of protein synthesis being unclear, it is evident that the specific enzymes and proteins provide a "defending shell' for other proteins contributing to overall cell stability and vitality. The further study of the cohort of long-term protein survivors would provide a clue for the mechanisms of *Mtb* persistence in the host organism and finding of new targets for the development of new drugs to combat latent tuberculosis.

DATA AVAILABILITY STATEMENT

The datasets generated for this study can be found in: http://www.peptideatlas.org/PASS/PASS01450.

AUTHOR CONTRIBUTIONS

AK and KT conceived and designed the experiments, analyzed the data, and wrote the manuscript. MS, KT, GD, and GV performed the experiments. KT prepared figures and graphs. All authors read and approved the final manuscript.

FUNDING

This work was supported by Russian Science Foundation grant 16-15-00245-P. GV acknowledges the receipt of support from Ministry of Science and Higher Education of the Russian Federation.

ACKNOWLEDGMENTS

MALDI-TOFF analysis were carried out with the equipment of the Shared-Access Equipment Center Industrial Biotechnology of Federal Research Center Fundamentals of Biotechnology Russian Academy of Sciences.

SUPPLEMENTARY MATERIAL

The Supplementary Material for this article can be found online at: https://www.frontiersin.org/articles/10.3389/fcimb.2020.00026/full#supplementary-material

Table S1 | The proteins found in cytosol and membrane fractions of active and two types of dormant *M. tuberculosis* cells. Active cells were harvested from early stationary phase; dormant cells were obtained after gradual acidification in stationary phase followed by 4.5 months storage at room temperature (D1) and stored dormant cells were obtain after 13 months of storage (D2). 2D electrophoresis and protein analysis for cytosol and membrane (SDS extracts) were performed as described in the M&M. Density estimation of each protein spot was performed in two technical replicates of the pooled samples obtained from 4 independent biological replicates for active and dormant bacteria. The average results are shown. The relative error for density values of each spot did not exceed 5%. In the columns marked as "place," proteins were arranged according to their spot density from highest (1) to lowest (159 for active, 92 for D1 cells and 75 for D2 cells) representation in the proteome. Proteins which were virtually absent in the other proteome marked as "ND." If a protein with a particular accession number is found in several spots, the corresponding rank was assigned for a spot with maximum density. Column marked as "Mass values matched" shows a number of experimentally found peptides matched with theoretically predicted peptides for particular protein. Column marked as "coverage" shows percent coverage calculated by dividing the number of amino acids in all found peptides by the total number of amino acids in the entire protein sequence. Protein functional roles for Mtb were obtained from the Mycobrowser database (https://mycobrowser.epfl.ch).

Table S2 | The proteins found only in stored *Mtb* dormant cells proteome (13 months), but not in other types of cells.

Table S3 | Proteins with substantially changed abundance in dormant cells (D2) proteome. Proteins with increased and decreased abundance in D2 cells vs.

active cells (place for active cells proteome minus place for D2 > |10|) including proteins which were virtually absent in the other cells proteome (marked as "ND") are shown.

Table S4 | Distribution of the proteins found in the proteomic profile of stored *Mtb* dormant cells (13 months) by the categories in which they can participate.

Table S5 | "Consensus" proteins shared between the 3 *Mtb* dormancy models found in the first 200 most abundant. Published data for proteins amount in Loebel and Wayne dormancy models were converted to ranks (places).

Table S6 | Overlap between proteins in dormant *M. smegmatis* and *M. tuberculosis* D2 cells.

REFERENCES

Albrethsen, J., Agner, J., Piersma, S. R., Højrup, P., Pham, T. V., Weldingh, K., et al. (2013). Proteomic profiling of *Mycobacterium tuberculosis* identifies nutrient-starvation-responsive toxin–antitoxin systems. *Mol. Cell. Proteomics* 12, 1180–1191. doi: 10.1074/mcp.M112.018846

Anuchin, A. M., Goncharenko, A. V., Demina, G. R., Mulyukin, A. L., Ostrovsky, D. N., and Kaprelyants, A. S. (2010). The role of histone-like protein, Hlp, in *Mycobacterium smegmatis* dormancy. *FEMS Microbiol. Lett.* 308, 101–107. doi: 10.1111/j.1574-6968.2010.01988.x

Betts, J. C., Lukey, P. T., Robb, L. C., McAdam, R. A., and Duncan, K. (2002). Evaluation of a nutrient starvation model of *Mycobacterium tuberculosis* persistence by gene and protein expression profiling. *Mol. Microbiol.* 43, 717–731. doi: 10.1046/j.1365-2958.2002.02779.x

Budde, H., Flohé, L., Radi, R., Trujillo, M., Singh, M., Jaeger, T., et al. (2004). Multiple thioredoxin-mediated routes to detoxify hydroperoxides in *Mycobacterium tuberculosis*. *Arch. Biochem. Biophys.* 423, 182–191. doi: 10.1016/j.abb.2003.11.021

Chao, M. C., and Rubin, E. J. (2010). Letting sleeping dos lie: does dormancy play a role in tuberculosis? *Annu. Rev. Microbiol.* 64, 293–311. doi: 10.1146/annurev.micro.112408.134043

Connell, N. D. (1994). Mycobacterium: isolation, maintenance, transformation, and mutant selection. *Methods Cell Biol.* 45, 107–125. doi: 10.1016/S0091-679X(08)61848-8

Dass, B. K. M., Sharma, R., Shenoy, A. R., Mattoo, R., and Visweswariah, S. S. (2008). Cyclic AMP in mycobacteria: characterization and functional role of the Rv1647 ortholog in mycobacterium smegmatis. *J. Bacteriol.* 190, 3824–3834. doi: 10.1128/JB.00138-08

de Man, J. C. (1974). The probability of most probable numbers. *Eur. J. Appl. Microbiol.* 1, 67–78. doi: 10.1007/BF01880621

Devasundaram, S., Gopalan, A., Das, S. D., and Raja, A. (2016). Proteomics analysis of three different strains of *Mycobacterium tuberculosis* under *in vitro* hypoxia and evaluation of hypoxia associated antigen's specific memory T cells in healthy household contacts. *Front. Microbiol.* 7:1275. doi: 10.3389/fmicb.2016.01275

Dhillon, J., Lowrie, D. B., and Mitchison, D. A. (2004). *Mycobacterium tuberculosis* from chronic murine infections that grows in liquid but not on solid medium. *BMC Infect. Dis.* 4:51. doi: 10.1186/1471-2334-4-51

Diz, A. P., Truebano, M., and Skibinski, D. O. F. (2009). The consequences of sample pooling in proteomics: an empirical study. *Electrophoresis* 30, 2967–2975. doi: 10.1002/elps.200900210

Enany, S., Yoshida, Y., Tateishi, Y., Ozeki, Y., Nishiyama, A., Savitskaya, A., et al. (2017). Mycobacterial DNA-binding protein 1 is critical for long term survival of *Mycobacterium smegmatis* and simultaneously coordinates cellular functions. *Sci. Rep.* 7, 1–11. doi: 10.1038/s41598-017-06480-w

Florczyk, M. A., McCue, L. A., Stack, R. F., Hauer, C. R., and McDonough, K. A. (2001). Identification and characterization of mycobacterial proteins differentially expressed under standing and shaking culture conditions, including Rv2623 from a novel class of putative ATP-binding proteins. *Infect. Immun.* 69, 5777–5785. doi: 10.1128/IAI.69.9.5777-5785.2001

Flores, R. (1978). A rapid and reproducible assay for quantitative estimation of proteins using bromophenol blue. *Anal. Biochem.* 88, 605–611. doi: 10.1016/0003-2697(78)90462-1

Flynn, J. L., and Chan, J. (2001). Tuberculosis: latency and reactivation. *Infect. Immun.* 69, 4195–4201. doi: 10.1128/IAI.69.7.4195-4201.2001

Galagan, J. E., Minch, K., Peterson, M., Lyubetskaya, A., Azizi, E., Sweet, L., et al. (2013). The *Mycobacterium tuberculosis* regulatory network and hypoxia. *Nature* 499, 178–183. doi: 10.1038/nature12337

García, A. E., Blanco, C. F., Bigi, M. M., Vazquez, L. C., Forrellad, A. M., Rocha, R., et al. (2018). Characterization of the two component regulatory system PhoPR in *Mycobacterium bovis*. *Vet. Microbiol.* 222, 30–38. doi: 10.1016/j.vetmic.2018.06.016

Ignatov, D. V., Salina, E. G., Fursov, M. V., Skvortsov, T. A., Azhikina, T. L., and Kaprelyants, A. S. (2015). Dormant non-culturable *Mycobacterium tuberculosis* retains stable low-abundant mRNA. *BMC Genomics* 16:954. doi: 10.1186/s12864-015-2197-6

Kana, B. D., Weinstein, E. A., Avarbock, D., Dawes, S. S., Rubin, H., and Mizrahi, V. (2001). Characterization of the *cydAB*-encoded cytochrome *bd* oxidase from *Mycobacterium smegmatis*. *J. Bacteriol.* 183, 7076–7086. doi: 10.1128/JB.183.24.7076-7086.2001

Kang, C., Nyayapathy, S., Lee, J., Suh, J., and Husson, R. N. (2008). Wag31, a homologue of the cell division protein DivIVA, regulates growth, morphology and polar cell wall synthesis in mycobacteria. *Microbiology* 154, 725–735. doi: 10.1099/mic.0.2007/014076-0

Khomenko, A. G., and Golyshevskaya, V. (1984). Filtrable forms of *Mycobacteria tuberculosis*. *Z. Erkr. Atmungsorgane* 162, 147–154.

Lee, J. J., Kang, C. M., Lee, J. H., Park, K. S., Jeon, J. H., and Lee, S. H. (2014). Phosphorylation-dependent interaction between a serine/threonine kinase PknA and a putative cell division protein Wag31 in *Mycobacterium tuberculosis*. *New Microbiol.* 37, 525–533.

Loebel, R. O., Shorr, E., and Richardson, H. B. (1933). The influence of foodstuffs upon the respiratory metabolism and growth of human tubercle bacilli. *J. Bacteriol.* 26, 139–166. doi: 10.1128/JB.26.2.139-166.1933

Magnusson, L. U., Farewell, A., and Nyström, T. (2005). ppGpp: a global regulator in *Escherichia coli*. *Trends Microbiol.* 13, 236–242. doi: 10.1016/j.tim.2005.03.008

Mishra, A., and Sarkar, D. (2015). Qualitative and quantitative proteomic analysis of vitamin C induced changes in *Mycobacterium smegmatis*. *Front. Microbiol.* 6:451. doi: 10.3389/fmicb.2015.00451

Nguyen, L., Chinnapapagari, S., and Thompson, C. J. (2005). FbpA-dependent biosynthesis of trehalose dimycolate is required for the intrinsic multidrug resistance, cell wall structure, and colonial morphology of *Mycobacterium smegmatis*. *J. Bacteriol.* 187, 6603–6611. doi: 10.1128/JB.187.19.6603-6611.2005

O'Farrell, P. H. (1975). High resolution two-dimensional electrophoresis of proteins. *J. Biol. Chem.* 250, 4007–4021.

Pang, X., Samten, B., Cao, G., Wang, X., Tvinnereim, A. R., Chen, X. L., et al. (2013). MprAB regulates the espA operon in *Mycobacterium tuberculosis* and modulates ESX-1 function and host cytokine response. *J. Bacteriol.* 195, 66–75. doi: 10.1128/JB.01067-12

Parish, T., and Roberts, D. M. (2015). *Mycobacteria Protocols*. New York, NY: Humana Press. doi: 10.1007/978-1-4939-2450-9

Raman, S., Puyang, X., Song, T., Husson, R. N., Bardarov, S., and Jacobs, W. R. (2001). The alternative sigma factor sigH regulates major components of oxidative and heat stress responses in *Mycobacterium tuberculosis*. *J. Bacteriol.* 183, 6119–6125. doi: 10.1128/JB.183.20.6119-6125.2001

Rosenkrands, I., Slayden, A. R., Janne, C., Aagaard, C., Barry, C. E., and Andersen, P. (2002). Hypoxic response of *Mycobacterium tuberculosis* studied by metabolic labeling and proteome analysis of cellular and extracellular proteins. *J. Bacteriol.* 184, 3485–3491. doi: 10.1128/JB.184.13.3485-3491.2002

Rustad, T. R., Harrell, M. I., Liao, R., and Sherman, D. R. (2008). The enduring hypoxic response of *Mycobacterium tuberculosis*. *PLoS ONE* 3:e1502. doi: 10.1371/journal.pone.0001502

Sajid, A., Arora, G., Gupta, M., Singhal, A., Chakraborty, K., Nandicoori, V. K., et al. (2011). Interaction of *Mycobacterium tuberculosis* elongation factor Tu with GTP is regulated by phosphorylation. *J. Bacteriol.* 193, 5347–5358. doi: 10.1128/JB.05469-11

Schubert, O. T., Ludwig, C., Kogadeeva, M., Kaufmann, S. H. E., Sauer, U., Schubert, O. T., et al. (2015). Absolute proteome composition and dynamics during dormancy and resuscitation of *Mycobacterium tuberculosis*. *Cell Host Microbe*. 18, 1–13. doi: 10.1016/j.chom.2015.06.001

Shi, L., Sohaskey, C. D., Kana, B. D., Dawes, S., North, R. J., Mizrahi, V., et al. (2005). Changes in energy metabolism of *Mycobacterium tuberculosis* in mouse lung and under *in vitro* conditions affecting aerobic respiration. *Proc. Natl. Acad. Sci. U.S.A.* 102, 15629–15634. doi: 10.1073/pnas.0507850102

Shleeva, M., Goncharenko, A., Kudykina, Y., Young, D., Young, M., and Kaprelyants, A. (2013). Cyclic amp-dependent resuscitation of dormant mycobacteria by exogenous free fatty acids. *PLoS ONE* 8:e82914. doi: 10.1371/journal.pone.0082914

Shleeva, M., Trutneva, K., Shumkov, M., Demina, G., and Kaprelyants, A. (2018). A major protein Rv0341 in the membrane of dormant *Mycobacterium tuberculosis* binds DNA and reduces the rate of RNA synthesis. *FEBS Open Bio.* 8:400. doi: 10.1002/2211-5463.12453

Shleeva, M. O., Kondratieva, T. K., Demina, G. R., Rubakova, E. I., Goncharenko, A. V., Apt, A. S., et al. (2017a). Overexpression of adenylyl cyclase encoded by the *Mycobacterium tuberculosis* Rv2212 gene confers improved fitness, accelerated recovery from dormancy and enhanced virulence in mice. *Front. Cell. Infect. Microbiol.* 7:370. doi: 10.3389/fcimb.2017.00370

Shleeva, M. O., Kudykina, Y. K., Vostroknutova, G. N., Suzina, N. E., Mulyukin, A. L., and Kaprelyants, A. S. (2011). Dormant ovoid cells of *Mycobacterium tuberculosis* are formed in response to gradual external acidification. *Tuberculosis* 91, 146–154. doi: 10.1016/j.tube.2010.12.006

Shleeva, M. O., Trutneva, K. A., Demina, G. R., Zinin, A. I., Sorokoumova, G. M., Laptinskaya, P. K., et al. (2017b). Free trehalose accumulation in dormant *Mycobacterium smegmatis* cells and its breakdown in early resuscitation phase. *Front. Microbiol.* 8:524. doi: 10.3389/fmicb.2017.00524

Starck, J., Ka, G., Marklund, B., Andersson, D. I., and Thomas, A. (2004). Comparative proteome analysis of *Mycobacterium tuberculosis* grown under aerobic and anaerobic conditions. *Microbiology* 150, 3821–3829. doi: 10.1099/mic.0.27284-0

Sureka, K., Ghosh, B., Dasgupta, A., Basu, J., Kundu, M., and Bose, I. (2008). Positive feedback and noise activate the stringent response regulator rel in mycobacteria. *PLoS ONE* 3:e1771. doi: 10.1371/journal.pone.0001771

Trutneva, K., Shleeva, M., Nikitushkin, V., Demina, G., and Kaprelyants, A. (2018). Protein composition of *Mycobacterium smegmatis* differs significantly between active cells and dormant cells with ovoid morphology. *Front. Microbiol.* 9:2083. doi: 10.3389/fmicb.2018.02083

Vashist, A., Malhotra, V., Sharma, G., Tyagi, J. S., and Clark-Curtiss, J. E. (2018). Interplay of PhoP and DevR response regulators defines expression of the dormancy regulon in virulent *Mycobacterium tuberculosis*. *J. Biol. Chem.* 293, 16413–16425. doi: 10.1074/jbc.RA118.004331

Wayne, L. G. (1994). Dormancy of *Mycobacterium tuberculosis* and latency of disease. *Eur. J. Clin. Microbiol. Infect. Dis.* 13, 908–914. doi: 10.1007/BF02111491

Young, M., Mukamolova, G., and Kaprelyants, A. (2005). "Mycobacterial dormancy and its relation to persistence," in *Mycobacterium: Molecular Microbiology*, ed T. Parish (Norwich: Horizon Scientific Press), 265–320.

Zhang, P., Fu, J., Zong, G., Liu, M., Pang, X., and Cao, G. (2018). Novel MprA binding motifs in the phoP regulatory region in *Mycobacterium tuberculosis*. *Tuberculosis* 112, 62–68. doi: 10.1016/j.tube.2018.08.002

Zimmermann, M., Kuehne, A., Boshoff, H. I., Barry, C. E., Zamboni, N., and Sauer, U. (2015). Dynamic exometabolome analysis reveals active metabolic pathways in non-replicating mycobacteria. *Environ. Microbiol.* 17, 4802–4815. doi: 10.1111/1462-2920.13056

Conflict of Interest: The authors declare that the research was conducted in the absence of any commercial or financial relationships that could be construed as a potential conflict of interest.

The reviewer AM declared a shared affiliation, with no collaboration, with the authors to the handling editor at time of review.

frontiers in Cellular and Infection Microbiology

REVIEW
published: 25 February 2020
doi: 10.3389/fcimb.2020.00065

Mycobacterium tuberculosis Dissemination Plays a Critical Role in Pathogenesis

Madeleine G. Moule and Jeffrey D. Cirillo**

Department of Microbial Pathogenesis and Immunology, Texas A&M University Health Science Center, Bryan, TX, United States

Mycobacterium tuberculosis is primarily a respiratory pathogen. However, 15% of infections worldwide occur at extrapulmonary sites causing additional complications for diagnosis and treatment of the disease. In addition, dissemination of *M. tuberculosis* out of the lungs is thought to be more than just a rare event leading to extrapulmonary tuberculosis, but rather a prerequisite step that occurs during all infections, producing secondary lesions that can become latent or productive. In this review we will cover the clinical range of extrapulmonary infections and the process of dissemination including evidence from both historical medical literature and animal experiments for dissemination and subsequent reseeding of the lungs through the lymphatic and circulatory systems. While the mechanisms of *M. tuberculosis* dissemination are not fully understood, we will discuss the various models that have been proposed to address how this process may occur and summarize the bacterial virulence factors that facilitate *M. tuberculosis* dissemination.

Keywords: tuberculosis, *Mycobacterium*, dissemination, extrapulmonary, pathogenesis

OPEN ACCESS

Edited by:
Alexander S. Apt, Central Tuberculosis Research Institute (RAMS), Russia

Reviewed by:
Brian D. Robertson, Imperial College, United Kingdom
Erwin Schurr, McGill University, Canada

****Correspondence:***
Jeffrey D. Cirillo
jdcirillo@tamu.edu
Madeleine G. Moule
maddly@gmail.com

Specialty section:
This article was submitted to Molecular Bacterial Pathogenesis, a section of the journal Frontiers in Cellular and Infection Microbiology

Received: *04 December 2019*
Accepted: *07 February 2020*
Published: *25 February 2020*

Citation:
Moule MG and Cirillo JD (2020) Mycobacterium tuberculosis Dissemination Plays a Critical Role in Pathogenesis. Front. Cell. Infect. Microbiol. 10:65. doi: 10.3389/fcimb.2020.00065

INTRODUCTION

Tuberculosis is one of the oldest known human pathogens. The disease can be traced back through historical references and evidence of infections in human remains from some of the most ancient civilizations. Evidence of tuberculosis infections has been found in the necropoli of Ancient Egypt, Neolithic skeletons from burial sites in Europe, and mummies excavated from the Andes Mountains in South America (Formicola et al., 1987; Zink et al., 2001). The oldest confirmed human tuberculosis patient dates back an estimated 9,000 years ago, from submerged site in the Mediterranean near modern day Israel, but statistical models have estimated that the *Mycobacterium tuberculosis* complex may have evolved 40,000 years ago around the same time that human populations are thought to have begun to expand and migrate out of Africa (Hershkovitz et al., 2008; Wirth et al., 2008).

This bacterial pathogen has followed and affected humans throughout history, and has become an infection so familiar that it has taken root in our collective understanding of health and disease. References to a disease thought to be tuberculosis can be found in the Torah and the Old Testament of the Bible, and in written documents from China and India that are over 200 years old. Descriptions made by Hippocrates in Ancient Greece indicate that physicians and scientists have been attempting to study tuberculosis for as long as the practice of medicine has existed (Barberis et al., 2017). In more recent times the extremely high incidence of tuberculosis, or "consumption," in Europe and the Americas led to an extended campaign against what was termed the "White Plague,"

resulting in establishment of sanatoriums that were so ubiquitous that they are still commonly referenced in the literature and other media today (Martini et al., 2018).

Despite the long history of attempts to understand and cure tuberculosis, *M. tuberculosis* infections remain the leading cause of death by an infectious agent. Improvements in socioeconomic conditions and public health interventions led to a decline in tuberculosis cases in industrialized nations the early twentieth century, and the discovery of antibiotics provided therapeutic interventions that vastly improved clinical outcomes for tuberculosis patients. However, the emergence of antibiotic resistant MDR and XDR strains of tuberculosis and the resurgence of tuberculosis cases due to the HIV epidemic in the 1980s returned the disease to the spotlight (Porter and McAdam, 1994). At least a quarter of the world's population is currently infected with active or latent tuberculosis, with over 10 million new infections and 1.2 million deaths from tuberculosis occurring every year. Over 15% of tuberculosis cases occur in the form of extrapulmonary infections that can affect any tissue in the body and are particularly difficult to diagnose and treat (Behr et al., 2018, 2019; WHO, 2019). The challenges facing patients with extrapulmonary infections are indicative of how little we understand this deadly disease, in spite of the long history of research that has been undertaken on the subject. In this review, we will discuss the incidence and diversity of extrapulmonary infections, the role of *M. tuberculosis* dissemination in pathogenesis of by *M. tuberculosis*, and the potential mechanisms of dissemination that *M. tuberculosis* employs to cross the alveolar epithelium and disseminate to secondary sites of infection.

EXTRAPULMONARY TUBERCULOSIS: UNFAMILIAR PRESENTATIONS OF A FAMILIAR DISEASE

The clinical presentations of tuberculosis are well-known both in the medical literature and in popular culture. Active tuberculosis usually presents as a pulmonary infection consisting of a cough lasting longer than a few weeks, often associated with the production of bloody sputum and a myriad of other classic symptoms including chills, fever, weakness, unintentional weight loss, and night sweats. Latent tuberculosis generally does not produce any clinical symptoms, and patients may never know that they have been infected unless reactivation occurs (Esmail et al., 2014). What is less widely known is that in addition to these two extremes, tuberculosis is capable of causing infections in an extremely wide range of tissues and organs. In fact, ∼15% of tuberculosis infections worldwide are extrapulmonary infections, that may or may not be accompanied by pulmonary symptoms (WHO, 2019). Extrapulmonary infections pose additional clinical challenges as they do not necessarily mean a patient will test positive for tuberculosis using a sputum smear, the gold standard TB diagnostic (Zurcher et al., 2019). In addition, the presence of *M. tuberculosis* in extrapulmonary locations can result in a wide range of additional symptoms and can pose complications for treatment regimens which already face ongoing challenges in terms of efficacy, compliance, and problematic side effects.

The most common form of extrapulmonary infection in tuberculosis patients is lymphadenitis, most typically infection of the cervical lymph nodes (Peto et al., 2009). In extreme cases, these infections can lead to severe swelling resembling a growth or tumor on the neck. Mycobacterial lymphadenitis was historically referred to as scrofula or the "King's Evil," as it was widely believed in medieval England and France to be curable through the touch of royalty. This superstition was widespread enough to be referenced by Shakespeare in the play Macbeth (Grzybowski and Allen, 1995). Over time, superstition was gradually replaced by the theory that scrofula was caused by an infectious disease, but it was not until Robert Koch was able to demonstrate the presence of mycobacteria in infected lymph nodes in 1882 that scrofula was understood to be a form of extrapulmonary tuberculosis (Barberis et al., 2017).

Another presentation of extrapulmonary tuberculosis that was once considered to be a separate disease is Pott's Disease, first described by Dr. Percival Pott in 1779. Pott described a palsy of the lower limbs associated with a distinctive curvature of the spine, and an abscess between one or more vertebrae (Dobson, 1972). This condition could be progressive and spread to secondary sites, potentially resulting in paralysis. Today Pott's disease is considered to be synonymous with spinal tuberculosis, a condition so ancient that it has been identified in human mummies in Egypt dating back to 3,400 BC (Taylor et al., 2007). While spinal tuberculosis is the most common form of musculoskeletal tuberculosis, *M. tuberculosis* can also infect any of the bones or joints in the body, commonly described either as articular tuberculosis in which the hips or knee joints are affected, or extraspinal tuberculous osteomyelitis when other localized bone infections occur (Golden and Vikram, 2005).

Similar to infections of the cervical lymph nodes, the second most common form of extrapulmonary tuberculosis is also located in close proximity to the primary site of infection in the lungs. Pleural tuberculosis is an infection of the membranes lining the lungs, often in the form of pleural effusions, or buildup of fluid between the membranes and lung. It was previously thought that pleural effusions were the results of a hypersensitive immune response against pulmonary tuberculosis infections as the pleural fluid was not thought to contain bacteria, but improvements in diagnostic techniques have shown that despite a low bacterial load the pleura is indeed often an active site of extrapulmonary infection (Diacon et al., 2003). Pleural tuberculosis often responds well to treatment and can even resolve spontaneously, but is often associated with later reactivation (Shaw et al., 2018).

Historically, another common presentation of extrapulmonary tuberculosis was infection of the gastrointestinal tract. Interestingly, these infections are more commonly associated with the closely related species *Mycobacterium bovis,* rather than *M. tuberculosis,* most likely due to the consumption of contaminated milk products (de la Rua-Domenech, 2006). *M. bovis,* also known as bovine tuberculosis, is 99.5% genetically identical to *M. tuberculosis* and can be difficult to distinguish from the human pathogen both clinically and immunologically

despite the fact that they can be identified as distinct species using PCR and DNA sequencing techniques (Garnier et al., 2003). Despite the genetic and pathogenetic similarity, there is strong species tropism between the two organisms with *M. tuberculosis* being primarily a human pathogen while *M. bovis* naturally infects cattle, buffalo, deer, and even badger populations (Corner et al., 2012). Following the advent of pasteurization of milk products and improved screening methods, the number of gastrointestinal tuberculosis infections decreased dramatically, as this process is generally sufficient to kill mycobacteria (Chalmers, 1945).

A less common but potentially serious form of extrapulmonary tuberculosis is infection of the central nervous system (CNS). This can take the form of tuberculosis meningitis, encephalitis, or as an abscess or tuberculoma (Rock et al., 2008). The origin of infections within the meninges has been hypothesized to be a single focal caseous lesion known as the Rich focus that appears to pre-date the meningitis and is likely to be the source of bacteria that infiltrate the sub-arachnid space (Rich and McCordock, 1933). Tuberculosis infections of the CNS can mimic a number of other serious conditions including meningitis caused by more acute viral, bacterial, or even fungal pathogens or even brain cancer. Taken together with the fact that CNS tuberculosis often presents as non-specific symptoms such as headache, low grade fever, neck stiffness, vomiting, and occasionally cognitive changes, *M. tuberculosis* infections of the CNS can be a diagnostic challenge (Schaller et al., 2019). The prognosis of CNS tuberculosis is particularly poor compared to other forms of tuberculosis, with extremely high mortality rates that are dependent on the stage at which *M. tuberculosis* infection is diagnosed and ensuing complications such as infarctions and hydrocephaly (El Sahly et al., 2007).

The most severe form of extrapulmonary tuberculosis is a systemic infection caused by widespread hematogenous spread of the bacteria. Dissemination throughout the entire body through the bloodstream results in numerous small lesions that can occur on any type. Early physicians considered these ubiquitous lesions to resemble millet seeds, resulting in the term miliary tuberculosis. These lesions can and do occur in every tissue within the body, but are most predominant in organs that are highly vascularized including the lungs, liver, spleen, bone marrow and kidneys (Sharma et al., 2005). In the pre-antibiotic era, miliary tuberculosis was considered to be an infallibly fatal progression of tuberculosis, and as with most forms of extrapulmonary tuberculosis was most commonly seen in young children (Munro, 1889). However, miliary tuberculosis often responds well to modern treatment regimes, and current mortality rates range around 20%, dependent on the age of the patient and other complicating factors (Kim et al., 1990; Lee et al., 2018).

A defining feature of extrapulmonary tuberculosis in every clinical form is the overrepresentation of these infections in vulnerable populations such as children and individuals suffering from malnourishment (Cegielski and McMurray, 2004). In a recent study of pulmonary and extrapulmonary infections in patients in the US between 1988 and 2014, children under 14 years of age were found to be more than twice as likely to have extrapulmonary tuberculosis than pulmonary tuberculosis, despite extrapulmonary infections making up such a small percentage of total cases (Banta et al., 2019). Other risk factors that have been shown to increase the likelihood of extrapulmonary tuberculosis are homelessness, incarceration, and excessive alcohol consumption (Peto et al., 2009). However, the single largest factor influencing the prevalence of extrapulmonary tuberculosis in modern medicine has been the HIV epidemic. As the number of people infected with the HIV virus increased in the 1980's, a concurrent increase in extrapulmonary mycobacterial infections was also observed, often from species of mycobacteria such as *Mycobacterium avium* that rarely cause disease in immunocompetent individuals (ATS CDC, 1987). Although much of this increase is likely due to the overall increase in tuberculosis infections due to HIV co-infection, there is a positive correlation between HIV and extrapulmonary sites of disease (Naing et al., 2013). In a humanized mouse model, HIV infection has been shown to cause a decrease in lung interstitial CD4+ T cells during tuberculosis infections and significant increase in disseminated disease, suggesting a possible mechanism for this association (Corleis et al., 2019).

M. TUBERCULOSIS DISSEMINATION: RARE EVENT, OR MANDATORY PHASE OF INFECTION?

The vast majority of *M. tuberculosis* infections are transmitted through inhaled aerosols, making the lungs the primary site of infection. Therefore, it is widely accepted that dissemination out of the lung is a prerequisite step for most extrapulmonary infections. However, there is also a great deal of evidence that mycobacterial dissemination may be more than just a rare event leading to extrapulmonary tuberculosis. Case studies and pathology of human patients throughout medical history indicate that dissemination may in fact be an essential first step in establishing all active tuberculosis infections, even when these infections present as prototypical pulmonary infections. As early as 1935, Dr. Elizabeth Lincoln noted a trend in the literature away from the previous thinking that disseminated tuberculosis was a rare event inevitably leading to catastrophic outcomes such as miliary tuberculosis, but rather a potential intermediate step of infection (Lincoln, 1935).

The early events following *M.* tuberculosis infection are difficult to follow due to lack of clinical symptoms for most patients at this stage of the disease. Most of our understanding has come from case studies following a recent outbreak, literature from the pre-antibiotic era, and animal studies. Despite the paucity of information, it has long been noted that following initial aerosol infection with *M. tuberculosis* the majority of productive infections occur in a single infection site within one lobe of the lung (Ghon, 1916; Blacklock, 1932). The initial sites of infection are often described as a localized patch of pneumonia, and can occur in any part of the lung (Marais et al., 2004a). Anton Ghon, an Australian pathologist, was one of the first to describe a focus of infection that can occur during this initial

infection, lending his name to what is known commonly known as the Ghon's focus. He further described how these initial lesions could progress to include involvement of nearby lymph nodes, creating a cluster of infection known as the Ghon's complex. These primary lesions often calcify during the course of disease, resulting in a distinct pathology. This pattern of infection was once thought to be a hallmark of childhood tuberculosis, but in the modern era where adults in countries with low incidence of tuberculosis are less likely to have been exposed to *M. tuberculosis* it has become evident that this is instead the progression of *M. tuberculosis* infections in immune naive individuals who have not previously developed an immune response against mycobacteria (Loddenkemper et al., 2015).

In contrast to primary tuberculosis infections, secondary or "post-primary" infections that occur either following reactivation or in previously exposed patients often present as numerous foci of infection in the apical and subapical lobes of the lungs (Balasubramanian et al., 1994). This tropism for the apical regions of the lungs has long been noted in patient autopsies and has been a matter of speculation for much of modern medical science. In 1949, Smith and Abernathy reviewed the myriad of theories that could explain the apical localization of post-primary tuberculosis lesions, and added their own hypothesis that *M. tuberculosis* spreads from infected lymph nodes into the lymphatic system, eventually entering the bloodstream through the thoracic duct which empties into the left subclavian vein, entering the heart through the superior vena cava. Assuming minimal mixing of blood from the superior and inferior vena cava, bacilli entering through this route would seed the apical lobes of the lungs by transiting through the bloodstream via the pulmonary artery (Smith and Abernathy, 1949). The idea that *M. tuberculosis* spreads from an initial single lesion to the surrounding lymph nodes, and transits through the lymphatic and circulatory systems to reseed the lungs is supported by earlier observations from pediatric physicians, including Dr. A. Margaret C. Macpherson, who noted that pediatric patients with enlarged lymph nodes near the primary site of infection were more likely to progress to disseminated infections including miliary tuberculosis. Dr. Macpherson hypothesized that this progression was likely due to spread of the bacteria through the lymphatic system and into the bloodstream via the thoracic duct, resulting in hematogenous dissemination (Margaret and Macpherson, 1942). Wallgren made similar observations, hypothesizing that dissemination occurs early, and can result in excretion of bacilli in the urine, though it is seldom possible to culture bacteria from the blood (Wallgren, 1948). Overall, observations in humans, particularly those in children, suggests that hematogenous spread of bacteria occurs co-incident to primary disease (Marais et al., 2004a,b). Since it is reasonable to speculate that hematogenous spread is responsible for secondary lesions in the lung found in most if not all infections (Sweany et al., 1931; Medlar, 1948; Stead, 1989; Balasubramanian et al., 1994), it is likely that bacterial factors also play an important role in this process. This conclusion is supported by the fact that different *M. tuberculosis* strains vary in their ability to cause extrapulmonary infections (Garcia de Viedma et al., 2005). Lymphohematogenous spread remains the most likely path of disease progression for both pulmonary and extrapulmonary infections acquired through the respiratory route (**Figure 1**).

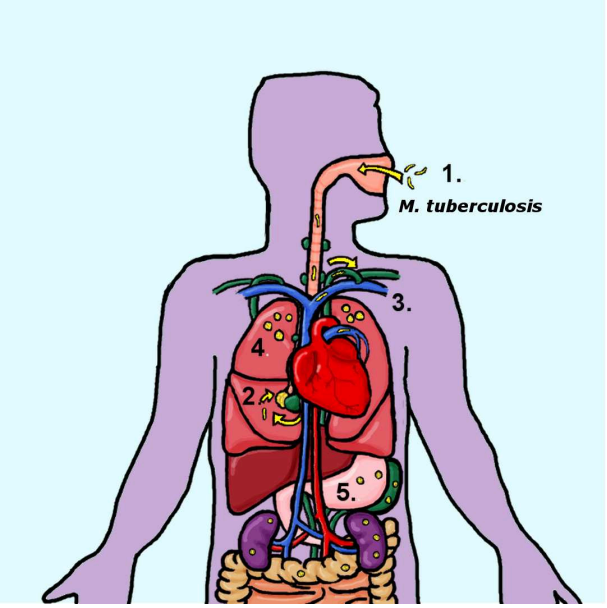

FIGURE 1 | Progression of human *M. tuberculosis* infections (1) Human tuberculosis infections are transmitted through the inhalation of contaminated aerosols. (2) Primary infections are established in the lungs, at a single site that develops into a primary granuloma. These initial sites of infection include involvement of the surrounding lymph nodes, forming a Ghon's complex. (3) Bacteria disseminate out of the lungs and into the lymphatic system, most likely entering the circulatory system through the entry of the thoracic duct into the subclavian vein. (4) Hematogenous reseeding of the lungs results in secondary granulomas located in the apical regions of the lungs and/or the extrapulmonary organs (5).

M. TUBERCULOSIS DISSEMINATION IN ANIMAL MODELS

A more detailed understanding of the course of *M. tuberculosis* dissemination must come from animal models. While mice are an obvious model for pathogenesis studies due to their ease of use, low cost, and the availability of tools, reagents and genetic knockouts, it is unclear how closely dissemination in this model mimics what occurs in humans. The morphology of the mycobacterial granulomas differs significantly between mice and humans, suggesting underlying differences in *M, tuberculosis* pathogenesis during mouse infections as compared to human patients (Flynn, 2006). Granulomas are a prototypical characteristic of tuberculosis infections. They are the lesions observed in the lungs and other organs where organized layers of host immune cells surround foci of bacteria, and have long been debated to be either a reservoir of bacteria or a quarantine site regulated by the host (Guirado and Schlesinger, 2013). Whereas, as previously described, the granulomas observed in human infections can be varied in composition including inert calcified lesions and necrotic, caseous granulomas, no

necrosis is observable in traditional mouse models (Medlar, 1948; Flynn, 2006). In contrast, the guinea pig model of infection displays two physiologically and immunologically distinct types of granulomas, more closely replicating what is observed in human infections (Ly et al., 2008).

Interestingly, the morphology and cytokine profiles of granulomas observed in the guinea pig model can be traced back to whether they are initial sites of bacterial seeding (primary granulomas), or subsequent secondary granulomas following reseeding of the lungs through lymphohematogenous spread (McMurray, 2003). Infecting animals with very low doses of *M. tuberculosis* results in the formation of a small number of granulomas that eventually become large and necrotic. Similar to what is observed in humans, the primary lesions resulting from the initial infection often become necrotic and calcify. Bacteria disseminate from the primary lesions very early during the course of infection, and within 2 weeks post-infection, bacteria can be found first in the lymph nodes adjacent to the lungs, and then later in the extrapulmonary organs including the spleen (Smith et al., 1970). Approximately 3–5 weeks post-infection, hematogenous dissemination re-seeds the lung, creating secondary lesions that develop primarily in the apical and subapical regions of the lung (Stead, 1989; Balasubramanian et al., 1994; McMurray, 2003). These secondary granulomas are smaller and do not become necrotic or calcify (Ho et al., 1978). Animals that have been vaccinated with BCG develop granulomas that are more similar to secondary granulomas from the onset, suggesting that the differences between these phenotypes is most likely due to the host immune response (Smith et al., 1975). Interestingly, dissemination in guinea pigs occurs in a temporal fashion that is very similar to that observed in mice (Kong et al., 2009). Overall, these observations suggest that the guinea pig model offers the opportunity to examine dissemination in more detail using a highly relevant system to human infections.

Rabbit models of tuberculosis have been useful for studying tuberculosis due to the characterization of both resistant and sensitive rabbit models. Lurie's sensitive rabbit model showed disease similar to that demonstrated in guinea pigs including extrapulmonary dissemination and distinct primary and secondary granulomas (Lurie, 1941). However, the majority of rabbit experiments were performed with *M. bovis* as rabbits do not develop severe disease or extrapulmonary infections from *M.* tuberculosis (Nedeltchev et al., 2009). Perhaps the ultimate model for studying *M. tuberculosis* dissemination and extrapulmonary spread is non-human primates who closely resemble human patients in terms of their susceptibility and immune response to *M. tuberculosis*. Similar to human infections, *M. tuberculosis* infections of cynomolgus macaques results in extrapulmonary infections in only a subset of animals. This allows more accurate modeling, but also makes studying extrapulmonary infections more complicated as they do not occur in every experimental animal. Interestingly, treating macaques with TNF neutralizing agents resulted in drastically increased extrapulmonary dissemination and the development of disseminated disease within 8 weeks post-infection (Lin et al., 2010). Moreover, similar to patterns of human infections in the pre-antibiotic era, macaques that do not show extrapulmonary infections in other organs still harbor persistent infections within their lymph nodes, suggesting that the lymphatic dissemination model is correct (Ganchua et al., 2018). The application of tools such as PET scans and genetic labeling of bacterial in non-human primate infections suggests that this model is likely to shed deeper insight into the mechanisms of *M. tuberculosis* dissemination in the future (Martin et al., 2017).

BREACHING THE BARRIER: A QUESTION OF MECHANISM

From what we have learned over the past century from both observations of human patients and experimental animal models, the likelihood of *M. tuberculosis* initiating infection from a single site and disseminating through the lymphatic and/or circulatory system is incredibly high. However, relatively little is understood about the molecular mechanisms of dissemination. Based on the correlation between susceptibility to severe disease and the frequency of extrapulmonary infections in various animal models, it can be assumed that the host immune response to infection plays a major role. This conclusion is further substantiated by the link between immunodeficiency and extrapulmonary tuberculosis in humans. However, there is also evidence that *M. tuberculosis* is not a passive player in this process and that bacterial virulence factors actively promote dissemination. There is evidence that *M. tuberculosis* strains from different phylogenetic lineages show different rates of extrapulmonary disease, and clinical isolates from extrapulmonary infections cause a greater degree of disseminated disease in animal models (Hernandez Pando et al., 2010; Be et al., 2011; Click et al., 2012). Furthermore, there is evidence that *M. tuberculosis* actively induces angiogenesis to promote dissemination through the formation of new blood vessels (Oehlers et al., 2015; Polena et al., 2016).

Of particular interest from a mechanistic viewpoint is the essential first step of extrapulmonary dissemination, the egress of *M. tuberculosis* out of the lung. For mycobacteria to gain access to interstitial tissues, it would first need to cross the epithelial barrier of the lung, circumventing the primary purpose of barrier epithelia. A number of models have been proposed regarding how non-motile bacteria could breach the lung epithelium, which we will discuss in more detail (**Figure 2**). One hypothesis is that as *M. tuberculosis* preferentially infect alveolar macrophages in high numbers, the bacteria could be transiting within these macrophages as they cross into and out of the lymphatic and circulatory systems. Another hypothesis is that *M. tuberculosis* directly infects the epithelial cells composing the barrier of the lung and is able to either translocate across these cells without disrupting the epithelium, or causes a breach in the monolayer by inducing cell death (Russell, 2001). Alternatively, dissemination could involve a role from a less ubiquitous cell type within the lung, dendritic cells, which are known to sample antigens from the alveoli and present them within the lymph nodes (Humphreys et al., 2006). Interestingly, there are genetic and phenotypic evidence available in the literature

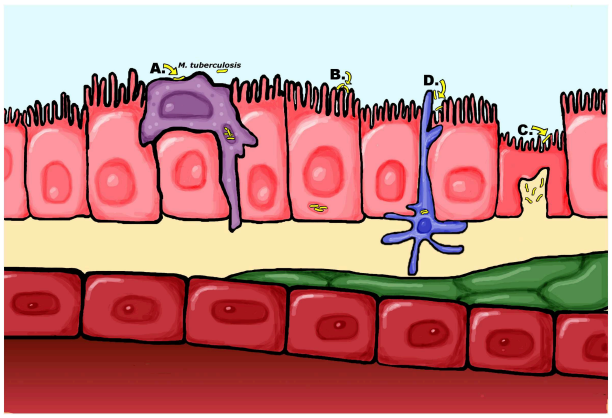

FIGURE 2 | Proposed mechanisms of *M. tuberculosis* dissemination across the airway epithelia **(A)** The "trojan horse" model of dissemination where *M. tuberculosis* is carried across the epithelial barrier within infected macrophages. **(B)** *M. tuberculosis* is capable of directly infecting epithelial cells, which could result in bacteria translocating across the barrier through the epithelial cells or inducing cell death to cause a breach in the barrier **(C)** Passage across the epithelium may occur in specialized M cells which actively translocate antigens to the interstitium for presentation to antigen presenting cells **(D)** Alternatively, dendritic cells sampling antigens in the alveoli may traffic live mycobacteria to the lymph nodes.

for all three hypotheses regarding routes of dissemination, possibly suggesting that in reality dissemination may occur by a combination of several or all of these pathways.

MACROPHAGE MIGRATION: THE TROJAN HORSE THEORY

The "trojan horse" theory of dissemination hypothesized that *M. tuberculosis* traffics within alveolar macrophages (AM) across the airway epithelium. This is an attractive theory, because it is well-established that AMs are one of the first and most numerous types cells to become infected with tuberculosis in both humans and animal models (Berthrong, 1970; Wagner, 1975; Srivastava et al., 2014). *M. tuberculosis* can survive and replicate within AMs, and the ability of this cell type to cross into and out of the circulatory and lymphatic systems is well-characterized. Moreover, this mechanism has been demonstrated in other bacterial pathogens, suggesting it could be a conserved mechanism for bacterial dissemination (Vazquez-Torres et al., 1999). However, the role of macrophages in *M. tuberculosis* dissemination and extrapulmonary spread is still not completely understood and knockouts in animal models are not usually specific enough to allow definitive demonstration of their role. Possibly, tissue-specific or lineage-specific knockouts in mice could allow careful analysis of their role in future studies.

Some evidence for trafficking of mycobacteria within macrophages comes from a zebrafish model using the related pathogen *Mycobacterium marinum*. Zebrafish provide a useful model to study to progression of mycobacterial infections because the natural transparency of the larvae allows the progress of infection to be followed in real time (Davis et al., 2002). Using this model, Davis and Ramakrishnan showed direct evidence of macrophage recruitment to *M. marinum* granulomas and subsequent migration of infected macrophages to new tissues (Davis and Ramakrishnan, 2009). The zebrafish model has also resulted in the identification and characterization of a number of bacterial factors that appear to play a role in dissemination of mycobacteria, including Zinc metalloprotease-1 (*zmp1*) *and* the regulatory gene *whiB6,* as well as the host factor CXC chemokine receptor 3 (CXCR3) (Torraca et al., 2015; Chen et al., 2016; Vemula et al., 2016). Interestingly, *M. marinum* mutants lacking the ESX-1 secretion locus, which is essential for full virulence in *M. tuberculosis* and *M. bovis* infections, were found to show decreased granuloma formation but increased dissemination within macrophages to remote tissues, suggesting an important role for this locus in dissemination.

While the zebrafish model provides evidence for the trojan horse theory of mycobacterial dissemination, this model cannot provide proof of dissemination across the alveolar epithelium or address the roles of the lymphatic system and adaptive immune system in dissemination. In addition, while *M. marinum* is a natural pathogen of fish and thus an excellent model for mycobacterial pathogenesis, it is divergent enough from *M. tuberculosis* that it will be important to confirm these findings in the actual human pathogen. A virulence factor that has been studied in relation to dissemination in both *M. marinum* and *M. tuberculosis* using a mammalian model is the virulence locus *mel2* that affects growth in activated macrophages as well as entry into host cells and dissemination (Subbian et al., 2007; Cirillo et al., 2009). The *mel2* locus affects susceptibility to reactive oxygen species (ROS) and this role may be the basis for effects on intracellular growth, but it is unclear whether this role is responsible for the effects on dissemination, since dissemination of a *mel2* mutant remains defective in phox$^{-/-}$ and iNOS$^{-/-}$ mice (Subbian et al., 2007; Cirillo et al., 2009).

Direct evidence for the trojan horse model in mammals was reported by Cohen et al. (2018). This study utilized an intratracheal antibody labeling assay to show that alveolar macrophages (AMs) infected with mCherry-labeled *M. tuberculosis* migrate from the lumen of the alveoli, where they typically reside, to the interstitium (Cohen et al., 2018). This was an exciting and interesting observation, as AMs have previously been described as sessile cells that remain closely associated with the epithelium even when stimulated (Westphalen et al., 2014). The authors investigated the genetics of this process, determining that migration is dependent on the *M. tuberculosis* virulence factor ESX-1, corroborating observations in the zebrafish model. Furthermore, using gene knockout mice, bone marrow chimeras, and adoptive transfer experiments, they demonstrated a role for the host IL-1R signaling pathway in dissemination through a mechanism that is dependent on non-hematopoietic cells, most likely epithelial cells. Not only is this a potentially important host-side mechanism in *M. tuberculosis* dissemination, but it suggests that mycobacterial dissemination may not be solely dependent on exploitation of a single host cell type, but rather the entire alveolar environment.

EPITHELIAL CELL INFECTION: THE DIRECT APPROACH

Perhaps the most direct strategy to breach the alveolar barrier is to directly infect the cells that make up the barrier. Once inside an epithelial cell, bacteria could translocate across the cells or induce apoptosis or necrosis, causing a break in the epithelium due to cell death. Mycobacteria has been known to be capable of infecting HeLa cells since the 1950's (Bloch, 1956; Shepard, 1957), and was shown to be capable of growth and replication in human lung epithelial cells over 20 years ago (Bermudez and Goodman, 1996; Mehta et al., 2006). The same year, the first *M. tuberculosis* adhesin, the heparin-binding hemagglutinin HbhA was identified and shown to be involved in adhesion of *M. tuberculosis* to epithelial cells (Menozzi et al., 2006). Infection of epithelial cells has also been shown to induce chemokine expression suggesting that this cell type could also play an important role in the immune response against *M. tuberculosis* (Lin et al., 1998; Wickremasinghe et al., 1999). Analysis of infected cells present in human sputum and in bronchiolar lavage samples shows that epithelial cells become infected with *M. tuberculosis* in human patients and in fact are one of the most commonly infected cell types after macrophages and neutrophils (Eum et al., 2010).

Transit of *M. tuberculosis* across epithelial cells has been demonstrated *in vitro* using polarized bilayers of epithelial and endothelial cells to recreate the airway barriers of the human lung in culture. In these three-dimensional models, epithelial cells and endothelial cells are cultured and allowed to polarize on opposite sides of a permeable transwell membrane. *M. tuberculosis* is then added to the apical chamber, and the basal chamber is monitored for bacteria that are able to translocate across the cell bilayer, showing that the bacteria is able to migrate across the epithelial and endothelial cell barriers (Birkness et al., 1999; Bermudez et al., 2002) In addition, Pethe et al. published a study in 2001 on the previously characterized adhesin HbhA that demonstrated a clear role for this gene in dissemination through interactions with epithelial cells. They showed that deletion of *hbhA* from either *M. tuberculosis* or the human vaccine strain *Mycobacterium bovis* BCG had no effect on the ability of the bacteria to infect or grow within the lung, but significantly impaired the ability to disseminate to the spleen following intranasal infection (Pethe et al., 2001). Moreover, they showed that *hbhA* mutants had no phenotype whatsoever in J774 macrophage cells, but were impaired in their ability to infect A549 human lung epithelial cells, consistent with the role of this gene in cell adhesion. Overall, these studies provide evidence for a direct role for epithelial cells in dissemination.

The role of *hbhA* in dissemination across epithelial cells has since been confirmed *in vitro* using the polarized bilayer models described above (Ryndak et al., 2016). However, these experiments do not address whether dissemination is due to translocation across epithelial cells, or cell death. Purified recombinant HbhA binds to the surface of polarized epithelial cells, induces actin reorganization, and can be internalized into cytoplasmic vacuoles via endocytosis. However, HbhA does not disrupt the integrity of cellular tight junctions or affect the permeability of epithelial cell monolayers (Menozzi et al., 2006). In contrast, infection of polarized monolayers with live bacteria does affect the isoelectric properties of epithelial cell monolayers, possibly by inducing TNFα expression, suggesting that there could be additional HbhA-independent mechanisms of barrier disruption (Zhang et al., 1997).

Another possible route of passage across epithelial cells could be through specialized epithelial cells known as microfold cells, or M cells. M cells are part of the epithelial barrier in mucosa-associated lymphoid tissues (MALT) including the gut and some parts of the respiratory system. Although M cells form tight junctions with other epithelial cells and are part of the epithelial barrier, they play an active role in taking up antigens and delivering them across the epithelia to antigen-presenting cells (Neutra et al., 1996). Due to this unique ability, M cells have been shown to be exploited by a large number of bacterial intestinal pathogens to invade deeper tissues (Owen et al., 1986; Grutzkau et al., 1990; Jones et al., 1994). The first suggestion that mycobacteria could also be using M cells as a route across the epithelia came in 1986, via demonstration of uptake of the *M. bovis* BCG vaccine strain by M cells in a rabbit ileum ligated loop model (Fujimura, 1986). A similar role for pulmonary M cells was later demonstrated in the guinea pig model using virulent *M. tuberculosis* (Teitelbaum et al., 1999).

Additional evidence for the role of M cells in mycobacterial dissemination was provided more recently using the mouse model to demonstrate that depletion of M cells decreases dissemination to the cervical lymph nodes, and an *in vitro* model using Caco-2 epithelial cells to show increased translocation when M cells are co-cultured in the monolayers (Nair et al., 2016). Taken together, these studies suggest that M cells are capable of translocating *M. tuberculosis* and likely play a role in dissemination. The only downside to this model of dissemination is that the prevalence of M cells in the human lung epithelium is unclear. Both nasal-associated lymphoid tissues (NALT) and bronchus-associated lymphoid tissues (BALT) are present in rodent models, but very little is known about these tissues in healthy human adults. They have been described as being primarily present in childhood and subsequently receding, perhaps inducible in response to infection or inflammation or only sparsely present (Bienenstock and McDermott, 2005). Therefore, it remains somewhat unclear what role M cells play in *M. tuberculosis* dissemination in humans, and it is likely that this is not the sole route that mycobacteria may disseminate through.

DENDRITIC CELL INFILTRATION: OPPORTUNISTIC HITCHHIKERS

Another candidate cell population suggested to play a role in *M. tuberculosis* dissemination are dendritic cells (Humphreys et al., 2006). These cells are particularly attractive candidates due to the established role of dendritic cells in active transport of antigens to the lymph nodes. Therefore, dendritic cells could provide a potential route of dissemination out of the primary site of infection for *M. tuberculosis* as they transport bacteria to the lymph nodes for presentation to immune cells. This hypothesis

is supported by data showing that infection of dendritic cells by BCG can occur within 48 h following intranasal infection of BALB/c mice, a timepoint that is relevant to early dissemination out of primary granulomas and formation of the Ghon's complex (Reljic et al., 2005). Moreover, infected inflammatory dendritic cells (iDCs) defined as CD11c+CD11b+Ly6C+ cells are capable of moving into and out of acute and chronic lesions induced by BCG in a CD11c-eYFP dendritic cell reporter mouse strain. Importantly, iDCs in dendritic cell reporter mice infected with BCG also migrate to peripheral sites at a much higher rate than in uninfected mice (Schreiber et al., 2011). Harding et al. also show that iDCs in the same reporter strain are recruited to *M. tuberculosis* granuloma-like lesions, after which they are found outside of the lesions interacting with populations of P25 cells and forming new regions of granulomatous inflammation (Harding et al., 2015).

Although these experiments establish a link between dendritic cells and dissemination, they have all been performed in mouse models that do not form structurally similar primary and secondary granulomas to those observed in humans. Many of these experiments also used the model organism *M. bovis* BCG, rather than virulent *M. tuberculosis,* so there remains a need to confirm the results of these novel experiments using *M. tuberculosis*. Interestingly, both human and mouse dendritic cell migration decreases across an epithelial barrier toward lymphatic chemokines following infection with the attenuated *M. tuberculosis* strain $mc^2$7000 or BCG (Roberts and Robinson, 2014; Harding et al., 2015). However, a computational model extrapolated from a data set consisting of blood and lung samples of non-human primates infected with the Erdman strain of *M. tuberculosis* also predicted an essential role for dendritic cells in dissemination, suggesting that dissemination within dendritic cells can occur in human tuberculosis (Marino and Kirschner, 2016).

Dendritic cells have also been described as playing a "trojan horse" role in transiting other respiratory pathogens to the lymph nodes, setting a precedent that could extend to *M. tuberculosis.* Cleret et al. observed transit of fluorescent-labeled *Bacillus anthracis* spores to the thoracic lymph nodes in GFP-labeled dendritic cells (Cleret et al., 2007). Subsequent studies suggest similar roles for DCs in trafficking *Streptococcus pneumoniae* and *Francisella tularensis* from initial infection sites in the lungs to the lymphatic system as well as roles for DCs in systemic dissemination of *Burkholderia pseudomallei* and *Salmonella typhimurium* (Bar-Haim et al., 2008; Rosendahl et al., 2013; Williams et al., 2014; Carden et al., 2017). Taken together, these studies suggest that dendritic cells play a prominent role in bacterial dissemination and that this may be a conserved mechanism across bacterial species.

DISCUSSION

Extrapulmonary tuberculosis accounts for a relatively small percentage of human tuberculosis cases in immunocompetent adults. However, the clinical impact of extrapulmonary tuberculosis is larger than this statistic may suggest as extrapulmonary infections are some of the most difficult to diagnose and treat. The gold standard for diagnosis of tuberculosis in many countries with the highest tuberculosis burdens remains sputum smear microscopy, but patients with extrapulmonary infections do not necessarily have bacteria in their sputum. Other assays that can be used to test for exposure to mycobacterial antigens, such as the tuberculin skin test and the QuantiFERON blood test are limited due to cross-reactivity with the BCG vaccine or environmental mycobacteria, respectively, and thus cannot be used to diagnose clinical tuberculosis. In 2010, GeneXpert was introduced and recommended by the WHO for pulmonary infections, but although this has the potential to address diagnostic challenges the test requires sophisticated and expensive equipment that is not always available in the places it is most needed and remains a sputum-based test (Walzl et al., 2018). Overall, this means that diagnosis strategies are lacking for extrapulmonary infections. The wide range of sites and symptoms associated with extrapulmonary tuberculosis means that it can masquerade as a number of different diseases and syndromes, such that tuberculosis may not even be suspected and tested for, delaying the time before appropriate treatment can be provided. Even when extrapulmonary tuberculosis is diagnosed in a timely manner, the recommended treatment regimen are primarily designed against pulmonary tuberculosis, and may or may not be effective depending on the presentation of extrapulmonary disease.

Extrapulmonary tuberculosis is associated with particularly high morbidity and mortality. This may be due to the fact that extrapulmonary forms of the disease often occur in some of the most vulnerable patients including young children and immunocompromised individuals. However, while they are no longer the death sentence that they once were, certain forms of extrapulmonary tuberculosis, particularly infection of the central nervous system such as meningitis and miliary tuberculosis, have very poor clinical outcomes. Diagnosis and morbidity/mortality are closely related in extrapulmonary tuberculosis, as early detection of infections can drastically improve the likelihood of the disease responding to treatment.

As most tuberculosis infections are contracted through the inhalation of aerosols containing *M. tuberculosis*, extrapulmonary infections occur through dissemination of the bacteria out of the lung into the surrounding lymphatic tissue, and subsequent distribution throughout the circulatory system. Secondary pulmonary granulomas are formed through reseeding of the lungs through the bloodstream. Therefore, understanding dissemination has broad implications for tuberculosis treatment and prevention. If these early steps can be blocked through vaccination or early intervention, it is conceivable that not only could extrapulmonary infections be prevented, but that reseeding the lungs could be blocked. This hypothesis is supported by the success of therapeutics designed to target the first known *M. tuberculosis* dissemination factor, *hbhA*. Immunization with purified recombinant HbhA protects mice from infection with *M. tuberculosis,* reducing the bacterial burden in both the lungs and extrapulmonary organs (Parra et al., 2004; Schepers et al., 2015). Boosting with this antigen also improves the efficacy of the BCG vaccine, suggesting a combined

regimen has the potential to protect against dissemination (Guerrero et al., 2010). HbhA has also been investigated as a potential diagnostic antigen and biomarker (De Maio et al., 2019), suggesting that work in this area can be applied in a number of novel ways.

It is not unreasonable to think that identification and characterization of additional dissemination factors could lead to the development of equally successful vaccines and therapeutics. However, since the identification of HbhA, research in this area has resulted in only a few new candidates being identified. Further investigation into identifying mycobacterial dissemination factors is needed. Identification of a comprehensive set of *M. tuberculosis* dissemination and extrapulmonary spread factors could improve our understanding of the molecular mechanisms involved, which will need to be confirmed and further evaluated in both small animal models and *in vitro* models. More sophisticated tracking of dissemination *in vivo* using modern imaging techniques could allow analysis of the longstanding belief that dissemination occurs via the lymphatic and circulatory systems. Moreover, further investigations into the interactions of *M. tuberculosis* with their host cells could help us better understand the mechanisms that the bacteria use to breach the alveolar barrier and cross into the lymphatic and/or circulatory systems.

Guidance on the future of *M. tuberculosis* dissemination research may come from the progress of research in other bacterial pathogens. The route through which enteric pathogens such as *Salmonella typhimurium* disseminate across the intestinal endothelial barrier to infect other tissues was once a hotly debated topic in bacteriology. Closely paralleling the current state of understanding of *M. tuberculosis* dissemination, the two major schools of thought were that *S. typhimurium* was either directly invading the epithelium though Microfold (M) cells, or hitching a ride within migrating macrophages. This debate was eventually addressed through experiments using bacterial genetics to address each hypothesis. First, *S. typhimurium* was demonstrated to exploit M cells by using bacterial adhesins to invade and colonize Peyer's Patches (Galan and Curtiss, 1989; Lee et al., 1992; Jones et al., 1994). A subsequent study showed that if all proposed epithelial cell adhesins were deleted from *S. typhimurium,* the resultant triple knockout mutant was still able to disseminate within a mouse model, though at a reduced level. Moreover, if the triple mutant was used to infect CD18 KO mice that lack a surface antigen expressed by macrophages and dendritic cells that dissemination to the liver and spleen was greatly reduced compared to wild-type mice (Garcia de Viedma et al., 2005). From these combined studies, it can be concluded that neither of these proposed mechanisms are mutually exclusive, and that *S. typhimurium* likely exploits both potential dissemination routes. To bring a similar sense of conclusion to the *M. tuberculosis* field, it will be necessary to perform similarly careful genetic studies that clarify the role of each proposed pathway in a relevant *in vivo* model such as non-human primates or the guinea pig model of infection. Using the history of enteric pathogen dissemination as a lesson, it seems likely that none of the proposed theories are mutually exclusive and that future evidence may reveal that mycobacteria are capable of utilizing more than one strategy to disseminate and establish extrapulmonary infections.

AUTHOR CONTRIBUTIONS

MM wrote the article and prepared the figures. JC provided the concept and critical review.

FUNDING

Research reported in this publication was supported by the National Institute of Allergy and Infectious Disease of the National Institutes of Health under award numbers R01AI104960 and F32AI120589.

REFERENCES

ATS and CDC (1987). Mycobacterioses and the acquired immunodeficiency syndrome. joint position paper of the american thoracic society and the centers for disease control. *Am. Rev. Respir. Dis.* 136, 492–496. doi: 10.1164/ajrccm/136.2.492

Balasubramanian, V., Wiegeshaus, E. H., and Smith, D. (1994). Pathogenesis of tuberculosis: pathways to apical localization. *Tuberc. Lung Dis.* 75, 168–178. doi: 10.1016/0962-8479(94)90002-7

Banta, J. E., Ani, C., Bvute, K. M., Lloren, J. I. C., and Darnell, T. A. (2019). Pulmonary vs. extra-pulmonary tuberculosis hospitalizations in the US [1998-2014]. *J. Infect. Public Health* 13, 131–139. doi: 10.1016/j.jiph.2019.07.001.

Barberis, I., Bragazzi, N. L., Galluzzo, L., and Martini, M. (2017). The history of tuberculosis: from the first historical records to the isolation of Koch's bacillus. *J. Prev. Med. Hyg.* 58, E9–E12.

Bar-Haim, E., Gat, O., Markel, G., Cohen, H., Shafferman, A., and Velan, B. (2008). Interrelationship between dendritic cell trafficking and *Francisella tularensis* dissemination following airway infection. *PLoS Pathog.* 4:e1000211. doi: 10.1371/journal.ppat.1000211

Be, N. A., Klinkenberg, L. G., Bishai, W. R., Karakousis, P. C., and Jain, S. K. (2011). Strain-dependent CNS dissemination in guinea pigs after *Mycobacterium tuberculosis* aerosol challenge. *Tuberculosis* 91, 386–389. doi: 10.1016/j.tube.2011.07.003

Behr, M. A., Edelstein, P. H., and Ramakrishnan, L. (2018). Revisiting the timetable of tuberculosis. *Brit. Med. J.* 362:k2738. doi: 10.1136/bmj.k2738

Behr, M. A., Edelstein, P. H., and Ramakrishnan, L. (2019). Is *Mycobacterium tuberculosis* infection life long? *Brit. Med. J.* 367:l5770. doi: 10.1136/bmj.l5770

Bermudez, L. E., and Goodman, J. (1996). *Mycobacterium tuberculosis* invades and replicates within type II alveolar cells. *Infect. Immun.* 64, 1400–1406. doi: 10.1128/IAI.64.4.1400-1406.1996

Bermudez, L. E., Sangari, F. J., Kolonoski, P., Petrofsky, M., and Goodman, J. (2002). The efficiency of the translocation of *Mycobacterium tuberculosis* across a bilayer of epithelial and endothelial cells as a model of the alveolar wall is a consequence of transport within mononuclear phagocytes and invasion of alveolar epithelial cells. *Infect. Immun.* 70, 140–146. doi: 10.1128/IAI.70.1.140-146.2002

Berthrong, M. (1970). The macrophage in tuberculosis. *Bibl. Tuberc.* 26, 1–27.

Bienenstock, J., and McDermott, M. R. (2005). Bronchus- and nasal-associated lymphoid tissues. *Immunol. Rev.* 206, 22–31. doi: 10.1111/j.0105-2896.2005.00299.x

Birkness, K. A., Deslauriers, M., Bartlett, J. H., White, E. H., King, C. H., and Quinn, F. D. (1999). An *in vitro* tissue culture bilayer model to examine early

events in *Mycobacterium tuberculosis* infection. *Infect. Immun.* 67, 653–658. doi: 10.1128/IAI.67.2.653-658.1999

Blacklock, J. W. (1932). The primary lung focus of tuberculosis in children. *Proc. R. Soc. Med.* 25, 725–733. doi: 10.1177/003591573202500557

Bloch, H. (1956). The propagation of tubercle bacilli in cultures of HeLa cells. *Zentralbl. Bakteriol. Orig.* 165, 385–390.

Carden, S. E., Walker, G. T., Honeycutt, J., Lugo, K., Pham, T., Jacobson, A., et al. (2017). Pseudogenization of the secreted effector gene ssei confers rapid systemic dissemination of *S. typhimurium* ST313 within migratory dendritic cells. *Cell Host Microbe* 21, 182–194. doi: 10.1016/j.chom.2017.01.009

Cegielski, J. P., and McMurray, D. N. (2004). The relationship between malnutrition and tuberculosis: evidence from studies in humans and experimental animals. *Int. J. Tuberc. Lung Dis.* 8, 286–298.

Chalmers, C. H. (1945). Tuberculosis and pasteurization of the milk supply. *Proc. Nutr. Soc.* 3, 186–194.

Chen, Z., Hu, Y., Cumming, B. M., Lu, P., Feng, L., Deng, J., et al. (2016). Mycobacterial whib6 differentially regulates ESX-1 and the dos regulon to modulate granuloma formation and virulence in zebrafish. *Cell Rep.* 16, 2512–2524. doi: 10.1016/j.celrep.2016.07.080

Cirillo, S. L., Subbian, S., Chen, B., Weisbrod, T. R., Jacobs, W. R. Jr, and Cirillo, J. D. (2009). Protection of *Mycobacterium tuberculosis* from reactive oxygen species conferred by the mel2 locus impacts persistence and dissemination. *Infect. Immun.* 77, 2557–2567. doi: 10.1128/IAI.01481-08

Cleret, A., Quesnel-Hellmann, A., Vallon-Eberhard, A., Verrier, B., Jung, S., Vidal, D., Mathieu, J., and Tournier, J. N. (2007). Lung dendritic cells rapidly mediate anthrax spore entry through the pulmonary route. *J. Immunol.* 178, 7994–8001. doi: 10.4049/jimmunol.178.12.7994

Click, E. S., Moonan, P. K., Winston, C. A., Cowan, L. S., and Oeltmann, J. E. (2012). Relationship between *Mycobacterium tuberculosis* phylogenetic lineage and clinical site of tuberculosis. *Clin. Infect. Dis.* 54, 211–219. doi: 10.1093/cid/cir788

Cohen, S. B., Gern, B. H., Delahaye, J. L., Adams, K. N., Plumlee, C. R., Winkler, J. K., et al. (2018). Alveolar macrophages provide an early *Mycobacterium tuberculosis* niche and initiate dissemination. *Cell Host Microbe* 24, 439–446.e4. doi: 10.1016/j.chom.2018.08.001

Corleis, B., Bucsan, A. N., Deruaz, M., Vrbanac, V. D., Lisanti-Park, A. C., Gates, S. J., et al. (2019). HIV-1 and SIV infection are associated with early loss of lung interstitial CD4+ T cells and dissemination of pulmonary tuberculosis. *Cell Rep.* 26, 1409–1418.e5. doi: 10.1016/j.celrep.2019.01.021

Corner, L. A., O'Meara, D., Costello, E., Lesellier, S., and Gormley, E. (2012). The distribution of *Mycobacterium bovis* infection in naturally infected badgers. *Vet. J.* 194, 166–172. doi: 10.1016/j.tvjl.2012.03.013

Davis, J. M., Clay, H., Lewis, J. L., Ghori, N., Herbomel, P., and Ramakrishnan, L. (2002). Real-time visualization of mycobacterium-macrophage interactions leading to initiation of granuloma formation in zebrafish embryos. *Immunity* 17, 693–702. doi: 10.1016/S1074-7613(02)00475-2

Davis, J. M., and Ramakrishnan, L. (2009). The role of the granuloma in expansion and dissemination of early tuberculous infection. *Cell* 136, 37–49. doi: 10.1016/j.cell.2008.11.014

de la Rua-Domenech, R. (2006). Human *Mycobacterium bovis* infection in the United Kingdom: incidence, risks, control measures and review of the zoonotic aspects of bovine tuberculosis. *Tuberculosis* 86, 77–109. doi: 10.1016/j.tube.2005.05.002

De Maio, F., Palmieri, V., De Spirito, M., Delogu, G., and Papi, M. (2019). Carbon nanomaterials: a new way against tuberculosis. *Expert Rev. Med. Devices* 16, 863–875. doi: 10.1080/17434440.2019.1671820

Diacon, A. H., Van de Wal, B. W., Wyser, C., Smedema, J. P., Bezuidenhout, J., Bolliger, C. T., and Walzl, G. (2003). Diagnostic tools in tuberculous pleurisy: a direct comparative study. *Eur. Respir. J.* 22, 589–591. doi: 10.1183/09031936.03.00017103a

Dobson, J. (1972). Percivall Pott. *Ann. R. Coll. Surg. Engl.* 50, 54–65.

El Sahly, H. M., Teeter, L. D., Pan, X., Musser, J. M., and Graviss, E. A. (2007). Mortality associated with central nervous system tuberculosis. *J. Infect.* 55, 502–509. doi: 10.1016/j.jinf.2007.08.008

Esmail, H., Barry, C. E., Young, D. B., and Wilkinson, R. J. (2014). The ongoing challenge of latent tuberculosis. *Philos. Trans. R. Soc. B.* 369:20130437. doi: 10.1098/rstb.2013.0437

Eum, S. Y., Kong, J. H., Hong, M. S., Lee, Y. J., Kim, J. H., Hwang, S. H. (2010). Neutrophils are the predominant infected phagocytic cells in the airways of patients with active pulmonary TB. *Chest* 137, 122–128. doi: 10.1378/chest.09-0903

Flynn, J. L. (2006). Lessons from experimental *Mycobacterium tuberculosis* infections. *Microbes Infect.* 8, 1179–1188. doi: 10.1016/j.micinf.2005.10.033

Formicola, V., Milanesi, Q., and Scarsini, C. (1987). Evidence of spinal tuberculosis at the beginning of the fourth millennium BC from Arene Candide cave (Liguria, Italy). *Am. J. Phys. Anthropol.* 72, 1–6. doi: 10.1002/ajpa.1330720102

Fujimura, Y. (1986). Functional morphology of microfold cells (M cells) in Peyer's patches. Phagocytosis and transport of BCG by M cells into rabbit Peyer's patches. *Gastroenterol. Jpn.* 21, 325–335. doi: 10.1007/BF02774129

Galan, J. E., and Curtiss, R. (1989). Cloning and molecular characterization of genes whose products allow *Salmonella typhimurium* to penetrate tissue culture cells. *Proc. Natl. Acad. Sci. U.S.A.* 86, 6383–6387. doi: 10.1073/pnas.86.16.6383

Ganchua, S. K. C., Cadena, A. M., Maiello, P., Gideon, H. P., Myers, A. J., Junecko, B. F., Klein, E. C., Lin, P. L., Mattila, J. T., and Flynn, J. L. (2018). Lymph nodes are sites of prolonged bacterial persistence during *Mycobacterium tuberculosis* infection in macaques. *PLoS Pathog.* 14:e1007337. doi: 10.1371/journal.ppat.1007337

Garcia de Viedma, D., Lorenzo, G., Cardona, P. J., Rodriguez, N. A., Gordillo, S., Serrano, M. J., and Bouza, E. (2005). Association between the infectivity of *Mycobacterium tuberculosis* strains and their efficiency for extrarespiratory infection. *J. Infect. Dis.* 192, 2059–2065. doi: 10.1086/498245

Garnier, T., Eiglmeier, K., Camus, J. C., Medina, N., Mansoor, H., Pryor, M., Duthoy, S. (2003). The complete genome sequence of *Mycobacterium bovis*. *Proc. Natl. Acad. Sci. U.S.A.* 100, 7877–7882. doi: 10.1073/pnas.1130426100

Ghon, A. (1916). *The Primary Lung Focus of Tuberculosis in Children*. London, JA: Churchill.

Golden, M. P., and Vikram H. R. (2005). Extrapulmonary tuberculosis: an overview. *Am. Fam. Physician* 72, 1761–1768.

Grutzkau, A., Hanski, C., Hahn, H., and Riecken, E. O. (1990). Involvement of M cells in the bacterial invasion of Peyer's patches: a common mechanism shared by Yersinia enterocolitica and other enteroinvasive bacteria. *Gut* 31, 1011–1015. doi: 10.1136/gut.31.9.1011

Grzybowski, S., and Allen, E. A. (1995). History and importance of scrofula. *Lancet* 346, 1472–1474. doi: 10.1016/S0140-6736(95)92478-7

Guerrero, G. G., Debrie, A. S., and Locht, C. (2010). Boosting with mycobacterial heparin-binding haemagglutinin enhances protection of *Mycobacterium bovis* BCG-vaccinated newborn mice against M. tuberculosis. *Vaccine* 28, 4340–4347. doi: 10.1016/j.vaccine.2010.04.062

Guirado, E., and Schlesinger, L. S. (2013). Modeling the *Mycobacterium tuberculosis* granuloma - the critical battlefield in host immunity and disease. *Front. Immunol.* 4:98. doi: 10.3389/fimmu.2013.00098

Harding, J. S., Rayasam, A., Schreiber, H. A., Fabry, Z., and Sandor, M. (2015). Mycobacterium-infected dendritic cells disseminate granulomatous inflammation. *Sci. Rep.* 5:15248. doi: 10.1038/srep15248

Hernandez Pando, R., Aguilar, D., Cohen, I., Guerrero, M., Ribon, W., Acosta, P. (2010). Specific bacterial genotypes of *Mycobacterium tuberculosis* cause extensive dissemination and brain infection in an experimental model. *Tuberculosis* 90, 268–277. doi: 10.1016/j.tube.2010.05.002

Hershkovitz, I., Donoghue, H. D., Minnikin, D. E., Besra, G. S., Lee, O. Y., Gernaey, A. M. (2008). Detection and molecular characterization of 9,000-year-old *Mycobacterium tuberculosis* from a neolithic settlement in the eastern mediterranean. *PLoS ONE* 3:e3426. doi: 10.1371/journal.pone.0003426

Ho, R. S., Fok, J. S., Harding, G. E., and Smith, D. W. (1978). Host-parasite relationships in experimental airborne tuberculosis. VII. Fate of *Mycobacterium tuberculosis* in primary lung lesions and in primary lesion-free lung tissue infected as a result of bacillemia. *J. Infect. Dis.* 138, 237–241. doi: 10.1093/infdis/138.2.237

Humphreys, I. R., Stewart, G. R., Turner, D. J., Patel, J., Karamanou, D., Snelgrove, R. J., and Young, D. B. (2006). A role for dendritic cells in the dissemination of mycobacterial infection. *Microbes Infect.* 8, 1339–1346. doi: 10.1016/j.micinf.2005.12.023

Jones, B. D., Ghori, N., and Falkow, S. (1994). Salmonella typhimurium initiates murine infection by penetrating and destroying the specialized epithelial M cells of the Peyer's patches. *J. Exp. Med.* 180, 15–23. doi: 10.1084/jem.180.1.15

Kim, J. H., Langston, A. A., and Gallis, H. A. (1990). Miliary tuberculosis: epidemiology, clinical manifestations, diagnosis, and outcome. *Rev. Infect. Dis.* 12, 583–590. doi: 10.1093/clinids/12.4.583

Kong, Y., Subbian, S., Cirillo, S. L., and Cirillo, J. D. (2009). Application of optical imaging to study of extrapulmonary spread by tuberculosis. *Tuberculosis* 89(Suppl. 1), S15–S17. doi: 10.1016/S1472-9792(09)70006-X

Lee, C. A., Jones, B. D., and Falkow, S. (1992). Identification of a Salmonella typhimurium invasion locus by selection for hyperinvasive mutants. *Proc. Natl. Acad. Sci. U.S.A.* 89, 1847–1851. doi: 10.1073/pnas.89.5.1847

Lee, J., Lim, J. K., Kim, E. J., Lee, D. H., Kim, Y. K., and Yoo, S. S. (2018). Comparison of clinical manifestations and treatment outcome according to age groups in adult patients with miliary tuberculosis. *J. Thorac. Dis.* 10, 2881–2889. doi: 10.21037/jtd.2018.04.139

Lin, P. L., Myers, A., Smith, L., Bigbee, C., Bigbee, M., and Fuhrman, C. (2010). Tumor necrosis factor neutralization results in disseminated disease in acute and latent *Mycobacterium tuberculosis* infection with normal granuloma structure in a cynomolgus macaque model. *Arthritis Rheum.* 62, 340–350. doi: 10.1002/art.27271

Lin, Y., Zhang, M., and Barnes, P. F. (1998). Chemokine production by a human alveolar epithelial cell line in response to *Mycobacterium tuberculosis*. *Infect. Immun.* 66, 1121–1126. doi: 10.1128/IAI.66.3.1121-1126.1998

Lincoln, E. M. (1935). Hematogenous tuberculosis in children. *Am. J. Dis. Child.* 50, 84–103. doi: 10.1001/archpedi.1935.01970070093008

Loddenkemper, R., Lipman, M., and Zumla, A. (2015). Clinical aspects of adult tuberculosis. *Cold Spring Harb. Perspect. Med.* 6:a017848. doi: 10.1101/cshperspect.a017848

Lurie, M. B. (1941). Heredity, constitution, and tuberculosis, and experimental study. *A. Rev. Tuberc.* 44(Suppl. 3), 1–125.

Ly, L. H., Russell, M. I., and McMurray, D. N. (2008). Cytokine profiles in primary and secondary pulmonary granulomas of Guinea pigs with tuberculosis. *Am. J. Respir. Cell Mol. Biol.* 38, 455–462. doi: 10.1165/rcmb.2007-0326OC

Marais, B. J., Gie, R. P., Schaaf, H. S., Hesseling, A. C., Obihara, C. C., and Nelson, L. J. (2004a). The clinical epidemiology of childhood pulmonary tuberculosis: a critical review of literature from the pre-chemotherapy era. *Int. J. Tuberc. Lung Dis.* 8, 278–285.

Marais, B. J., Gie, R. P., Schaaf, H. S., Hesseling, A. C., Obihara, C. C., and Starke, J. J. (2004b). The natural history of childhood intra-thoracic tuberculosis: a critical review of literature from the pre-chemotherapy era. *Int. J. Tuberc. Lung Dis.* 8, 392–402.

Margaret, A., and Macpherson, C. (1942). Primary tuberculosis of the lung and some of its consequences. *Postgrad. Med. J.* 18, 139–141. doi: 10.1136/pgmj.18.201.139

Marino, S., and Kirschner, D. E. (2016). A multi-compartment hybrid computational model predicts key roles for dendritic cells in tuberculosis infection. *Computation*. 4:39. doi: 10.3390/computation4040039

Martin, C. J., Cadena, A. M., Leung, V. W., Lin, P. L., Maiello, P., Hicks, N., et al. (2017). Digitally barcoding *Mycobacterium tuberculosis* reveals *in vivo* infection dynamics in the macaque model of tuberculosis. *MBio* 8:e00312-17. doi: 10.1128/mBio.00312-17

Martini, M., Gazzaniga, V., Behzadifar, M., Bragazzi, N. L., and Barberis, I. (2018). The history of tuberculosis: the social role of sanatoria for the treatment of tuberculosis in Italy between the end of the 19th century and the middle of the 20th. *J. Prev. Med. Hyg.* 59, E323–E327. doi: 10.15167/2421-4248/jpmh2018.59.4.1103

McMurray, D. N. (2003). Hematogenous reseeding of the lung in low-dose, aerosol-infected guinea pigs: unique features of the host-pathogen interface in secondary tubercles. *Tuberculosis* 83, 131–134. doi: 10.1016/S1472-9792(02)00079-3

Medlar, E. M. (1948). The pathogenesis of minimal pulmonary tuberculosis: a study of 1225 necropsies in cases of sudden and unexpected death. *Am. Rev. Tuberc.* 58, 583–611. doi: 10.1164/art.1948.58.6.583

Mehta, P. K., Karls, R. K., White, E. H., Ades, E. W., and Quinn, F. D. (2006). Entry and intracellular replication of *Mycobacterium tuberculosis* in cultured human microvascular endothelial cells. *Microb. Pathog.* 41, 119–124. doi: 10.1016/j.micpath.2006.05.002

Menozzi, F. D., Reddy, V. M., Cayet, D., Raze, D., Debrie, A. S., Dehouck, M. P., et al. (2006). *Mycobacterium tuberculosis* heparin-binding haemagglutinin adhesin (HBHA) triggers receptor-mediated transcytosis without altering the integrity of tight junctions. *Microbes Infect.* 8, 1–9. doi: 10.1016/j.micinf.2005.03.023

Munro, J. C. (1889). *Report of Twenty-Four Cases of Acute Miliary Tuberculosis*. American Clinical and Climatological Association.

Naing, C., Mak, J. W., Maung, M., Wong, S. F., and Kassim, A. I. (2013). Meta-analysis: the association between HIV infection and extrapulmonary tuberculosis. *Lung* 191, 27–34. doi: 10.1007/s00408-012-9440-6

Nair, V. R., Franco, L. H., Zacharia, V. M., Khan, H. S., Stamm, C. E., You, W., et al. (2016). Microfold cells actively translocate *Mycobacterium tuberculosis* to initiate infection. *Cell Rep.* 16, 1253–1258. doi: 10.1016/j.celrep.2016.06.080

Nedeltchev, G. G., Raghunand, T. R., Jassal, M. S., Lun, S., Cheng, Q. J., and Bishai, W. R. (2009). Extrapulmonary dissemination of *Mycobacterium bovis* but not *Mycobacterium tuberculosis* in a bronchoscopic rabbit model of cavitary tuberculosis. *Infect. Immun.* 77, 598–603. doi: 10.1128/IAI.01132-08

Neutra, M. R., Frey, A., and Kraehenbuhl, J. P. (1996). Epithelial M cells: gateways for mucosal infection and immunization. *Cell* 86, 345–348. doi: 10.1016/S0092-8674(00)80106-3

Oehlers, S. H., Cronan, M. R., Scott, N. R., Thomas, M. I., Okuda, K. S., Walton, E. M., et al. (2015). Interception of host angiogenic signalling limits mycobacterial growth. *Nature* 517, 612–615. doi: 10.1038/nature13967

Owen, R. L., Pierce, N. F., Apple, R. T., and Cray, W. C. Jr (1986). M cell transport of Vibrio cholerae from the intestinal lumen into peyer's patches: a mechanism for antigen sampling and for microbial transepithelial migration. *J. Infect. Dis.* 153, 1108–1118. doi: 10.1093/infdis/153.6.1108

Parra, M., Pickett, T., Delogu, G., Dheenadhayalan, V., Debrie, A. S., Locht, C., et al. (2004). The mycobacterial heparin-binding hemagglutinin is a protective antigen in the mouse aerosol challenge model of tuberculosis. *Infect. Immun.* 72, 6799–6805. doi: 10.1128/IAI.72.12.6799-6805.2004

Pethe, K., Puech, V., Daffe, M., Josenhans, C., Drobecq, H., Locht, C., et al. (2001). *Mycobacterium smegmatis* laminin-binding glycoprotein shares epitopes with *Mycobacterium tuberculosis* heparin-binding haemagglutinin. *Mol. Microbiol.* 39, 89–99. doi: 10.1046/j.1365-2958.2001.02206.x

Peto, H. M., Pratt, R. H., Harrington, T. A., LoBue, P. A., and Armstrong, L. R. (2009). Epidemiology of extrapulmonary tuberculosis in the United States, 1993-−2006. *Clin. Infect. Dis.* 49, 1350–1357. doi: 10.1086/605559

Polena, H., Boudou, F., Tilleul, S., Dubois-Colas, N., Lecointe, C., Rakotosamimanana, N., et al. (2016). *Mycobacterium tuberculosis* exploits the formation of new blood vessels for its dissemination. *Sci. Rep.* 6:33162. doi: 10.1038/srep33162

Porter, J. D., and McAdam, K. P. (1994). The re-emergence of tuberculosis. *Annu. Rev. Public Health* 15, 303–323. doi: 10.1146/annurev.pu.15.050194.001511

Reljic, R., Di Sano, C., Crawford, C., Dieli, F., Challacombe, S., and Ivanyi, J. (2005). Time course of mycobacterial infection of dendritic cells in the lungs of intranasally infected mice. *Tuberculosis* 85, 81–88. doi: 10.1016/j.tube.2004.09.006

Rich, A. R., and McCordock, H. A. (1933). The pathogenesis of tuberculous meningitis. *Bull. Johns Hopkins Hosp.* 52, 2–37

Roberts, L. L., and Robinson, C. M. (2014). *Mycobacterium tuberculosis* infection of human dendritic cells decreases integrin expression, adhesion and migration to chemokines. *Immunology* 141, 39–51. doi: 10.1111/imm.12164

Rock, R. B., Olin, M., Baker, C. A., Molitor, T. W., and Peterson, P. K. (2008). Central nervous system tuberculosis: pathogenesis and clinical aspects. *Clin. Microbiol. Rev.* 21, 243–261. doi: 10.1128/CMR.00042-07

Rosendahl, A., Bergmann, S., Hammerschmidt, S., Goldmann, O., and Medina, E. (2013). Lung dendritic cells facilitate extrapulmonary bacterial dissemination during pneumococcal pneumonia. *Front. Cell. Infect. Microbiol.* 3:21. doi: 10.3389/fcimb.2013.00021

Russell, D. G. (2001). TB comes to a sticky beginning. *Nat. Med.* 7, 894–895. doi: 10.1038/90926

Ryndak, M. B., Chandra, D., and Laal S. (2016). Understanding dissemination of *Mycobacterium tuberculosis* from the lungs during primary infection. *J. Med. Microbiol.* 65, 362–369. doi: 10.1099/jmm.0.000238

Schaller, M. A., Wicke, F., Foerch, C., and Weidauer, S. (2019). Central nervous system tuberculosis : etiology, clinical manifestations and neuroradiological features. *Clin. Neuroradiol.* 29, 3–18. doi: 10.1007/s00062-018-0726-9

Schepers, K., Dirix, V., Mouchet, F., Verscheure, V., Lecher, S., Locht, C., et al. (2015). Early cellular immune response to a new candidate

mycobacterial vaccine antigen in childhood tuberculosis. *Vaccine* 33, 1077–1083. doi: 10.1016/j.vaccine.2014.12.011

Schreiber, H. A., Harding, J. S., Hunt, O., Altamirano, C. J., Hulseberg, P. D., Stewart, D., et al. (2011). Inflammatory dendritic cells migrate in and out of transplanted chronic mycobacterial granulomas in mice. *J. Clin. Invest.* 121, 3902–3913. doi: 10.1172/JCI45113

Sharma, S. K., Mohan, A., Sharma, A., and Mitra, D. K. (2005). Miliary tuberculosis: new insights into an old disease. *Lancet Infect. Dis.* 5, 415–430. doi: 10.1016/S1473-3099(05)70163-8

Shaw, J. A., Irusen, E. M., Diacon, A. H., and Koegelenberg, C. F. (2018). Pleural tuberculosis: a concise clinical review. *Clin. Respir. J.* 12, 1779–1786. doi: 10.1111/crj.12900

Shepard, C. C. (1957). Growth characteristics of tubercle bacilli and certain other mycobacteria in HeLa cells. *J. Exp. Med.* 105, 39–48. doi: 10.1084/jem.105.1.39

Smith, D. T., and Abernathy, R. S. (1949). Selective localization of pulmonary emboli: an explanation for the apical localization of reinfection tuberculosis. *Trans. Am. Clin. Climatol. Assoc.* 61, 191–220.

Smith, D. W., Fok, J. S., Ho, R. S., Harding, G. E., Wiegeshaus, E., and Arora, P. K. (1975). Influence of BCG vaccination on the pathogenesis of experimental airborne tuberculosis. *J. Hyg. Epidemiol. Microbiol. Immunol.* 19, 407–417.

Smith, D. W., McMurray, D. N., Wiegeshaus, E. H., Grover, A. A., and Harding, G. E. (1970). Host-parasite relationships in experimental airborne tuberculosis. *IV*. Early events in the course of infection in vaccinated and nonvaccinated guinea pigs. *Am. Rev. Respir. Dis.* 102, 937–949. doi: 10.1164/arrd.1970.102.6.937

Srivastava, S., Ernst, J. D., and Desvignes, L. (2014). Beyond macrophages: the diversity of mononuclear cells in tuberculosis. *Immunol. Rev.* 262, 179–192. doi: 10.1111/imr.12217

Stead, W. W. (1989). Pathogenesis of tuberculosis: clinical and epidemiological perspectives. *Rev. Infect. Dis.* 11(Suppl. 2), S366–S368. doi: 10.1093/clinids/11.Supplement_2.S366

Subbian, S., Mehta, P. K., Cirillo, S. L., and Cirillo, J. D. (2007). The *Mycobacterium marinum mel2* locus displays similarity to bacterial bioluminescence systems and plays a role in defense against reactive oxygen and nitrogen species. *BMC Microbiol.* 7:4. doi: 10.1186/1471-2180-7-4

Sweany, H. C., Cook, C. E., and Kegerreis, R. (1931). A study of the position of primary cavities in pulmonary tuberculosis. *Am. Rev. Tuberc.* 24, 558–582.

Taylor, G. M., Murphy, E., Hopkins, R., Rutland, P., and Chistov, Y. (2007). First report of *Mycobacterium bovis* DNA in human remains from the Iron Age. *Microbiology* 153(Pt 4), 1243–1249. doi: 10.1099/mic.0.2006/002154-0

Teitelbaum, R., Schubert, W., Gunther, L., Kress, Y., Macaluso, F., Pollard, J. W., et al. (1999). The M cell as a portal of entry to the lung for the bacterial pathogen *Mycobacterium tuberculosis*. *Immunity* 10, 641–650. doi: 10.1016/S1074-7613(00)80063-1

Torraca, V., Cui, C., Boland, R., Bebelman, J. P., van der Sar, A. M., Smit, M. J., et al. (2015). The CXCR3-CXCL11 signaling axis mediates macrophage recruitment and dissemination of mycobacterial infection. *Dis. Model. Mech.* 8, 253–269. doi: 10.1242/dmm.017756

Vazquez-Torres, A., Jones-Carson, J., Baumler, A. J., Falkow, S., Valdivia, R., Brown, W., et al. (1999). Extraintestinal dissemination of *Salmonella* by CD18-expressing phagocytes. *Nature* 401, 804–808. doi: 10.1038/44593

Vemula, M. H., Medisetti, R., Ganji, R., Jakkala, K., Sankati, S., Chatti, K., et al. (2016). *Mycobacterium tuberculosis* zinc metalloprotease-1 assists mycobacterial dissemination in zebrafish. *Front. Microbiol.* 7:1347. doi: 10.3389/fmicb.2016.01347

Wagner, W. H. (1975). Host-parasite interactions with peritoneal macrophages of mice and rats *in vitro* and *in vivo*. *Infect. Immun.* 12, 1295–1306. doi: 10.1128/IAI.12.6.1295-1306.1975

Wallgren, A. (1948). The time-table of tuberculosis. *Tubercle* 29, 245–251. doi: 10.1016/S0041-3879(48)80033-4

Walzl, G., McNerney, R., du Plessis, N., Bates, M., McHugh, T. D., Chegou, N. N., et al. (2018). Tuberculosis: advances and challenges in development of new diagnostics and biomarkers. *Lancet Infect. Dis.* 18, e199–e210. doi: 10.1016/S1473-3099(18)30111-7

Westphalen, K., Gusarova, G. A., Islam, M. N., Subramanian, M., Cohen, T. S., Prince, A. S., et al. (2014). Sessile alveolar macrophages communicate with alveolar epithelium to modulate immunity. *Nature* 506, 503–506. doi: 10.1038/nature12902

WHO (2019). *Global Tuberculosis Report 2019*. Geneva: World Health Organization.

Wickremasinghe, M. I., Thomas, L. H., and Friedland, J. S. (1999). Pulmonary epithelial cells are a source of IL-8 in the response to *Mycobacterium tuberculosis*: essential role of IL-1 from infected monocytes in a NF-kappa B-dependent network. *J. Immunol.* 163, 3936–3947.

Williams, N. L., Morris, J. L., Rush, C. M., and Ketheesan, N. (2014). Migration of dendritic cells facilitates systemic dissemination of Burkholderia pseudomallei. *Infect. Immun.* 82, 4233–4240. doi: 10.1128/IAI.01880-14

Wirth, T., Hildebrand, F., Allix-Beguec, C., Wolbeling, F., Kubica, T., Kremer, K., et al. (2008). Origin, spread and demography of the *Mycobacterium tuberculosis* complex. *PLoS Pathog.* 4: e1000160. doi: 10.1371/journal.ppat.1000160

Zhang, M., Kim, K. J., Iyer, D., Lin, Y., Belisle, J., McEnery, K., et al. (1997). Effects of *Mycobacterium tuberculosis* on the bioelectric properties of the alveolar epithelium. *Infect. Immun.* 65, 692–698. doi: 10.1128/IAI.65.2.692-698.1997

Zink, A., Haas, C. J., Reischl, U., Szeimies, U., and Nerlich, A. G. (2001). Molecular analysis of skeletal tuberculosis in an ancient Egyptian population. *J. Med. Microbiol.* 50, 355–366. doi: 10.1099/0022-1317-50-4-355

Zurcher, K., Ballif, M., Kiertiburanakul, S., Chenal, H., Yotebieng, M., Grinsztejn, B., et al. (2019). Diagnosis and clinical outcomes of extrapulmonary tuberculosis in antiretroviral therapy programmes in low- and middle-income countries: a multicohort study. *J. Int. AIDS Soc.* 22: e25392. doi: 10.1002/jia2.25392

Conflict of Interest: The authors declare that the research was conducted in the absence of any commercial or financial relationships that could be construed as a potential conflict of interest.

frontiers in Cellular and Infection Microbiology

PERSPECTIVE
published: 08 April 2020
doi: 10.3389/fcimb.2020.00139

Challenges of Immune Response Diversity in the Human Population Concerning New Tuberculosis Diagnostics, Therapies, and Vaccines

Abul K. Azad[1], *Christopher Lloyd*[1], *Wolfgang Sadee*[2] *and Larry S. Schlesinger*[1]*

[1] *Host-Pathogen Interaction Program, Texas Biomedical Research Institute, San Antonio, TX, United States,* [2] *Department of Cancer Biology and Genetics, Center for Pharmacogenomics, College of Medicine, The Ohio State University, Columbus, OH, United States*

Universal approaches to the prevention and treatment of human diseases fail to take into account profound immune diversity resulting from genetic variations across populations. Personalized or precision medicine takes into account individual lifestyle, environment, and biology (genetics and immune status) and is being adopted in several disease intervention strategies such as cancer and heart disease. However, its application in infectious diseases, particularly global diseases such as tuberculosis (TB), is far more complex and in a state of infancy. Here, we discuss the impact of human genetic variations on immune responses and how they relate to failures seen in current TB diagnostic, therapy, and vaccine approaches across populations. We offer our perspective on the challenges and potential for more refined approaches going forward.

Keywords: tuberculosis, immunity, diagnostics, therapy, vaccine, genetics, genetic diversity

OPEN ACCESS

Edited by:
Igor Kramnik,
Boston University, United States

Reviewed by:
Surya Prakash Pandey,
University of Pittsburgh, United States
Maria Lerm,
Linköping University, Sweden

***Correspondence:**
Larry S. Schlesinger
lschlesinger@txbiomed.org

Specialty section:
This article was submitted to Microbes and Innate Immunity, a section of the journal Frontiers in Cellular and Infection Microbiology

Received: *11 December 2019*
Accepted: *17 March 2020*
Published: *08 April 2020*

Citation:
Azad AK, Lloyd C, Sadee W and Schlesinger LS (2020) Challenges of Immune Response Diversity in the Human Population Concerning New Tuberculosis Diagnostics, Therapies, and Vaccines. Front. Cell. Infect. Microbiol. 10:139. doi: 10.3389/fcimb.2020.00139

THE CLOSE LINK BETWEEN HUMAN EVOLUTIONARY BIOLOGY AND IMMUNE DIVERSITY

Human evolutionary biology is thought to have a pronounced influence on genetic diversity, particularly in regards to the immune system. Disease-risk alleles that are predominantly deleterious by loss of function represent a subset of global human genetic diversity. Their occurrence, frequency, and population distribution are shaped by evolutionary forces such as purifying selection, genetic drift, and migration (Tishkoff and Verrelli, 2003; Quintana-Murci, 2016). On the other hand, genetic variants that convey protection and resilience can be under positive selection, reaching high allele frequencies, observed in genes affecting immunity and host defense, under the enduring selection pressure of microbes.

Large inter-individual variation observed in human immune responses has been attributed to genetic factors (Azad et al., 2012; Sanz et al., 2018; Scepanovic et al., 2018) and environmental influence (Macgillivray and Kollmann, 2014), subject to both human adaptation and rapid evolution of the pathogens (Kodaman et al., 2014). Admixture with ancient hominins introduced advantageous immune variants into the modern human population (Racimo et al., 2015), and it is unlikely that the population distribution of common susceptibility alleles results from neutral processes alone (Corona et al., 2013; Quintana-Murci, 2016). The innate immune system is the critical primary target for protection against infections, with a large portion of the human population exposed to a variety of infections, one prominent one being *Mycobacterium tuberculosis* (*M.tb*). However, ramping up the innate immune system—necessary under increasingly crowded

living conditions—engenders susceptibility to autoimmune diseases (Waldner, 2009; Azad et al., 2012). As a result, genetic variants in innate immune genes often accumulate to high allele frequency until the negative and positive effects cancel each other. This type of genetic variant under balancing selection is largely regulatory, requiring distinct methods for discovery compared to variants that change the amino acid sequence. Because multiple pathways can lead to resistance against various infectious agents and their subspecies, we expect pronounced differences in genetic adaptation between populations, and, in parallel, genetic risk of diseases such as type 2 diabetes, biliary liver cirrhosis, psoriasis, inflammatory bowel disease, and systemic lupus erythematosus (Corona et al., 2013). These relationships lead to pervasive overlap between positively selected genomic regions and genes associated with traits or diseases in genome-wide association studies (GWAS) that comprise multiple regions associated with infectious and autoimmune disease risks, including tuberculosis (TB) and leprosy (Grossman et al., 2013). Medications that target chemokines and cytokines—principal actors of the innate immune response—hence carry warning labels not to be used when an infection such as TB is detected, highlighting the nexus between autoimmune disease and infection. In the context of how human evolution has acted upon immune phenotypes and diversity, it is important to consider that adapted immune traits can be transmitted across generations not only through genetics but also *via* environmental and cultural factors (Danchin et al., 2011).

IMPORTANCE OF INTER-INDIVIDUAL HUMAN IMMUNE RESPONSE VARIATION IN INFECTIOUS DISEASES SUCH AS TB

When humans are exposed to pathogenic microbes, immune responses are initiated to protect the host, and these responses are highly variable among humans, even between healthy individuals within and across populations (Scepanovic et al., 2018). In the case of TB, *M.tb* infection is followed by a spectrum of responses and outcomes (Lin and Flynn, 2018). Very few infected individuals proceed to develop clinical disease. Instead, the majority of those infected maintain latent TB infection (LTBI), with only 5–10% later developing clinical disease, usually within 2 years of infection (Dodd and Schlesinger, 2017; Behr et al., 2018).

Human TB cell-based experimentation studies and vaccine trials highlight the significant hurdle of substantial human-to-human variation in cellular and immunological responses to antigen stimulation (Azad et al., 2012; Tameris et al., 2013; Zumla et al., 2016; Fava and Schurr, 2017). We posit that knowing the root causes of differential human immune responses will enable better design of effective therapies and vaccines that encompass the majority of recipients. While several factors contribute to natural differences in human immunity to disease, this PERSPECTIVE article focuses mainly on host genetic factors as one of the main drivers for outcomes of infectious diseases, specifically TB (Abel et al., 2014). In the current state, the BCG vaccine for TB elicits highly variable protection in different human populations, and anti-TB drugs might work well in one person but be less effective or cause serious side effects in another (Bloom et al., 2017). Therefore, knowing the underlying relationship between genetics and biology will enable us to identify those individuals who will benefit maximally from designed therapies and vaccines.

GLOBAL DATABASE ON TB INCIDENCE AT A GLANCE

According to recent WHO report (2019), an estimated 10.0 million (range, 9.0–11.1 million) people fell ill with TB in 2018 (WHO, 2019). Globally, the average rate of decline in the TB incidence rate was 1.6% per year in the period 2000–2018, and 2.0% between 2017 and 2018. The global reduction in the number of TB deaths between 2015 and 2018 was 11%. Co-infection (for example, with HIV) bears influence on TB mortality. There were 1.2 million TB deaths among HIV-negative people globally in 2018, but an additional 251,000 deaths were reported among HIV-positive people. Since 8.6% of all TB cases were also living with HIV, it appears that co-infection with HIV increases the death rate. Geographically, most TB incidences in 2018 were in the WHO regions of developing countries of South-East Asia (44%), Africa (24%) and the Western Pacific (18%), with smaller shares in most developed countries of the Eastern Mediterranean (8%), the Americas (3%) and Europe (3%). In 2017, 69% of international donor funding for TB was provided by the Global Fund. The US government was the second largest donor, which contributed US$ 249 million (23% of the global total) via the Global Fund (WHO, 2019).

CHALLENGES OF UNIVERSAL MEDICINE AND THE PROSPECT OF MORE PERSONALIZED TREATMENTS FOR TB

M.tb infection leads to significant up-regulation of many immune and metabolic response genes (Barreiro et al., 2012). However, if the individual carries functional genetic variants [most commonly single nucleotide polymorphisms (SNPs)] in key immune or metabolic response genes, primary immune responses that defend against *M.tb* infection can be rendered more or less robust (Barreiro et al., 2012). Likewise, if genetic variants significantly alter drug metabolism, a standard drug formulation could fail or cause side effects in carriers (Ahmed et al., 2016). In the ideal situation, each individual's personal set of immune and metabolic characteristics should be considered to provide the most effective treatment for TB and other infectious diseases. This challenge is already being addressed in deciding on cancer immunotherapy regimens (Liu and Guo, 2018). Serious problems may arise for immune-variant individuals when universal medicine, the provision of identical forms of treatment to all individuals who present with the same disease, is exercised; yet, our ability to predict immune competence with respect to infectious diseases is quite limited. Heterogeneity between ethnic groups contributes to the challenge of developing biomarker panels guiding therapy.

For example, 16–21% of genes involved in generating Toll-like receptor (TLR) ligands and other immune responses differ between African and European subjects (Sanz et al., 2018). Such findings suggest that immunity across different populations will differ enough to render treatments that are effective in one region ineffective in others, further illustrating the need to optimize treatments to personal characteristics. Similarly, frequent variants exist in genes encoding drug-metabolizing enzymes, for example, N-acetyltransferase 2 (NAT2), which plays a role in the metabolism of the anti-TB drug isoniazid (INH) (Klein et al., 2016) (see below). To date, genetic predictors are not being used in the clinic for diagnostic and therapeutic purposes in infectious diseases, which is in stark contrast to their pervasive use in cancer and other diseases (Thanassoulis and Vasan, 2010; Tian et al., 2012; Verma, 2012; Demkow and Wolanczyk, 2017; Giudicessi et al., 2017).

For these reasons, we argue that new treatments and vaccines designed on a more personal basis in infectious diseases including TB should be considered going forward, so-called personalized or precision medicine. Improved genetic sequencing technologies, functional genomics strategies, and systems biology approaches developed in recent years make this feasible to consider (Poland et al., 2013; Jensen and Van Hal, 2017; Ladner et al., 2019). Such approaches have allowed for fast and reliable sequencing of both human and pathogen genomes, providing increased knowledge of host-pathogen interactions, particularly the underlying mechanisms for disease pathogenesis, which can be used as the foundation for developing more personalized treatments, particularly relevant when considering host-directed therapies (Simmons et al., 2018). There has been a recent discussion on the development of precision medicine for drug-resistant TB (Cox et al., 2018; Groschel et al., 2018; Mahomed et al., 2019). However, interpretation of human genomics data in the context of susceptibility to infections is currently far from sufficient to develop clinical decision tools. In part, this shortcoming may have arisen from the emphasis of research on those of European descent (Popejoy and Fullerton, 2016), biasing conclusions and missing opportunities to learn from the global variation of the human immune system.

Although the concept and application of personalized medicine are attractive and hold promise for avoiding unnecessary and inappropriate treatment options, there are indeed drawbacks. Apart from ethical issues, the introduction of personalized medicine will be difficult to institute in endemic regions, especially in developing countries, where poverty, lawlessness, and internal strife exist. According to many critics, the application of personalized medicine theory in developing countries is considered uncertain or impossible (So and Joly, 2013; Gameiro et al., 2018). In addition to the limited global financial support for the development of new costly medicine, collected genomic data remain insufficient for many ethnic groups. Current GWAS go a long way to cover ethnic diversity, but often lack sufficient size to advance the field substantially. While it can be reasonably argued that personalized medicine cannot yet be broadly applied to the individual, we submit that more emphasis should be placed on initiatives to progress precision medicine principles on a regionalized scale, covering the majority of ethnic populations, and leading to novel insights into relevant disease risk pathways in those populations.

HUMAN GENETIC POLYMORPHISMS IN TB-ASSOCIATED INNATE IMMUNE GENES, GWAS, FUNCTIONAL GENOMICS, AND PHARMACOGENOMICS

Functional variants in host innate immune genes are frequent and include both gain- and loss-of-function mutations under strong selection pressure. Key genes affected are likely to be shared across all ethnicities. However, we can further expect that multiple variants have arisen in each gene locus, that interact with each other, with substantially different allele frequencies between ethnic groups—a challenge for geneticists assessing functional consequences. Host genetic risk in TB also depends on the mycobacterial genetic background, highlighting the importance of studying the interaction between host and *M.tb* genomes (Omae et al., 2017). TB-associated innate immune genes encode pattern recognition receptors, inflammatory factors, nuclear receptors, surfactant proteins, oxidative response proteins, cytokines, chemokines, etc., (Azad et al., 2012; Fol et al., 2015). A majority of TB-associated SNPs have been derived from GWAS, taking advantage of massive genomics data sets across populations, leading to inferences of candidate genes contributing to human immune variation and susceptibility or resistance to diseases in general (Uren et al., 2017). However, GWAS-significant SNPs mostly do not reveal the underlying mechanisms of a potential functional variant or even the causative genes, as regulatory variants can reside at a long distance from their target genes, acting by chromatin looping mechanisms (Sadee et al., 2014; Gallagher and Chen-Plotkin, 2018). Therefore, GWAS-significant SNPs are often only marker SNPs that vary greatly in frequency between ethnic groups. Moreover, since TB is a complex multi-genic disorder, each genetic variant alone contributes but a small fraction of overall risk which can, in part, be addressed with polygenic risk scores reflecting all marker SNPs (Wray et al., 2013). However, this approach neglects dynamic interactions between genes and pathways and with the environment. Much larger datasets are needed to begin to address these crucial questions (currently under development in multiple countries) making it difficult at the current time to identify any single SNP or combination of SNPs affecting gene product(s) that can be targeted for therapy or vaccine development (Jin et al., 2019; Luo et al., 2019). On the other hand, a rapidly expanding source of large functional genomic databases is now publicly available enabling identification of causal variants and genes, using expression quantitative trait locus analysis presented in GTEx (Consortium, 2013), and the Encyclopedia of DNA Elements (ENCODE) (Consortium, 2012), followed by experimental validation using molecular biology tools. The field of pharmacogenomics has embraced functional genomics platforms for some time, identifying causal functional variants

that alter drug metabolism, thereby applying personalized medicine concepts to individualizing drug treatment (Potamias et al., 2014) (see below).

Current GWAS for TB are still limited by sample size, ethnic stratification of the sample population, and difficulties in acquiring accurate medical history records such as information about past exposure to disease and treatment (Barreiro et al., 2012). As a result of hidden population stratification, GWAS-hit SNPs are often spurious, requiring mandatory replication in the same ethnic population and across ethnic groups—where SNPs may vary, but candidate genes may overlap. A particular hurdle in GWAS is a large number of variants tested, up to 4 million per chip plus imputations, each to be considered a separate hypothesis—hence, genome-wide significance requires a *p*-value as low as 10^{-8} under Bonferroni correction. Clearly, many valid functional variants remain hidden using this conservative cutoff. Therefore, one can use prior knowledge to focus on a genomic region around a known strong candidate immune gene, greatly reducing the number of SNPs tested and hence allowing for a higher *p*-value, under the assumption that a causative variant is often located near its immune target gene (e.g., within 200-kb of the gene's transcription starting site in either direction) (Barreiro et al., 2012). To search for more than one functional variant per gene locus, one needs to address the linkage disequilibrium (LD) structure (as available in the 1,000 genomes database) to determine which LD block carries independently active variants (Uren et al., 2017) and how these could interact with each other (Lee et al., 2018; Joiret et al., 2019).

IMMUNE DIVERSITY AND THE CHALLENGE OF GLOBAL TB DIAGNOSTICS AND VACCINES

Variability in immune responses can contribute to the difficulty of TB diagnosis. Currently, the tuberculin skin test and blood IFNγ release assay are used to assess TB infection (Sharma et al., 2017). Due to the different mechanisms by which these tests operate, results do not always agree (Gallant et al., 2010). In addition, the presence of immune-related genetic variants likely affects test results of immune responses as indicators of *M.tb* infection. A report of the influence of genetic variance and shared environment on the production of IFNγ is an example in this context (Tao et al., 2013).

Genetic variability between individuals also poses a challenge to developing a universal TB vaccine (Gong et al., 2018). Substantial variability in response to the current BCG vaccine is attributed to individual differences in age, sex, dosage, method of vaccination, and nutritional status, among others (Castiblanco and Anaya, 2015; Newport, 2015). Genetic variants that influence the expression of TLRs, HLAs, and cytokines and their receptors can induce differential host responses to the BCG vaccine (Newport, 2015). For example, IFNγ responses in Gambian neonates after BCG vaccination demonstrate a bell-shaped curve distribution, indicating that the vaccine does not induce immunity across all individuals in a population (Newport, 2015). A twin study in Gambian infants indicates that IFNγ and IL-13 responses to tetanus, pertussis, and some BCG vaccine antigens are 39–65% heritable (Newport et al., 2004), supporting the view that immune response to vaccines is strongly influenced by genetics and that the genetic profile of individuals should be taken into account when developing effective TB vaccines. This critical issue compels a robust effort to understand the underlying biology and genetics, which are currently insufficiently resolved to guide vaccine optimization.

Current TB vaccine design strategies generally target enhanced cell-mediated immunity, whereas antibody-based approaches have been largely dismissed until recently (Achkar and Casadevall, 2013; Cywes-Bentley et al., 2018; Kawahara et al., 2019; Tanner et al., 2019). Recent evidence also supports the contribution of trained innate immunity to vaccine protection (Khader et al., 2019; Koeken et al., 2019). Since infants and the elderly are at high risk of infectious diseases, researchers are beginning to focus on understanding age-specific immunity to design workable vaccines for those age-groups (Keener, 2019). Future vaccine approaches will need to consider the different immune mechanisms in these contexts but will also need to consider strategies to identify subsets of individuals, populations, or regions in order to determine the best vaccine type or adjuvant combination to administer. Such efforts will also further clarify the degree of susceptibility or resistance to *M.tb* infection and progression to TB.

DO GENETIC VARIANTS OF THE HOST INFLUENCE TB DRUG EFFICACY, TOXICITY, AND RESISTANCE?

Host genetic mutations are not typically associated with the development of drug resistance, which is most commonly attributed to bacterial gene mutations under the selection pressure of prolonged drug exposure. However, genetic polymorphisms in host drug-metabolizing enzymes may render drugs less active or inactive, reduce drug levels that can promote bacterial mutation, or cause drug toxicity *via* increased formation of reactive metabolites (Motta et al., 2018). Such polymorphisms may contribute to differences in the incidence of anti-TB drug-induced hepatotoxicity (ATDH) between different populations. Among the anti-TB drugs, INH metabolism and disposition are strongly impacted by genetic factors. A few reports suggest a role for genetic polymorphisms with respect to rifampicin (RFP) metabolism, while less is known regarding the influence of genetic polymorphisms on the metabolism of other first- and second-line anti-TB drugs (Ramachandran and Swaminathan, 2012). Two major host enzymes involved in INH metabolism are NAT2 and cytochrome P450 family 2 subfamily E member 1 (CYP2E1). Frequent *NAT2* variants convey a rapid and slow acetylator phenotype, which inactivates INH as an anti-TB drug and results in substantial differences in drug exposure for the same dose. In addition, the main metabolite downstream of acetylation is acetylhydrazide, which is subsequently oxidized to toxic products. Since acetylhydrazide itself is further inactivated to diacetylhydrazide by NAT2, the relationship between NAT2 metabolizer status and liver toxicity

results from the interplay of multiple pathways—an illustration that genetic effects can be complex even in a seemingly simple drug-effect relationship. A review by Klein et al. (2016) suggests that INH dose reduction in slow acetylators relative to rapid acetylators does not reduce anti-TB efficacy while likely reducing liver toxicity. Another recent study has reported an association between anti-TB drugs and *CYP2B6* polymorphisms and the risk of ATDH in a Chinese population (Wang et al., 2017). In their review of pharmacokinetics and pharmacogenetics of anti-TB drugs, Motta et al. (2018) suggest that increasing the RFP doses in individuals with SLCO1B1 loss of function alleles is a promising strategy—SLCO1B1 is a transporter of drugs into hepatic cells. More robust clinical prospective studies are needed to evaluate the contribution of these polymorphisms in the occurrence of liver toxicity during anti-TB treatment. Thus, we feel that there is a need to incorporate pharmacogenomics into clinical trials of TB to understand the factors impacting therapeutic success and occurrence of adverse drug effects.

DISCUSSION AND FUTURE DIRECTIONS

Inter-individual variability in human immune responses to TB and other infectious diseases will continue to create a challenge as improvements in drugs and vaccines are discovered and implemented. Although currently viewed as provocative and difficult to achieve in infectious diseases, particularly in developing countries, we feel that the study and development of more personalized treatments and vaccines targeting specific immune characteristics of individuals, populations, or regions will become more important going forward. These more personalized approaches are likely to become commonplace as discoveries and innovations continue to be made in functional genomics and systems biology as applied to differential immune responses to disease. Currently, these innovations are being incorporated clinically in the fields of cancer, cardiovascular disorders, and brain diseases (Twilt, 2016).

The emergence and rapid dissemination of multi-drug, extremely drug, and totally drug-resistant strains *of M.tb* remains a severe global threat (Parida et al., 2015; Oppong et al., 2019); thus, development of new treatments and an effective vaccine(s) is paramount. We feel that it is also imperative to better understand the genetics underlying human variations in immune responses to TB, not only to aid in more personalized approaches to administration but also to advance host-directed or gene-targeted (e.g., CRISPR gene editing) therapeutic approaches that hold promise for overriding TB drug resistance.

Next-generation sequencing, increasing public availability of large-scale genomic and other "omic" data sets, and robust analytics need to be integrated into the diagnosis, treatment, and control of TB. Genomic data must be integrated with clinical and radiological data to compose complete individualized biological databases. Global challenges exist in differences between cultures, legal frameworks, economic conditions, and health priorities that have the potential to lead to a diversity of personalized medicine models throughout the globe, especially applicable to infectious diseases. To provide scientific evidence that will turn the concept and promise of personalized medicine into a reality for TB, the development of rigorous research programs, and both medical and non-medical multidisciplinary teams are required. If the correct policies and technologies are used, personalized medicine has the potential to improve treatment outcomes and decrease the transmission of TB for a greater proportion of the population.

In focusing on genetic studies, we note that the majority of SNPs associated with TB susceptibility have been found in intergenic regions of the genome, or non-coding regions of candidate genes (introns and UTRs), suggesting that they are regulatory genes (Azad et al., 2012; Uren et al., 2017). Recently, it has become possible to predict the function of these non-coding genetic variations by using software such as RegulomeDB or Variant Effect Predictor (Uren et al., 2017). The potential to identify the function of regulatory genes will allow for future studies to target those that lead to immune function changes and can be compensated with corrective drugs or supplements. These methods have already been used in the search for cures to diseases such as late-onset Alzheimer's, cardiovascular disease, and aging, suggesting that they could be used in the study of infectious diseases like TB as well (Rosenthal et al., 2014; Haider and Faisal, 2015; Bastami et al., 2016; Cavalli et al., 2016). Lastly, we propose that future clinical studies of TB therapy must link pharmacogenomics data with TB treatment outcomes.

We acknowledge that the concepts and ideas put forth in this PERSPECTIVE piece represent a leap for infectious diseases and TB in particular, and several significant roadblocks exist at the current time, including cost, technological tools, the feasibility of global data access and integration, etc. However, infectious diseases contribute substantially to global mortality and morbidity (Dye, 2014), and projections are for the impact of these diseases to increase (Holmes et al., 2017). TB alone has thus far killed over 1.4 billion people over human history, far greater than any other single infectious disease, and prevalence of drug resistance, toxicity of complicated drug regimens, and the absence of an effective vaccine that consistently generates protection in the majority of recipients portends continued challenges for TB control in the foreseeable future. These serious issues make it necessary that we continue to harness and embrace new intervention approaches.

AUTHOR CONTRIBUTIONS

All authors listed have made a substantial, direct and intellectual contribution to the work, and approved it for publication.

REFERENCES

Abel, L., El-Baghdadi, J., Bousfiha, A. A., Casanova, J. L., and Schurr, E. (2014). Human genetics of tuberculosis: a long and winding road. *Philos. Trans. R. Soc. Lond B Biol. Sci.* 369:20130428. doi: 10.1098/rstb.2013.0428

Achkar, J. M., and Casadevall, A. (2013). Antibody-mediated immunity against tuberculosis: implications for vaccine development. *Cell Host. Microbe.* 13, 250–262. doi: 10.1016/j.chom.2013.02.009

Ahmed, S., Zhou, Z., Zhou, J., and Chen, S. Q. (2016). Pharmacogenomics of drug metabolizing enzymes and transporters: relevance to precision medicine. *Genom. Proteom. Bioinform.* 14, 298–313. doi: 10.1016/j.gpb.2016.03.008

Azad, A. K., Sadee, W., and Schlesinger, L. S. (2012). Innate immune gene polymorphisms in tuberculosis. *Infect. Immun.* 80, 3343–3359. doi: 10.1128/IAI.00443-12

Barreiro, L. B., Tailleux, L., Pai, A. A., Gicquel, B., Marioni, J. C., and Gilad, Y. (2012). Deciphering the genetic architecture of variation in the immune response to *Mycobacterium tuberculosis* infection. *Proc. Natl. Acad. Sci. U. S. A.* 109, 1204–1209. doi: 10.1073/pnas.1115761109

Bastami, M., Nariman-Saleh-Fam, Z., Saadatian, Z., Nariman-Saleh-Fam, L., Omrani, M. D., Ghaderian, S. M. H., et al. (2016). The miRNA targetome of coronary artery disease is perturbed by functional polymorphisms identified and prioritized by in-depth bioinformatics analyses exploiting genome-wide association studies. *Gene* 594, 74–81. doi: 10.1016/j.gene.2016.08.054

Behr, M. A., Edelstein, P. H., and Ramakrishnan, L. (2018). Revisiting the timetable of tuberculosis. *BMJ* 362:k2738. doi: 10.1136/bmj.k2738

Bloom, B. R., Atun, R., Cohen, T., Dye, C., Fraser, H., Gomez, G. B., et al. (2017). "Tuberculosis," in *Major Infectious Diseases*, eds R. D. Holmes, K. K. Bertozzi, S. B. R. Bloom, and P. Jha (Washington, DC: World bank Group), 233–313. doi: 10.1596/978-1-4648-0524-0_ch11

Castiblanco, J., and Anaya, J. M. (2015). Genetics and vaccines in the era of personalized medicine. *Curr Genomics* 16, 47–59. doi: 10.2174/1389202916666141223220551

Cavalli, M., Pan, G., Nord, H., and Wadelius, C. (2016). Looking beyond GWAS: allele-specific transcription factor binding drives the association of GALNT2 to HDL-C plasma levels. *Lipids Health Dis.* 15:18. doi: 10.1186/s12944-016-0183-x

Consortium, E. P. (2012). An integrated encyclopedia of DNA elements in the human genome. *Nature* 489, 57–74. doi: 10.1038/nature11247

Consortium, G. (2013). The Genotype-Tissue Expression(GTEx) project. *Nat. Genet.* 45, 580–585. doi: 10.1038/ng.2653

Corona, E., Chen, R., Sikora, M., Morgan, A. A., Patel, C. J., Ramesh, A., et al. (2013). Analysis of the genetic basis of disease in the context of worldwide human relationships and migration. *PLoS Genet.* 9:e1003447. doi: 10.1371/journal.pgen.1003447

Cox, H., Hughes, J., Black, J., and Nicol, M. P. (2018). Precision medicine for drug-resistant tuberculosis in high-burden countries: is individualised treatment desirable and feasible? *Lancet Infect. Dis.* 18, e282–7. doi: 10.1016/S1473-3099(18)30104-X

Cywes-Bentley, C., Rocha, J. N., Bordin, A. I., Vinacur, M., Rehman, S., Zaidi, T. S., et al. (2018). Antibody to Poly-N-acetyl glucosamine provides protection against intracellular pathogens: mechanism of action and validation in horse foals challenged with *Rhodococcus equi*. *PLoS Pathog.* 14:e1007160. doi: 10.1371/journal.ppat.1007160

Danchin, E., Charmantier, A., Champagne, F. A., Mesoudi, A., Pujol, B., and Blanchet, S. (2011). Beyond DNA: integrating inclusive inheritance into an extended theory of evolution. *Nat. Rev. Genet.* 12, 475–486. doi: 10.1038/nrg3028

Demkow, U., and Wolanczyk, T. (2017). Genetic tests in major psychiatric disorders-integrating molecular medicine with clinical psychiatry-why is it so difficult? *Transl. Psychiatry* 7:e1151. doi: 10.1038/tp.2017.106

Dodd, C. E., and Schlesinger, L. S. (2017). New concepts in understanding latent tuberculosis. *Curr. Opin. Infect. Dis.* 30, 316–321. doi: 10.1097/QCO.0000000000000367

Dye, C. (2014). After 2015: infectious diseases in a new era of health and development. *Philos. Trans. R Soc. Lond. B Biol. Sci.* 369:20130426. doi: 10.1098/rstb.2013.0426

Fava, V. M., and Schurr, E. (2017). Evaluating the impact of LTA4H genotype and immune status on survival from tuberculous meningitis. *J. Infect. Dis.* 215, 1011–1013. doi: 10.1093/infdis/jix052

Fol, M., Druszczynska, M., Wlodarczyk, M., Ograczyk, E., and Rudnicka, W. (2015). Immune response gene polymorphisms in tuberculosis. *Acta Biochim. Pol.* 62, 633–640. doi: 10.18388/abp.2015_1130

Gallagher, M. D., and Chen-Plotkin, A. S. (2018). The post-GWAS era: from association to function. *Am. J. Hum. Genet.* 102, 717–730. doi: 10.1016/j.ajhg.2018.04.002

Gallant, C. J., Cobat, A., Simkin, L., Black, G. F., Stanley, K., Hughes, J., et al. (2010). Tuberculin skin test and *in vitro* assays provide complementary measures of antimycobacterial immunity in children and adolescents. *Chest* 137, 1071–1077. doi: 10.1378/chest.09-1852

Gameiro, G. R., Sinkunas, V., Liguori, G. R., and Auler-Junior, J. O. C. (2018). Precision medicine: changing the way we think about healthcare. *Clinics* 73:e723. doi: 10.6061/clinics/2017/e723

Giudicessi, J. R., Kullo, I. J., and Ackerman, M. J. (2017). Precision cardiovascular medicine: state of genetic testing. *Mayo Clin. Proc.* 92, 642–662. doi: 10.1016/j.mayocp.2017.01.015

Gong, W., Liang, Y., and Wu, X. (2018). The current status, challenges, and future developments of new tuberculosis vaccines. *Hum. Vaccin Immunother.* 14, 1697–1716. doi: 10.1080/21645515.2018.1458806

Groschel, M. I., Walker, T. M., Van Der Werf, T. S., Lange, C., Niemann, S., and Merker, M. (2018). Pathogen-based precision medicine for drug-resistant tuberculosis. *PLoS Pathog.* 14:e1007297. doi: 10.1371/journal.ppat.1007297

Grossman, S. R., Andersen, K. G., Shlyakhter, I., Tabrizi, S., Winnicki, S., and Yen, A., et al. (2013). Identifying recent adaptations in large-scale genomic data. *Cell* 152, 703–713. doi: 10.1016/j.cell.2013.01.035

Haider, S. A., and Faisal, M. (2015). Human aging in the post-GWAS era: further insights reveal potential regulatory variants. *Biogerontology* 16, 529–541. doi: 10.1007/s10522-015-9575-y

Holmes, K. K., Bertozzi, S., Bloom, B. R., Jha, P., Gelband, H., Demaria, L. M., et al. (2017). "*Major Infectious Diseases: Key Messages from Disease Control Priorities. 3rd Edn*," in *Major Infectious Diseases*, eds R. D. Holmes, K. K. Bertozzi, S. B. R. Bloom, and P. Jha (Washington, DC: World Bank Group), 1–27. doi: 10.1596/978-1-4648-0524-0_ch1

Jensen, S. O., and Van Hal, S. J. (2017). Personalized medicine and infectious disease management. *Trends Microbiol.* 25, 875–876. doi: 10.1016/j.tim.2017.09.006

Jin, H. S., Cho, J. E., and Park, S. (2019). Association between CD53 genetic polymorphisms and tuberculosis cases. *Genes Genomics* 41, 389–395. doi: 10.1007/s13258-018-0764-3

Joiret, M., Mahachie John, J. M., Gusareva, E. S., and Van Steen, K. (2019). Confounding of linkage disequilibrium patterns in large scale DNA based gene-gene interaction studies. *BioData Min* 12:11. doi: 10.1186/s13040-019-0199-7

Kawahara, J. Y., Irvine, E. B., and Alter, G. (2019). A case for antibodies as mechanistic correlates of immunity in tuberculosis. *Front. Immunol.* 10:996. doi: 10.3389/fimmu.2019.00996

Keener, A. (2019). Tailoring vaccines for older people and the very young. *Nature* 575, S48–S50. doi: 10.1038/d41586-019-03638-6

Khader, S. A., Divangahi, M., Hanekom, W., Hill, P. C., Maeurer, M., Makar, K. W., et al. (2019). Targeting innate immunity for tuberculosis vaccination. *J. Clin. Invest.* 129, 3482–3491. doi: 10.1172/JCI128877

Klein, D. J., Boukouvala, S., Mcdonagh, E. M., Shuldiner, S. R., Laurieri, N., Thorn, C. F., et al. (2016). PharmGKB summary: isoniazid pathway, pharmacokinetics. *Pharmacogenet. Genom.* 26, 436–444. doi: 10.1097/FPC.0000000000000232

Kodaman, N., Sobota, R. S., Mera, R., Schneider, B. G., and Williams, S. M. (2014). Disrupted human-pathogen co-evolution: a model for disease. *Front. Genet.* 5:290. doi: 10.3389/fgene.2014.00290

Koeken, V., Verrall, A. J., Netea, M. G., Hill, P. C., and Van Crevel, R. (2019). Trained innate immunity and resistance to *Mycobacterium tuberculosis* infection. *Clin. Microbiol. Infect.* 25, 1468–1472. doi: 10.1016/j.cmi.2019.02.015

Ladner, J. T., Grubaugh, N. D., Pybus, O. G., and Andersen, K. G. (2019). Precision epidemiology for infectious disease control. *Nat. Med.* 25, 206–211. doi: 10.1038/s41591-019-0345-2

Lee, S. H., Ahn, W. Y., Seweryn, M., and Sadee, W. (2018). Combined genetic influence of the nicotinic receptor gene cluster CHRNA5/A3/B4 on nicotine dependence. *BMC Genom.* 19:826. doi: 10.1186/s12864-018-5219-3

Lin, P. L., and Flynn, J. L. (2018). The end of the binary era: revisiting the spectrum of tuberculosis. *J. Immunol.* 201, 2541–2548. doi: 10.4049/jimmunol.1800993

Liu, M., and Guo, F. (2018). Recent updates on cancer immunotherapy. *Precis Clin. Med.* 1, 65–74. doi: 10.1093/pcmedi/pby011

Luo, Y., Suliman, S., Asgari, S., Amariuta, T., Baglaenko, Y., Martinez-Bonet, M., et al. (2019). Early progression to active tuberculosis is a highly heritable trait driven by 3q23 in Peruvians. *Nat. Commun.* 10:3765. doi: 10.1038/s41467-019-11664-1

Macgillivray, D. M., and Kollmann, T. R. (2014). The role of environmental factors in modulating immune responses in early life. *Front. Immunol.* 5:434. doi: 10.3389/fimmu.2014.00434

Mahomed, S., Padayatchi, N., Singh, J., and Naidoo, K. (2019). Precision medicine in resistant tuberculosis: treat the correct patient, at the correct time, with the correct drug. *J. Infect.* 78, 261–268. doi: 10.1016/j.jinf.2019.03.006

Motta, I., Calcagno, A., and Bonora, S. (2018). Pharmacokinetics and pharmacogenetics of anti-tubercular drugs: a tool for treatment optimization? *Expert. Opin. Drug Metab. Toxicol.* 14, 59–82. doi: 10.1080/17425255.2018.1416093

Newport, M. J. (2015). The genetic regulation of infant immune responses to vaccination. *Front. Immunol.* 6:18. doi: 10.3389/fimmu.2015.00018

Newport, M. J., Goetghebuer, T., Weiss, H. A., Whittle, H., Siegrist, C. A., Marchant, A., et al. (2004). Genetic regulation of immune responses to vaccines in early life. *Genes Immun.* 5, 122–129. doi: 10.1038/sj.gene.6364051

Omae, Y., Toyo-Oka, L., Yanai, H., Nedsuwan, S., Wattanapokayakit, S., Satproedprai, N., et al. (2017). Pathogen lineage-based genome-wide association study identified CD53 as susceptible locus in tuberculosis. *J. Hum. Genet.* 62, 1015–1022. doi: 10.1038/jhg.2017.82

Oppong, Y. E. A., Phelan, J., Perdigao, J., Machado, D., Miranda, A., Portugal, I., et al. (2019). Genome-wide analysis of Mycobacterium tuberculosis polymorphisms reveals lineage-specific associations with drug resistance. *BMC Genom.* 20:252. doi: 10.1186/s12864-019-5615-3

Parida, S. K., Axelsson-Robertson, R., Rao, M. V., Singh, N., Master, I., Lutckii, A., et al. (2015). Totally drug-resistant tuberculosis and adjunct therapies. *J. Intern. Med.* 277, 388–405. doi: 10.1111/joim.12264

Poland, G. A., Kennedy, R. B., Mckinney, B. A., Ovsyannikova, I. G., Lambert, N. D., Jacobson, R. M., et al. (2013). Vaccinomics, adversomics, and the immune response network theory: individualized vaccinology in the 21st century. *Semin. Immunol.* 25, 89–103. doi: 10.1016/j.smim.2013.04.007

Popejoy, A. B., and Fullerton, S. M. (2016). Genomics is failing on diversity. *Nature* 538, 161–164. doi: 10.1038/538161a

Potamias, G., Lakiotaki, K., Katsila, T., Lee, M. T., Topouzis, S., Cooper, D. N., et al. (2014). Deciphering next-generation pharmacogenomics: an information technology perspective. *Open Biol.* 4:e140071. doi: 10.1098/rsob.140071

Quintana-Murci, L. (2016). Understanding rare and common diseases in the context of human evolution. *Genome Biol.* 17:225. doi: 10.1186/s13059-016-1093-y

Racimo, F., Sankararaman, S., Nielsen, R., and Huerta-Sanchez, E. (2015). Evidence for archaic adaptive introgression in humans. *Nat. Rev. Genet.* 16, 359–371. doi: 10.1038/nrg3936

Ramachandran, G., and Swaminathan, S. (2012). Role of pharmacogenomics in the treatment of tuberculosis: a review. *Pharmgenom. Pers Med.* 5, 89–98. doi: 10.2147/PGPM.S15454

Rosenthal, S. L., Barmada, M. M., Wang, X., Demirci, F. Y., and Kamboh, M. I. (2014). Connecting the dots: potential of data integration to identify regulatory SNPs in late-onset Alzheimer's disease GWAS findings. *PLoS ONE* 9:e95152. doi: 10.1371/journal.pone.0095152

Sadee, W., Hartmann, K., Seweryn, M., Pietrzak, M., Handelman, S. K., and Rempala, G. A. (2014). Missing heritability of common diseases and treatments outside the protein-coding exome. *Hum. Genet.* 133, 1199–1215. doi: 10.1007/s00439-014-1476-7

Sanz, J., Randolph, H. E., and Barreiro, L. B. (2018). Genetic and evolutionary determinants of human population variation in immune responses. *Curr. Opin. Genet. Dev.* 53, 28–35. doi: 10.1016/j.gde.2018.06.009

Scepanovic, P., Alanio, C., Hammer, C., Hodel, F., Bergstedt, J., Patin, E., et al. (2018). Human genetic variants and age are the strongest predictors of humoral immune responses to common pathogens and vaccines. *Genome Med.* 10:59. doi: 10.1186/s13073-018-0568-8

Sharma, S. K., Vashishtha, R., Chauhan, L. S., Sreenivas, V., and Seth, D. (2017). Comparison of TST and IGRA in diagnosis of latent tuberculosis infection in a high TB-burden setting. *PLoS ONE* 12:e0169539. doi: 10.1371/journal.pone.0169539

Simmons, J. D., Stein, C. M., Seshadri, C., Campo, M., Alter, G., Fortune, S., et al. (2018). Immunological mechanisms of human resistance to persistent *Mycobacterium tuberculosis* infection. *Nat. Rev. Immunol.* 18, 575–589. doi: 10.1038/s41577-018-0025-3

So, D., and Joly, Y. (2013). Commercial opportunities and ethical pitfalls in personalized medicine: a myriad of reasons to revisit the myriad genetics saga. *Curr. Pharmacogenom. Person Med.* 11, 98–109. doi: 10.2174/1875692111311020003

Tameris, M. D., Hatherill, M., Landry, B. S., Scriba, T. J., Snowden, M. A., Lockhart, S., et al. (2013). Safety and efficacy of MVA85A, a new tuberculosis vaccine, in infants previously vaccinated with BCG: a randomised, placebo-controlled phase 2b trial. *Lancet* 381, 1021–1028. doi: 10.1016/S0140-6736(13)60177-4

Tanner, R., Villarreal-Ramos, B., Vordermeier, H. M., and Mcshane, H. (2019). The humoral immune response to BCG vaccination. *Front. Immunol.* 10:1317. doi: 10.3389/fimmu.2019.01317

Tao, L., Zalwango, S., Chervenak, K., Thiel, B., Malone, L. L., Qiu, F., et al. (2013). Genetic and shared environmental influences on interferon-gamma production in response to Mycobacterium tuberculosis antigens in a Ugandan population. *Am. J. Trop. Med. Hyg.* 89, 169–173. doi: 10.4269/ajtmh.12-0670

Thanassoulis, G., and Vasan, R. S. (2010). Genetic cardiovascular risk prediction: will we get there? *Circulation* 122, 2323–2334. doi: 10.1161/CIRCULATIONAHA.109.909309

Tian, Q., Price, N. D., and Hood, L. (2012). Systems cancer medicine: towards realization of predictive, preventive, personalized and participatory (P4) medicine. *J. Intern. Med.* 271, 111–121. doi: 10.1111/j.1365-2796.2011.02498.x

Tishkoff, S. A., and Verrelli, B. C. (2003). Patterns of human genetic diversity: implications for human evolutionary history and disease. *Annu. Rev. Genom. Hum. Genet.* 4, 293–340. doi: 10.1146/annurev.genom.4.070802.110226

Twilt, M. (2016). Precision medicine: the new era in medicine. *EBioMedicine* 4, 24–25. doi: 10.1016/j.ebiom.2016.02.009

Uren, C., Henn, B. M., Franke, A., Wittig, M., Van Helden, P. D., Hoal, E. G., et al. (2017). A post-GWAS analysis of predicted regulatory variants and tuberculosis susceptibility. *PLoS ONE* 12:e0174738. doi: 10.1371/journal.pone.0174738

Verma, M. (2012). Personalized medicine and cancer. *J. Pers Med.* 2, 1–14. doi: 10.3390/jpm2010001

Waldner, H. (2009). The role of innate immune responses in autoimmune disease development. *Autoimmun. Rev.* 8, 400–404. doi: 10.1016/j.autrev.2008.12.019

Wang, Y., Xiang, X., Wu, S. Q., Chen, G., Zhang, M. M., Wang, M. G., et al. (2017). Association of CYP2B6 gene polymorphisms and anti-tuberculosis drug-induced hepatotoxicity in a Chinese population. *Infect. Genet. Evol.* 51, 198–202. doi: 10.1016/j.meegid.2017.04.001

WHO. (2019). *Global Tuberculosis Report 2019*. Geneva.

Wray, N. R., Yang, J., Hayes, B. J., Price, A. L., Goddard, M. E., and Visscher, P. M. (2013). Pitfalls of predicting complex traits from SNPs. *Nat. Rev. Genet.* 14, 507–515. doi: 10.1038/nrg3457

Zumla, A., Rao, M., Wallis, R. S., Kaufmann, S. H., Rustomjee, R., Mwaba, P., et al. (2016). Host-directed therapies for infectious diseases: current status, recent progress, and future prospects. *Lancet Infect. Dis.* 16, e47–e63. doi: 10.1016/S1473-3099(16)00078-5

Conflict of Interest: The authors declare that the research was conducted in the absence of any commercial or financial relationships that could be construed as a potential conflict of interest.

frontiers in Cellular and Infection Microbiology

ORIGINAL RESEARCH
published: 16 April 2020
doi: 10.3389/fcimb.2020.00150

Small Animal Model of Post-chemotherapy Tuberculosis Relapse in the Setting of HIV Co-infection

*Matthew B. Huante[1], Tais B. Saito[2], Rebecca J. Nusbaum[3], Kubra F. Naqvi[2], Sadhana Chauhan[1], Robert L. Hunter[4], Jeffrey K. Actor[4], Jai S. Rudra[5], Mark A. Endsley[1], Joshua G. Lisinicchia[2], Benjamin B. Gelman[2] and Janice J. Endsley[1]**

[1] Department of Microbiology and Immunology, University of Texas Medical Branch, Galveston, TX, United States, [2] Department of Pathology, University of Texas Medical Branch, Galveston, TX, United States, [3] Department of Microbiology, University of Pennsylvania, Philadelphia, PA, United States, [4] Department of Pathology and Laboratory Medicine, University of Texas Health Sciences Center, Houston, TX, United States, [5] Department of Biomedical Engineering, Washington University in St. Louis, St. Louis, MO, United States

OPEN ACCESS

Edited by:
Igor Kramnik, Boston University, United States

Reviewed by:
Selvakumar Subbian, Public Health Research Institute (PHRI), United States
Eric Nuermberger, Johns Hopkins University, United States

***Correspondence:**
Janice J. Endsley
jjendsle@utmb.edu

Specialty section:
This article was submitted to Clinical Microbiology, a section of the journal Frontiers in Cellular and Infection Microbiology

Received: *05 October 2019*
Accepted: *23 March 2020*
Published: *16 April 2020*

Citation:
Huante MB, Saito TB, Nusbaum RJ, Naqvi KF, Chauhan S, Hunter RL, Actor JK, Rudra JS, Endsley MA, Lisinicchia JG, Gelman BB and Endsley JJ (2020) Small Animal Model of Post-chemotherapy Tuberculosis Relapse in the Setting of HIV Co-infection. Front. Cell. Infect. Microbiol. 10:150. doi: 10.3389/fcimb.2020.00150

Tuberculosis relapse following drug treatment of active disease is an important global public health problem due to the poorer clinical outcomes and increased risk of drug resistance development. Concurrent infection with HIV, including in those receiving anti-retroviral therapy (ART), is an important risk factor for relapse and expansion of drug resistant *Mycobacterium tuberculosis* (*Mtb*) isolates. A greater understanding of the HIV-associated factors driving TB relapse is important for development of interventions that support immune containment and complement drug therapy. We employed the humanized mouse to develop a new model of post-chemotherapy TB relapse in the setting of HIV infection. Paucibacillary TB infection was observed following treatment with Rifampin and Isoniazid and subsequent infection with HIV-1 was associated with increased *Mtb* burden in the post-drug phase. Organized granulomas were observed during development of acute TB and appeared to resolve following TB drug therapy. At relapse, granulomatous pathology in the lung was infrequent and mycobacteria were most often observed in the interstitium and at sites of diffuse inflammation. Compared to animals with HIV mono-infection, higher viral replication was observed in the lung and liver, but not in the periphery, of animals with post-drug TB relapse. The results demonstrate a potential role for the humanized mouse as an experimental model of TB relapse in the setting of HIV. Long term, the model could facilitate discovery of disease mechanisms and development of clinical interventions.

Keywords: TB, HIV, TB and HIV co-infection, TB relapse, pathology, TB chemotherapy, immune response, tuberculosis

INTRODUCTION

Tuberculosis (TB) caused by *Mycobacterium tuberculosis* (*Mtb*) infection is the leading cause of infectious disease-related mortality, with the World Health Organization estimating 10 million cases of TB and 1.45 million deaths in 2018 (WHO, 2019). Completion of combination drug therapy leads to clinical cure in most subjects, however, a spectrum of incomplete cures that

range from latent infection to active TB occur frequently (Dooley et al., 2011; Rockwood et al., 2016; McIvor et al., 2017) and play an important role in the global TB burden (Chao and Rubin, 2010; Mirsaeidi and Sadikot, 2018). In those with bacteriological evidence of cure following drug therapy, recurrent TB can occur due to endogenous reactivation (relapse) or re-infection. DNA fingerprint analysis of case samples demonstrates that at least half of recurrent TB in endemic sites occurs due to relapse of a persisting *Mtb* strain and not a new infection (Marx et al., 2014). Recurrent TB that develops within the first year following the completion of antibiotic treatment is most often a relapse event (Sonnenberg et al., 2001; Shen et al., 2006; Crampin et al., 2010; Narayanan et al., 2010; Unis et al., 2014) and is associated with greatly increased risk for resistance to front line TB drugs (Yoshiyama et al., 2004; Munje et al., 2015). The emergence of multi (MDR)- and extensively (XDR)-drug resistant isolates in a growing number of geographical regions is an important factor contributing to the global health crisis of TB (WHO, 2019).

Risk factors associated with TB recurrence include cavitary disease, sputum positivity after the intensive phase of treatment (Lee and Kim, 2014), HIV infection, malnutrition, or treatment with immunosuppressive therapies (see reviews; Braun et al., 1989; Cisneros and Murray, 1996; Douglas et al., 1996; Rajagopalan and Yoshikawa, 2000; Bresnihan and Cunnane, 2003; Gideon and Flynn, 2011; Ernst, 2012; Esmail and Barry, 2012). Among these risk factors, HIV infection is one of the most significant due to the epidemiological overlap of the afflicted populations, loss or dysfunction of immunity, and several other poorly understood mechanisms for synergistic pathogenesis (Pulido et al., 1997; Pawlowski et al., 2012; Unis et al., 2014). People living with HIV (PLWH) are more likely to experience: TB chemotherapy failure, TB relapse following treatment, and reactivation of latent TB (Khan et al., 2010; Unis et al., 2014; Trinh et al., 2015).

Clinical management of TB and HIV co-infection is challenging and can impact TB treatment outcomes (Mirsaeidi and Sadikot, 2018; Tornheim and Dooley, 2018). There are several clinically relevant scenarios whereby co-infection with HIV could increase risk for TB relapse including: non-diagnosed HIV infection, new HIV infection during or following the standard 6 month TB treatment phase, or poor ART access or compliance during or following TB chemotherapy. In endemic regions, the potential for HIV-associated factors to impact treatment is even greater for those undergoing drug therapy for multi-drug resistant TB due the 18–24 month treatment period (Falzon et al., 2017). The strong association between TB and HIV includes biological mechanisms of pathogen synergy as well as many non-biological factors (e.g., socioeconomic) and clinical issues as recently reviewed (Huante et al., 2019). A greater understanding of the complex interplay between *Mtb* and HIV in the setting of *in vivo* drug treatment is needed to inform development of new approaches to reduce TB relapse.

An animal model of post-drug TB relapse in the setting of HIV, or SIV, has not been described to date. As a result, our current understanding is based on extrapolations from clinical outcomes in *Mtb*/HIV co-infected human subjects and models of latent TB infection (LTBI) reactivation due to SIV infection in non-human primates (NHP) (Diedrich et al., 2010; Mehra et al., 2011). The loss of $CD4^+$T cells is a well-established deficiency in PLWH whose HIV infection has progressed to the acquired immune deficiency syndrome (AIDS) stage. Reduced production of effector molecules (e.g., IFN-γ, TNF-α) due to the effects of HIV on both loss and cellular function of $CD4^+$T cells has been linked to poor immune containment of *Mtb* infection (see reviews Diedrich and Flynn, 2011; Pawlowski et al., 2012). Increasingly, though, the risk for TB relapse has been shown to occur along a spectrum of $CD4^+$T cell loss, including in those subjects virally suppressed following ART (Sonnenberg et al., 2005; Walker et al., 2013). As observed in human subjects, reactivation of LTBI due to SIV in NHP has been shown to be associated with both $CD4^+$T cell loss-dependent and independent mechanisms (Diedrich et al., 2010; Foreman et al., 2016). Development of a small animal model amenable to infection with human HIV isolates would facilitate mechanistic studies to understand the immunological and microbiological alterations that promote post-drug TB relapse and provide a system to test clinical interventions.

Our results demonstrate the potential to use the human immune system (HIS) mouse model of TB (Calderon et al., 2013; Nusbaum et al., 2016) to investigate TB relapse *in vivo* in animals co-infected with HIV-1. Consistent with observations of greater TB relapse in PLWH, infection of HIS mice with HIV increased *Mtb* burden following drug treatment with RIF and INH. The increased HIV viral load observed in animals with TB relapse also further suggests that *Mtb* infection may provide a favorable niche for viral replication in tissue compartments. These results support further exploration of the HIS mouse models for discovery of disease mechanisms for TB relapse due to HIV co-infection and as a platform for development and testing of therapeutic interventions. The current model investigated the effects of HIV infection when introduced at the end of TB drug therapy. Further adaptation could facilitate mechanistic investigations of several important clinical scenarios including the effects of chronic HIV, or HIV infection suppressed by ART, on TB treatment outcomes.

MATERIALS AND METHODS

Ethics Statement

The experimental procedures using mice were approved by the University of Texas Medical Branch Institutional Animal Care and Use Committee under protocols 1604017 and 1501001. Mice were housed in HEPA filtered cages in a climate controlled facility designed to maintain optimal temperature, humidity, and light cycle. Food and water were provided *ad libitum*, in addition to nesting material. Animals were monitored daily by trained animal resource center staff with oversight by staff veterinarians. Upon showing signs of severe disease beyond the point of recovery the mice were humanely euthanized. De-identified human tissue specimens used in the development of humanized mice were obtained from Advanced Bioscience Resources, Alameda, CA as previously described (Calderon et al., 2013). Tissues were confirmed to be free of specific infectious agents including HIV, Hepatitis B, and Hepatitis C virus.

Generation of Humanized Mice

All infection experiments were performed using HIS bone marrow, liver, and thymus (or BLT) mice that were generated using the NOD-SCID/γ_c^{null} (NSG) mouse as previously described (Calderon et al., 2013; Nusbaum et al., 2016). Reconstitution of a human immune system was validated using flow cytometric detection of human leukocytes including T cell (CD4 and CD8) and myeloid cell (monocytes, macrophages, and dendritic cell) populations as we described (Calderon et al., 2013). Animals that displayed evidence of graft vs. host disease (GVHD) such as allopecia that can occur in extended studies with HIS mouse models, as described (Greenblatt et al., 2012; Karpel et al., 2015), were excluded from analysis. Losses/exclusions due to GVHD were 30–40% of animals in the two studies due to the length of the studies. Mice from two HIS mouse groups were used to establish paucibacillary TB and assess the potential to study relapse following HIV infection. Excluding animals that developed GVHD, data from 12 animals is shown in study 1 including non-infected control ($n = 2$), post-infection and post-rifampicin confirmation of infection and bacterial reduction ($n = 4$, with 2 animals per timepoint), TB relapse ($n = 3$) and TB/HIV relapse ($n = 3$) groups. In study 2, excluding GVHD animals, data analysis is from 18 animals including non-infected control ($n = 3$), post-infection and post-rifampicin confirmation of infection and bacterial reduction ($n = 4$, with 1 animal per timepoint), TB relapse ($n = 4$), TB/HIV relapse ($n = 4$), and HIV infection ($n = 3$) groups.

Infections With *Mtb*

Mycobacterial infections were performed after assignment of HIS mice to treatment groups including mock (PBS) or *Mtb* infection using the H37Rv strain via an intranasal (i.n.) route of infection as described (Calderon et al., 2013). A growth stock of *Mtb* H37Rv was propagated in Middlebrook 7H9 and suspended in PBS for use as inoculum to deliver *Mtb* to the lung compartment by intranasal distillation of 40 μl (20 μl/nare). Bacterial enumeration was performed using limiting dilutions of the innoculum plated on 7H11 agar plates to estimate the *Mtb* infection dose that was administered as described (Endsley et al., 2006). The estimated i.n. dose, based on CFU of plated inoculum was 10^2 CFU/mouse in study 1, and 10^3 CFU/mouse in study 2. Tissues from non-infected control mice generated from the same HIS production groups were used to establish normal tissue histology and immune analyte baselines. The HIS mice infected with only HIV-1 in study 2 received mock *Mtb* infection (PBS).

Drug Treatment to Generate Paucibacillary Infection

A Cornell-like model of paucibacillary TB that was previously described in the C57BL/6J mouse (Radaeva et al., 2005) was reproduced in HIS mice. Following development of clinical signs of active TB at 8 and 4 weeks post-infection in study 1 and 2, respectively, TB chemotherapy was initiated for 8 weeks. Treatment consisted of daily oral gavage for seven days a week with 750 ug of both rifampin (RIF) and isoniazid (INH) purchased from Sigma-Aldrich and dissolved in 100 μl of sterile water. Stock solutions of RIF were dissolved in a low volume DMSO and final concentration of DMSO in the delivered dose was <0.01%. Chemotherapy was provided to all treatment groups (including non-infected and HIV-infected groups) to control for drug and carrier effects and potential carryover of weak antiviral activity that is described for RIF (Clark, 1971; Moshkowitz et al., 1971). Upon development of clinical signs (e.g., weight loss) following 4–8 weeks of *Mtb* infection and upon completion of 8 weeks of TB chemotherapy, the bacterial burden was determined in randomly selected animals using CFU enumeration of disrupted tissue. Tissue specimens were also preserved for histopathology and histochemistry analysis.

Infections With HIV

At the completion of TB chemotherapy, HIS mice were infected with 2,500 $TCID_{50}$ of HIV-1 (JR-CSF strain, UCLA Center for AIDS Research) or mock infected (PBS) as we previously described (Nusbaum et al., 2016). Virus stock was diluted in PBS and infections performed by i.v. delivery of 100 μl via the tail vein. Blood was collected prior to infection and at necropsy and plasma was frozen for subsequent assessment of viral infection.

Determination of Viral and Bacterial Burden

Animals were humanely euthanized at the designated timepoints or the observations of clinical signs of disease (e.g., weight loss, lethargy). Randomly selected animals were euthanized prior to initiation of TB drug therapy to confirm development of active *Mtb* infection and following 8 week of drug therapy to demonstrate drug efficacy. The left lung lobe and the median liver lobe was preserved in formalin and embedded in paraffin for use in hisopathological analysis and detection of acid fast bacilli (AFB) using the Ziehl-Neelson method. The right lung superior, inferior, and post-caval lung lobes and the left liver lobe were disrupted using a tissue grinder (Kendall, Inc) to determine mycobacterial burden by CFU enumeration following limiting dilution and growth on 7H11 agar plates as described (Endsley et al., 2006). At necropsy, blood and tissues (lung and liver) were collected from the mice. Tissue were disrupted in 1 ml of sterile PBS using a tissue grinder (Kendell, Inc) and aliquots of the tissue homogenate were used for limiting dilution analysis of CFU as described (Endsley et al., 2006). The limit of detection of *Mtb* CFU using this enumeration method is 30 bacilli. Supernatants collected from tissue homogenates in study 2 were used for assessment of viral load and cytokine and chemokine profiles. Viral load was determined by measurement of HIV p24 capsid protein levels in the plasma, lung, and liver, using an ELISA (Zeptometrix Corporation).

Histopathology and RNA Scope Analysis

Formalin-fixed and paraffin embedded tissue sections were cut, dewaxed, and stained using hematoxylin and eosin (H&E) for histopathology analysis (UTMB Research Histopathology Core Facility) and the Ziehl-Neelson method to detect AFB. Additional tissue sections were used for analysis of viral RNA in the lung using RNA scope (ACD Bio) using *in situ* hybridization with probes specific to the HIV-1 *gag* gene in accordance with manufacturer's instructions.

Cytokine and Chemokine Quantification

Supernatants harvested from disrupted lung were stored at −80°C and inactivated by exposure to 5 MRAD γ-irradiation on dry ice using a JL Shepherd Model 109–68 Cobalt-60 Research Irradiator (JL Shepherd & Associates, San Fernando, CA). Sterility was confirmed by lack of CFU following 3 weeks of growth on 7H11 agar. Analysis of lung cytokines and chemokines affected by treatment was performed with a human multiplex ELISA (Bio-rad Bio-plex Pro™ human cytokine 27-plex kit) according to the manufacturer's instructions as previously described (Nusbaum et al., 2016). Results from molecules with cross-reactivity between human detection reagents and mouse cytokines (e.g., VEGF, IL-13) were excluded from the analysis to reduce confounding outcomes. Values that were out of range high were not observed in any of the samples tested. The out of range low values were set to zero and data from tissue analytes where many values were out of range low are not presented. Analytes were quantified by generating a standard curve using validated standards and values were determined by linear regression to the standard curve as described (Nusbaum et al., 2016).

Statistics

Microbiological and immunological data from animal studies are shown as mean ± SEM. One-way ANOVA followed by a Bonferroni's multiple comparison test was used for multiple group comparisons (GraphPad Software v7.0).

RESULTS

Paucibacillary TB and Granuloma Resolution Following TB Chemotherapy

We previously developed a HIS mouse model of TB (Calderon et al., 2013) and acute TB/HIV co-infection (Nusbaum et al., 2016) in the BLT mouse. Here we further adapted this *in vivo* system to model TB relapse in a Cornell-like model of disease (Radaeva et al., 2005) in order to permit exploration of the effects of HIV co-infection on relapse. The experimental approach for outcomes following low dose infection (study 1) is diagrammed in **Figure 1A**. The data shown in **Figures 1**, **2**, and **Supplemental Figure 1** were from experiments conducted with this design.

Representative images of the pathology observed among the mice following low dose *Mtb* infection and treatment with TB chemotherapy is shown in **Figure 1**. Following 8 weeks of *Mtb* infection, the lungs of HIS mice were characterized by large areas of granulomatous inflammation including some areas of necrosis and caseous necrosis (**Figure 1B**). Within the granulomatous lesions, bacilli were abundant as detected with Ziehl-Neelson staining for AFB (**Figure 1C**). As shown in **Figure 1D**, normal lung architecture is observed in non-infected HIS mice. Assessment of mouse lung tissue by CFU enumeration (**Figure 1E**) confirmed the presence of an established infection at 8 weeks post-*Mtb* infection. The bacterial load in the mice was below the limit of detection, however, following 8 weeks of daily oral TB chemotherapy with 750 μg daily RIF and INH (**Figure 1E**).

An interesting observation made in the lungs of HIS mice 8 weeks after TB chemotherapy was the lack of residual granulomatous lesions. Areas of persisting interstitial inflammation as shown in **Figure 1F**, however, were frequently observed, and were generally devoid of detectable AFB as shown in **Figure 1G**. Very rare bacilli were observed in brightfield microscopy analysis of lung following TB chemotherapy, as illustrated with one AFB detected in a foamy alveolar macrophage in **Figure 1H**. Taken together, these results indicate that a paucibacillary state of *Mtb* infection in HIS mice occurs coincident with apparent resolution of granulomatous lung pathology following drug treatment.

Pulmonary TB Relapse in HIS Mice Co-infected With HIV-1

Following 8 weeks of TB drug therapy, HIS mice were subsequently assigned to TB and TB/HIV treatment groups as diagrammed in **Figure 1A**. The animals in the TB/HIV group were infected i.v. with 2,500 $TCID_{50}$ of a human clinical HIV-1 isolate (JR-CSF) as diagrammed in **Figure 1**. At 8 weeks following cessation of TB drug therapy and infection with HIV, the development of relapse was assessed. As shown in **Figure 2A**, CFU enumeration revealed a significant increase in pulmonary mycobacterial burden of mice with HIV, as compared to mock, co-infection. In lungs of HIV naïve mice, bacilli were below the limit of detection for growth on solid media.

Analysis of the lung histology demonstrated that the interstitial inflammation observed at the completion of drug treatment (**Figure 1F**) may have partially resolved by 8 weeks after drug treatment cessation (**Figure 2B**). Surprisingly, a fairly similar histological appearance was observed in the lung of mice from both the TB and TB/HIV treatment groups as shown with representative images in **Figures 2B–H**. This included areas of normal alveolar architecture and areas with small foci of inflammation in the alveolar walls as shown in **Figure 2B**. Foamy alveolar macrophages (**Figure 2C**) that were lacking AFB (**Figure 2D**) were also observed. Areas with interstitial or paraseptal inflammatory cells (**Figure 2E**) were also frequently seen. Rare AFB were observed at these sites of mild inflammatory cell accumulation in the lung of mice from both the TB and TB/HIV groups as shown in **Figure 2F**. Some areas of moderate inflammation associated with small pockets of AFB were occasionally observed as shown in **Figures 2G,H**.

Hepatic TB in HIS Mice Following Drug Treatment and HIV Infection

To determine whether HIV infection may promote TB growth or regrowth at a common site of *Mtb* dissemination and viral replication in the HIS mouse, an analysis of hepatic tissue was performed. HIV infects liver tissue (Housset et al., 1990) and extra-pulmonary TB presentation is more commonly observed in PLWH as compared to those with negative HIV status (Leeds et al., 2012). Following low dose *Mtb* infection in study 1, dissemination of *Mtb* to the liver was observed (**Supplemental Figure 1A**) at

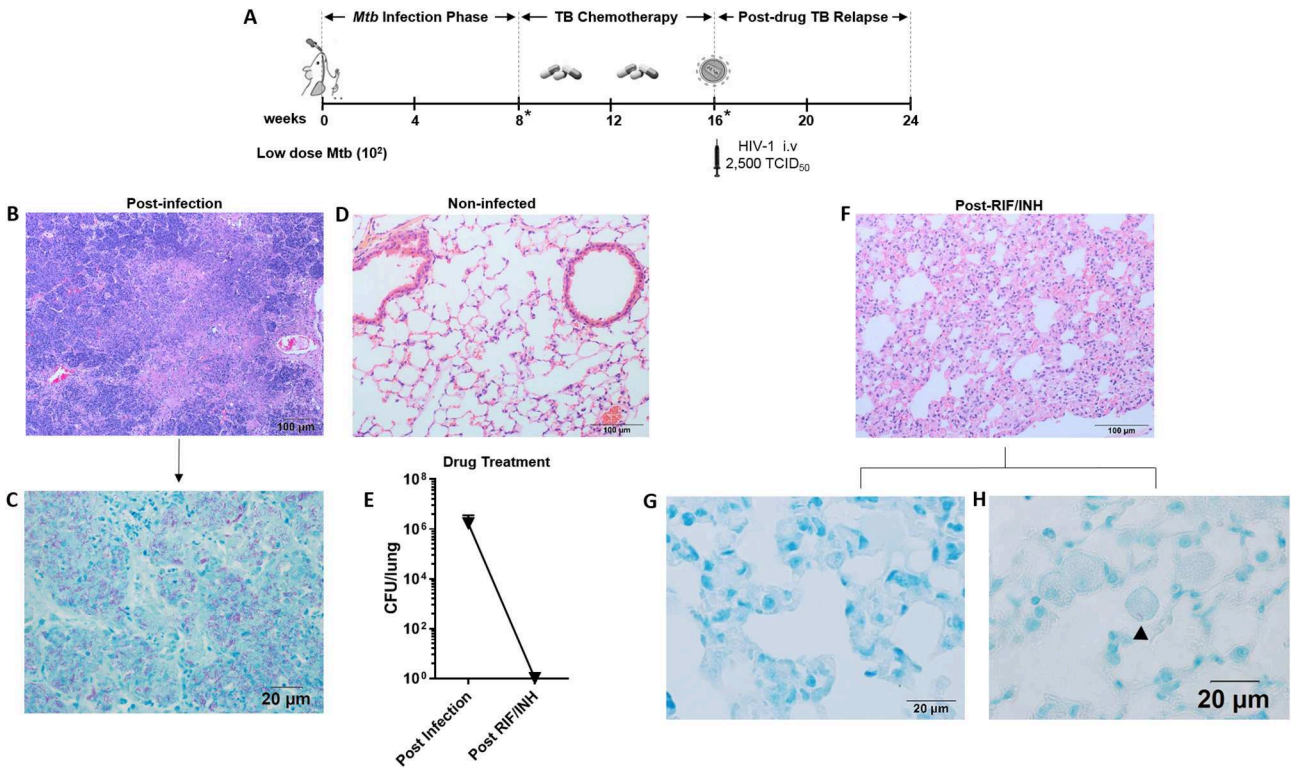

FIGURE 1 | Paucibacillary TB and granuloma resolution following TB chemotherapy. **(A)** Experimental design for study 1. HIS BLT mice were generated and infected i.n. with 10^2 CFU of *Mtb* H37Rv for 8 weeks followed by treatment with RIF and INH by oral gavage (750 µg/day) for 8 weeks. Drug treatment was terminated and HIS mice were assigned to i.v. infection with 2,500 $TCID_{50}$ of HIV-1 (JR-CSF) or mock (PBS) using 3 mice per group. Relapse of TB was assessed at 8 weeks post-HIV infection. Infection with *Mtb* and drug efficacy was confirmed by CFU enumeration in tissues of 2 animals per designated (*) time point with a limit of detection of 30 organisms. Representative images from histological findings as visualized with H&E and Ziehl-Neelson staining and brightfield microscopy. **(B)** Granulomatous pathology characteristic of active TB in HIS mouse lung and **(C)** corresponding AFB present in the inflamed tissue. **(D)** Healthy lung from a non-infected mouse. **(E)** Mycobacterial burden in the lung, as determined by CFU enumeration following 8 weeks of infection and 8 weeks of drug treatment with RIF and INH. **(F)** Residual interstitial inflammation observed in lung following drug treatment, including **(G)** AFB negative inflammatory cells frequently observed in interstitium, and **(H)** Rare AFB observed in alveolar macrophage.

8 weeks post-infection. Consistent with this outcome, small AFB positive lesions were a frequent observation in microscopy analysis of liver specimens as shown in **Supplemental Figures 1B,C**.

Similar to the lung, chemotherapy with RIF and INH reduced culturable bacilli in the liver to below the limit of detection by 8 weeks (**Supplemental Figure 1A**). The liver was mostly non-remarkable following drug treatment (**Supplemental Figure 1D**) and AFB were not observed in liver parenchyma (**Supplemental Figure 1E**). In contrast to the lung, culturable bacilli were detected in the liver of animals from both the TB and TB/HIV groups at 8 weeks post-drug cessation (**Supplemental Figure 1F**) although no significant treatment differences were observed. The liver tissue from both treatment groups was generally unremarkable at this endpoint (**Supplemental Figure 1G**) and only rare AFB were detected (**Supplemental Figure 1H**). These data suggest the HIS mouse can effectively model the effects of HIV infection in the liver on TB relapse at sites of dissemination.

Pulmonary TB Relapse Following High Dose *Mtb* Infection

A subsequent experiment (study 2) was conducted as detailed in **Figure 3A** in which sufficient HIS mice were generated from the same tissue source to permit inclusion of an HIV mono-infection group. This study differs from study 1 in that animals were infected with a higher estimated dose (10^3 CFU) of *Mtb*. The shorter treatment phases shown in **Figure 3A** are due to the associated acceleration of TB disease progression that required earlier drug intervention following *Mtb* infection, and earlier endpoint collection in the relapse phase, respectively. As shown in **Figure 3B**, treatment with RIF and INH progressively reduced the pulmonary bacterial load to below the limit of detection by 8 weeks. In contrast to study 1, relapse TB in study 2 was indicated by detection of culturable bacilli in both the TB and TB/HIV groups (**Figure 3C**). A trend toward increased pulmonary burden ($p = 0.09$) was observed in lung of mice from the TB/HIV group, although this effect did not reach significance.

Active TB, as characterized by significant areas of granulomatous inflammation and abundant AFB in lung

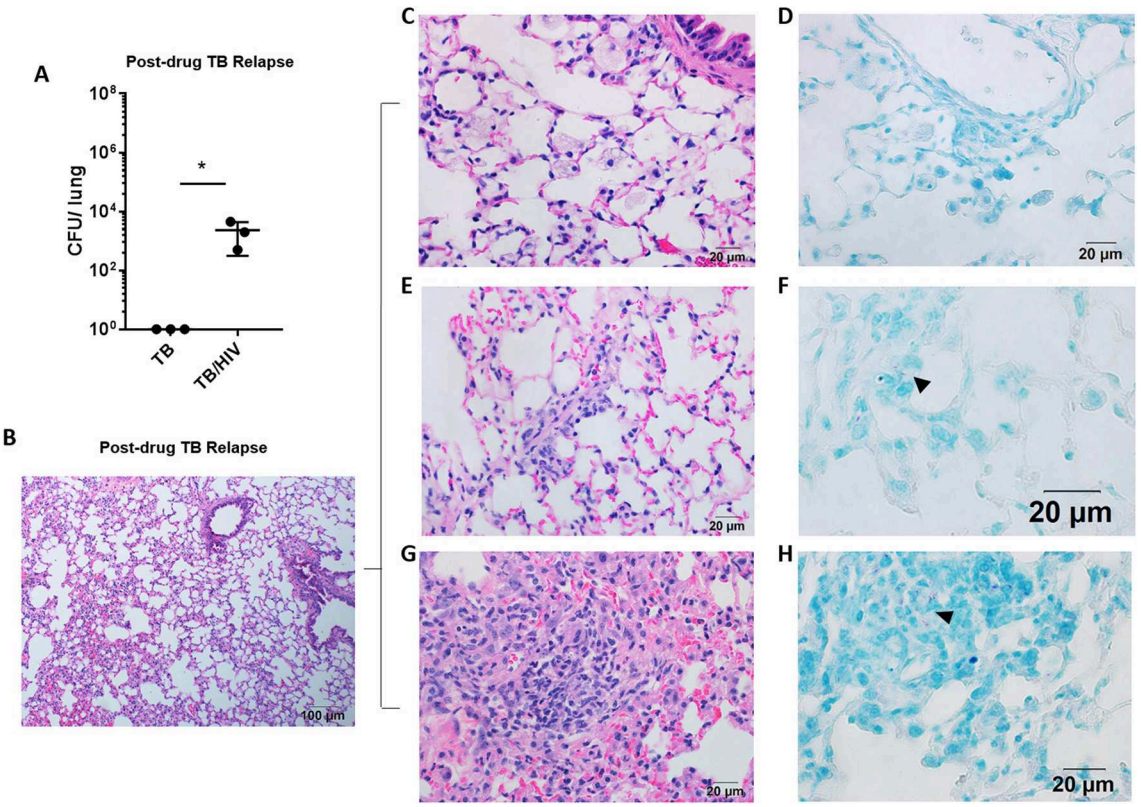

FIGURE 2 | Pulmonary TB relapse in HIS mice co-infected with HIV-1. Pulmonary TB relapse outcomes in the setting of HIV infection in study 1. Following establishment of paucibacillary *Mtb* infection with chemotherapy, HIS mice were co-infected i.v. with mock (PBS) or HIV-1 (2,500 $TCID_{50}$ JR-CSF). Experiments were terminated at 8 weeks post HIV or mock infection to assess TB relapse. **(A)** Lung bacterial burden during the relapse phase in TB and TB/HIV infection groups. Histological appearance of lung as shown with representative images from animals in both TB and TB/HIV groups. **(B)** Non-remarkable lung with occasional pockets of inflammation and frequent areas of interstitial inflammation that include features illustrated in C-H. **(C)** Foamy alveolar macrophages that are **(D)** lacking AFB. **(E)** Paraseptal and interstitial inflammation with **(F)** occasional AFB positive (arrowhead) inflammatory cells in interstitium. **(G)** Larger areas of inflammation containing **(H)** pockets of AFB (arrowhead). Data shown in **(A)** is the mean ± SEM and statistically significant differences between treatment groups are shown as $^*p < 0.05$.

tissue was observed 4 weeks post-infection (**Figures 3D,E**) and was similar to observations in study 1 (**Figures 1B,C**) at 8 weeks post-infection. At 4 weeks into the 8 week drug treatment, diffuse inflammation was the most common finding as shown in **Supplemental Figure 2A** while small clusters of AFB were visible throughout the inflamed areas (**Supplemental Figure 2B**). By 8 weeks of RIF and INH treatment (**Figure 3F**), a pattern of interstitial inflammation similar to study 1 (**Figure 1F**) was observed. Rare AFB were seen in cells within these pockets of inflammation (**Figure 3G**), consistent with the observations in study 1 (**Figure 2H**).

At relapse, the histological appearance of the lung tissue in mice from the TB and TB/HIV groups was similar. Areas characterized as non-remarkable or as having mild inflammatory infiltrate were observed similar to study 1. In contrast to study 1, larger areas of interstitial and perivascular inflammation (**Figure 3H**) and infrequent areas of granulomatous inflammation (**Figure 3J**), were also noted. Small pockets of AFB were observed in areas of diffuse inflammation (**Figure 3I**) while more abundant AFB were seen in granulomas (**Figure 3K**).

Hepatic Dissemination and Relapse Following High Dose *Mtb* Infection

Treatment with RIF and INH progressively reduced the mycobacterial burden in the liver to below the limit of detection by 8 weeks (**Figure 4A**). Organized inflammatory lesions were frequently observed in the liver parenchyma (**Figure 4B**) and contained AFB positive cells (**Figure 4C**). Following drug treatment, lesions containing inflammatory cells and multinucleated giant cells (MGC) were a common finding (**Figure 4D**). MGC are a characteristic feature of TB pathology that is not observed in several small animal models. Similar to study 1, AFB were not detected in these liver lesions (**Figure 4E**) or other areas of the liver at 8 weeks post-drug treatment.

Relapse was observed in liver of mice from both the TB and TB/HIV groups and a significant increase in CFU was observed due to HIV infection (**Figure 4F**). A caveat to note is that liver CFU data from one animal in the TB/HIV group was lost due to fungal contamination of the agar plate. The lung CFU result from this mouse was intermediate among the four animals in the TB/HIV group. In contrast to study 1 (**Supplemental Figure 1**), residual inflammation including the

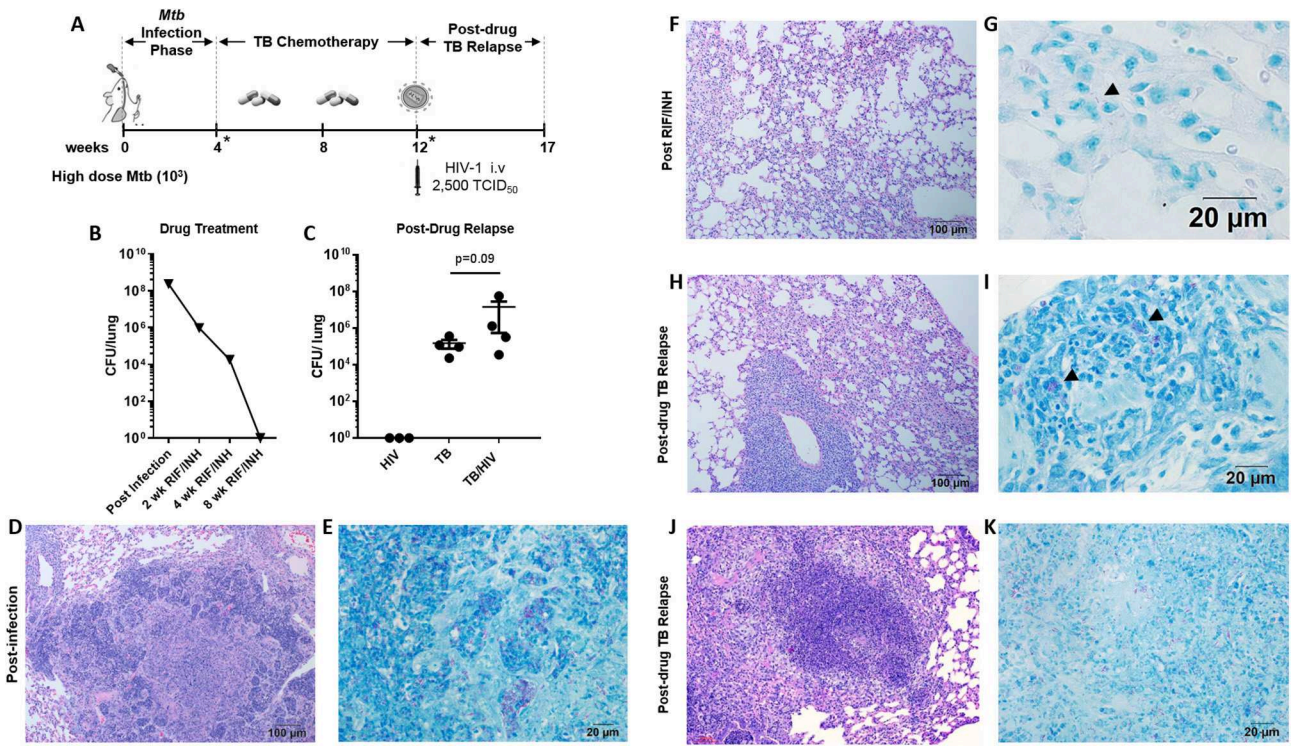

FIGURE 3 | Pulmonary TB relapse following high dose *Mtb* exposure and HIV infection **(A)** Experimental overview for study 2. HIS BLT mice were infected i.n. with an estimated 10^3 CFU of *Mtb* H37Rv for 4 weeks and subsequently treated with RIF and INH by oral gavage (750 μg/day) for 8 weeks. Drug treatment was terminated and HIS mice were assigned to i.v. infection with 2,500 $TCID_{50}$ of HIV-1 (JR-CSF) or mock (PBS) using 4 HIS mice per group. Relapse of TB was assessed at 5 weeks post-HIV infection due to observation of signs of disease (e.g., weight loss). *Denotes confirmation of infection and drug activity in selected animals. **(B)** Confirmation of infection and drug efficacy prior to, during, and at the completion of TB chemotherapy ($n = 4$, with 1 animal per time point). **(C)** Bacterial burden 5 weeks post-HIV or mock infection in the TB and TB/HIV groups. Histological appearance of tissue from HIS mice following *Mtb* infection, drug treatment with RIF/INH, and at TB relapse is shown in **(D–K)**. **(D)** Granulomatous inflammation at 4 weeks post-infection with *Mtb* and **(E)** abundant AFB positive areas within the granuloma. **(F)** Residual interstitial inflammation and **(G)** rare AFB (arrowhead) in inflammatory cells in the interstitium, after 8 weeks of RIF and INH. Similar histological appearance of lung following relapse in TB and TB/HIV experimental groups is shown with representative images in **(H–K)**. **(H)** Frequently observed areas that include non-remarkable lung, interstitial inflammation, and perivascular inflammation and **(I)** AFB in small pockets of inflammation. **(J)** Infrequent granulomatous lesion and **(K)** AFB in a granuloma center.

presence of MGC was observed in liver of animals from both groups (**Figure 4G**) post-drug therapy. MGC were also observed in the liver of a mouse harvested after 4 weeks of RIF and INH treatment as shown in **Supplemental Figure 2C**. At this stage of treatment, only rare AFB+ cells were observed in hepatic tissue (**Supplemental Figure 2D**). Despite the differences in liver bacterial burden in the relapse phase (**Figure 4F**), similar histological features were seen among tissue from animals in both the TB and TB/HIV treatment groups (**Figure 4G**) including the presence of MGC and cells containing AFB (**Figure 4H**).

HIV Replication in Lung and Liver During TB Relapse

Increased viral replication has been described in the bronchoalveolar lavage of those with TB and HIV co-infection (Nakata et al., 1997). To determine if *Mtb* infection could alter viral replication in the periphery or tissues, the viral load and distribution of cells harboring viral RNA was assessed in HIS mice (**Figure 5**). An HIV mono-infection treatment group, naïve for *Mtb* exposure, was mock infected i.n. with PBS, treated with RIF/INH to control for potential drug effects, and subsequently infected with HIV. Similarly, control animals naïve for *Mtb* and HIV infection were also provided the RIF and INH regimen and tissues collected at the study end to provide baseline values. It is important to note that animals in the non-infected and HIV mono-infection treatment groups were generated in the same HIS mouse production batch (i.e., matched tissues/cells) as the other animals used in study 2.

As shown in **Figure 5A**, productive infection with HIV-1 was observed in blood and tissues of HIS mice from both the HIV and TB relapse/HIV groups at 5 weeks post HIV infection. Plasma levels of HIV proteins measured by a commercial diagnostic ELISA did not differ between HIV and TB/HIV infection groups (**Figure 5A**). Interestingly, the viral load was significantly increased in both the lung and the liver of mice with TB/HIV

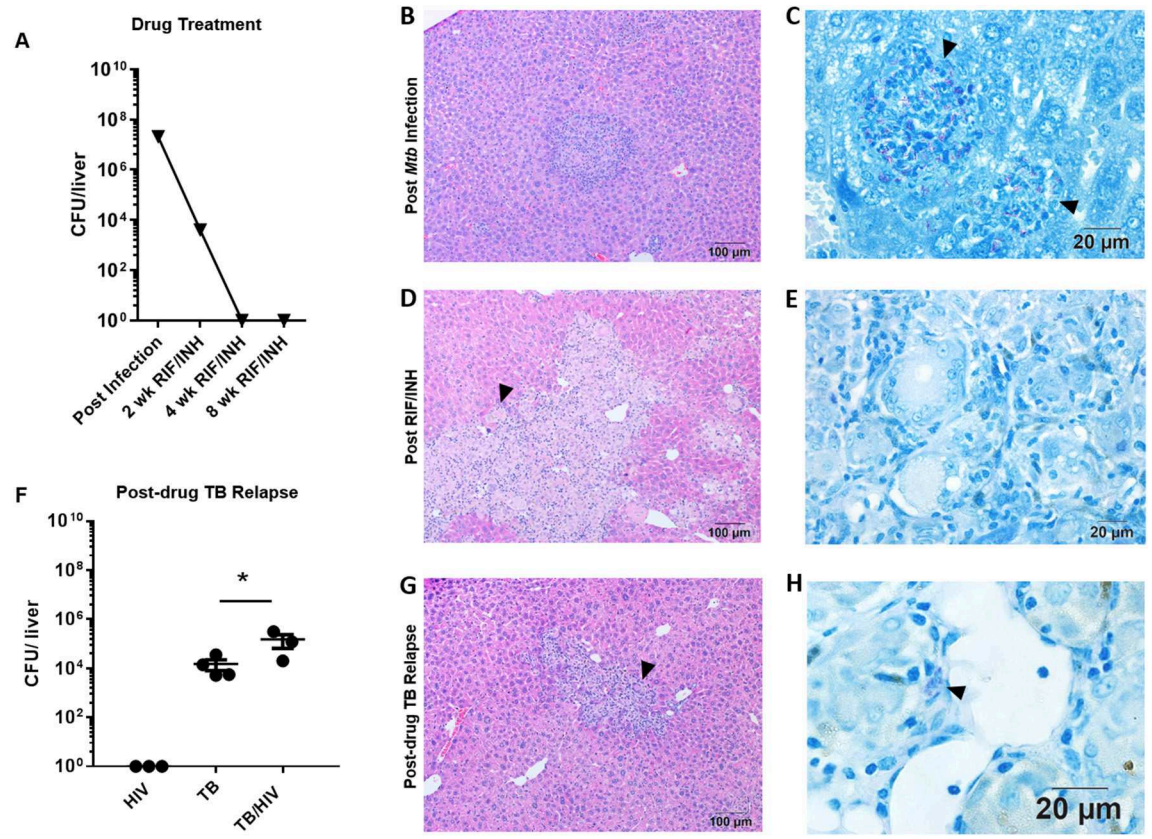

FIGURE 4 | Hepatic TB relapse in the setting of HIV co-infection. Infection, drug treatment and TB relapse outcomes in liver of HIS mice given high dose (10^3 CFU) *Mtb* infection in study 2. **(A)** CFU in the liver 4 weeks after i.n. infection with *Mtb* and after 2, 4, and 8 weeks of TB chemotherapy with RIF/INH. **(B)** Inflammatory foci containing **(C)** clusters of AFB (arrowheads) in the liver of mice following infection with *Mtb*. **(D)** Lesions with frequent multi-nucleated giant cells (arrowheads) observed following 8 weeks of TB chemotherapy which **(E)** lack detectable AFB. **(F)** Hepatic mycobacterial burden (CFU) in the TB relapse phase in HIV mono-infected, and *Mtb* and drug treated mice with mock (TB) or HIV (TB/HIV) co-infection. **(G)** Inflammatory foci similarly evident in liver from both TB and TB/HIV relapse in which **(H)** rare AFB are observed in the TB relapse phase. Data in B are means ± SEM with statistically significant differences between treatments shown as $^*p < 0.05$.

co-infection compared to the group mono-infected with HIV (**Figure 5A**).

Histopathology and RNA scope analysis were employed to further characterize HIV infection of the lung and liver. As shown in **Figure 5B**, cellular syncytia due to HIV infection was observed in bright field microscopy analysis of HIS mouse lung. This is an important cellular pathology observed in human tissue of those with HIV and is associated with cell to cell transfer of virus (Bracq et al., 2017) that we now demonstrate in the HIS mouse. RNA scope analysis further demonstrated limited areas of viral RNA in lung and liver of HIV mono-infected mice that were observed to be randomly distributed throughout the lung parenchyma (**Figure 5C**) and near portal tracts in the liver (**Figure 5D**). At TB relapse in co-infected animals, viral RNA was also detected in the lung parenchyma, and further found to be localized to interstitial spaces characterized by mild inflammatory infiltrate (**Figure 5E**), as well as the periphery of TB lesions (**Figure 5F**). In the liver of co-infected mice, HIV RNA was observed near portal tracts and in proximity to vessels (**Figure 5G**).

Pulmonary Immune Microenvironment of TB and TB/HIV Relapse

To identify the immune signature of HIS mice in the TB relapse phase, in the presence or absence of HIV co-infection, multiplex ELISA assessment of lung, liver, and plasma was performed on animals from study 2. In general, HIV mono-infection did not significantly affect pulmonary cytokines and chemokines production, compared to non-infected animals (**Figure 6**). Lung of mice with TB relapse was characterized by moderate increases in several cytokines and chemokines with important roles in host immunity to *Mtb* (e.g., IL-1β, TNF-α, IL-17, and IFN-γ) and promotion of HIV pathogenesis (IL-1β, TNF-α, IL-6, and CCL2). Additional chemokines with roles in host defense against *Mtb* and HIV (CXCL10 and CCL4) were also elevated in lung, although increases in CCL4 did not reach significance. Expression of CCL2 remained elevated in lung of animals with co-infection while moderate, though non-significant, reductions of IL-1β and IL-6 were observed compared to the TB group.

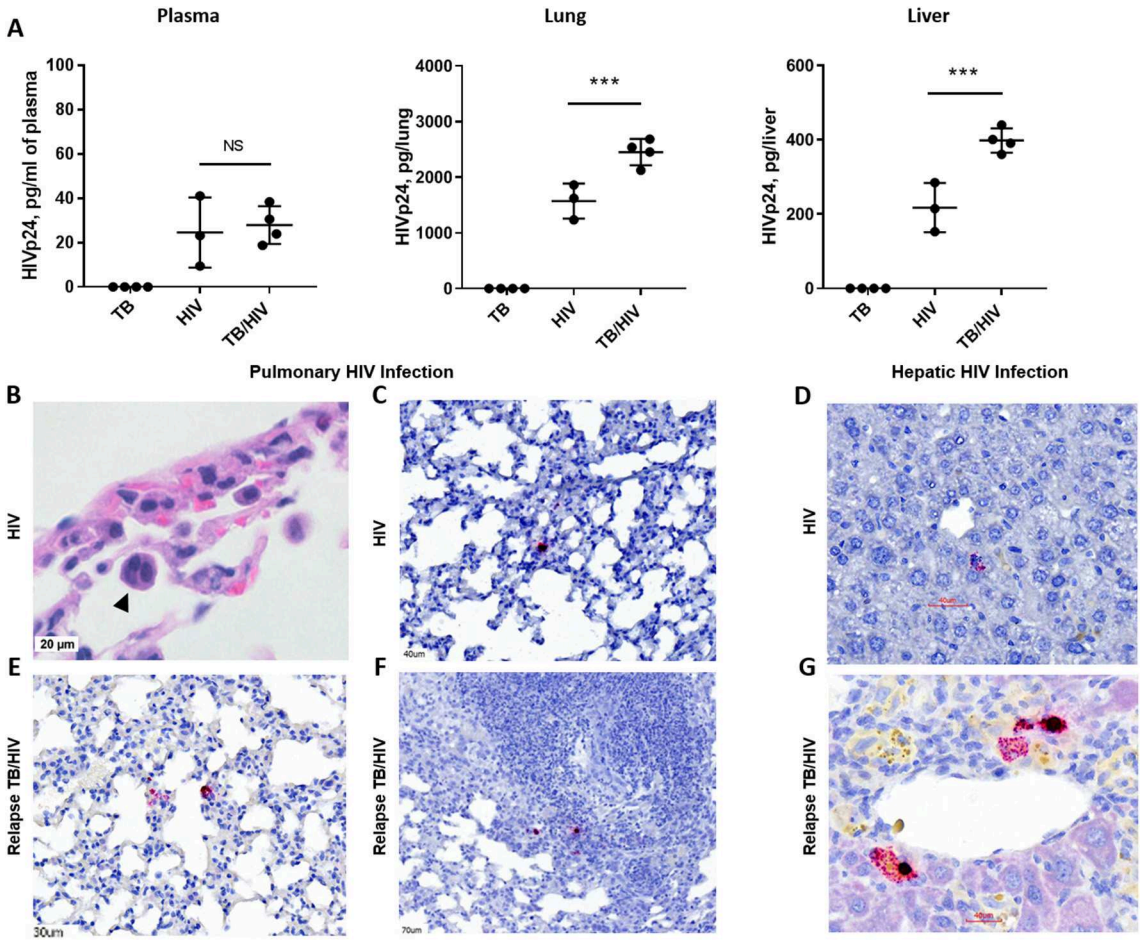

FIGURE 5 | HIV replication in lung and liver during TB relapse. Viral load and distribution of HIV+ cells in the periphery and tissues in the TB relapse phase in study 2. **(A)** Viral load in the plasma, lung, and liver as measured by ELISA (Zeptometrix) specific to HIV p24 capsid protein. **(B)** Detection of a cellular syncytia (arrowhead) characteristic of HIV infection as observed in bright field microscopy following visualization with H&E. **(C–G)** HIV infected cells were detected with RNA-Scope specific to HIV gag. **(C,D)** HIV+ cells in the lung interstitium and near portal tracts in the liver of a HIS mouse with HIV mono-infection. **(E–G)** HIV+ cells were observed in inflamed interstitium **(E)** and in the periphery of TB lesions **(F)**, as well as near blood vessels in the liver **(G)**, of TB/HIV co-infected mice at TB relapse. Data shown in **(A)** are means ± SEM with statistically significant differences between indicated treatment groups shown as $^{***}p < 0.001$.

Activation of IL-17 in mice with TB relapse, however, was significantly suppressed due to HIV infection.

Several cytokines and chemokines were at or below the limit of detection in the lung including IL-2, IL-4, IL-5, IL-7, and IL-15. Increased G-CSF, and a trend ($p = 0.06$) for increased IL-10, was observed in lung of mice with HIV mono-infection as shown in **Supplemental Figure 3**. The levels of other detectable analytes did not significantly differ among treatment groups.

Cytokine and Chemokine Signatures in Liver and Periphery

The cytokine/chemokine profile of the liver tissue was also assessed to identify microenvironment signatures associated with hepatic TB relapse or *Mtb*-driven viral replication. In general, the liver microenvironment was less activated compared to the lung as shown in the treatment group comparisons in **Supplemental Figure 4**. Similar to the lung, the expression of several analytes (IL-2, IL-4, IL-5, IL-7, and IL-15) was below or near the limit of detection. A signal for several other individual cytokines was detectable and demonstrated that there were no significant differences among treatment groups for most analytes measured. Exceptions included GM-CSF, levels of which decreased in all infection groups while co-infection was associated with a significantly more marked suppression (**Supplemental Figure 4**). An interesting pattern of activation and suppression was observed for IL-1ra, CCL4, CXCL10, and IL-17 (**Supplemental Figure 4**). Increased production was observed in liver of mice from the TB group. Co-infection with HIV, however, was associated with a suppression of these cytokines/chemokines in comparison to TB (**Supplemental Figure 4**).

Plasma was further assessed to explore biomarkers that may reflect the disease and immune responses of the tissue compartments. As compared to the lung and liver, fewer

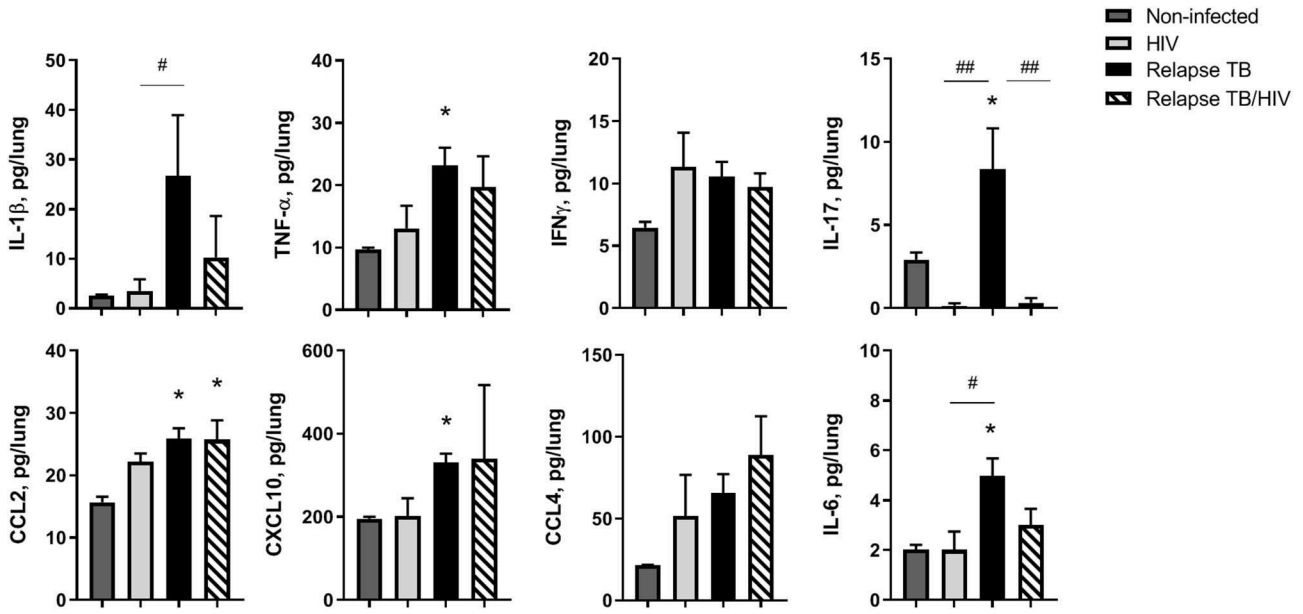

FIGURE 6 | Pulmonary immune microenvironment of TB and TB/HIV relapse. Lung supernatants were harvested from disrupted lung tissue to assess differences in the immune microenvironment at TB relapse, in the presence or absence of HIV. Analysis of lung cytokines and chemokines was performed with a human multiplex ELISA (Bio-rad Bio-plex Pro™ human cytokine 27-plex kit. Shown are results from selected cytokines or chemokines at the TB relapse endpoint from study 2. Data are the means ± SEM with statistically significant differences compared to non-infected controls designated as follows: *$p < 0.05$. Significant differences between the indicated infection groups are shown as #$p < 0.05$; ##$p < 0.01$.

cytokines and chemokines were above the limit of detection and the levels of detectable analytes were generally low (**Supplemental Figure 5**). Few cytokines were significantly altered due to treatment with the exception of activation of CXCL10 in the TB group. Some cytokines were observed to be decreased in all infection groups including IL-9, FGF, and PDGF. As observed in the lung and liver, CXCL10 was significantly reduced in the TB/HIV, compared to the TB, treatment group. TB/HIV was associated with a significant suppression of CCL4, G-CSF, and a trend toward suppression of TNF-α ($p = 0.06$), compared to TB.

DISCUSSION

TB recurrence due to relapse, reinfection, or reactivation of a latent *Mtb* infection continues to be a critical obstacle in the control and eradication of tuberculosis. HIV infection is an important contributing factor for: the current incidence of TB treatment failure or post-therapy relapse (Pulido et al., 1997; Crampin et al., 2010; Narayanan et al., 2010; Unis et al., 2014; Gadoev et al., 2017); the probability of death as a result of recurrent TB (Alvaro-Meca et al., 2014); and the development of *Mtb* drug resistance following relapse (Yoshiyama et al., 2004; McIvor et al., 2017). The challenges to investigations in human subjects and lack of experimental models has resulted in a poor understanding of the mechanisms for relapse TB in those with HIV.

Our work contributes, to the best of our knowledge, the first candidate small animal model of post-drug treatment relapse of TB amenable to the study of HIV co-infection. Use of HIS mice overcomes the challenge of human host restriction by HIV that otherwise limits investigations of TB relapse to correlative clinical studies of co-infected human subjects and extrapolations from studies of LTBI reactivation in SIV-infected NHP. Importantly, the HIS mouse model would also permit investigations of the $CD4^+$T cell-independent mechanisms of disease due to HIV infection that are not reproduced through generalized immune suppression with aminoguanidine or glucocorticoids, *in vivo* $CD4^+$T cell subset depletion, or use of mouse strains with immune defects (Scanga et al., 1999; Botha and Ryffel, 2002; Cheigh et al., 2010).

In the current study, HIV infection was implemented at the end of TB drug therapy to focus the investigation on the effects of HIV during the post-drug phase. This allowed us to reduce potentially confounding effects of chronic HIV on immunity and tissue mycobacterial burden at the end of TB chemotherapy on interpretation of results. HIV infections are an important risk for several TB disease scenarios in endemic regions (Tornheim and Dooley, 2018) including during development of active disease as well as during TB treatment and follow up. Acute HIV develops rapidly in the first few weeks after infection (Cohen et al., 2011) while chronic infection, including in those virally suppressed, perturbs the immune system (see reviews; Morou et al., 2014; Younas et al., 2016). Several other important clinical scenarios that could be modeled in HIS mice include: the effects of chronic HIV infection on the length of drug treatment needed

to achieve clearance; the persistence of immune defects despite ART suppression of viral load; and the effects of ART and TB drug interactions on treatment windows and rates of relapse.

Our results demonstrate that paucibacillary TB can be generated in HIS mice following treatment with standard TB drugs and treatment timelines similar to the Cornell or Cornell-like approaches used in other murine models (McCune et al., 1966; Radaeva et al., 2005). The relapse kinetics we observed following HIV co-infection or high dose *Mtb* infection were more similar to those observed in genetically susceptible (e.g., I/St) as compared to resistant (e.g., C57BL/6) mouse strains (Radaeva et al., 2005). Our results suggest the infectious dose or human host genetics may result in different relapse outcomes, or different kinetics of relapse, regardless of the apparent development of paucibacillary disease observed following drug treatment. Based on our observations, 4 weeks of infection is sufficient to establish a bacterial burden that is paucibacillary following 8 weeks of drug treatment. The disease outcomes affected by HIV in the model may also be more discernible after lower dose infections (e.g., $\leq 10^2$ CFU). Further model development will be needed to determine the range of relapse kinetics in HIS mice developed from diverse human stem cell donors and in cord blood models. Once fully developed, these model systems would allow for hypothesis-driven investigations of disease susceptibility through generation of mice with stem cells from sources with known genetic backgrounds.

Post-drug TB relapse, or reactivation from latency, is often postulated to be the result of HIV-related or other immune disturbances which cause breakdown of an existing granuloma and permit dissemination (Diedrich and Flynn, 2011). These paradigms are generally well-supported by observations in NHP models of TB latency and latent TB reactivation due to immune suppression such as following TNF blockade therapy or SIV infection (Diedrich et al., 2010; Mehra et al., 2011; Foreman et al., 2016). In NHPs that have developed LTBI, necropsy reveals well-organized lesions persisting in the lung despite the absence of detectable bacilli (Hudock et al., 2017). In an elegant study of latent TB reactivation in the NHP due to TNF-α blockade, fluorescence labeling of metabolic hotspots along with PET CT imaging of granulomas demonstrated activity in previously affected areas of the lung (Lin et al., 2016). In that study, new granulomas did also develop simultaneously with, or in advance of apparent reactivation of the residual granulomatous areas, suggesting events beyond a breach of lesion containment also occur. To date, similar studies of post-drug relapse due to SIV infection have not been described in an NHP model.

Analysis of granulomatous inflammation outcomes related to *Mtb* containment following TB drug treatment is challenging in many murine models due to the limited development of granulomatous pathology. Compared to standard murine TB models, a strength of the HIS mouse is the spectrum of granulomas that develop including large necrotizing, and caseous lesions (Calderon et al., 2013; Nusbaum et al., 2016) with similarities to those observed in C3HeB/FeJ mice (Pan et al., 2005; Kramnik and Beamer, 2016). Lesions persist following TB drug treatment in C3HeB/FeJ, and other susceptible models such as the I/St, mouse (Kondratieva et al., 2018; Xu et al., 2019). In the current study, an apparent resolution of these granulomatous lesions was observed following TB chemotherapy in HIS mice. At relapse, the most consistent observation was that of moderate to significant interstitial inflammation and presence of AFB in these inflamed interstitial spaces. Our observations of pulmonary pathology in the HIS mouse thus further support the concept that TB relapse may also occur via mechanisms independent of granuloma integrity breakdown similar to those observed during LTBI reactivation in NHP (Lin et al., 2016). Further investigation is needed to determine if the outcomes observed in the HIS mouse are unique to the model or may represent a spectrum of events that occur in TB relapse in human lung and advanced animal models such as NHP. Our initial findings in the setting of co-infection suggest that HIV infection promotes greater mycobacterial proliferation in the post-chemotherapy stage independent of effects on granuloma integrity.

Pulmonary viremia was previously demonstrated to be increased in PLWH that had active TB compared to those without TB (Nakata et al., 1997). Our results are consistent with these observations and demonstrate the first preliminary evidence, to our knowledge, that these polymicrobial outcomes in the lung could be modeled in the HIS mouse. The observations that HIV+ cells localized to the sites of interstitial inflammation and *Mtb* proliferation further suggest potential mechanisms of microbial synergy in the lung. The inflammatory immune response that restrains *Mtb* propagation in lesions may recruit new targets and establish activation conditions favorable for HIV replication. Likewise, the suppression of immunity due to local effects of HIV infection could promote *Mtb* proliferation. Importantly, our results suggest that these tissue events of co-infection may differ from those in the periphery, as described in one report of human subjects (Nakata et al., 1997). We observed increased viral replication in the lung and liver in the setting of *Mtb* co-infection while plasma viral loads were similar among HIV and HIV/TB groups. These differences in viremia between the blood and tissues could suggest that blood-based diagnostics may not fully reflect the *in vivo* disease process in those with co-infection with regard to the impact on viral load or viral reservoirs.

Multiplex analysis of lung analytes from HIS mice with relapse demonstrated a moderate activation of many cytokines and chemokines including pro-inflammatory molecules. HIV infection is known to promote a pro-inflammatory bias in the infected host (Nou et al., 2016) while several inflammatory mechanisms are associated with increased *Mtb* pathogenesis (Tobin, 2015; Wallis and Hafner, 2015). In the current study, HIV mono-infection generally presented with only moderate and non-significant activation of cytokines and chemokines in the tissues and plasma compared to non-infected animals. Infection with *Mtb* in the post-drug relapse phase, however, was associated with pulmonary activation of several pro-inflammatory cytokines and chemokines that have established roles in enhancing HIV replication including IL-1β, IL-6, TNF-α, and CCL-2 (Swingler et al., 1994; Kumar et al., 2013; Nou et al., 2016; Pasquereau et al., 2017). CCL2 was recently shown to further support HIV pathogenesis by promoting virion release from infected host cells (Ajasin et al., 2019). Increased proliferation

of HIV in lung of persons with *Mtb* co-infection has been previously associated with increased TNF-α and CCL2 levels in bronchoalveolar lavage (Mayanja-Kizza et al., 2009; Kumar et al., 2013). Further exploration in HIS models may demonstrate if the production of these pro-viral molecules at sites of *Mtb*-driven inflammation favor HIV replication through a variety of potential mechanisms including recruitment of inflammatory target cells, direct activation of the HIV LTR, and augmented virion release from productively infected host cells.

Effector cytokines with anti-mycobacterial function (e.g., IFN-γ, TNF-α, and IL-17) (Ernst, 2012) were also observed to be moderately activated in the lung microenvironment at relapse. Co-infection with HIV did not significantly reduce the activation of IFN-γ or TNF-α at *Mtb* regrowth endpoints, suggesting lack of a generalized immune suppression. In contrast, HIV infection reduced production of pulmonary IL-17 following activation by *Mtb* regrowth. These preliminary results may suggest an interesting candidate mechanism of microbial synergy for further exploration. The Th17 subset of $CD4^+$T cells are very permissive to HIV infection due to lack of RNases (Christensen-Quick et al., 2016). Impairment and depletion of Th17 cells in PLWH is also known to occur in the early stages of infection (El Hed et al., 2010; Prendergast et al., 2010; Murray et al., 2018). IL-17 produced by multiple cell populations is important for host immunity to *Mtb* (Lockhart et al., 2006; Umemura et al., 2007; Okamoto Yoshida et al., 2010; Torrado and Cooper, 2010; Shen and Chen, 2018) and is elevated in persons with latent TB compared to healthy controls (Coulter et al., 2017; Devalraju et al., 2018). In support of our observations, reduced IL-17 was also associated with TB regrowth in a BALB/c mouse model of post-drug TB relapse (de Steenwinkel et al., 2013).

The overall pattern of cytokine and chemokine activation in the liver was similar, but muted, compared to the lung. This outcome is consistent with the lower pathogen burden in this site of dissemination. Similarly, even fewer significant differences in cytokine and chemokine levels were observed in the plasma at relapse. An interesting exception was the activation of CXCL10 observed in the lung, liver, and plasma of animals in the TB relapse group. CXCL10 has been previously described as a biomarker capable of distinguishing active and latent TB and predicting the risk for TB chemotherapy failure (Hong et al., 2014; Wergeland et al., 2015). In contrast to the observations in human subjects that CXCL10 predicted TB disease state irrespective of HIV status (Wergeland et al., 2015), we observed a significant reduction of CXCL10 in the liver and plasma, but not the lung, of HIS mice in the setting of co-infection. Further studies are needed to validate the biomarker potential of CXCL10 and other immune molecules to inform TB relapse outcomes and identify the effect of HIV on these biomarkers. Our preliminary findings support the potential for this small animal model to reproduce important immune outcomes in a system where mechanistic investigations of the lung and other tissue compartments can be undertaken and therapeutic interventions can be tested.

There are several challenges to use of HIS mice that should be noted despite the obvious advantages for study of HIV and co-infections such as HIV and *Mtb*. Animals are expensive to generate and maintain, and often require 2 to 3 months for development of immune reconstitution following irradiation and engraftment of human stem cells. The chimeric nature of the system means that immune outcomes include both human adaptive and innate, as well as murine innate, responses. There are additionally suboptimal development of some immune responses such as humoral immunity in HIS mice (Karpel et al., 2015). In the NSG mouse strain used to generate BLT mice in the current study, development of GVHD is a known issue (Greenblatt et al., 2012) that led to losses in animal numbers in the prolonged study design required to reproduce TB treatment and relapse as reported here. Recent regulatory and legal issues have further restricted production of, and funding for, the BLT HIS model in many states and institutions. Nonetheless, the outcomes of the current study are important to guide development of models of co-infection including HIV-associated TB relapse in newer HIS models. Cord blood stem cells can generate HIS mice with similar reconstitution efficiency to the BLT (Wunderlich et al., 2018) while further refinements in these models can expand different immune compartments and reduce development of GVHD (Iwabuchi et al., 2018).

In conclusion, our findings describe a candidate small animal model of TB relapse in the setting of HIV infection that reproduces aspects of clinical disease, including microbial synergy and immune activation, observed in co-infected persons. Long term, HIS mouse models of TB relapse may serve an important pre-clinical role for discovery and translation of therapeutics prior to final evaluation in NHP models. Investigations in models capable of supporting co-infections are critical to improving TB treatment outcomes in HIV+ persons.

DATA AVAILABILITY STATEMENT

All datasets generated for this study are included in the article/**Supplementary Material**.

ETHICS STATEMENT

The animal study was reviewed and approved by the University of Texas Medical Branch Institutional Animal Care and Use Committee.

AUTHOR CONTRIBUTIONS

Investigations into the feasibility and application of the HIS mouse to study TB relapse in the setting of HIV were carried out by MH, TS, RN, KN, SC, JR, ME, JL, BG, and JE. Data generated from these investigations was analyzed by MH, RN, KN, SC, RH, JA, BG, and JE. MH and JE prepared the manuscript and upon careful review by TS, RN, KN, SC, JR, and BG. ME edited the document for submission.

FUNDING

This work was supported by grants to BG and JE from the NIH (R56 HL129881 and R01 A1HL129881) and the UTMB Institute

for Human Infections and Immunity. Fellowship support for MH was provided through the American Society for Microbiology Robert D. Watkins Graduate Research Fellowship Program. RN and KN were supported by Pre-doctoral Fellowships through the UTMB James W. McLaughlin Endowment.

ACKNOWLEDGMENTS

We wish to express our sincere gratitude to Mark Griffin, manager of the UTMB Flow Cytometry and Cell Sorting Core Facility, for his assistance with flow cytometry experiments. We truly appreciate the team of dedicated individuals affiliated with the UTMB Animal Resource Center for animal husbandry during the lengthy infection studies.

SUPPLEMENTARY MATERIAL

The Supplementary Material for this article can be found online at: https://www.frontiersin.org/articles/10.3389/fcimb.2020.00150/full#supplementary-material

REFERENCES

Ajasin, D. O., Rao, V. R., Wu, X., Ramasamy, S., Pujato, M., Ruiz, A. P., et al. (2019). CCL2 mobilizes ALIX to facilitate Gag-p6 mediated HIV-1 virion release. *Elife* 8:e35546. doi: 10.7554/eLife.35546

Alvaro-Meca, A., Rodriguez-Gijon, L., Diaz, A., Gil, A., and Resino, S. (2014). Incidence and mortality of tuberculosis disease in Spain between 1997 and 2010: impact of human immunodeficiency virus (HIV) status. *J. Infect.* 68, 355–362. doi: 10.1016/j.jinf.2013.12.003

Botha, T., and Ryffel, B. (2002). Reactivation of latent tuberculosis by an inhibitor of inducible nitric oxide synthase in an aerosol murine model. *Immunology* 107, 350–357. doi: 10.1046/j.1365-2567.2002.01511.x

Bracq, L., Xie, M., Lambele, M., Vu, L. T., Matz, J., Schmitt, A., et al. (2017). T cell-macrophage fusion triggers multinucleated giant cell formation for HIV-1 spreading. *J. Virol.* 91:e01237-17. doi: 10.1128/JVI.01237-17

Braun, M. M., Truman, B. I., Maguire, B., DiFerdinando, G. T. Jr., Wormser, G., Broaddus, R., et al. (1989). Increasing incidence of tuberculosis in a prison inmate population. *Association with HIV infection. JAMA* 261, 393–397. doi: 10.1001/jama.1989.03420030067031

Bresnihan, B., and Cunnane, G. (2003). Infection complications associated with the use of biologic agents. *Rheum. Dis. Clin. North Am.* 29, 185–202. doi: 10.1016/S0889-857X(02)00101-1

Calderon, V. E., Valbuena, G., Goez, Y., Huante, M., Sutjita, P., Johnston, K., et al. (2013). A humanized mouse model of tuberculosis. *PLoS ONE* 8:e63331. doi: 10.1371/journal.pone.0063331

Chao, M. C., and Rubin, E. J. (2010). Letting sleeping dos lie: does dormancy play a role in tuberculosis? *Annu. Rev. Microbiol.* 64, 293–311. doi: 10.1146/annurev.micro.112408.134043

Cheigh, C. I., Senaratne, R., Uchida, Y., Casali, N., Kendall, L. V., and Riley, L. W. (2010). Posttreatment reactivation of tuberculosis in mice caused by Mycobacterium tuberculosis disrupted in mce1R. *J. Infect. Dis.* 202, 752–759. doi: 10.1086/655224

Christensen-Quick, A., Lafferty, M., Sun, L., Marchionni, L., DeVico, A., and Garzino-Demo, A. (2016). Human Th17 cells lack hiv-inhibitory rnases and are highly permissive to productive HIV infection. *J. Virol.* 90, 7833–7847. doi: 10.1128/JVI.02869-15

Cisneros, J. R., and Murray, K. M. (1996). Corticosteroids in tuberculosis. *Ann. Pharmacother.* 30, 1298–1303. doi: 10.1177/106002809603001115

Clark, R. J. (1971). Antiviral action of rifampin. *N. Engl. J. Med.* 284:675. doi: 10.1056/NEJM197103252841219

Cohen, M. S., Shaw, G. M., McMichael, A. J., and Haynes, B. F. (2011). Acute HIV-1 Infection. *N. Engl. J. Med.* 364, 1943–1954. doi: 10.1056/NEJMra1011874

Coulter, F., Parrish, A., Manning, D., Kampmann, B., Mendy, J., Garand, M., et al. (2017). IL-17 Production from T helper 17, mucosal-associated invariant t, and gammadelta cells in tuberculosis infection and disease. *Front. Immunol.* 8:1252. doi: 10.3389/fimmu.2017.01252

Crampin, A. C., Mwaungulu, J. N., Mwaungulu, F. D., Mwafulirwa, D. T., Munthali, K., Floyd, S., et al. (2010). Recurrent TB: relapse or reinfection? The effect of HIV in a general population cohort in Malawi. *AIDS* 24, 417–426. doi: 10.1097/QAD.0b013e32832f51cf

de Steenwinkel, J. E., de Knegt, G. J., M. T., ten Kate, Verbrugh H. A., Hernandez-Pando, R., Leenen, P. J., et al. (2013). *Tuberculosis* 93, 213–221. doi: 10.1016/j.tube.2012.11.006

Devalraju, K. P., Neela, V. S. K., Ramaseri, S. S., Chaudhury, A., Van A, Krovvidi, S. S., Vankayalapati, R., et al. (2018). IL-17 and IL-22 production in HIV+ individuals with latent and active tuberculosis. *BMC Infect. Dis.* 18:321. doi: 10.1186/s12879-018-3236-0

Diedrich, C. R., and Flynn, J. L. (2011). HIV-1/mycobacterium tuberculosis coinfection immunology: how does HIV-1 exacerbate tuberculosis? *Infect. Immun.* 79, 1407–1417. doi: 10.1128/IAI.01126-10

Diedrich, C. R., Mattila, J. T., Klein, E., Janssen, C., Phuah, J., Sturgeon, T. J., et al. (2010). Reactivation of latent tuberculosis in cynomolgus macaques infected with SIV is associated with early peripheral T cell depletion and not virus load. *PLoS ONE* 5:e9611. doi: 10.1371/journal.pone.0009611

Dooley, K. E., Lahlou, O., Ghali, I., Knudsen, J., Elmessaoudi, M. D., Cherkaoui I, and and El Aouad, R. (2011). Risk factors for tuberculosis treatment failure, default, or relapse and outcomes of retreatment in Morocco. *BMC Public Health* 11:140. doi: 10.1186/1471-2458-11-140

Douglas, A. S., Strachan, D. P., and Maxwell, J. D. (1996). Seasonality of tuberculosis: the reverse of other respiratory diseases in the UK. *Thorax* 51, 944–946. doi: 10.1136/thx.51.9.944

El Hed, A., Khaitan, A., Kozhaya, L., Manel, N., Daskalakis, D., Borkowsky, W., et al. (2010). Susceptibility of human Th17 cells to human immunodeficiency virus and their perturbation during infection. *J. Infect. Dis.* 201, 843–854. doi: 10.1086/651021

Endsley, J. J., Endsley, M. A., and Estes, D. M. (2006). Bovine natural killer cells acquire cytotoxic/effector activity following activation with IL-12/15 and reduce Mycobacterium bovis BCG in infected macrophages. *J. Leukoc. Biol.* 79, 71–79. doi: 10.1189/jlb.0505239

Ernst, J. D. (2012). The immunological life cycle of tuberculosis. *Nat. Rev. Immunol.* 12, 581–591. doi: 10.1038/nri3259

Esmail, H., Barry, C. E. III and Wilkinson, R. J. (2012). Understanding latent tuberculosis: the key to improved diagnostic and novel treatment strategies. *Drug Discov. Today* 17, 514–521. doi: 10.1016/j.drudis.2011.12.013

Falzon, D., Schünemann, H. J., Harausz, E., González-Angulo, L., Lienhardt, C., Jaramillo, E., et al. (2017). World Health Organization treatment guidelines for drug-resistant tuberculosis, 2016 update. *Eur. Respir. J.* 49:1602308. doi: 10.1183/13993003.02308-2016

Foreman, T. W., Mehra, S., LoBato, D. N., Malek, A., Alvarez, X., Golden, N. A., et al. (2016). CD4+ T-cell-independent mechanisms suppress reactivation of latent tuberculosis in a macaque model of HIV coinfection. *Proc. Natl. Acad. Sci. U.S.A.* 113, E5636–E5644. doi: 10.1073/pnas.1611987113

Gadoev, J., Asadov, D., Harries, A. D., Parpieva, N., Tayler-Smith, K., Isaakidis, P., et al. (2017). Recurrent tuberculosis and associated factors: a five - year countrywide study in Uzbekistan. *PLoS ONE* 12:e0176473. doi: 10.1371/journal.pone.0176473

Gideon, H. P., and Flynn, J. L. (2011). Latent tuberculosis: what the host "sees"? *Immunol. Res.* 50, 202–212. doi: 10.1007/s12026-011-8229-7

Greenblatt, M. B., Vrbanac, V., Tivey, T., Tsang, K., Tager, A. M., and Aliprantis, A. O. (2012). Graft versus host disease in the bone marrow,

liver and thymus humanized mouse model. *PLoS ONE* 7:e44664. doi: 10.1371/journal.pone.0044664

Hong, J. Y., Lee, H. J., Kim, S. Y., Chung, K. S., Kim, E. Y., Jung, J. Y., et al. (2014). Efficacy of IP-10 as a biomarker for monitoring tuberculosis treatment. *J Infect.* 68, 252–258. doi: 10.1016/j.jinf.2013.09.033

Housset, C., Lamas, E., and Brechot, C. (1990). Detection of HIV1 RNA and p24 antigen in HIV1-infected human liver. *Res. Virol.* 141, 153–159. doi: 10.1016/0923-2516(90)90017-D

Huante, M. B., Nusbaum, R. J., and Endsley, J. J. (2019). "Co-infection with TB and HIV: converging epidemics, clinical challenges, microbial synergy," in *Tuberculosis Host-Pathogen Interactions,* eds J. D. Cirillo and Y. H. Kang (Basel: Elsevier), 123–153.

Hudock, T. A., Foreman, T. W., Bandyopadhyay, N., Gautam, U. S., Veatch, A. V., LoBato, D. N., et al. (2017). Hypoxia sensing and persistence genes are expressed during the intragranulomatous survival of *Mycobacterium tuberculosis*. *Am. J. Respir. Cell Mol. Biol.* 56, 637–647. doi: 10.1165/rcmb.2016-0239OC

Iwabuchi, R., Ikeno, S., Kobayashi-Ishihara, M., Takeyama, H., Ato, M., Tsunetsugu-Yokota, Y., et al. (2018). Introduction of human Flt3-L and GM-CSF into humanized mice enhances the reconstitution and maturation of myeloid dendritic cells and the development of Foxp3(+)CD4(+) T Cells. *Front. Immunol.* 9:1042. doi: 10.3389/fimmu.2018.01042

Karpel, M. E., Boutwell, C. L., and Allen, T. M. (2015). BLT humanized mice as a small animal model of HIV infection. *Curr. Opin. Virol.* 13, 75–80. doi: 10.1016/j.coviro.2015.05.002

Khan, F. A., Minion, J., Pai, M., Royce, S., Burman, W., Harries, A. D., et al. (2010). Treatment of active tuberculosis in HIV-coinfected patients: a systematic review and meta-analysis. *Clin. Infect. Dis.* 50, 1288–1299. doi: 10.1086/651686

Kondratieva, T. K., Kapina, M. A., Rubakova, E. I., Kondratieva, E. V., Nikonenko, B. V., Majorov, K. B., et al. (2018). A new model for chronic and reactivation tuberculosis: infection with genetically attenuated Mycobacterium tuberculosis in mice with polar susceptibility" *Tuberculosis* 113, 130–138. doi: 10.1016/j.tube.2018.10.003

Kramnik, I., and Beamer, G. (2016). Mouse models of human TB pathology: roles in the analysis of necrosis and the development of host-directed therapies. *Semin. Immunopathol.* 38, 221–237. doi: 10.1007/s00281-015-0538-9

Kumar, A., Abbas, W., and Herbein, G. (2013). TNF and TNF receptor superfamily members in HIV infection: new cellular targets for therapy? *Mediat. Inflamm.* 2013:484378. doi: 10.1155/2013/484378

Lee, H., and Kim, J. (2014). A study on the relapse rate of tuberculosis and related factors in Korea using nationwide tuberculosis notification data. *Osong Public Health Res. Perspect* 5, S8–S17. doi: 10.1016/j.phrp.2014.11.001

Leeds, I. L., Magee, M. J., Kurbatova, E. V., del Rio, C., Blumberg, H. M., Leonard, M. K., et al. (2012). Site of extrapulmonary tuberculosis is associated with HIV infection. *Clin. Infect. Dis.* 55, 75–81. doi: 10.1093/cid/cis303

Lin, P. L., Maiello, P., Gideon, H. P., Coleman, M. T., Cadena, A. M., Rodgers, M. A., et al. (2016). PET CT identifies reactivation risk in cynomolgus macaques with latent *M. tuberculosis. PLoS Pathog.* 12:e1005739. doi: 10.1371/journal.ppat.1005739

Lockhart, E., Green, A. M., and Flynn, J. L. (2006). IL-17 production is dominated by gammadelta T cells rather than CD4 T cells during *Mycobacterium tuberculosis* infection. *J. Immunol.* 177, 4662–4669. doi: 10.4049/jimmunol.177.7.4662

Marx, F. M., Dunbar, R., Enarson, D. A., Williams, B. G., Warren, R. M., G. D., et al. (2014). The temporal dynamics of relapse and reinfection tuberculosis after successful treatment: a retrospective cohort study. *Clin. Infect. Dis.* 58, 1676–1683. doi: 10.1093/cid/ciu186

Mayanja-Kizza, H., Wu, M., Aung, H., Liu, S., Luzze, H., Hirsch, C., et al. (2009). The interaction of monocyte chemoattractant protein-1 and tumour necrosis factor-alpha in *Mycobacterium tuberculosis*-induced HIV-1 replication at sites of active tuberculosis. *Scand. J. Immunol.* 69, 516–520. doi: 10.1111/j.1365-3083.2009.02246.x

McCune, R. M., Feldmann, F. M., Lambert, H. P., and McDermott, W. (1966). Microbial persistence. I. The capacity of tubercle bacilli to survive sterilization in mouse tissues. *J. Exp. Med.* 123, 445–468. doi: 10.1084/jem.123.3.445

McIvor, A., Koornhof, H., and Kana, B. D. (2017). Relapse, re-infection and mixed infections in tuberculosis disease. *Pathog. Dis.* 75:ftx020. doi: 10.1093/femspd/ftx020

Mehra, S., Golden, N. A., Dutta, N. K., Midkiff, C. C., Alvarez, X., Doyle, L. A., et al. (2011). Reactivation of latent tuberculosis in rhesus macaques by coinfection with simian immunodeficiency virus. *J. Med. Primatol.* 40, 233–243. doi: 10.1111/j.1600-0684.2011.00485.x

Mirsaeidi, M., and Sadikot, R. T. (2018). Patients at high risk of tuberculosis recurrence. *Int. J. Mycobacteriol.* 7, 1–6. doi: 10.4103/ijmy.ijmy_164_17

Morou, A., Palmer, B. E., and Kaufmann, D. E. (2014). Distinctive features of CD4+ T cell dysfunction in chronic viral infections. *Curr. Opin. HIV AIDS* 9, 446–451 doi: 10.1097/COH.0000000000000094

Moshkowitz, A., Goldblum, N., and Heller, E. (1971). Studies on the antiviral effect of rifampicin in volunteers. *Nature* 229:422. doi: 10.1038/229422a0

Munje, R., Deshmukh, R., and Tumane, K. (2015). Multidrug-resistant TB among previously treated TB cases: a retrospective study in Nagpur, India. *Indian J. Tuberc.* 62, 207–210. doi: 10.1016/j.ijtb.2015.11.002

Murray, L. W., Satti, I., Meyerowitz, J., Jones, M., Willberg, C. B., Ussher, J. E., et al. (2018). Human immunodeficiency virus infection impairs th1 and th17 mycobacterium tuberculosis-specific T-cell responses. *J. Infect. Dis.* 217, 1782–1792. doi: 10.1093/infdis/jiy052

Nakata, K., Rom, W. N., Honda, Y., Condos, R., Kanegasaki, S., Cao, Y., et al. (1997). *Mycobacterium tuberculosis* enhances human immunodeficiency virus-1 replication in the lung. *Am. J. Respir. Crit. Care Med.* 155, 996–1003. doi: 10.1164/ajrccm.155.3.9117038

Narayanan, S., Swaminathan, S., Supply, P., Shanmugam, S., Narendran, G., Hari, L., et al. (2010). Impact of HIV infection on the recurrence of tuberculosis in South India. *J. Infect. Dis.* 201, 691–703. doi: 10.1086/650528

Nou, E., Lo, J., and Grinspoon, S. K. (2016). Inflammation, immune activation, and cardiovascular disease in HIV. *AIDS* 30, 1495–1509. doi: 10.1097/QAD.0000000000001109

Nusbaum, R. J., Calderon, V. E., Huante, M. B., Sutjita, P., Vijayakumar, S., Lancaster, K. L., et al. (2016). Pulmonary tuberculosis in humanized mice infected with HIV-1. *Sci. Rep.* 6:21522. doi: 10.1038/srep21522

Okamoto Yoshida, Y., Umemura, M., Yahagi, A., O'Brien, R. L., Ikuta, K., Kishihara, K., et al. (2010). Essential role of IL-17A in the formation of a mycobacterial infection-induced granuloma in the lung. *J. Immunol.* 184, 4414–4422. doi: 10.4049/jimmunol.0903332

Pan, H., Yan, B. S., Rojas, M., Shebzukhov, Y. V., Zhou, H., Kobzik, L., et al. (2005). Ipr1 gene mediates innate immunity to tuberculosis. *Nature* 434, 767–772. doi: 10.1038/nature03419

Pasquereau, S., Kumar, A., and Herbein, G. (2017). Targeting TNF and TNF receptor pathway in HIV-1 infection: from immune activation to viral reservoirs. *Viruses* 9:64. doi: 10.3390/v9040064

Pawlowski, A., Jansson, M., Skold, M., Rottenberg, M. E., and Kallenius, G. (2012). Tuberculosis and HIV co-infection. *PLoS Pathog.* 8:e1002464. doi: 10.1371/journal.ppat.1002464

Prendergast, A., Prado, J. G., Kang, Y. H., Chen, F., Riddell, L. A., Luzzi, G., et al. (2010). HIV-1 infection is characterized by profound depletion of CD161+ Th17 cells and gradual decline in regulatory T cells. *AIDS* 24, 491–502. doi: 10.1097/QAD.0b013e3283344895

Pulido, F., Pena, J. M., Rubio, R., Moreno, S., Gonzalez, J., Guijarro, C., et al. (1997). Relapse of tuberculosis after treatment in human immunodeficiency virus-infected patients. *Arch. Intern. Med.* 157, 227–232. doi: 10.1001/archinte.1997.00440230105014

Radaeva, T. V., Nikonenko, B. V., Mischenko, V. V., Averbakh, M. M. Jr. and Apt, A. S. (2005). Direct comparison of low-dose and Cornell-like models of chronic and reactivation tuberculosis in genetically susceptible I/St and resistant B6 mice. *Tuberculosis* 85, 65–72. doi: 10.1016/j.tube.2004.09.014

Rajagopalan, S., and Yoshikawa, T. T. (2000). Tuberculosis in long-term-care facilities. *Infect. Control Hosp. Epidemiol.* 21, 611–615. doi: 10.1086/501816

Rockwood, N., du Bruyn, E., Morris, T., and Wilkinson, R. J. (2016). Assessment of treatment response in tuberculosis. *Expert Rev. Respir. Med.* 10, 643–654. doi: 10.1586/17476348.2016.1166960

Scanga, C. A., Mohan, V. P., Joseph, H., Yu, K., Chan, J., and Flynn, J. L. (1999). Reactivation of latent tuberculosis: variations on the Cornell murine model. *Infect. Immun.* 67, 4531–4538. doi: 10.1128/IAI.67.9.4531-4538.1999

Shen, G., Xue, Z., Shen, X., Sun, B., Gui, X., Shen, M., et al. (2006). The study recurrent tuberculosis and exogenous reinfection, Shanghai, China. *Emerg. Infect. Dis.* 12, 1776–1778. doi: 10.3201/eid1211.051207

Shen, H., and Chen, Z. W. (2018). The crucial roles of Th17-related cytokines/signal pathways in M. *tuberculosis infection. Cell Mol. Immunol.* 15, 216–225. doi: 10.1038/cmi.2017.128

Sonnenberg, P., Glynn, J. R., Fielding, K., Murray, J., Godfrey-Faussett, P., and Shearer, S. (2005). How soon after infection with HIV does the risk of tuberculosis start to increase? A retrospective cohort study in South African gold miners. *J. Infect. Dis.* 191, 150–158. doi: 10.1086/426827

Sonnenberg, P., Murray, J., Glynn, J. R., Shearer, S., Kambashi, B., and Godfrey-Faussett, P. (2001). HIV-1 and recurrence, relapse, and reinfection of tuberculosis after cure: a cohort study in South African mineworkers. *Lancet* 358, 1687–1693. doi: 10.1016/S0140-6736(01)06712-5

Swingler, S., Morris, A., and Easton, A. (1994). Tumour necrosis factor alpha and interleukin-1 beta induce specific subunits of NFKB to bind the HIV-1 enhancer: characterisation of transcription factors controlling human immunodeficiency virus type 1 gene expression in neural cells. *Biochem. Biophys. Res. Commun.* 203, 623–630. doi: 10.1006/bbrc.1994.2228

Tobin, D. M. (2015). Host-directed therapies for tuberculosis. *Cold Spring Harb. Perspect. Med.* 5:a021196. doi: 10.1101/cshperspect.a021196

Tornheim, J. A., and Dooley, K. E. (2018). Challenges of TB and HIV co-treatment: updates and insights. *Curr. Opin. HIV AIDS* 13, 486–491. doi: 10.1097/COH.0000000000000495

Torrado, E., and Cooper, A. M. (2010). IL-17 and Th17 cells in tuberculosis. *Cytokine Growth Factor Rev.* 21, 455–462. doi: 10.1016/j.cytogfr.2010.10.004

Trinh, Q. M., Nguyen, H. L., Nguyen, V. N., Nguyen, T. V., Sintchenko, V., and Marais, B. J. (2015). Tuberculosis and HIV co-infection-focus on the Asia-Pacific region. *Int. J. Infect. Dis.* 32, 170–178. doi: 10.1016/j.ijid.2014.11.023

Umemura, M., Yahagi, A., Hamada, S., Begum, M. D., Watanabe, H., Kawakami, K., et al. (2007). IL-17-mediated regulation of innate and acquired immune response against pulmonary *Mycobacterium bovis* bacille Calmette-Guerin infection. *J. Immunol.* 178, 3786–3796. doi: 10.4049/jimmunol.178.6.3786

Unis, G., Ribeiro, A. W., Esteves, L. S., Spies, F. S., Picon, P. D., Dalla Costa, E. R., et al. (2014). Tuberculosis recurrence in a high incidence setting for HIV and tuberculosis in Brazil. *BMC Infect. Dis.* 14:548. doi: 10.1186/s12879-014-0548-6

Walker, N. F., Meintjes, G., and Wilkinson, R. J. (2013). HIV-1 and the immune response to TB. *Future Virol.* 8, 57–80. doi: 10.2217/fvl.12.123

Wallis, R. S., and Hafner, R. (2015). Advancing host-directed therapy for tuberculosis. *Nat. Rev. Immunol.* 15, 255–263. doi: 10.1038/nri3813

Wergeland, I., Pullar, N., Assmus, J., Ueland, T., Tonby, K., Feruglio, S., et al. (2015). IP-10 differentiates between active and latent tuberculosis irrespective of HIV status and declines during therapy. *J. Infect.* 70, 381–391 doi: 10.1016/j.jinf.2014.12.019

WHO (2019). *2019 Global Tuberculosis Report*. Geneva: World Health Organization.

Wunderlich, M., Chou, F. S., Sexton, C., Presicce, P., Chougnet, C. A., Aliberti, J., et al. (2018). Improved multilineage human hematopoietic reconstitution and function in NSGS mice. *PLoS ONE* 13:e0209034. doi: 10.1371/journal.pone.0209034

Xu, J., Li, S., Almeida, D. V., Tasneen, R., Barnes-Boyle, K., Converse, P. J., Upton, A. M., et al. (2019). Contribution of pretomanid to novel regimens containing bedaquiline with either linezolid or moifloxacin and pyrazinamide in murine models of tuberculosis. *Antimicrob. Agents Chemother.* 63:e00021-19. doi: 10.1128/AAC.00021-19

Yoshiyama, T., Yanai, H., Rhiengtong, D., Palittapongarnpim, P., Nampaisan, O., Supawitkul, S., et al. (2004). Development of acquired drug resistance in recurrent tuberculosis patients with various previous treatment outcomes. *Int. J. Tuberc. Lung Dis.* 8, 31–38.

Younas, M., Psomas, C., Reynes, J., and Corbeau, P. (2016). Immune activation in the course of HIV-1 infection: causes, phenotypes and persistence under therapy. *HIV Med.* 17, 89–105. doi: 10.1111/hiv.12310

Conflict of Interest: The authors declare that the research was conducted in the absence of any commercial or financial relationships that could be construed as a potential conflict of interest.

frontiers in Cellular and Infection Microbiology

ORIGINAL RESEARCH
published: 15 May 2020
doi: 10.3389/fcimb.2020.00226

3D Imaging of the Transparent *Mycobacterium tuberculosis*-Infected Lung Verifies the Localization of Innate Immune Cells With Granuloma

Gyeong-Yi Kang[1,2†], *Hyeong-Jun Rhyu*[3†], *Hong-Hee Choi*[4], *Sung Jae Shin*[2,4,5*] and *Young-Min Hyun*[1,2*]

[1] Department of Anatomy, Yonsei University College of Medicine, Seoul, South Korea, [2] BK21 PLUS Project for Medical Science, Yonsei University College of Medicine, Seoul, South Korea, [3] Department of Medicine, Yonsei University College of Medicine, Seoul, South Korea, [4] Department of Microbiology, Yonsei University College of Medicine, Seoul, South Korea, [5] Institute for Immunology and Immunological Disease, Yonsei University College of Medicine, Seoul, South Korea

OPEN ACCESS

Edited by:
David Neil McMurray,
Texas A& M Health Science Center,
United States

Reviewed by:
Selvakumar Subbian,
Public Health Research Institute (PHRI), United States
Michiel Van Der Vaart,
Leiden University, Netherlands

***Correspondence:**
Sung Jae Shin
sjshin@yuhs.ac
Young-Min Hyun
ymhyun@yuhs.ac

[†] These authors have contributed equally to this work

Specialty section:
This article was submitted to Microbes and Innate Immunity, a section of the journal Frontiers in Cellular and Infection Microbiology

Received: 18 February 2020
Accepted: 22 April 2020
Published: 15 May 2020

Citation:
Kang G-Y, Rhyu H-J, Choi H-H, Shin SJ and Hyun Y-M (2020) 3D Imaging of the Transparent Mycobacterium tuberculosis-Infected Lung Verifies the Localization of Innate Immune Cells With Granuloma. Front. Cell. Infect. Microbiol. 10:226. doi: 10.3389/fcimb.2020.00226

Using a novel tissue-clearing method, we aimed to visualize the three-dimensional (3D) distribution of immune cells within *Mycobacterium tuberculosis* (Mtb)-infected mice lungs. Ethyl cinnamate-based tissue clearing of Mtb-infected mice lungs was performed to obtain transparent lung samples, which were then imaged using a light sheet fluorescence microscope. Using the 3D images, we performed quantitative analysis of the immune cell population within multiple granulomas. In addition, to compare the data from the tissue clearing method, we performed histopathological and immunofluorescence analyses, and flow cytometry. We then created 3D images of the Mtb-infected lung that successfully demonstrated the distribution of blood vessels, immune cells, and granulomas. Since the immune cells within a granuloma could be separately selected and counted, the immune cell population within a specific lesion could be quantified. In addition, macroscopic analysis, e.g., the size or shape of a granuloma, as well as microscopic analysis could be performed as intact lung samples were used. The use of the tissue clearing method in infected lungs could be a novel modality for understanding the role of the immune system in the pathogenesis of tuberculosis.

Keywords: granuloma, innate immunity, lung, tissue clearing, tuberculosis

INTRODUCTION

Tuberculosis (TB), a pulmonary disease caused by a group of infectious agents named *Mycobacterium tuberculosis* (Mtb) complex, remains one of the major health concerns worldwide. World Health Organization (WHO) reported that nearly 10.4 million people were infected, and 1.7 million deaths were caused by the contagious disease in 2016 (Floyd et al., 2018). The standard treatment for TB includes multiple anti-TB drugs, i.e., isoniazid, rifampin, ethambutol, and pyrazinamide (Tiberi et al., 2018). However, with the advent of drug-resistant TB, which exhibits resistance against one or more of the drugs in the initial regimen, chemotherapy alone has not been demonstrated to control the disease completely (Tiberi et al., 2018). Therefore, novel therapeutic approaches for TB are required.

In light of this need for a new treatment, several researches have attempted to elucidate the role of the innate immune system in the pathogenesis of the disease. The primary cells involved in the initial immune response against TB infection are macrophages, including resident alveolar and monocyte derived macrophages, and neutrophils (Schlesinger, 1996). The defense mechanism of macrophages against the infective agent is relatively well-known. As Mtb enter the alveoli, alveolar macrophages phagocytose the bacteria and subsequently produce various cytokines, recruiting monocytes from the blood and leading to mobilization of monocyte derived macrophages. This is followed by production of reactive oxygen species (ROS) and apoptosis of the recruited macrophages (Pieters, 2008). Recently, several counteractive actions of Mycobacteria against macrophages have also been found (Lerner et al., 2015). In contrast, several findings have identified a controversial role of neutrophils in regard to their interaction with the pathogen (Lowe et al., 2012). Being the most prominent immune cells in human TB, neutrophils are also the most common leukocytes in human blood (Eum et al., 2010). Animal studies have demonstrated that neutrophils play a crucial role in the initial defense against TB (Pedrosa et al., 2000; Fulton et al., 2002; Sugawara et al., 2004). Recruitment of neutrophils results in decreased colony forming units (CFU) while their depletion causes the opposite (Sugawara et al., 2004). One of the known antibacterial actions of neutrophils is its formation of a DNA scaffold, named neutrophil extracellular traps (NET) that entraps pathogens and facilitates bactericidal actions (Papayannopoulos, 2018). However, it has also been reported that there was no difference in the disease course in granulocyte-depleted mice and normal mice (Seiler et al., 2000). Additionally, the contribution of neutrophils is limited to the early stages of the disease (Petrofsky and Bermudez, 1999; Pedrosa et al., 2000; Sugawara et al., 2004; Zhang et al., 2009). In chronic TB infection, neutrophil depletion was shown to be correlated with a decrease in CFU (Zhang et al., 2009). Data from patients also suggest that higher neutrophil count is associated with worse prognosis in well-established TB (Barnes et al., 1988). To summarize, these findings indicate that the role of neutrophils in the immune response of TB remains to be clarified and studying their functions at different stages of the disease may provide a deeper understanding of the pathogenesis.

One possible approach to interpret the complicated immune reaction is to observe the spatial distribution of the immune cells. It has been reported that Mtb-infected macrophages become highly mobile and egress from the primary granuloma, consequently becoming a source of new granulomas in zebrafish and mouse (Davis and Ramakrishnan, 2009; Cohen et al., 2018). This implies that the physical distribution of Mtb-infected macrophages, or how they translocate out of the granuloma, can affect the progress of the disease. In contrast, the local influx of neutrophils has been correlated with worse prognosis while suppressing it by chemokine modulation has a better outcome (Condos et al., 1998; Nandi and Behar, 2011). These findings show that the course of the disease is closely linked with the distribution of the immune cells, such as neutrophils and macrophages. Traditionally, several modalities, e.g., hematoxylin and eosin (H&E) staining, immunohistochemistry, and fluorescence microscopy, have been used to localize cells in a pathologic condition. However, all these methods provide limited information, since the data are mostly 2D images with the possibility of omitting cells. Recently, total organ imaging enabled by a method that makes an organ transparent, namely tissue clearing, is emerging as a novel technique in various fields of research (Chung et al., 2013; Klingberg et al., 2017). One of tissue clearing methods, PACT (passive clarity technique), has also been used for fluorescence-labeled Mtb in the Mtb-infected mouse lungs (Cronan et al., 2015). In this study, we used the another tissue clearing technique using Ethyl cinnamate (ECi) to visualize immune cells within the pathologic tissue. We used 3D imaging technique of the tissue-cleared lung to localize neutrophils and macrophages in Mtb-infected mice lungs. Providing data on the spatial distribution of these immune cells and granulomas, we propose a new modality in understanding the role of the innate immune system in the pathogenesis of TB.

Abbreviations: CFU, colony-forming units; ECi, ethyl cinnamate; FACS, fluorescence-activated cell sorting; FBS, fetal bovine serum; FDA, U.S. Food and Drug Administration; GFP, green fluorescent protein; H&E, hematoxylin and eosin; LFMS, light sheet fluorescence microscopy; Mtb, Mycobacterium tuberculosis; OADC, oleic acid albumin dextrose catalase; PBS, phosphate-buffered saline; TB, tuberculosis; WHO, World Health Organization.

METHODS

Mice

C57BL/6 mice were purchased from Japan SLC Inc. (Shizuoka, Japan). C57BL/6, CX3CR1-GFP (green fluorescent protein) (Jung et al., 2000) and LysM-GFP (Faust et al., 2000) mice were maintained under specific-pathogen-free conditions at the Avison Biomedical Research Center, Yonsei University College of Medicine. In order to minimize the unintended loss in leukocyte motility or its bactericidal function, heterogenetic (+/–) LysM-GFP and CX3CR1-GFP mice were used in the experiments. All animal experiments were performed with the approval by the animal ethics committee of Yonsei University College of Medicine (2016-0178 and 2018-0218).

Infection of Mice

Mice were infected under strict barrier conditions in a BSL-3 facility at the Avison Biomedical Research Center, Yonsei College of Medicine. Briefly, mice were challenged with the pre-calibrated Mtb H37Rv (ATCC 27294) via aerosol using an airborne infection apparatus (Glas-Col, USA), and ∼200 viable bacteria were delivered. Mice at 4 weeks post-infection were used. For the bacterial growth analysis, the lungs were homogenized, and serially diluted samples were plated onto Middlebrook 7H11 agar plates (Becton Dickinson, USA) supplemented with 10% OADC (oleic acid albumin dextrose catalase; Difco Laboratories, USA), 2 μg/mL 2-thiophenecarboxylic acid hydrazide (Sigma-Aldrich, USA), and amphotericin B (Sigma-Aldrich). The bacterial colonies were counted after 3–4 weeks of incubation period at 37°C. The animal ethics committee of Yonsei University

College of Medicine approved all of the experimental protocols used (2016-0178 and 2018-0218).

Histopathological and Immunofluorescence Studies

The naïve and Mtb-infected mice lungs were isolated and fixed in 10% formalin overnight. Fixed lungs were serially dehydrated using ethanol and then infiltrated with paraffin. The lungs were then embedded into the paraffin wax block. Paraffin blocks were sectioned by 4–5 μm thickness, and then stained using H&E. Samples were observed using Olympus BX51 microscope (Olympus, Japan). For immunofluorescence imaging, antigen retrieval was performed using Tris-EDTA. Immune cells were labeled using anti-CD3 (T cells; BioLegend, USA), anti-Ly-6G (neutrophils; Biolegend, USA), and anti-F4/80 (macrophages; BioLegend, USA) antibodies and nuclei were stained using DAPI (4',6-diamidino-2-phenylindole). The slides were observed using the LSM700 confocal microscope (Carl Zeiss, Germany). Volocity Software (Quorum Technologies, Canada) software was used for data analysis.

Flow-Cytometry

The lung samples were minced into 2-4 mm pieces using scissors. The samples were then incubated in 3 mL of cellular dissociation buffer [RPMI medium; Biowest, France)], which contained 0.1% collagenase type IV (Worthington Biochemical Corporation, USA) and 1 mM $CaCl_2$ and 1 mM $MgCl_2$ for 30 min at 37°C. The dissociated cells were then filtered using a 40 μm cell strainer (BD Biosciences, USA) in RPMI medium supplemented with 2% fetal bovine serum (FBS, Biowest, France), and the erythrocytes were removed by incubating the samples in red blood cell lysis buffer (Sigma-Aldrich, USA) for 3 min at room temperature. Finally, the single cells were washed twice in RPMI medium supplemented with 2% FBS before analysis. For flow-cytometric analysis, cells were first washed with 2% FBS containing PBS and anti-CD16/32 antibodies were treated for blocking function at 4°C for 20 min. Surface molecules were labeled with fluorochrome-conjugated anti-CD45 (immune cells), anti-Siglec-F (alveolar macrophages), anti-Ly-6G (neutrophils) (BD bioscience, USA), anti-F4/80 (macrophages), anti-CD11b (monocytes/macrophages, granulocytes) (eBioscience, USA), anti-CD64 (monocyte-derived macrophages), and anti-CD11c (monocytes/macrophages) (Biolegend, USA) antibodies and using the LIVE/DEAD Fixable Dead Cell Stain Kit (Molecular Probes, USA) at 4°C for 30 min. The cells were then washed with PBS, fixed with Intracellular (IC) fixation buffer (eBioscience, USA) for flow cytometry analysis. The cells were subsequently analyzed using a CytoFLEX S Flow Cytometer (Beckman Coulter, USA).

ECi (Ethyl Cinnamate)-Based Tissue Clearing

LysM-GFP and CX3CR1-GFP mice were used for visualization of the immune cells, and FSD-647 *Lycopersicon esculentum* (*L. esculentum*) lectin (BioActs, Korea) was intravenously injected to label glycocalyx in the basal membrane of the endothelial cells. ECi clearing method was selected as it has benefits such as minimizing sample shrinkage and preserving endogenous fluorescence for fluorescence imaging (Klingberg et al., 2017). In addition, the method is not toxic, and has been approved by the U.S. Food and Drug Administration (FDA). The aqueous buffer clearing method was excluded as it can make samples inadequately clear and may cause the samples to swell giving them a jelly-like texture. Before conducting tissue clearing using the ECi solution, the mice were perfused with 1X PBS and 4% formaldehyde via the myocardial route. Perfusion using this method enables effective fixation of mice lungs by utilizing the circulatory system of the animal. The intact lungs were then fixed in 4% formaldehyde solution for 2 h and dehydrated in alkaline solutions for 12 h (50/70/100% ethanol, 4 h each). Finally, the samples were cleared using the ECi solution (Alfa Aesar, USA) for 30 min at room temperature. All incubation processes were conducted away from light. The cleared samples were stored in polypropylene tubes till the imaging was done. Light sheet fluorescence microscopy (LFMS) was performed using UltraMicroscope II (LaVison BioTec, Germany). The samples were fixed with and immersed in absolute ECi solution in the mounting chamber during the imaging. Dual side illumination was used, and each plane was obtained every 7 μm. Imaris software (Bitplane, Switzerland) was used to analyze the whole-organ 3D images. The cell counts, volume and area of the granulomas were measured.

Statistical Analysis

The cell count data were described as either mean ± standard deviation (flow cytometric studies) or mean ± standard error of the mean (histopathological and immunofluorescence studies, and tissue clearing). Prism version 7 (GraphPad Software, USA) was used for statistics and Student's *t*-test was used for analysis.

RESULTS

Flow cytometric studies were performed in order to quantify three types of immune cells: neutrophils, alveolar macrophages, and infiltrating macrophages, in both naïve and Mtb-infected mice lungs (**Figure 1**). All the Mtb-infected mice used in this study were in their fourth week post-infection, at which point the total CFU of the Mtb (T = 4 weeks) showed a higher increase than that at the first day of infection (T = 1 day) (**Figure 1A**). As described in **Figure 1B**, flow cytometric studies of both naïve and Mtb-infected mice lungs were performed to compare the population of neutrophils ($CD45^+$ and $Ly6G^+$), alveolar macrophages ($CD45^+$ and $Siglec\text{-}F^+$), and infiltrating macrophages ($CD45^+$ and $CD64^+$) between two groups. The proportion of the immune cells showed a notable difference between two groups (**Figure 1C**). In the naïve group, resident alveolar macrophages ($CD45^+$ and $Siglec\text{-}F^+$) was the predominant cell type (3.97%). Neutrophils and infiltrating macrophages represented 2.74% and 1.77% of the cell population, respectively. In contrast, neutrophils were the most abundant cell type in Mtb-infected lung (8.10%). This was followed by infiltrating macrophages (4.26%), while the proportion of alveolar macrophages was relatively insignificant

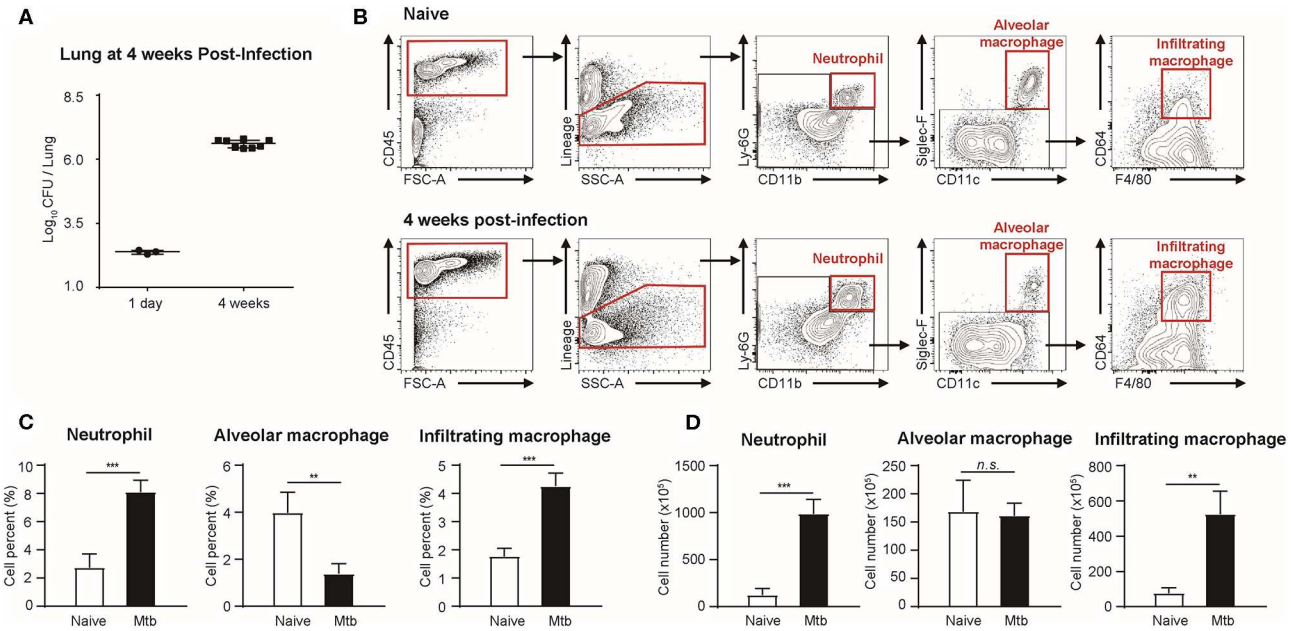

FIGURE 1 | Quantitative analysis of immune cell population in naïve and Mtb (*Mycobacterium tuberculosis*)-infected mice lungs (4 weeks post-infection). **(A)** colony-forming units (CFU) 1 h after (T = 1 day, $n = 3$) and 4 weeks after (T = 4 weeks, $n = 4$) infection with Mtb. **(B)** Gating strategy of immune cells. **(C)** The proportion (%) and **(D)** the absolute count ($\times 10^5$) of different subtypes of immune cells were quantified and compared between naïve and Mtb-infected groups [four mice per group, mean ± standard deviation (SD)]. Statistical analysis was performed using the Student's *t*-test. $^{**}P < 0.01$, $^{***}P < 0.005$. n.s., not significant.

(1.37%). The actual cell count of alveolar macrophages, however, showed no difference between two groups (**Figure 1D**). Instead the total cell number in the infected group was larger, making the relative proportion of alveolar macrophages smaller. Both neutrophils and infiltrating macrophages were drastically increased in the infected lung. The mean number of neutrophils was nearly 7 times larger than that of the uninfected lungs, and the mean number of infiltrating macrophages was more than 5 times larger than that of the uninfected lung. These data suggest that both neutrophils and macrophages mediate the host immune reaction against Mtb infection.

The morphology and the immune cell population were compared between the naïve and Mtb-infected mice lungs (**Figure 2**). At low magnification, the whole lung section could be viewed (**Figure 2A**, upper panel). The granulomas were well-demarcated from the surrounding tissue. At higher magnification, the granulomas showed a highly cellular lesion lacking the normal alveolar structure seen in the naïve lung (**Figure 2A**). This is consistent with a previous finding that granulomas in C57BL/6 mouse are exclusively cellular without any necrosis or hypoxia (Medina and North, 1998). In order to classify the types of cells in this highly cellular structure, immunofluorescence (IF) microscopy was performed (**Figure 2B**). Neutrophils, macrophages, and T lymphocytes were distinguished and counted. Since the lung samples were not perfused, most of the immune cells in the naïve mice were located within the alveolar vessels and the non-granulomatous area of the infected mice showed a similar distribution. In contrast, both neutrophils and macrophages were dispersed irregularly throughout the granuloma. The cell number of each subtype of immune cells was counted (**Figure 2C**). A slight difference in the immune cell population was observed between the granulomas and naive mice lungs, but the difference was not significant (**Figure 2C**). However, compared with the non-granulomatous area, the infected group contained a larger number of all three subtypes of immune cells than the naïve group (**Figure 2C**). As stated above, both H&E and immunofluorescence images reveal a limited view of the organ, as they are 2D sectioned images. The sectioned view represents only a part of the whole lesion, making it challenging to quantitatively compare normal and pathologic conditions.

To overcome the limit of 2D analytical methods, 3D whole-lung imaging was performed in each of the cleared samples (**Figure 3**). In order to observe macrophages, the fluorescence was obtained using CX3CR1-GFP mice that produce green fluorescence protein (GFP) largely in macrophages (Jung et al., 2000) (**Figure 3A** and **Supplementary Videos 1**, **2**). In order to visualize neutrophils, LysM-GFP mice that has GFP in their neutrophils were used (Faust et al., 2000) (**Figure 3B** and **Supplementary Videos 3**, **4**). As the lung tissue itself has an auto-fluorescence (Ramanujam, 2000), the structures of the lungs such as the pleura or the bronchus could be identified along with the fluorescent cells (**Figures 3A,B** and **Supplementary Videos 1–4**). Multiple granulomas, whose intact shape and size were preserved, were detected in the infected lungs and their distribution in the entirety of the

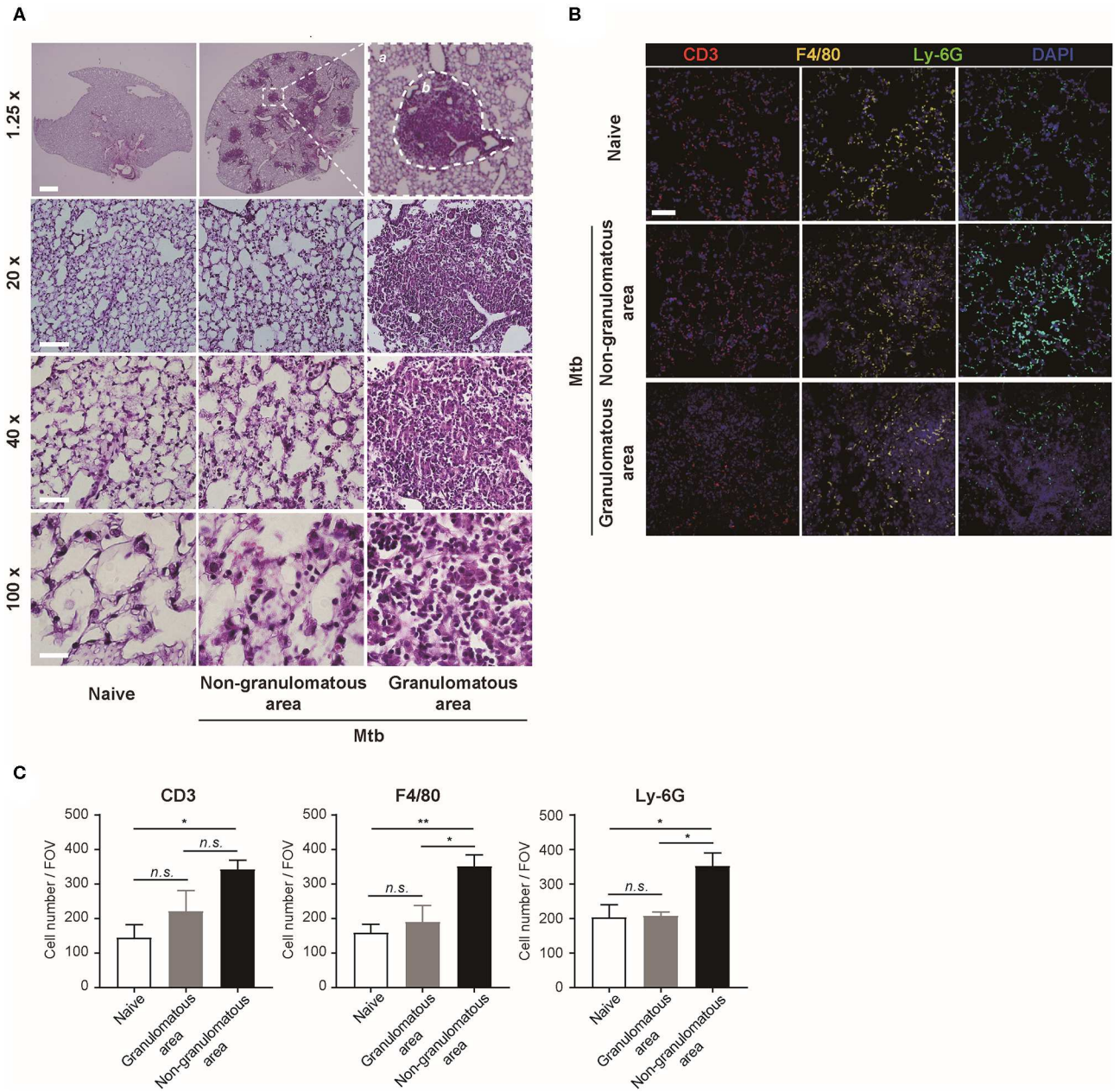

FIGURE 2 | Microscopic morphology and immune cell distribution in naïve and Mtb-infected mice's lungs **(A)** Hematoxylin and eosin (H&E) staining of naïve and Mtb-infected mice lungs (Scale bar, 1.25X: 1 mm, 20X: 100 μm, 40X: 50 μm, 100X: 20 μm). The magnified image contains a single granulomatous area (b) separating it from the non-granulomatous area (a) via a dotted line. **(B)** Immunofluorescence staining of naïve and Mtb-infected mice lungs to verify specific immune cell subtypes. Scale bar, 50 μm. **(C)** The cell counts were compared between the naïve and Mtb-infected group, including granulomatous and non-granulomatous area. Manual counting of each of the immunofluorescence-stained sections was performed [three fields per section, three sections per mouse, three mice per group, mean ± standard error of mean (SEM)]. Statistical analysis was performed using the Student's *t*-test. $^{*}P < 0.05$, $^{**}P < 0.01$. Field of view (FOV): 10.24 mm². n.s., not significant.

lungs could be visualized (**Figures 3A,B**). Both neutrophils and macrophages were aggregated near the granulomas. Using zoomed-in images, a single granuloma could be selected and reconstructed into a graphic mass (green), whose volume could be measured (**Figure 3C** and **Supplementary Video 5**). Since the fluorescence of the background tissues could be deleted by modulating the field of intensity, the cellular components could be separately selected. The cells were marked as spots (green; **Figure 3C**). We analyzed the cell counts, specifically those within the borders of the granuloma in the infected samples and divided it by the volume of each granuloma. The number of macrophages were significantly higher in

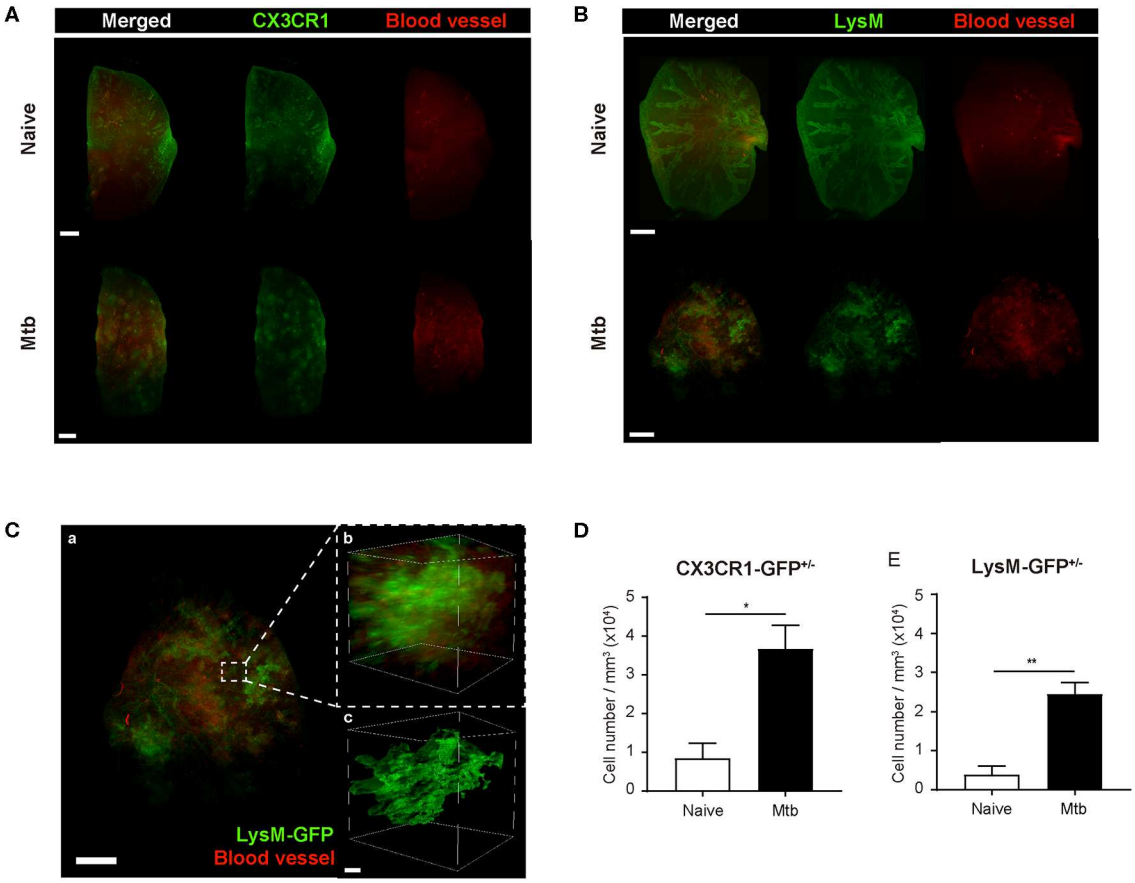

FIGURE 3 | Three-dimensional visualization of the cleared naïve and Mtb-infected mice lung. **(A,B)** Granulomas were clearly detected using CX3CR1-GFP (green fluorescent protein) and LysM-GFP mice. The formation of the blood vessels around the granulomas was also observed. **(C)** The zoomed-in image, containing a single granuloma, was reconstructed as an image of a graphic mass, representing the granuloma, and spots, representing the fluorescent immune cells, for quantitative analysis. **(D,E)** The number of macrophages and neutrophils per volume was compared between naïve and infected group (three granulomas per mouse, three mice per group, mean ± SEM). Statistical analysis was performed using the Student's *t*-test. $^{*}P < 0.05$, $^{**}P < 0.01$.

the Mtb-infected granuloma (**Figure 3D**). In addition, the number of neutrophils were higher in the infected group than the naïve group (**Figure 3E**). These results were similar to that obtained by the flow cytometric studies. However, since the cell count was limited to the granulomas, this result is more reliable in regard to the analysis of the granulomatous lesions.

To map the vascular distribution of the organ, florescent-labeled *L. esculentum* lectin was infused via the retro-orbital vein to visualize blood vessels prior to sample preparation. It has been reported that uncontrolled angiogenesis occurs in the lungs following Mtb infection (Cronan et al., 2015; Oehlers et al., 2015). Consistent with this report, the vascular distribution differed between the naïve and Mtb-infected mouse's lungs (**Figure 3**). In the naïve mouse's lung, the vasculature was distributed evenly over the entire organ, showing typical alveolar structures (**Figures 3A,B**, upper right panels). However, in the Mtb-infected lungs, the vessels showed a more concentrated distribution around the granulomas (**Figures 3A,B**, lower right panels). In a zoomed-in image of a granuloma (**Figure 3C**), the vessels appeared to form an outer layer of the lesion, which suggests that the angiogenesis around the granulomas can cause a difference in vascular distribution.

DISCUSSION

In this study, we employed a tissue-clearing method using ECi solution that preserves the fluorescence of fluorescent proteins, such as GFP, while making an intact organ transparent (Klingberg et al., 2017). Through this procedure, we were able to generate 3D images of the whole mouse lungs containing granulomatous lesions. We demonstrated the distribution of immune cells within each of the selected granulomas and performed a quantitative analysis comparing the immune cell population between Mtb-infected and naïve mouse lungs. The novelty of this study lies in its innovative approach to visualize the immune reactions during TB infection. Compared to the conventional methods such as H&E staining, FACS (fluorescence-activated cell sorting),

clearing of the whole lung has a clear advantage of visualizing how the immune cells with fluorescence are located within the pathologic lesion. This allows an accurate counting of specific subtypes of immune cells, which is limited using 2D-sectioned images. In addition, since lung clearing uses the whole lung sample, macroscopic analysis, e.g., shape, volume, distribution of granuloma, can be performed simultaneously with the microscopic analysis. This method can be used in a variety of studies aiming to interpret or modulate the immune response against Mtb infection and should be further evaluated for its application in studying other diseases. For 3D images for the tissue-cleared lungs captured by light sheet microscopy, we employed low magnitude objective lens to acquire the larger area imaging including multiple granulomas, which may result in low-resolution images. To avoid a bias of manual counting of cell numbers from the image data, we performed cell counting by the Imaris software depending on the size and the intensity of the fluorescent cells. Although we just used only 4 weeks period of TB infection for immune cells counting in this study, as an innovative modality to visualize and quantify the immune reactions in TB infection, the whole lung clearing could be a versatile tool to find better clue for therapeutics against TB in combination with other experimental techniques.

DATA AVAILABILITY STATEMENT

All datasets generated for this study are included in the article/**Supplementary Material**.

ETHICS STATEMENT

The animal study was reviewed and approved by Yonsei University College of Medicine.

AUTHOR CONTRIBUTIONS

G-YK and H-JR performed the experiments and wrote the manuscript. H-HC provided essential reagents for the experiments. SS and Y-MH conceived the study and wrote the manuscript.

FUNDING

This study was supported by the National Research Foundation of Korea (NRF) grant funded by the Korea government (MSIT) (NRF-2019R1A2C2003204, SS and NRF-2019R1A2C2008481, Y-MH) Republic of Korea.

SUPPLEMENTARY MATERIAL

The Supplementary Material for this article can be found online at: https://www.frontiersin.org/articles/10.3389/fcimb.2020.00226/full#supplementary-material

Supplementary Video 1 | 3D clearing imaging of naïve CX3CR1-GFP$^{+/-}$ mouse's lung. Green and red fluorescence represents CX3CR1$^{+/-}$ cells and blood vessels, respectively.

Supplementary Video 2 | 3D clearing imaging of Mtb-infected CX3CR1-GFP$^{+/-}$ mouse's lung. Green and red fluorescence represents CX3CR1$^{+/-}$ cells and blood vessels, respectively. Blood vessels are aggregated around the granulomas.

Supplementary Video 3 | 3D clearing imaging of naïve LysM-GFP$^{+/-}$ mouse's lung. Green and red fluorescence represents LysM-GFP$^{+/-}$ cells and blood vessels, respectively.

Supplementary Video 4 | 3D view of Mtb-infected LysM-GFP$^{+/-}$ mouse's lung. Green and red fluorescence represents LysM-GFP$^{+/-}$ cells and blood vessels, respectively. Blood vessels are clumped around the granuloma lesion.

Supplementary Video 5 | A single granuloma of Mtb-infected LysM-GFP$^{+/-}$ mouse's lung. For analysis, a single granulomatous area was reconstructed into a graphic mass, and volume could be measured, also LysM-GFP$^{+/-}$ cells could be defined as green dots.

REFERENCES

Barnes, P. F., Leedom, J. M., Chan, L. S., Wong, S. F., Shah, J., Vachon, L. A., et al. (1988). Predictors of short-term prognosis in patients with pulmonary tuberculosis. *J. Infect. Dis.* 158, 366–371. doi: 10.1093/infdis/158.2.366

Chung, K., Wallace, J., Kim, S. Y., Kalyanasundaram, S., Andalman, A. S., Davidson, T. J., et al. (2013). Structural and molecular interrogation of intact biological systems. *Nature* 497, 332–337. doi: 10.1038/nature12107

Cohen, S. B., Gern, B. H., Delahaye, J. L., Adams, K. N., Plumlee, C. R., Winkler, J. K., et al. (2018). Alveolar macrophages provide an early *Mycobacterium tuberculosis* niche and initiate dissemination. *Cell Host Microbe* 24, 439–446.e434. doi: 10.1016/j.chom.2018.08.001

Condos, R., Rom, W. N., Liu, Y. M., and Schluger, N. W. (1998). Local immune responses correlate with presentation and outcome in tuberculosis. *Am. J. Respir. Crit. Care Med.* 157, 729–735. doi: 10.1164/ajrccm.157.3.9705044

Cronan, M. R., Rosenberg, A. F., Oehlers, S. H., Saelens, J. W., Sisk, D. M., Jurcic Smith, K. L., et al. (2015). CLARITY and PACT-based imaging of adult zebrafish and mouse for whole-animal analysis of infections. *Dis. Model Mech.* 8, 1643–1650. doi: 10.1242/dmm.021394

Davis, J. M., and Ramakrishnan, L. (2009). The role of the granuloma in expansion and dissemination of early tuberculous infection. *Cell* 136, 37–49. doi: 10.1016/j.cell.2008.11.014

Eum, S. Y., Kong, J. H., Hong, M. S., Lee, Y. J., Kim, J. H., Hwang, S. H., et al. (2010). Neutrophils are the predominant infected phagocytic cells in the airways of patients with active pulmonary TB. *Chest* 137, 122–128. doi: 10.1378/chest.09-0903

Faust, N., Varas, F., Kelly, L. M., Heck, S., and Graf, T. (2000). Insertion of enhanced green fluorescent protein into the lysozyme gene creates mice with green fluorescent granulocytes and macrophages. *Blood* 96, 719–726. doi: 10.1182/blood.V96.2.719

Floyd, K., Glaziou, P., Zumla, A., and Raviglione, M. (2018). The global tuberculosis epidemic and progress in care, prevention, and research: an overview in year 3 of the End TB era. *Lancet Respir. Med.* 6, 299–314. doi: 10.1016/S2213-2600(18)30057-2

Fulton, S. A., Reba, S. M., Martin, T. D., and Boom, W. H. (2002). Neutrophil-mediated mycobacteriocidal immunity in the lung during Mycobacterium bovis BCG infection in C57BL/6 mice. *Infect. Immun.* 70, 5322–5327. doi: 10.1128/IAI.70.9.5322-5327.2002

Jung, S., Aliberti, J., Graemmel, P., Sunshine, M. J., Kreutzberg, G. W., Sher, A., et al. (2000). Analysis of fractalkine receptor CX(3)CR1 function by targeted deletion and green fluorescent protein reporter gene insertion. *Mol. Cell Biol.* 20, 4106–4114. doi: 10.1128/MCB.20.11.4106-4114.2000

Klingberg, A., Hasenberg, A., Ludwig-Portugall, I., Medyukhina, A., Mann, L., Brenzel, A., et al. (2017). Fully automated evaluation of total glomerular number and capillary tuft size in nephritic kidneys using lightsheet microscopy. *J. Am. Soc. Nephrol.* 28, 452–459. doi: 10.1681/ASN.2016020232

Lerner, T. R., Borel, S., and Gutierrez, M. G. (2015). The innate immune response in human tuberculosis. *Cell Microbiol.* 17, 1277–1285. doi: 10.1111/cmi.12480

Lowe, D. M., Redford, P. S., Wilkinson, R. J., O'Garra, A., and Martineau, A. R. (2012). Neutrophils in tuberculosis: friend or foe? *Trends Immunol.* 33, 14–25. doi: 10.1016/j.it.2011.10.003

Medina, E., and North, R. J. (1998). Resistance ranking of some common inbred mouse strains to *Mycobacterium tuberculosis* and relationship to major histocompatibility complex haplotype and Nramp1 genotype. *Immunology* 93, 270–274. doi: 10.1046/j.1365-2567.1998.00419.x

Nandi, B., and Behar, S. M. (2011). Regulation of neutrophils by interferon-gamma limits lung inflammation during tuberculosis infection. *J. Exp. Med.* 208, 2251–2262. doi: 10.1084/jem.20110919

Oehlers, S. H., Cronan, M. R., Scott, N. R., Thomas, M. I., Okuda, K. S., Walton, E. M., et al. (2015). Interception of host angiogenic signalling limits mycobacterial growth. *Nature* 517, 612–615. doi: 10.1038/nature13967

Papayannopoulos, V. (2018). Neutrophil extracellular traps in immunity and disease. *Nat. Rev. Immunol.* 18, 134–147. doi: 10.1038/nri.2017.105

Pedrosa, J., Saunders, B. M., Appelberg, R., Orme, I. M., Silva, M. T., and Cooper, A. M. (2000). Neutrophils play a protective nonphagocytic role in systemic *Mycobacterium tuberculosis* infection of mice. *Infect. Immun.* 68, 577–583. doi: 10.1128/IAI.68.2.577-583.2000

Petrofsky, M., and Bermudez, L. E. (1999). Neutrophils from Mycobacterium avium-infected mice produce TNF-alpha, IL-12, and IL-1 beta and have a putative role in early host response. *Clin. Immunol.* 91, 354–358. doi: 10.1006/clim.1999.4709

Pieters, J. (2008). *Mycobacterium tuberculosis* and the macrophage: maintaining a balance. *Cell Host Microbe* 3, 399–407. doi: 10.1016/j.chom.2008.05.006

Ramanujam, N. (2000). Fluorescence spectroscopy of neoplastic and non-neoplastic tissues. *Neoplasia* 2, 89–117. doi: 10.1038/sj.neo.7900077

Schlesinger, L. S. (1996). Entry of *Mycobacterium tuberculosis* into mononuclear phagocytes. *Curr. Top Microbiol. Immunol.* 215, 71–96. doi: 10.1007/978-3-642-80166-2_4

Seiler, P., Aichele, P., Raupach, B., Odermatt, B., Steinhoff, U., and Kaufmann, S. H. (2000). Rapid neutrophil response controls fast-replicating intracellular bacteria but not slow-replicating *Mycobacterium tuberculosis*. *J. Infect. Dis.* 181, 671–680. doi: 10.1086/315278

Sugawara, I., Udagawa, T., and Yamada, H. (2004). Rat neutrophils prevent the development of tuberculosis. *Infect. Immun.* 72, 1804–1806. doi: 10.1128/IAI.72.3.1804-1806.2004

Tiberi, S., Walzl, G., Vjecha, M. J., Rao, M., Ntoumi, F., Mfinanga, S., et al. (2018). Tuberculosis: progress and advances in development of new drugs, treatment regimens, and host-directed therapies. *Lancet Infect. Dis.* 18, e183–e198. doi: 10.1016/S1473-3099(18)30110-5

Zhang, X., Majlessi, L., Deriaud, E., Leclerc, C., and Lo-Man, R. (2009). Coactivation of Syk kinase and MyD88 adaptor protein pathways by bacteria promotes regulatory properties of neutrophils. *Immunity* 31, 761–771. doi: 10.1016/j.immuni.2009.09.016

Conflict of Interest: The authors declare that the research was conducted in the absence of any commercial or financial relationships that could be construed as a potential conflict of interest.

frontiers in Cellular and Infection Microbiology

REVIEW
published: 03 June 2020
doi: 10.3389/fcimb.2020.00263

Myeloid C-Type Lectin Receptors in Tuberculosis and HIV Immunity: Insights Into Co-infection?

*Kubra F. Naqvi and Janice J. Endsley**

Department of Microbiology and Immunology, The University of Texas Medical Branch, Galveston, TX, United States

C-type lectin receptors (CLRs) are carbohydrate binding pattern recognition receptors (PRRs) which play a central role in host recognition of pathogenic microorganisms. Signaling through CLRs displayed on antigen presenting cells dictates important innate and adaptive immune responses. Several pathogens have evolved mechanisms to exploit the receptors or signaling pathways of the CLR system to gain entry or propagate in host cells. CLR responses to high priority pathogens such as *Mycobacterium tuberculosis (Mtb),* HIV, Ebola, and others are described and considered potential avenues for therapeutic intervention. *Mtb* and HIV are the leading causes of death due to infectious disease and have a synergistic relationship that further promotes aggressive disease in co-infected persons. Immune recognition through CLRs and other PRRs are important determinants of disease outcomes for both TB and HIV. Investigations of CLR responses to *Mtb* and HIV, to date, have primarily focused on single infection outcomes and do not account for the potential effects of co-infection. This review will focus on CLRs recognition of *Mtb* and HIV motifs. We will describe their respective roles in protective immunity and immune evasion or exploitation, as well as their potential as genetic determinants of disease susceptibility, and as avenues for development of therapeutic interventions. The potential convergence of CLR-driven responses of the innate and adaptive immune systems in the setting of *Mtb* and HIV co-infection will further be discussed relevant to disease pathogenesis and development of clinical interventions.

Keywords: tuberculosis, HIV, TB and HIV co-infection, innate immunity, C-type lectin receptors

OPEN ACCESS

Edited by:
Alexander S. Apt, Central Tuberculosis Research Institute (RAMS), Russia

Reviewed by:
Supriya Shukla, Case Western Reserve University, United States
Konstantin Neumann, Hannover Medical School, Germany

****Correspondence:***
Janice J. Endsley
jjendsle@utmb.edu

Specialty section:
This article was submitted to Microbes and Innate Immunity, a section of the journal Frontiers in Cellular and Infection Microbiology

Received: *07 January 2020*
Accepted: *04 May 2020*
Published: *03 June 2020*

Citation:
Naqvi KF and Endsley JJ (2020) Myeloid C-Type Lectin Receptors in Tuberculosis and HIV Immunity: Insights Into Co-infection? Front. Cell. Infect. Microbiol. 10:263. doi: 10.3389/fcimb.2020.00263

INTRODUCTION

TB and HIV are the leading causes of death by infectious agents globally (WHO, 2019a,b). In 2018, an estimated 10 million people fell ill with TB and 1.2 million deaths occurred among HIV-negative people globally (WHO, 2019a). Approximately 37.9 million people are currently living with HIV/AIDS and 1.1 million die each year (WHO, 2019b). Tuberculosis remains a large risk factor for people living with HIV (PLWH)/AIDS and HIV-associated TB was the cause of an additional 251,000 deaths in 2018. The co-infection of *Mycobacterium tuberculosis* (*Mtb)* and HIV contributes to the large burden on healthcare systems of endemic areas and have increased the priority of improved co-infection therapeutic strategies (WHO, 2019a,b).

Cell mediated immunity (CMI), especially that mediated by $CD4^{+}$T cells, is essential for host resistance to *Mtb* (Cooper, 2009). HIV infection drives progressive depletion and

dysfunction of leukocytes of the CMI response (Pawlowski et al., 2012) including defects that persist following anti-retroviral therapy (ART). A synergistic deterioration of the immune system is associated with aggressive disease in those with co-infection through mechanisms that are incompletely characterized. Although the loss of protective immunity in PLWH is primarily attributed to $CD4^+$T cell loss and dysfunction in the progression to AIDS, those with co-infection nonetheless display immune disturbance prior to significant T cell loss (Sharma et al., 2005; de Noronha et al., 2008; Sester et al., 2010).

Innate and adaptive immune cells which are resistant to direct infection display functional defects in the setting of HIV infection due to indirect effects on cell toxicity and immune signaling networks by viral mediators (Mazzuca et al., 2016; Garg and Joshi, 2017). Myeloid cell populations including monocytes, macrophages and dendritic cells are targets for HIV infection; macrophages in particular are an important viral reservoir (Igarashi et al., 2001; Heesters et al., 2015; Honeycutt et al., 2017). As the primary hosts for *Mtb* propagation, the direct and indirect effects of HIV infection on myeloid cell innate function are an important and poorly understood factor for the outcome of co-infection.

Signaling through myeloid cell PRRs dictates important innate recognition and responses to *Mtb* and HIV molecular patterns that may direct the progression of disease in co-infection scenarios. Engagement of PRRs such as toll-like receptors (TLR), nod-like receptors (NLR) and CLRs, and the downstream immune responses that are elicited is critical for dictating outcomes of individual disease during TB or HIV as previously reviewed (Mesman and Geijtenbeek, 2012; Hossain and Norazmi, 2013; Mortaz et al., 2015). In brief, TLRs interact with specific mycobacterial ligands to initiate phagosome maturation, pro-inflammatory, and anti-inflammatory cytokine secretion (e.g., IL-12, IL-18, and IL-10) (Kim et al., 2019). The resulting induction of IFN-γ further activates antimicrobial pathways of infected macrophages (Hossain and Norazmi, 2013; Mortaz et al., 2015). HIV infection activates TLR signaling pathways (Meier et al., 2007; Lester et al., 2008) that contribute to host restriction through induction of antiviral interferons or activation of cytokines that promote viral transcription (Mesman and Geijtenbeek, 2012).

Nod-like receptors are cytosolic PRRs which recognize intracellular bacterial and viral pathogens to further mediate macrophage activation. NOD-1 and 2 signaling following *Mtb* infection facilitates mycobacterial survival by suppressing apoptosis of macrophages (Mortaz et al., 2015). Additionally, NLRP3-dependent inflammasome activation of macrophages exposed *in vitro* to *Mtb* promotes IL-1β secretion and cell death (Mortaz et al., 2015). Inflammasome activation by NOD-like receptors is also a major mechanism of pyroptotic $CD4^+$T cell depletion due to HIV in *ex vivo* models of infection (Doitsh et al., 2014; Tomalka et al., 2016). HIV genomic RNA and newly synthesized mRNA in infected macrophages is also detected by the Rig-I like receptors (RLR) in the cytosol. RLRs drive the production of type-1 IFNs following recognition of intracellular pathogens (Bergantz et al., 2019), inducing expression of interferon stimulated genes and eliciting an antiviral response. However, HIV can evade this mechanism through degradation of RIG-I by a viral protease (Bergantz et al., 2019).

The surface bound CLRs, especially abundant on innate leukocytes of the myeloid lineage, also bind to molecular patterns of *Mtb* and HIV (Turville et al., 2003; Mishra et al., 2017). The characteristic glycosylation of the mycobacterial cell wall and HIV envelope protein gp120 (Turville et al., 2001; Guttman et al., 2015; Ishikawa et al., 2017), engage CLRs, which recognize carbohydrate motifs. Molecular recognition through CLRs triggers a myriad of downstream signaling events that modulate ligand and CLR-specific immune outcomes (Geijtenbeek and Gringhuis, 2009). Our understanding of the role of CLRs in TB and HIV mono-infections is rapidly evolving through active investigation. In contrast, the effect of co-infection to exacerbate, confound, or otherwise perturb signaling through CLR pathways is largely uncharacterized.

This review will discuss the current state of knowledge regarding CLRs with described roles in innate immune recognition of *Mtb* and HIV. The contribution of these CLR pathways to protective and non-protective immune outcomes will be discussed in the context of mono- and or co-infection settings. Finally, the potential to exploit CLR pathways for clinical interventions that prevent or reduce disease due to this important dual pandemic will be discussed.

CLRS REGULATE PROTECTIVE AND PATHOGENIC OUTCOMES OF TB AND HIV

Dendritic cells (DCs) and macrophages are sentinel antigen presenting cells (APC) and are therefore well equipped with PRRs to engage molecular motifs of *Mtb* or HIV during infection. The CLRs of antigen presenting cells bind self and non-self-antigens to activate and/or suppress immune function and internalize pathogens (McGreal et al., 2005). CLRs can be classified based on structural, carbohydrate recognition and signaling features (Dambuza and Brown, 2015). The carbohydrate recognition domain is a compact structural motif of CLRs which determines carbohydrate specificity and binds ligands in Ca^{2+} dependent or independent manner (Geijtenbeek and Gringhuis, 2009).

The transmembrane CLRs are further divided into groups, the type I mannose receptor family and the type II asialoglycoprotein receptor family which includes further subfamilies (dectin 1 and DCIR) (Geijtenbeek and Gringhuis, 2009). The signaling motifs of CLRs can also be used to categorize these receptors further. Transmembrane CLRs can include immunoreceptor tyrosine-based activation (ITAM) or inhibitory (ITIM) motifs while some CLRs signal through a single tyrosine-based motif termed hem-ITAM (Osorio and Reis e Sousa, 2011). Many transmembrane and soluble CLRs carry out essential functions in immune homeostasis and innate responses against a wide variety of pathogens. This review will focus on CLRs associated with *Mtb* and HIV infections including the mannose receptor, Mincle, Dectins 1 and 2, Mannose Binding Lectin, DC-SIGN, Langerin and DCIR (**Figure 1**).

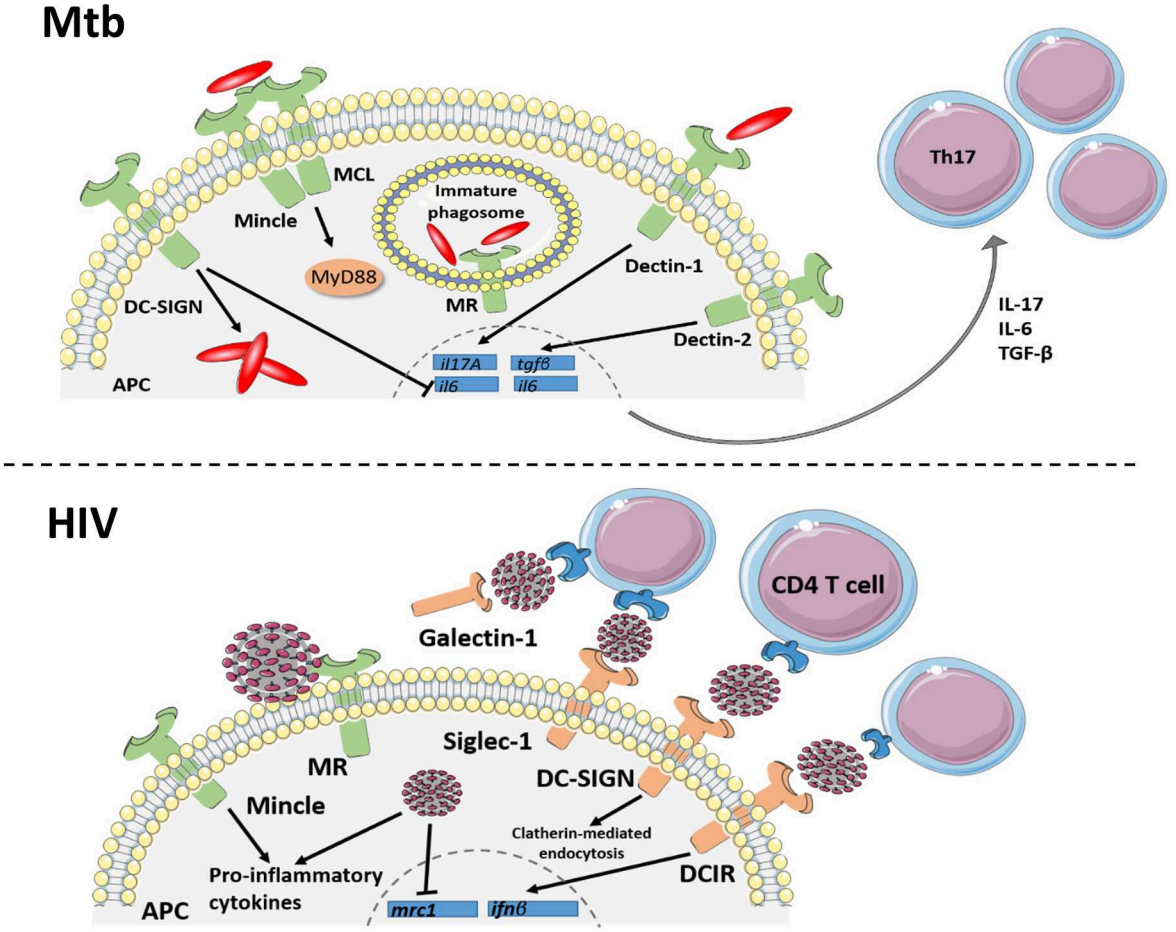

FIGURE 1 | C-type lectin receptor signaling in TB and HIV. Signaling through C-type lectins is an important driver of innate and adaptive responses against *Mtb* infection. Dectin 1 and 2 signaling within APCs results in expression of *il17A, il6* and *tgfβ* transcript for the differentiation of Th17 cell subsets. DC-SIGN can inhibit the IL-6 response of Dectin-1, producing an anti-inflammatory environment, which favors *Mtb* intracellular growth. Mincle, which binds to mycobacterial TDM, forms a heterodimer with another CLR, MCL, to induce protective cytokine responses through the MyD88 signaling pathway. Mannose receptor (MR), binding to mannosylated *Mtb*, initiates phagocytosis while also inhibiting phagosome maturation within macrophages. Additionally, C-type lectin receptors bind to the HIV envelope protein, gp120, to mediate or restrict viral transmission and regulate inflammatory responses. The transmembrane CLRs, DC-SIGN, DCIR and siglec-1 facilitate trans-infection of HIV to $CD4^{+}$T cells through the lymphatics. Additionally, the soluble CLR, galectin-1, improves HIV binding to the CD4 receptor. Signaling of dendritic cell receptors, DC-SIGN and DCIR, also aid in host defense against HIV by internalizing viral particles and initiating an antiviral type I interferon response, respectively. As another mechanism of host defense, the macrophage mannose receptor restricts viral particle budding, although HIV can evade this mechanism by downregulating the *mrc1* gene. HIV also increases Mincle-induced pro-inflammatory cytokine production in *in vitro* models of infection. Together, these CLRs demonstrate the multifaceted role of receptor binding in HIV protection and pathogenesis and regulating the innate immune response to *Mtb*.

MANNOSE RECEPTOR

The mannose receptor (MR, CD206) is a type I transmembrane CLR present on alveolar macrophages, M2 macrophages and dendritic cells. Binding of MR to sulfated and mannosylated sugars results in internalization of antigen and delivery to the MHC II and CD1b pathways (Martinez-Pomares, 2012). Receptor engagement by *Mtb* has served as a model system to characterize MR signaling outcomes and further define an innate immune role in TB. Virulent *Mtb* induces PPAR-γ-dependent inflammatory responses, including IL-8 and cyclooxygenase 2 expression, through a MR dependent pathway (Rajaram et al., 2010). MR binds to *Mtb* liparabinomannan and mannosylated proteins, resulting in interaction with the FcRγ-chain which mediates surface localization and activation of the Grb2 adaptor molecule required for phagocytosis (Rajaram et al., 2017). MR recruitment of the tyrosine phosphatase, SHP-1, however, limits the PI(3)P production needed for maturation of the *Mtb*-containing phagosome (Rajaram et al., 2017). As currently understood, recognition of *Mtb* PAMPs through MR activates important inflammatory and phagocytic function of APCs, but may also promote intracellular *Mtb* survival through inhibition of phagosome-lysosome fusion.

The distribution of MR as a phenotypic marker of alternatively activated, or M2, macrophages in unique subsets and disease processes has also informed our understanding of its immune

role. MR is a selective marker of perivascular macrophages in human and non-human primate CNS tissue and a marker of phenotypic switch (CD206+ to CD206-) during HIV neuroinflammation (Holder et al., 2014). Expression of MR on peripheral macrophages can also serve as a potential biomarker to identify those with dual HIV strain infections. MR expression decreases following ART treatment for patients with HIV-1 or HIV-2, and remains constant in those with dual infection despite treatment (Andersen et al., 2018). Cellular expression of MR also contributes to sexual transmission of HIV as an alternative entry receptor in vaginal epithelial cells, the primary site of male-to-female transmission (Jadhav et al., 2013).

Binding of MR to HIV gp120 induces production of matrix metalloproteinase (MMPs) breaking down the extracellular matrix and permitting HIV to cross the epithelial barrier to gain access to sub-epithelial $CD4^+$ cells (Fanibunda et al., 2011). In addition to expression on vaginal epithelial cells, MR expression on sperm cells has been shown *in vitro* to mediate infection to susceptible cells, suggesting a possible role for sperm cells as vectors for sexual transmission of HIV (Fanibunda et al., 2008; Cardona-Maya et al., 2011). Binding of HIV gp120 to MR is further enhanced by oligomerization of the receptor on macrophages and dendritic cells, further promoting trans-infection of $CD4^+$T lymphocytes (Lai et al., 2009). An anti-viral role for MR has also been described and occurs through prevention of HIV particle release from infected cells (Sukegawa et al., 2018). Interestingly, HIV counteracts this antiviral activity by repressing MR transcription (Sukegawa et al., 2018).

The role for MR in the innate function of APCs in response to *Mtb* or HIV is increasingly understood to be complex; activating important antimicrobial mechanisms and serving as an avenue for immune exploitation. To date, studies in the setting of experimental co-infection that would show how simultaneous or synergistic activation through MR signaling could impact myeloid cell function are lacking. These are important given the potential for co-infection signaling events to influence disease processes. Speculatively, the *Mtb*-driven MR signaling of inflammation could augment viral replication driven through cytokine pathways known to activate the HIV promoter (Jiang and Dandekar, 2015). Similarly, activation of MMPs by HIV signaling through MR could affect the development and maintenance of *Mtb* granulomas which are important for mycobacterial containment (Al Shammari et al., 2015; Sabir et al., 2019).

MINCLE

Macrophage-inducible C-type lectin (Mincle, Clec4e), is a type II transmembrane CLR expressed by myeloid cells, such as macrophages, and contains a single carbohydrate recognition domain. Mincle binds both foreign and self-antigens including motifs found on fungal and bacterial surfaces and damaged-self antigens including SAP130 and β-glucosylceramide that are released from necrotic cells (Miyake et al., 2010; Nagata et al., 2017). Binding of Mincle to fungal pathogens such as *C. albicans* and Malassezia species is an important component of anti-fungal immunity mediated through TNF-α induction. The binding of Mincle to trehalose-6,6'-dimycolate (TDM) of the mycobacterial membrane activates macrophages to produce nitric oxide(NO) and inflammatory cytokines that contribute to antibacterial function and granuloma formation, respectively (Miyake et al., 2010). Consistent with other CLRs, Mincle deficiency does not alter the disease outcome in experimental murine TB. The inflammatory response that occurs upon *in vitro* binding of Mincle by TDM (Lang, 2013) is also fully compensated for *in vivo* (Heitmann et al., 2013).

In contrast to Mincle, the macrophage C-type lectin (MCL) co-receptor for Mincle has been shown to be indispensable for protective TB immunity (Wilson et al., 2015). $MCL^{-/-}$ mice exhibit increased mortality, bacterial burden and pulmonary inflammation following *Mtb* infection, compared to WT. MCL shares high AA sequence homology with Mincle and is also expressed by myeloid populations (Miyake et al., 2013, 2015). Mincle expression is positively regulated by MCL, an outcome postulated to reflect the heteromeric complex formation of Mincle and MCL (Miyake et al., 2015). Formation of the Mincle/MCL complex occurs downstream of Mincle-dependent MyD88 signaling and contributes to protective anti-mycobacterial responses (Kerscher et al., 2016).

A role for Mincle in HIV disease outcomes has not been described to date. Similarly, the contribution of Mincle signaling to co-infection outcomes is poorly understood due to a lack of knowledge related to HIV activation and paucity of investigations of experimental co-infections. A recent study, however, suggested that peripheral blood myeloid cells from HIV+ subjects respond differently to *Mtb* Mincle agonists (Zapata et al., 2019). Interestingly, *in vitro* activation of Mincle using a TDM analog promoted increased pro-inflammatory responses by peripheral blood monocytes from HIV+ and aged subjects (Zapata et al., 2019). These results suggest that HIV infection may disturb Mincle signaling in the setting of co-infection with *Mtb* and potentially alter immune outcomes.

DECTIN 1

The type II transmembrane CLR, Dectin-1, is expressed on myeloid cells including monocytes, macrophages, dendritic cells and neutrophils, and binds to β-glucans commonly found on fungal cell walls (Tsoni and Brown, 2008). Ligand binding of Dectin-1 induces a downstream signaling response which results in phagocytosis, respiratory burst, and a pro-inflammatory response that promotes fungal clearance (Brown, 2006; Dennehy and Brown, 2007). In addition to regulating innate immune responses to pathogens, Dectin-1-induced cytokines modulate subsequent adaptive responses (Brown, 2006). Blocking Dectin-1 signaling in a human PBMC model of *in vitro Mtb* infection reduced production of IL-17A through a mechanism that required co-signaling with TLR4 and endogenous IL-1 (van de Veerdonk et al., 2010). The IL-17 producing helper T cells (Th17) are among the essential $CD4^+$T cell subsets that direct anti-mycobacterial responses of the adaptive immune system.

The Dectin-1 pathway could thus be exploited as a novel vaccination strategy to activate Th17 cell memory to *Mtb* and other important pathogens that rely on IL-17 for protective immunity (Scriba et al., 2008).

Similar to Mincle, the immune functions activated through Dectin-1 appear to have redundant mechanisms, as Dectin 1-deficient mice display similar immune response and pulmonary disease as wild type counterparts (Marakalala et al., 2011). Deficiency of a single signaling intermediate rarely results in markedly increased pulmonary TB. An exception is deficiency of CARD9, the central adaptor for many CLRs including both Mincle and Dectin-1. *Mtb*-infected mice lacking CARD9 display severe pyogenic and neutrophilic pneumonia, and fatal TB disease (Dorhoi et al., 2010). Interestingly, deficiency in CARD9 did not impair the *in vitro* antimicrobial activity of macrophages and did not alter Th17 or other T cell responses *in vivo* (Dorhoi et al., 2010). The substantial influx of neutrophils observed in *Card9*$^{-/-}$ mice is consistent with observations that loss of signaling through MCL or CTLR (Clec9a) compromises the regulation of IL-1 and CXCL8 responses of *Mtb*-infected macrophages (Wilson et al., 2015; Cheng et al., 2017).

In contrast to the activation of protective immune responses to *Mtb*, HIV engagement of Dectin-1 promotes viral replication by facilitating *cis*-infection of immature DCs (Cote et al., 2013). Dectin-1 engagement by opportunistic pathogens can also promote viral pathogenesis. Binding of Dectin-1 by β-glucans of fungal pathogens such as histoplasmosis results in reduced leukotriene B4 levels (Sorgi et al., 2009). An imbalance between leukotrienes and prostaglandins favors HIV proliferation and establishment of opportunistic infection due to the role of PGE2 in inhibiting microbial killing (Sorgi et al., 2009). The balance between leukotrienes and prostaglandins also influences survival in experimental models of TB and are identified as a correlate of TB-diabetes co-morbidity (Tobin et al., 2012; Mayer-Barber et al., 2014; Shivakoti et al., 2019).

DECTIN-2

Dectin-2, present on tissue macrophages, some DC subsets including Langerhans cells, and peripheral blood monocytes, recognizes numerous fungal and bacterial pathogens (Graham and Brown, 2009). Dectin-2 binds zymosan of fungal species such as *Candida albicans* and mannose rich glycolipids such as lipoarabinomannan (Man-LAM) of *Mtb* (Decout et al., 2018). Binding of Dectin-2 to Man-LAM activates pro-inflammatory (IL-6 and TNF-α) and immune regulatory (IL-10 and TGF- β) cytokines (Yonekawa et al., 2014). Consistent with the roles of IL-6 and TGF- β to promote Th17 differentiation, binding of Man-LAM by Dectin-2 drives generation of *Mtb*-specific Th17 cells (Decout et al., 2018).

Although other Dectin-2 family CLRs, such as DCIR, are associated with HIV transmission, a role for Dectin-2 signaling in HIV mono-infection and co-infections with *Mtb* has not been described. The function of both Dectin 1 and 2 to promote differentiation of Th17 cells during the adaptive response to other pathogens such as *Mtb,* however, may have consequences in the setting of HIV co-infection. Activated CD4^{+}T cells with a memory phenotype are more susceptible to HIV infection and support greater viral replication than resting T cell counterparts. Among various CD4^{+}T cell populations, the Th17 populations are especially susceptible to HIV infection, lacking inhibitory RNAses that limit viral replication in other cells (Sun et al., 2015; Christensen-Quick et al., 2016; Lee and Lichterfeld, 2016; Fernandes et al., 2017). Th17 cells expressing CCR6 were recently described to function as a long lived HIV reservoir that persists in PLWH despite ART pressure (Sun et al., 2015; Fernandes et al., 2017; Gosselin et al., 2017). CLR-dependent pathways that promote differentiation of *Mtb*-specific Th17 cells may thus contribute to HIV proliferation and persistence. Depletion and compromise of Th17 cells due to HIV infection could similarly compromise protective function of the cell mediated immune response to *Mtb*.

MANNOSE BINDING LECTIN

Mannose binding lectin (MBL) belongs to a family of secreted proteins known as collectins and primarily circulates through serum, synovial and amniotic fluid. MBL ligand binding is Ca^{2+} dependent and selective for terminal mannose, fucose and N-acetylgalactosamine (GalNAC)(Ip et al., 2009). Due to the broad ligand binding and presence in the serum, MBL is an important receptor for opsonization of pathogens to clear infection and prevent recurrent infections (Ip et al., 2009). MBL binding to *Mycobacterium avium* was previously reported (Polotsky et al., 1997), while recent studies have demonstrated a broader role in mycobacterial immunity. Ligation of MBL to *Mtb* and the related *M. bovis*, results in enhanced phagocytosis, lectin pathway activation and agglutination of bacteria (Bartlomiejczyk et al., 2014). Additionally, binding of MBL to *Mtb* activates MASP1 homodimers to catalyze activation of MASP2 and ultimately generation of C3 convertase (Klassert et al., 2018) in the immune complement cascade. The function and expression of MBL is dependent on polymorphisms in the *MBL2* gene, which encodes the receptor. Polymorphisms in *MBL2* are associated with susceptibility to pulmonary and extra-pulmonary TB in various human populations (da Cruz et al., 2013; Nisihara et al., 2018).

The HIV envelope displays several conserved glycan residues that are epitopes for broadly neutralizing antibodies (bnAb) produced by B cells of the acquired immune system. MBL present in human serum is able to block binding of the 2G12 bnAb to HIV, and as a result, increase virus infectivity (Marzi et al., 2007). Serum concentrations of MBL may thus limit the efficacy of neutralizing antibody-based prevention or treatment strategies for HIV. The outcome of MBL signaling in the setting of co-infection has not been described to date. Activation of MBL by *Mtb* exposure could be explored as a potential mechanism for the increased viral replication observed in those with dual infection. Similarly, increased HIV replication due to inhibition of bnAb by MBL could further compromise CMI to *Mtb*.

DC-SIGN

The CLR which has been most extensively studied in *Mtb* and HIV infections is DC-SIGN. This mannose-binding type II CLR is present on dermal DCs, interstitial DCs of the mucosa, and macrophages (van Kooyk and Geijtenbeek, 2003). DC-SIGN interacts with the LPS structure of *Klebsiella pneumonia* and *Helicobacter pylori* to internalize and target these pathogens for antigen presentation (van Kooyk and Geijtenbeek, 2003). In experimental TB, selective knockout of the murine homolog for human DC-SIGN (Tanne and Neyrolles, 2010), SIGNR1, only partially impairs host resistance to *Mtb*. However, deficiency in both SIGNR1 and murine MR results in increased lung inflammation and larger foci of bacilli 5 months post-infection (Court et al., 2010). These disease outcomes are moderate, however, compared to those in mice lacking the essential cytokine pathways (TNF, IL-1 or IFN-γ) which lack compensatory mechanisms and are unable to control *Mtb* (Court et al., 2010).

Although DC-SIGN is primarily expressed on dendritic cells, expression on immunoregulatory macrophages has been shown in the pleural cavity of human patients and lung tissue from NHPs with active TB (Lugo-Villarino et al., 2018). The functional outcome of DC-SIGN signaling within *Mtb*-exposed myeloid cells remains to be fully characterized, however, modulation of the Dectin-1 driven pro-inflammatory responses has been observed in a subset of M2 macrophages (Lugo-Villarino et al., 2018). Further investigations are required to determine if DC-SIGN pathways may work in concert with other CLRs or PRRs to regulate damaging pro-inflammatory responses to *Mtb*.

DC-SIGN also serves as an entry receptor for several viral pathogens including Dengue virus, Ebola virus, hepatitis C virus and cytomegalovirus (van Kooyk and Geijtenbeek, 2003). A role for DC-SIGN in trans-infection with HIV and the closely related simian immunodeficiency virus (SIV) has been well-documented in human and non-human primate cells, respectively (Geijtenbeek et al., 2001). Adhesion of gp120 to DC-SIGN promotes viral transmission via the lymphatics while expression of DC-SIGN by placental Hofbauer cells permits vertical transmission of HIV (Soilleux et al., 2001; da Silva R. C. et al., 2011). Expression of DC-SIGN has also been described on HIV-susceptible tissues such as colonic mucosa (Preza et al., 2014) and foreskin epithelium (Hirbod et al., 2010) as a potential mechanism of HIV transmission to and from those sites.

The function of DC-SIGN in viral infection and transmission highlights the specificity and overlap of the CLR interactions with HIV. Although DC-SIGN promotes trans-infection of HIV, many other CLRs carry out a similar function independent of DC-SIGN. As previously discussed, MR facilitates HIV transmission by binding to mannose moieties of gp120 through a mechanism inhibited by pre-incubation of cells with mannan (Nguyen and Hildreth, 2003). The heavy glycosylation of HIV gp120 also contains sialic acid residues which are recognized by siglecs. These sialic acid binding lectins, present on macrophages and DCs, facilitate viral adhesion and infection of R5-tropic viruses to macrophages (Zou et al., 2011). In particular, siglec-1 expressed on mature DCs of the cervical mucosa enhances viral uptake and trans-infection, thus enabling systemic viral spread (Izquierdo-Useros et al., 2014; Perez-Zsolt et al., 2019).

Soluble CLRs, such as galectin-1, are exploited by HIV to enhance binding of gp120 and the CD4 receptor to facilitate viral infection of T cells (St-Pierre et al., 2011). CLRs which bind to HIV gp120 are also able to competitively inhibit viral binding to DC-SIGN and thus, block trans-infection. The CLR surfactant protein SP-D, present in mucosal tissue, inhibits viral entry and DC-SIGN interaction by competitively binding HIV gp120 (Dodagatta-Marri et al., 2017). In short, CLR binding to gp120 and other carbohydrate rich molecular motifs is an important mechanism for HIV pathogenesis as well as a potential avenue for clinical intervention.

The association of DC-SIGN in immune evasion strategies employed by *Mtb* and HIV has been characterized as previously reviewed (Kaufmann and Schaible, 2003; van Kooyk et al., 2003). In brief, during co-infection with *Mtb*, DC-SIGN mediated Raf-1 signaling has been shown to be critical for HIV transcription elongation and can even enhance viral replication (Gringhuis et al., 2010). Additional studies of the antigen uptake mechanism of DC-SIGN have identified the involvement of membrane cholesterol and dynamin for endocytosis and the clatherin-dependent HIV internalization into dendritic cells (Cambi et al., 2009).

LANGERIN

The CLR Langerin is specifically expressed by Langerhans immature DC of the epidermis and mucosal tissues (de Witte et al., 2008). Langerin is a type II transmembrane receptor which binds mannose, fucose, and GlcNAC in a Ca^{2+} dependent manner (van der Vlist and Geijtenbeek, 2010). As a consequence of broad spectrum carbohydrate recognition, Langerin recognizes a number of PAMPs including those expressed by *Candida albicans* and *Mycobacterium leprae*. To date, the subsequent downstream signaling events triggered by Langerin binding are poorly characterized. Additionally, although it is likely that Langerin recognizes components of the glycosylated *Mtb* cell wall, direct binding has not been described (van der Vlist and Geijtenbeek, 2010).

Langerhans cells are among the first innate immune cells to encounter mucosal pathogens and are therefore important gatekeepers to prevent infection at those sites (van der Vlist and Geijtenbeek, 2010). To that effect, binding of Langerin to HIV initiates a TRIM5α dependent pathway which targets HIV for autophagic degradation (Ribeiro et al., 2016). Interestingly, DC-SIGN engagement abrogates this restriction pathway by causing a dissociation of TRIM5α from the receptor and thus, permitting infection (Ribeiro et al., 2016). These findings highlight the synergistic ability of DC CLRs to dictate the outcome of HIV infection by permitting or restricting pathogen replication and immune responses. Additionally, therapeutic strategies which block DC-SIGN may in turn augment the protective function of Langerin signaling during HIV infection. Identification of *Mtb* binding by Langerin could suggest avenues whereby Langerin

and DC-SIGN signaling convergence, or interference, may impact immune outcomes in co-infected individuals.

DCIR

Dendritic cell immunoreceptor (DCIR) is highly expressed on peripheral blood leukocytes including monocyte-derived DCs, macrophages, neutrophils, and plasmacytoid DCs (Graham and Brown, 2009). DCIR contains an immunoreceptor tyrosine-based inhibition motif (ITIM) associated with downregulation of pro-inflammatory signaling. Similar to other related CLRs, DCIR-dependent internalization targets antigens for presentation on APCs, thus promoting T-cell proliferation (Graham and Brown, 2009). As mentioned previously, the DCIR related CLR, Dectin-2, promotes Th17 responses upon engagement with *Mtb* antigen (Decout et al., 2018). Similarly, recognition of *Mtb* by DCIR promotes Th17 T cell differentiation while also activating the IFNR-associated JAK-STAT pathway to sustain type I IFN signaling and reduce Th1 responses. Expectedly, knockout of DCIR improves *Mtb* control but also results in increased pulmonary pathology (Troegeler et al., 2017). More interesting, however, is the immune activating nature of DCIR in TB immunity which is unexpected for an ITIM-containing CLR, although this mechanism is yet to be determined (Troegeler et al., 2017).

Analogous to DC-SIGN, DCIR plays an important role in promoting HIV viral capture and replication within $CD4^{+}$T cells through activating phosphorylation of the receptor ITIM domain (Lambert et al., 2008, 2011). Blocking of DCIR has been employed as a therapeutic strategy to prevent HIV transmission and may be an effective strategy to improve Th1 responses against *Mtb* in a co-infection scenario. The role of DCIR to promote Th17 differentiation, similar to Dectin 1 and 2, may increase viral replication and persistence due to the susceptibility of Th17 cells to HIV.

GENETIC POLYMORPHISMS OF CLRs AS DISEASE PREDICTORS

Polymorphisms of PRR genes within the human population have been increasingly associated with disease resistance and susceptibility. Functional polymorphisms in CLR genes that result in receptor impairment have been linked to increased susceptibility to infections such as invasive pneumonia and hepatitis (Eisen and Minchinton, 2003), as well as chronic diseases such as Crohn's disease (Marquez et al., 2009). The population diversity of several CLRs, especially MR, Mincle, and MBL, has been further linked to increased susceptibility to HIV and *Mtb* within endemic areas through diverse mechanisms including: modulation of immune outcomes, improved pathogen transmission, and associated co-morbidities.

Recognition of Man-LAM by MR plays a key role in innate immunity to *Mtb* (Kang et al., 2005). A single nucleotide polymorphism (SNP) of the *MRC1* gene which encodes the MR was recently identified as a candidate for genetic susceptibility to *Mtb*. A cohort of 222 Chinese subjects with pulmonary TB was compared to 232 healthy controls and analyzed for six SNPs in exon 7 of the *MRC1* gene. In both frequency of genotype and allele, the G1186A site was significantly different between those with pulmonary TB compared to healthy controls (Zhang et al., 2012). These observations identify the G1186A mutation as a potential risk factor for the development of pulmonary TB. Speculatively, functional changes in MR due to the G1186A SNP may temper the pro-inflammatory or phagocytic outcomes of MR signaling upon *Mtb* infection, or alternatively, further inhibit phagosome maturation. To date, MR SNP that are linked to susceptibility to HIV and HIV/*Mtb* co-infections have not been described.

Polymorphisms in the *CLEC4E* gene that encodes Mincle have been associated with susceptibility to *Mtb,* although limited results to date suggest racial or other population differences. Mincle binding of mycobacterial TDM is strongly associated with TB granuloma formation. Four *CLEC4E* SNPs (rs10841845, rs10841847, rs10841856, and rs4620776) were identified in an African patient cohort of 416 confirmed TB cases and 405 healthy controls (Bowker et al., 2016). No significant association between these four SNP and TB disease was identified in this comparison (Bowker et al., 2016). A more recent study in a population from northern China further characterized these CLEC4E polymorphisms in association with pulmonary TB disease (Kabuye et al., 2019). Interestingly, studies in this population identified significantly increased variants of rs10841845 and rs10841847 in the 214 control patients compared to the 202 pulmonary TB patients. This suggests that functional polymorphism of CLEC4E may confer protection against pulmonary *Mtb* infection in this population (Kabuye et al., 2019). To date, *MRC1 and CLEC4E* SNP that are linked to risk for HIV infection or HIV/*Mtb* co-infections have not been described.

Human MBL, encoded by the *MBL2* gene, belongs to a family of soluble CLRs known as collectins that initiate complement activation. Polymorphisms of *MBL2* and the downstream signaling components which initiate the complement lectin pathway (Klassert et al., 2018), are associated with susceptibility to both pulmonary and extra-pulmonary TB across various populations (Denholm et al., 2010). In a cohort from the northeastern region of Brazil, *MBL2* promoter polymorphisms were linked with increased susceptibility to pulmonary TB. Interestingly, no significant correlations were observed between *MBL2* polymorphisms and extra pulmonary TB (da Cruz et al., 2013). Conversely, a relationship with extra-pulmonary TB was identified in a cohort of Chinese patients. In this analysis, MBL2 polymorphisms were found to correlate with a diagnosis of spinal TB (Zheng et al., 2018).

MBL2 polymorphisms have also been associated with reduced levels of serum MBL, although the implications for *Mtb* susceptibility remain to be fully characterized (da Cruz et al., 2013). In one study of patients with ankylosing spondylitis (AS), a rheumatic disease characterized by low MBL levels, a significant correlation was identified between MBL deficiency and TB. The increased TB risk in those with low serum MBL was independent of either TNF therapy or latent infection in the patient medical history (Nisihara et al., 2018).

Susceptibility to HIV infection is also associated with MBL polymorphisms. In a 2011 study of a cohort from Southern Brazil, variant alleles of MBL were associated with increased susceptibility to HIV-1 infection (da Silva G. K. et al., 2011). Genotyping of HIV-infected patients of European and African descent in the cohort further revealed a difference in *MBL2* SNP frequencies and serum levels between ethnic groups. Interestingly, HIV-positive patients of European descent had low MBL serum levels whereas those of African descent had elevated MBL levels. The basis for this dichotomy is unknown and suggests that the full scope of immune responses regulated by *MBL2* are not yet understood.

In one report, *MBL2* alleles and genotypes were assessed in a Western European population for association with co-infection. Interestingly, HIV/TB dual disease was associated with low or non-producer alleles in comparisons with TB negative subjects including those with a positive HIV status (Garcia-Laorden et al., 2006). MBL deficiency may thus be associated with active TB in HIV co-infection. These findings demonstrate the broad spectrum of *MBL2* polymorphisms associated with HIV and TB disease across various populations, including those with co-infection.

CLR BASED THERAPEUTIC STRATEGIES

The function of C-type lectin receptor signaling to shape innate and adaptive immune responses is exploited in recent approaches to develop novel therapeutics. CLR receptors are efficiently engaged by *Mtb* and HIV PAMPs and several of the resulting immune outcomes are characterized (**Figure 2**). As a result, mycobacterial and viral antigens that bind CLR have many therapeutic applications ranging from immune activation to cell targeted delivery. Competitive inhibition of CLR binding to viral particles also holds promise as a strategy for antiviral therapy.

Vaccine Adjuvants

The glycosylation of both the mycobacterial cell wall and HIV virion is an important factor for recognition by CLRs and initiates downstream immune responses. Engagement of Mincle by TDM (Ishikawa et al., 2009) and phosphatidylinositol mannosides (Mosaiab et al., 2018) of mycobacteria induces robust pro-inflammatory cytokine response (IL-6 and TNF-α) and NO production *in vivo* (Ishikawa et al., 2009). Activation of Mincle signaling using TDM derivatives has been employed as an adjuvant strategy for TB vaccines (Desel et al., 2013; Decout et al., 2017) as well as for vaccines for unrelated pathogens (Azuma and Seya, 2001; Drummond et al., 2011). Of note, the adjuvant effect of TDM is dependent not only on Mincle, but also its co-receptor, MCL, constitutively expressed on myeloid cells (Tanne and Neyrolles, 2010; Miyake et al., 2013). Adjuvant outcomes could thus be tailored as needed for specific immune responses through strategies that target individual or multiple CLR pathways.

The choice of antibody subclass can also be modulated through CLR signaling. Generation of balanced IgG2a/IgG1 antibody subclasses specific to HIV is an important goal of DNA immunization. Activation of CLR signaling by HIV envelope was shown to regulate the antibody subclass response, as demonstrated by immunization of *Card9*$^{-/-}$ mice (Hess et al., 2019). In contrast, antibody subclasses were not altered in *Myd88/Trif*$^{-/-}$ mice that lack functional TLR signaling (Hess et al., 2019). Application of CLR-targeting molecules for vaccine adjuvants is at an early stage of development. These early outcomes show promise to "fine-tune" the immune response as relevant to different microbial threats.

Cell Targeted Delivery

Not only are CLRs capable of eliciting protective cytokine responses, but they also function as internalization receptors for delivery to antigen presentation pathways. Thus, the inclusion of CLR targets is increasingly employed to improve cellular uptake of drugs or vaccines. In a recent report, CLR-targeted delivery was shown to improve inhaled delivery of lipid nanoparticles loaded with rifampicin, a first line TB drug (Maretti et al., 2019). Decoration of lipid nanoparticles with novel mannose derivatives targeted the particle for uptake by MR. The result was improved efficiency of drug uptake by alveolar macrophages, the host cell for *Mtb* (Maretti et al., 2019).

A nanoparticle vaccine strategy that incorporated CLR targeted oligosaccharides has also been employed as a novel vaccination strategy for HIV. Co-delivery of mannose-enriched ligands that target DC-SIGN, with HIV peptides, increased the generation of antigen-specific $CD8^+$ and $CD4^+$T-cell responses (Climent et al., 2018). Targeting antigens to DCs through DC-SIGN has also been employed for TB vaccination. Conjugation of anti-DC-SIGN antibodies to the *Mtb* antigen Ag85B molecule elicited strong antigen-specific and polyfunctional (IFN-γ+, IL-2+, and TNF-α+) $CD4^+$T cell responses (Velasquez et al., 2018). These strategies to target DC-SIGN may increase uptake and targeting to antigen presentation pathways as well as activate immune danger signals that promote development of polyfunctional T cell memory.

Receptor Antagonists

The function of CLRs as potent endocytic receptors and innate immune activators is frequently exploited by pathogens for transmission and pathogenesis. Inhibition of these interactions thus provides opportunities for therapeutic intervention. Recently, blocking CLR-mediated viral transmission to naïve host cells was shown to serve as a host-directed therapeutic strategy for HIV. Galectin-1, a soluble CLR used by HIV for attachment and entry, may also serve as a target for anti-retroviral therapy. Treatment with carbohydrate lactoside compounds competitively inhibit the galectin-1 interaction with human $CD4^+$T cells and HIV, and thus preventing attachment to uninfected cells (St-Pierre et al., 2012). Direct carbohydrate inhibitors are effective treatment strategies for CLRs with unique ligands. The carbohydrate recognition motifs shared by different CLRs are more challenging to target through inhibition strategies. For example, DC-SIGN shares ligand homology with Langerin. DC-SIGN is exploited by HIV to

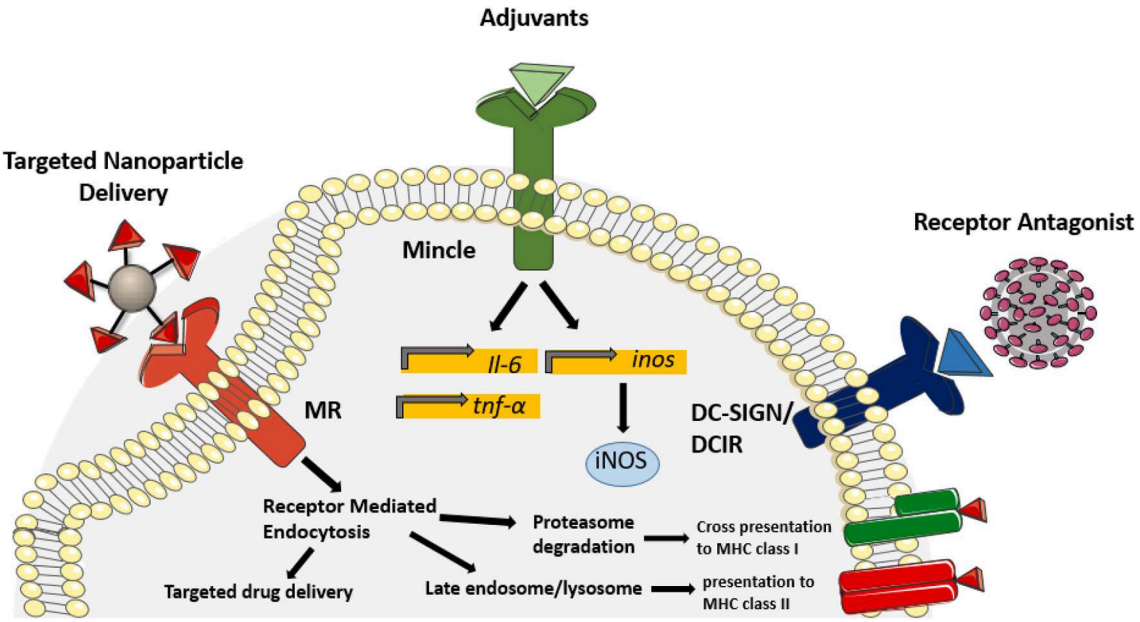

FIGURE 2 | Therapeutic application of CLR ligands. In recent years, known CLR ligands have been used as therapeutic targets to improve uptake of drugs and vaccines, modulate protective immune responses and block receptor binding. Incorporating mannose derivatives on nanoparticles targets uptake through the mannose receptor, thus targeting antigen presentation pathways and improving drug delivery into alveolar macrophages. Due to the potent inflammatory response initiated by Mincle binding, derivatives of TDM have been incorporated as adjuvants to improve antigen-specific protective immunity during vaccination. Glycan derivatives have also been used as a mechanism to antagonize receptor binding of the HIV envelope, thus preventing viral transmission. Competitive inhibition of galectin-1, DC-SIGN and DCIR have shown efficacy in reducing HIV transmission to $CD4^+$T cells. Targeting CLR signaling and binding has proven efficacious in various therapeutic applications and demonstrates the potential for CLR ligands in the treatment of infectious diseases.

facilitate viral transmission while Langerin directs protective outcomes (de Witte et al., 2008; van der Vlist and Geijtenbeek, 2010).

One potential strategy is the use of glycomimetic technology to synthesize receptor targeted inhibitors specific for individual CLRs. Use of a glycomimetic to inhibit DC-SIGN binding reduced HIV trans-infection of T cells in human explant tissue models (Varga et al., 2014). At low μM concentration, these functionalized multivalent ligands also inhibited *in vitro* HIV trans-infection in isolated $CD4^+$T cells (Varga, Sutkeviciute et al.). Blocking of other receptors which facilitate trans-infection of HIV, such as DCIR, have also shown efficacy in decreasing viral infection of $CD4^+$T cells (Lambert et al., 2011). Use of glycomimetics and other CLR inhibitors thus have potential to reduce infections and may also have applications to modulate disease outcomes.

CONCLUDING REMARKS

CLRs are essential PRR pathways of the innate immune response with diverse roles in immunity to *Mtb* and HIV. Our understanding of the roles of individual CLRs and the downstream immune responses in *Mtb* and HIV infection, and especially co-infection, is still evolving. Several CLRs bind *Mtb* ligands and activate innate, often pro-inflammatory, immune responses. There is redundancy in CLR function, as individual CLRs are generally dispensable with regards to TB disease outcomes in murine models. The roles for CLRs in HIV infection are less characterized due to the limitations for animal models. As currently understood, CLRs can generate protective anti-viral responses as well as serves as mechanisms for viral transmission. In the setting of co-infection, simultaneous signaling could drive convergent processes that differ from mono-infection and contribute to aggressive disease through mechanisms that are not yet understood. These overlapping mechanisms may also extend into other opportunistic infections and co-morbidities associated with *Mtb* or HIV infections, which may modulate innate immune signaling of CLRs. On-going applications that target CLR pathways demonstrate recognition of the translational potential for development of interventions for TB and HIV.

AUTHOR CONTRIBUTIONS

KN and JE both contributed conception and design of the review. KN wrote the first draft of the manuscript and developed the figure graphics. JE wrote sections of the manuscript and provided overall editing. All authors contributed to manuscript revision, read and approved the submitted version.

FUNDING

This work was supported by funding from NIH, NIAID to JE (R61AI138328). Fellowship support for KN was provided by a pre-doctoral award from the James W. McLaughlin Endowment.

REFERENCES

Al Shammari, B., Shiomi, T., Tezera, L., Bielecka, M. K., Workman, V., Sathyamoorthy, F., et al. (2015). The extracellular matrix regulates granuloma necrosis in tuberculosis. *J. Infect. Dis.* 212, 463–473. doi: 10.1093/infdis/jiv076

Andersen, M. N., Honge, B. L., Jespersen, S., Medina, C., da Silva Te, D., Laursen, A., et al. (2018). Soluble macrophage mannose receptor (sCD206/sMR) as a biomarker in human immunodeficiency virus infection. *J. Infect. Dis.* 218, 1291–1295. doi: 10.1093/infdis/jiy318

Azuma, I., and Seya, T. (2001). Development of immunoadjuvants for immunotherapy of cancer. *Int. Immunopharmacol.* 1, 1249–1259. doi: 10.1016/S1567-5769(01)00055-8

Bartlomiejczyk, M. A., Swierzko, A. S., Brzostek, A., Dziadek, J., and Cedzynski, M. (2014). Interaction of lectin pathway of complement-activating pattern recognition molecules with mycobacteria. *Clin. Exp. Immunol.* 178, 310–319. doi: 10.1111/cei.12416

Bergantz, L., Subra, F., Deprez, E., Delelis, O., and Richetta, C. (2019). Interplay between intrinsic and innate immunity during hiv infection. *Cells* 8:E922. doi: 10.3390/cells8080922

Bowker, N., Salie, M., Schurz, H., van Helden, P. D., Kinnear, C. J., Hoal, E. G., et al. (2016). Polymorphisms in the pattern recognition receptor mincle gene (CLEC4E) and association with tuberculosis. *Lung* 194, 763–767. doi: 10.1007/s00408-016-9915-y

Brown, G. D. (2006). Dectin-1: a signalling non-TLR pattern-recognition receptor. *Nat. Rev. Immunol.* 6, 33–43. doi: 10.1038/nri1745

Cambi, A., Beeren, I., Joosten, B., Fransen, J. A., and Figdor, C. (2009). The C-type lectin DC-SIGN internalizes soluble antigens and HIV-1 virions via a clathrin-dependent mechanism. *Eur. J. Immunol.* 39, 1923–1928. doi: 10.1002/eji.200939351

Cardona-Maya, W., Velilla, P. A., Montoya, C. J., Cadavid, A., and Rugeles, M. T. (2011). *In vitro* human immunodeficiency virus and sperm cell interaction mediated by the mannose receptor. *J. Reprod. Immunol.* 92, 1–7. doi: 10.1016/j.jri.2011.09.002

Cheng, A. C., Yang, K. Y., Chen, N. J., Hsu, T., Hsieh, S.L., et al. (2017). CLEC9A modulates macrophage-mediated neutrophil recruitment in response to heat-killed *Mycobacterium tuberculosis* H37Ra. *PLoS ONE* 12:e0186780. doi: 10.1371/journal.pone.0186780

Christensen-Quick, A., Lafferty, M., Sun, L., Marchionni, L., deVico, A., and Garzino-Demo, A. (2016). Human Th17 cells lack HIV-inhibitory RNases and are highly permissive to productive HIV infection. *J. Virol.* 90, 7833–7847. doi: 10.1128/JVI.02869-15

Climent, N., Garcia, I., Marradi, M., Chiodo, F., Miralles, L., Maleno, M., et al. (2018). Loading dendritic cells with gold nanoparticles (GNPs) bearing HIV-peptides and mannosides enhance HIV-specific T cell responses. *Nanomedicine* 14, 339–351. doi: 10.1016/j.nano.2017.11.009

Cooper, A. M. (2009). Cell-mediated immune responses in tuberculosis. *Annu. Rev. Immunol.* 27, 393–422. doi: 10.1146/annurev.immunol.021908.132703

Cote, S. C., Plante, A., Tardif, M. R., and Tremblay, M. J. (2013). Dectin-1/TLR2 and NOD2 agonists render dendritic cells susceptible to infection by X4-using HIV-1 and promote cis-infection of CD4(+) T cells. *PLoS ONE* 8:e67735. doi: 10.1371/journal.pone.0067735

Court, N., Vasseur, V., Vacher, R., Fremond, C., Shebzukhov, Y., Yeremeev, V., et al. (2010). Partial redundancy of the pattern recognition receptors, scavenger receptors, and C-type lectins for the long-term control of *Mycobacterium tuberculosis* infection. *J. Immunol.* 184, 7057–7070. doi: 10.4049/jimmunol.1000164

da Cruz, H. L., da Silva, R. C., Segat, L., de Carvalho, M. S., Brandao, L. A., Guimaraes, R. L., et al. (2013). MBL2 gene polymorphisms and susceptibility to tuberculosis in a northeastern Brazilian population. *Infect. Genet. Evol.* 19, 323–329. doi: 10.1016/j.meegid.2013.03.002

da Silva, G. K., Guimaraes, R., Mattevi, V. S., Lazzaretti, R. K., Sprinz, E., Kuhmmer, R., et al. (2011). The role of mannose-binding lectin gene polymorphisms in susceptibility to HIV-1 infection in Southern Brazilian patients. *AIDS* 25, 411–418. doi: 10.1097/QAD.0b013e328342fef1

da Silva, R. C., Segat, L., and Crovella, S. (2011). Role of DC-SIGN and L-SIGN receptors in HIV-1 vertical transmission. *Hum. Immunol.* 72, 305–311. doi: 10.1016/j.humimm.2011.01.012

Dambuza, I. M., and Brown, G. D. (2015). C-type lectins in immunity: recent developments. *Curr. Opin. Immunol.* 32, 21–27. doi: 10.1016/j.coi.2014.12.002

de Noronha, A. L., Bafica, A., Nogueira, L., Barral, A., and Barral-Netto, M. (2008). Lung granulomas from *Mycobacterium tuberculosis*/HIV-1 co-infected patients display decreased in situ TNF production. *Pathol. Res. Pract.* 204, 155–161. doi: 10.1016/j.prp.2007.10.008

de Witte, L., Nabatov, A., and Geijtenbeek, T. B. (2008). Distinct roles for DC-SIGN+-dendritic cells and Langerhans cells in HIV-1 transmission. *Trends Mol. Med.* 14, 12–19. doi: 10.1016/j.molmed.2007.11.001

Decout, A., Silva-Gomes, S., Drocourt, D., Barbe, S., Andre, I., Cueto, F., et al. (2017). Rational design of adjuvants targeting the C-type lectin mincle. *Proc. Natl. Acad. Sci. U.S.A.* 114, 2675–2680. doi: 10.1073/pnas.1612421114

Decout, A., Silva-Gomes, S., Drocourt, D., Blattes, E., Riviere, M., Prandi, J., et al. (2018). Deciphering the molecular basis of mycobacteria and lipoglycan recognition by the C-type lectin Dectin-2. *Sci. Rep.* 8:16840. doi: 10.1038/s41598-018-35393-5

Denholm, J. T., McBryde, E. S., and Eisen, D. P. (2010). Mannose-binding lectin and susceptibility to tuberculosis: a meta-analysis. *Clin. Exp. Immunol.* 162, 84–90. doi: 10.1111/j.1365-2249.2010.04221.x

Dennehy, K. M., and Brown, G. D. (2007). The role of the beta-glucan receptor dectin-1 in control of fungal infection. *J. Leukoc. Biol.* 82, 253–258. doi: 10.1189/jlb.1206753

Desel, C., Werninghaus, K., Ritter, M., Jozefowski, K., Wenzel, J., Russkamp, N., et al. (2013). The Mincle-activating adjuvant TDB induces MyD88-dependent Th1 and Th17 responses through IL-1R signaling. *PLoS ONE* 8:e53531. doi: 10.1371/journal.pone.0053531

Dodagatta-Marri, E., Mitchell, D. A., Pandit, H., Sonawani, A., Murugaiah, V., Idicula-Thomas, S., et al. (2017). Protein-protein interaction between surfactant protein D and DC-SIGN via C-type lectin domain can suppress HIV-1 transfer. *Front. Immunol.* 8:834. doi: 10.3389/fimmu.2017.00834

Doitsh, G., Galloway, N. L., Geng, X., Yang, Z., Monroe, K., Zepeda, O., et al. (2014). Cell death by pyroptosis drives CD4 T-cell depletion in HIV-1 infection. *Nature* 505, 509–514. doi: 10.1038/nature12940

Dorhoi, A., Desel, C., Yeremeev, V., Pradl, L., Brinkmann, V., Mollenkopf, H., et al. (2010). The adaptor molecule CARD9 is essential for tuberculosis control. *J. Exp. Med.* 207, 777–792. doi: 10.1084/jem.20090067

Drummond, R. A., Saijo, S., Iwakura, Y., and Brown, G., D. (2011). The role of Syk/CARD9 coupled C-type lectins in antifungal immunity. *Eur. J. Immunol.* 41, 276–281. doi: 10.1002/eji.201041252

Eisen, D. P., and Minchinton, R. M. (2003). Impact of mannose-binding lectin on susceptibility to infectious diseases. *Clin. Infect. Dis.* 37, 1496–1505. doi: 10.1086/379324

Fanibunda, S. E., Modi, D. N., Gokral, J. S., and Bandivdekar, A. (2011). HIV gp120 binds to mannose receptor on vaginal epithelial cells and induces production of matrix metalloproteinases. *PLoS ONE* 6:e28014. doi: 10.1371/journal.pone.0028014

Fanibunda, S. E., Velhal, S. M., Raghavan, V. P., and Bandivdekar, A. (2008). CD4 independent binding of HIV gp120 to mannose receptor on human spermatozoa. *J. Acquir. Immune Defic. Syndr.* 48, 389–397. doi: 10.1097/QAI.0b013e318179a0fb

Fernandes, J. R., Berthoud, T. K., Kumar, A., and Angel, J. B. (2017). IL-23 signaling in Th17 cells is inhibited by HIV infection and is not restored by HAART: implications for persistent immune activation. *PLoS ONE* 12:e0186823. doi: 10.1371/journal.pone.0186823

Garcia-Laorden, M. I., Pena, M. J., Caminero, J. A., Garcia-Saavedra, A., Campos-Herrero, M. I., et al. (2006). Influence of mannose-binding lectin on HIV infection and tuberculosis in a western-European population. *Mol. Immunol.* 43, 2143–2150. doi: 10.1016/j.molimm.2006.01.008

Garg, H., and Joshi, A. (2017). Host and viral factors in HIV-mediated bystander apoptosis. *Viruses* 9:E237. doi: 10.3390/v9080237

Geijtenbeek, T. B., and Gringhuis, S. I. (2009). Signalling through C-type lectin receptors: shaping immune responses. *Nat. Rev. Immunol.* 9, 465–479. doi: 10.1038/nri2569

Geijtenbeek, T. B., Koopman, G., van Duijnhoven, G. C., van Vliet, S. van Schijndel, A. C., Engering, A., et al. (2001). Rhesus macaque and chimpanzee DC-SIGN act as HIV/SIV gp120 trans-receptors, similar to human DC-SIGN. *Immunol. Lett.* 79, 101–107. doi: 10.1016/S0165-2478(01)00279-6

Gosselin, A., Wiche Salinas, T. R., Planas, D., Wacleche, V. S., Zhang, Y., Fromentin, R., et al. (2017). HIV persists in CCR6+CD4+ T cells from colon and blood during antiretroviral therapy. *AIDS* 31, 35–48. doi: 10.1097/QAD.0000000000001309

Graham, L. M., and Brown, G. D. (2009). The dectin-2 family of C-type lectins in immunity and homeostasis. *Cytokine* 48, 148–155. doi: 10.1016/j.cyto.2009.07.010

Gringhuis, S. I., van der Vlist, M., van den Berg, L. M., den Dunnen, J., Litjens, M., and Geijtenbeek, T. B. (2010). HIV-1 exploits innate signaling by TLR8 and DC-SIGN for productive infection of dendritic cells. *Nat. Immunol.* 11, 419–426. doi: 10.1038/ni.1858

Guttman, M., Varadi, C., Lee, K. K., and Guttman, A. (2015). Comparative glycoprofiling of HIV gp120 immunogens by capillary electrophoresis and MALDI mass spectrometry. *Electrophoresis* 36, 1305–1313. doi: 10.1002/elps.201500054

Heesters, B. A., Lindqvist, M., Vagefi, P. A., Scully, E. P., Schildberg, F. A., Altfel, M., et al. (2015). Follicular dendritic cells retain infectious HIV in cycling endosomes. *PLoS Pathog.* 11:e1005285. doi: 10.1371/journal.ppat.1005285

Heitmann, L., Schoenen, H., Ehlers, S., Lang, R., and Holscher, C. (2013). Mincle is not essential for controlling *Mycobacterium tuberculosis* infection. *Immunobiology* 218, 506–516. doi: 10.1016/j.imbio.2012.06.005

Hess, R., M. Storcksdieck G. B., Lapuente, D., Maaske, A., Kirschning, C., Ruland, J., Lepenies, B., et al. (2019). Glycosylation of HIV env impacts IgG subtype responses to vaccination. *Viruses* 11:E153. doi: 10.3390/v11020153

Hirbod, T., Bailey, R. C., Agot, K., Moses, S., Ndinya-Achola, J., Murugu, R., Andersson, J., et al. (2010). Abundant expression of HIV target cells and C-type lectin receptors in the foreskin tissue of young Kenyan men. *Am. J. Pathol.* 176, 2798–2805. doi: 10.2353/ajpath.2010.090926

Holder, G. E., McGary, C. M., Johnson, E. M., Zheng, R., John, V. T., Sugimoto, C., et al. (2014). Expression of the mannose receptor CD206 in HIV and SIV encephalitis: a phenotypic switch of brain perivascular macrophages with virus infection. *J. Neuroimmune Pharmacol.* 9, 716–726. doi: 10.1007/s11481-014-9564-y

Honeycutt, J. B., Thayer, W. O., Baker, C. E., Ribeiro, R., Lada, S. M., Cao, Y. et al. (2017). HIV persistence in tissue macrophages of humanized myeloid-only mice during antiretroviral therapy. *Nat. Med.* 23, 638–643. doi: 10.1038/nm.4319

Hossain, M. M., and Norazmi, M., N. (2013). Pattern recognition receptors and cytokines in *Mycobacterium tuberculosis* infection–the double-edged sword? *Biomed. Res. Int.* 2013:179174. doi: 10.1155/2013/179174

Igarashi, T., Brown, C. R., Endo, Y., Buckler-White, A., Plishka, R., Bischofberger, N., et al. (2001). Macrophage are the principal reservoir and sustain high virus loads in rhesus macaques after the depletion of CD4+ T cells by a highly pathogenic simian immunodeficiency virus/HIV type 1 chimera (SHIV), implications for HIV-1 infections of humans. *Proc. Natl. Acad. Sci. U.S.A.* 98, 658–663. doi: 10.1073/pnas.98.2.658

Ip, W. K., Takahashi, K., Ezekowitz, R. A., and Stuart, L. M. (2009). Mannose-binding lectin and innate immunity. *Immunol. Rev.* 230, 9–21. doi: 10.1111/j.1600-065X.2009.00789.x

Ishikawa, E., Ishikawa, T., Morita, Y. S., Toyonaga, K., Yamada, H., Takeuchi, O., et al. (2009). Direct recognition of the mycobacterial glycolipid, trehalose dimycolate, by C-type lectin Mincle. *J. Exp. Med.* 206, 2879–2888. doi: 10.1084/jem.20091750

Ishikawa, E., Mori, D., and Yamasaki, S. (2017). Recognition of mycobacterial lipids by immune receptors. *Trends Immunol.* 38, 66–76. doi: 10.1016/j.it.2016.10.009

Izquierdo-Useros, N., Lorizate, M., McLaren, P. J., Telenti, A., Krausslich, H., Martinez-Picado, J. (2014). HIV-1 capture and transmission by dendritic cells: the role of viral glycolipids and the cellular receptor Siglec-1. *PLoS Pathog.* 10:e1004146. doi: 10.1371/journal.ppat.1004146

Jadhav, S. K., Velhal, S. M., Deshpande, A., and Bandivdekar, A. H. (2013). Association of human mannose receptor in sexual transmission of human immunodeficiency virus in serodiscordant couples. *AIDS Res. Hum. Retroviruses* 29, 156–163. doi: 10.1089/aid.2012.0101

Jiang, G., and Dandekar, S. (2015). Targeting NF-kappaB signaling with protein kinase C agonists as an emerging strategy for combating HIV latency. *AIDS Res. Hum. Retroviruses* 31, 4–12. doi: 10.1089/aid.2014.0199

Kabuye, D., Chu, Y., Lao, W., Jin, G., and Kang, H. (2019). Association between CLEC4E gene polymorphism of mincle and pulmonary tuberculosis infection in a northern Chinese population. *Gene* 710, 24–29. doi: 10.1016/j.gene.2019.05.011

Kang, P. B., Azad, A. K., Torrelles, J. B., Kaufman, T., Beharka, A., Tibesar, E., et al. (2005). The human macrophage mannose receptor directs *Mycobacterium tuberculosis* lipoarabinomannan-mediated phagosome biogenesis. *J. Exp. Med.* 202, 987–999. doi: 10.1084/jem.20051239

Kaufmann, S. H., and Schaible, U. E. (2003). A dangerous liaison between two major killers: *Mycobacterium tuberculosis* and HIV target dendritic cells through DC-SIGN. *J. Exp. Med.* 197, 1–5. doi: 10.1084/jem.20021964

Kerscher, B., Dambuza, I. M., Christofi, M., Reid, D. M., Yamasaki, S., Willment, J. A., et al. (2016). Signalling through MyD88 drives surface expression of the mycobacterial receptors MCL (Clecsf8, Clec4d) and Mincle (Clec4e) following microbial stimulation. *Microbes Infect.* 18, 505–509. doi: 10.1016/j.micinf.2016.03.007

Kim, J. S., Kim, Y. R., and Yang, C. S. (2019). Latest comprehensive knowledge of the crosstalk between TLR signaling and mycobacteria and the antigens driving the process. *J. Microbiol. Biotechnol.* 29, 1506–1521. doi: 10.4014/jmb.1908.08057

Klassert, T. E., Goyal, S., Stock, M., Driesch, D., Hussain, A., Berrocal-Almanza, L., et al. (2018). AmpliSeq screening of genes encoding the C-type lectin receptors and their signaling components reveals a common variant in MASP1 associated with pulmonary tuberculosis in an indian population. *Front. Immunol.* 9:242. doi: 10.3389/fimmu.2018.00242

Lai, J., Bernhard, O. K., Turville, S. G., Harman, A., Wilkinson, J., and Cunningham, A. L. (2009). Oligomerization of the macrophage mannose receptor enhances gp120-mediated binding of HIV-1. *J. Biol. Chem.* 284, 11027–11038. doi: 10.1074/jbc.M809698200

Lambert, A. A., Barabe, F., Gilbert, C., and Tremblay, M., J. (2011). DCIR-mediated enhancement of HIV-1 infection requires the ITIM-associated signal transduction pathway. *Blood* 117, 6589–6599. doi: 10.1182/blood-2011-01-331363

Lambert, A. A., Gilbert, C., Richard, M., Beaulieu, A. D., and Tremblay, M. (2008). The C-type lectin surface receptor DCIR acts as a new attachment factor for HIV-1 in dendritic cells and contributes to trans- and cis-infection pathways. *Blood* 112, 1299–1307. doi: 10.1182/blood-2008-01-136473

Lang, R. (2013). Recognition of the mycobacterial cord factor by Mincle: relevance for granuloma formation and resistance to tuberculosis. *Front. Immunol.* 4:5. doi: 10.3389/fimmu.2013.00005

Lee, G. Q., and Lichterfeld, M. (2016). Diversity of HIV-1 reservoirs in CD4+ T-cell subpopulations. *Curr. Opin. HIV AIDS* 11, 383–387. doi: 10.1097/COH.0000000000000281

Lester, R. T., Yao, X. D., Ball, T. B., McKinnon, L., Kaul, R., Wachihi, C., et al. (2008). Toll-like receptor expression and responsiveness are increased in viraemic HIV-1 infection. *AIDS* 22, 685–694. doi: 10.1097/QAD.0b013e3282f4de35

Lugo-Villarino, G., Troegeler, A., Balboa, L., Lastrucci, C., Duval, C., Mercier, I., et al. (2018). The C-type lectin receptor DC-SIGN has an anti-inflammatory role in human M(IL-4) macrophages in response to *Mycobacterium tuberculosis*. *Front. Immunol.* 9:1123. doi: 10.3389/fimmu.2018.01123

Marakalala, M. J., Guler, R., Matika, L., Murray, G., Jacobs, M., Brombacher, F., et al. (2011). The Syk/CARD9-coupled receptor Dectin-1 is not required for host resistance to *Mycobacterium tuberculosis* in mice. *Microbes Infect.* 13, 198–201. doi: 10.1016/j.micinf.2010.10.013

Maretti, E., Costantino, L., Buttini, F., Rustichelli, C., Leo, E., Truzzi, E., et al. (2019). Newly synthesized surfactants for surface mannosylation of respirable SLN assemblies to target macrophages in tuberculosis therapy. *Drug Deliv. Transl. Res.* 9, 298–310. doi: 10.1007/s13346-018-00607-w

Marquez, A., Varade, J., Robledo, G., Martinez, A., Mendoza, J. L., Taxonera, C., Fernandez-Arquero, M., et al. (2009). Specific association of a CLEC16A/KIAA0350 polymorphism with NOD2/CARD15(-) Crohn's disease patients. *Eur. J. Hum. Genet.* 17, 1304–1308. doi: 10.1038/ejhg.2009.50

Martinez-Pomares, L. (2012). The mannose receptor. *J. Leukoc. Biol.* 92, 1177–1186. doi: 10.1189/jlb.0512231

Marzi, A., Mitchell, D. A., Chaipan, C., Fisch, T., Doms, R., Carrington, M., Desrosiers, R. C., et al. (2007). Modulation of HIV and SIV neutralization sensitivity by DC-SIGN and mannose-binding lectin. *Virology* 368, 322–330. doi: 10.1016/j.virol.2007.07.004

Mayer-Barber, K. D., Andrade, B. B., Oland, S. D., Amaral, E., Barber, D. L., Gonzales, J., et al. (2014). Host-directed therapy of tuberculosis based on interleukin-1 and type I interferon crosstalk. *Nature* 511, 99–103. doi: 10.1038/nature13489

Mazzuca, P., Caruso, A., and Caccuri, F. (2016). HIV-1 infection, microenvironment and endothelial cell dysfunction. *New Microbiol.* 39, 163–173.

McGreal, E. P., Miller, J. L., and Gordon, S. (2005). Ligand recognition by antigen-presenting cell C-type lectin receptors. *Curr. Opin. Immunol.* 17, 18–24. doi: 10.1016/j.coi.2004.12.001

Meier, A., Alter, G., Frahm, N., Sidhu, H., Li, B., Bagchi, A., et al. (2007). MyD88-dependent immune activation mediated by human immunodeficiency virus type 1-encoded Toll-like receptor ligands. *J. Virol.* 81, 8180–8191. doi: 10.1128/JVI.00421-07

Mesman, A. W., and Geijtenbeek, T. B. (2012). Pattern recognition receptors in HIV transmission. *Front. Immunol.* 3:59. doi: 10.3389/fimmu.2012.00059

Mishra, A., Akhtar, S., Jagannath, C., and Khan, A. (2017). Pattern recognition receptors and coordinated cellular pathways involved in tuberculosis immunopathogenesis: emerging concepts and perspectives. *Mol. Immunol.* 87: 240–248. doi: 10.1016/j.molimm.2017.05.001

Miyake, Y., Ishikawa, E., Ishikawa, T., and Yamasaki, S. (2010). Self and nonself recognition through C-type lectin receptor, Mincle. *Self Nonself* 1, 310–313. doi: 10.4161/self.1.4.13736

Miyake, Y., Masatsugu, O. H., and Yamasaki, S. (2015). C-type lectin receptor MCL facilitates mincle expression and signaling through complex formation. *J. Immunol.* 194, 5366–5374. doi: 10.4049/jimmunol.1402429

Miyake, Y., Toyonaga, K., Mori, D., Kakuta, S., Hoshino, Y., Oyamada, A., et al. (2013). C-type lectin MCL is an FcRgamma-coupled receptor that mediates the adjuvanticity of mycobacterial cord factor. *Immunity* 38, 1050–1062. doi: 10.1016/j.immuni.2013.03.010

Mortaz, E., Adcock, I. M., Tabarsi, P., Masjedi, M. R., Mansouri, D., Velayati, A. A., et al. (2015). Interaction of pattern recognition receptors with mycobacterium tuberculosis. *J. Clin. Immunol.* 35, 1–10. doi: 10.1007/s10875-014-0103-7

Mosaiab, T., Boiteux, S., Zulfiker, A. H. M., Wei, M. Q., Kiefel, M. J., and Houston, T. A. (2018). A simple glycolipid mimic of the phosphatidylinositol mannoside core from *Mycobacterium tuberculosis* inhibits macrophage cytokine production. *Chembiochem* 19, 1476–1481. doi: 10.1002/cbic.201800150

Nagata, M., Izumi, Y., Ishikawa, E., Kiyotake, R., Doi, R., Iwai, S., et al. (2017). Intracellular metabolite beta-glucosylceramide is an endogenous Mincle ligand possessing immunostimulatory activity. *Proc. Natl. Acad. Sci. U.S.A.* 114, E3285–E3294. doi: 10.1073/pnas.1618133114

Nguyen, D. G., and Hildreth, J., E. (2003). Involvement of macrophage mannose receptor in the binding and transmission of HIV by macrophages. *Eur. J. Immunol.* 33, 483–493. doi: 10.1002/immu.200310024

Nisihara, R., Skare, T., Maestri, V., Alegretti, J. S., Campos, A., and Messias-Reason, I. (2018). Mannose-binding lectin (MBL) deficiency and tuberculosis infection in patients with ankylosing spondylitis. *Clin. Rheumatol.* 37, 555–558. doi: 10.1007/s10067-017-3813-4

Osorio, F., and Reis e Sousa, C. (2011). Myeloid C-type lectin receptors in pathogen recognition and host defense. *Immunity* 34, 651–664. doi: 10.1016/j.immuni.2011.05.001

Pawlowski, A., Jansson, M., Skold, M., Rottenberg, M. E., and Kallenius, G. (2012). Tuberculosis and HIV co-infection. *PLoS Pathog.* 8:e1002464. doi: 10.1371/journal.ppat.1002464

Perez-Zsolt, D., Cantero-Perez, J., Erkizia, I., Benet, S., Pino, M., Serra-Peinado, C., et al. (2019). Dendritic cells from the cervical mucosa capture and transfer HIV-1 via siglec-1. *Front. Immunol.* 10:825. doi: 10.3389/fimmu.2019.00825

Polotsky, V. Y., Belisle, J. T., Mikusova, K., Ezekowitz, R. A., and Joiner, K. A. (1997). Interaction of human mannose-binding protein with *Mycobacterium avium*. *J. Infect. Dis.* 175, 1159–1168. doi: 10.1086/520354

Preza, G. C., Tanner, K., Elliott, J., Yang, O. O., Anton, P., Ochoa, M. T. (2014). Antigen-presenting cell candidates for HIV-1 transmission in human distal colonic mucosa defined by CD207 dendritic cells and CD209 macrophages. *AIDS Res. Hum. Retroviruses* 30, 241–249. doi: 10.1089/aid.2013.0145

Rajaram, M. V., Brooks, M. N., Morris, J. D., Torrelles, J., Azad, A. Z., and Schlesinger, L. S. (2010). *Mycobacterium tuberculosis* activates human macrophage peroxisome proliferator-activated receptor gamma linking mannose receptor recognition to regulation of immune responses. *J. Immunol.* 185, 929–942. doi: 10.4049/jimmunol.1000866

Rajaram, M. V. S., Arnett, E., Azad, A. K., Guirado, E., Ni, B., Gerberick, A. D., et al. (2017). *M. tuberculosis*-initiated human mannose receptor signaling regulates macrophage recognition and vesicle trafficking by FcRgamma-chain, Grb2, and SHP-1. *Cell Rep.* 21, 126–140. doi: 10.1016/j.celrep.2017.09.034

Ribeiro, C. M., Sarrami-Forooshani, R., Setiawan, L. C., Zijlstra-Willems, E. M., van Hamme, L. J., Tigchelaar, W., et al. (2016). Receptor usage dictates HIV-1 restriction by human TRIM5alpha in dendritic cell subsets. *Nature* 540, 448–452. doi: 10.1038/nature20567

Sabir, N., Hussain, T., Mangi, M. H., Zhao, D., and Zhou, X. (2019). Matrix metalloproteinases: expression, regulation and role in the immunopathology of tuberculosis. *Cell Prolif.* 52:e12649. doi: 10.1111/cpr.12649

Scriba, T. J., Kalsdorf, B., Abrahams, D. A., Isaacs, F., Hofmeister, J., Black, G., et al. (2008). Distinct, specific IL-17- and IL-22-producing CD4+ T cell subsets contribute to the human anti-mycobacterial immune response. *J. Immunol.* 180, 1962–1970. doi: 10.4049/jimmunol.180.3.1962

Sester, M., Giehl, C., McNerney, R., Kampmann, B., Walzl, G., Cuchi, P., et al. (2010). Challenges and perspectives for improved management of HIV/*Mycobacterium tuberculosis* co-infection. *Eur. Respir. J.* 36, 1242–1247. doi: 10.1183/09031936.00040910

Sharma, S. K., Mohan, A., and Kadhiravan, T. (2005). HIV-TB co-infection: epidemiology, diagnosis & management. *Indian J. Med. Res.* 121, 550–567.

Shivakoti, R., Dalli, J., Kadam, D., Gaikwad, S., Barthwal, M., Colas, R., et al. (2019). Lipid mediators of inflammation and resolution in individuals with tuberculosis and tuberculosis-Diabetes. *Prostag. Oth. Lipid M.* 147:106398. doi: 10.1016/j.prostaglandins.2019.106398

Soilleux, E. J., Morris, L. S., Lee, B., Pohlmann, S., Trowsdale, J., Doms, R. W., et al. (2001). Placental expression of DC-SIGN may mediate intrauterine vertical transmission of HIV. *J. Pathol.* 195, 586–592. doi: 10.1002/path.1026

Sorgi, C. A., Secatto, A., Fontanari, C., Turato, W. M., Belanger, C., de Medeiros, A. I., et al. (2009). Histoplasma capsulatum cell wall {beta}-glucan induces lipid body formation through CD18, TLR2, and dectin-1 receptors: correlation with leukotriene B4 generation and role in HIV-1 infection. *J. Immunol.* 182, 4025–4035. doi: 10.4049/jimmunol.0801795

St-Pierre, C., Manya, H., Ouellet, M., Clark, G. F., Endo, T., Tremblay, M. J., et al. (2011). Host-soluble galectin-1 promotes HIV-1 replication through a direct interaction with glycans of viral gp120 and host CD4. *J. Virol.* 85, 11742–11751. doi: 10.1128/JVI.05351-11

St-Pierre, C., Ouellet, M., Giguere, D., Ohtake, R., Roy, R., Sato, S., et al. (2012). Galectin-1-specific inhibitors as a new class of compounds to treat HIV-1 infection. *Antimicrob. Agents Chemother.* 56, 154–162. doi: 10.1128/AAC.05595-11

Sukegawa, S., Miyagi, E., Bouamr, F., Farkasova, H., and Strebel, K. (2018). Mannose receptor 1 restricts HIV particle release from infected macrophages. *Cell Rep.* 22, 786–795. doi: 10.1016/j.celrep.2017.12.085

Sun, H., Kim, D., Li, X., Kiselinova, M., Ouyang, Z., Vandekerckhove, L., Shang, H., et al. (2015). Th1/17 Polarization of CD4 T cells supports HIV-1 persistence during antiretroviral therapy. *J. Virol.* 89, 11284–11293. doi: 10.1128/JVI.01595-15

Tanne, A., and Neyrolles, O. (2010). C-type lectins in immune defense against pathogens: the murine DC-SIGN homologue SIGNR3 confers early protection against *Mycobacterium tuberculosis* infection. *Virulence* 1, 285–290. doi: 10.4161/viru.1.4.11967

Tobin, D. M., Roca, F. J., Oh, S. F., McFarland, R., Vickery, T. W., Ray, J. P., et al. (2012). Host genotype-specific therapies can optimize the inflammatory response to mycobacterial infections. *Cell* 148, 434–446. doi: 10.1016/j.cell.2011.12.023

Tomalka, J., Ghneim, K., Bhattacharyya, S., Aid, M., Barouch, D. H., Sekaly, R. P., et al. (2016). The sooner the better: innate immunity as a path toward the HIV cure. *Curr. Opin. Virol.* 19, 85–91. doi: 10.1016/j.coviro.2016.07.003

Troegeler, A., Mercier, I., Cougoule, C., Pietretti, D., Colom, A., Duval, C., et al. (2017). C-type lectin receptor DCIR modulates immunity to tuberculosis by sustaining type I interferon signaling in dendritic cells. *Proc. Natl. Acad. Sci. U.S.A.* 114, E540–E549. doi: 10.1073/pnas.1613254114

Tsoni, S. V., and Brown, G. D. (2008). beta-Glucans and dectin-1. *Ann. N. Y. Acad. Sci.* 1143, 45–60. doi: 10.1196/annals.1443.019

Turville, S., Wilkinson, J., Cameron, P., Dable, J., and Cunningham, A., L. (2003). The role of dendritic cell C-type lectin receptors in HIV pathogenesis. *J. Leukoc. Biol.* 74, 710–718. doi: 10.1189/jlb.0503208

Turville, S. G., Cameron, P. U., Arthos, J., MacDonald, K., Clark, G., Hart, D., et al. (2001). Bitter-sweet symphony: defining the role of dendritic cell gp120 receptors in HIV infection. *J. Clin. Virol.* 22, 229–239. doi: 10.1016/S1386-6532(01)00194-9

van de Veerdonk, F. L., Teirlinck, A. C., Kleinnijenhuis, J., Kullberg, B. J., van Crevel, R., van der Meer, J. W., et al. (2010). *Mycobacterium tuberculosis* induces IL-17A responses through TLR4 and dectin-1 and is critically dependent on endogenous IL-1. *J. Leukoc. Biol.* 88, 227–232. doi: 10.1189/jlb.0809550

van der Vlist, M., and Geijtenbeek, T., B. (2010). Langerin functions as an antiviral receptor on Langerhans cells. *Immunol. Cell Biol.* 88, 410–415. doi: 10.1038/icb.2010.32

van Kooyk, Y., Appelmelk, B., and Geijtenbeek, T. B. (2003). A fatal attraction: *Mycobacterium tuberculosis* and HIV-1 target DC-SIGN to escape immune surveillance. *Trends Mol. Med.* 9, 153–159. doi: 10.1016/S1471-4914(03)00027-3

van Kooyk, Y., and Geijtenbeek, T., B. (2003). DC-SIGN: escape mechanism for pathogens. *Nat. Rev. Immunol.* 3, 697–709. doi: 10.1038/nri1182

Varga, N., Sutkeviciute, I., Ribeiro-Viana, R., Berzi, A., Ramdasi, R., Daghetti, A., et al. (2014). A multivalent inhibitor of the DC-SIGN dependent uptake of HIV-1 and Dengue virus. *Biomaterials* 35, 4175–4184. doi: 10.1016/j.biomaterials.2014.01.014

Velasquez, L. N., Stuve, P., Gentilini, M. V., Swallow, M., Bartel, J., Lycke, N. Y., et al. (2018). Targeting *Mycobacterium tuberculosis* antigens to dendritic cells via the DC-specific-ICAM3-grabbing-nonintegrin receptor induces strong T-helper 1 immune responses. *Front. Immunol.* 9:471. doi: 10.3389/fimmu.2018.00471

WHO (2019a). *Global Tuberculosis Report.* Available online at: https://www.who.int/tb/publications/global_report/en/ (Retrieved April 27, 2020).

WHO (2019b). *HIV/AIDS Data and Statistics.* Available online at: http://www.who.int/hiv/data/en/ (Retrieved April 27, 2020).

Wilson, G. J., Marakalala, M. J., Hoving, J. C., van Laarhoven, A., Drummond, R. A., Brown, G. D., et al. (2015). The C-type lectin receptor CLECSF8/CLEC4D is a key component of anti-mycobacterial immunity. *Cell Host Microbe* 17, 252–259. doi: 10.1016/j.chom.2015.01.004

Yonekawa, A., Saijo, S., Hoshino, Y., Miyake, Y., Ishikawa, E., Suzukawa, M., et al. (2014). Dectin-2 is a direct receptor for mannose-capped lipoarabinomannan of mycobacteria. *Immunity* 41, 402–413. doi: 10.1016/j.immuni.2014.08.005

Zapata, H. J., Van Ness, P. H., Avey, S., Siconolfi, B., Allore, H., Tsang, S., et al. (2019). Impact of Aging and HIV infection on the function of the C-type lectin receptor MINCLE in monocytes. *J. Gerontol. A Biol. Sci. Med. Sci.* 74, 794–801. doi: 10.1093/gerona/gly209

Zhang, X., Jiang, F., Wei, L., Li, F., Liu, J., Wang, C., et al. (2012). Polymorphic allele of human MRC1 confer protection against tuberculosis in a Chinese population. *Int. J. Biol. Sci.* 8, 375–382. doi: 10.7150/ijbs.4047

Zheng, M., Shi, S., Wei, W., Zheng, Q., Wang, Y., Ying, X., et al. (2018). Correlation between MBL2/CD14/TNF- α gene polymorphisms and susceptibility to spinal tuberculosis in Chinese population. *Biosci. Rep.* 38:BSR20171140. doi: 10.1042/BSR20171140

Zou, Z., Chastain, A., Moir, S., Ford, J., Trandem, K., Martinelli, E., et al. (2011). Siglecs facilitate HIV-1 infection of macrophages through adhesion with viral sialic acids. *PLoS ONE* 6:e24559. doi: 10.1371/journal.pone.0024559

Conflict of Interest: The authors declare that the research was conducted in the absence of any commercial or financial relationships that could be construed as a potential conflict of interest.

frontiers in Cellular and Infection Microbiology

ORIGINAL RESEARCH
published: 27 August 2020
doi: 10.3389/fcimb.2020.00432

A TLR2-Activating Fraction From *Mycobacterium abscessus* Rough Variant Demonstrates Vaccine and Diagnostic Potential

Vincent Le Moigne[1], Anne-Laure Roux[1], Aude Jobart-Malfait[1], Landry Blanc[2], Karima Chaoui[2], Odile Burlet-Schiltz[2], Jean-Louis Gaillard[1], Stéphane Canaan[3], Jérôme Nigou[2] and Jean-Louis Herrmann[1,4]*

[1] Université Paris-Saclay, UVSQ, Inserm, Infection et inflammation, Montigny-le-Bretonneux, France, [2] Institut de Pharmacologie et de Biologie Structurale, Université de Toulouse, CNRS, Université Paul Sabatier, Toulouse, France, [3] Université Aix-Marseille, CNRS, LISM, IMM FR3479, Marseille, France, [4] APHP, GHU Paris-Saclay, Hôpital Raymond Poincaré, Service de Microbiologie, Garches, France

OPEN ACCESS

Edited by:
David Neil McMurray, Texas A&M Health Science Center, United States

Reviewed by:
Ashu Sharma, University at Buffalo, United States
Ramon A. Juste, NEIKER Basque Institute for Agricultural Research and Development, Spain

***Correspondence:**
Vincent Le Moigne
vincent.le-moigne@uvsq.fr

Specialty section:
This article was submitted to Microbes and Innate Immunity, a section of the journal Frontiers in Cellular and Infection Microbiology

Received: *28 January 2020*
Accepted: *14 July 2020*
Published: *27 August 2020*

Citation:
Le Moigne V, Roux A-L, Jobart-Malfait A, Blanc L, Chaoui K, Burlet-Schiltz O, Gaillard J-L, Canaan S, Nigou J and Herrmann J-L (2020) A TLR2-Activating Fraction From Mycobacterium abscessus Rough Variant Demonstrates Vaccine and Diagnostic Potential. Front. Cell. Infect. Microbiol. 10:432. doi: 10.3389/fcimb.2020.00432

Mycobacterium abscessus is a prevalent pathogenic mycobacterium in cystic fibrosis (CF) patients and one of the most highly drug resistant mycobacterial species to antimicrobial agents. It possesses the property to transition from a smooth (S) to a rough (R) morphotype, thereby influencing the host innate immune response. This transition from the S to the R morphotype takes place in patients with an exacerbation of the disease and a persistence of *M. abscessus*. We have previously shown that the exacerbation of the Toll-like receptor 2 (TLR2)-mediated inflammatory response, following this S to R transition, is essentially due to overproduction of bacilli cell envelope surface compounds, which we were able to extract by mechanical treatment and isolation by solvent partition in a fraction called interphase. Here, we set up a purification procedure guided by bioactivity to isolate a fraction from the R variant of *M. abscessus* cells which exhibits a high TLR2 stimulating activity, referred to as TLR2-enriched fraction (TLR2eF). As expected, TLR2eF was found to contain several lipoproteins and proteins known to be stimuli for TLR2. Vaccination with TLR2eF showed no protection toward an *M. abscessus* aerosol challenge, but provided mild protection in ΔF508 mice and their FVB littermates when intravenously challenged by *M. abscessus*. Interestingly however, antibodies against TLR2eF compounds were detected during disease in CF patients. In conclusion, we show the potential for compounds in TLR2eF as vaccine and diagnostic candidates, in order to enhance diagnosis, prevent and/or treat *M. abscessus*-related infections.

Keywords: *Mycobacterium abscessus*, cystic fibrosis, lipoprotein TLR2, vaccine adjuvant, diagnosis

INTRODUCTION

Mycobacterium abscessus, a rapid growing mycobacterium (RGM), is emerging as a difficult-to-treat pathogen in cystic fibrosis (CF) patients. *Mycobacterium abscessus* is responsible for muco-cutaneous (Viana-Niero et al., 2008) and pulmonary infections (Griffith et al., 1993; Olivier et al., 2003; Roux et al., 2009). Severe and often fatal infections have been described

and are able to persist for decades in selected infected hosts (Cullen et al., 2000; Jönsson et al., 2007; Catherinot et al., 2009; Qvist et al., 2015). Above all, it is also the most resistant bacterium to antibiotics, with well documented therapeutic failures (Sanguinetti et al., 2001).

Mycobacterium abscessus is able to transition from a smooth (S) to a rough (R) morphotype. This S to R transition is linked to genetic insertions/deletions (Pawlik et al., 2013), which results in the arrest of synthesis and/or transport of glycopeptidolipids (GPL) at the cell surface (Ripoll et al., 2007). This event, occurring throughout the course of the disease, modifies completely the intensity of the inflammatory response triggered by *M. abscessus* S or R *in vivo* (Catherinot et al., 2007, 2009). The loss of GPL in the R variant is compensated by the increased synthesis and exposure at the cell surface of numerous lipoproteins, such as LpqH, LprA, and LprG (Roux et al., 2011). After isolating a fraction enriched in lipoproteins from the cell surface of the *M. abscessus* R variant, we found this fraction was responsible for TLR2 activation pathway provoking an important inflammatory response (Roux et al., 2011). This cell envelope remodeling was responsible for the TLR2-mediated hyper-pro-inflammatory phenotype of virulent R variants (Roux et al., 2011).

Major TLR2-activators are found among mycobacterial compounds, including lipoproteins (Brightbill et al., 1999; Thoma-Uszynski et al., 2000, 2001), lipomannan (LM) and phosphatidylinositol-mannosides (PIMs) (Gilleron et al., 2003; Quesniaux et al., 2004), in addition to several other proteins, including some heat shock proteins (HSP) (Jo et al., 2007).

The immune response triggered by the various mycobacterial glycolipids or lipoproteins in antigen-presenting cells is balanced, depending on the pattern recognition receptors (TLRs, DC-SIGN, Mannose Receptor, …) engaged, between a protective inflammatory response characterized by the synthesis of IL-12 and Interferon gamma (IFNɣ), and a response with anti-inflammatory IL-10 release leading to an impaired T cell response (Nigou et al., 2001; Tailleux et al., 2002; Geijtenbeek et al., 2003; Kaufmann and Schaible, 2003).

The use of TLR activation strategies induced by lipoproteins was previously proposed in the context of vaccine development, with the goal of amplifying antibacterial defense mechanisms and immune responses (Brightbill et al., 1999). TLR agonists have potent immunomodulatory activities and can promote adaptive immune responses to co-administered antigens. Consequently, they have been exploited as adjuvants in vaccines for other infectious diseases and cancers as anti-tumor immunotherapy (Conroy et al., 2008; Higgins and Mills, 2010).

In the present study, we evaluated both the vaccine and diagnostic potential in *M. abscessus* infection of a TLR2-activating fraction purified from *M. abscessus* R variant.

MATERIALS AND METHODS

Bacterial Strain Culture

Mycobacterium abscessus R variant was grown in 7H9 medium containing 1% glucose and cells were collected by centrifugation. Pellets were weighted and conserved at −30°C until extraction. For bacterial experimental infections, batches were prepared after centrifugation by washing pellets with phosphate-buffered saline (PBS), centrifuged and finally suspended in PBS with 10% glycerol, and dissociated by repeated passage through a 29.5-gauge needle. Then, 1-ml aliquot bacterial batches were frozen and conserved at −80°C until they were required and titrated.

Fraction Extraction and Purification by Reverse-Phase Chromatography

Mycobacterium abscessus pellets (40 g) were delipidated by several extractions with $CHCl_3/CH_3OH$. The first one with 180 mL $CHCl_3/CH_3OH$ (1:2, v/v) and incubated 150 min at 50°C in a glass jar with agitation as previously described (Nigou et al., 1997). The suspension was then centrifuged 15 min at 800 g at room temperature and the supernatant (lipids) was removed. The pellet was suspended in 200 mL of $CHCl_3/CH_3OH$ (1:1, v/v) and incubated for 90 min as previously. After a second centrifugation (15 min at 800 g, room temperature), the supernatant was removed. The pellet was resuspended in 200 mL $CHCl_3/CH_3OH$ (1:1, v/v) and shacked overnight at room temperature. After centrifugation, the supernatant was added to the two previously supernatants. Delipidated cells were then disrupted by sonication. Proteins were further extracted by refluxing the broken cells in 160 mL of 50% ethanol at 65°C for 90 min. The supernatant was recovered and, following the same procedure, a second extraction was then performed on the remaining pellet. Finally, both supernatants were mixed. The resulting ethanol/water extract was evaporated with a Rotavap up to 4 mL final volume and to allow to solubilize proteins, eventually stuck on the glass tube, the flask was rinsed with 4 mL of water and sonicated. A final volume of 8 mL was then recovered, frozen and lyophilized. DNAse and RNAse digestion was then performed onto the dried extract in 3 mL of 20 mM Tris-HCl, 1 mM $MgCl_2$, pH 7.5 containing 130 U of DNAse and 130 U of RNase (8 h at 37°C). Dialysis (MW cut-off 6–8 kDa) against water was then performed followed by α-amylase digestion to remove glycans in a phosphate buffer 50 mM (pH 7.5) with 2% (w:w) for the enzyme (8 h, room temperature). A second dialysis (MW cut-off 6–8 kDa) against water was then performed. A total of 20 mg protein was obtained as determined by Bradford assay.

The protein fraction was resuspended at a concentration of 1 mg/mL in water and loaded onto a PuriFlash C_4 bonded silica column (15 µm particles, porosity 200 Å; Interchim) pre-equilibrated with Limulus Amoebocyte Lysate (LAL) tested water containing 0.1% Trifluoroacetic acid (TFA). A first wash of the column with 10 mL of water/0.1% TFA was then performed. The charged column was then placed onto the chromatograph in which all of the pipes have been filled previously with eluents, firstly 99% acetonitrile/water LAL 1%/0.1% TFA (buffer B), then 99.9% LAL water/0.1% TFA (buffer A). The gradient used to elute the different products of interest, with a flow rate of 2 mL/min, was: from 100% buffer A to 25% buffer A/75% buffer B in 15 min; 25% buffer A/75% buffer B to 100% buffer B in 10 min; 100% buffer B for 10 min; 100% buffer B to 100% buffer A in 5 min; 100% buffer A for 5 min. About 1 mL of the fractions from the final volume were collected in 90 glass tubes for 45 min to complete elution. Glass tubes were previously treated at 160°C

for at least 2 h to remove any traces of LPS. Collected fractions of 1 mL were dried in a speedvac, resuspended in 110 μL of water, and protein concentration was determined.

HEK-TLR2 Experiments

As described previously (Roux et al., 2011), HEK-Blue^{TM}-TLR2 cells (InvivoGen, France), derivatives of HEK293 cells that stably express the human TLR2 and CD14 genes along with a NF-κB-inducible reporter system (secreted alkaline phosphatase), were maintained in Dulbecco's modified Eagle's medium (DMEM, Gibco) containing 10% Fetal Bovine Serum (FBS, Gibco), 4.5 g/L glucose, 2 mM L-glutamine, 100 U/mL penicillin, 100 μg/mL streptomycin (Sigma). Protein fraction (0.1 μL) and HEK-TLR2 cells (5×10^4 cells per well) were added to 96-well plates. A cells stimulation control was realized with the synthetic triacylated lipopeptide Pam3CSK4 in a range from 0.01 to 100 ng/mL. Reporter cells were stimulated for 18 h and alkaline phosphatase activity was measured by mixing 20 μL of the culture supernatant and 180 μL of Quanti-Blue^{TM} (InvivoGen) and reading O.D. at 630 nm.

Human Monocytes Derived Dendritic Cells (DCs) and Cytokines Quantification

Peripheral blood mononuclear cells were isolated from freshly collected blood samples obtained from healthy voluntary blood donors (Ambroise Paré Hospital, France) by density gradient centrifugation using a lymphocyte separation medium (GE Healthcare Bio-Sciences, Sweden) as previously described (Dulphy et al., 2007; Talpin et al., 2014). Monocytes were purified by positive selection using anti-CD14-coated magnetic micro beads (Miltenyi Biotec, Bergisch Gladbach, Germany). Sorted monocytes were morphogically homogeneous with 90% of CD14+ cells, as determined by flow cytometry. Monocytes were differentiated into DCs for 7 days in RPMI medium supplemented with 10% FCS 100 U/mL penicillin, 100 μg/mL streptomycin, 500 UI/mL GM-CSF, and 500 UI/mL IL-4 (Miltenyi Biotec, Germany R&D Systems, Abingdon, UK). At day 2, fresh medium supplemented with GM-CSF and IL-4 was added to culture and supplemented with IL-4 only at day 6. For stimulation assays, cells were harvested and cultured for an additional 2 days in fresh culture medium supplemented with either *Escherichia coli* LPS (250 ng/mL, Sigma, Saint-Louis, MI, USA) or with various concentrations of the TLR2eF (0.1–10 μg/mL). Supernatants from immature DCs stimulated with or without bacterial products were harvested at 48 h as previously described (Dulphy et al., 2007). TNF-α was quantified by ELISA with kits provided by R&D Systems (Abingdon, UK).

Tandem Mass Spectrometry Analysis

Protein samples were partially air-dried in a *speed-vac* device, reconstituted in 1× final Laemmli buffer, and loaded on a one-dimensional SDS-PAGE gel. The electrophoretic migration was stopped as soon as the proteins entered the separating gel, in order to isolate all proteins in a single gel band. This band was washed, subjected to in-gel tryptic digestion and analyzed by nanoLC-MS/MS using an UltiMate 3000 RSLCnano system (Dionex, Amsterdam, The Netherlands) as previously described (Martinez-Pinna et al., 2014) except that peptides were eluted using a 5–50% gradient of solvent B (80% acetonitrile, 0.2% formic acid) during 5 h at 300 nL/min flow rate. The nanoLC system was coupled to an Orbitrap Fusion^{TM} Tribrid^{TM} Mass Spectrometer (Thermo Scientific, Bremen, Germany) operated in a data-dependent acquisition mode with the XCalibur software. Survey scan MS were acquired in the Orbitrap on the 300–2,000 m/z range with the resolution set to a value of 120,000. During data dependent acquisition, Orbitrap survey spectra were scheduled for execution at least every 3 s, with the embedded control system determining the number of MS/MS acquisitions executed during this period. Dynamic exclusion was employed within 60 s to prevent repetitive selection of the same peptide. Quadruplicate technical LC-MS measurements were performed.

Bioinformatic Processing of Mass Spectrometry Data

Raw mass spectrometry files were processed with the MaxQuant software (version 1.5.0) for database search with the Andromeda search engine and for quantitative analysis. Data were searched for against *M. abscessus* entries of the Uniprot-Swissprot-TrEMBL protein database (October 2019 version). Carbamidomethylation of cysteines was set as a fixed modification, whereas oxidation of methionine, protein N-terminal acetylation was set as variable modifications. Specificity of trypsin digestion was set for cleavage after K or R, and two missed trypsin cleavage sites were allowed. The precursor mass tolerance was set to 20 ppm for the first search and 5 ppm for the main Andromeda database search. The mass tolerances MS/MS mode was set to 0.6 Da. Minimum peptide length was set to seven amino acids, and the minimum number of peptides was set to one. Andromeda results were validated by the target-decoy approach using a reverse database at a both a peptide and protein FDR of 1%. The iBAQ metric, which corresponds to the sum of all the peptide intensities divided by the number of observable peptides of a protein (Schwanhäusser et al., 2011), was used to estimate absolute protein abundance. A threshold of iBAQ $>6 \times 10^8$ was applied as it corresponds to an abrupt stall of the slope of the curve of iBAQ values.

Vaccination and Infectious Challenge

Animal experiments were performed as previously described (Le Moigne et al., 2015), according to institutional and national ethical guidelines and approved by the Comité d'éthique en experimentation animale No. 047 with agreement A783223 under the reference APAFIS#11465. Briefly, ΔF508 FVB mice and their wild type FVB littermates (van Doorninck et al., 1995) (INRA, Jouy en Josas, France) were housed in a bio-confinement level 2 facility and CF mice supplemented with movicol (Norgine, The Netherlands). Mice were immunized by subcutaneous (SC) injection with 20 μg of the TLR2eF diluted in PBS in a final volume of 200 μL following a prime/boost scheme (days 0, 21, and 42) as described (Le Moigne et al., 2015). Control mice received PBS only. Two weeks after the third immunization, mice were challenged by aerosol (4×10^8 bacterial cells/mL of CIP S) or intravenously (IV) (10^6 bacteria/mice) as previously described (Catherinot et al., 2007; Bernut et al., 2014; Bakala N'Goma et al.,

2015). At various time-points post infection (Day 1, 12, and 21 for the aerosol challenge and Day 1 and 26 for the IV challenge), mice were sacrificed, and CFU counts were performed on lungs, spleen, and liver as described previously (Le Moigne et al., 2015). For each time-point, a total of 5–7 mice were infected. A control group of mice were sacrificed on the first day after infection (D1) allowing checking the inoculum. Blood samples were collected from the retro-orbital sinus for measurement of antibody levels by an ELISA approach. Samples were warmed at 37°C for 1 h and then centrifuged (10,000 g, 10 min). Collected sera were stored at −80°C until use.

ELISA Assay

Plates were coated with 1 μg/mL of TLR2eF in 100 μL of carbonate-bicarbonate buffer (0.1 M, pH 9.6) overnight at 4°C. Plates were then washed with PBS-Tween 20 (PBS-T) (0.05% v/v) and blocked with PBS-T containing 0.5% bovine serum albumin (PBS-T-BSA) 1 h at 37°C. Sera previously obtained (Roux et al., 2009) were added at dilution of 1:400 in PBS-T-BSA, and were incubated 90 min at 37°C. After four washes, goat anti-human total IgG alkaline phosphatase-conjugated (Southern biotechnology, Birmingham, USA) was added and plates were incubated again 90 min at 37°C. After four washes, 100 μL of 1 mg/mL of *p*-nitrophenylphosphate (Sigma, Saint Quentin Fallavier, France) in diethanolamine buffer (pH 9.8) was added, and incubated at room temperature in the dark for 2 h. Plates were read at 405 nm with a Biorad PR 3100 TSC instrument (Biorad France, Marnes-la-Coquette, France).

Western-Blot

Fifteen μg of TLR2eF per well with Laemmli buffer was electrophoresed on a 15% acrylamide SDS-PAGE. The gel was then transferred on a nitrocellulose membrane. After blocking with TBS-5% skimmed milk, the membrane was cut into bands corresponding to each well and each band was incubated for 2 h with a serum from a CF patient or a control serum diluted 1/500th in TBS-Tween 20 (0.1% v/v)−1% milk. After three washes in TBS-Tween, strips were incubated for two additional hours with goat anti-human IgG-HRP conjugated (CliniSciences, France). After three new washes, peroxidase activity was revealed with HRP substrate (WesternBright ECL, Advansta, CA, USA).

Statistical Analysis

For mice experiments, where two groups were compared, Student's *t*-test was used. A p-value < 0.05 was considered to be significant (ns = non-significant, $^{*}P < 0.05$; $^{**}P < 0.01$; $^{***}P < 0.001$; $^{****}P < 0.0001$). In ELISA experiments, for comparison of the mean values of multiple groups, data that appeared to be statistically significant were compared by analysis of variance and non-parametric analysis using GraphPad Prism 6.0 software (GraphPad Software, La Jolla, CA, USA). A p-value < 0.05 was considered to be significant. (ns = non-significant, $^{*}P < 0.05$; $^{**}P < 0.01$; $^{***}P < 0.001$; $^{****}P < 0.0001$). The technical values of the test in terms of sensitivity and specificity were calculated on the basis of ROC curves.

RESULTS

Purification of a Pro-inflammatory TLR2-Activating Fraction

Mycobacterium abscessus S and R variants differ in the magnitude of the TLR2-mediated inflammatory response they trigger. We used *M. abscessus* R cells to extract cell wall components and to purify, using a cell-based bioassay, the most stimulating TLR2 fractions by reverse-phase chromatography. Elution fractions (EF) were tested for their ability to induce TLR2 signaling in a reporter cell line and their protein concentration was measured in parallel (**Figure 1A**). EFs 48–59 show the highest TLR2 stimulating activity, while containing a low amount of proteins, as shown in **Figure 1A**. These EFs were then pooled to allow subsequent experiments to be carried out. This pooled fraction (called TLR2eF for TLR2-enriched fraction) was separated by SDS-PAGE, showing an enrichment in 4 major proteins (indicated by a star) (**Figure 1B**). We next confirmed that TLR2eF was capable of inducing in a dose-dependent fashion the production of TNF-α by human dendritic cells (**Figure 1C**).

Protein Composition of TLR2eF

We previously showed that the surface fraction overexpressed in *M. abscessus* R variant was enriched in lipoproteins (Roux et al., 2011). To identify the main proteins found in TLR2eF, we performed a proteomic analysis by mass spectrometry of (i) TLR2eF as a whole (**Table 1** and **Supplementary Table 1**), and (ii) the proteins under the four predominant bands illustrated in **Figure 1B**, after their extraction from the SDS-PAGE. Proteomic analysis of the whole TLR2eF identified many proteins, among which the first thirty most abundant, as determined by calculation of the iBAQ metric, are listed in **Table 1**. Three lipoproteins, namely LpqN (MAB_4924) and LprG (MAB_2806) and the conserved 19 kDa lipoantigen family protein (MAB_0885c), were detected. Importantly, it is worth noting that tryptic digestion of lipoproteins is always suboptimal; therefore, the relative abundance of the lipoprotein in such analysis is often underestimated relatively to non-acylated proteins. Several potential lipoproteins or putative lipoprotein precursors of *M. abscessus* were also identified: LppK (MAB_2160c), LprB (MAB_1416), LpqE (MAB_0567c), and three potential lipoproteins LpqH precursors (MAB_0885c, MAB_2379, and MAB_3261c) (**Table 1**). Another putative lipoprotein belonging to the imelysin family protein (MAB_1162c) and the putative lipoprotein MAB_3983c, have also be identified. *Mycobacterium abscessus* homologs of other *Mycobacterium tuberculosis* proteins described to induce signaling *via* TLR2 were also found abundant in TLR2eF, such as Hsp65, Hsp70, and GroEL (**Table 1**) (Floto et al., 2006; Jo et al., 2007; Heo et al., 2011; Basu et al., 2012). Although described as TLR2 ligands (Basu et al., 2007; Palucci et al., 2016), no PE_PGRS proteins were detected in TLR2eF, albeit one WXG100 type VII secretion target family protein (MAB_3754c; EsxU) was observed (**Table 1**). Finally, protein representatives of the Ag85 complex (85A and 85C), in addition to a porin (MSPA; MAB_1080) were also detected, although nothing is presently known regarding their potential recognition by TLR2. Analysis of

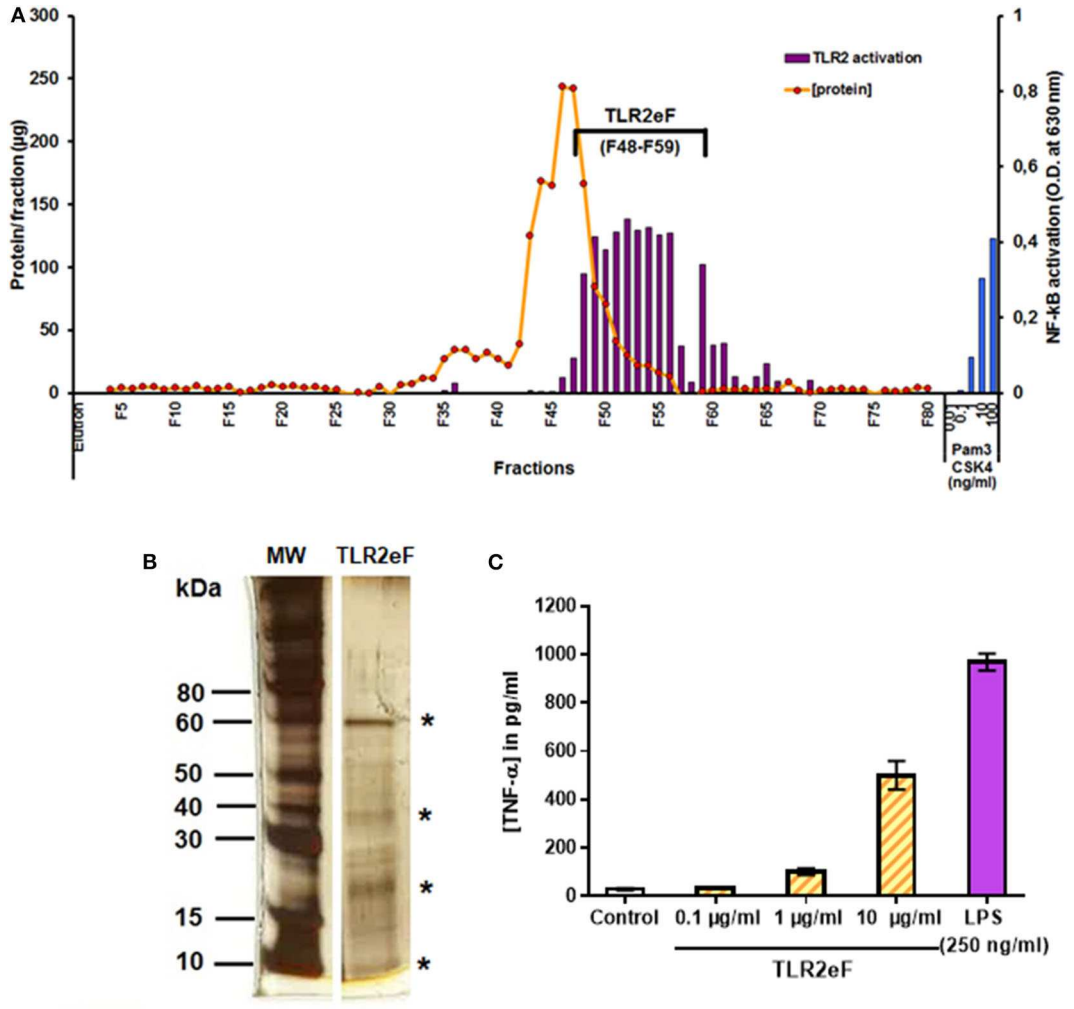

FIGURE 1 | Purification of a TLR2-enriched fraction (TLR2eF) from *M. abscessus* R variant. **(A)** Proteins were extracted by ethanol/water treatment of delipidated *M. abscessus* bacteria and were further resolved by reverse-phase chromatography using a C_4 column eluted by a gradient of acetonitrile in water. The fractions collected were assayed for TLR2-stimulating activity using a HEK-TLR2 reporter cell line and protein concentration of each fraction was measured. The blue bars on the right represent the control stimulation of HEK-TLR2 cells with PamCSK4 in the range of 0.01–100 ng/mL. **(B)** The TLR2eF (F48-F59) were pooled together and the resulting mix was submitted to SDS-PAGE and stained by nitrate silver method. Stars indicate the most important proteins in terms of quantity. **(C)** Production of TNF-α by human dendritic cells (DCs) stimulated by TLR2eF. Human DCs were obtained after 7 days of differentiation from peripheral blood purified monocytes and stimulated by different concentrations of TLR2eF (from 0.1 to 10 µg/mL) or LPS (250 ng/mL) as a control. Production of the inflammatory cytokine TNF-α was measured in the culture supernatant after 48 h of incubation.

the four individual bands excised from the gel identified many of the proteins listed in **Table 1** and did not allow to assign a specific protein to each band (not shown), because of the still complex mixture of proteins composing TLR2eF.

TLR2eF Provides a Partial Protection Against an *M. abscessus* IV Challenge in Mice

Mice were vaccinated three times (Day 1, 21, and 42) subcutaneously (SC) at doses of 20 µg of TLR2eF, and then challenged 2 weeks after the third immunization, as previously described (Le Moigne et al., 2015). ΔF508-CFTR mutated mice (ΔF508-FVB) and their wild-type littermates (FVB mice) were challenged either by aerosol (**Figure 2A**) or by the intravenous (IV) routes (**Figure 2B**) by *M. abscessus* (Le Moigne et al., 2015). *Mycobacterium abscessus* CFU counts were measured per organ (liver, spleen, and lung) at different time points (**Figure 2**).

After an aerosol challenge, we could not see any significant difference in the numbers of viable bacteria in lungs in all evaluated mice (**Figure 2A**). As previously described (Bernut et al., 2014; Le Moigne et al., 2015), CFU in mouse spleen and liver after an aerosol infection were below the sensitivity limit to be counted.

In contrast, *M. abscessus* challenge by an intravenous route allowed recovery of sufficient CFUs in all organs. At day 1

TABLE 1 | Proteins detected in TLR2eF by mass spectrometry.

Gene name	Protein description	Molecular weight (kDa)	Sequence coverage (%)	iBAQ values	Presence in the 4 tryptic-digested band from Targeted MS
MAB_1080	Porin, (partial), MspA	20	36.8	3.16E+09	All
MAB_3731c	60 kDa chaperonin 1 (GroEL protein 1)	56.3	93.3	2.39E+09	All
MAB_0175	Antigen 85-C precursor	33.7	75.2	2.29E+09	All
MAB_0405c	Hypothetical protein MA4S0206_2016/Hypothetical protein MAB_0405c	19.2	47.3	2.11E+09	All
MAB_0176	Antigen 85-A precursor	35	59	2.00E+09	All
MAB_2373	LysM domain protein/Putative mannose-specific lectin precursor	19.6	70.2	1.94E+09	All
MAB_0126c	Putative bacterioferritin BfrB	20.1	91.7	1.90E+09	All
MAB_1439c	Hypotetical protein L835_4095	18.2	50.3	1.85E+09	All
MAB_2824c	Putative integration host factor (MihF)	11.5	61	1.57E+09	18 + 11 kDa bands
MAB_0177	Antigen 85-A/B/C precursor	32.9	77.3	1.45E+09	All
MAB_2806*	Lipoprotein LprG precursor (27 kDa lipoprotein)	23.2	87.6	1.29E+09	All
MAB_1616	Hypothetical protein MA4S0116S_0600/MAB_1616	16.8	76	1.13E+09	All
MAB_3848c	Elongation factor Tu (EF-Tu)	43.5	88.9	1.10E+09	All
MAB_3243	Soluble secreted antigen MPT53 precursor	16	71.3	1.06E+09	All
MAB_4924*	Putative lipoLpqN family protein	21	74.6	1.01E+09	All
MAB_2352	Hypothetical protein L835_4919 (Putative 3-methyladenine DNA glycosylase)	7.5	14.3	9.8E+08	All
MAB_2871c	Hypothetical protein I544_0303	14.4	62	9.69E+08	All
MAB_0218c	Major membrane protein I—mmpI	33.7	91.5	9.35E+08	All
MAB_4184c	Superoxide dismutase [Cu-Zn] precursor—SodC	19.9	73.2	8.97E+08	All
MAB_2329c	Hypothetical protein MBOL_21430	18.3	39.7	8.62E+08	All
MAB_3754c	WXG100 type VII secretion target family protein/EsxU	10.5	98.9	8.27E+08	All
MAB_4203	Aldehyde dehydrogenase family protein	50.9	75.2	8.04E+08	All
MAB_1506c	Putative enoyl-CoA hydratase 1/(MaoC-like dehydratase)	16.6	94.7	7.18E+08	All
MAB_2560	LGFP repeat family protein/Conserved hypothetical protein	17.3	73.5	7.01E+08	All
MAB_2190	Hypothetical protein I542_0868	4.1	94.6	6.79E+08	40 + 18 + 11 kDa bands
MAB_3355	GDSL-like Lipase/Acylhydrolase family protein	25.4	63.9	6.75E+08	All
MAB_4543c	Hypothetical protein L835_2328	18.3	70.8	6.74E+08	40 + 18 kDa bands
MAB_2017	divIVA domain protein (Hypothetical immunogenic protein antigen 84)	30.0	87.6	6.65E+08	All
MAB_0885c*	Conserved 19 kDa lipoantigen family protein/Hypothetical lipoprotein lpqH precursor	14.9	62.7	6.56E+08	18 + 11 kDa bands
MAB_1453	ATP synthase subunit beta AtpD	50.5	90.1	6.45E+08	All
MAB_4273c	Chaperone protein DnaK (Hsp 70)	66.4	77.7	3.90E+08	All
MAB_2379*	Hypothetical lipoprotein LpqH precursor	15.6	56.8	3.27E+08	18 kDa band
MAB_0650	60 kDa chaperonin 2 (Protein Cpn60 2) (GroEL)	56	87.6	2.94E+08	All
MAB_3261c*	Probable lipoprotein LpqH precursor	13.2	76.2	2.37E+08	18 kDa band
MAB_0567c*	Putative lipoprotein lpqE precursor	20.9	55.1	7.86E+07	18 + 11 kDa bands
MAB_2160c*	Putative lipoprotein LppK precursor	19.5	53.6	6.82E+07	18 kDa band
MAB_1162c*	Imelysin family protein Putative lipoprotein	40.1	63.3	4.97E+07	40 + 18 + 11 kDa bands
MAB_1416*	Putative lipoprotein LprB precursor	18.8	55.4	3.54E+07	18 kDa band
MAB_3983c*	Hypothetical protein MAB_3983c/Putative lipoprotein	19.9	57.4	5.83E+06	18 kDa band

**Lipoproteins.*

post-infection the CFU count was comparable in all organs. However, at day 26 post-infection, TLR2eF-vaccinated FVB and ΔF508-FVB mice had significantly fewer mycobacteria in the liver ($P \leq 0.05$) and in the lungs ($P \leq 0.05$) as compared to non-vaccinated control FVB and ΔF508-FVB mice (**Figure 2B**). These results suggest that TLR2eF administration before infection, can induce partial protection against *M. abscessus* IV challenge in mice.

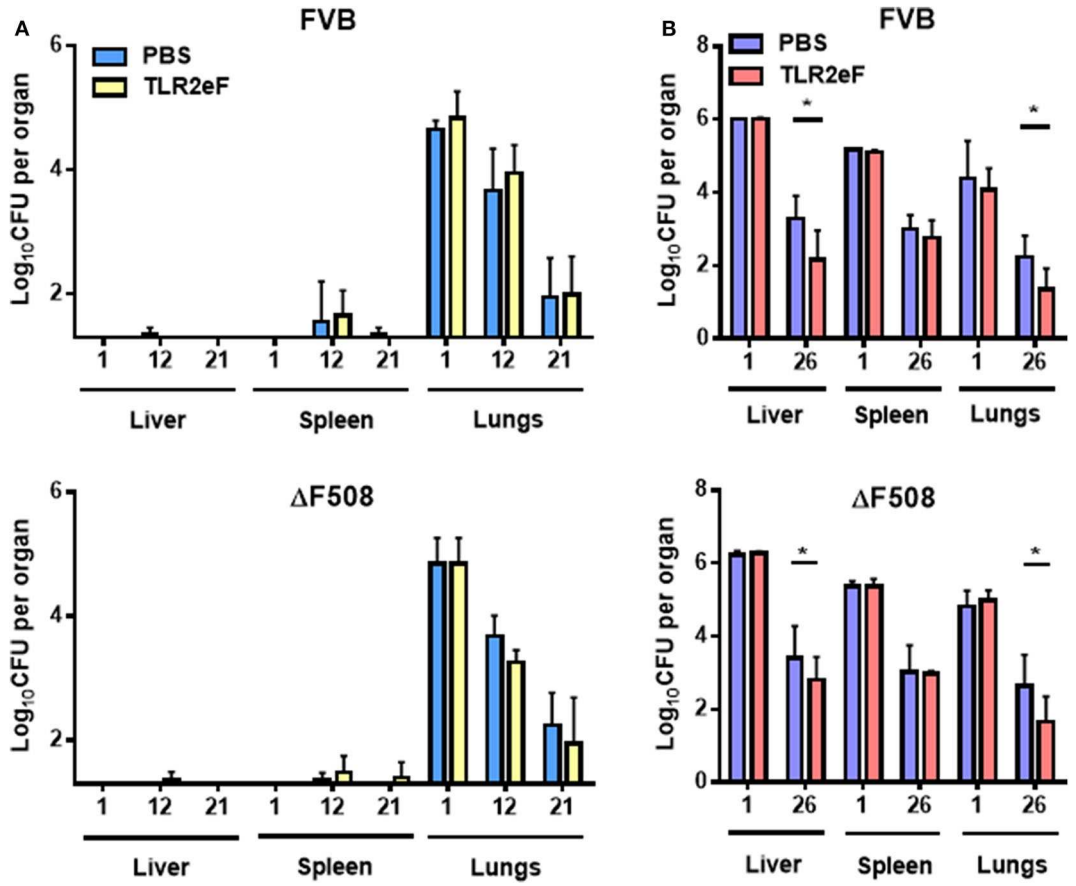

FIGURE 2 | Bacterial load of *M. abscessus* CIP S after aerosol **(A)** or IV **(B)** infections in liver, spleen, and lungs of TLR2eF vaccinated or control-PBS vaccinated wild-type FVB and ΔF508-FVB mice. Lungs, spleen, and liver of mice, infected with an aerosolized solution containing 4×10^8 bacteria/mL of CIP S or intravenously infected with 10^6 bacteria/mice, were collected and homogenized by dislocation. Homogenates were serially diluted and plated on VCAT medium plates for CFU count. Results are expressed as the log units of CFU for TLR2eF-vaccinated mice [yellow **(A)** and red **(B)** bars] or PBS vaccinated mice [control group, light blue **(A)**, and blue **(B)** bars] at days 1, 12, and 21 post-infection for aerosol infection and days 1 and 26 for IV infection. Statistical values for FVB and ΔF508-FVB were; $P = 0.019$ and $P = 0.033$, respectively in their liver; $P = 0.374$ and $P = 0.298$, respectively in the spleens and $P = 0.023$ and $P = 0.045$, respectively in the lungs. For each time-point, a total of 5–7 mice were infected (ns = non-significant, $^*P < 0.05$).

TLR2eF Is Recognized by Mice and Human Sera

TLR2eF was further used as an antigen source in an ELISA assay aimed at diagnosis of *M. abscessus* infection. Firstly, the intensity of the antibody response generated by TLR2eF-immunized mice was compared to the response generated in the *M. abscessus* phospholipase C (PLC)-vaccinated mice (Le Moigne et al., 2015). As a negative control of the antibody response, we used mouse sera sampled at day 1 post-immunization. As shown in **Figure 3A**, we were able to detect an antibody response against TLR2eF in vaccinated mice. However, the intensity of the antibody response was inferior to the intensity of the antibody response obtained in PLC-vaccinated mice (**Figure 3A**).

We then evaluated the antibody response in human sera from CF patients, either infected with non-tuberculous mycobacterial (NTM) or not (**Figure 3B**). In order to develop the test, we have chosen from the collection of sera from a prevalence survey carried out in a population of CF patients in France (Roux et al., 2009), 10 CF patients culture positive for *M. abscessus*, five CF patients culture positive for *Mycobacterium avium* and five CF patients culture positive for *Mycobacterium intracellulare*. As a control population, we selected 20 CF patients from the same study who were NTM negative, and *Pseudomonas aeruginosa* positive or negative in culture. The serological response for patients infected with NTM was higher than in those NTM uninfected or infected with another bacterium such as *P. aeruginosa* ($P < 0.001$ and $P < 0.0001$, respectively) (**Figure 3B**). Nevertheless, when the NTM group is separated according to the mycobacterial species, we observe a true separation between positive and negative by this serological approach, from the population of CF-positive patients in culture to *M. abscessus* or *M. intracellulare* as compared to *M. avium* (**Figure 3C**); with six patients notably showing a response similar to that observed in control patients (4 out of 5 *M. avium*, 1 out of 5 *M. intracellulare*,

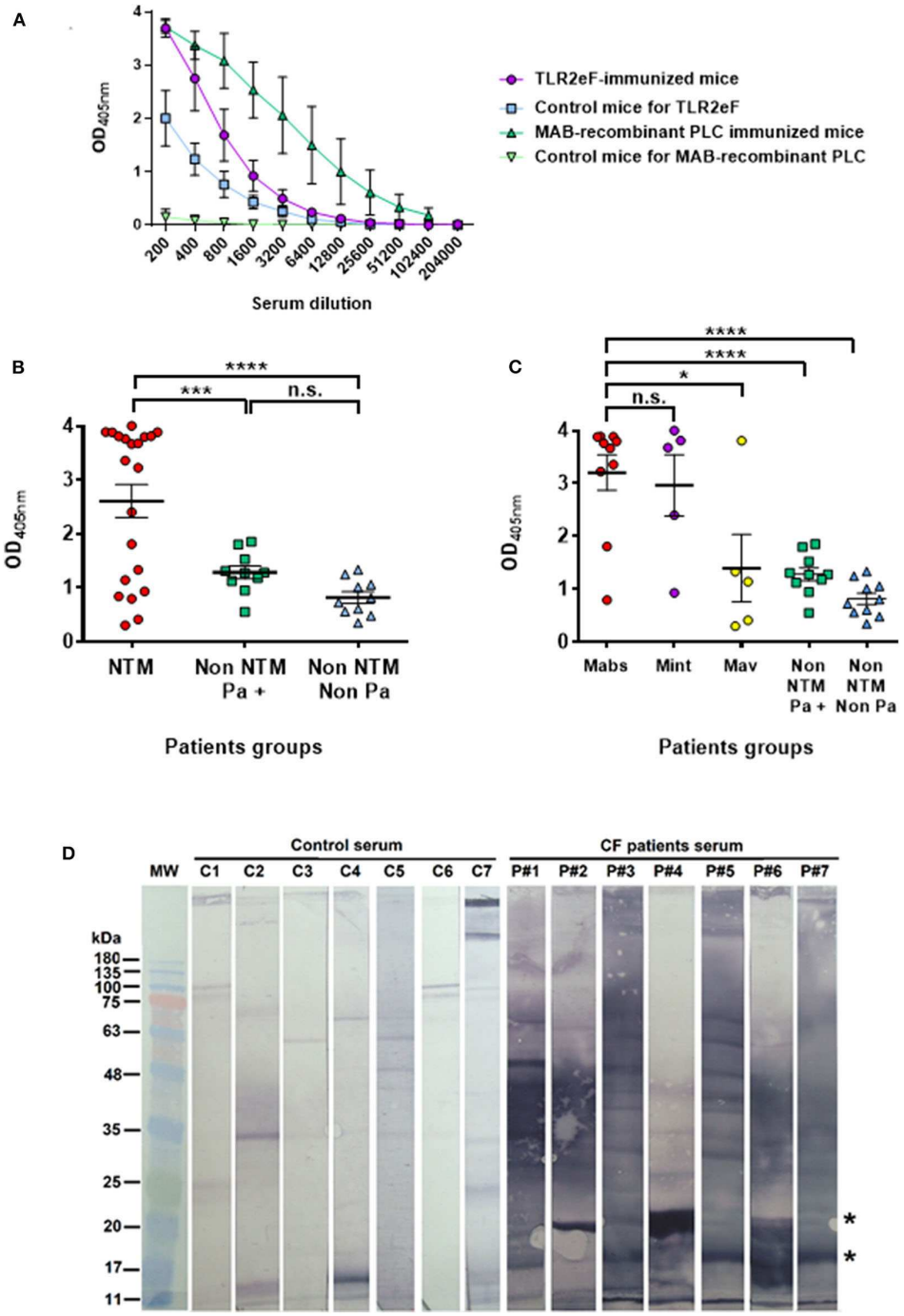

FIGURE 3 | (A) ELISA response from mice immunized with TLR2eF (purple) or control group (blue) against the TLR2eF pool. In green we present the response obtained after the same protocol of immunization with a purified recombinant *M. abscessus* phospholipase C (PLC) and tested in ELISA in the same way. The responses of 4 mice per group were analyzed. **(B)** Specific anti-TLR2eF antibody response in sera from cystic fibrosis patients. Sera were tested in ELISA for the presence of IgG isotype antibodies against TLR2eF components. The results are shown for sera diluted at 1:400. "NTM" group (red circles) corresponds to CF patients infected by non-tuberculous mycobacteria, including *M. abscessus.* "Non-NTM Pa+" (green squares) and "Non-NTM Non-Pa" (blue triangles) groups correspond to CF patients not infected by non-tuberculous mycobacteria, and infected or not by *Pseudomonas aeruginosa*, respectively. Results are mean ± SEM and were analyzed by two-way ANOVA. ***$P < 0.001$; ****$P < 0.0001$. **(C)** Specific anti-TLR2eF antibody response in sera from cystic fibrosis patients. Same results as in **(B)** but "NTM" group is splitted in three groups according NTM infection: CF patients infected by *M. abscessus* (red circles), infected by *M. intracellulare* (purple circles), and by *M. avium* (yellow circles). "Non-NTM Pa+" (green squares) and "Non-NTM Non-Pa" (blue triangles) are as in **(B)**. Results are mean ± SEM and were analyzed by two-way ANOVA. ns, non-significant, *$P < 0.05$; ***$P < 0.001$; ****$P < 0.0001$. **(D)** Anti-TLR2eF antibody response of sera from cystic fibrosis patients observed in Western Blot. Sera from seven of the best CF patients responders (P#1–P#7) against TLR2eF in ELISA were diluted at 1/500th and tested in western-blot against 15 μg of TLR2eF resolved on a 15% acrylamide gel and transferred to a nitrocellulose membrane. Serum from seven non-CF persons (C1–C7) were used as a control.

and 1 out of 10 *M. abscessus*). The technical values of the test in terms of sensitivity and specificity were calculated on the basis of ROC (not shown, AUC = 0.779) curves allowing the determination of a threshold value of 1.803. The test sensitivity was 70% (95% CI 45.7 to 88.1%) and the specificity 95% (95% CI 75.1 to 99.9%).

In order to determine by western blot which proteins in TRL2eF might be recognized by CF patient antibodies, we used seven positive CF sera, used in the ELISA assay, as examples. Although two proteins with apparent molecular weights between 17 and 20 kDa, which might correspond to one of the major proteins observed in SDS-PAGE (**Figure 1B**), were commonly recognized in six tested sera (indicated by two stars in **Figure 3D**), each serum showed a different pattern.

DISCUSSION

Mycobacterial species that are pathogenic for humans and animals have a specific ability to both positively and negatively regulate innate and adaptive immune responses in the host (Kaufmann, 2001; Abel et al., 2002). One deleterious consequence is the persistence of pathogens within the infected host. Pathogenic mycobacteria have turned this to their own advantage, striking a balance with their hosts, and making it difficult or even impossible to eradicate (Zahrt, 2003). The peculiar mycobacterial cell envelope plays a key role in such modulation. The outer layers, composed of the capsule and the mycomembrane, confer protection against antiseptics and antibiotics, and contain many (glyco)lipids that are inflammatory triggers, although some other (glyco)lipids might modulate the intensity of the response via anti-inflammatory or masking properties.

Mycobacterium abscessus possesses the advantageous property of an interchangeable morphology, as described for some other mycobacterial species *in vitro* (Fregnan and Smith, 1962). However, the *M. abscessus* transition from S to R morphology was mainly observed *in vivo*, during infection in CF patients (Catherinot et al., 2009), or in mouse models (Rottman et al., 2007). The consequences are often catastrophic for CF patients and result in exacerbations of disease with acute respiratory distress syndrome (Catherinot et al., 2009). The main pathological mechanisms are (i) a hyper-proinflammatory response, due a very high TLR2 activation and the synthesis of proinflammatory cytokines and (ii) a very rapid extracellular growth (Salvator et al., 2018) with the formation of cords (Bernut et al., 2014).

In order to combat infection with this multi-resistant mycobacterium, our goal here was to evaluate the vaccine and diagnostic potentials of a still crude cell envelope fraction, TRL2eF, showing a high TLR2-stimulating activity. Although the serological response observed was of interest, the protective response after immunization was disappointing.

Despite being prepared using different techniques, TRL2eF and the so-called interphase fraction reported in Roux et al. (2011) show a similar protein composition, most particularly regarding lipoproteins. Of course, the composition of such crude fractions may be slightly different from one batch to another, but our first goal was to prove the usefulness and the potency of the TLR2-stimulating compounds overexpressed in the *M. abscessus* R variant, as a whole fraction.

TLR2eF showed no protection toward an aerosol challenge, and only a partial protection in the liver and the lungs toward an IV *M. abscessus* challenge. In fact, immunization with the TLR2eF, might be insufficient to activate the adaptive immune response required to make a vaccine, as we also need potent antigens. Consequently, do we confer an antigen-dependent protection or simply boost innate immunity that results in an improvement in infection outcome via the IV route only?

Signals from TLR2 are required for phagosome maturation (Blander and Medzhitov, 2004) and reduction of *M. tuberculosis* viability inside macrophages (Thoma-Uszynski et al., 2001). However, the intense inflammatory response observed in CF patients infected with *M. abscessus* during the emergence of the R variant (Catherinot et al., 2009), rather results in a lack of infection control. The TLR2-induced response might be suboptimal due to the presence of TLR2 lipid antagonists in TLR2eF. For instance, complex *M. tuberculosis* glycolipids have been described as TLR2 antagonists (Blanc et al., 2017), but such lipids have been removed during the purification procedure of TLR2eF (see experimental section). We cannot exclude the presence of TLR2 protein antagonists in TLR2eF, as described for ESAT-6 (EsxA), which inhibits TLR2-mediated NF-kB and IRFs activation (Pathak et al., 2007). In fact, we found a protein of this ESX family in the main proteins of our TLR2eF: EsxU (MAB_3754c). A Tn library screening, recently described for *M. abscessus* (Dubois et al., 2018; Laencina et al., 2018) and *M. tuberculosis* (Blanc et al., 2017) might allow a more precise characterization of such antagonists.

Finally, we argue that the immune response required to control bacterial infection might be different with regard to the route of *M. abscessus* administration. A B-cell response might preferentially act to inhibit bacterial respiratory infection in mice, through the secretion of immunoglobulin-A (IgA) in the lungs. However, lipoprotein inhibition of MHC-II presentation might be responsible for the induction of a suboptimal B cell response (Harding and Boom, 2010). As we have seen a weaker antibody response after TLR2eF immunization in mice, as compared to PLC vaccinated mice, the fact that we did not observe protection after aerosol challenge could be due to the partial inhibition of this humoral response, an important factor to circumvent pathogen invasion in the context of lung infection. Comparatively, a predominant antigen-specific $CD8^+$ T cell (CTL) response is observed in the systemic compartment, when boosted by TLR2-ligands (Deres et al., 1989; Jackson et al., 2004; Borsutzky et al., 2006). This might explain the more rapid elimination of *M. abscessus* seen repeatedly in the TLR2eF-vaccinated IV infected mice.

Despite a disappointing protective response, it was interesting to evaluate whether individual components in TLR2eF were recognized by the immune system in CF patients infected with *M. abscessus*. This latter point was highlighted by a recent clinical study showing the importance of detecting *M. abscessus* infection in CF patients (Qvist et al., 2015). Therefore, clinical values obtained in our study are very promising for the detection of patients who have been in contact with NTM and have developed an antibody response. What is fundamentally interesting is that

the lowest optical density values, similar to those of control patients, are obtained for patients infected with *M. avium*. Four of the six patients with the lowest values are infected with *M. avium*. By improving the technical values of our serological test, we will therefore be able to differentiate between CF patients infected with *M. avium* and those infected with *M. abscessus*. On the contrary, meeting the initial objective of having a reagent allowing to discriminate NTMs, the goal is reached. Additional studies should be undertaken to know if there is common antigens or TLR2-ligands between *M. abscessus* and *M. intracellulare* and inversely to explain the absence of response with *M. avium*. From a diagnostic point of view, it may make it possible to detect this patient group, and to better evaluate them clinically and microbiologically in order to adapt treatment to prevent progressive infection. In addition to detecting CF patients infected by *M. abscessus*, the presence of high antibody responses, as seen in several patients against TLR2eF, might allow the differentiation of CF patients infected with the R morphotype, responsible for the most severe form of the disease, and with an imperative for early treatment.

Based on this study, we will pursue our efforts to evaluate the use of TLR2eF as a serological tool, more particularly to determine its potential for identifying NTM infections in CF patients in the context of microbiological diagnosis during epidemiological studies.

DATA AVAILABILITY STATEMENT

All datasets generated for this study are included in the article/**Supplementary Material**.

ETHICS STATEMENT

The studies involving human participants were reviewed and approved by the OMA (Observatoire des mycobactéries atypiques) group. The patients/participants provided their written informed consent to participate in this study. The animal study was reviewed and approved by Comité d'éthique en experimentation animale N°047 with agreement A783223.

AUTHOR CONTRIBUTIONS

VL, J-LG, JN, and J-LH designed the project and experiments. VL, A-LR, AJ-M, LB, KC, and OB-S performed the experiments. VL, JN, SC, and J-LH wrote and corrected the manuscript. All authors contributed to the article and approved the submitted version.

FUNDING

This work was supported by grants from the Association Vaincre la Mucoviscidose (RF20110600446/1/3/130) and the Région Île-de-France (post-doctoral fellowship for VL).

ACKNOWLEDGMENTS

We gratefully acknowledge Dr. Jacques Prandi and Ms. Sophie Zuberogoitia (IPBS) for helpful assistance with reverse phase chromatography. We also acknowledge Dr. B. Marshall (Southampton University, UK) for helpful comments and critical reading of the manuscript. This work has benefited from the facilities and expertise of the proteomic platform of IMM FR3479 CNRS.

SUPPLEMENTARY MATERIAL

The Supplementary Material for this article can be found online at: https://www.frontiersin.org/articles/10.3389/fcimb.2020.00432/full#supplementary-material

REFERENCES

Abel, B., Thieblemont, N., Quesniaux, V. J., Brown, N., Mpagi, J., Miyake, K., et al. (2002). Toll-like receptor 4 expression is required to control chronic *Mycobacterium tuberculosis* infection in mice. *J. Immunol.* 169, 3155–3162. doi: 10.4049/jimmunol.169.6.3155

Bakala N'Goma, J. C., Le Moigne, V., Soismier, N., Laencina, L., Le Chevalier, F., Roux, A.-L., et al. (2015). *Mycobacterium abscessus* phospholipase C expression is induced during coculture within amoebae and enhances *M. abscessus* virulence in mice. *Infect. Immun.* 83, 780–791. doi: 10.1128/IAI.02032-14

Basu, J., Shin, D. M., and Jo, E. K. (2012). Mycobacterial signaling through toll-like receptors. *Front. Cell. Infect. Microbiol.* 2:145. doi: 10.3389/fcimb.2012.00145

Basu, S., Pathak, S. K., Banerjee, A., Pathak, S., Bhattacharyya, A., Yang, Z., et al. (2007). Execution of macrophage apoptosis by PE_PGRS33 of *Mycobacterium tuberculosis* is mediated by Toll-like receptor 2-dependent release of tumor necrosis factor-alpha. *J. Biol. Chem.* 282, 1039–1050. doi: 10.1074/jbc.M604379200

Bernut, A., Le Moigne, V., Lesne, T., Lutfalla, G., Herrmann, J.-L., and Kremer, L. (2014). *In vivo* assessment of drug efficacy against *Mycobacterium abscessus* using the embryonic zebrafish test system. *Antimicrob. Agents Chemother.* 58, 4054–4063. doi: 10.1128/AAC.00142-14

Blanc, L., Gilleron, M., Prandi, J., Song, O. R., Jang, M. S., and Gicquel, B. (2017). *Mycobacterium tuberculosis* inhibits human innate immune responses via the production of TLR2 antagonist glycolipids. *Proc. Natl. Acad. Sci. U.S.A.* 114, 11205–11210. doi: 10.1073/pnas.1707840114

Blander, J. M., and Medzhitov, R. (2004). Regulation of phagosome maturation by signals from toll-like receptors. *Science* 304, 1014–1018. doi: 10.1126/science.1096158

Borsutzky, S., Ebensen, T., Link, C., Becker, P. D., Fiorelli, V., Cafaro, A., et al. (2006). Efficient systemic and mucosal responses against the HIV-1 Tat protein by prime/boost vaccination using the lipopeptide MALP-2 as adjuvant. *Vaccine* 24, 2049–2056. doi: 10.1016/j.vaccine.2005.11.025

Brightbill, H. D., Libraty, D. H., Krutzik, S. R., Yang, R. B., Belisle, J. T., Bleharski, J. R., et al. (1999). Host defense mechanisms triggered by microbial lipoproteins through toll-like receptors. *Science* 285, 732–736. doi: 10.1126/science.285.5428.732

Catherinot, E., Clarissou, J., Etienne, G., Ripoll, F., Emile, J.-F., Daffé, M., et al. (2007). Hypervirulence of a rough variant of the *Mycobacterium abscessus* type strain. *Infect. Immun.* 75, 1055–1058 doi: 10.1128/IAI.00835-06

Catherinot, E., Roux, A.-L., Macheras, E., Hubert, D., Matmar, M., Dannhoffer, L., et al. (2009). Acute respiratory failure involving an R variant of *Mycobacterium abscessus*. *J. Clin. Microbiol.* 47, 271–274. doi: 10.1128/JCM.01478-08

Conroy, H., Marshall, N. A., and Mills, K. H. (2008). TLR ligand suppression or enhancement of Treg cells? A double-edged sword in immunity to tumours. *Oncogene* 27, 168–180. doi: 10.1038/sj.onc.1210910

Cullen, A. R., Cannon, C. L., Mark, E. J., and Colin, A. A. (2000). *Mycobacterium abscessus* infection in cystic fibrosis. Colonization or infection? *Am. J. Respir. Crit. Care Med.* 161, 641–645. doi: 10.1164/ajrccm.161.2.9903062

Deres, K., Schild, H., Wiesmuller, K. H., Jung, G., and Rammensee, H. G. (1989). *In vivo* priming of virus-specific cytotoxic T lymphocytes with synthetic lipopeptide vaccine. *Nature* 342, 561–564. doi: 10.1038/342561a0

Dubois, V., Viljoen, A., Laencina, L., Le Moigne, V., Bernut, A., Dubar, F., et al. (2018). $MmpL8_{MAB}$ controls *Mycobacterium abscessus* virulence and production of a previously unknown glycolipid family. *Proc. Natl. Acad. Sci. U.S.A.* 115, E10147–E10156. doi: 10.1073/pnas.1812984115

Dulphy, N., Herrmann, J.-L., Nigou, J., Réa, D., Boissel, N., Puzo, G., et al. (2007). Intermediate maturation of *Mycobacterium tuberculosis* LAM-activated human dendritic cells. *Cell. Microbiol.* 9, 1412–1425. doi: 10.1111/j.1462-5822.2006.00881.x

Floto, R. A., MacAry, P. A., Boname, J. M., Mien, T. S., Kampmann, B., Hair, J. R., et al. (2006). Dendritic cell stimulation by mycobacterial Hsp70 is mediated through CCR5. *Science* 314, 454–458. doi: 10.1126/science.1133515

Fregnan, G. B., and Smith, D. W. (1962). Description of various colony forms of mycobacteria. *J. Bacteriol.* 83, 819–827. doi: 10.1128/JB.83.4.819-827.1962

Geijtenbeek, T. B., van Vliet, S. J., Koppel, E. A., Sanchez-Hernandez, M., Vandenbroucke-Grauls, C. M., Appelmelk, B., et al. (2003). Mycobacteria target DC-SIGN to suppress dendritic cell function. *J. Exp. Med.* 197, 7–17. doi: 10.1084/jem.20021229

Gilleron, M., Quesniaux, V. F., and Puzo, G. (2003). Acylation state of the phosphatidylinositol hexamannosides from *Mycobacterium bovis* bacillus Calmette Guerin and *Mycobacterium tuberculosis* H37Rv and its implication in Toll-like receptor response. *J. Biol. Chem.* 278, 29880–29889. doi: 10.1074/jbc.M303446200

Griffith, D. E., Girard, W. M., and Wallace, R. J. Jr. (1993). Clinical features of pulmonary disease caused by rapidly growing mycobacteria. An analysis of 154 patients. *Am. Rev. Respir. Dis.* 147, 1271–1278. doi: 10.1164/ajrccm/147.5.1271

Harding, C. V., and Boom, W. H. (2010). Regulation of antigen presentation by *Mycobacterium tuberculosis*: a role for Toll-like receptors. *Nat. Rev. Microbiol.* 8, 296–307. doi: 10.1038/nrmicro2321

Heo, D. R., Shin, S. J., Kim, W. S., Noh, K. T., Park, J. W., Son, K. H., et al. (2011). *Mycobacterium tuberculosislpdC*, Rv0462, induces dendritic cell maturation and Th1 polarization. *Biochem. Biophys. Res. Commun.* 411, 642–647. doi: 10.1016/j.bbrc.2011.07.013

Higgins, S. C., and Mills, K. H. (2010). TLR, NLR agonists, and other immune modulators as infectious disease vaccine adjuvants. *Curr. Infect. Dis. Rep.* 12, 4–12. doi: 10.1007/s11908-009-0080-9

Jackson, D. C., Lau, Y. F., Le, T., Suhrbier, A., Deliyannis, G., Cheers, C., et al. (2004). A totally synthetic vaccine of generic structure that targets Toll-like receptor 2 on dendritic cells and promotes antibody or cytotoxic T cell responses. *Proc. Natl. Acad. Sci. U.S.A.* 101, 15440–15445. doi: 10.1073/pnas.0406740101

Jo, E. K., Yang, C. S., Choi, C. H., and Harding, C. V. (2007). Intracellular signalling cascades regulating innate immune responses to Mycobacteria: branching out from Toll-like receptors. *Cell. Microbiol.* 9, 1087–1098. doi: 10.1111/j.1462-5822.2007.00914.x

Jönsson, B. E., Gilljam, M., Lindblad, A., Ridell, M., Wold, A. E., and Welinder-Olsson, C. (2007). Molecular epidemiology of *Mycobacterium abscessus*, with focus on cystic fibrosis. *J. Clin. Microbiol.* 45, 1497–1504. doi: 10.1128/JCM.02592-06

Kaufmann, S. H. (2001). How can immunology contribute to the control of tuberculosis? *Nat. Rev. Immunol.* 1, 20–30. doi: 10.1038/35095558

Kaufmann, S. H., and Schaible, U. E. (2003). A dangerous liaison between two major killers: *Mycobacterium tuberculosis* and HIV target dendritic cells through DC-SIGN. *J. Exp. Med.* 197, 1–5. doi: 10.1084/jem.20021964

Laencina, L., Dubois, V., Le Moigne, V., Viljoen, A., Majlessi, L., Pritchard, J., et al. (2018). Identification of genes required for *Mycobacterium abscessus* growth *in vivo* with a prominent role of the ESX-4 locus. *Proc. Natl. Acad. Sci. U.S.A.* 115, E1002–E1011. doi: 10.1073/pnas.1713195115

Le Moigne, V., Rottman, M., Goulard, C., Barteau, B., Poncin, I., Soismier, N., et al. (2015). Bacterial phospholipases C as vaccine candidate antigens against cystic fibrosis respiratory pathogens: the *Mycobacterium abscessus* model. *Vaccine* 33, 2118–2124. doi: 10.1016/j.vaccine.2015.03.030

Martinez-Pinna, R., Gonzalez de Peredo, A., Monsarrat, B., Burlet-Schiltz, O., and Martin-Ventura, J. L. (2014). Label-free quantitative proteomic analysis of human plasma-derived microvesicles to find protein signatures of abdominal aortic aneurysms. *Proteomics Clin. Appl.* 8, 620–625. doi: 10.1002/prca.201400010

Nigou, J., Gilleron, M., Cahuzac, B., Bounéry, J. D., Herold, M., Thurnher, M., et al. (1997). The phosphatidyl-myo-inositol anchor of the lipoarabinomannans from *Mycobacterium bovis* bacillus Calmette Guérin. Heterogeneity, structure, and role in the regulation of cytokine secretion. *J. Biol. Chem.* 272, 23094–23103. doi: 10.1074/jbc.272.37.23094

Nigou, J., Zelle-Rieser, C., Gilleron, M., Thurnher, M., and Puzo, G. (2001). Mannosylated lipoarabinomannans inhibit IL-12 production by human dendritic cells: evidence for a negative signal delivered through the mannose receptor. *J. Immunol.* 166, 7477–7485. doi: 10.4049/jimmunol.166.12.7477

Olivier, K. N., Weber, D. J., Wallace, R. J. Jr., Faiz, A. R., Lee, J. H., Zhang, Y., et al. (2003). Nontuberculous mycobacteria. I: multicenter prevalence study in cystic fibrosis. *Am. J. Respir. Crit. Care Med.* 167, 828–834. doi: 10.1164/rccm.200207-678OC

Palucci, I., Camassa, S., Cascioferro, A., Sali, M., Anoosheh, S., Zumbo, A., et al. (2016). PE_PGRS33 contributes to *Mycobacterium tuberculosis* entry in macrophages through interaction with TLR2. *PLoS ONE* 11:e0150800. doi: 10.1371/journal.pone.0150800

Pathak, S. K., Basu, S., Basu, K. K., Banerjee, A., Pathak, S., Bhattacharyya, A., et al. (2007). Direct extracellular interaction between the early secreted antigen ESAT-6 of *Mycobacterium tuberculosis* and TLR2 inhibits TLR signaling in macrophages. *Nat. Immunol.* 8, 610–618. doi: 10.1038/ni1468

Pawlik, A., Garnier, G., Orgeur, M., Tong, P., Lohan, A., Le Chevalier, F., et al. (2013). Identification and characterization of the genetic changes responsible for the characteristic smooth-to-rough morphotype alterations of clinically persistent *Mycobacterium abscessus*. *Mol. Microbiol.* 90, 612–629. doi: 10.1111/mmi.12387

Quesniaux, V. J., Nicolle, D. M., Torres, D., Kremer, L., Guérardel, Y., Nigou, J., et al. (2004). Toll-like receptor 2 (TLR2)-dependent-positive and TLR2-independent-negative regulation of proinflammatory cytokines by mycobacterial lipomannans. *J. Immunol.* 172, 4425–4434. doi: 10.4049/jimmunol.172.7.4425

Qvist, T., Pressler, T., Taylor-Robinson, D., Katzenstein, T. L., and Høiby, N. (2015). Serodiagnosis of *Mycobacterium abscessus* complex infection in cystic fibrosis. *Eur. Respir. J.* 4, 707–716. doi: 10.1183/09031936.00011815

Ripoll, F., Deshayes, C., Pasek, S., Laval, F., Beretti, J. L., Biet, F., et al. (2007). Genomics of glycopeptidolipid biosynthesis in *Mycobacterium abscessus* and *M. chelonae*. *BMC Genomics* 8:114. doi: 10.1186/1471-2164-8-114

Rottman, M., Catherinot, E., Hochedez, P., Emile, J.-F., Casanova, J.-L., Gaillard, J.-L., et al. (2007). Importance of T cells, gamma interferon, and tumor necrosis factor in immune control of the rapid grower *Mycobacterium abscessus* in C57BL/6 mice. *Infect. Immun.* 75, 5898–5907. doi: 10.1128/IAI.00014-07

Roux, A.-L., Catherinot, E., Ripoll, F., Soismier, N., Macheras, E., Ravilly, S., et al. (2009). Multicenter study of prevalence of nontuberculous mycobacteria in patients with cystic fibrosis in France. *J. Clin. Microbiol.* 47, 4124–4128. doi: 10.1128/JCM.01257-09

Roux, A.-L., Ray, A., Pawlik, A., Medjahed, H., Etienne, G., Rottman, M., et al. (2011). Overexpression of proinflammatory TLR-2-signalling lipoproteins in hypervirulent mycobacterial variants. *Cell. Microbiol.* 13, 692–704. doi: 10.1111/j.1462-5822.2010.01565.x

Salvator, H., Berti, E., Catherinot, E., Rivaud, E., Chabrol, A., Nguyen, S., et al. (2018). Pulmonary alveolar proteinosis and *Mycobacterium abscessus* lung infection related to ruxolitinib after allogeneic stem cell transplantation. *Eur. Respir. J.* 51:1701960. doi: 10.1183/13993003.01960-2017

Sanguinetti, M., Ardito, F., Fiscarelli, E., La Sorda, M., D'Argenio, P., Ricciotti, G., et al. (2001). Fatal pulmonary infection due to multidrug-resistant *Mycobacterium abscessus* in a patient with cystic fibrosis. *J. Clin. Microbiol.* 39, 816–819. doi: 10.1128/JCM.39.2.816-819.2001

Schwanhäusser B., Busse D., Li N., Dittmar G., Schuchhardt J., Wolf J. et al. (2011). Global quantification of mammalian gene expression control. *Nature.* 473, 337–342. doi: 10.1038/nature10098

Tailleux, L., Schwartz, O., Herrmann, J. L., Pivert, E., Jackson, M., Amara, A., et al. (2002). DC-SIGN is the major *Mycobacterium tuberculosis* receptor on human dendritic cells. *J. Exp. Med.* 197, 119–125. doi: 10.1084/jem.20021468

Talpin, A., Costantino, F., Bonilla, N., Leboime, A., Letourneur, F., Jacques, S., et al. (2014). Monocyte-derived dendritic cells from HLA-B27+ axial spondyloarthritis (SpA) patients display altered functional capacity and deregulated gene expression. *Arthritis Res. Ther.* 16:417. doi: 10.1186/s13075-014-0417-0

Thoma-Uszynski, S., Kiertscher, S. M., Ochoa, M. T., Bouis, D. A., Norgard, M. V., Miyake, K., et al. (2000). Activation of toll-like receptor 2 on human dendritic cells triggers induction of IL-12, but not IL-10. *J. Immunol.* 165, 3804–3810. doi: 10.4049/jimmunol.165.7.3804

Thoma-Uszynski, S., Stenger, S., Takeuchi, O., Ochoa, M. T., Engele, M., Sieling, P. A., et al. (2001). Induction of direct antimicrobial activity through mammalian Toll-like receptors. *Science* 291, 1544–1547. doi: 10.1126/science.291.5508.1544

van Doorninck, J. H., French, P. J., Verbeek, E., Peters, R. H., Morreau, H., Bijman, J., et al. (1995). A mouse model for the cystic fibrosis delta F508 mutation. *EMBO J.* 14, 4403–4411. doi: 10.1002/j.1460-2075.1995.tb00119.x

Viana-Niero, C., Lima, K. V. B., Lopes, M. L., da Silva Rabello, M. C., Marsola, L. R., Brilhante, V. C. R., et al. (2008). Molecular characterization of *Mycobacterium massiliense* and *Mycobacterium bolletii* in isolates collected from outbreaks of infections after laparoscopic surgeries and cosmetic procedures. *J. Clin. Microbiol.* 46, 850–855. doi: 10.1128/JCM.02052-07

Zahrt, T. C. (2003). Molecular mechanisms regulating persistent *Mycobacterium tuberculosis* infection. *Microbes Infect.* 5, 159–167. doi: 10.1016/S1286-4579(02)00083-7

Conflict of Interest: The authors declare that the research was conducted in the absence of any commercial or financial relationships that could be construed as a potential conflict of interest.

Advantages of publishing in Frontiers

OPEN ACCESS
Articles are free to read for greatest visibility and readership

FAST PUBLICATION
Around 90 days from submission to decision

HIGH QUALITY PEER-REVIEW
Rigorous, collaborative, and constructive peer-review

TRANSPARENT PEER-REVIEW
Editors and reviewers acknowledged by name on published articles

Frontiers
Avenue du Tribunal-Fédéral 34
1005 Lausanne | Switzerland

Visit us: www.frontiersin.org
Contact us: info@frontiersin.org | +41 21 510 17 00

REPRODUCIBILITY OF RESEARCH
Support open data and methods to enhance research reproducibility

DIGITAL PUBLISHING
Articles designed for optimal readership across devices

FOLLOW US
@frontiersin

IMPACT METRICS
Advanced article metrics track visibility across digital media

EXTENSIVE PROMOTION
Marketing and promotion of impactful research

LOOP RESEARCH NETWORK
Our network increases your article's readership